


DELHI COLLEGE OF ENGINEERING



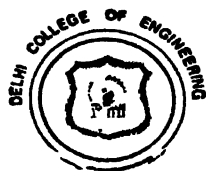
BAWANA ROAD, DELHI-42

LIBRARY

Class No. 6213133

Book No BEW'

Accession No 21884



**Borrower is requested
to check the book and
get the signatures on
the torned pages, if any.**

Alternating Current Machinery



THE MACMILLAN COMPANY
NEW YORK • BOSTON • CHICAGO
DALLAS • ATLANTA • SAN FRANCISCO

MACMILLAN AND CO. LIMITED
LONDON • BOMBAY • CALCUTTA
MADRAS • MELBOURNE

**THE MACMILLAN COMPANY
OF CANADA LIMITED**
TORONTO

L. V. BEWLEY PROFESSOR AND DIRECTOR OF THE CURRICULUM
IN ELECTRICAL ENGINEERING, MITCHELL UNIVERSITY

Alternating Current Machinery

THE MACMILLAN COMPANY *New York 1949*

COPYRIGHT, 1949, BY THE MACMILLAN COMPANY

All rights reserved no part of this book may be reproduced in any form without permission in writing from the publisher, except by a reviewer who wishes to quote brief passages in connection with a review written for inclusion in magazine or newspaper.

PRINTED IN THE UNITED STATES OF AMERICA

To my Father and Mother

Frank W. Bewley

Sadie M. Bewley

Preface

The justification for another book on alternating current machinery lies in the real need for a modern text that will present the more recent advances in theory and methods of analysis, and which will break away from some of the false premises and artificial concepts that have plagued this subject for half a century. The present text does not pretend to be a comprehensive treatment covering all types of electric apparatus, but rather a general method of analysis applied to the more important kinds of alternating current machinery. In Chapter 3 certain general equations applicable to all electrical machines are developed. This is followed by specific chapters on the polyphase induction motor, single phase induction motor, a-c commutator motors, synchronous machines, and synchronous converters. In the Appendices, a very general and comprehensive analysis is offered for the benefit of those who would pursue machine theory beyond an elementary point of view. Each chapter follows the same pattern. In the chapter introductions are given the definitions, discussion of purposes and uses, and perhaps some classifications. In the section on principles of operation are established the physical concepts and simplest basic relationships, devoid of mathematical ramifications or refinements. This is followed by a brief discussion of structural details and types of construction. After these preliminaries, the more complete theory is developed, usually in the order: magnetomotive forces (or

armature reactions), permeances, flux densities, fluxes, voltages, currents, power, torque, and performance characteristics.

In certain respects the methods of this text differ radically from those found in standard treatises. Its key features are a general *equation of voltage* which recognizes the simultaneous movement of the conductors, displacement of the flux, and pulsation of the flux, and which includes as special cases all the processes of voltage induction to be found in any machine; and a general *equation of armature reaction* which applies to any machine, a-c or d-c. From the point of view of these general equations one machine differs from another only in the presence or absence of specific terms, and thus great unification of concept ensues.

My original intention in writing this book had been to base the whole of machine theory on these two general concepts; but as the work progressed it became apparent that many of the accepted methods of machine analysis would fall by the wayside if a completely unified method of attack were followed too strictly. It seemed better, therefore, while preserving the central theme of a general method of attack, to weave into the analysis the older and more widely known procedures. Nevertheless, I believe that machine theory ultimately will become much more condensed by strict adherence to the general method, and abandonment of some of the old scaffolding on which many of our concepts have been built.

Other features representing essential departures from traditional treatment may be mentioned. The concept of a fictitious winding in a transformer (the consolidated eddy current circuits) to account for the core loss permits the equivalent circuit to be derived from the differential equations as well as by the traditional Steinmetz method, and there is no need to apologize for the failure of the core loss term to materialize. The parallel piecemeal development of the equations, vector diagrams, and equivalent circuits employed in the treatment of the transformer, and of the polyphase induction motor, are believed to offer a clearer and cleaner approach to the study of these machines than is otherwise possible. The treatment of multiple winding transformer circuits is of great power and utility, and the underlying philosophy is applicable to any other type of circuit. The sharp distinction between *time* and *space* vector diagrams, employed in some detail in the cross-field theory of the single-phase induction motor, is essential to a real understanding of machine theory. The reader may encounter certain other methods of approach, of both an analytical and a pedagogical nature, which deviate from the normal.

This text does not try to avoid long mathematical manipulations in cases where such are essential to a reasonably complete understanding of electrical machinery. However, it must be pointed out that most of them involve nothing more than simple trigonometric and algebraic transformations. They are time consuming, but not difficult. It is not possible to delve very far beneath the surface of machine theory without becoming involved in a considerable mass of symbols. All too often this is avoided by making such simplifying assumptions as to vitiate the results. For example, the usual simplifying assumptions made in analyzing the armature reaction of a synchronous converter are such as to ignore completely the most important terms!

Certain aspects of machine theory, such as the flux distribution in slots, air gaps, and around field poles; eddy-current loss in conductors; and other field problems have not been included, as they have been dealt with adequately in a companion text "Two Dimensional Fields in Electrical Engineering."

No attempt has been made in this text to include the mercury arc rectifier or other electronic devices, since to treat them with a completeness comparable to that given machines would require excessive space in a book devoted primarily to machinery. An adequate treatment of such electronic devices, along with their controls, should require a separate course and text in industrial electronics.

Highly specialized machines, such as eddy current and hysteresis motors, have not been touched upon, in spite of their growing importance for very small power outputs and in instrumentation. Nor have such machines as the capacitor motor been included, since their theories are essentially adaptations of the general principles developed in the text for the more basic types of machines.

I have refrained from using the MKS system of units, in spite of its growing popularity, because the majority of present day design engineers think and work in terms of the older units.

The subject matter of this text has been given over the past few years as a two-semester course in Alternating Current Machinery at Lehigh University. The first part, comprising transformers, polyphase and single-phase induction motors, and a-c commutating motors, is given to second semester juniors (EE 36). The second part, comprising synchronous generators, motors, and converters, is given to first semester seniors (EE 38), and is intended as background for an advanced course in electrical machines (EE 137) given to second semester seniors in the Power Option. The book was written with the dual intention of pro-

viding a text for the immediate needs of the above courses, and of supplying a reference source for further study. The arrangement was dictated by the first requirement, the level by both requirements.

I wish to thank Mr. Alton P. Dieffenbach and Mr. Richard T. Smith for reading the proofs, and Miss Elsie Davis for typing the manuscript.

L. V. Bewley

BETHLEHEM, PENNSYLVANIA

Contents

	<i>Page</i>
1. General Principles and Common Features	
1. Introduction	<i>1</i>
2. Electromagnetic Phenomena in Machines	<i>4</i>
3. The Magnetic Circuit	<i>5</i>
2. The Transformer	
1. Introduction	<i>10</i>
2. Principles of Operation	<i>12</i>
3. Transformer Construction	<i>15</i>
4. The Magnetic Circuit	<i>25</i>
5. Effect of Saturation and Hysteresis on Wave Form	<i>26</i>
6. Hysteresis Loss	<i>28</i>
7. Eddy-Current Loss in Iron Core	<i>29</i>
8. Separation of Hysteresis and Eddy-Current Loss	<i>30</i>
9. General Equations, Vector Diagram, and Equivalent Circuit	<i>32</i>
10. Approximate Equivalent Circuit	<i>37</i>
11. Differential Equation Approach	<i>38</i>
12. Transformer Constants and Tests	<i>40</i>
13. Performance Calculations, Regulation, and Efficiency	<i>44</i>
14. The Generalized Constants of the Transformer	<i>47</i>
15. Referred Quantities and Per-unit Values	<i>49</i>
16. Autotransformer	<i>52</i>
17. Three-winding Transformer	<i>56</i>
18. Instrument Transformers	<i>57</i>
19. Constant-Current Transformer	<i>60</i>
20. Parallel Operation of Transformers	<i>61</i>
21. Transformer Connections	<i>63</i>
22. Multiwinding Transformer Circuits	<i>65</i>
23. Windings in Series	<i>68</i>
24. Windings with Independent Connections	<i>70</i>
25. Windings in Parallel	<i>71</i>
26. Coupling Windings	<i>73</i>
27. The Simple Autotransformer	<i>74</i>
28. Forked Autotransformer	<i>75</i>
	xi

	<i>Page</i>
29. Regulating Transformer	76
30. Single-Phase Connections	77
31. Polyphase Connections	78
32. The Y-Y Connection	79
33. Delta-delta Connection	85
34. Open-delta Connection	87
35. Delta-wye and Wye-delta Connection	88
36. The T-T Connection	88
37. The Scott Connection	89
38. Double Zigzag Phase-shift Autotransformer	90
39. Wye-Delta-Zigzag Connection	92
40. Leakage Flux Problems	93
41. Leakage reactance	94

3. General Principles of Rotating Machines

1. Introduction	103
2. Armature Windings	104
3. Induced Voltages	111
4. Armature Reaction	123
5. Reactances	129

4. The Polyphase Induction Motor

1. Introduction	136
2. Principles of Operation	137
3. Construction	139
4. The Rotating Field	145
5. The Vector Diagram and Equivalent Circuit	148
6. Power Equations	150
7. Torque	154
8. Determination of Constants	155
9. The Circle Diagram	160
10. Analytical Derivation of Exact Circle Diagram	163
11. The Design Constants	164
12. The Core Loss	164
13. The Magnetizing Current	164
14. The Winding Resistance	165
15. The Leakage Reactances	165
16. Performance Calculations	168
17. Effect of Harmonics	169

	<i>Page</i>
18. Starting of Polyphase Induction Motors	<i>171</i>
19. Line Start Motors	<i>172</i>
20. Autotransformer or Compensator Starting	<i>172</i>
21. Wye-delta Starting	<i>174</i>
22. Wound-rotor Motor with External Resistor	<i>174</i>
23. The Double Squirrel-cage Induction Motor	<i>179</i>
24. Speed Control	<i>181</i>
25. Changing Number of Poles	<i>181</i>
26. Changing Applied Frequency	<i>181</i>
27. Rotor Rheostatic Control	<i>182</i>
28. Concatenation	<i>182</i>
29. Speed Control by Applied Rotor Voltage	<i>186</i>
30. The Leblanc Control System	<i>186</i>
31. The Kramer Control System	<i>187</i>
32. The Scherbius System	<i>189</i>
33. Mechanical Speed Control	<i>190</i>
34. The Induction Generator	<i>190</i>

5. Single Phase Induction Motor

1. Introduction	<i>194</i>
2. Principles of Operation	<i>194</i>
3. The Double-Revolving Field Theory	<i>195</i>
4. General Equations from the Revolving Field Theory	<i>197</i>
5. The Equivalent Circuit of the Revolving Field Theory	<i>198</i>
6. Single phase Constants from Three-phase Measurements	<i>199</i>
7. Transformer and Speed Voltages	<i>201</i>
8. Cross-field Theory of the Single phase Induction Motor	<i>204</i>
9. Starting of Single phase Induction Motors	<i>208</i>
10. Shaded-pole Motors	<i>208</i>
11. Split-phase Motors	<i>210</i>
12. The Capacitor Motor	<i>210</i>

6. Alternating Current Commutator Machines

1. Introduction	<i>217</i>
2. General Principles	<i>218</i>
3. The Series Motor	<i>220</i>
4. The Repulsion Motor	<i>225</i>

7. The Synchronous Generator and Motor

1. Introduction	<i>230</i>
2. Principles of Operation	<i>231</i>

	<i>Page</i>
3 Construction	238
4 Analysis of Synchronous Machines	249
5 Flux Distribution Due to Field Pole Excitation	250
6 Armature Reaction	251
7 Flux Distribution Due to Armature Reaction	254
8 Induced Voltage	256
9 Reactances	258
10 Vector Diagrams of Synchronous Machines	260
11 Regulation and Excitation of an Alternator	266
12 The Potier Diagram	268
13 The I MI Method	269
14 The Old AII I Method	270
15 The MMI Method	271
16 The ASA Method	272
17 The General Method	273
18 Salient Pole Machines	274
19 Comparison of the Different Methods	275
20 Power Transfer between Two Voltage Sources	279
21 Power Transfer between Round Rotor Machines	281
22 Power Transfer between Salient Pole Machines	282
23 Power Transfer between Salient Pole Machines (saturated)	283
24 Power Equation (round rotor)	288
25 Power Equations (salient pole)	290
26 Excitation Characteristics (round rotor)	292
27 Excitation Characteristics (salient pole motor)	291
28 Mechanical Oscillations in Synchronous Machines	296
29 Starting of Synchronous Motors	301
30 Synchronizing	307
31 Parallel Operation of Synchronous Machines	310
32 Circle Diagrams of the Synchronous Motor (round rotor)	313
33 Losses and Efficiency	320

8 The Synchronous Converter

1 Introduction	323
2 Principles of Operation	326
3 Construction	333
4 The Voltage Ratio	333
5 The Current Ratio	337
6 Armature Heating	338
7 Armature Reaction	342

	<i>Page</i>
8. Voltage Control	345
9. Hunting and Commutation	346
10. Inverters	347
11. Starting	348
Appendix I. The Distribution Summations	
The Distribution Summations	350
Appendix II. Armature Reaction	
1. The Magnetomotive Force of a Single Coil	352
2. The Armature Reaction of a Group of Coils	354
3. The Armature Reaction of a Polyphase Winding	355
Appendix III. Permeances and Flux Density	
1. Uniform Air Gaps	360
2. Nonuniform Air Gap	361
3. Flux Density Due to Armature Reaction	362
Appendix IV. Induced Voltages	
1. Induced Voltage of a Single Coil	364
2. Induced Voltage of a Group of Coils	366
3. Induced Voltage of a Synchronous Machine	367
4. The Round Rotor Machine	370
5. The Direct and Quadrature Reactances	371
INDEX	373

1 General Principles and Common Features

1. Introduction

The term *electrical machinery* includes any apparatus which is used to convert mechanical to electrical energy (or conversely) through the agency of current-carrying conductors moving with respect to a magnetic field, and thus embraces all generators and motors. The term also includes rotating apparatus used to convert one form of electrical energy to another form, as in converting alternating to direct current, or in changing frequency. In such cases a double conversion may be considered to take place—electrical to mechanical and mechanical to electrical. Rotary converters, frequency changers, boosters, rotating phase converters, motor generators, and dynamotors are in this category. The alternating current transformer, used to transform voltage and current, is a purely static device, and strictly speaking is not a machine, but by common usage is considered as such, because its analysis has much in common with that of true electrical machinery. The mercury arc rectifier, another static device for the conversion of alternating to direct current, is also usually included under electrical machinery, as a matter of convenience. On the other hand, relays, control devices, and instruments which have moving parts, and whose torques result from the reaction between conductors and magnetic fields, while true machines, are not considered in a text on electrical machinery, because their primary purpose is not the production or transformation of power.

For our purpose, then, we are led to the following classification of electrical machinery:

	APPARATUS	TYPE OF CONVERSION		
		Mech. \rightarrow Elec.	Elec. \rightarrow Mech.	Elec. \rightarrow Elec.
Static	Transformer			Voltage and Current
	Rectifier			Number of Phases
Dynamic	D-c Generators	Mech. to D-c		A-c to D-c
	Synchronous Generator	Mech. to A-c		
	Induction Generator	Mech. to A-c		
	D-c Motors		D-c to Mech.	
	A-c Motors		A-c to Mech.	
	Rotary Converters			A-c to D-c
	Frequency Changers			f_1 to f_2

The different machines have much in common, both in principle and in construction. In every electrical machine we may identify:

1. A *magnetic circuit* for the main, or useful, flux.
2. *Exciting windings* which produce the flux.
3. *Power or armature windings* in which voltages are induced by the flux, and in which currents react on the flux to produce forces, torque, and power.
4. *Connections* which provide paths for the currents, and combine voltages in the desired fashion.

Furthermore, in every rotating machine we have:

5. The *stator*, or stationary member, consisting of a magnetic core or yoke, and usually a set of windings. The stator may carry either the field poles and field windings, as in d-c machines, or the armature windings as in rotating field synchronous machines, or no winding at all.
6. The *rotor*, or moving member, consisting of a magnetic core and, usually, a set of windings. The rotor may carry either the field or the armature windings, or (as in the case of an inductor alternator) no windings at all.
7. The *air gap* separating the stator and the rotor, which gap must be crossed by the main flux.
8. *Slots and teeth* in which the windings are embedded.

9. *Mechanical features* such as shafts and bearings, frame and bed-plates, clamps, etc.

There are certain phenomena which occur in practically all types of electrical machinery, among which may be mentioned:

1. The *magnetomotive force drops* through the magnetic circuit.
2. The *distribution of flux* in various parts of the machine.
3. *Hysteresis loss* in the *iron* due to alternating flux.
4. *Eddy-current loss* in the *iron* due to alternating flux.
5. *Eddy-current loss* in the *copper* conductors due to alternating flux.
6. *Armature reaction* due to currents in the windings.
7. *Induction of voltages* by the variation of flux and by the movement of conductors through flux.
8. *Flow of currents* in the windings.
9. Production of *forces* and *torques* due to the reaction of the currents on the field.
10. Creation of *leakage reactance* fluxes by the currents, causing undesirable voltage drops.

There are three standard methods emphasized in the analysis of any electrical machine:

1. *General equations* for voltages, currents, torques, power, and motion. These may be derived from many different points of view.
2. *Vector diagrams* showing graphically the time and space relationships between the various electrical quantities. In many cases these relationships are such that a range of values may be shown by means of *circle diagrams*.
3. *Equivalent circuits* which duplicate the electrical characteristics of the actual machine, and which may be analyzed by ordinary circuit methods.

It is sometimes possible to develop each of the above methods independently, although in the more complicated cases the vector diagrams and equivalent circuits must be discovered from the general equations. Maximum understanding and clarity results when all three methods are developed progressively side by side. The general equation method is the most general and inclusive. The vector diagram gives a visual impression of the phenomena. The equivalent circuit is usually the most useful for routine calculation of characteristics, or when the machine is to be studied with respect to other external connections, such as when it is considered as part of a system.

From the foregoing it is evident that the different types of electrical machinery are actually quite similar in both theory and construction. Indeed, from one point of view all machines may be considered as special cases of a single set of generalized equations, differing from each other only in the manner of their connections.* But we shall not carry the generalization to this extreme. It will, however, save a great deal of time if the common features and theory of rotating machines in general be disposed of once for all in Chapter 3, after which detailed consideration for each special machine will be given in a separate chapter. In these

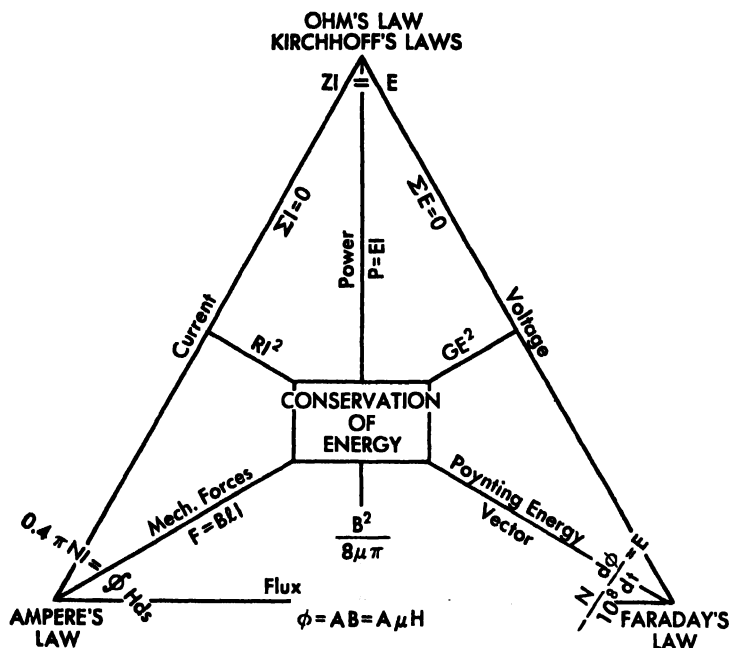


Fig. 1 The interrelationship of the electromagnetic quantities.

subsequent chapters, the procedure will follow the pattern: (a) definition and general description of the machine; (b) construction and structural details; (c) basic principles of operation; (d) analysis; and (e) calculation and discussion of characteristics.

2. Electromagnetic Phenomena in Machines

The complete analysis of any electrical machine involves the determination of fluxes, voltages, and currents; and therefrom the torque,

* Bewley, L. V., "Induced Voltage of Electrical Machines," *IEEE Transactions*, Vol. 49 (1930).

power, and losses. The calculation of power factor, efficiency, regulation, and other characteristics is then routine. It may happen that the fluxes are given, and we are required to proceed from there. In another case, the voltages are specified. In any event, the quantities are related in rather simple fashion by the laws of electromagnetic theory. It is in the application of these laws to actual machines that complications may arise which demand simplifying approximations.

The way in which the few laws of electromagnetic theory essential to our needs are interrelated is depicted in Fig. 1. Ampere's law relates the magnetomotive force (mmf) and magnetic intensity H . The flux density is then $B = \mu H$, and the flux for uniform density is $\phi = AB$. The induced voltage follows by Faraday's law. Currents are then found from Ohm's (generalized) law and the application of Kirchhoff's laws. Thus currents, fluxes, and voltages are interrelated by a triumvirate of laws, Fig. 1. If we now invoke the law of conservation of energy, we arrive at the following: With respect to current alone, the rate of energy loss RI^2 ; with respect to voltage alone, the rate of energy loss GI^2 ; with respect to flux, the density of energy storage $B^2/8\mu\pi$; with respect to voltage and current, the power $p = EI$; with respect to current and flux, the mechanical force $F = BI$; with respect to flux and voltage, the Poynting energy vector.

3. The Magnetic Circuit

One of the two principal foundation stones of electromagnetic theory is Ampere's law

$$\oint H \cdot ds = 0.4\pi NI \quad (1)$$

which states that the total work done in carrying unit pole completely around a magnetic circuit is 0.4π times the ampere-turns enclosed, or linked, by that circuit. If the magnetic circuit, Fig. 2, consists of several parts of lengths l_1, l_2, l_3, \dots with corresponding average magnetic intensities H_1, H_2, H_3, \dots , then the integral becomes

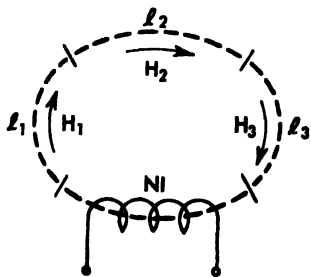


Fig. 2

$$\sum H_n l_n = H_1 l_1 + H_2 l_2 + H_3 l_3 + \dots = 0.4\pi NI \quad (2)$$

Putting $H = B/\mu$ and A for the average cross-sectional area of the flux path, (2) becomes

$$\begin{aligned}
 A_1 B_1 \frac{l_1}{\mu_1 A_1} + A_2 B_2 \frac{l_2}{\mu_2 A_2} + A_3 B_3 \frac{l_3}{\mu_3 A_3} + \dots \\
 = \phi R_1 + \phi R_2 + \phi R_3 + \dots = 0.4\pi N I
 \end{aligned}
 \quad (3)$$

in which $\phi = AB$ is the flux, and $R = l/\mu A$ is the reluctance of the path. The total ampere-turns are consumed by the several reluctances in series, just as in the analogous series electric circuit, and thus (3) corresponds to Kirchhoff's first law $\sum e = 0$ around a circuit. Moreover, the magnetomotive force consumed by a single reluctance is

$$F = 0.4\pi N I = R\phi \quad (4)$$

and this is exactly analogous to Ohm's law $e = ri$. Finally, for several magnetic paths in parallel, Fig. 3, it is clear that

$$\begin{aligned}
 \phi &= \phi_1 + \phi_2 + \phi_3 + \dots \\
 &= 0.4\pi N I \left(\frac{1}{R_1} + \frac{1}{R_2} + \frac{1}{R_3} + \dots \right) \\
 &= 0.4\pi N I (P_1 + P_2 + P_3 + \dots)
 \end{aligned}
 \quad (5)$$

in which the reciprocal of reluctance, $P = 1/R$, is the *permeance* of the path, and is analogous to conductance, the reciprocal of resistance. Equation (5) is seen to correspond to Kirchhoff's first law $\sum i = 0$ at the branch point.

Thus there is complete analogy between the magnetic and d-c circuits, so that:

MAGNETIC CIRCUIT		ELECTRIC CIRCUIT	
flux	ϕ	i	current
mmf	$F = 0.4\pi N I$	e	emf
reluctance	$R = \frac{l}{\mu A}$	$r = \frac{l\rho}{A}$	resistance
permeability	μ	$1/\rho$	1 resistivity
permeance	$P = \frac{1}{R}$	$g = \frac{1}{r}$	conductance
series circuits	$\sum F = 0$	$\sum e = 0$	Kirchhoff's law
parallel circuits	$\sum \phi = 0$	$\sum i = 0$	Kirchhoff's law

In the electric circuit the resistivity varies slightly with the temperature, but otherwise is constant with respect to current, so that resistances may be considered constant in a circuit analysis, and thus the current in a series circuit is arrived at readily. This is not so in

magnetic circuits involving iron, because the permeability μ varies greatly with the flux density. It is not possible, then, to solve (3) directly. However, a solution can be obtained by trial with the aid of the magnetic

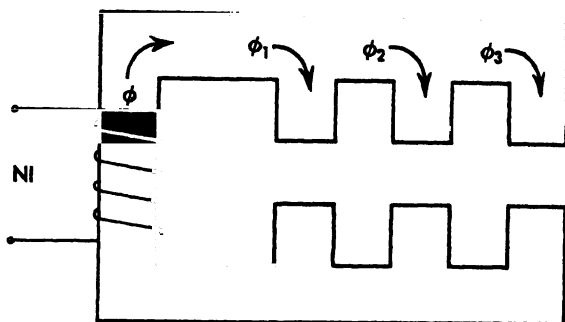


Fig. 3

characteristics of the iron. Figure 4 shows such a characteristic, in which flux density B , in any desired units, is plotted against intensity H , or ampere-turns per unit length of circuit. Such characteristics, or "saturation curves," exhibit a slight reverse curvature initially, followed by a relatively straight-line portion, then a rather abrupt curvature called the "knee" of the saturation curve, and then a "region of saturation" in which the flux density increases only slowly with an increase in intensity.

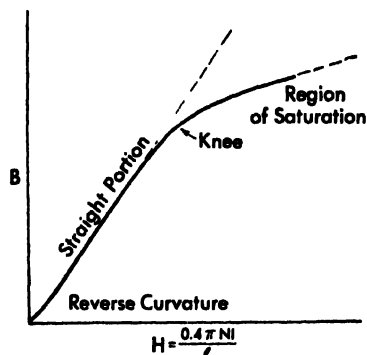


Fig. 4 Saturation curve.

In design practice, it is customary to make use of curves in which flux density in lines per square inch are plotted against magnetizing ampere-turns per inch. Figure 5 shows a set of such curves for the different kinds of iron used in an alternating current generator.

Figure 6 shows the magnetic circuits of a four pole machine, in which A_1, A_2, A_3, A_4, A_5 are, respectively, the effective cross sectional areas of the armature, teeth, air gap, pole, and yoke, and l_1, l_2, l_3, l_4, l_5 are the corresponding mean lengths of these parts.

The pole arc, $\alpha\tau$ (usually about two thirds of the pole pitch τ or distance between center lines of adjacent poles), is either of different curva-

ture, or chamfered with respect to the armature, so that the air gap is greater at the pole tips than at the pole center - perhaps four times as

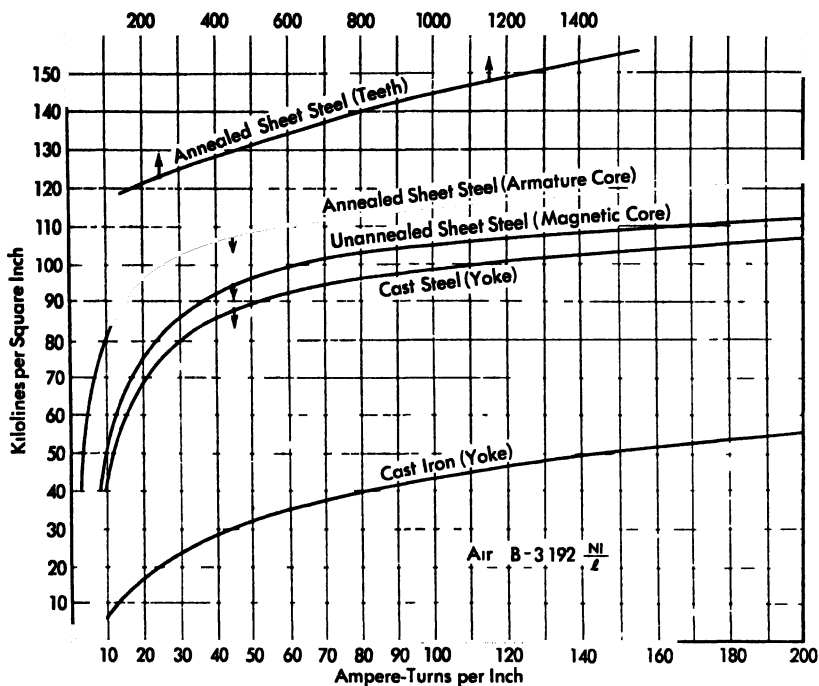


Fig. 5 Magnetizing characteristics

great. Also, there is fringing of the flux at the pole tips. The accurate determination of the total flux crossing the gap, and its form, is a matter of flux plotting¹ or involved mathematical calculation. In design

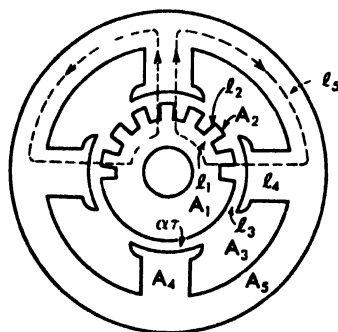


Fig. 6

offices, curves are available showing the average gap in terms of the ratio of maximum to minimum gaps, assuming the total flux is confined to the pole arc. From such curves the average length of gap is readily determined. A typical curve is shown in Fig. 7.

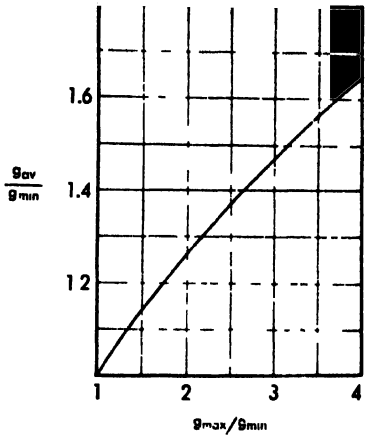
The armature surface is not smooth, it is interrupted by the coil slots. The flux fringing at the teeth can be determined by calculation or flux plot

* Bewley, L. V., *Two dimensional Fields in Electrical Engineering* The Macmillan Company, New York, 1948

ting, and design curves prepared from such plots. Figure 8 gives the ratio of the actual flux Φ to the flux Φ_0 which would be calculated on the assumption of a uniform flux density over the tooth width. Thus the fringing depends on the ratio of tooth width to slot width, and on the ratio of gap to slot width. The *effective* width of the teeth may be taken as

$$l_{eff} = \frac{\Phi}{\Phi_0} l_{total}$$

in which the ratio Φ/Φ_0 is called the *fringing coefficient*.



$$\frac{g_{av}}{g_{min}} = \frac{\sqrt{\frac{g_{max}}{g_{min}} + \frac{g_{min}}{g_{max}} - 1}}{\tan^{-1} \sqrt{\frac{g_{max}}{g_{min}} - 1}} \cong \frac{2}{3} + \frac{1}{3} \frac{g_{max}}{g_{min}}$$

Fig. 7 Average gap for a field pole

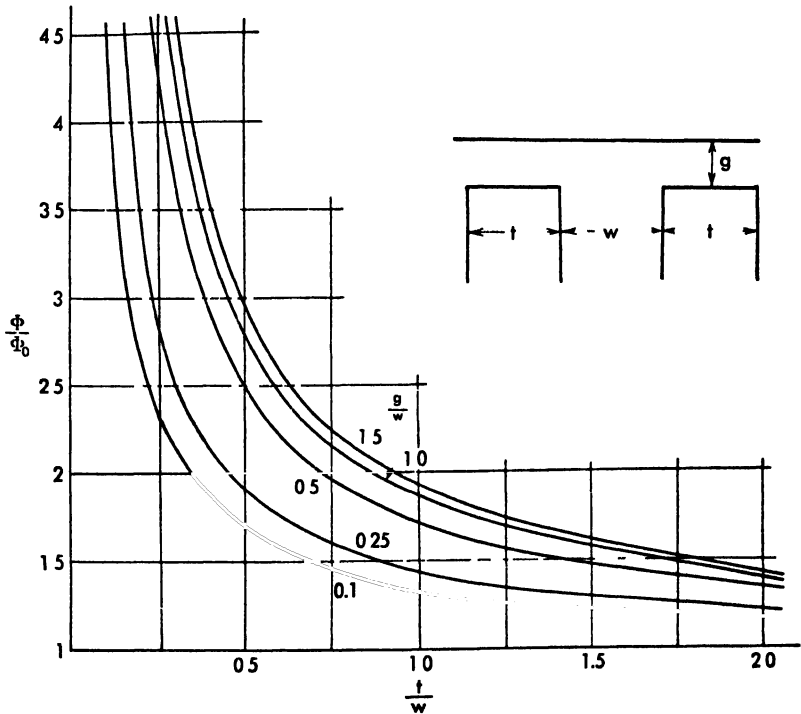


Fig. 8 Fringing factor for teeth and slots

2 The Transformer

1. Introduction

The alternating current transformer is a static device for transforming electrical energy of one voltage and current to electrical energy of another voltage and current at a fixed frequency. It is the "universal link" of electrical systems, for it can be used to tie together parts of a system operating at different voltages and permit the transfer of power between them in either direction. It provides a "gear ratio" between the source and receiver of electric power.

Transformers may be classified with respect to their application, and with respect to their structural features. The latter will be dealt with in the section on construction. Concerning their use, they are classified as: power, distribution, tie in, step-up, step down, instrument, and special-purpose transformers.

Power transformers comprise the large units used at the generating and switching stations of power systems, or at the sending and receiving ends of transmission lines, and at the substations of consumers of large blocks of power (industrial plants, railways, etc.). They are usually of greater than 500 kva capacity. The larger ones are practically all custom-built and designed to special specifications. This practice which has developed in the electrical power industry is unfortunate from an economical standpoint, since it has retarded standardization and added greatly to the cost of power transformers. The practice is not necessary and

enormous economies could be effected if the industry would agree to standardize the ratings and characteristics of power transformers.

Distribution transformers include the familiar pole-type transformers of a few kilovolt-ampere capacity, distribution network transformers installed in street vaults, and transformers in small unattended substations supplying residential districts or industrial consumers of small blocks of power. The design of distribution-type transformers has been highly standardized, and semi-mass production methods are employed in their manufacture. Transformers of standard kilovolt-ampere and voltage ratings are carried in stock by the manufacturers. There is no difference in principle between a power and distribution transformer, but the lower voltages and smaller ratings of the latter, and the need for designs which can be produced more cheaply and in quantity has resulted in striking differences in construction. Furthermore, economy dictates a different ratio of copper and iron losses in the two types. These differences result in somewhat different characteristics.

Tie-in transformers are used to link together two parts of a system so that power may be transformed in either direction. They hold the two parts of the system in rigid phase and synchronism. Multiwinding transformers may be used to link together more than two systems. Tie in transformers may be provided with extra windings and taps for phase shifting purposes. A transformer capable of changing taps while under load (usually by automatic relay control) is called a *load ratio control* transformer.

Step-up transformers are those used to increase the voltage in the direction of power flow. Higher voltages than it is feasible to generate directly are necessary for the economical transmission of power, and thus step-up transformers are used at generating stations supplying power over long transmission lines.

Step-down transformers are necessary to reduce high voltages to safe, or more convenient, voltages for application to the load. Step down transformers are found at the receiver ends of transmission lines and distribution circuits. Generally there are several step down transformers between the transmission receiver substation and the ultimate load. For example, the main receiver substation may reduce a transmission line voltage from 220,000 volts down to 66,000 volts for secondary transmission, and these lines may terminate at substations where the voltage is further reduced to 4,000 volts for primary distribution, and finally distribution transformers reduce the voltage to 110 or 220 volts for household use.

Instrument transformers are of two types—potential and current transformers. The former is used to reduce a voltage to a value suitable and safe for application to a voltmeter or the potential coil of a wattmeter. The latter is used in connection with ammeters and the current coils of wattmeters. Instrument transformers are also used to supply power to relays.

2. Principles of Operation

Essentially, the simple 2-winding transformer consists of a *magnetic core* of laminated iron carrying a mutual flux linked with a *primary winding* connected to the source of power, and a *secondary winding* connected to an external load. In accordance with Faraday's law, the variation of the flux induces a counter electromotive force E_1 in the primary, opposing and practically equal to the applied voltage V_1 , and an induced voltage E_2 in the secondary practically equal to its terminal voltage. Thus

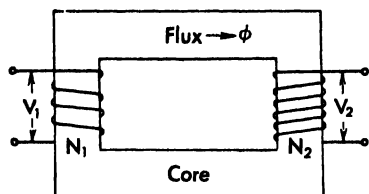


Fig. 1 Simple two-winding transformer.

$$E_1 = -\frac{N_1}{10^8} \frac{d\phi}{dt}$$

$$E_2 = -\frac{N_2}{10^8} \frac{d\phi}{dt}$$

$$\therefore \frac{E_1}{E_2} = \frac{N_1}{N_2} = \text{transformation ratio} \quad (1)$$

With the secondary winding open-circuited, only a small primary (magnetizing) current flows, sufficient to produce the flux ϕ according to Ampere's law, thus

$$\phi = \frac{0.4\pi N_1 I_1}{R} = \frac{\text{mmf}}{\text{reluctance}}$$

If it were not for the small impedance drop of this current in the primary winding we would have $V_1 = E_1$ exactly, and the two differ actually by only a fraction of a per cent. Now if the secondary is connected to an external load, a secondary current I_2 will flow, and this current will produce a magnetomotive force which, according to Lenz's law, will oppose the core flux. But as long as the primary applied voltage is constant, the flux must remain substantially constant (since $E_1 \propto \phi$), and therefore

the primary winding will draw from the supply an additional current of such value as will nullify the mmf of the secondary current; that is, the net ampere-turns $N_1 I_0$ must remain invariant to the secondary load current if impedance drops are neglected,

$$N_1 I_1 + N_2 I_2 = N_1 I_0$$

Now the no-load current I_0 is always small (of the order of a few per cent) compared with the full-load current I_1 . If we neglect I_0 we have, numerically,

$$N_1 I_1 \cong N_2 I_2 \quad (2)$$

It follows from (1) and (2) that

$$E_2 I_2 \cong \frac{N_2}{N_1} E_1 I_1 \cong E_1 I_1 \quad (3)$$

and therefore the law of conservation of volt-amperes holds approximately in a transformer.

If the secondary voltage E_2 is consumed by an impedance Z_2 as $E_2 = Z_2 I_2$, then by (1) and (2)

$$E_1 = \frac{N_1}{N_2} E_2 = \frac{N_1}{N_2} Z_2 I_2 = \left(\frac{N_1^2}{N_2} Z_2 \right) \left(\frac{N_2}{N_1} I_2 \right) = \left(\frac{N_1^2}{N_2} Z_2 \right) I_1 \quad (4)$$

The impedance $\left(\frac{N_1^2}{N_2} Z_2 \right)$ is said to be the secondary impedance Z_2 *referred to the primary*, since it gives primary voltage when multiplied by primary current.

We then arrive at four *approximate* relationships in a transformer:

1. Voltages are transformed *directly* as the turn ratio, $\frac{E_2}{E_1} \cong \frac{N_2}{N_1}$
2. Currents are transformed *inversely* as the turn ratio, $\frac{I_2}{I_1} \cong \frac{N_1}{N_2}$
3. Volt-amperes are *conserved*, $E_1 I_1 \cong E_2 I_2$
4. Impedances are transformed as the *square* of the turn ratio,

$$\frac{Z_1}{Z_2} = \left(\frac{N_1}{N_2} \right)^2$$

In a subsequent section more exact relationships will be derived, but the foregoing provides a basis for qualitative reasoning and understanding of the phenomena which occur in a transformer.

There are many problems in connection with transformer theory. They may be classified as follows:

1. Main flux
 - Saturation curves and magnetizing characteristics
 - Hysteresis loss and harmonics due to hysteresis loops
 - Eddy-current loss in iron cores
 - Induced voltages
2. Leakage flux
 - Flux paths and permeances
 - Reactances of concentric and interleaved windings
 - Mechanical forces on windings and clamps
 - Stray loss in tank, clamps, cooling coils and shields
 - Eddy current loss in conductors, and reduction by transpositions
3. Circuit problems
 - Vector diagrams
 - Equivalent circuits
 - Parallel operation
 - Multiple windings
 - Connections of windings and phases
 - Voltage taps and load-ratio-control circuits
4. Insulation
 - Breakdown volt time characteristics
 - Stresses under 60 cycles and impulse or surge conditions
 - Stress control by shielding
 - Puncture and creepage structures
 - Deterioration with temperature, age, moisture, etc.
5. Heating and cooling
 - Core temperature distribution (hot spot and average)
 - Winding temperatures (effect of insulation and cooling surfaces)
 - Oil temperatures and oil circulation
 - Radiation and cooling by tanks, tubes, and cooling coils
6. Other problems
 - Economical division of copper and iron losses
 - Mechanical design — clamps, tanks, accessories
 - Manufacture and assembly

An adequate treatment of some of these problems is outside the scope of the present text, but references will be cited at suitable points.

3 Transformer Construction

From a structural point of view transformers may be classified with respect to the type of magnetic core arrangement of the windings coil connections and methods of cooling

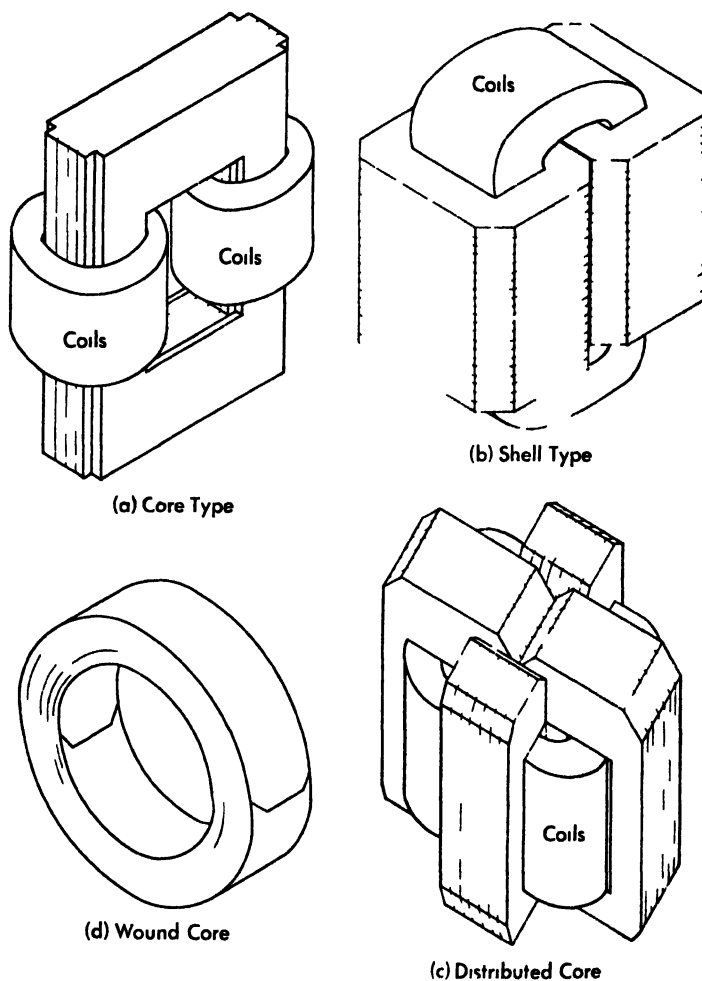


Fig 2 Type of transformer core

In the *core type* transformer Fig 2(a) the flux has a single path around the legs. *Concentric type* windings around each vertical leg are common in core type design.

In the *shell type* transformer Fig 2(b) the flux through the center leg splits and return through two outside yokes. *Interleaved type* windings

in which the high-voltage winding is sandwiched between sections of the low-voltage winding, are common in shell-type designs.

In the *distributed-core-type* transformer, Fig. 2(c), the coils are wound on a central leg, and the flux returns through four outside legs. This type (also called a cruciform core) is favored in smaller ratings, such as pole top distribution transformers.

In the *wound-core-type* transformer, Fig. 2(d), the core consists of a continuous strip of steel rolled into a tight spiral.

The magnetic core, which carries the main flux, is made up of thin sheets, or laminations, of silicon steel 0.014-inch thick for 60-cycle and 0.020-inch thick for 25-cycle transformers. These laminations are insulated from each other by coats of baked-on varnish, approximately 0.001 inch thick. It is necessary to laminate the core in order to reduce the eddy current loss which occurs in the iron. The laminations are stamped out as rectangular, E-shaped, and L shaped punchings, and assembled in packets held together by channel iron clamps and bolts. The punchings are assembled with the joints of adjacent layers alternated, so as to reduce the reluctance of the magnetic circuit. Even so, the joints consume an appreciable part of the total magnetomotive force required to magnetize the core. Both lap and butt joints are used, the latter facilitating assembly and giving a better space factor. Transformer steel has a high silicon content and is very brittle and hard to punch or shear. An appreciable change in magnetic properties may be occasioned by rough handling of the sheets. The sheets are rolled so that the grain is in the direction of the magnetic flux.

There are two types of windings employed in transformer construction, the *concentric* and the *interleaved*. The former is usually associated with core type and the latter with shell type designs. The insulation structure is also quite different for these two types, and incidentally (since each type in larger sizes is sponsored by competing manufacturers) even the bushings are of different types!

Each type of core and coils has certain advantages and disadvantages. The core type uses relatively less iron but more copper. The shell-type gives better coil protection but less accessibility and its rectangular coils are not as strong against change of shape due to short circuit forces. The shell type is better adapted to air blast cooling. It is easier to obtain low reactances with shell type interleaved coil construction. Actually, however, both types are used universally, and the arguments advanced in favor of one or the other are to a certain extent purely commercial propaganda.

Transformer insulation is classified as *major* and *minor* insulation. The former insulates a winding from ground (the core and tank) and from other windings, and comprises the insulating cylinders, flange collars and barriers between windings. Minor insulation includes the paper cotton-covered turn and strand insulation, the varnish cambric taping around individual coil sections, and the barrier sheets between adjacent sections of the same winding. Oil serves both as an insulator and a cooling medium.

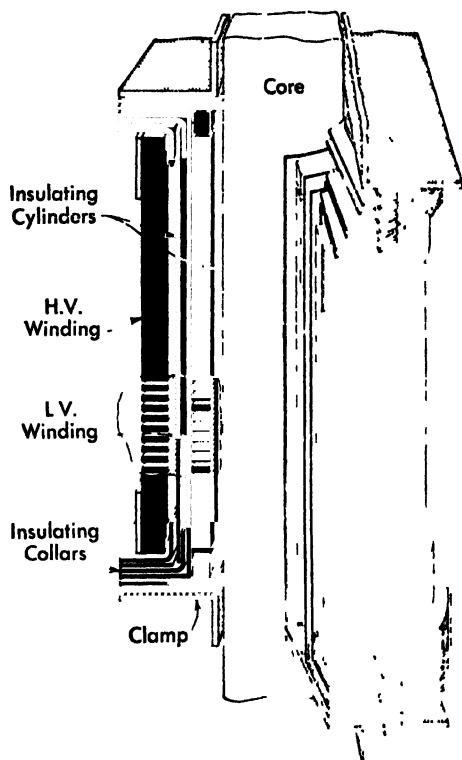


Fig. 3 Cutaway view of concentric coils showing insulating cylinders and flanged collar.

Figure 3 is a cutaway view of a concentric-coil core type construction. The low-voltage coil is usually a circular helix or barrel of heavy rectangular copper conductor wound on a hard molded insulating cylinder of varnished paper from 3 16 to 3 4 inch thick. The conductors themselves are insulated with varnished paper held in place by cotton tape, and may be spaced apart to facilitate heat dissipation to the surrounding oil. The high voltage winding consists of a stack of sections, each con-

Fig. 5 Partly wound low voltage helical coil (General Electric Company)

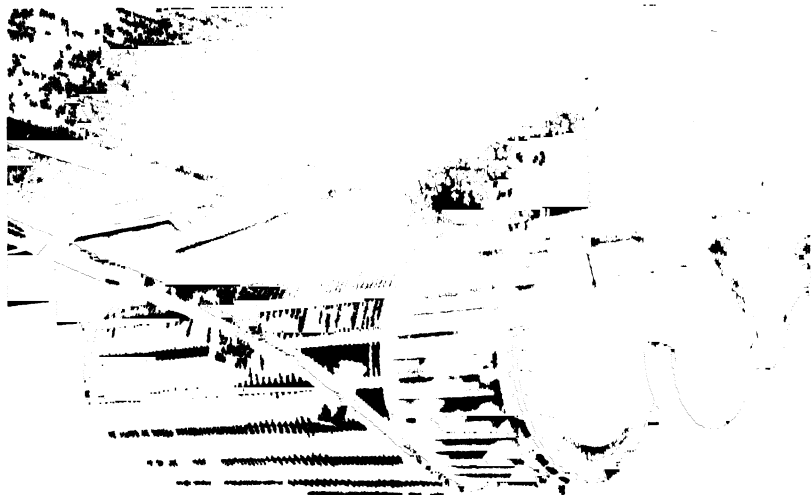


Fig. 4 Single phase 3 leg core
(General Electric Company)

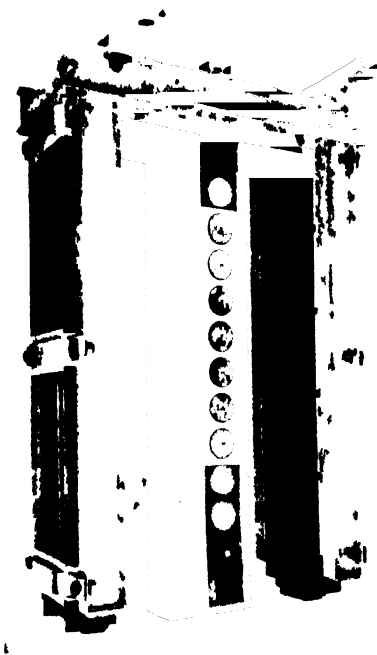
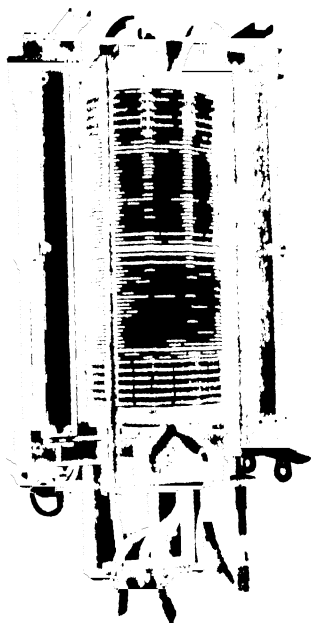


Fig. 6 Assembled core and coils
concentric type design
(General Electric Company)



taining from a few to many turns. The sections are alternately connected by inside and outside crossovers, and are separated by oil ducts and insulating pressboard barriers; proper distances between sections are maintained by spacers. The high-voltage coil stack is supported on insulating paper cylinders, the number depending on the voltage rating. Molded flange collars comprise the insulation at the ends of the stack. The line end sections usually are wrapped with extra insulation, as are the line end turns, as protection against incoming surges.* The coils and insulating structure are held in place by channel or angle iron clamps.

Figure 4 shows the construction of a 3-leg transformer core, consisting of the top and bottom yokes, the vertical legs, the windows, and the clamps. The joints between punchings are alternated. Vertical oil ducts are provided to assist in cooling the core. In assembling the transformer, the legs and bottom yoke are built up first, then the coils are slipped over the center leg, and finally the top yoke completed by sandwiching the rectangular punchings between those of the legs. The cross-section of the legs is usually stepped rather than rectangular, so as to more nearly approximate a circular form and permit the maximum amount of iron inside a circular coil. The bolts and clamps holding the core together must be insulated so that there are no completed circuits; for otherwise currents would flow in such circuits causing additional losses and heating.

Figure 5 shows a partly wound low-voltage helical coil on the winding form. The pressboard spacers and the spacing strips are shown. The low-voltage coil is made up of a large number of strands, and these strands are transposed through the coil stack in order to reduce the eddy-current loss in the conductors.

Figure 6 shows an assembled core and coils of a 3-leg transformer. The manner of bringing out the leads should be noted. The wide conductors at the two ends of the coil stack are electrostatic shields for surge protection.

Figure 7 shows an external view of a completely assembled 20,000-kva transformer. Radiators are provided to give additional cooling surface. The conservator tank above the radiators is an oil reservoir which assures that the transformer tank will always be full, even though the volume of the oil changes with temperature variation. A relief pipe, seen over the conservator tank, offers protection in case of gas caused by internal trouble. Mounted on top of the transformer tank are the bushings and

* Certain other provisions for surge protection, such as static plates and electrostatic shields, are not shown, as consideration of them is beyond the scope of this book. See Bewley, L. V., *Traveling Waves on Transmission Systems*, John Wiley and Sons, New York, 1937.

integral lightning arrestors The box like structures on the side of the transformer house the load ratio control contactors and mechanism. The entire transformer is mounted on a truck. Certain gauges and conduits and other accessories are clear in the illustration.



Fig 7 Internal view of a modern power transformer showing radiators, oil conservator tank, relief pipe, bushings, lightning arrester, and housing for load ratio control equipment. (General Electric Company)

Figure 8 is a cutaway view of an interleaved coil shell type three phase transformer showing the core and coil arrangement, leads, high voltage protective links, and condenser bushings. This transformer has the so called form fit tank construction. Note the well defined path for the circulation of the cooling oil—up through the coils and down through the radiators, with no bypass between the coil and tank. This construction is ideally suited for the application of a forced oil circulation.

Figure 9 shows a cross-section through one coil group. Note the static shield at the high-voltage end of the coil, the insulating barriers and channels, and the cooling oil ducts. Wide coils of this type can be shielded adequately against high-voltage surges by a simple static plate.

Figure 10 shows the completely assembled high voltage and low voltage coils of a transformer having four coil groups.

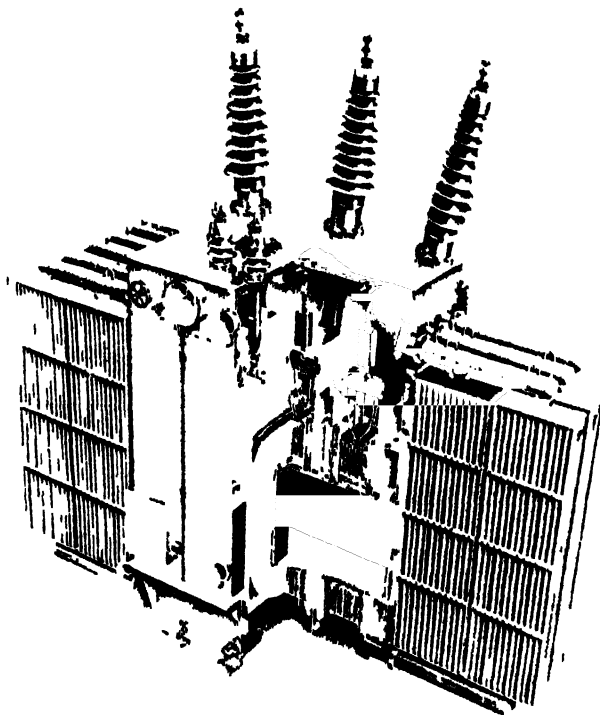


Fig. 8 Cutaway view of a shell type transformer. (Westinghouse Electric Corporation)

Figure 11(a) is a cutaway view of an oil filled bushing showing the porcelain shell, ground sleeve, insulating barriers, and oil reservoir. The lower part of the bushing, which will be immersed in the oil of the tank, need not be so long as the upper portion, since the striking and creepage distances in oil are much less than in air for the same voltage. Figure 11(b) is a cutaway view of the condenser type bushing. In this type bushing

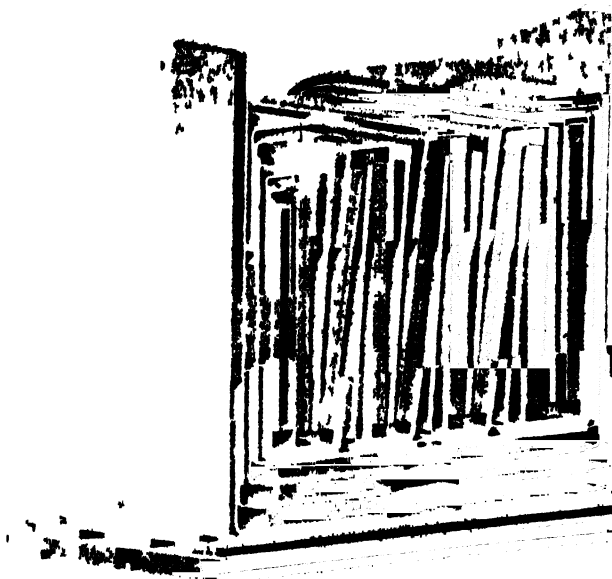


Fig 9 Cutaway view through a coil group of an interleaved design. (Westinghouse Electric Corporation)

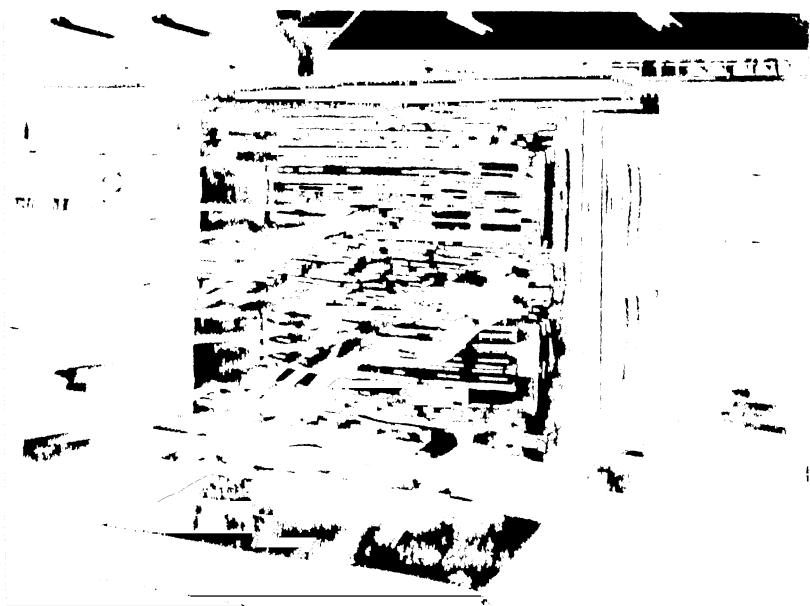


Fig 10 Completely assembled HV and LV coils of a shell type transformer (Westinghouse Electric Corporation)

the radial gradients are made approximately uniform by inserting a series of concentric aluminum-foil cylinders in the paper insulation around the lead. These cylinders act as a series of condensers of such

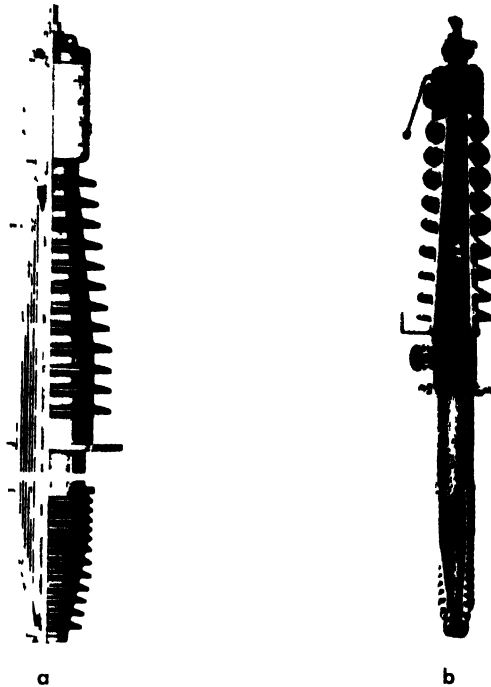


Fig. 11 High voltage bushings
a Oil filled type (General Electric Company)
b Condenser type (Westinghouse Electric Corporation)

capacitance as to equalize the voltage distribution. Condenser type bushings are of smaller diameter, but greater length, than oil filled bushings for the same voltage. Sometimes the bushing is surrounded by a current transformer, and it is then a great advantage, for reasons of accurate current measurement, to use a bushing of minimum diameter. Condenser-type bushings are also used where additional capacitance is required for capacitance coupling with external devices.

A general classification of transformers with respect to their utilization and construction is given in the following table.

TABLE 1
TRANSFORMER CLASSIFICATIONS

Utilization	Construction
Power	Magnetic circuit
step-up	core type
step-down	shell type
tie-in	cruciform
phase-shifting	wound (spiral) core
load-ratio-control	
multiple-winding	Windings
autotransformer	concentric disk
	interleaved (pancake)
Distribution	barrel (helical)
pole type	Insulation
unit substation	cylinders
street vault	flange collars
Instruments	barriers (press-board)
potential	turn (d.c.c. paper and enamel)
current	layer (paper)
	section (paper and tape)
Special purpose	oil
starting compensator	Bushings
constant current	condenser type
welding	oil-filled
rectifiers and converters	solid (paper) insulation
electric furnace	
high-voltage testing	Cooling
Connections	water-cooled (cooling coils)
wye	air-blast
delta	self-cooled (tubes and radiators)
zig-zag	
double-delta (hexagon)	Tanks
stub-delta	round
extended-delta	oval
quadruple zig-zag	square

4. The Magnetic Circuit

Consider, Fig. 12, a magnetic core of permeance P_0 excited by a coil of N -turns carrying a current i_0 . The magnetomotive force is then $0.4\pi Ni_0$ and the flux is

$$\phi_0 = 0.4\pi Ni_0 P_0 = B_0 l \quad (5)$$

in which B_0 is the flux density and l the cross-sectional area of the core.

The permeance P_0 is not a constant, but depends on the flux density. This dependence is shown by the typical saturation curve of Fig. 13, which is usually plotted as flux density against ampere turns per inch.

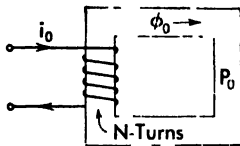


Fig. 12

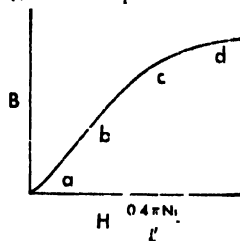


Fig. 13

It is characterized by: (a) a slight reverse curvature at low values of flux density, (b) a near linear or straight line portion, (c) the "knee," or region of abrupt curvature, and (d) the region of saturation over which large increases of magnetomotive force result in only small increases in flux density. Obviously, there is little to gain by extending the working range far into the region of saturation. Moreover, as will be shown later, operation at high flux densities results in excessive losses due to hysteresis and eddy currents, and introduces objectionable harmonics into the exciting current or voltage. For these reasons, transformers are usually designed to operate at from 70,000 to 90,000 lines per square inch maximum flux density.

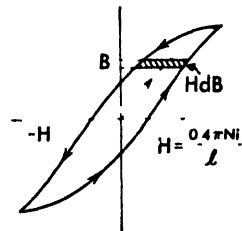


Fig. 14 Hysteresis loop.

Now if the current is alternating, the flux density, instead of following a simple saturation curve, will describe a *hysteresis loop*, Fig. 14. When the current is first applied, with the core unmagnetized, the flux density, B , increases along the saturation curve (shown dotted) until it reaches a maximum simultaneous with maximum current. But when the current decreases, the flux density follows at a higher value than on the saturation curve, and at current zero there is a residual flux in the core. In fact, if the current ceases at this point, the core remains mag-

netized. The remaining magnetism does not reach zero until the current becomes negative. As the current continues to decrease, the flux density also decreases until it reaches a negative maximum equal to its positive

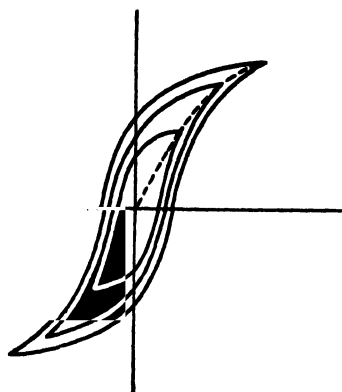


Fig. 15 Nest of hysteresis loops.
The maxima points of the loops lie on the normal saturation curve.

maximum. As the current increases and completes its cycle, the loop is closed. Such a hysteresis loop is symmetrical about the origin, so that the positive and negative half-loops are similar.

If a number of hysteresis loops are constructed from test data for different values of maximum flux densities, it will be found that they are nested together with the higher density loops surrounding the lower density loops. The locus of the

5. Effect of Saturation and Hysteresis on Wave Form

Suppose that the voltage applied to the coil of Fig. 12 contains a number of harmonics and is represented by the Fourier series

$$\begin{aligned} e &= E_1 \sin(\omega t + \alpha_1) + E_3 \sin(3\omega t + \alpha_3) + E_5 \sin(5\omega t + \alpha_5) + \dots \\ &= \sum E_k \sin(k\omega t + \alpha_k) \quad \text{where } k = 1, 3, 5, \dots \end{aligned} \quad (6)$$

The flux variation in the core must be such as to induce a counter electromotive force equal and opposite to the applied voltage (6). The relation-

ship between flux and voltage is given by Faraday's law, $e = -\frac{N}{10^8} \frac{d\phi}{dt}$, or conversely

$$\begin{aligned} \phi &= -\frac{10^8}{N} \int e dt = -\frac{10^8}{N} \int \sum E_k \sin(k\omega t + \alpha_k) dt \\ &= +\frac{10^8}{N\omega} \sum \frac{E_k}{k} \cos(k\omega t + \alpha_k) \\ &= \frac{10^8}{N\omega} \left\{ E_1 \cos(\omega t + \alpha_1) + \frac{E_3}{3} \cos(3\omega t + \alpha_3) + \frac{E_5}{5} \cos(5\omega t + \alpha_5) + \dots \right\} \end{aligned} \quad (7)$$

Comparison of (6) and (7) shows that the harmonics in the flux wave are successively smaller than those in the voltage wave, and each flux harmonic leads the corresponding voltage harmonic by 90 degrees.

On the other hand, if the flux wave is specified as a Fourier series, the corresponding voltage wave is easily found by Faraday's law. Usually, the applied voltage wave is free of harmonics, and consequently the flux wave must also be sinusoidal. But harmonics then appear in the current due to saturation and hysteresis.

The current wave could be found if the relationship between the current and flux, as given by the saturation curve or hysteresis loop, could be expressed analytically. While certain empirical expressions have been proposed for this relationship, in general they are not satisfactory. It is more profitable to obtain a graphical solution for the current, as shown in Fig. 16.

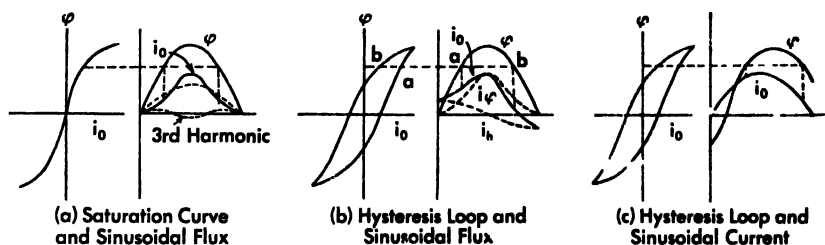


Fig. 16

Figure 16a shows the variation of flux ϕ and current i_0 according to a simple saturation curve. For a sinusoidal flux wave, the value of current for each value of flux is picked from the saturation curve and transferred to the time diagram. The resulting current wave is peaked and symmetrical about its maximum. It is composed essentially of a fundamental and a third harmonic, although higher harmonics are present.

For a sinusoidal flux wave, the current wave due to hysteresis, Fig. 16b, is not symmetrical. But if the fundamental in-phase component of the current i_h is subtracted, the remaining current i_ϕ is symmetrical. It is the *magnetizing current*. The in-phase current component is an energy component and accounts for the hysteresis loss discussed in the next section.

For a sinusoidal current, the flux wave becomes flat-topped, and the voltage wave correspondingly peaked, Fig. 16c.

The problem of determining the exact voltage and current wave shapes in circuits containing saturable iron cores is extremely complex, even in the most simple cases—say a sinusoidal voltage applied to a series R - L circuit. Step-by-step and graphical methods, or calculating machines, must be used. Fortunately, in transformer calculations, either a sinusoidal voltage or a sinusoidal current may be assumed, depending on

the connections. The effect of the connections on third harmonics will be discussed later.

6. Hysteresis Loss

Referring to the magnetic core of Fig. 12, assume that the flux density varies according to the hysteresis loop of Fig. 14. The voltage induced in the coil of N turns by this flux is, by Faraday's law and (5),

$$e = -\frac{N}{10^8} \frac{d\phi_0}{dt} = -\frac{NA}{10^8} \frac{dB_0}{dt} \quad (8)$$

The instantaneous power loss is equal to the product of the voltage and the current, and the energy loss per cycle (or one hysteresis loop) then is, by (5) and (8),

$$\begin{aligned} W &= \int e i_0 dt = \int \frac{NA}{10^8} i_0 dB_0 \\ &= \frac{Al}{10^8} \int \left(\frac{N i_0}{l} \right) dB_0 = \frac{V}{10^8} \int \frac{H}{0.4\pi} dB_0 = \frac{V}{4\pi 10^8} (\text{area of hysteresis loop}) \end{aligned} \quad (9)$$

in which $V = Al$ is the volume of the iron core. Since there are f loops per second, if f is the frequency of the applied voltage, the hysteresis power loss is

$$P_h = \frac{Vf}{4\pi 10^8} (\text{area of hysteresis loop}) \text{ watts} \quad (10)$$

Thus the hysteresis loss is directly proportional to the volume of the iron, to the frequency, and to the area of the loop. Transformer iron having a narrow loop is therefore desirable. This loss amounts to about two-thirds of the total core loss in a transformer, the other one-third being eddy-current loss.

Steinmetz has given an empirical formula for the hysteresis loss. It is

$$P_h = \eta f V B_{\max}^a 10^{-3} \text{ watts} \quad (11)$$

in which $a = 1.5$ to 1.7 (1.6 average value)

$\eta = 0.001$ to 0.003 erg per cu in. for annealed steel

$= 0.0005$ to 0.0008 erg per cu in. for silicon steel

B_{\max} = maximum flux density in lines per sq in.

The exponent a can be determined by measuring the hysteresis loss at different flux densities and plotting the curve of watts loss *vers* flux density on logarithmic paper. Then the constant η is found from (11).

In terms of the area S of the hysteresis loop, upon equating (10) and (11), there are for two different flux densities

$$\left(\frac{B_1}{B_2}\right)^a = \frac{S_1}{S_2} \quad \text{or} \quad a = \frac{\log (S_1 / S_2)}{\log (B_1 / B_2)}$$

and

$$\eta = \frac{S_1}{4\pi B_1^a} = \frac{S_2}{4\pi B_2^a}$$

7. Eddy-Current Loss in Iron Core

The flux in the transformer core induces voltages which cause parasitic currents to flow in the iron, causing losses. It is to reduce these eddy current losses that the core is built up of laminations insulated from each other by a coating of baked-on enamel. Even so, the eddy currents confined to the individual laminations contribute about one third of the core losses of a transformer. A complete analysis of this problem, taking into account the actual paths traversed by the currents, and the redistribution of flux and currents caused by them, is rather involved.* But results

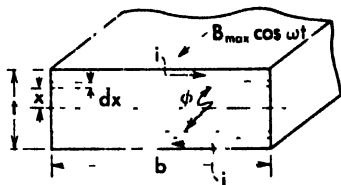


Fig. 17 Flux and eddy current paths in a lamination.

of great accuracy may be obtained on the simplifying assumptions: (1) that the eddy currents flow parallel and symmetrically above and below the center line of the lamination, (2) the flux density is uniform throughout the cross section of the lamination; (3) the circuit of the current is completed at the ends of the sheets. Referring to Fig. 17, which shows a cross section of a lamination of width b and thickness t carrying a maximum flux density B_{\max} , and considering the elementary path distance x from the center line, it is clear that the total flux linked with this path is

$$\phi = 2bx B_{\max} \cos \omega t \quad (12)$$

This flux will induce in the path a voltage

$$e = - \frac{1}{10^8} \frac{d\phi}{dt} = \frac{2bx}{10^8} \omega B_{\max} \sin \omega t \quad (13)$$

If ρ is the resistivity of the iron, the resistance of the path of width dx and length l (in direction of B) is

$$r = \frac{2b\rho}{ldx} \quad (14)$$

* Bewley, L. V., *Two-dimensional Fields in Electrical Engineering*, The Macmillan Company, New York, 1948

Neglecting the small reduction in the flux which would be occasioned by the magnetomotive force due to any current that flows in the lamination, the rms current in the path is the rms voltage divided by the resistance, and the eddy-current loss in the lamination therefore is by (13) and (14)

$$\begin{aligned} P_e &= \frac{\omega^2 B_{\max}^2}{\rho 10^{16}} bl \int_0^{t/2} x^2 dx \\ &= \frac{\pi^2 l}{6\rho 10^{16}} f^2 b l^3 B_{\max}^2 = \frac{\pi^2}{6\rho 10^{16}} V f^2 B_{\max}^2 t^2 \end{aligned} \quad (15)$$

This equation shows that the eddy-current loss varies as the squares of the frequency, flux density, and *thickness of the lamination*. Therefore, thin laminations result in low loss. In practice, the thickness of laminations for 60-cycle machines has been standardized at 0.014 inch, and flux densities rarely exceed 90,000 lines per square inch. The resistivity of transformer steel increases with the percentage of silicon. The ideal steel would have high resistivity to keep down the eddy-current loss; a low constant and narrow hysteresis loop to limit the hysteresis loss; a high permeability to reduce the magnetizing current; low saturation to limit third harmonics; stability against aging and rough handling; mechanical workability; and would be inexpensive truly an intriguing problem for the metallurgist!

8. Separation of Hysteresis and Eddy-Current Losses

The total core loss is the sum of the hysteresis and eddy-current losses as given by (11) and (15), or

$$\begin{aligned} P &= P_h + P_e = \eta V f B_{\max}'' 10^{-7} + k V f^2 B_{\max}^2 \\ &= k' f B_{\max}'' + k'' f^2 B_{\max}^2 \end{aligned} \quad (16)$$

As there are three unknowns (a , k' , k''), a minimum of three sets of power measurements at different values of the independent variables f and B are necessary. Let power be measured under the three conditions (f_1 , B_1), (f_2 , B_2), and (f_1 , B_2). Then (16) gives

$$\left. \begin{aligned} P_1 &= k' f_1 B_1'' + k'' f_1^2 B_1^2 \\ P_2 &= k' f_2 B_2'' + k'' f_2^2 B_2^2 \\ P_3 &= k' f_1 B_2'' + k'' f_1^2 B_2^2 \end{aligned} \right\} \quad (17)$$

Eliminating k'' between the second and third equations of (17), there results

$$f_1^2 P_2 - f_2^2 P_3 = k' f_1 f_2 (f_1 - f_2) B_2'' \quad (18)$$

Eliminating k'' between the first and second equations of (17), there results

$$f_2^2 B_2^2 P_1 - f_1^2 B_1^2 P_2 = k' (f_2^2 f_1 B_2^2 B_1^a - f_1^2 f_2 B_1^2 B_2^a) \quad (19)$$

Eliminating k' between (18) and (19), there results after some rearrangement

$$\left(\frac{B_1}{B_2}\right)^a = \frac{f_2(f_1 - f_2)B_2^2 P_1 + f_1(f_1 P_2 - f_2 P_3)B_1^2}{B_2^2(f_1^2 P_2 - f_2^2 P_3)} \quad (20)$$

From (20) the exponent a is found as

$$a = \frac{\log \left[\frac{1 - \beta^2 P_3 P_2}{\beta(1 - \beta)(P_1 P_2) + (B_1 B_2)^2(1 - \beta P_3 P_2)} \right]}{\log (B_2 B_1)} \quad (21)$$

in which $\beta = f_2 f_1$.

Having determined the exponent, k' follows immediately from (18) as

$$k' = \frac{f_1^2 P_2 - f_2^2 P_3}{f_1 f_2 (f_1 - f_2) B_2^a} \quad (22)$$

And upon eliminating k' between the second and third equations of (17),

$$k'' = \frac{f_1 P_3 - f_2 P_3}{f_1 f_2 (f_2 - f_1) B_2^2} \quad (23)$$

Usually the exponent is taken as $a = 1.6$ and the two constants then follow from (22) and (23) without finding a from (21).

Example: A transformer has the following losses corresponding to three conditions:

$$B_1 = 25,800 \text{ lines per sq in.}, \quad f_1 = 30, \quad P_1 = 270$$

$$B_2 = 64,500 \text{ lines per sq in.}, \quad f_2 = 60, \quad P_2 = 2920$$

$$B_3 = 64,500 \text{ lines per sq in.}, \quad f_1 = 30, \quad P_3 = 1250$$

Then by (21), since $\beta = 2$,

$$a = \frac{\log \left[\frac{1 - 4 \times 0.428}{2(1 - 2) 0.0925 + 0.4^2 (1 - 2 \times 0.428)} \right]}{\log 2.50} = 1.615$$

By (22) and (23)

$$k' = \frac{30 \times 30 \times 2920 - 60 \times 60 \times 1250}{30 \times 60 (30 - 60) 64,500^{1.615}} = 0.60 \times 10^{-8}$$

$$k'' = \frac{30 \times 2920 - 60 \times 1250}{30 \times 60 (60 - 30) 64,500^2} = 0.56 \times 10^{-10}$$

Hence the core loss for this transformer is

$$P = \frac{0.60}{10^6} \int B_{\max}^{1.616} + \frac{0.56}{10^{10}} \int^2 B_{\max}^2$$

9. General Equations, Vector Diagram, and Equivalent Circuit

The traditional method of analyzing a 2-winding transformer, attributed to C. P. Steinmetz, assumes a power source on one winding, the primary, and a load on the other winding, the secondary, and the core loss is taken into account by including an in phase component in the exciting current. Two departures from these premises will be made in

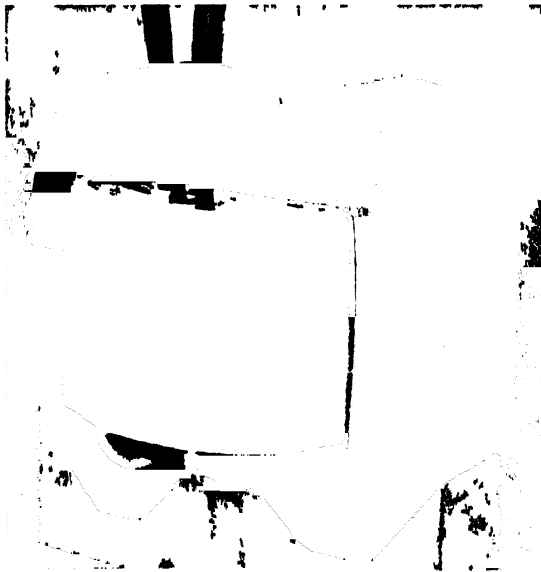


Fig. 18 Wound core transformer, 15 kva 2400 to 120-240 volts (General Electric Company)

the present treatment. First, since power may flow in either direction, and since in multiple winding transformers no one winding has a preferential status, it will be assumed here that each winding is connected to a voltage source and positive current direction will be taken as that which assists in magnetization of the core. Second, the core loss will be accounted for as occurring in the resistance of a fictitious third winding having the same number of turns, N_1 , as one of the windings. This latter artifice will permit the transformer problem to be approached from the alternative differential equation point of view without having to apologize for the absence of core loss in the results.

Referring to Fig. 19, there is shown a simple 2-winding transformer. For clarity the two windings are shown on separate core legs, but in practice there would be a primary and a secondary winding on each leg. The two windings have N_1 and N_2 turns, and resistances R_1 and R_2 , respectively. Voltages V_1 and V_2 cause currents I_1 and I_2 to flow in the windings, as a result of which there is a mutual flux ϕ_0 through the permeance P_0 of the iron core. In addition, the winding magnetomotive forces cause leakage fluxes ϕ_{1l} and ϕ_{2l} through the permeances P_1 and P_2 of the air paths. The mutual flux ϕ_0 in the iron core causes hysteresis and eddy current losses in the laminations. The former is proportional to the 1.6 power and the latter to the square of the flux density. If, as a legitimate approximation, both losses are assumed to be proportional to the square of the flux, then the iron losses and the demagnetizing effect of the eddy currents can be taken into account most appropriately by introducing a fictitious winding (shown dotted in Fig. 19) of N_1 turns and a conductance G_0 , to be determined, carrying a current I_{h+c} , such that $I_{h+c}^2 G_0$ is equal to the core loss. This fictitious winding is assumed to have no leakage flux. It will be assumed further that currents and voltages vary sinusoidally. There are thus three magnetomotive forces acting on the core (where I_1 , I_2 , I_{h+c} designate effective values for the currents):

$$M_1 = 0.4\pi \sqrt{2} N_1 I_1 e^{j\omega t} \quad (24)$$

$$M_2 = 0.4\pi \sqrt{2} N_2 I_2 e^{j\omega t} \quad (25)$$

$$M_3 = 0.4\pi \sqrt{2} N_1 I_{h+c} e^{j\omega t} \quad (26)$$

The resultant magnetomotive force is

$$\begin{aligned} M_0 &= M_1 + M_2 + M_3 \\ &= 0.4\pi \sqrt{2} (N_1 I_1 + N_2 I_2 + N_1 I_{h+c}) e^{j\omega t} \\ &= 0.4\pi \sqrt{2} N_1 I_\phi e^{j\omega t} \end{aligned} \quad (27)$$

in which, putting $a = N_1 N_2$,

$$I_\phi = I_1 + I_2 + \frac{I_{h+c}}{a} \quad (28)$$

is an equivalent current flowing in N_1 turns and which produces the same magnetomotive force as the three actual currents.

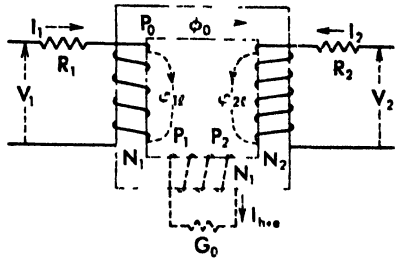


Fig. 19 Idealized transformer.

These magnetomotive forces produce the leakage fluxes ϕ_{1l} and ϕ_{2l} , as well as the mutual flux ϕ_0 , whose crest values are

$$\phi_{1l} = M_1 P_1 = 0.4\pi\sqrt{2}N_1 P_1 I_1 e^{j\omega t} \quad (29)$$

$$\phi_{2l} = M_2 P_2 = 0.4\pi\sqrt{2}N_2 P_2 I_2 e^{j\omega t} \quad (30)$$

$$\phi_0 = M_0 P_0 = 0.4\pi\sqrt{2}N_1 P_0 I_\phi e^{j\omega t} = \Phi_0 e^{j\omega t} \quad (31)$$

and, by Faraday's law, these fluxes induce the instantaneous voltages

$$e_{1l} = -\frac{N_1}{10^8} \frac{d\phi_{1l}}{dt} = -j \frac{0.4\pi N_1^2 P_1 \omega \sqrt{2}}{10^8} I_1 e^{j\omega t} \quad (32)$$

$$e_{2l} = -\frac{N_2}{10^8} \frac{d\phi_{2l}}{dt} = -j \frac{0.4\pi N_2^2 P_2 \omega \sqrt{2}}{10^8} I_2 e^{j\omega t} \quad (33)$$

$$e_1 = -\frac{N_1}{10^8} \frac{d\phi_0}{dt} = -j \frac{0.4\pi N_1^2 P_0 \omega \sqrt{2}}{10^8} I_\phi e^{j\omega t} \quad (34)$$

$$e_2 = -\frac{N_2}{10^8} \frac{d\phi_0}{dt} = -j \frac{0.4\pi N_1 N_2 P_0 \omega \sqrt{2}}{10^8} I_\phi e^{j\omega t} \quad (35)$$

in which (32) and (33) are the leakage flux voltages. In terms of rms values, they define the primary and secondary leakage reactances,

$$X_1 = \frac{0.4\pi N_1^2 P_1 \omega}{10^8} \quad (36)$$

$$X_2 = \frac{0.4\pi N_2^2 P_2 \omega}{10^8} \quad (37)$$

The induced voltages (34) and (35), in terms of the mutual flux Φ_0 defined in (31), have rms values

$$E_1 = -j \frac{\omega N_1 \Phi_0}{10^8 \sqrt{2}} = -j \frac{4.44}{10^8} f N_1 \Phi_0 \quad (38)$$

$$E_2 = -j \frac{\omega N_2 \Phi_0}{10^8 \sqrt{2}} = -j \frac{4.44}{10^8} f N_2 \Phi_0 \quad (39)$$

and the ratio of transformation is

$$\frac{E_1}{E_2} = \frac{N_1}{N_2} = a \quad (40)$$

Any secondary voltage multiplied by this ratio is said to be referred to the primary. Likewise, as is evident from (28), any secondary current divided by this ratio is said to be referred to the primary. Referred quantities are primed, for example, $E_2' = aE_2$ and $I_2' = I_2/a$.

Since only I_1 and I_2 are measurable currents, it is customary to write from (28)

$$I_0 = I_\phi - I_{h+c} = I_1 + I_2' \quad (41)$$

and this current I_0 , having a magnetizing component I_ϕ and an energy loss component I_{h+r} , is called the *exciting current* of the transformer.

Since the fictitious winding of N_1 turns has only a conductance G_0 and no leakage reactance, its induced voltage (38) must be consumed entirely by this conductance, or

$$I_{h+r} = G_0 E_1 \quad (42)$$

and since it is in phase with E_1 , thus lags the mutual flux Φ_0 by 90 degrees. The value of G_0 is such that

$$\frac{I_{h+r}^2}{G_0} = G_0 E_1^2 = \text{core loss} \quad (43)$$

The net magnetizing current I_ϕ must be in phase with the flux Φ_0 , that is proportional to E_1 and leading E_1 by 90 degrees. Let this proportionality factor be B_0 . Then by (41) and (42)

$$\begin{aligned} I_0 &= I_1 + I_2' = I_\phi + I_{h+r} \\ &= -(G_0 - jB_0)E_1 = -Y_0 E_1 \\ &= Y_0 E_0 \end{aligned} \quad (44)$$

in which $Y_0 = G_0 - jB_0$ is called the exciting admittance of the transformer, and $E_0 = -E_1$.

The secondary terminal voltage is consumed by the secondary resistance drop $R_2 I_2$, the leakage reactance drop $jX_2 I_2$, and the component to overcome the induced voltage E_2 ,

$$V_2 = R_2 I_2 + jX_2 I_2 - E_2 = Z_2 I_2 - E_2 \quad (45)$$

where $Z_2 = R_2 + jX_2$

This may be referred to the primary by multiplying both sides of (45) by the turn ratio a

$$\begin{aligned} aV_2 &= aZ_2 I_2 - aE_2 \\ &= (a^2 Z_2) \frac{I_2}{a} - aE_2 \end{aligned} \quad (46)$$

Then using primes for referred quantities and putting $E_0 = -E_1 = -aE_2$

$$V_2' = Z_2' I_2' + E_0 \quad (47)$$

where $Z_2' = a^2 Z_2$, $I_2' = I_2 / a$, and $V_2' = aV_2$

Thus secondary impedances must be multiplied by a^2 when referred to the primary.

The primary terminal voltage is consumed by the resistance drop

$R_1 I_1$, the leakage reactance drop $jX_1 I_1$ and the component to overcome the induced voltage E_1 ,

$$V_1 = R_1 I_1 + jX_1 I_1 - E_1 = Z_1 I_1 + E_0 \quad (48)$$

Equations (38), (39), (41), (44), (47), and (48) constitute the fundamental equations of the transformer. These equations may be interpreted as vector diagrams, or as those of an equivalent circuit, developed piecemeal and concurrently in Fig. 20. To begin with, let the mutual

VECTOR DIAGRAM	EQUATIONS	EQUIVALENT CIRCUIT
	$E_1 = -j 4.44 f N_1 \Phi_0 10^{-8}$ $E_2 = -j 4.44 f N_2 \Phi_0 10^{-8}$ $E_0 = -E_1 = -\alpha E_2$ $I_2' = I_2 / \alpha$ $I_0 = I_1 + I_2'$ $= I_w + I_{h.w.}$ $= Y_0 E_0$	<p>(a)</p>
	$V_2 = Z_2 I_2 - E_2$ $V_2' = Z_2' I_2' + E_0$ $V_2' = \alpha V_2$ $I_2' = I_2 / \alpha$ $Z_2' = \alpha^2 Z_2$	<p>(b)</p>
	$V_1 = Z_1 I_1 + E_0$	<p>(c)</p>
	$V_1 = \left(Z_1 + j \frac{1}{\frac{Y_0}{Z_2'} + Y_0} \right) I_1$ $+ \frac{V_2'}{1 + Y_0 Z_2'}$ $I_1' = -I_2'$ $I_1 = I_0 + I_1'$	<p>(d)</p>

Fig. 20

flux Φ_0 be taken as reference vector and drawn vertical. Then by (38) and (39) the induced voltages E_1 and E_2 lag Φ_0 by 90 degrees and the voltage E_0 to overcome these induced voltages must lead Φ_0 by 90 degrees.

The exciting current I_0 , made up of the magnetizing component I_ϕ in phase with Φ_0 and the core loss component $-I_w$, in phase with E_0 , is the resultant of the primary and secondary currents I_1 and I_2' , by (41). The element of the equivalent circuit, Fig. 20a, satisfies the current relationships.

The secondary voltage equation, (46), is easily recognized by (47) as a simple series circuit, Fig. 20b.

The primary voltage equation, (48), is likewise a simple series circuit, Fig. 20c.

Finally, since the three separate parts of the equivalent circuit have the same voltage E_0 , and satisfy the conditions of current continuity, they may be joined at their common terminals to form the complete equivalent circuit, Fig. 20d.

As a check, upon eliminating E_0 , I_0 and I_2' between (44), (47), and (48) there results, after some rearrangement,

$$V_1 = \left(Z_1 + \frac{1}{Y_0 + \frac{1}{Z_2'}} \right) I_1 + \frac{V_2'}{1 + Y_0 Z_2'} - Z_1 I_1 + \frac{V_2'}{1 + Y_0 Z_2'} \quad (49)$$

If $V_2' = 0$, the equivalent impedance in (49) is seen to be that of the circuit, Fig. 20d. Or if $I_1 = 0$, the voltage V_1 as given by (49) is the same as would be obtained from the equivalent circuit.

10. Approximate Equivalent Circuit

The primary impedance drop, $Z_1 I_1$, rarely exceeds 5 per cent of the applied voltage, and being also out of phase with the voltage, it is almost always permissible to take $E_0 \cong V_1$ in calculating the exciting current I_0 . Furthermore, the current I_0 is only a few per cent of the load current I_1 , so that it adds very little to the impedance drop, $Z_1 I_1$. Therefore, the exciting admittance branch Y_0 may be moved to the line terminals, and the equivalent circuit and its vector diagram reduces to that of Fig. 21. This simplified diagram is sufficient for all practical purposes. There are neglected factors (saturation, harmonics, and others) of far greater importance than the error

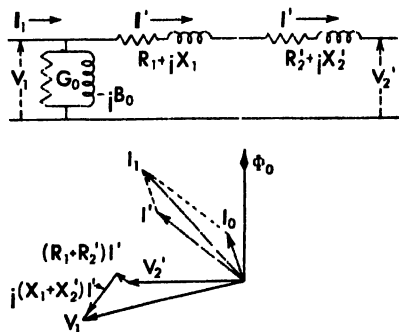


Fig. 21 The approximate equivalent circuit and vector diagram of the transformer.

committed in going over to the approximate equivalent circuit. In most problems involving power transformers the exciting admittance may be ignored entirely in calculating regulation and division of load, although the core loss must be included in determining the efficiency.

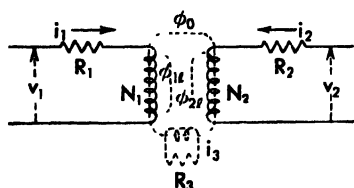


Fig. 22

11. Differential Equation Approach

The schematic diagram of a 2-winding transformer with its fictitious "core loss" winding is shown in Fig. 22. The differential equations of this circuit, in terms of self and mutual inductances, are

$$\left. \begin{aligned} v_1 &= R_1 i_1 + L_1 \frac{di_1}{dt} + M_{12} \frac{di_2}{dt} + M_{13} \frac{di_3}{dt} \\ v_2 &= R_2 i_2 + L_2 \frac{di_2}{dt} + M_{21} \frac{di_1}{dt} + M_{23} \frac{di_3}{dt} \\ 0 &= R_3 i_3 + L_3 \frac{di_3}{dt} + M_{31} \frac{di_1}{dt} + M_{32} \frac{di_2}{dt} \end{aligned} \right\} \quad (50)$$

Assuming all quantities to vary sinusoidally, and using rms values,

$$\left. \begin{aligned} i_1 &= I_1 e^{j\omega t} \\ i_2 &= I_2 e^{j\omega t} \\ i_3 &= I_3 e^{j\omega t} \\ v_1 &= V_1 e^{j\omega t} \\ v_2 &= V_2 e^{j\omega t} \\ v_3 &= 0 \end{aligned} \right\} \quad (51)$$

In terms of the permeances, the inductance coefficients are defined as

$$\left. \begin{aligned} L_1 &= 0.4\pi N_1^2 (P_1 + P_0) 10^{-9} = L_1' + M \\ L_2 &= 0.4\pi N_2^2 (P_2 + P_0) 10^{-9} = L_2' + M a^2 \\ L_3 &= 0.4\pi N_1^2 P_0 10^{-9} = M \\ M_{12} &= 0.4\pi N_1 N_2 P_0 10^{-9} = M' a \\ M_{23} &= 0.4\pi N_2 N_1 P_0 10^{-9} = M' a \\ M_{31} &= 0.4\pi N_1 N_1 P_0 10^{-9} = M \end{aligned} \right\} \quad (52)$$

in which L_1' and L_2' are leakage inductances.

Substituting (51) in (50), cancelling the $e^{j\omega t}$ factor, and making use of (52)

$$\begin{aligned}
 V_1 &= R_1 I_1 + j\omega L_1 I_1 + j\omega M_{12} I_2 + j\omega M_{13} I_3 \\
 &= R_1 I_1 + j\omega (L_1' + M) I_1 + j\omega \frac{M}{a} I_2 + j\omega M I_3 \\
 &= R_1 I_1 + j\omega L_1' I_1 + j\omega M \left(I_1 + \frac{I_2}{a} + I_3 \right) \\
 &= R_1 I_1 + jX_m I_1 + jX_m \left(I_1 + \frac{I_2}{a} + I_3 \right) \quad (53)
 \end{aligned}$$

$$\begin{aligned}
 V_2 &= R_2 I_2 + j\omega L_2 I_2 + j\omega M_{21} I_1 + j\omega M_{23} I_3 \\
 &= R_2 I_2 + j\omega \left(L_2' + \frac{M}{a^2} \right) I_2 + j\omega \frac{M}{a} I_1 + j\omega \frac{M}{l} I_3 \\
 &= R_2 I_2 + j\omega L_2' I_2 + j\omega \frac{M}{a} \left(I_1 + \frac{I_2}{a} + I_3 \right) \\
 &= R_2 I_2 + jX_m I_2 + j \frac{X_m}{c} \left(I_1 + \frac{I_2}{a} + I_3 \right) \quad (54)
 \end{aligned}$$

$$\begin{aligned}
 0 &= R_3 I_3 + j\omega L_3 I_3 + j\omega M_{31} I_1 + j\omega M_{32} I_2 \\
 &= R_3 I_3 + j\omega M I_3 + j\omega M I_1 + j\omega \frac{M}{a} I_2 \\
 &= R_3 I_3 + jX_m \left(I_1 + \frac{I_2}{a} + I_3 \right) \quad (55)
 \end{aligned}$$

Let

$$I_\phi = I_1 + \frac{I_2}{a} + I_3 = \text{net magnetizing current} \quad (56)$$

$$E_0 = jX_m I_\phi = \text{induced voltage due to mutual flux} \quad (57)$$

$$I_2' = \frac{I_2}{a} = \text{reflected secondary current}$$

Then (53), (54), (55), and (57) may be written

$$V_1 = Z_1 I_1 + E_0 \quad (58)$$

$$V_2 = Z_2 I_2 + \frac{E_0}{a} \quad \text{or} \quad aV_2 = (a^2 Z_2) \frac{I_2}{a} + E_0 \quad (59)$$

$$0 = R_3 I_3 + E_0 \quad \text{or} \quad I_3 = -\frac{E_0}{R_3} = G_0 E_0 \quad (60)$$

$$I_\phi = \frac{E_0}{jX_m} = -jB_0 E_0 \quad (61)$$

$$I_0 = I_\phi - I_3 = (G_0 - jB_0) E_0 = Y_0 E_0 \quad (62)$$

These equations are identical ($I_3 = I_{h+}$) with those derived in Sec. 9, and thus lead to the same vector diagrams and equivalent circuits. It is to be noted that core loss has been included, but would not have appeared in this development had the fictitious core loss circuit of resistance R_3 been omitted.

12. Transformer Constants and Tests

The equivalent circuits of Figs. 20 and 21 contain six constants: $R_1, X_1, R_2, X_2, G_0, B_0$, in terms of which the transformer performance may be calculated. These constants may be determined either from design formulas and data, or from test. The former procedure is:

1. The d-c resistances of the windings are calculated from the resistivity, cross-sectional areas and lengths of the conductors, and are then corrected for the operating temperature.
2. The eddy current loss in the conductors is calculated, and the winding resistances are increased to include this extra loss as a load loss (proportional to the current squared).
3. The stray loss in the tank and clamps is estimated, and the winding resistances are increased to include this extra loss as a load loss.
4. The core loss is determined from core loss curves for the appropriate flux densities and type of steel, corrected by test probability curves, and attributed to a conductance loss $G_0 E_0^2$.
5. The magnetizing current is determined from saturation curves, corrected for the number and type of joints in the core, and attributed to a susceptance, $B_0 = I_\phi / E_0$.
6. Leakage reactances are calculated from appropriate formulas and apportioned equally to X_1 and X_2' .

Obviously, the necessary information to carry out an analytical determination of the constants, particularly the all important empirical corrections, will be available only in the design office of the manufacturer.

But it is relatively simple to determine the constants experimentally. Two basic tests, the short-circuit and the open-circuit, are necessary.

The *short-circuit test*, Fig. 23, is made with the secondary winding short circuited and at reduced primary voltage (just sufficient to circulate rated current). Measurements are made of voltage, current, and power input. The primary voltage is adjusted so that approximately rated current flows through the transformer. Since the transformer impedance drop rarely exceeds 12 per cent of rated voltage, this means that the voltage is only that per cent of normal. The main flux is just

sufficient to produce rated secondary current. The exciting current at such low voltage is only a fraction of a per cent of rated load current. Consequently the exciting admittance of the equivalent circuit, Fig. 20 or 21, may be ignored as indicated by dotted outlines, and the equivalent circuit is that shown in Fig. 23b. Then

$$\cos \theta_{sc} = \frac{W_{sc}}{V_{sc} I_{sc}} \quad (63)$$

$$Z_{sc} = \sqrt{(R_1 + R_2')^2 + (X_1 + X_2')^2} = \frac{V_{sc}}{I_{sc}} \quad (64)$$

$$R_1 + R_2' = \frac{W_{sc}}{I_{sc}^2} = Z_{sc} \cos \theta_{sc} \quad (65)$$

$$X_1 + X_2' = \sqrt{Z_{sc}^2 - (R_1 + R_2')^2} = Z_{sc} \sin \theta_{sc} \quad (66)$$

But this test does not show how the total resistance is to be split between the primary and the secondary, nor how the total reactance is to be apportioned between X_1 and X_2' . It will be remembered that R_1 and R_2' are greater than the d-c resistances—perhaps as much as 25 per cent greater—because of the eddy loss in the conductors and the stray loss in the tank and clamps. If the d-c resistances of the two windings, as measured by the drop-of-potential method or by a bridge, are r_1 and r_2 , it is sufficient to assume R_1 and R_2' to be in the ratio $R_1 : R_2' = r_1 : a^2 r_2$ and substituting in (65) for R_2' gives

$$R_1 = \left(\frac{r_1}{r_1 + a^2 r_2} \right) \left(\frac{W_{sc}}{I_{sc}^2} \right) \quad (67)$$

The reactances X_1 and X_2' may be taken in the same ratio, or more usually as equal to each other. It is not feasible by test methods to separate the total reactance into primary and secondary components X_1 and X_2' , although the two parts may be calculated separately from design data.

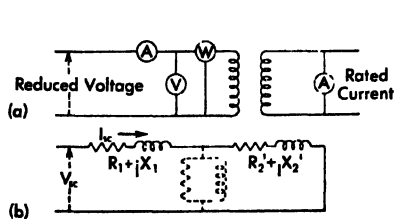


Fig. 23 Short-circuit test.

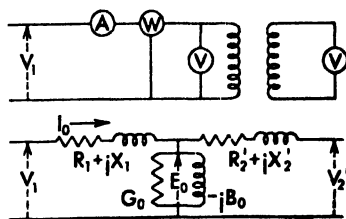


Fig. 24 Open-circuit test.

The *open-circuit test*, Fig. 24, is made with the secondary open-circuited and with rated voltage applied to the primary. Measurements are made of voltage, current, and power input. The no-load or exciting current I_0

is only a fraction to a few per cent of normal rated current, and its voltage drop in the primary winding is quite negligible. Therefore, in the equivalent circuit under this condition, the voltage E_0 across the exciting admittance is substantially the same as the applied voltage, so that

$$Y_0 = \frac{I_0}{E_0} = \frac{I_0}{|V_1 - (R_1 + jX_1)I_0|} \cong \frac{I_0}{V_1} \quad (68)$$

$$G_0 = \frac{W_{oc}}{E_0^2} = \frac{R_1 I_0^2}{V_1^2} \cong \frac{W_{oc}}{V_1^2} \quad (69)$$

$$B_0 = \sqrt{Y_0^2 - G_0^2} \quad (70)$$

These equations have been written so that one can readily verify that the impedance drop $(R_1 + jX_1)I_0$ may be ignored completely in determining G_0 and B_0 . In (68), as a sufficiently good approximation, I_0 may be taken as lagging V_1 by 90 degrees, that is $I_0 = -jI_0$.

Under the open-circuit test the no-load current will contain a pronounced third harmonic due to saturation (see Fig. 17). This harmonic current, flowing through any impedance between the generator or voltage source and the transformer under test, will result in a third harmonic voltage on the transformer terminals and may change the core loss considerably. Precautions should be taken to insure that the test voltage wave form is a pure sinusoid, or else that measuring instruments are used which will correct for any distortion in the flux wave (the flux voltmeter).

In testing small transformers, corrections must be made for the currents taken by the measuring instruments.

The turn ratio is obtainable from either the short-circuit or open-circuit tests, if the secondary current and voltage are taken, thus

$$\frac{N_1}{N_2} = \left(\frac{I_2}{I_1} \right) = \left(\frac{V_1}{V_2} \right) \quad (71)$$

Example: The short-circuit and open-circuit tests on a power transformer rated 60 cycles, 12,000 kva, 132-22 kv are as follows:

	SHORT-CIRCUIT	OPEN-CIRCUIT
Voltage, primary	10,900	132,000
Voltage, secondary	0	22,020
Current, primary	90.9	0.95
Current, secondary	545.5	0
Kw, input	71.4	54.5

The primary and secondary d-c resistances at 75 C are: $r_1 = 4.11$, $r_2 = 0.0975$ ohms.

$$(a) \text{ By (71): } \frac{N_1}{N_2} = \frac{545.5}{90.9} = 6.00$$

$$\frac{N_1}{N_2} = \frac{132,000}{22,020} = 5.99$$

$$(b) \text{ By (63) } \cos \theta_{sc} = \frac{71,400}{10,900 \times 90.9} = 0.0721$$

$$\sin \theta_{sc} = 0.9974$$

$$\theta_{sc} = -85.85^\circ$$

$$(c) \text{ By (64) } Z_{sc} = \frac{10,900}{90.9} = 120 \text{ ohms}$$

$$(d) \text{ By (65) } R_{sc} = \frac{71,400}{90.9^2} = 8.65 \text{ ohms}$$

$$(e) \text{ By (66) } X_{sc} = \sqrt{120^2 - 8.65^2} = 119.6 \text{ ohms}$$

$$(f) \text{ By (67) } R_1 = \frac{4.11 \times 8.65}{4.11 + 0.0975 \times 36} = 4.67$$

$$R_2' = 8.65 - 4.67 = 3.98$$

$$R_2 = 3.98 \div 36 = 0.1106 \text{ ohms}$$

$$X_1 = \frac{4.11 \times 119.6}{7.62} = 64.5 \text{ ohms}$$

$$X_2' = 119.6 - 64.5 = 55.1 \text{ ohms}$$

$$X_2 = 55.1 \div 36 = 1.53 \text{ ohms}$$

$$\cos \theta_m = \frac{54,500}{132,000 \times 0.95} = 0.435$$

$$\sin \theta_m = 0.9002 \quad \theta_m = -64.2^\circ$$

$$E_0 = 132,000 - (64.7 \times 85.85^\circ) (0.95 / -64.2^\circ) = 131,943 - j23$$

$$(g) \text{ By (68) } I_0 = \frac{0.95}{131,944} = 7.20 \times 10^{-6}$$

$$(h) \text{ By (69) } G_0 = \frac{54,500 - 4.67 \times 0.95^2}{131,944} = 3.13 \times 10^{-6}$$

$$(i) \text{ By (70) } B_0 = \sqrt{7.20^2 - 3.13^2} \times 10^{-6} = 6.49 \times 10^{-6}$$

Note how insignificant is the effect of the impedances in determining I_0 and G_0 .

13. Performance Calculations, Regulation, and Efficiency

The performance calculations for the transformer include the determination of its regulation; losses; efficiency; primary, secondary, and exciting currents; voltages; power factor; division of load with other transformers during parallel operation; and temperature rises. All except the last of these may be calculated from the equivalent circuit in terms of the six parameters $R_1, X_1, R_2', X_2', G_0, B_0$. Either the exact, Fig. 20d, or the approximate, Fig. 21, equivalent circuit may be used. The latter is much simpler and quite adequate for calculations on power or distribution transformers. On instrument transformers, the performance is almost always determined from test. In high-voltage potential transformers, the capacitance effect is of far greater importance than any differences between the two equivalent circuits.

Per cent regulation is defined as

$$\% \text{ Reg} = \frac{V_2(\text{no load}) - V_2(\text{full load})}{V_2(\text{full load})} \times 100 \quad (72)$$

based on rated voltage, current, and frequency at full load and a specified power factor (pf) (usually 0.80 and 1.00), with sine wave voltages, and a winding temperature of 75°C . The no-load voltage is usually taken as $V_2(\text{no load}) = V_1 a$, since the primary impedance drop of the exciting current is negligible. Using the approximate equivalent circuit (referred to the secondary), taking the voltage V_2 as reference vector, and the load current I_2 at a lagging pf angle θ_2 ,

$$\begin{aligned} V_1/a &= (R + jX)I_2(\cos \theta_2 - j \sin \theta_2) + V_2 \\ &= (V_2 + RI_2 \cos \theta_2 + XI_2 \sin \theta_2) + j(XI_2 \cos \theta_2 - RI_2 \sin \theta_2) \end{aligned} \quad (73)$$

The absolute value of the primary voltage then is

$$V_1/a = \sqrt{V_2^2 + (R^2 + X^2)I_2^2 + 2V_2(RI_2 \cos \theta_2 + XI_2 \sin \theta_2)} \quad (74)$$

and the regulation therefore is

$$\text{Reg} = \sqrt{1 + \frac{(R^2 + X^2)I_2^2}{V_2^2} + \frac{2}{V_2}(RI_2 \cos \theta_2 + XI_2 \sin \theta_2)} - 1 \quad (75)$$

But the second and third terms under the radical are small compared to unity, and therefore by expanding the radical by the binomial theorem and rejecting terms beyond the square, there finally results

$$\text{Reg} = \frac{RI_2 \cos \theta_2 + XI_2 \sin \theta_2}{V_2} + \frac{1}{2} \left(\frac{XI_2 \cos \theta_2 - RI_2 \sin \theta_2}{V_2} \right)^2 \quad (76)$$

Equation (76) is the American Institute of Electrical Engineers rule for calculating regulation.

Efficiency is defined as

$$\begin{aligned} \text{Eff} &= \frac{\text{output}}{\text{input}} = \frac{\text{output}}{\text{output} + \text{losses}} = 1 - \frac{\text{losses}}{\text{input}} \\ &= \frac{V_2 I_2 \cos \theta_2}{V_2 I_2 \cos \theta_2 + R_1 I_1^2 + R_2 I_2^2 + G_0 E_0^2} \end{aligned} \quad (77)$$

and for all practical purposes we may take $E_0 \cong V_1$.

For distribution transformers, where full load is carried for only a small part of the day, but the core loss is continuous, the *all-day* efficiency is of importance. Let the iron losses be W , watts per hour, and t_1, t_2, \dots be the hours per day at which the transformer carries $\alpha_1, \alpha_2, \dots$ fractions of full-load current I . Then the all-day efficiency is (assuming constant pf through the day)

$$\eta = \frac{V_2 I \cos \theta_2 (\alpha_1 t_1 + \alpha_2 t_2 + \alpha_3 t_3 + \dots)}{V_2 I \cos \theta_2 (\alpha_1 t_1 + \alpha_2 t_2 + \dots) + R I^2 (\alpha_1^2 t_1 + \alpha_2^2 t_2 + \dots) + 24W} \quad (78)$$

This is a maximum for $\frac{d\eta}{dI} = 0$, which gives

$$R I^2 (\alpha_1^2 t_1 + \alpha_2^2 t_2 + \dots) = 24W \quad (79)$$

If the transformer is fully loaded all of the time, this equation shows that the copper and iron losses should be equal for maximum efficiency. But otherwise, the iron losses should be less than the full load copper losses.

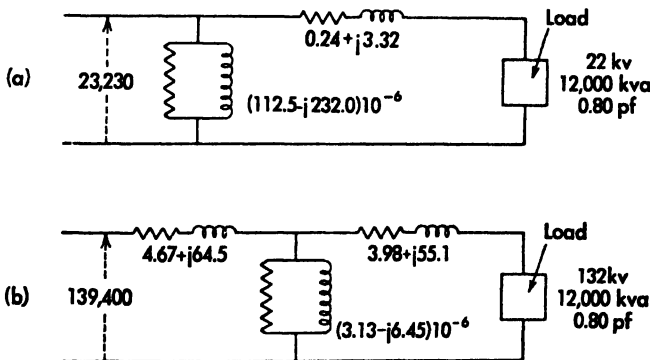


Fig. 25

Nomographs are often used in design offices for the rapid calculation of regulation and efficiency.

Example: Consider the same transformer as in the example of Sec. 12, the approximate equivalent circuit for which (referred to the low-voltage side) is

shown in Fig. 25a. The secondary load is 12,000 kva at 0.80 pf lag, and 22 kv. Full load current is

$$I_2 = \frac{12,000}{22} = 545.5 \text{ amp}$$

The regulation, by (76), is

$$\begin{aligned} \text{Reg} &= \frac{0.24 \times 545.5 \times 0.80 + 3.32 \times 545.5 \times 0.60}{22,000} + \\ &\quad \frac{1}{2} \left(\frac{3.32 \times 545.5 \times 0.80 - 0.24 \times 545.5 \times 0.60}{22,000} \right)^2 = 0.0561 \end{aligned}$$

The losses are

$$\frac{0.24 \times 545.5^2}{1000} + \frac{112.5}{10^6} \times \frac{22,000^2}{1000} = 71.4 + 54.4 = 125.8 \text{ kw}$$

The output is $12,000 \times 0.80 = 9600 \text{ kw}$

The efficiency then is

$$\eta = 1 - \frac{125.8}{9600 + 125.8} = 0.987$$

Suppose this transformer has a daily load cycle in which it carries 20 per cent overload for 2 hours, full load for 6 hours, 75 per cent load for 8 hours, and 50 per cent load for 8 hours. What is its all day efficiency? By (78)

$$\begin{aligned} \eta &= \frac{22,000 \times 545.5 \times 0.80 (1.20 \times 2 + 1.00 \times 6 + 0.75 \times 8 + 0.50 \times 8)}{\left\{ 22,000 \times 545.5 \times 0.80 (1.20 \times 2 + 1.00 \times 6 + 0.75 \times 8 + 0.50 \times 8) \right.} \\ &\quad \left. + 24 \times 54,500 \right\} \\ &\quad \left\{ + 0.24 \times 545.5^2 (1.20^2 \times 2 + 1.00^2 \times 6 + 0.75^2 \times 8 + 0.50^2 \times 8) \right\} \\ &= 0.9865 \end{aligned}$$

The primary current is

$$\begin{aligned} I_1 &= \frac{1}{6} \left[545.5 (0.8 - j0.6) + \left(\frac{112.5 - j232.0}{10^6} \right) 23,230 \right] \\ &= 73.0 - j55.3 \end{aligned}$$

The primary voltage is

$$\begin{aligned} V_1 &= 6 [22,000 + (0.24 + j3.32) 545.5 (0.8 - j0.6)] \\ &= 139,150 + j8220 = 139,400 \angle 3.4^\circ \end{aligned}$$

By way of comparison, it is instructive to carry out detailed calculations for the exact equivalent circuit, Fig. 25b.

$$I_2' = \frac{12,000}{132} (0.8 - j0.6) = 72.7 - j54.5 = 90.8 \angle -36.9^\circ$$

$$\begin{aligned} E_0 &= 132,000 + (72.7 - j54.5) (3.98 + j55.1) \\ &= 135,290 + j3793 = 135,300 \angle 1.6^\circ \end{aligned}$$

$$I_0 = \left(\frac{3.13}{10^6} - j6.45 \right) (135,290 + j3793) = 0.45 - j0.86 = 0.97 \angle -62.4^\circ$$

$$I_1 = (72.7 - j54.5) + (0.45 - j0.86) = 73.2 - j55.4 = 91.9 \angle -37.1^\circ$$

$$V_1 = (135,290 + j3793) + (4.67 + j64.5)(73.2 - j55.4) \\ = 139,207 + j8254 = 139,400 \angle 3.4^\circ$$

$$\text{Reg} = \frac{139,400 - 132,000}{132,000} = 0.0561$$

$$\text{Losses} = \frac{4.67 \times 91.9^2}{10^3} + \frac{3.98 \times 91.8^2}{10^3} + \frac{3.13}{10^6} \times \frac{135,300^2}{10,000} = 129.7 \text{ kw}$$

$$\text{Eff} = 1 - \frac{129.7}{12,000 + 129.7} = 0.989$$

It is evident that the approximate and exact equivalent circuits give the same results within slide rule accuracy. In transformers with high exciting currents and high leakage impedance, the differences become more pronounced. It happens, however, that high exciting currents and high impedances do not go together in commercial designs. The per cent exciting current is larger for small distribution transformers, but the per cent impedance is low. On large high voltage power transformers just the reverse is true. In fact, it is possible for a very high voltage, small capacity transformer to draw a leading no load current, because of the charging current.

14. The Generalized Constants of the Transformer

The external behavior of a 4 terminal network with linear characteristics, Fig. 26, may be specified in terms of its so-called *generalized constants* A, B, C, D and the terminal voltages V_1, V_2 and currents I_1, I_2 . These constants are of great utility in the analysis of transmission systems. The generalized equations are

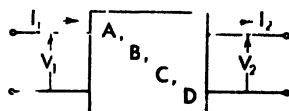


Fig. 26

$$\begin{cases} V_1 = AV_2 + BI_2 \\ I_1 = CV_2 + DI_2 \end{cases} \quad (80)$$

or conversely, solving for V_2 and I_2

$$\begin{cases} V_2 = A'V_1 + B'I_1 \\ I_2 = C'V_1 + D'I_1 \end{cases} \quad (81)$$

in which

$$\left. \begin{aligned} A' &= D/(AD - BC) \\ B' &= -B/(AD - BC) \\ C' &= -C/(AD - BC) \\ D' &= A/(AD - BC) \end{aligned} \right\} \quad (82)$$

Other combinations could just as well be worked out, for example V_1 as a linear function of V_2 and I_1 , but the forms (80) and (81) are of the greatest use.

The generalized constants may be determined quite readily from short-circuit and open-circuit tests, or by analysis if the network is known.

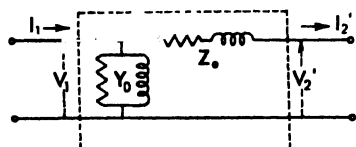


Fig. 27

Suppose, now, that the network in the box of Fig. 26 is a 2-winding transformer, the approximate equivalent circuit of which is Fig. 27. If the secondary is short-circuited, $V_2 = 0$ and under this condition, Fig. 27 gives

$$I_2' = \frac{V_1}{Z_0} \quad \text{or} \quad V_1 = Z_0 I_2' + \frac{Z_1}{a} I_2$$

$$I_1 = Y_0 V_1 + I_2' = Y_0 \left(Z_0 I_2' + \frac{Z_1}{a} I_2 \right) + I_2' = \frac{Y_0 Z_0}{a} I_2 + \left(1 + \frac{Y_0 Z_1}{a} \right) I_2'$$

hence comparison with (80) shows that

$$B = \frac{Z_0}{a} = \left(\frac{V_1}{I_2'} \right)_{V_2=0}$$

$$D = \frac{Y_0 Z_0}{a} + 1 = \left(\frac{I_1}{I_2'} \right)_{V_2=0}$$

On open circuit test, $I_2 = 0$ and under this condition Fig. 27 gives

$$V_1 = V_2' + a V_2$$

$$I_1 = Y_0 V_1 = Y_0 a V_2$$

and comparison with (80) shows that

$$A = a = \left(\frac{V_1}{V_2} \right)_{I_2=0}$$

$$C = Y_0 a = \left(\frac{I_1}{V_2} \right)_{I_2=0}$$

Therefore, (80) may be written in specific equivalent circuit or test data terms as

$$\left. \begin{aligned} V_1 &= aV_2 + \frac{Z_1}{a} I_2 = \left(\frac{V_1}{V_2} \right)_{oc} V_2 + \left(\frac{V_1}{I_2} \right)_{sc} I_2 \\ I_1 &= Y_0 a V_2 + \frac{Y_0 Z_1 + 1}{a} I_2 = \left(\frac{I_1}{V_2} \right)_{oc} V_2 + \left(\frac{I_1}{I_2} \right)_{sc} I_2 \end{aligned} \right\} \quad (83)$$

The same procedure could have been carried through for the exact equivalent circuit, but the extra complication is not justifiable.

Example: Referring to the test data in the example of Sec. 12.

$$A = \left(\frac{V_1}{V_2} \right)_{oc} = \frac{132,000}{22,020} = 5.99$$

$$B = \left(\frac{V_1}{I_2} \right)_{sc} = \frac{10,900}{545.5} = 19.85.85^\circ$$

$$C = \left(\frac{I_1}{V_2} \right)_{oc} = \frac{0.95}{22,020} = 43.2 \times 10^{-6} \quad 64.1^\circ$$

$$D = \left(\frac{I_1}{I_2} \right)_{sc} = \frac{90.9}{545.5} = 1.66$$

Or, from the same example, using the deduced constants of the equivalent circuit

$$A = a = 6.00$$

$$B = \frac{Z_1}{a} = \frac{12.0}{6} \angle 85.85^\circ = 2.0 \angle 85.85^\circ$$

$$C = Y_0 a = \frac{6 \times 7.20}{10^6} \angle -64.10^\circ = 43.2 \times 10^{-6} \angle -64.10^\circ$$

$$D = \frac{1 + Y_0 Z_1}{a} = \frac{1 + 7.20 \times 10^{-6} \angle -64.10^\circ}{6.00} \angle 120.85.85^\circ \approx \frac{1}{6.00}$$

Note that the constant D , as calculated from the test data, does not contain any phase difference between the currents I_1 and I_2 , although this very small correction may be taken into account in terms of the equivalent circuit constants. Finally

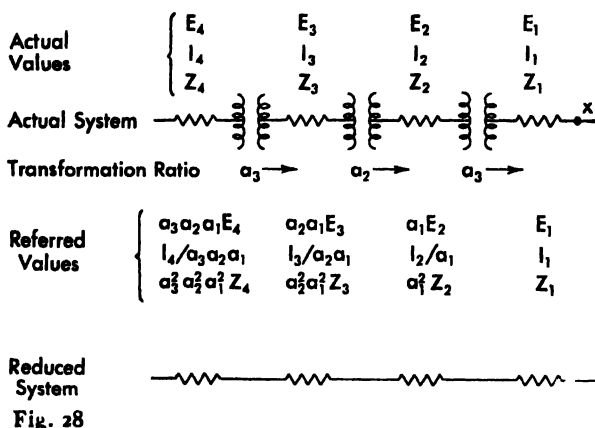
$$V_1 = 6.00 V_2 + 20 \angle 85.85^\circ I_2$$

$$I_1 = \frac{43.2}{10^6} \angle -64.1^\circ V_2 + \frac{1}{6.00} I_2$$

15. Referred Quantities and Per-unit Values

It has been shown that voltages, currents, and impedances as given on one side of a transformer may be transferred to the other side upon

multiplication by a , a^{-1} , and a^2 respectively, where a is the transformation ratio. If there are several such transformations in succession a_1, a_2, a_3, \dots this process permits all quantities on the system to be *referred* to a particular point, as indicated in Fig. 28, where the actual system has been referred to point x and in the reduced system there are no transformers.



However, in the analysis of an extensive system this process is not only awkward and unwieldy, but is a source of error. It is so very easy to use a transformation ratio upside down! The difficulties and pitfalls can be avoided by introducing the concept of *per unit values*, which are simply the ratios of actual quantities to arbitrary standard or *base* quantities. Consider the simple series circuit of Fig. 29, in which

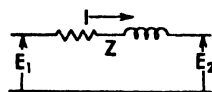


Fig. 29

$$E_1 = E_2 + ZI \quad (84)$$

Suppose that a perfectly arbitrary voltage E_b and a current I_b be selected as *base* quantities. Then upon dividing each side of (84) by E_b

$$\left(\frac{E_1}{E_b} \right) = \left(\frac{E_2}{E_b} \right) + \left(\frac{ZI}{E_b} \right) = \left(\frac{E_2}{E_b} \right) + \left(\frac{ZI_b}{E_b} \right) \left(\frac{I}{I_b} \right) \quad (85)$$

The voltage ratios, (E_1/E_b) and (E/E_b) , which are the actual voltages expressed as fractions of the base voltages, are called *per-unit voltages* (abbreviated pu). The ratio of the actual current I to the base current I_b is the *per unit current*. And the ratio of the impedance drop produced by base current to the base voltage, (ZI_b/E_b) , is the *per unit impedance*. The equation may be rewritten in terms of these definitions as

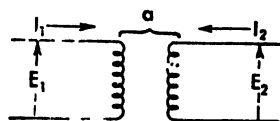
$$\text{pu } E_1 = \text{pu } E_2 + (\text{pu } Z)(\text{pu } I) \quad (86)$$

or the *pu* understood and dispensed with. The per-unit equation then looks exactly like a volt-ampere-ohm equation. Usually it is more convenient to select a base *kva* instead of a base current, in which case

$$I_b = \frac{(kva)_b}{(kv)_b} \quad (87)$$

$$pu \ Z = \frac{Z(\text{ohms}) I_b(\text{amps})}{E_b(\text{volts})} = \frac{Z(\text{ohms})}{1000} \cdot \frac{(kva)_b}{(kv)_b^2} \quad (88)$$

The great utility of per-unit quantities lies in the fact that they have the same value referred to either side of a transformer. Moreover, the per-unit impedance of an electrical machine is rather definite within narrow limits, whereas the ohmic value may be almost anything, depending on the voltage and size of the apparatus. For example, the impedance of a power transformer is between 5 and 10 per cent, or 0.05 and 0.10 per unit. Consider the ideal transformer of Fig. 30, in which voltages, currents, and impedances on the secondary side have been referred to the primary by the transformation ratio *a*. Also, the secondary base voltage E_{b2} and current I_{b2} have been referred. Then the per-unit quantities on the primary side are seen to reduce to identities with the per unit quantities on the secondary side, thus



$$\left. \begin{aligned} E_1 &= a E_2 \\ I_1 &= I_2 / a \\ Z_1 &= a^2 Z_2 \\ E_{b1} &= a E_{b2} \\ I_{b1} &= I_{b2} / a \end{aligned} \right\} \begin{aligned} E_2 \\ I_2 \\ Z_2 \\ E_{b2} \\ I_{b2} \end{aligned}$$

Fig. 30

$$\left. \begin{aligned} \frac{E_1}{E_{b1}} &= \frac{a E_2}{a E_{b2}} = \frac{E_2}{E_{b2}} \\ \frac{I_1}{I_{b1}} &= \frac{I_2 / a}{I_{b2} / a} = \frac{I_2}{I_{b2}} \\ \frac{Z_1 I_{b1}}{E_{b1}} &= \frac{a^2 Z_2 I_{b2} / a}{a E_{b2}} = \frac{Z_2 I_{b2}}{E_{b2}} \end{aligned} \right\} \quad (89)$$

Per cent values are merely *per-unit* (*pu*) values multiplied by 100 and are usually written %*E* or %*I* or %*ZI*.

Now it often happens that one or more bases have to be changed in order that all impedances in a system be expressed on a common base. For example, the impedances of individual generators and transformers are usually expressed in terms of their own rated *kva* and *kv* as base quantities. Let primed quantities denote a new base. Then a transfer of base is effected by the equations

$$(pu I') = \frac{I}{I_b'} = \frac{I}{I_b} \frac{I_b}{I_b'} = (pu I) \frac{I_b}{I_b'} = (pu I) \left(\frac{kva}{kv} \right)_b \left(\frac{kv}{kva} \right)' \quad (90)$$

$$(pu E') = \frac{E}{E_b'} = \frac{E}{E_b} \frac{E_b}{E_b'} = (pu E) \frac{E_b}{E_b'} = (pu E) \left(\frac{kv}{kv'} \right)_b \quad (91)$$

$$(pu Z') = \frac{ZI_b'}{E_b'} = \frac{ZI_b}{E_b} \frac{E_b}{E_b'} \frac{I_b'}{I_b} = (pu Z) \frac{E_b}{E_b'} \frac{I_b'}{I_b} = (pu Z) \left(\frac{kv^2}{kva} \right)_b \left(\frac{kva}{kv^2} \right)' \quad (92)$$

Example: What are the per-unit resistance, reactance, and impedance of the transformer in the example of Sec. 13 on its own kva and kv base? By definition

$$pu R = \frac{8.65 \times 90.9}{132,000} = 0.00595$$

$$pu X = \frac{119.6 \times 90.9}{132,000} = 0.0824$$

$$pu Z = \frac{120 \times 90.9}{132,000} = 0.0826$$

If this transformer is part of a large system which is being analyzed, and the bases of the system have been selected as 200,000 kva and 138 kv, what is its per-unit impedance on the new base? By (92)

$$pu Z' = 0.0826 \frac{132^2}{12,000} \frac{200,000}{138^2} = 1.26$$

16. Autotransformer

An arrangement, such as Fig. 31, in which the primary and secondary windings of a transformer are interconnected electrically as well as inductively is called an *autotransformer*. There are many variations of this simplest autotransformer connection, some of which involve three windings and three phase connections. The great advantages of the autotransformer as compared to the ordinary transformer are: (1) higher efficiency, particularly when the voltages on the high and low side do not differ much; (2) greatly reduced size for the same output; and (3) only a fraction of the leakage impedance. The disadvantages are: (1) the two circuits are not isolated electrically; and (2) the currents and mechanical forces due to a short-circuit are many times greater. Autotransformers are used where a relatively small ratio of transformation – rarely more than 2 to 1 – is required. They are used a great deal for starting poly-phase induction motors, in which case they are called *starting compensators*.

In theory, the autotransformer of Fig. 31 is still a 2-winding transformer in which the current in the *series* winding of N_1 turns is the same as the high-voltage current, while the current in the *common* winding is the difference of the high-voltage and low-voltage currents. Basically then, for an ideal transformer, the induced voltages in the two windings are in the ratio of the turns, the ampere-turns balance, and the kva is conserved.

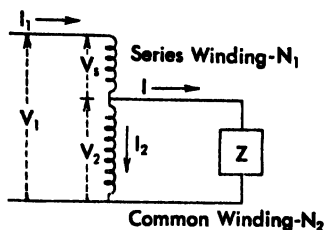


Fig. 31 Autotransformer.

The ratio of the induced voltages in the series and common windings is the *transformer ratio*

$$\frac{E_1}{E_2} = \frac{N_1}{N_2} = a \quad (93)$$

while the *autotransformer ratio* is defined as

$$\frac{E_1 + E_2}{E_2} = \frac{N_1 + N_2}{N_2} = 1 + \frac{N_1}{N_2} = 1 + a = b \quad (94)$$

The exciting current may be accounted for in the usual way by an exciting admittance,

$$I_0 = -Y_0(E_1 + E_2) = -bY_0E_2 \quad (95)$$

The ampere-turn balance is

$$N_1I_1 + N_2I_2 = (N_1 + N_2)I_0 \quad (96)$$

Dividing through by N_2 and making use of (93), (94) and (95)

$$aI_1 + I_2 = bI_0 = -b^2Y_0E_2 \quad (97)$$

$$\text{The load current is } I = I_1 - I_2 \quad (98)$$

The voltage equations for the series and common windings then are

$$V_1 = -E_1 + Z_1I_1 \quad (99)$$

$$V_2 = -E_2 + Z_2I_2 = ZI = Z(I_1 - I_2) \quad (100)$$

Adding these two equations gives the primary voltage

$$V_1 = V_1' + V_2 = -E_1 - E_2 + Z_1I_1 + Z_2I_2 = -bE_2 + Z_1I_1 + Z_2I_2 \quad (101)$$

Eliminating E_2 and I_2 between (97), (100) and (101) there results, after some rearrangement,

$$\begin{aligned} \frac{V_1}{I_1} &= Z_1 + \frac{-aZ_2 + \frac{b^2Y_0ZZ_2 + abZ_2 + b^2Z}{1 + b^2Y_0(Z_2 + Z)}}{1 + b^2Y_0(Z_2 + Z)} \\ &= Z_1 - aZ_2 + \frac{b^2Y_0Z_2(bZ + aZ_2) + abZ_2 + b^2Z}{1 + b^2Y_0(Z_2 + Z)} \end{aligned} \quad (102)$$

Putting $Z_0 = 1/Y_0$ and rearranging, since $b^2 = b(1 + a)$,

$$\frac{V_1}{I_1} = Z_1 - aZ_2 + \frac{(bZ_2 + Z_0)(abZ_2 + b^2Z)}{abZ_2 + bZ_2 + b^2Z + Z_0} \quad (103)$$

The equivalent circuit corresponding to (103) is easily recognized as that of Fig. 32a, and if the exciting impedance branch is moved to the line terminals there results the approximate equivalent circuit of Fig. 32b.

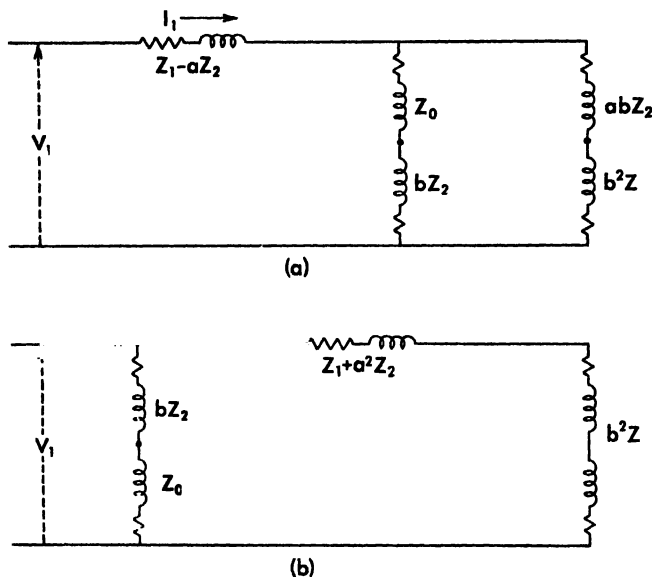


Fig. 32 Equivalent circuits of the autotransformer.

It is clear that:

1. Load impedances are referred to the high voltage by the square of the autotransformer ratio, b^2 .
2. The common winding impedance is referred to the high voltage by the square of the transformer ratio, a^2 .

In order to compare the autotransformer with a transformer for the same load and power supply conditions, the following assumptions will be made:

1. Both are designed for the same current density in each winding.
2. Reactance varies as the square of the number of turns. (This is not quite true, since a greater number of turns would require more winding space, and therefore result in additional reactance.)
3. Exciting current is negligible.

Figure 33a shows a transformer of primary voltage V_1 and secondary voltage V_2 . Let the resistance of the N_1 turns be R_1 and the reactance X_1 ohms. Then the transformer impedance referred to the primary is

$$Z_{trans} = R_1 + \frac{R_2}{a^2} + j \left(\frac{X_1 + X_2}{a} \right) \quad \lambda_1 + j b \lambda_2$$

By assumption (1) $b^2 R_2$ is equal to the primary resistance, and by assumption (2) $b^2 X_2 = (b/a)^2 X_1$. Hence

$$Z_{trans} = 2 \frac{b}{a} R_1 + j 2 \frac{b^2}{a^2} X_1 \quad (104)$$

Now for the autotransformer, the current in the common winding is only a fraction ($I_2/I_1 = a$) of the current in the series winding, and therefore at the same current density the resistance per turn of the common winding is $(1/a)$ times as great as in the series winding. Consequently, the autotransformer impedance referred to the primary is

$$\begin{aligned} Z_{auto} &= Z_1 + a^2 Z_2 \\ &= R_1 + a^2 \frac{R_2}{a^2} + j \lambda_1 + j a^2 \lambda_2 \\ &= R_1 + R_1 + j \lambda_1 + j a^2 \left(\frac{\lambda_2}{\lambda_1} \right)^2 \lambda_1 \\ &= 2R_1 + j 2 \lambda_1 \end{aligned} \quad (105)$$

Hence the ratios of effective resistances and reactances are

$$\frac{R_{auto}}{R_{trans}} = \frac{a}{b} \quad (106)$$

$$\frac{X_{auto}}{X_{trans}} = \left(\frac{a}{b} \right)^2 \quad (107)$$

Thus the copper losses in the autotransformer are only (a/b) those in the transformer, and the reactance only $(a/b)^2$ as great.

The equivalent transformer size of the autotransformer (the average of the volt-amperes in its two windings) is

$$\frac{1}{2} (V_1 I_1 + V_2 I_2) = \frac{1}{2} \left(a V_1 I_1 + \frac{V_1}{b} a I_1 \right) = \frac{a}{b} (V_1 I_1) \quad (108)$$

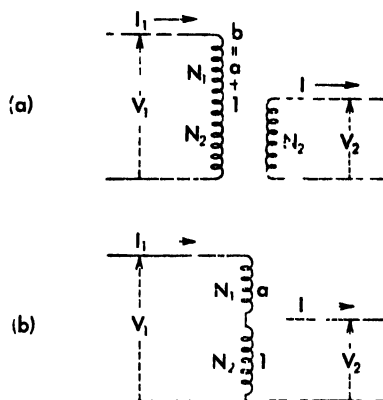


Fig. 33 Transformer and autotransformer

Sometimes an autotransformer is tested as an ordinary transformer, using the series winding as the primary and the common winding as the secondary (or conversely). The measured ohms impedance then is $(Z_1 + a^2 Z_2)$, the same as for the autotransformer impedance as shown in Fig. 32b. However, the per-unit impedance is (b/a) times as great, since

$$pu Z_{\text{trans}} = (Z_1 + a^2 Z_2) \frac{I_1}{V_1} \quad (109)$$

$$pu Z_{\text{auto}} = (Z_1 + a^2 Z_2) \frac{I_1}{V_1} = \frac{a}{b} (pu Z_{\text{trans}}) \quad (110)$$

Example: A 100 kva, 2300 volt, 80% pf load is to be supplied from a 4000 volt circuit. An ordinary transformer for this job has $\%I^2R = 4.10$, $\%JR = 1.06$ and 860 watts core loss. If an autotransformer is substituted, how will its characteristics compare with those of the transformer?

TRANSFORMER		AUTOTRANSFORMER	
$b = \frac{4000}{2300} = 1.74$	ratio	$a = \frac{4000 - 2300}{2300} = 0.74$	
1.69 ohms	R	by (106) $\frac{0.74}{1.74} 1.69 = 0.72$	
6.55 ohms	X	by (107) $\left(\frac{0.74}{1.74}\right)^2 6.55 = 1.19$	
4.23%	$\%IZ$		0.87%
$1.69 \times 25^2 = 1060$	Copper loss	$0.72 \times 25^2 = 450$	
860	Core loss	860	
1920	Total loss	1310	
97.65%	Efficiency	98.39%	
100	Relative size	42.6	

17. Three-winding Transformer

An appreciable percentage of the large power transformers built today have three windings. The third winding is called a *tertiary* winding and may be used for a number of purposes, for example: (1) to supply a load at other than secondary voltage; (2) to connect a synchronous condenser for the regulation of a transmission line; (3) to tie-in with another system; (4) to provide a low impedance for the flow of third harmonic or zero-sequence currents; (5) for the excitation of a regulating transformer; (6) as a fork on an autotransformer connection. Whatever the reason, it is obvious that wherever more than one secondary voltage is required, it can be secured more economically from a third winding rather than from an additional transformer.

A 3-winding transformer is indicated in Fig. 34a. Let the per-unit impedances between the windings of this transformer, taking one pair at a time and with the remaining winding open-circuited, be Z_{12} , Z_{13} , and Z_{23} . Then, ignoring the exciting current, it is easy to show that the equivalent circuit is that of Fig. 34b. To determine the branch impedances Z_1 , Z_2 , and Z_3 of this

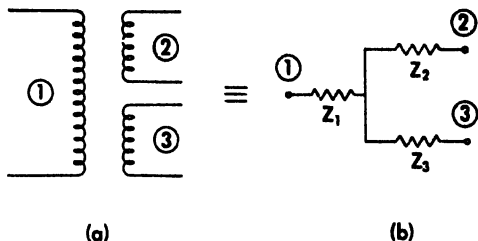


Fig. 34 The 3-winding transformer and its equivalent circuit.

of the leakage impedances of the actual transformer, each corresponding terminal in succession is open-circuited and the impedance between the other two terminals must then be the same for the equivalent circuit as for the transformer, thus

$$\left. \begin{aligned} \text{No. 1 open: } Z_{23} &= Z_2 + Z_3 \\ \text{No. 2 open: } Z_{13} &= Z_1 + Z_3 \\ \text{No. 3 open: } Z_{12} &= Z_1 + Z_2 \end{aligned} \right\} \quad (111)$$

Solving these three simultaneous equations, there results

$$\left. \begin{aligned} Z_1 &= \frac{1}{2}(Z_{12} + Z_{23} + Z_{31}) - Z_{23} \\ Z_2 &= \frac{1}{2}(Z_{12} + Z_{23} + Z_{31}) - Z_{13} \\ Z_3 &= \frac{1}{2}(Z_{12} + Z_{23} + Z_{31}) - Z_{12} \end{aligned} \right\} \quad (112)$$

If it is desired to include the exciting current, an exciting impedance branch Z_0 may be connected from the wye-point of the equivalent circuit to neutral, or from the line terminal of the primary to neutral. This refinement is rarely used or necessary.

It is interesting to note that the reactive component of one of the branch impedances of the equivalent circuit may be negative (capacitive).

18. Instrument Transformers

Instrument (potential and current) transformers are used to supply power to voltmeters, wattmeters, ammeters, relays, control devices, and the solenoids of circuit breakers. They serve the two-fold purpose of (1) reducing the measured quantity to a low value which can be indicated by standard instruments (usually 150-volts and 5 amperes), and (2) insulating the instruments from high-voltage sources, as a safety precaution.

A typical diagram of connections is shown in Fig. 36. Depending on the *burden* (the name for the load of an instrument transformer), instrument

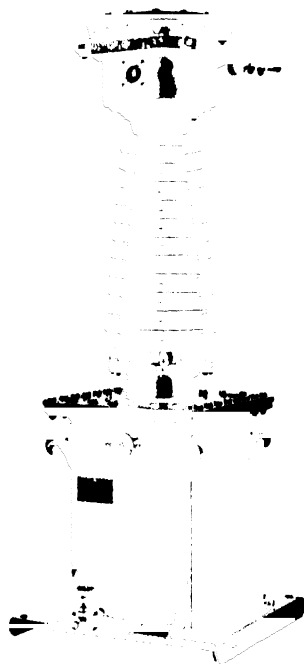


Fig. 35 Instrument current transformer 115,000 volt circuit, 200-400 to 5 amperes (General Electric Company)

transformers are rated from 25 to 500 volt-amperes, but may be 2 to 6 times as large as a distribution transformer of the same rating. The ideal instrument transformer would be one which would provide an exact ratio and no-phase displacement between the primary and secondary sides, regardless of the burden (load impedance). Actually, however, both ratio and phase-angle errors which vary with the burden are present, and no practicable means are available for the complete elimination or compensation of these errors. Instrument transformers do not differ in theory from ordinary power transformers; they have the same vector diagram and equivalent circuit, Fig. 37. It is clear from this vector diagram that the secondary impedance drop causes a phase displacement α , and the primary impedance drop a phase displacement β ; while the exciting current I_0 causes a further phase displacement γ , so that the angle between the secondary voltage and current is $(\theta_2 + \alpha + \beta + \gamma)$ as compared with an angle θ_2 between the secondary voltage and current. Thus the transformer introduces a phase-angle error $(\alpha + \beta + \gamma)$. Moreover, V_1 and V_2 will be only approximately in the ratio of the number of turns. The significance of these errors is indicated in Fig. 38. Calibration curves of this type are furnished by the manufacturer. In order to nullify or reduce the errors,

transformers are rated from 25 to 500 volt-amperes, but may be 2 to 6 times as large as a distribution transformer of the same rating.

The ideal instrument transformer would be one which would provide an exact ratio and no-phase displacement between the primary and secondary sides, regardless of the burden (load impedance). Actually, however, both ratio and phase-angle errors which vary with the burden are present, and no practicable means are available for the complete elimination or compensation of these errors. Instrument transformers do not differ in theory from ordinary power transformers; they have the same vector diagram and equivalent circuit, Fig. 37. It is clear from this vector diagram that the secondary impedance drop causes a phase displacement α , and the primary impedance drop a phase displacement β ; while the exciting current I_0 causes a further phase displacement γ , so that the angle between the secondary voltage and current is $(\theta_2 + \alpha + \beta + \gamma)$ as compared with an angle θ_2 between the secondary voltage and current. Thus the transformer introduces a phase-angle error $(\alpha + \beta + \gamma)$. Moreover, V_1 and V_2 will be only approximately in the ratio of the number of turns. The significance of these errors is indicated in Fig. 38. Calibration curves of this type are furnished by the manufacturer. In order to nullify or reduce the errors,

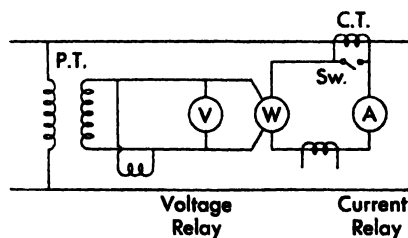


Fig. 36 Instrument transformers.

instrument transformers are designed with (1) small leakage reactances and low resistances - - which reduce angles α and β ; (2) low flux densities

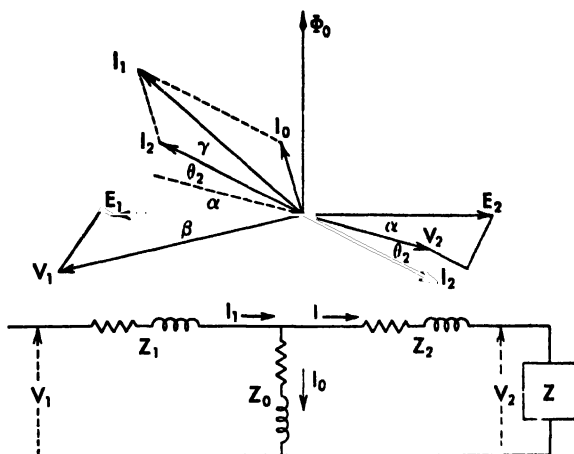


Fig. 37 Phase-angle displacements in an instrument transformer

and good transformer iron which reduce the exciting current I_0 and therefore angle γ ; and (3) less than nominal turn ratio which compensates for the ratio error. Compensating impedances may also be provided, so that the burden can be kept constant as instruments are put in or out of the circuit. For a constant burden, the instruments may be calibrated, or corrected, against the load.

Provision must be made to short-circuit the secondary of a current transformer before removing any instruments, for otherwise high voltages dangerous to life may ensue. It is clear from the equivalent circuit of Fig. 37 that if the secondary is open-circuited, the primary current, of fixed magnitude as determined by the load, must flow through the exciting impedance and act entirely as a magnetizing current to the transformer. This results in high flux density and correspondingly high voltage. Oscillograms of such a voltage show it to be very peaked by a dominating third harmonic, as would be expected.

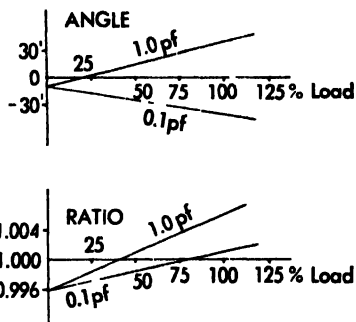


Fig. 38

19. The Constant-Current Transformer

Constant-current transformers were developed in the early days of street lighting when arc lamps were operated in series. Arc lamps are rarely seen nowadays, but there are street lighting systems employing incandescent lamps in series and other circuits requiring approximately constant current. One scheme for obtaining approximately constant current regulation from a transformer is simply to construct the transformer with very high leakage reactance, either by putting its windings on opposite legs, or by using a magnetic shunt, Fig. 39a. The current in the circuit of resistance R (load resistance plus transformer resistance) then is

$$I = \frac{V_1}{\sqrt{R^2 + X^2}} = \frac{V_1}{X} \left(1 + \frac{R^2}{X^2} \right)^{-1/2} = \frac{V_1}{X} \left(1 - \frac{R^2}{2X^2} + \frac{3}{8} \frac{R^4}{X^4} - \dots \right) \quad (113)$$

Hence if X is large compared with R , the current is substantially constant and equal to V_1/X .

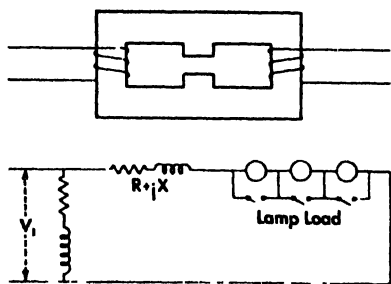


Fig. 39

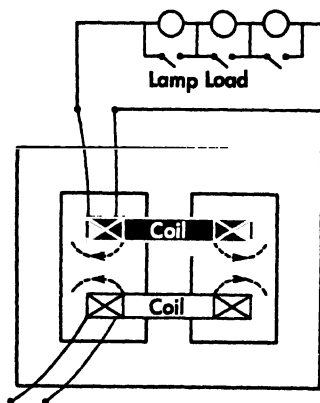


Fig. 40

But it is also evident from (113) that if X could be varied so that $(R^2 + X^2)$ is constant for all values of load, then the current would remain constant. Such a transformer is shown in Fig. 40. One coil, the primary, is stationary, while the secondary coil is movable and counter-balanced by weights. The electromagnetic repulsion between the coils is proportional to the product of the currents: therefore the movable coil automatically will take such position as to maintain constant current. Any change in the load conditions tending to change the current will result in a movement of the coil such as to reestablish the constant current of the system; for inasmuch as force is proportional to the

product of the currents, and since the force of the counterweights is constant, the product of the currents (and thus each individually) must remain constant.

20. Parallel Operation of Transformers

For the purpose of calculating the division of load between transformers operated in parallel on both the high- and low-voltage sides, it is sufficient to disregard the exciting admittances entirely. Then if the ratios of transformation are all exactly alike, the loads divide inversely proportional to the impedances, and the loads will be properly proportioned if all per-unit impedances, when based on the individual transformer ratings, are equal. But if the ratios are not alike, circulating currents upset the division of load. Referring to Fig. 41, suppose that the transformation ratios of the n transformers in parallel are a_1, a_2, \dots, a_n and their impedances (referred to the secondary side) are Z_1, Z_2, \dots, Z_n ohms respectively. The common primary voltage is V_1 , and the common secondary voltage is V . The individual transformer secondary currents are I_1, I_2, \dots, I_n , which combine to form the load current I flowing in the load impedance Z ohms. Then the individual transformer currents (referred to the secondary), in terms of admittances $Y_1 = 1/Z_1, Y_2 = 1/Z_2$, etc., are

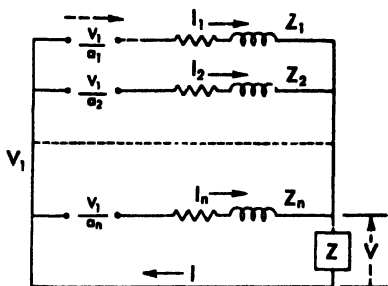


Fig. 41

$$\left. \begin{aligned} I_1 &= Y_1 \left(\frac{V_1}{a_1} - V \right) \\ I_2 &= Y_2 \left(\frac{V_1}{a_2} - V \right) \\ &\dots\dots\dots \\ I_n &= Y_n \left(\frac{V_1}{a_n} - V \right) \end{aligned} \right\} \quad (114)$$

The sum of these currents is the total load current

$$I = I_1 + I_2 + \dots + I_n = \sum_1^n Y_i \left(\frac{V_1}{a_i} - V \right) \quad (115)$$

Solving this equation for the primary voltage, there is

$$V_1 = \frac{I + V \sum Y_k}{\sum (Y_k/a_k)} \quad (116)$$

Then any transformer current of (114) is

$$I_r = \frac{(Y_r/a_r)I}{\sum (Y_k/a_k)} + \left[\frac{\sum Y_k}{\sum (Y_k/a_k)} - a_r \right] \frac{Y_r}{a_r} V \quad (117)$$

This equation shows that any individual transformer current consists of the superposition of two parts: One part, the first term in the right-hand side of (117) represents the normal division of the load current according to the admittances, as in any parallel circuit; and the other part, the second term, represents the circulating current occasioned by the differences in transformer ratios.

Example: Three transformers having the characteristics shown in the following table are operated in parallel supplying a 6500-kva, 2250-volt, 0.80-pf lagging load. Determine the primary voltage and the division of load.

	KVA	HV	LV	$\%IR$	$\%IX$	RATED AMPS	a
No. 1	1250	33,000	2300	1.1	5.3	543	14.34
No. 2	3000	33,000	2350	0.8	4.7	1275	14.04
No. 3	2500	31,500	2200	0.9	6.2	1136	14.32

The impedances (in ohms) referred to the low-voltage side are, by (88),

$$Z_1 = \frac{1000 \times 2.3^2}{1250} (0.011 + j0.053) = 0.0466 + j0.2247 = 0.230 \angle 78.3^\circ$$

$$Z_2 = \frac{1000 \times 2.35^2}{3000} (0.008 + j0.047) = 0.0148 + j0.0866 = 0.088 \angle 80.3^\circ$$

$$Z_3 = \frac{1000 \times 2.2^2}{2500} (0.009 + j0.062) = 0.0174 + j0.1203 = 0.122 \angle 81.8^\circ$$

Changing impedances to admittances according to (117)

$$Y_1 = 0.88 - j4.25 = 4.35 \angle -78.3^\circ$$

$$Y_2 = 1.92 - j11.22 = 11.36 \angle -80.3^\circ$$

$$Y_3 = 1.17 - j8.11 = 8.20 \angle -81.8^\circ$$

$$\sum Y_k = 3.97 - j23.58 = 23.90 \angle -80.4^\circ$$

$$Y_1/a_1 = 0.0612 - j0.296 = 0.303 \angle -78.3^\circ$$

$$Y_2/a_2 = 0.1370 - j0.800 = 0.810 \angle -80.3^\circ$$

$$Y_3/a_3 = 0.0818 - j0.566 = 0.572 \angle -81.8^\circ$$

$$\sum (Y_k/a_k) = 0.2800 - j1.662 = 1.685 \angle -80.4^\circ$$

Taking $V = 2250 + j0$ as reference vector, the load current is

$$I = \frac{6500}{2.25} (0.80 - j0.60) = 2885 - 36.9^\circ$$

The individual transformer currents then are

$$I_1 = \frac{0.303 - 78.3^\circ}{1.685 - 80.4^\circ} 2885 - 36.9^\circ + \left[\frac{23.90 - 80.4^\circ}{1.685 - 80.4^\circ} - 14.34 \right] (0.303 - 78.3^\circ) 2250$$

$$= 407 - j203 = 455 - 26.6^\circ$$

$$I_2 = \frac{0.810 - 80.3^\circ}{1.685 - 80.4^\circ} 2885 - 36.86^\circ + \left[\frac{23.90 - 80.4^\circ}{1.685 - 80.4^\circ} - 14.04 \right] (0.810 - 80.3^\circ) 2250$$

$$= 1164 - j1120 = 1615 - 43.8^\circ \text{ (over-loaded)}$$

$$I_3 = \frac{0.572 - 81.8^\circ}{1.685 - 80.4^\circ} 2885 - 36.86^\circ + \left[\frac{23.90 - 80.4^\circ}{1.685 - 80.4^\circ} - 14.32 \right] (0.572 - 81.8^\circ) 2250$$

$$= 748 - j453 = 875 - 31.2^\circ$$

21. Transformer Connections

As a preliminary to the analysis of transformer—particularly poly-phase—circuits, it is necessary to have a clear understanding of several concepts relating to windings and directions. These are: (1) the tracing direction, (2) the direction of winding, (3) the winding designations, (4) the direction of voltage, (5) the direction of current, (6) the connection diagram, (7) phase rotation, (8) angular displacement, and (9) polarity. Brief definitions will be given in this section and then expanded in subsequent applications.

The *tracing direction* is the (arbitrary) positive direction in which it is agreed to trace through a circuit. It need not have anything to do with the direction of the voltage or current in that circuit. As indicated in Fig. 42, the tracing direction may be by an arrow, by letters (*A*, *B*, *C*), by numbers (1, 2, 3), or by any combination of these.

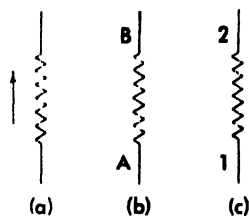


Fig. 42 Tracing direction.

The *direction of winding* relates not only to the relative physical arrangement of the winding with respect to the core, but also as to which terminals are designated as "start" and "finish." Thus in Fig. 43a both windings have the same physical direction of winding with respect to the core and the "start" and "finish" terminals (as indicated by 1 and 2 respectively)

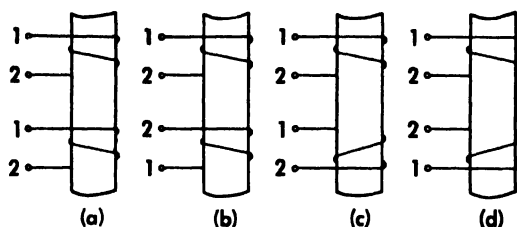


Fig. 43 Winding directions.

show that the tracing direction is the same for each; consequently they are said to have the *same* direction of winding. In Fig. 43b the low-voltage terminal designations have been reversed, and the winding directions become *opposite*. In Fig. 43c the windings are physically reversed, and the terminal designations are such that the winding directions are *opposite*. Finally in Fig. 43d both the physical windings and the terminal designations are reversed, and this makes the winding direction the *same*.

The American Standards Association (ASA) prescribes the letters *H*, *X*, and *Y* for high-voltage, low voltage, and tertiary windings respectively. Subscripts are then employed to indicate the direction of induced voltages.

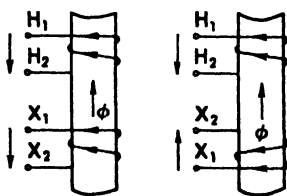


Fig. 44 Direction of voltage.

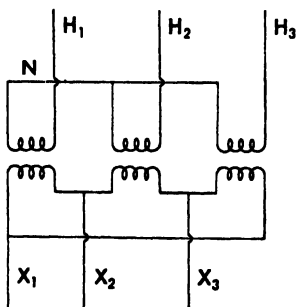


Fig. 45 Connection diagram.

The *direction of current* is the direction of the current due to the induced voltage; it opposes the flux, as indicated by the arrows on the windings in Fig. 44 or as H_1 to H_2 and X_1 to X_2 . Since the current and voltage directions are related, it is not necessary to show both.

The *connection diagram* is simply a sketch showing how the windings

are interconnected, and labelled to show the direction of winding. Figure 45 shows a connection diagram for a $\Gamma\Delta$ transformer.

Phase rotation relates to the relative vector diagrams of the windings. In single-phase transformers the voltages are either in phase or in phase opposition, and the notation H_1H_2 and X_1X_2 on the connection diagram is sufficient. But in polyphase connections, either the connection diagram with polarity markings or vector diagrams are required. Standard phase rotation is taken as ccw . AIEE Standardization Rules specify that the leads must be marked in such a way that $H_1H_2H_3$ and $X_1X_2X_3$ have the same phase rotation. Figure 46 shows the vector diagram corresponding to Fig. 45. The *angular displacement* is the angle between H_1N and X_1N . In Fig. 46 it is 30 degrees.

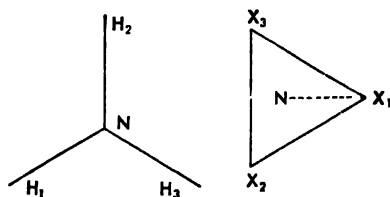


Fig. 46 Phase rotation.

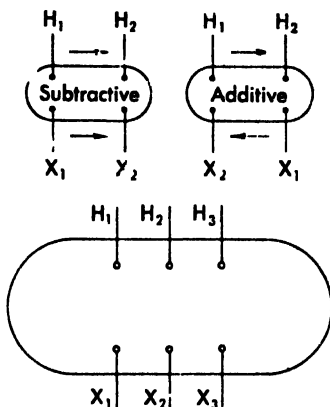


Fig. 47 Polarity

Polarity refers to the phase relations between high voltage and low-voltage terminals as brought out of the case, Fig. 47, and has nothing to do with winding directions or internal connections inside the tank. Factory markings are such that as the observer faces the tank on the high-voltage side, the H_1 terminal is always on his right. If the X_1 terminal of the low-voltage is also on his right the polarity is *subtractive*. But if the X_1 terminal is on his left, the polarity is *additive*. Another way of telling polarity is simply to walk around the tank clockwise and note whether X_1X_2 subtracts or adds to H_1H_2 . The polarity markings corresponding to the $\Gamma\Delta$ transformer of Fig. 45 are shown in Fig. 47.

22. Multiwinding Transformer Circuits

Modern power transformers may have three or more windings interconnected in different ways. Moreover, various kinds of interconnections

between transformers, both single and polyphase, present a bewildering array of circuit problems demanding a unified method of attack. The present section is concerned with the development of the necessary equations and procedure to solve any of the multiwinding transformer circuits which may arise in practice.*

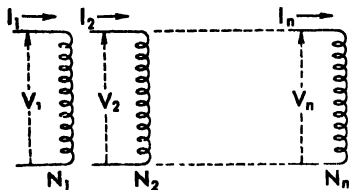


Fig. 48 Multiwinding transformer.

Consider a transformer, Fig. 48, having n windings numbered $1, \dots, n$ and having N_1, \dots, N_n turns respectively. These windings carry currents I_1, \dots, I_n and have terminal voltages V_1, \dots, V_n . At this stage of the description there are $2n$ unknowns—the n currents and the n voltages, and consequently $2n$ additional specifications and simultaneous equations are required. It will be shown that half of these are supplied by the *n-canonical equations* which are completely independent of the way in which the windings may be interconnected or connected to generators or outside loads; while the remaining half depend entirely on the *n equations of constraint* which describe the connections (Kirchhoff's equations). It is to be understood that a specification, such as winding No. 6 is connected to a generator of known voltage V_g , is equivalent to an equation of constraint $V_6 = V_g$. (The above terminology and the subsequent procedure are borrowed from dynamics.) Let winding No. 1 of N_1 turns be selected as the reference winding. Then the *inverse* transformation ratios of the other windings with respect to the reference winding are

$$n_2 = \frac{N_2}{N_1}, \dots, n_n = \frac{N_n}{N_1} \quad (118)$$

Now consider only two of the windings, say a and b , to carry currents, all other windings being open circuited, and let

$z_{aa} = r_{aa} + j\omega L_{aa}$ self-impedance of winding a

$z_{bb} = r_{bb} + j\omega L_{bb}$ self-impedance of winding b

$z_{ab} = j\omega M_{ab}$ mutual inductance between a and b

Then ignoring the exciting current, there are

$$0 = N_a I_a + N_b I_b \quad \text{or} \quad I_b = -\frac{n_a}{n_b} I_a \quad (119)$$

$$V_a = z_{aa} I_a + z_{ab} I_b = \left(z_{aa} - \frac{n_a}{n_b} z_{ab} \right) I_a \quad (120)$$

* Bewley, L. V., "Tensor Algebra in Transformer Circuits," *Electrical Engineering*, Nov. 1930

$$V_b = z_{ba}I_a + z_{bb}I_b = \begin{pmatrix} z_{ba} - \frac{n_a}{n_b}z_{ab} \\ z_{bb} \end{pmatrix} I_a \quad (121)$$

Multiplying (120) by $(1/n_a)$ and (121) by $(1/n_b)$ and subtracting

$$\frac{V_a/n_a - V_b/n_b}{n_a I_a - n_b I_b} = \frac{z_{aa}}{n_a^2} - \frac{z_{bb}}{n_b^2} - \frac{2z_{ab}}{n_a n_b} = Z'_{a-b} \quad (122)$$

The construction of this equation shows that the voltages and current have all been referred to the reference winding; hence the impedance is the leakage impedance between windings a and b referred to the reference winding (No. 1).

But if all windings are active, and exciting current is ignorable, the equations become

$$0 = I_1 + \sum_2^n n_i I_i, \quad k = 2, \dots, n \quad (123)$$

$$V_j = z_{j1}I_1 + \sum_2^n z_{j2}I_2 = \sum_2^n (z_{j1} - n_j z_{11})I_2 \quad (124)$$

$$V_1 = z_{11}I_1 + \sum_2^n z_{12}I_2 = \sum_2^n (z_{11} - n_i z_{11})I_k \quad (125)$$

Subtracting n_j times (125) from (124) and rearranging

$$\begin{aligned} V_j - n_j V_1 &= \sum_2^n (z_{j2} - n_j z_{12} - n z_{11} + n n_i z_{11})I_k \\ &= \sum_2^n n n_i \left[\frac{1}{2} \left(z_{11} + \frac{z_{ii}}{n} - 2 \frac{z_{1i}}{n} \right) \right. \\ &\quad \left. + \frac{1}{2} \left(z_{11} + \frac{z_{ii}}{n_i} - 2 \frac{z_{1i}}{n} \right) \right. \\ &\quad \left. - \frac{1}{2} \left(\frac{z_{ii}}{n_j} + \frac{z_{ii}}{n} - 2 \frac{z_{1i}}{n n_i} \right) \right] I_i \end{aligned} \quad (126)$$

Comparing the terms in parentheses in (126) with (122) it is clear that they are the leakage impedances, so that (126) may be re-written

$$V_j - n_j V_1 = \sum_2^n n n_i \frac{1}{2} (Z'_{1i} + Z'_{i1} - Z'_{j1}) I_i = \sum_2^n n n_i Z'_{ji} I_i \quad (127)$$

$$j = 2, \dots, n$$

Dividing through by n_j , putting $I_i' = n_i I_i$, and $V_j' = V_j/n_j$, this equation becomes

$$V_j' - V_1 = \sum_2^n \frac{1}{2} (Z'_{1i} + Z'_{i1} - Z'_{j1}) I_i' = \sum_2^n Z'_{ji} I_i' \quad (128)$$

$$j = 2, \dots, n$$

in which all quantities have now been referred to the reference winding, and the impedance

$$Z_{jk}' = \frac{1}{2}(Z'_{1-j} + Z'_{1-k} - Z'_{j-k}) \quad (129)$$

made up of three leakage impedances, is called the *branch impedance*. It has the same form as the impedance branches in the equivalent circuit of the 3-winding transformer (112).

Equations (127) or (128), together with (123), constitute the n canonical equations. They may be written regardless of any subsequent connections or interconnections between windings. Equation (128) is equally true in terms of *per-unit* quantities.

The *equations of constraint*, which specify the way in which the windings are interconnected with each other or to external circuits, are supplied by Kirchhoff's laws:

$$\sum(\text{currents at a junction}) = 0 \quad (130)$$

$$\sum(\text{voltages around a loop}) = 0 \quad (131)$$

This general method will be applied to a number of practical cases in subsequent sections. Sometimes the algebra involved is long and tedious and brings out nothing new from a circuit analysis point of view. In such cases final results will be given without showing detailed algebraic reductions.

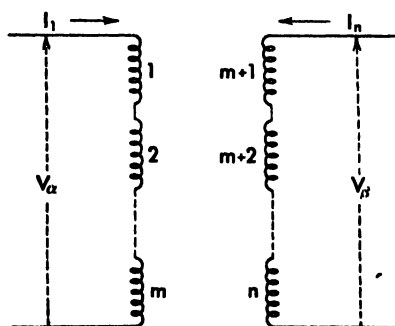


Fig. 49 Windings in series.

23. Windings in Series

Figure 49 shows m windings in series on the high-voltage side and $(n - m)$ windings in series on the low-voltage side. The *equations of constraint* are

$$I_1 = I_2 = \dots = I_m \quad (132)$$

$$I_{m+1} = \dots = I_n \quad (133)$$

$$V_1 + V_2 + \dots + V_m = V_a \quad (134)$$

$$V_{m+1} + \dots + V_n = V_b \quad (135)$$

By (132) and (133), (123) becomes

$$(n_1 + \dots + n_m)I_1 + (n_{m+1} + \dots + n_n)I_n = 0 \quad (136)$$

hence
$$I_n = - \left(\frac{n_1 + \dots + n_m}{n_{m+1} + \dots + n_n} \right) I_1 = -a I_1 \quad (137)$$

Then (127) may be written

$$\begin{aligned} V_j - n_j V_1 &= \sum_2^n n_j n_k Z_{jk}' I_k \\ &= I_1 \sum_2^m n_j n_k Z_{jk}' - a I_1 \sum_{m+1}^n n_j n_k Z_{jk}'; \quad j = 2, \dots, n \end{aligned} \quad (138)$$

Substituting (138) in (134) and (135), respectively, there results

$$V_\alpha - V_1 \sum_1^m n_j = I_1 \sum_2^m \left(\sum_2^m - a \sum_{m+1}^n \right) n_j n_k Z_{jk}' \quad (139)$$

$$V_\beta - V_1 \sum_{m+1}^n n_j = I_1 \sum_{m+1}^n \left(\sum_2^m - a \sum_{m+1}^n \right) n_j n_k Z_{jk}' \quad (140)$$

Subtracting a times (140) from (139) and making use of (137)

$$V_\alpha - a V_\beta = I_1 \left(\sum_2^m - a \sum_{m+1}^n \right) \left(\sum_2^m - a \sum_{m+1}^n \right) n_j n_k Z_{jk}' \quad (141)$$

In terms of leakage impedances (129), it may be shown (but it is quite an algebraic exercise!) that (141) reduces to

$$\begin{aligned} V_\alpha - a V_\beta &= \left(- \sum_1^m \sum_1^m \frac{n_j n_k}{2} Z'_{j-k} - \sum_{m+1}^n \sum_{m+1}^n \frac{a^2 n_j n_k}{2} Z'_{j-k} \right. \\ &\quad \left. + \sum_1^m \sum_{m+1}^n a n_j n_k Z'_{j-k} \right) I_1 \end{aligned} \quad (142)$$

in which all impedances have been referred to No. 1 winding.

The special case of a single primary winding and two windings in series on the secondary is of great practical importance. In this case $m = 1$, $n = 3$, and (142) reduces to

$$\begin{aligned} V_\alpha - \frac{n_1}{n_2 + n_3} V_\beta &= \left[- \frac{n_1 n_1}{2} Z'_{1-1} - \frac{a^2}{2} (n_2^2 Z'_{2-2} + 2n_2 n_3 Z'_{2-3} + n_3^2 Z'_{3-3}) \right. \\ &\quad \left. + a n_1 (n_2 Z'_{1-2} + n_3 Z'_{1-3}) \right] I_1 \end{aligned} \quad (143)$$

But the leakage impedance of a winding to itself is zero, by (122), also $n_1 = 1$, and therefore (143) simplifies to

$$V_\alpha - \frac{1}{n_2 + n_3} V_\beta = [a n_2 Z'_{1-2} + a n_3 Z'_{1-3} - a^2 n_2 n_3 Z'_{2-3}] I_1 \quad (144)$$

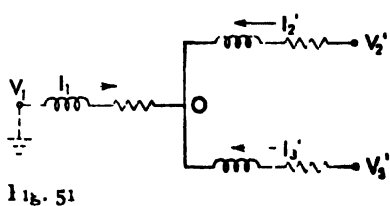
Example: A 3-winding transformer has the following data:

Winding No.	1	2	3
kva	20,000	15,000	5,000
kv	132	33	11

for in terms of V_1 and the currents I_2, \dots, I_n . Or writing the equations with all quantities referred to No. 1 winding, as in (128),

$$\begin{aligned} V_2' - V_1 &= Z_{12}' I_2' + \frac{1}{2}(Z_{12}' + Z_{21}') - Z_{22}' I_2' \\ V_3' - V_1 &= \frac{1}{2}(Z_{13}' + Z_{31}') - Z_{22}' I_2' + Z_{31}' I_3' \end{aligned} \quad (151)$$

To identify equations (151) with the 3 winding equivalent circuit reproduced in Fig. 51, put $V_1 = 0$ in both (151) and Fig. 51. Then with terminal No. 3 open circuited, $I_3' = 0$, and the voltage at the open terminal must be the same as that at the neutral 0, that is the



$$\begin{aligned} \text{Also } \left. \begin{aligned} V_1' &= -\frac{1}{2}(Z_{11}' + Z_{11}') - Z_{11}' I_1' \\ V_2' &= -Z_{12}' I_1' - Z_{11}' I_2' \\ V_3' &= -Z_{13}' I_1' - (Z_{11}' + Z_{11}') I_2' \end{aligned} \right\} \quad (152)$$

Solving these equations there results

$$\begin{aligned} Z_1 &= \frac{1}{2}(Z_{11}' + Z_{11}') - Z_{11}' \\ Z_2 &= Z_{12}' - Z_{11}' + Z_{11}' + Z_{11}' - Z_{11}' \\ Z_3 &= Z_{13}' - Z_{11}' + \frac{1}{2}(Z_{11}' + Z_{11}') - Z_{11}' \end{aligned} \quad (153)$$

which agree with the findings in Sec. 17

25. Windings in Parallel, Fig. 52

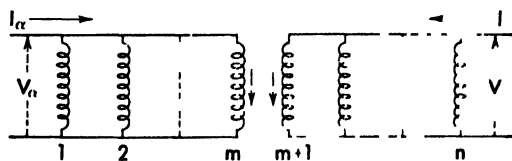


Fig. 52 Windings in parallel

Suppose the primary consists of m windings in parallel numbered $(1, \dots, m)$, and the secondary consists of $(n - m)$ windings in parallel numbered $(m + 1, \dots, n)$ inclusive. The equations of constraint are

$$V_m = V_1 = V \quad (154)$$

But the last three terms in the denominator add up to zero, as is clearly evident in terms of the self and mutual inductances of (122), thus

$$\begin{aligned} 2Z_{1-4} - Z_{1-2} - Z_{3-4} &= 2z_{11} + \frac{2z_{11}}{n^2} - \frac{4}{n} z_{14} \\ &\quad - z_{11} - z_{22} + 2z_{12} \\ &\quad - \frac{z_{33}}{n^2} - \frac{z_{11}}{n^2} + 2\frac{z_{31}}{n^2} \end{aligned} \quad (162)$$

Now $z_{22} = z_{11}$, $z_{33} = z_{44}$ and the mutual inductances $z_{14} = z_{12} = z_{34} = z_{31}$.

Hence

$$I = \frac{-nV_a}{Z + \frac{n^2}{2} Z'_{1-3}} \quad (163)$$

and $\frac{n^2}{2} Z'_{1-3}$ is the effective impedance of the transformer referred to the load.

26. Coupling Windings, Fig. 54

Coupling windings are sometimes used in transformers as a means of reducing the reactance. They are merely pairs of windings in parallel with no external load. It is convenient to number the coupling windings of each pair by odd and even numbers, $(2s-1)$ and $(2s)$, as shown in Fig. 54. The equations of constraint are

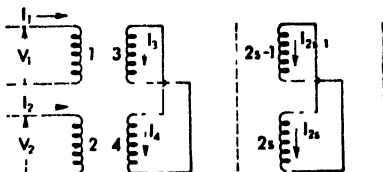


Fig. 54 Coupling windings

$$\left. \begin{aligned} n_{2s-1} &= n_{2s} \\ V_{2s-1} &= V_{2s} \\ 0 &= I_{2s-1} + I_{2s} \end{aligned} \right\} \quad (164)$$

Then since the ampere-turns of each pair of coupling windings cancel, $(n_{2s-1}I_{2s-1} + n_{2s}I_{2s} = 0)$, equation (123) reduces to

$$0 = I_1 + n_2 I_2 \quad (165)$$

Equation (127) may be written

$$V_j - n_j V_1 = n_j Z'_{j2} I_2 + \sum_2^{n-2} n_j n_{2s} [Z'_{j(2s)} - Z'_{j(2s-1)}] I_{2s} \quad (166)$$

Rewriting (166), substituting $(2r-1)$ for j , and again with $(2r)$ for j ,

noting that $n_{2r-1} = n_{2r}$, and subtracting

$$0 = n_2 n_2 [Z'_{(2r)2} - Z'_{(2r-1)2}] I_2 + \sum_2^{n-2} n_2 n_2 [Z'_{(2r)(2s)} + Z'_{(2r-1)(2s-1)} - Z'_{(2r-1)2s} - Z'_{(2r)(2s-1)}] I_{2s} \quad (167)$$

$$r = 2, \dots, n-2$$

Also writing (166) for $j = 2$

$$V_2 - n_2 V_1 = n_2^2 Z'_{22} I_2 + \sum_2^{n-2} n_2 n_2 [Z'_{2(2s)} - Z'_{2(2s-1)}] I_{2s} \quad (168)$$

Equations (165), (167), and (168) supply the necessary simultaneous equations from which all quantities may be determined in terms of any two quantities.

As an example, consider a transformer having only one pair of coupling windings. Then (167) and (168) reduce to

$$0 = n_2 n_2 (Z'_{22} - Z'_{32}) I_2 + n_1^2 (Z'_{11} + Z'_{33} - 2Z'_{31}) I_1 \quad (169)$$

$$V_2 - n_2 V_1 = n_2^2 Z'_{22} I_2 + n_2 n_1 (Z'_{21} - Z'_{31}) I_1 \quad (170)$$

Suppose the secondary winding is short circuited, $V_2 = 0$, and eliminate I_1 and I_2 between (165), (169), and (170) yielding

$$\frac{V_1}{I_1} = \frac{Z'_{22} - (Z'_{21} - Z'_{31})^2}{(Z'_{11} + Z'_{33} - 2Z'_{31})} \quad (171)$$

Substituting leakage impedances this becomes

$$\frac{V_1}{I_1} = Z'_{12} = \frac{(Z'_{11} - Z'_{12} - Z'_{13} + Z'_{23})^2}{4Z'_{34}} \quad (172)$$

Had there been no coupling winding the impedance would have been simply Z'_{12} , and thus it is evident that the coupling winding has reduced the short circuit impedance of the transformer.

27. The Simple Autotransformer, Fig. 55

The equations for the simple autotransformer were derived in Sec. 16.

In the present section they will be obtained by the general method of Sec. 22. Referring to Fig. 55, the equations of constraint are seen to be

$$V_2 = -ZI \quad (173)$$

$$V_a = V_1 + V_2 \quad (174)$$

$$I_2 = I_1 + I \quad (175)$$

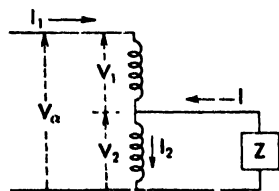


Fig. 55 Autotransformer

Equations (123) and (127) become

$$0 = I_1 + n_2 I_2 \quad (176)$$

$$V_2 - n_2 V_1 = n_2^2 Z_{22}' I_2 = n_2^2 Z_{12}' I_2 \quad (177)$$

The elimination of I_2 , I and V_2 between these equations leads to

$$\frac{V_a}{I_1} = \left(\frac{1 + n_2}{n_2} \right)^2 Z + Z_{12}' = b^2 Z + Z_{12}' \quad (178)$$

showing that the load impedance transfers to the high-voltage side by the square of the transformation ratio, and that the impedance contributed by the autotransformer is the same as the impedance between windings No. 1 and No. 2; that is, as if tested as a transformer. Also from (176) and (175)

$$I_1 = -n_2 I_2 = -\frac{n_2}{1 + n_2} I \quad (179)$$

28. Forked Autotransformer, Fig. 56

Autotransformers are sometimes built with a third winding forming a fork, as in Fig. 56. Either or both tines of the fork may be provided with taps for voltage regulation. The equations of constraint are

$$V_a = V_1 + V_2 \quad (180)$$

$$V_a = V_2 + V_3 = -Z I_3 \quad (181)$$

$$I_2 = I_1 + I_3 \quad (182)$$

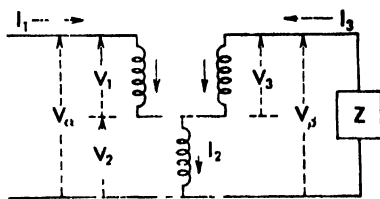


Fig. 56 Forked autotransformer.

And the general equations (123) and (127) are

$$0 = I_1 + n_2 I_2 + n_3 I_3 \quad (183)$$

$$V_2 - n_2 V_1 = n_2^2 Z_{22}' I_2 + n_2 n_3 Z_{23}' I_3 \quad (184)$$

$$V_3 - n_3 V_1 = n_2 n_3 Z_{23}' I_2 + n_3^2 Z_{33}' I_3 \quad (185)$$

Eliminating V_2 , V_3 , I_2 , I_3 between these equations there results

$$\frac{V_a}{I_1} = \frac{n_2^2(1 - n_3)^2 Z_{22}' + n_3^2(1 + n_2)^2 Z_{33}' + 2n_2 n_3(1 - n_3)(1 + n_2) Z_{23}' + (1 + n_2)^2 Z}{(n_2 + n_3)^2} \quad (186)$$

Substituting leakage impedances, the total impedance is

$$\frac{V_a}{I_1} = \left\{ \frac{n_2(1 - n_3)}{n_2 + n_3} Z_{12}' + \frac{n_3(1 + n_2)}{n_2 + n_3} Z_{13}' - \frac{n_2 n_3(1 - n_3)(1 + n_2)}{(n_2 + n_3)^2} Z_{12}' \right\} + \left(\frac{1 + n_2}{n_2 + n_3} \right)^2 Z \quad (187)$$

Thus the load impedance Z is transferred to the primary side by the square of the voltage ratio between the primary and the load. The terms in braces $\{\}$ represent the impedance contributed by the forked autotransformer.

Putting $n_2 = 0$, the circuit of Fig. 56 is that of an ordinary transformer, and (187) reduces to $(Z'_1 + Z'_3)$, as would be expected.

Putting $n_3 = 0$, the circuit of Fig. 56 is that of the simple autotransformer of Fig. 55, and (187) reduces to $Z'_1 + \left(\frac{1+n_2}{n_2}\right)^2 Z$ agreeing with (178).

29. Regulating Transformer, Fig. 57

An arrangement such as shown in Fig. 57 consisting of a main 3-winding transformer, the tertiary of which excites a regulating unit which in turn supplies a series transformer, is often used to provide variable voltage to a load. Taps, usually with automatic load-ratio control, are on the regulating unit. The tap range can be doubled by reversing the connections to the regulating unit.

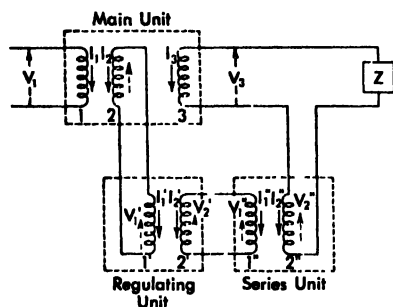


Fig. 57 Regulating transformer

Let the windings be numbered as shown on the sketch. In subsequent equations unprimed voltages, currents, and impedances refer to the main transformer; single-primed quantities, to the regulating unit; and double-primed quantities, to the series unit. The equations of constraint are

$$V_1' = V_2 \quad (188)$$

$$V_2' = V_1'' \quad (189)$$

$$V_3 + V_2'' = -Z I_3 \quad (190)$$

$$0 = I_2 + I_1' \quad (191)$$

$$0 = I_2' + I_1'' \quad (192)$$

$$I_3 = I_2'' \quad (193)$$

The general equations for the main transformer are

$$0 = I_1 + n_2 I_2 + n_3 I_3 \quad (194)$$

$$V_2 - n_2 V_1 = n_2^2 Z_{22} I_2 + n_2 n_3 Z_{23} I_3 \quad (195)$$

$$V_3 - n_3 V_1 = n_2 n_3 Z_{32} I_2 + n_3^2 Z_{33} I_3 \quad (196)$$

The general equations for the regulating transformer are

$$0 = I_1' + n_2' I_2' \quad (197)$$

$$V_2' - n_2' V_1' = n_2' n_2' Z_{22}' I_2' \quad (198)$$

The general equations for the series transformer are

$$0 = I_1'' + n_2'' I_2'' \quad (199)$$

$$V_2'' - n_2'' V_1'' = n_2'' n_2'' Z_{22}'' I_2'' \quad (200)$$

From (191), (192), (193), (194), (197), and (199) the current relationships are found to be

$$\begin{aligned} I_1 &= - \frac{n_3 + n_2 n_2' n_2''}{n_2' n_2''} I_2 = - (n_3 + n_2 n_2' n_2'') I_2 \\ &= \frac{n_3 + n_2 n_2' n_2''}{n_2' n_2''} I_1' = - \frac{n_3 + n_2 n_2' n_2''}{n_2''} I_2' \\ &= \frac{n_3 + n_2 n_2' n_2''}{n_2''} I_1'' = - (n_3 + n_2 n_2' n_2'') I_2'' \end{aligned} \quad (201)$$

Eliminating all variables except V_1 and I_1 there result

$$\begin{aligned} \frac{V_1}{I_1} &= \\ &= \frac{(n_2 n_2' n_2'')^2 Z_{22} + 2 n_3 n_2 n_2' n_2'' Z_{32} + n_3^2 Z_{33} + (n_2' n_2'')^2 Z_{22}' + (n_2'')^2 Z_{22}'' + Z}{(n_3 + n_2 n_2' n_2'')^2} \end{aligned} \quad (202)$$

In terms of leakage impedances this becomes

$$\begin{aligned} \frac{V_1}{I_1} &= \frac{n_2 n_2' n_2'' Z_{1-2} + n_3 Z_{1-3}}{n_3 + n_2 n_2' n_2''} \\ &+ \frac{- n_3 n_2 n_2' n_2'' Z_{2-3} + (n_2' n_2'')^2 Z_{1-2}' + (n_2'')^2 Z_{2-1}'' + Z}{(n_3 + n_2 n_2' n_2'')^2} \end{aligned} \quad (203)$$

The ratio of transformation between the load and the primary is evidently $(n_3 + n_2 n_2' n_2'')$. Putting $n_2 = 0$, or $n_2' = 0$, or $n_2'' = 0$, converts the circuit to that of a simple 2-winding transformer, and the impedance according to (203) reduces to $(Z_{1-3} + Z n_3^2)$ as it should. Reversing the connections on the regulating unit is equivalent to changing the sign of n_2' .

30. Single-phase Connections, Fig. 58

Distribution transformers often have two similar primary and two similar secondary coils, enabling the transformer to be connected for four different voltage-current combinations, Fig. 58. As indicated by the

dotted lines in Fig. 58, the series groupings also permit bringing out a neutral, which may or may not be grounded.

The polarity is usually marked; but if not, it may be tested for by connecting a high-voltage and a low-voltage terminal together (say H_2 and X_2), applying a reduced voltage across the high-voltage (H_1 to H_2),

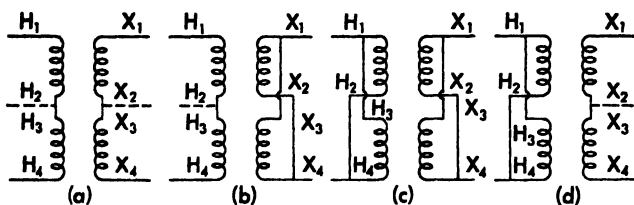


Fig. 58 Single phase connections.

and measuring the voltage between the other high-voltage and low-voltage terminals (H_1 to X_1). If this voltage is less than the applied voltage the polarity is subtractive, otherwise additive. In making this test, the voltmeter selected must have a range that is at least equal to the sum of the high-voltage and low-voltage potentials.

31. Polyphase Connections

The primary and secondary windings of single-phase transformers may be interconnected in a variety of ways for polyphase power. The more common polyphase transformer and autotransformer connections are shown in Table II on pages 80 and 81.

The connection used in any particular case is governed by the following considerations:

- (1) Number of phases of the power supply (primary side)
- (2) Number of secondary phases required (2, 3, 4, 6, 12, 24)
- (3) Is a neutral connection required (for grounding, relaying, or load connection)?
- (4) Path for third harmonic (exciting) currents
- (5) Path for zero-sequence (fault) currents
- (6) Insulation to ground and voltage stresses
- (7) Need for partial capacity with one unit out of service
- (8) Operation in parallel with existing transformers
- (9) Operation under unbalanced load or fault conditions
- (10) Economic factors (cost, size, weight, efficiency)
- (11) Voltage regulation (taps and load-ratio-control)
- (12) Phase displacement or control

In analyzing any polyphase transformer circuit it is sufficient to remember that:

- (1) The theory, equations, equivalent circuit, and vector relationships in any individual transformer of the group are the same as though that transformer were by itself.
- (2) Exciting currents may be neglected, except insofar as third-harmonic current paths must be provided, or else third harmonic voltages tolerated.
- (3) The ampere-turns on any magnetic core must balance out to zero (hereby secondary currents are readily determined in terms of primary currents).
- (4) Kirchhoff's laws always apply.
- (5) In many practical cases simple vector diagrams, in conjunction with (3) above, are all that are necessary for an understanding and description of the circuit.
- (6) In complicated cases, particularly where circuit impedances or detailed current and voltage distributions must be determined, an appeal to the general method of Sec. 22 can always be made.

In subsequent sections, the more common types of connections will be taken up in detail.

32. The Y-Y Connection

Because of certain disadvantages, which will be brought out, the Y-Y connection is rarely used. If the primary coils are connected in Y, there are two possible ways of forming the Y for the secondary coils, as

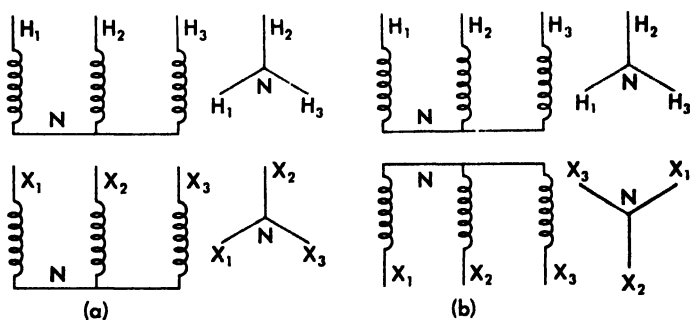


Fig. 59 Wye-wye transformer.

shown in Fig. 59. In the first case the phase displacement is zero. In the second case it is 180 degrees. The phase rotation is standard (positive sequence) in both cases. The line voltage H_1H_2 is $(H_1V) + (NH_2)$

TABLE II
TYPICAL TRANSFORMER CONNECTIONS

	TRANSFORMERS		AUTOTRANSFORMERS
	PRIMARY	SECONDARY	
2 ϕ to 2 ϕ			
		3 Wire	
		4 Wire	
3 ϕ to 3 ϕ	Wye	Wye	Wye
	Delta	Delta	Inverted Delta
	Wye	Delta	Extended Delta
	Delta	Wye	Stub Delta
	Open-Delta	Open Delta	Open Delta
	Tee	Tee	Tee
	or Delta	Zigzag	Zigzag
2 ϕ to 3 ϕ		Scott	
		0.155	

TABLE II (Continued)

	TRANSFORMERS		AUTOTRANSFORMERS
	PRIMARY	SECONDARY	
3 ϕ to 2 ϕ		Taylor	
		Fortescue	
		Arnold	
	or	Woodbridge	
3 ϕ to 6 ϕ	or	Diametrical	
	or	Double Wye	
	or	Double Delta	
	or	Hexagon	Hexagon
		Double Tee	Inverted Zigzag
	or	Double Zigzag	Double Zigzag
3 ϕ to 12 ϕ	or	Quadruple Zigzag	
	or	Double Cord	

$= (I_1 V) - (I_2 V)$, thus $\sqrt{3}$ times as great as the voltage to neutral, but the line and winding currents are the same. If the neutral is grounded, each transformer need be insulated for only $1/\sqrt{3} = 0.58$ of the line voltage. This fact, together with the availability of the neutral, is the principal advantage of a wye connection.

If the neutral is isolated, no third-harmonic current is permitted to flow (since the third-harmonic currents in each transformer are in time phase), and consequently third-harmonic exciting voltages appear across each transformer, but cancel out in the line voltage. If the neutral is grounded, and a similar grounded neutral exists elsewhere on the line, third harmonic currents, limited only by the impedance of the line and ground return circuit, may flow; but they cause telephone interference, and in some cases relay malfunctioning.

If the neutral is isolated on both sides, no zero-sequence currents can flow. If the neutral is grounded on one side only, small zero-sequence currents limited by the exciting impedance may flow on that side. If both neutrals are grounded, and return paths through ground are offered elsewhere on both sides of the system, then zero sequence currents flowing to the neutral encounter the leakage impedance of the transformer.

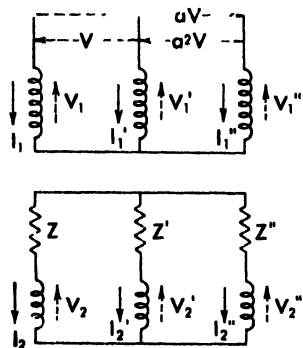


Fig. 60 The Y-Y connection with unbalanced loads

V, a^2V, aV where $a = e^{j120^\circ} = 120^\circ$ is the unit vector which rotates any vector with which it is multiplied by 120° . Of course, $a^2 = 240^\circ$ and the sequence $(1, a^2, a)$ represents standard positive phase rotation. The equations of constraint are seen to be

$$V = V_1 = V_1' \quad (204)$$

$$aV = V'' = V_1' \quad (205)$$

$$0 = V_1 = V_1' + ZI = Z'I' \quad (206)$$

$$0 = V_2'' - V_2' + Z'' I_2'' - Z' I_2' \quad (207)$$

$$0 = I_1 + I_1' + I_1'' \quad (208)$$

$$0 = I_2 + I_2' + I_2'' \quad (209)$$

The general equations (123) and (127) for the three transformers are

$$0 = I_1 + n_2 I_2 \quad (210)$$

$$0 = I_1' + n_2' I_2' \quad (211)$$

$$0 = I_1'' + n_2'' I_2'' \quad (212)$$

$$V_2 - n_2 V_1 = n_2 n_2 Z_{22} I_2 \quad (213)$$

$$V_2' - n_2' V_1' = n_2' n_2' Z_{22}' I_2' \quad (214)$$

$$V_2'' - n_2'' V_1'' = n_2'' n_2'' Z_{22}'' I_2'' \quad (215)$$

Note that the above equations allow for entirely dissimilar transformers having different impedances and different turn ratios and an unbalanced load. From the current equations (208), (209), (210), (211), and (212) there results

$$\begin{aligned} I_1 &= - \frac{n_2 n_2' - n_2''}{n_2' n_2 - n_2''} I_1' & \frac{n_2 n_2' - n_2''}{n_2'' n_2 - n_2'} I_1'' \\ &= n_2 \frac{n_2' - n_2''}{n_2 - n_2''} I_1' & \frac{n_2 n_2' - n_2''}{n_2 - n_2'} I_1'' = -n_2 I_2 \end{aligned} \quad (216)$$

Eliminating V_1' , V_1 , and V_1'' between (204), (206), (213), and (214), and eliminating V_1'' , V_1' , and V_2'' between (205), (207), (214), and (215) yields two simultaneous equations from which I_1 and V_1 may be found,

$$I_1 = \frac{n_2 n_2' - n_2''}{z(n_2' - n_2'') + z''(n_2' - n_2) + z'(n_2 - n_2'')^2} [n_2' n_2'' a' + n_2(n_2' + a n_2'')] V \quad (217)$$

$$V_1 = \frac{(n_2' - n_2'')(n_2' + a n_2'')z + n_2'(n_2' - n_2)z'' + n_2''(n_2 - n_2'')az'}{(n_2' - n_2'')^2 z + (n_2' - n_2)^2 z'' + (n_2 - n_2'')^2 z'} V \quad (218)$$

in which

$$\left. \begin{aligned} z &= n_2 n_2 Z_{22} + Z \\ z' &= n_2' n_2' Z_{22}' + Z' \\ z'' &= n_2'' n_2'' Z_{22}'' + Z'' \end{aligned} \right\} \quad (219)$$

Then V_1' may be found from (204), V_1'' from (205), V_2 from (213), V_2' from (214), V_2'' from (215), and any current from (216).

However, if any two of the turn ratios are identical, such as $n_2' = n_2''$, it is evident from either (216) or (217) that $I_1 = 0$, and by (218) the voltage V_1 may reach very large values (but limited by saturation).

If all three turn ratios are identical, the above solutions are indetermi-

nate, and a new solution must be sought by putting $n = n_2 = n_2' = n_2''$ in equations (204) to (215) inclusive. It is then found that

$$I_1 = -nI_2 = \frac{z'' - az'}{zz' + zz'' + z'z''} n^2V \quad (220)$$

$$I_1' = -nI_2' = \frac{a^2z - z''}{zz' + zz'' + z'z''} n^2V \quad (221)$$

$$I_1'' = -nI_2'' = \frac{az' - a^2z}{zz' + zz'' + z'z''} n^2V \quad (222)$$

If the transformer impedances are equal and the load is balanced, these currents are seen to reduce to balanced symmetrical 3-phase currents. The individual transformer voltages $V_1, V_2, V_1', V_2', V_1'', V_2''$ cannot be determined, since both neutrals are free and may take on any potentials. Potential differences are found easily: ($V_1 - V_1'$) from (204), ($V_1'' - V_1$) from (205), ($V_2 - V_2'$) from (206), and ($V_2'' - V_2'$) from (207).

Interesting features of the Y-Y connection with isolated neutrals are brought out by the following table, based on equations (220), (221), and (222).

	Balanced load $z = z' = z''$	S C of one load $z = 0, z' = z''$	O C of one load $z = \infty, z' = z''$
I_1	$\frac{1}{\sqrt{3}} \frac{n^2V}{z''}$	$\sqrt{3} \frac{n^2V}{z''}$	0
I_1'	$\frac{1}{\sqrt{3}} \frac{n^2V}{z''}$	$\frac{n^2V}{z''}$	$\frac{1}{2} \frac{n^2V}{z''}$
I_1''	$\frac{1}{\sqrt{3}} \frac{n^2V}{z''}$	$\frac{n^2V}{z''}$	$\frac{1}{2} \frac{n^2V}{z''}$

If it is desired to investigate the division of load and the neutral shift under the condition of the load neutral and transformer secondary neutral connected together, or what is the same thing, with the transformers supplying independent single phase loads, equations (206), (207), and (209) must be replaced by

$$V_2 = -ZI_2 \quad (223)$$

$$V_2' = -Z'I_2' \quad (224)$$

$$V_2'' = -Z''I_2'' \quad (225)$$

Solution of the simultaneous equations then gives

$$I_2 = -\frac{I_1}{n_2} = n_2(an_2''n_2'z' - n_2'n_2'z'') \frac{V}{D} \quad (226)$$

$$I_2' = -\frac{I_1'}{n_2'} = n_2'(n_2 n_2 z'' - a^2 n_2'' n_2'' z) \frac{V}{D} \quad (227)$$

$$I_2'' = -\frac{I_1''}{n_2''} = n_2''(a^2 n_2' n_2' z - a n_2 n_2 z') \frac{V}{D} \quad (228)$$

$$V_1 = z(n_2' n_2' z'' - a n_2'' n_2'' z') \frac{V}{D} \quad (229)$$

$$V_1' = z'(a^2 n_2'' n_2'' z - n_2 n_2 z') \frac{V}{D} \quad (230)$$

$$V_1'' = z''(a n_2 n_2 z' - a^2 n_2' n_2' z) \frac{V}{D} \quad (231)$$

$$\text{where} \quad D = n_2' n_2' z z'' + n_2 n_2 z' z'' + n_2'' n_2'' z z' \quad (232)$$

The neutral shift is readily found for any specified loads or turn ratios. If all turn ratios are alike, $n_2 = n_2'$, and two of the secondary load circuits are open-circuited, say $z' = z'' = \infty$; then (229) shows that $V_1 = 0$, while (230) and (231) show that $V_1' = -V$ and $V_1'' = aV$; and the neutral has shifted to a corner of the applied voltage triangle. On the other hand, if the loads are balanced and the transformers identical, $z = z' = z''$; (229), (230), and (231) give $V_1 = (1-a)V/3$, $V_1' = (a^2-1)V/3$, and $V_1'' = a(1-a)V/3$; and the neutral is seen to be at the center of the applied voltage triangle.

Equations (226), (227), and (228) become identical with (220), (221), and (222) when the turn ratios are equal; for under this condition $I_2 + I_2' + I_2'' = -(I_1 + I_1' + I_1'')/n = 0$, and no current flows in the neutral.

A great deal of space has been devoted in this section to the consideration of neutral shift and instability. The matter is of considerable practical importance.

33. Delta-delta Connection, Fig. 61

There are two ways in which transformers may be connected *delta-delta*, as shown in Fig. 61. The first case has zero angular displacement, subtractive polarity, and positive phase rotation. The second case has 180-degree angular displacement, additive polarity, and positive phase rotation. With the delta connection the coil and line voltages are identical, but the line currents are $\sqrt{3}$ times the coil currents. The presence of a delta permits the flow of the third-harmonic exciting current (since the currents in each coil are in phase), and therefore neither third-harmonic currents nor voltages will appear on the line. But the

delta is a block to the flow of zero-sequence currents. The analysis may be carried out by reference to Fig. 62, which shows three dissimilar trans-

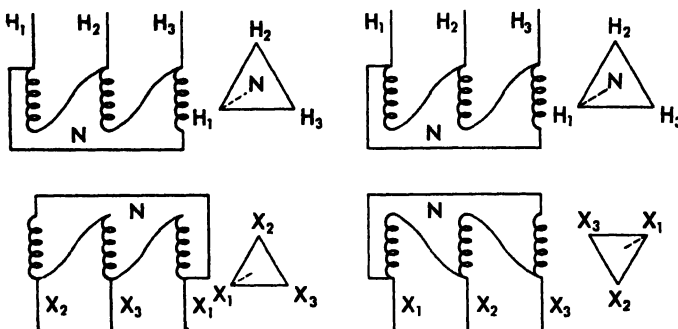


Fig. 61 Delta-delta connections.

formers (different impedances and different turn ratios) supplying an unbalanced wye-connected load. The equations of constraint are

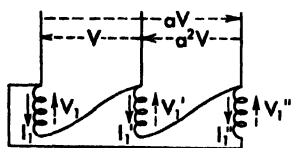


Fig. 62

$$V_1 = V \quad (233)$$

$$V_1' = a^2 V \quad (234)$$

$$V_1'' = a V \quad (235)$$

$$V_2 = Z''(I_2'' - I_2) - Z(I_2 - I_2') \quad (236)$$

$$V_2' = Z(I_2 - I_2') - Z'(I_2' - I_2'') \quad (237)$$

$$V_2'' = Z'(I_2' - I_2'') - Z''(I_2'' - I_2) \quad (238)$$

The general equations (123) and (127) are

$$0 = I_1 + n_2 I_2 \quad (239)$$

$$0 = I_1' + n_2' I_2' \quad (240)$$

$$0 = I_1'' + n_2'' I_2'' \quad (241)$$

$$V_2 - n_2 V_1 = n_2 n_2 Z_{22} I_2 \quad (242)$$

$$V_2' - n_2' V_1' = n_2' n_2' Z_{22}' I_2' \quad (243)$$

$$V_2'' - n_2'' V_1'' = n_2'' n_2'' Z_{22}'' I_2'' \quad (244)$$

These equations yield three simultaneous equations for the currents

$$-n_2 V = (n_2 n_2 Z_{22} + Z'' + Z) I_2 - Z I_2' - Z'' I_2'' \quad (245)$$

$$-a^2 n_2' V = (n_2' n_2' Z_{22}' + Z + Z') I_2' - Z I_2 - Z' I_2'' \quad (246)$$

$$-a n_2'' V = (n_2'' n_2'' Z_{22}'' + Z' + Z'') I_2'' - Z' I_2' - Z'' I_2 \quad (247)$$

Explicit solutions for the currents from the above three equations result

in long and cumbersome expressions showing nothing of interest. In a specific case it is just as easy to substitute numerical values and solve (245), (246), (247) directly.

34. Open-delta Connection, Fig. 63

A principal advantage of the delta-delta connection is that it may continue to operate on 3-phase circuits with one transformer removed, although at only 58 per cent of the capacity. The diagram of connections is shown in Fig. 63. Assuming dissimilar transformers, the equations of constraint and the general equations are the same as (233) to (244) inclusive, with $I_2'' = 0$ and $Z_{22}'' = \infty$, and with (238), (241), and (244) deleted. The solution of these equations then yields

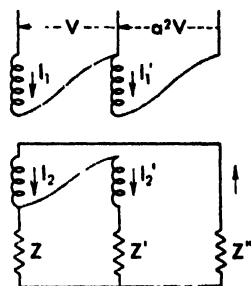


Fig. 63 Open 'delta.

$$I_2 = -\frac{I_1}{n_2} = \frac{[-n_2 n_2' n_2' Z_{22}' - n_2(Z + Z') - n_2' a^2 Z]V}{(n_2 n_2 Z_{22} + Z + Z'')(n_2' n_2' Z_{22}' + Z + Z') - Z^2} \quad (248)$$

$$I_2' = -\frac{I_1'}{n_2'} = \frac{[-n_2' n_2 n_2 Z_{22} a^2 - n_2' a^2(Z + Z'') - n_2 Z]V}{(n_2 n_2 Z_{22} + Z + Z'')(n_2' n_2' Z_{22}' + Z + Z') - Z^2} \quad (249)$$

For similar transformers ($Z_{22} = Z_{22}'$ and $n_2' = n_2$) and balanced load impedances ($Z = Z' = Z''$), the ratio of these currents is

$$\frac{I_2}{I_2'} = \frac{I_1}{I_1'} = \frac{(n_2^2 Z_{22} + 2Z) + a^2 Z}{a^2(n_2^2 Z_{22} + 2Z) + Z} = 1 e^{j\alpha} \quad (250)$$

This equation shows that if the impedances contain both resistances and reactances, then the magnitude of the ratio is different than unity and the phase displacement may be anything. Thus the currents do not divide equally, even though the circuit of Fig. 63 is itself perfectly balanced and symmetrical. Reversal of the phase rotation of the applied voltage transfers the larger current from one transformer to the other. If the circuit contains no resistance, then the current magnitudes are equal. Also, on short circuit ($Z = 0$) they are equal. This phenomenon occurs in certain other transformer circuits, and in the case of the quadruple zigzag may reach exaggerated proportions.

The capacity of an open-delta bank is usually given in terms of equal balanced currents in a resistance load, as shown in Fig. 64. The load voltages are then in phase with the load currents, but the line, or transformer, voltages are $\sqrt{3}$ times as great and 30 degrees out of phase with

the currents. The output of the open-delta bank therefore is

$$P = VI \cos 30^\circ + VI \cos (-30^\circ) = \sqrt{3}VI$$

The total transformer capacity is $2VI$. Hence the *capacity ratio* is only 0.866. The open-delta bank can carry $\sqrt{3}VI/3VI = 0.58$ of the capacity of a delta-delta bank. But if the load consists of simple impedances, and possesses no inherent phase-balancing characteristics, the currents of an open-delta will not be of equal magnitude, and the capacity of the bank may be considerably less than the ideal 0.866 given above.

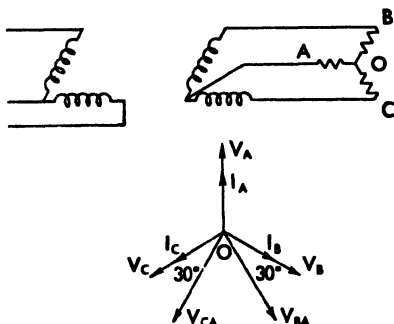


Fig. 64 Open delta.

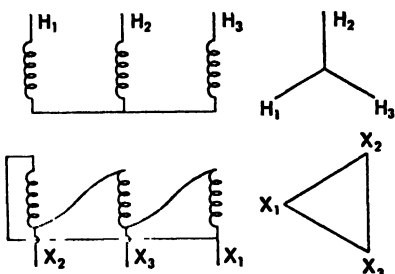


Fig. 65 Wye-delta transformer.

35. Delta-wye and Wye-delta Connections, Fig. 65

These are the most popular and generally satisfactory of all 3-phase transformer connections. The wye is used on the high-voltage side to profit from the advantage of being able to use a transformer of lower voltage than line voltage, and to provide for a grounded neutral. The delta provides a path for third harmonic exciting currents, and permits zero sequence currents to flow to ground on the wye side by encountering only leakage impedance.

Every wye-delta or delta-wye transformer connection can be reduced to the same vector diagram, Fig. 65, by a proper interchange in the numbering of the leads. This is not possible with wye-wye or delta-delta connections.

On transmission systems, delta-wye connections at the generator end and wye-delta connections at the receiving end are almost universal.

36. The T-T Connection, Fig. 66

This connection may be used to transform 3-phase to 3-phase with two transformers. The voltage of the *teaser* winding OC is only 0.866

that of the *main* winding AB . The output for a balanced resistance load is

$$P = \frac{VI}{2} \cos 30^\circ + \frac{VI}{2} \cos (-30^\circ) + \frac{\sqrt{3}}{2} VI = \sqrt{3} VI$$

The transformer rating is $VI + 0.866VI = 1.866VI$. Hence the *capacity ratio* is $1.732/1.866 = 0.926$. This is somewhat better than the open-delta connection.

A complete analysis will not be undertaken, as the connection is rarely used and then only in small power installations.

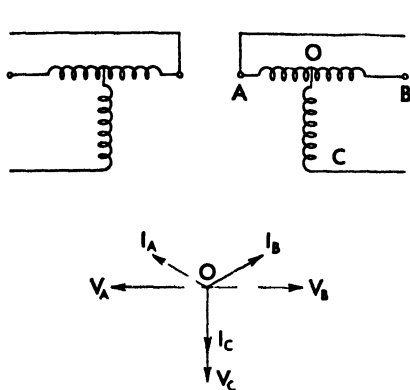


Fig. 66 The T T connection

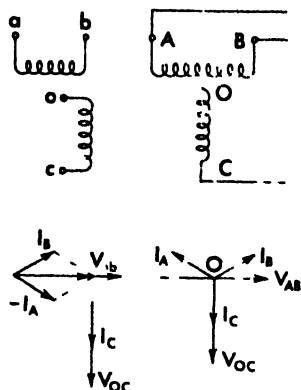


Fig. 67 The Scott connection

37. The Scott Connection, Fig. 67

This connection is used to transform from 2 phase to 3 phase or conversely. Of the great number of transformer connections that have been used, this is one of the few named after its inventor. It is a simple T. The idealized connection and vector diagrams are shown in Fig. 67. The power output to a balanced resistance load is $\sqrt{3}VI$. The rating of the windings is $1.866VI$, and capacity ratio is therefore 0.926.

Figure 68 shows the Scott connection used to transform 3-phase power to a 2 phase load. Let the main winding on the 3-phase side be regarded as the windings $1'$ and $3'$. Then the equations of constraint are

$$V_2 = -Z_2 I_2 \quad (251)$$

$$V_2' = -Z_2' I_2' \quad (252)$$

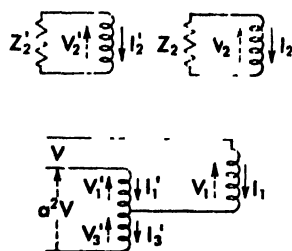


Fig. 68

$$a^2 V = V_1' + V_3' \quad (253)$$

$$V = V_1 - V_1' \quad (254)$$

$$0 = I_1 + I_1' - I_3' \quad (255)$$

The general equations are

$$0 = I_1 + n_2 I_2 \quad (256)$$

$$V_2 - n_2 V_1 = n_2 n_2' Z_{22} I_2 \quad (257)$$

$$0 = I_1' + n_2' I_2' + n_3' I_3' \quad (258)$$

$$V_2' - n_2' V_1' = n_2' n_2' Z_{22}' I_2' + n_2' n_3' Z_{23}' I_3' \quad (259)$$

$$V_3' - n_3' V_1' = n_3' n_2' Z_{32}' I_2' + n_3' n_3' Z_{33}' I_3' \quad (260)$$

Let

$$\left. \begin{aligned} z_1 &= n_3' n_2' Z_{32}' - (n_2' n_2' Z_{22}' + Z_2')(1 + n_3') n_2' \\ z_2 &= n_3' n_3' Z_{33}' - n_2' n_3' Z_{23}'(1 + n_3') n_2' \\ z_3 &= (n_2 n_2' Z_{22} + Z_2) n_2' n_2^2 + (n_2' n_2' Z_{22}' + Z_2') n_2' \\ z_4 &= (n_2 n_2' Z_{22} + Z_2)(1 + n_3') n_2^2 + n_3' Z_{23}' \end{aligned} \right\} \quad (261)$$

Then the solution of (251) to (260) for the currents yields

$$I_2' = \frac{a^2 z_1 - z_2}{z_1 z_2 - z_2 z_3} V \quad (262)$$

$$I_3' = \frac{z_1 - a^2 z_3}{z_1 z_2 - z_2 z_3} V \quad (263)$$

$$I_1' = - \frac{n_2'(a^2 z_1 - z_2) + n_3'(z_1 - a^2 z_3)}{z_1 z_2 - z_2 z_3} V \quad (264)$$

$$I_1 = -n_2 I_2 = \frac{(1 + n_3') z_1 - n_2' z_2 - (n_3 z_3 - z_3 - n_2' z_1) a^2}{z_1 z_2 - z_2 z_3} V \quad (265)$$

In practical cases $n_2' = n_3'$ and the solutions simplify somewhat.

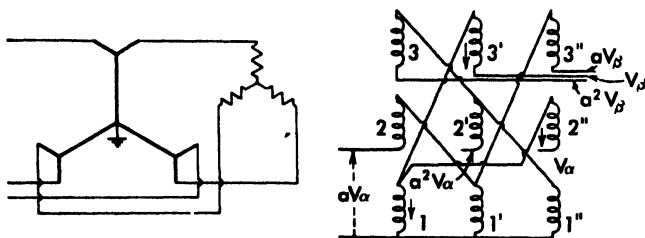


Fig. 69 Double zigzag autotransformer.

38. Double Zigzag Phase-shift Autotransformer, Fig. 69

This connection is used to tie two systems together where it is desirable to adjust the phase angle between them, and perhaps to effect

simultaneously small changes in the voltage ratios. The connection diagram is shown in Fig. 69. There are 3 windings on each core (or core leg in the case of a 3-phase core). Assuming balanced conditions, the phase voltages may be taken as (V_a, aV_a, a^2V_a) on one side and $(V_\beta, aV_\beta, a^2V_\beta)$ on the other. The currents will likewise be balanced.

The equations of constraint are

$$I_1 + I_2'' + I_3' = I_1 + a^2I_2 + aI_3 = 0 \quad (266)$$

$$V_1 - V_2'' = V_1 - a^2V_2 = V_a \quad (267)$$

$$V_1 - V_3' = V_1 - aV_3 = V_\beta \quad (268)$$

The general equations (123) and (127) for the first core are

$$0 = I_1 + n_2I_2 + n_3I_3 \quad (269)$$

$$V_2 - n_2V_1 = n_2n_2Z_{22}I_2 + n_2n_3Z_{23}I_3 \quad (270)$$

$$V_3 - n_3V_1 = n_3n_2Z_{32}I_2 + n_3n_3Z_{33}I_3 \quad (271)$$

Taking the load quantities V_β and I_3 as given, (266) and (269) give

$$I_1 = \frac{an_2}{a^2 - n_2} I_3 \quad (272)$$

$$I_2 = \frac{n_1 - a}{a^2 - n_2} I_3 \quad (273)$$

while (268), (270), and (271) yield

$$V_1 = \frac{1}{1 - an_3} V_\beta + \frac{an_3}{1 - an_3} \left(n_2 \frac{n_3 - a}{a^2 - n_2} Z_{32} + n_3 Z_{33} \right) I_3 \quad (274)$$

$$V_2 = \frac{n_2}{1 - an_3} V_\beta + \left[n_2^2 \frac{n_3 - a}{a^2 - n_2} Z_{22} + \frac{an_2n_3^2}{1 - an_3} Z_{33} \right. \\ \left. + \frac{n_2n_3(a^2 - n_3 + an_2 + 2an_2n_3)}{(1 - an_3)(a^2 - n_2)} Z_{23} \right] I_3 \quad (275)$$

$$V_3 = \frac{n_3}{1 - an_3} V_\beta + \frac{n_3}{1 - an_3} \left(n_2 \frac{n_3 - a}{a^2 - n_2} Z_{32} + n_3 Z_{33} \right) I_3 \quad (276)$$

$$V_a = \frac{1 - a^2n_2}{1 - an_3} V_\beta + \left[\frac{n_3^2(a - n_2)}{1 - an_3} Z_{33} - a^2n_2^2 \frac{n_3 - a}{a^2 - n_2} Z_{22} \right. \\ \left. + \frac{n_2n_3(-n_3 - 2n_2n_3 - n_2 + 1)}{(1 - an_3)(a^2 - n_2)} Z_{23} \right] I_3 \quad (277)$$

The short-circuit impedance of the autotransformer is found by putting $V_\beta = 0$ in (277), substituting I_3 in terms of I_2 from (273), and rearranging as

$$\frac{aV_a}{-I_2} = n_2^2 Z_{22} + \frac{1 + n_2 + n_2^2}{1 + n_3 + n_3^2} n_3^2 Z_{33} + \frac{2n_2n_3 + n_2 + n_3 - 1}{1 + n_3 + n_3^2} n_2n_3 Z_{23} \quad (278)$$

The above procedure for the analysis of the double zigzag phase-shifting autotransformer is typical of the method of solution for such circuits as the inscribed, extended, stub delta, semi-stub delta, inverted double zigzag phase shift, and hexagon autotransformers shown in Table II.

39. Wye-Delta-Zigzag Connection, *Fig. 70*

With this connection there are four windings for each magnetic circuit or core leg. Suppose that the balanced load impedance is on the zigzag

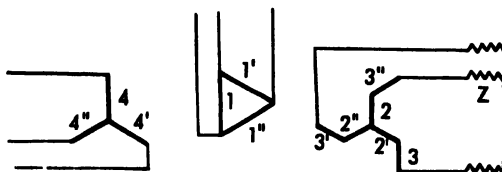


Fig. 70 Wye-delta-zigzag transformer.

winding, and that the wye and delta windings are connected to generators or fixed voltage sources. The three transformers will be considered as entirely similar, and to be operating under balanced conditions, so that any single primed voltage or current is displaced 120 degrees from the corresponding unprimed quantity, and any double-primed voltage or current is displaced 240 degrees from the corresponding unprimed quantity. Then using the phase sequence $(1, a, a^2)$ the constraints are seen to be

$$V_2 - V_3'' = V_2 - a^2 V_3 = -Z I_2 \quad (279)$$

$$I_3'' = a^2 I_3 = -I_2 \quad (280)$$

The general equations (123) and (127) become

$$0 = I_1 + n_2 I_2 + n_3 I_3 + n_4 I_4 \quad (281)$$

$$V_2 - n_2 V_1 = n_2 n_2 Z_{22} I_2 + n_2 n_3 Z_{23} I_3 + n_2 n_4 Z_{24} I_4 \quad (282)$$

$$V_3 - n_3 V_1 = n_3 n_2 Z_{32} I_2 + n_3 n_3 Z_{33} I_3 + n_3 n_4 Z_{34} I_4 \quad (283)$$

$$V_1 - n_4 V_1 = n_4 n_2 Z_{12} I_2 + n_4 n_3 Z_{13} I_3 + n_4 n_4 Z_{14} I_4 \quad (284)$$

Solving for the currents in terms of voltages V_1 and V_4 assumed to be known, there results

$$I_2 = -a^2 I_3 = [(V_4 - n_4 V_1)(n_2 n_4 Z_{21} - a^2 n_3 n_4 Z_{34}) - (a^2 n_3 - n_2) V_1 n_4^2 Z_{11}] D^{-1} \quad (285)$$

$$I_4 = [(a^2 n_3 - n_2) V_1 (n_2 n_4 Z_{42} - a n_4 n_3 Z_{43}) - (V_4 - n_4 V_1)(n_2 n_2 Z_{22} + n_3 n_3 Z_{33} + n_2 n_3 Z_{23} + Z)] D^{-1} \quad (286)$$

$$I = (an_3 - n_2)I_2 - n_4I_4 \quad (287)$$

in which

$$D = (n_2n_1Z_{24})^2 + (n_3n_4Z_{31})^2 + n_2n_3n_1^2Z_{31}Z_{24} \\ - n_4^2Z_{44}(n_2^2Z_{22} + n_3^2Z_{33} + n_2n_3Z_{23} + Z) \quad (288)$$

If there is a load Z_4 on the wye winding (instead of a generator) the above solutions hold upon substituting $(n_4^2Z_{44} + Z_4)$ for $n_4^2Z_{44}$ and putting $V_4 = 0$.

40. Leakage Flux Problems

The transfer of power between windings of a transformer is effected by the mutual flux confined to the iron core, and this flux is responsible for the hysteresis and eddy-current losses in the laminations. There is also, however, an appreciable flux (from 2 to 12 per cent of that in the core, depending on the size and voltage rating of the transformer) external to the core, and this *leakage* flux has four generally undesirable effects:

- (1) By interlinkage with one winding and not with the other, or only partially with the other, it constitutes a *leakage reactance* flux resulting in an induced reactance voltage drop which causes poorer regulation, poorer power-factor, and influences the division of load on parallel operation.
- (2) By interlinkage with the tank, clamps, bolts, and other accessories it induces currents in them which account for as much as 20 per cent of the total losses in the transformer. These losses are called *stray losses*, and are extremely difficult to calculate or estimate. Copper or aluminum shields are sometimes introduced to reduce tank losses.
- (3) By interlinkage with the individual conductors it induces voltage differences over the cross-section of the conductor which cause an unequal distribution of current in the conductors, resulting in *skin effect* or conductor *eddy-current losses*. In effect, these eddy currents increase the effective resistance of the conductor to as much as 20 per cent more than its d-c value, thereby adding materially to the copper losses. In order to control this extra loss, the conductors are stranded and transposed.
- (4) By interaction with the currents in the conductors it gives rise to *mechanical forces* which tend to burst the windings asunder, or, in the case of dissymmetry, to displace the winding axially. Under

short-circuit conditions these mechanical forces may become destructive, and must be braced against by suitable clamps and supports.

As a matter of fact, the leakage fluxes present by far the most difficult and involved problems in transformer design. They are field rather than circuit problems, and therefore require more advanced analytical methods. It will not be possible to give more than superficial attention to these problems here. However, a detailed mathematical treatment of leakage fluxes and reactances, eddy-current loss, and mechanical forces will be found in a companion text.*

41. Leakage Reactance

The calculation of the leakage flux and reactance between a pair of windings is based on the assumption that the primary and secondary ampere-turns are equal and opposite; that is, the magnetizing ampere-turns are neglected, $N_1 I_1 + N_2 I_2 = 0$. Also, depending upon the type of winding and the core construction, certain other simplifying assumptions are usually made in order to carry out the mathematical calculations. Even where the most precise and involved methods are used, it is usually necessary to make minor empirical corrections based on design experience for reliable design calculations.

Figure 71 shows a simple concentric winding, core-type design, in which the high-voltage winding of $N_1 I_1$ ampere-turns is on the outside and the low-voltage winding of $N_2 I_2$ ampere-turns is on the inside. The leakage flux distribution follows curved elliptical-shaped paths, as indicated by the light lines, but these actual paths can be determined only by the use of advanced mathematics, and by ignoring the proximity of the tank and other distorting effects. It is sufficient

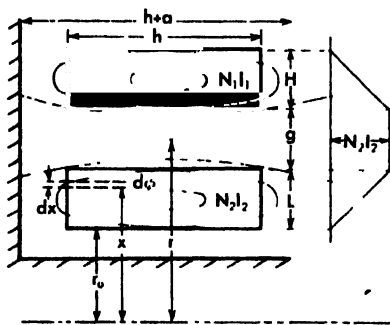


Fig. 71

for most purposes to assume the flux parallel to the core, and of a length $(h + a)$, where h is the height of the coil stack and a is an empirical correction which accounts for the return path of the flux. The ampere-turn distribution is trapezoidal, building up linearly through the low-

* Bewley, L. V., *Two dimensional Fields in Electrical Engineering*, The Macmillan Company, New York, 1948.

voltage winding to a maximum of $N_2 I_2$ and then linearly back to zero as the ampere-turns of the high-voltage subtract. The procedure in calculating leakage reactance is in three steps: (1) the flux $d\phi$ in an elementary path is found by dividing the magnetomotive force with which the path is linked by the reluctance of the path; (2) the flux linkages are found as the integral of the products of the fluxes $d\phi$ and the linked magnetomotive forces; (3) the reactance is found by dividing flux linkages by the square of the total current. Referring to Fig. 71, and assuming the flux to go straight across and return through the core, the flux in the elemental path dx at radius x in the low-voltage winding is

$$d\phi_2 = \frac{\text{mmf}}{\text{reluctance}} = \frac{0.4\pi N_2 I_2 (x - r_0) L}{(h + a) 2\pi x dx}$$

interlinking with $N_2 I_2 (x - r_0) L$ turns, and the total interlinkages are

$$\lambda_2 = \frac{0.8\pi^2 N_2^2 I_2^2}{(h + a) L^2} \int_{r_0}^{r_0 + L} (x - r_0)^2 x dx = \frac{0.8\pi^2 N_2^2 I_2^2 L}{(h + a)} \left(\frac{r_0}{3} + \frac{L}{4} \right) \quad (289)$$

The flux in the gap between the coils links with the low-voltage winding. The total interlinkages are

$$\begin{aligned} \lambda_g &= \frac{0.8\pi^2 N_2^2 I_2^2}{h + a} \int_{r_0 + L}^{r_0 + L + g} x dx \\ &= \frac{0.8\pi^2 N_2^2 I_2^2 g}{h + a} \left(r_0 + L + \frac{g}{2} \right) \end{aligned} \quad (290)$$

Finally, the flux in an elemental path dx at radius x in the high voltage winding is due to all of the low-voltage ampere turns and part of the high-voltage ampere-turns, or since $N_1 I_1 = -N_2 I_2$

$$N_2 I_2 + N_1 I_1 \left(\frac{x - r_0 - L - g}{H} \right) = N_2 I_2 \left(\frac{r_0 + L + g + H - x}{H} \right)$$

and the total interlinkages of the flux in the high-voltage winding are

$$\begin{aligned} \lambda_1 &= \frac{0.8\pi^2 N_2^2 I_2^2}{(h + a) H^2} \int_{r_0 + L + g}^{r_0 + L + g + H} (r_0 + L + g + H - x)^2 x dx \\ &= \frac{0.8\pi^2 N_2^2 I_2^2}{(h + a)} H \left(\frac{r_0 + L + g}{3} + \frac{H}{12} \right) \end{aligned} \quad (291)$$

The total flux linkages then are

$$\lambda = \lambda_2 + \lambda_g + \lambda_1 = \frac{0.8\pi^2 N_2^2 I_2^2}{(h + a)} \left(\frac{L}{3} r_2 + g r + \frac{H}{3} r_1 \right) \quad (292)$$

in which

$$r_2 = r_0 + \frac{3}{4} L \quad = \text{effective radius of low-voltage winding}$$

$$r = r_0 + L + \frac{g}{2} = \text{effective radius of the gap}$$

$$r_1 = r_0 + L + g + \frac{H}{4} = \text{effective radius of high-voltage winding}$$

Now by the definition of reactance,

$$X = \frac{\omega \sum N \phi}{10^8 I_2} = \frac{\omega \lambda}{10^8 I_2^2} = \frac{1.6 \pi^2 f N_2^2}{10^8 (h + a)} \left(\frac{L r_2}{3} + g r + \frac{H r_1}{3} \right) \text{ ohms} \quad (293)$$

in which dimensions are in centimeters. If the windings on the two legs of the transformer are alike and are in series, the reactance of the transformer is double this value (if N_2 are the turns per leg). If the 2 legs are in parallel, the transformer reactance is half of (293). In design work, it is usually sufficient to take $r_1 \cong r$ and $r_2 \cong r$ and put $2\pi r = \text{mean length of turn (mlt)}$. Then

$$X = \frac{8 \pi^2 f N_2^2 (\text{mlt})}{10^8 (h + a)} \left(\frac{L}{3} + g + \frac{H}{3} \right) \quad (294)$$

Problems

1. A hydroelectric station generates at 13.2 kv and transmits over a long line at 220 kv to a switching station from which radiate three secondary transmission lines at 66 kv to main substations. Distribution lines leave the substations at 13.2 kv and supply feeder substations which distribute at 4 kv to pole-top transformers that reduce the voltage to 220 110 volts for domestic use. Draw a single-line diagram showing the system, and indicate on the sketch the location, voltages, and classification of all transformers.
2. List and discuss the advantages and disadvantages of the different types of construction features found in transformers. (Consult other texts and manufacturers' bulletins.)
3. Great economies accrue from the use of standardized ratings. Consult the ASA (American Standards Association) and the NELA (National Electric Light Association) bulletins, and submit a list of standard voltage ratings for (a) power and (b) distribution transformers. Indicate if any of these standard voltages are to be preferred.
4. A single-phase transformer has 1200 primary and 200 secondary turns, and supplies a 640 kw load at 6600 volts and 0.80 pf. What is its ratio of transformation, and approximately the voltage, current, and kva on each winding?
5. The 60-cycle voltage applied to a coil of 663 turns is

$$e = 160 \sin 377t + 60 \sin (1131t - 45^\circ) - 20 \sin (1885t + 75^\circ)$$
 (a) Plot the voltage and flux wave forms and their harmonic components.

- (b) Repeat, when the signs of the harmonics in the voltage wave are reversed.

6. A sample of transformer steel has the following hysteresis loop:

Kilolines per sq. in.	0	10	20	30	40	50	60	64.5
Ampere-turns per in. (up)	+0.85	1.00	1.17	1.45	1.86	2.50	3.50	4.00
Ampere-turns per in. (down)	-0.85	-0.73	-0.60	-0.35	0.05	0.80	2.55	

Let $N = 800$ turns, $l = 1.30$ in., $A = 100$ sq. in., $f = 60$ cycles.

- Assuming a sinusoidal flux density wave, plot the magnetizing current and determine its harmonics by Fourier analysis.
 - What is the in-phase (energy loss) component of this current?
 - Assuming a sinusoidal current wave, plot the flux density wave and determine its harmonics.
 - Determine the induced voltage wave shape and plot it.
 - What is the energy loss for this hysteresis loop?
 - What is the coefficient in the Steinmetz formula if the exponent is 1.6?
7. The core loss (hysteresis and eddy-current) of a sample of iron at a certain flux density is known for 25 and for 60 cycles. Derive a formula which will give the loss for any other frequency at the same flux density.
8. A 6600-volt, 60-cycle transformer has 0.22 kw hysteresis loss and 3.81 kw eddy-current loss. Assume the hysteresis exponent as $a = 1.6$.
- If this transformer is used on a 50-cycle supply at the same voltage, what will its losses be?
 - If the voltage is reduced to 6200 volts at 50 cycle, what will the losses be?
9. The transformer of problem 8 is operating at a maximum flux density of 75,000 lines per square inch at 60 cycles. Plot curves showing how its core loss will vary with (a) applied voltage at constant frequency, (b) frequency at constant voltage, (c) flux density at constant frequency.

10. Core-loss tests on a sample of iron give the following corresponding values:

f	30	30	60	cycles
B	4000	10,000	10,000	gausses
P	1.80	8.30	19.48	watts

Determine the exponent a and the coefficients k' and k'' in the core-loss equation (16), Chap. 2.

11. A transformer has the following constants:

$N_1 = 1200$ turns	$N_2 = 120$ turns	$f = 60$ cycles
$R_1 = 20$ ohms	$R_2 = 0.2$ ohms	$G_0 = 1.00 \times 10^{-6}$ mho
$X_1 = 110$ ohms	$X_2 = 1.1$ ohms	$B_0 = 6.00 \times 10^{-6}$ mho

The secondary voltage is $V_2 = 6600$ volts, and the secondary current is $I_2 = 150$ amperes. Draw to scale, the vector diagrams for the following secondary power factor angles: $\theta_2 = 90^\circ$ lag, 45° lag, 0° , 45° lead, 90° lead. Comment on the ratio of V_1 V_2 in each case.

12. The following table gives the characteristics of some typical 60-cycle transformers.

No.	RATING		SHORT-CIRCUIT TEST			OPEN-CIRCUIT TEST		
	Kva	Voltages	V_1	I_1	W_1	V_1	I_0	W_0
1								
2	10	2,300 : 220	115	4.35	204	2,300	0.045	71
3	100	4,000 : 220	164	25.00	1,060	4,000	0.90	860
4	500	13,200 : 2,200	725	37.90	4,550	13,200	1.06	4,250
5	1,000	66,000 : 2,200	5,150	15.15	7,220	66,000	0.48	9,100
6	5,000	13,200 : 2,200	1,070	379	38,100	13,200	15.9	29,000
7	10,000							
8	20,000							
9	30,000							
10	50,000							

For transformer No. listed in the above table:

- Determine the constants R_1 , X_1 , Z_1 , R_2 , X_2 , Z_2 , G_0 , B_0 , Y_0 .
- Show and label the exact and approximate equivalent circuits.
- Calculate and plot the *Regulation* at unity, 80% lagging and 80% leading pf.
- Calculate and plot the *Efficiency* at 25% , 50% , 75% , 100% , 125% load, at 80% lagging, 80% leading and unity pf.
- Calculate the currents, voltages, and phase angles for full load, 80% lagging pf conditions.
- Draw the vector diagram to scale.
- Calculate the A , B , C , D constants, and write the voltage and current equations.

13. The daily load cycle for transformer No. 2 of problem 12 is

Time	0600	0800	1200	1300	1700	1800	2100	0100
	0800	1200	1300	1700	1800	2100	2400	0600
$\%$ Load	30	90	50	80	30	50	60	10

- What is its *all-day* efficiency?
- What is its maximum efficiency, and at what load?
- If a replacement were ordered, what ratio of iron to copper losses at full load should be specified?

14. Derive the A , B , C , D constants corresponding to the exact equivalent circuit of the transformer.

15. Plot a set of curves showing how the *regulation* varies with the per cent reactance ($\%XI_2 = 100 XI_2 V_2$) for different load power factors (0.80 lead, 1.00, 0.80 lag). Assume that $R/X = 0.1$ in all cases, and take the per cent reactance range from 2% to 16% .

16. (a) Derive equation (76) from (75), showing all steps in detail.

(b) Itemize and count the number of operations in each formula.

(c) Do you believe (76) has an advantage over (75) in speed or accuracy for slide rule computations? Is the alleged advantage easily circumvented

if one knows that $\sqrt{1+s} \cong 1 + \frac{s}{2}$ when s is small?

17. Of the several alternative expressions for efficiency in (77), which will give the best slide rule results? Why?

18. Suppose that you have already calculated the regulation of a transformer and found it to be 5.6% . The secondary voltage (referred) is $V_2' = 13,000$ volts. What would you use for E_0 in (77) if you wanted very precise results but did not want to go to the trouble of solving the exact equivalent circuit?

19. Show the detailed derivation of (79) from (78).

20. The daily load cycle of a 10 kw distribution transformer is

Time	0600	0700	1100	1200	1300	1700	1800	2100	2300
	0700	1100	1200	1300	1700	1800	2100	2300	0600
$\%$ Load	90	60	110	15	30	95	30	60	5

What should be the optimum ratio of the full load copper-to-iron losses for this transformer?

21. Two different manufacturers submit bids for the above transformer. "A" offers a transformer having 0.75% iron losses and 2.25% copper losses at full load. "B" offers a transformer having 0.80% iron and 2.10% copper losses.

(a) At the same price which bid should be accepted?

(b) If power is selling at 9 mills per kw hr, what should be the price differential between these two bids to make them equally attractive? Assume fixed charges at 12% per year.

22. A 60-cycle, 2500-kva, 66,000-4000-volt transformer shows the following test results (high-voltage side):

	VOLTS	AMPS	WATTS
Short-circuit	5575	37.9	14,880
No-load	66,000	0.7	7600

- (a) Calculate the 6 transformer constants.
- (b) Draw the exact and approximate equivalent circuits and label with the proper impedance values.
- (c) If this transformer is carrying 1600 kw at 0.80 pf lagging and at 4000 volts on the load, calculate for both the exact and approximate equivalent circuits:
- (1) all currents (I_2 , I_2' , I_0 , I_1) and their phase angles
 - (2) all voltages (V_2 , V_2' , E_0 , V_1) and their phase angles
 - (3) regulation
 - (4) losses (segregated into primary and secondary copper and iron losses)
 - (5) efficiency
- (d) Draw the vector diagram (referred to the high-voltage) to scale of 10,000 volts per inch and 10 amps per inch.
- (e) If the load current remains the same, but the primary voltage is held to 66 kv, what are the results under (c) above?
- (f) At full load how many reactive kva does this transformer contribute to the system?
- (g) What are its A , B , C , D constants?
23. Construct the vector diagram for the autotransformer.
24. Carry out in detail the development of equations (102) and (103).
25. An autotransformer rated 1250 kva, 6900-4000 volts is tested as an ordinary transformer with the generator on the series winding. The test data are:
- | SECONDARY | S C | O C |
|---------------|-------|------|
| Primary volts | 125 | 2900 |
| amps | 131.1 | 2.75 |
| kw | 7.25 | 7.45 |
- (a) Determine the transformer constants in *ohms* and in *per cent*.
- (b) Determine the autotransformer constants in *ohms* and in *per cent*.
- (c) Neglecting the exciting current, what are the currents in the series and common windings and to the load?
- (d) What are the *kva* capacities of each winding?
- (e) Calculate the losses and efficiency of the autotransformer at full load and 0.80 pf lagging.
- (f) Calculate the regulation at full load and 0.80 pf.
- (g) What would be the relative size, efficiency and per cent impedance of a transformer for the same job?
26. (a) Reduce the following system to a "single-line diagram" with all loads, voltages, and impedances expressed in *per cent values* based on 50,000 kva, and 13.2 kv at load A.

- (b) Calculate the voltages and currents at all points in "per cent" and convert to actual kilovolts and amperes.

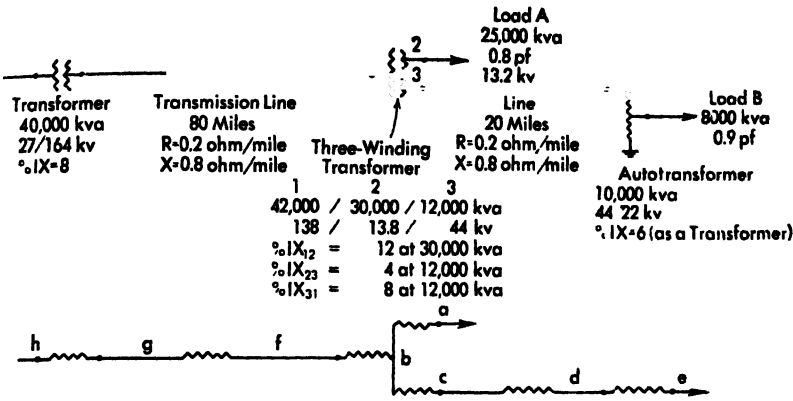


Fig. 72

27. Two transformers operated in parallel on a 140-volt lagging 0.80 pf load have the following characteristics:

	KVA	VOLTAGES	$\epsilon_1 IR$	$\epsilon_1 IX$
No. 1	200	230 / 440	0.9	3.5
No. 2	100	240 / 480	1.1	3.8

- (a) What load can be carried without overloading either transformer?
(b) What load can be carried if the voltage ratio of No. 2 is the same as that of No. 1?
(c) What load can be carried if the pu impedance of No. 2 is the same as that of No. 1?
(d) Draw to scale the vector diagram for (a) above.
(e) What is the circulating current between these two transformers at no-load?
28. (a) If three or more transformers are operated in parallel is it possible for one transformer to be free of circulating current?
(b) If all the transformers have different ratios is it possible for more than one of them to be free of circulating current?
(c) If several transformers having identical ratios are to be operated in parallel, show that maximum load can be carried without overloading any one transformer if $\frac{R_1}{X_1} = \frac{R_2}{X_2} = \frac{R_3}{X_3} = \text{etc.}$

29. Solve equation (114) together with $I = I_1 + I_2 + \dots + I_n$ for $n = 3$ by determinants and compare solution with (117).

- (a) Does the determinant solution bring out the “physics” of the problem, that is, does it show clearly the distinction between division of load current and circulating currents?
- (b) Does the determinant solution have anything to recommend it from the point of view of facilitating the numerical calculations?

3 General Principles of Rotating Machines

1. Introduction

There are a number of features and characteristics which are common to practically every electrical rotating machine, and it will accordingly save much duplication of treatment if these common factors are disposed of once for all in a preliminary chapter on rotating machines. Thus the types of windings used in both d.c. and a.c. machines are generally similar; and therefore the processes of voltage induction are the same, as are the magnetomotive force or armature reaction fluxes developed by these windings.*

Windings are rarely lumped or concentrated, but made up of a series of coils displaced in space from each other, so that each individual coil may be situated in a different field of flux at any given instant. Moreover, each side of a coil may be cutting a flux of different density. The arrangements and dispositions of windings then leads to certain

* Note to the instructor:

A thorough understanding of the contents of this chapter is essential to the treatment of the synchronous generator and motor given in Chapter 6, and the synchronous converter given in Chapter 7, and a.c. commutating machines given in Chapter 5. However, the chapters on the polyphase and single-phase induction motors may be considered independent of the present chapter if a complete understanding of skew, pitch and distribution factors is not insisted on until after the study of synchronous machines is undertaken. In that event it will suffice to explain to the student that these coefficients are simply factors which account for the fact that the winding is not a full pitch concentrated coil. This procedure permits the transformer and polyphase and single phase induction motors to be treated in the first semester, and to take up the more involved aspects under synchronous machines the second semester.

reduction factors which enter into the calculation of induced voltages and armature reaction. It is the purpose of the present chapter to describe the usual types of windings encountered in rotating machines, and then to derive the equations of voltage and armature reaction for these windings. Finally, there is offered a brief discussion of the various leakage reactances found in such machines.

2. Armature Windings

The armature windings of most a-c machines may be classified with respect to:

- | | |
|-----------------------------|--|
| a. Number of phases | single or polyphase |
| b. Connections | star (wye) or mesh (delta) |
| c. Parallel paths | single or multiple |
| d. Layers | single (half-coil) or double (whole-coil) |
| e. End connections | lap, wave, spiral (concentric), and chain (basket) |
| f. Slots per pole per phase | integer or fraction |
| g. Coil pitch | full or fraction (chorded) |
| h. Phase belt span | 60 or 120 degrees for 3-phase |

Modern synchronous generators and motors, polyphase induction motors, and other a-c motors above the fractional horsepower class usually have double layer, wye-connected, lap windings with short-pitch coils but there are many exceptions.

The essential difference between single and polyphase windings is illustrated in Fig. 1 for the case of a *bipolar* generator with concentrated phase windings. Each diamond-shaped coil has two "coil sides," a and a' , and may consist of any number of turns. The sinusoidally distributed flux of the revolving field cuts the coil sides and induces sinusoidal voltages in them. The coil side voltages, being in series, combine to produce the coil voltage represented by the wave or the vector V_a . Suppose, now, that an additional winding bb' is added to the stator 90 degrees in *space* ahead (in the direction of rotation) of the winding aa' . The voltage of this new coil will reach its maximum at a later instant 90 degrees in *time* after the maximum of coil aa' occurred, as indicated by the wave or vector V_b . This arrangement constitutes a *2-phase* winding. If there are three windings aa' , bb' , cc' on the stator, 120-degrees apart in *space*, the three induced voltages are obviously 120-degrees apart in *time*, as indicated by the waves or vectors V_a , V_b , V_c , and the arrangement constitutes a *3 phase* winding. Obviously, an m -phase winding may be constructed by placing m windings on the stator dis-

tributed with an angle of $360/m$ electrical degrees between coils. There are 360 electrical degrees per pair of poles, and consequently, in the case of a multipolar machine,

$$(\text{electrical degrees}) = \frac{(\text{number of poles})}{2} (\text{mechanical degrees})$$

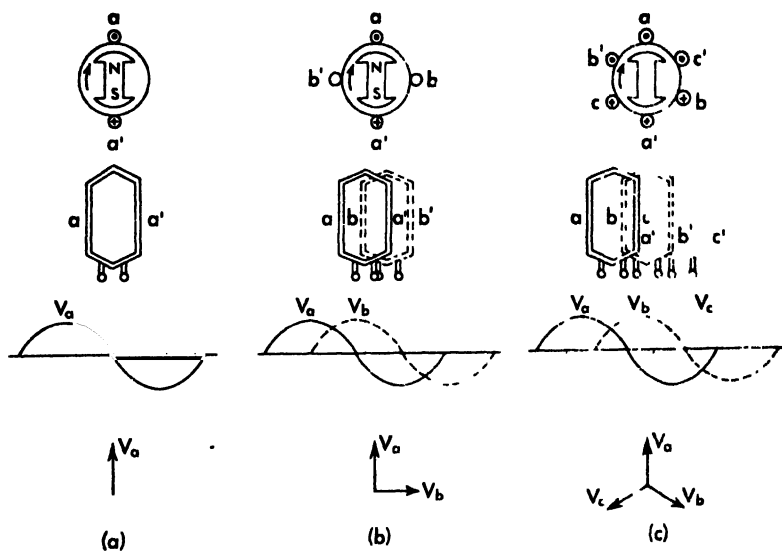


Fig. 1 Induced voltages in concentrated windings *a* single phase, *b* two phase, *c* three phase

Thus there are 1080 electrical degrees in one revolution of a 6 pole machine, and in such a machine the voltage alternates 6 times for each complete revolution of the field

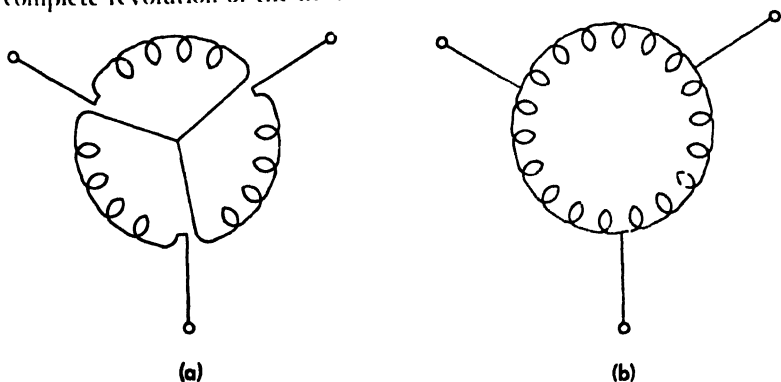


Fig. 2 Phase connections.
a Star or wye. *b* Mesh or delta

Both ends of each individual phase winding are rarely brought out to the terminal board of the machine, but are interconnected inside the machine to the other phase windings, either in star (wye, open-circuit) or mesh (delta, closed-circuit) as illustrated in Fig. 2. The majority of modern machines are star-connected, although rotary converters and a-c commutating machines have mesh-connected armatures similar to those of d-c machines, and some alternators are delta-connected.

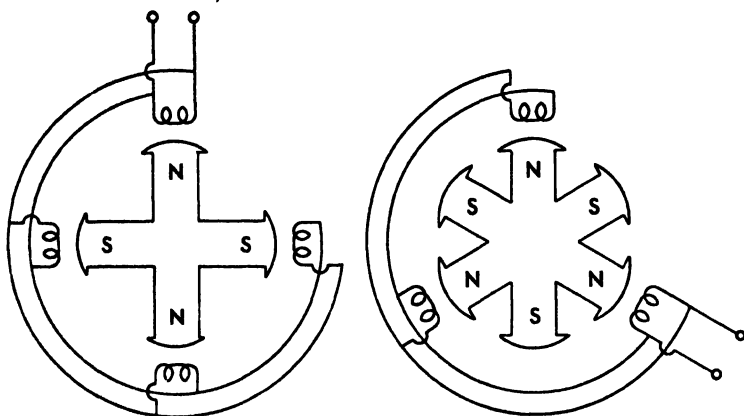


Fig. 3 Multiple circuits providing paths in parallel.

In multipolar machines, as shown in Fig. 3, the armature windings opposite similar poles may be connected in parallel to provide multiple current paths

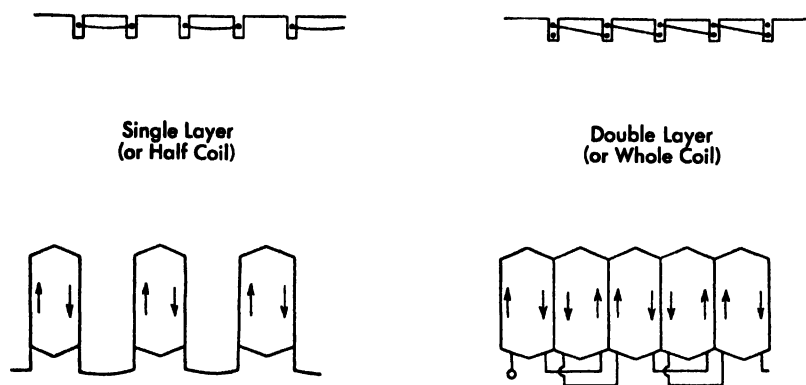


Fig. 4 Single and double layer windings

Figure 4a shows a *single-layer* or *half-coil* winding in which there is only one coil side per slot, and consequently only half as many coils as slots. This type of winding is used in small induction motors. It is

not much used in polyphase machines. The *double-layer* or *whole-coil* winding of Fig. 4 is standard in most machines, as it permits the use of fractional pitch coils, and identical diamond-shaped coils. There are as many coils as slots. Typical diamond-shaped coils are shown in Fig. 5.

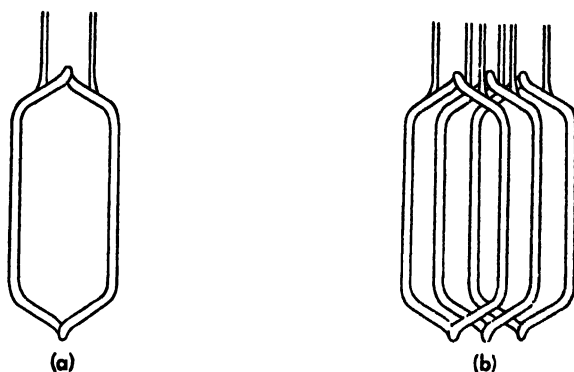


Fig. 5 Diamond-shaped coils.

Three basic types of end connections are shown in Fig. 6. The *lap* winding, Fig. 6a, is the most generally used. It permits the use of

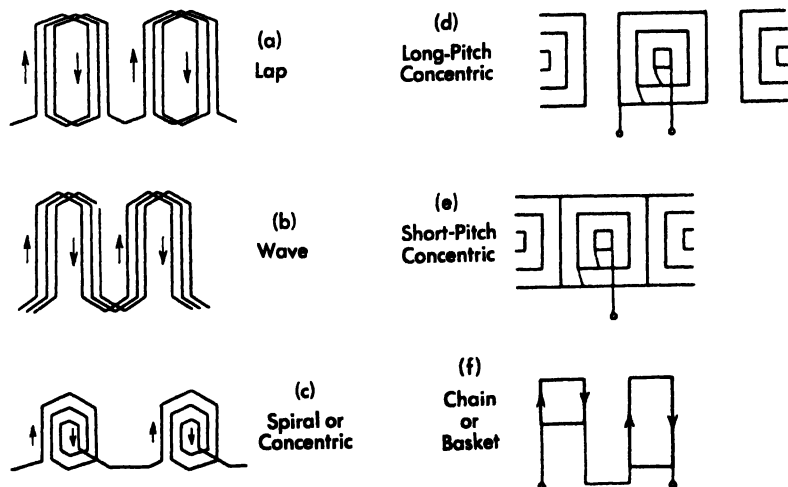


Fig. 6 Types of windings.

identical diamond-shaped coils throughout. Coil groups may be connected in series or in parallel with other groups. The end connections are comparatively easy to brace.

The *wave* winding, Fig. 6b, is rarely used in a-c machines, except for

the rotor of wound-rotor induction motors. It has fewer end connections than the lap winding. The lap and wave windings of a-c machines are identical in construction with those of d-c machines.

The *spiral* or *concentric* winding, Fig. 6c, is sometimes used in large high-voltage generators. It is more popular in Europe than in the United States. Variations of this type of winding are shown as the full-pitch winding of Fig. 6d, and the short-pitch winding of Fig. 6e. In polyphase windings of this type, the coils must be made with different length end-extensions, which gives the winding the appearance of links of a chain. Such windings are sometimes called *chain* or *basket* windings. The field windings of turbo alternators are usually the concentric type.

All of the above windings are electrically identical and indistinguishable.

Fractional-slot windings, which do not have an integer number of slots per pole per phase, are the rule rather than the exception. Their use not only simplifies manufacturing by minimizing the number of standard armature punchings which need be stocked, but they also are of real benefit in reducing the undesirable higher harmonics in the induced voltage. In fact, certain higher harmonics which would cause telephone interference cannot be eliminated except either by fractional slot windings or skewing. In slow speed machines with a large number of poles, it may be difficult to provide more than two slots per pole per phase, and in such machines fractional slot windings are just about universal. In such windings it is necessary to connect the phase groups under several poles in series, and some of these phase groups will have one more coil side than the others. However, the winding repeats itself in a *repeatable group* of poles. In order to avoid repetition, a special case will be developed along with the general equations.* Let in a single-layer winding,

$$Q = \text{total number of slots} = 42$$

$$P = \text{total number of poles} = 10$$

$$m = \text{number of phases} = 3$$

Then since the total number of slots must be equally divided among the phases, Q/m must be an integer. Suppose that Q/m and P are each divisible by a common integer factor k . Then the slots per pole per phase are

$$q = \frac{Q}{mP} = \frac{Q}{P} \frac{m}{k} = \frac{q'}{P'} = \frac{1}{8}$$

where $k = \text{number of repeatable groups in the winding} = 2$

* For comparison purposes, the same example is discussed here as in Langsdorf, Alexander F., *Theory of Alternating Current Machinery*, p. 316, McGraw-Hill Book Co

$$P' = \frac{P}{k} = \text{number of poles in a repeatable group} = 5$$

$$q' = \frac{()}{mk} = \text{slots per phase in a repeatable group} = 7$$

The angle between adjacent slots is

$$\beta = \frac{P}{()} 180^\circ = \frac{180^\circ}{mq} = 42\frac{6}{7}^\circ$$

If phases *I, II, III, ...* occupy successive $180^\circ/m$ arcs on the armature, then a single-layer winding may be arranged as in Fig. 7 (shown for a 3-phase winding and 60 degree arcs)

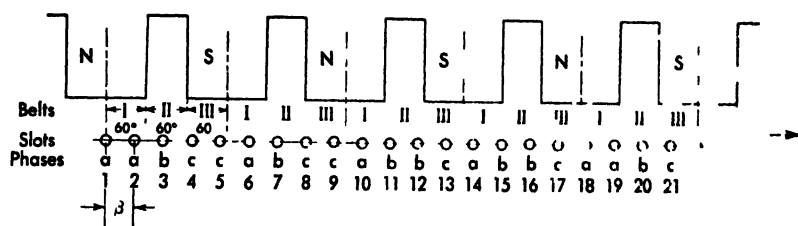


Fig. 7 Three-phase winding with 7 slots per pole per phase

The n th slot is located at an angle

$$(n-1)\beta = (n-1) \frac{180^\circ}{mq} = (n-1) 42\frac{6}{7}^\circ$$

from the center line of the first pole, and belongs to phase λ if

$$\left(h + \frac{\lambda}{m}\right) 180^\circ > (n-1) \frac{180^\circ}{mq} \geq \left(h + \frac{\lambda-1}{m}\right) 180^\circ$$

where h is any integer of the sequence 0, 1, 2, ..., $P' - 1$. The inequality may be rearranged as

$$(X + mh)q + 1 > n \geq (X + mh - 1)q + 1$$

Hereby the conductors belonging to any phase λ may be readily found. The conductor will be under an N or S pole depending on whether h is even (including zero) or odd. For $\lambda = 1$, $m = 3$, and $q = 7$ 5 there is

$(1 + 3h) \frac{7}{5} + 1 \geq n > (3h \frac{7}{5} + 1)$				
$h = 0$	$2\frac{2}{5}$	1, 2	1	N pole
$h = 1$	$6\frac{3}{5}$	6	$5\frac{1}{5}$	S pole
$h = 2$	$10\frac{4}{5}$	10	$9\frac{2}{5}$	N pole
$h = 3$	15	14	$13\frac{3}{5}$	S pole
$h = 4$	$19\frac{1}{5}$	18, 19	$17\frac{4}{5}$	N pole

Thus the phase-1 slots are 1, 2, 6, 10, 14, 18, 19.

The angle corresponding to any conductor n is $(n-1)180^\circ/mq$ and it is displaced from the center of the nearest trailing pole by the angle

$$(n-1) \frac{180^\circ}{mq} - h 180^\circ = \left(\frac{n-1}{m} \frac{P'}{q'} - h \right) 180^\circ$$

Now the latter expression is obviously divisible by $(180/mq')$, the quotient being the integer $[(n-1)P' - mhq']$, and therefore $(180/mq')$ is the angle of progression of the winding. There will be q' slots belonging to each phase in P' pole pitches, and since the conductors under an N pole are in series with those under an S pole, the whole single-layer winding is equivalent to a uniformly distributed winding having q' slots per pole per phase, as shown in Fig. 8. For the case in hand the angles from the pole centers of the conductors of phase 1 are 0, 42.6°, 34.2°, 25.5°, 17.1°, 8.4°, 51.3°, and the sequence may be arranged in the order 0, 8.4°, 17.1°, 25.5°, 34.2°, 42.6°, 51.3°, thus showing $q' = 7$ slots distributed by the regular angle $180/mq' = 180/21 = 8.4^\circ$.

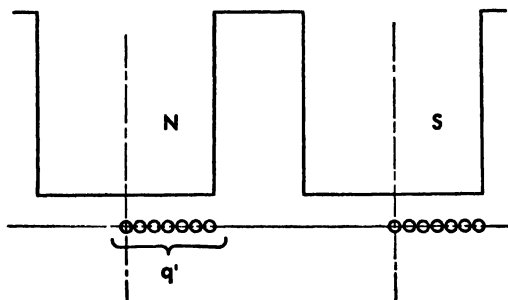


Fig. 8

For a 2-layer winding, the coil sides in the top of the slots are distributed as for a single-layer winding, and the coil sides in the bottom of slots have an identical distribution of one coil pitch further along.

The ideal flux distribution in the air gap of an electrical machine is a simple sinusoid, for such a flux distribution will induce a pure sine wave of voltage. Any deviation from a sinusoid in the flux distribution will cause undesirable harmonics to appear in the voltage wave. These harmonics not only cause telephone interference, but increase the losses and may impose greater insulation stresses. Various expedients are adopted to give as nearly a sinusoidal flux as possible, such as chamfered field poles and distributed field windings. Nevertheless, the no-load field form is usually far from sinusoidal, and armature reaction further

distorts it. There are several methods employed to eliminate or reduce the induced voltage harmonics. The armature conductors may be *skewed* as shown in Fig. 9. Skewing is used on small motors, but is too expensive on large machines.

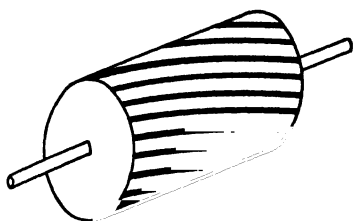


Fig. 9 Skewed conductors.

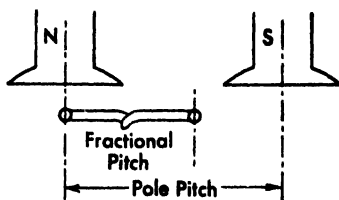


Fig. 10 Fractional pitch coil.

The coils may be made with *fractional pitch* as shown in Fig. 10. A fractional pitch coil can be made to eliminate or greatly reduce certain harmonics without materially affecting the fundamental. Moreover, short pitch coils result in shorter end connections and a saving in copper. Their use is practically universal. Finally, harmonics may be eliminated or reduced by *distribution* of the winding in several slots per pole per phase. If this distribution is in fractional slots per pole per phase, there is a vernier effect equivalent to a high order of uniform distribution. The effects of skew, pitch, and distribution will be investigated in detail under the section on induced voltages below.

3. Induced Voltages

Faraday's law states that the voltage induced in a closed circuit is proportional to the time rate of increase of the flux linked with that circuit,

$$e = - \frac{N}{10^8} \frac{d\phi}{dt} \quad (1)$$

The negative sign is occasioned by Lenz's law, which recognizes that any current which is permitted to flow as a result of this voltage will oppose the original flux change.

Consider a coil, Fig. 11a, embedded in the slots of a movable armature A , and a movable field structure F whose poles are excited by magnetizing ampere-turns $N_f i_f$. Evidently there are three distinct ways in which the flux linked with the coil may be caused to vary:

- (1) With both armature and field structure stationary the current in the field coils can be varied, thereby causing the flux ϕ itself to vary. The voltage due to this action is called *transformer electro-*

motive force. It is the common means of induction in transformers, and is present in some forms of a-c motors.

- (2) With the field structure stationary and the field excitation constant, the armature can be moved so that the coil cuts through the flux, thereby changing its flux linkages. The voltage due to this action is sometimes called a *motional* or *speed electromotive force*, and the process is referred to as *cutting action*. It is the common means of voltage induction in d-c machines.

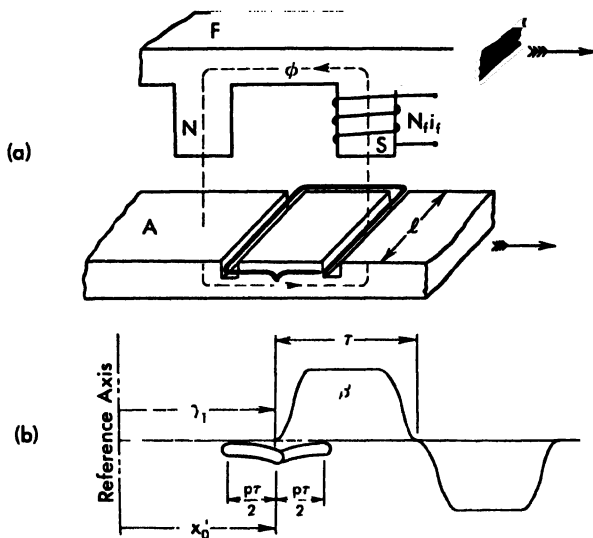


Fig. 11

- (3) With the armature stationary and the field excitation constant, the field structure can be moved past the coil, thereby changing the flux linked with it. This also is a *speed electromotive force*, since it is the *relative* motion between field and armature which counts, and it is immaterial whether the armature or the field has the absolute motion. A moving field is the more common means of voltage induction in revolving field synchronous machines and in polyphase induction motors.

Of course, all three processes may occur simultaneously. It is quite easy to develop a general equation for this contingency.* Such an equation has the great advantage of unifying electrical machine theory

* "Induced Voltages of Electrical Machinery," by L. A. Bewley, AIEE Trans., Vol. 48, 1930.

and of permitting a more critical examination of the processes of induction which occur in particular machines. Referring to Fig. 11b, let the flux density distribution be specified by the Fourier series

$$B = \sum \beta_k \sin k \left(\frac{\pi x}{\tau} \pm \gamma_k \right) \quad (2)$$

in which

k = order of the space harmonic

β_k = amplitude of the k th harmonic (a function of time)

γ_k = phase angle (position) of the k th harmonic (a function of time)

2τ = pitch (wave length) of the fundamental

x = distance measured from an arbitrary stationary reference axis

Now it is clear that the *location* of this flux density may be shifted (that is, caused to move) by changing the values of the phase angles γ_k . Indeed, there is no reason why the relative positions of the several harmonics cannot be disturbed, so as to cause a change in the shape of the distribution, as well as its location. If, for example, the γ_k are functions of time, a particular point on the sinusoid of the k th harmonic is given by

$$\frac{\pi x}{\tau} \pm \gamma_k = \text{constant} \quad (3)$$

and by differentiation
$$\frac{dx}{dt} = \mp \frac{\tau}{\pi} \frac{d\gamma_k}{dt} \quad (4)$$

that is, the particular point is *travelling in the positive or negative direction with a linear velocity* $\mp \frac{\tau}{\pi} \frac{d\gamma_k}{dt}$. The *direction* of travel is positive for $- \gamma_k$

and negative for $+ \gamma_k$. Thus (2) defines a system of travelling sinusoidal waves if the γ_k are functions of time.

It is also clear that the amplitudes β_k may be functions of time. For example

$$\beta_k = B_k \cos n\omega t \quad (5)$$

Such a pulsation would give rise to a transformer component of induced voltage.

Thus (2) represents a distribution of flux density which may pulsate in place; or move along as a rigid distribution, or break up into individual harmonics pulsating at different rates and travelling in either direction at different speeds.

The next operation is to find the flux which such a distribution causes to link with the (movable) coil at a given instant. This is also quite easy to do. Again referring to Fig. 11b, let the mid-point of the coil be located a distance x_0' from the reference axis, and suppose the coil pitch is $p\tau$ where p is some fraction. The coil is then said to have a *fractional pitch*. Let l be the axial length of the coil along the armature, perpendicular to the motion. The flux linked with the coil then is

$$\begin{aligned}\phi &= \int_{x_0' - p\tau/2}^{x_0' + p\tau/2} l \beta dx = \int_{x_0' - p\tau/2}^{x_0' + p\tau/2} l \sum_{\nu} \beta_{\nu} \sin \left(\frac{\pi x}{\tau} \pm \gamma_{\nu} \right) dx \\ &= \frac{2}{\pi} l \sum \sin \frac{k p \pi}{2} \frac{\beta_{\nu}}{k} \sin k \left(\frac{\pi x_0'}{\tau} \pm \gamma_{\nu} \right)\end{aligned}\quad (6)$$

Thus the flux linked with the coil has the same sinusoidal distribution as the flux density, but the amplitudes have been reduced as their order. For instance, the fifth harmonic, $k = 5$, of flux is reduced to $\frac{1}{5}$ th the relative amplitude of the fifth harmonic of flux density. Moreover, if $p \neq 1$, each harmonic of flux is further reduced by the coefficient

$$K_{p\nu} = \sin \frac{k p \pi}{2} \quad (7)$$

This factor is called the *pitch coefficient*. It may have a value anywhere between -1 and $+1$, depending upon the pitch, p , and the harmonic order, k , as shown in Fig. 12 for several space harmonics. It may reduce,

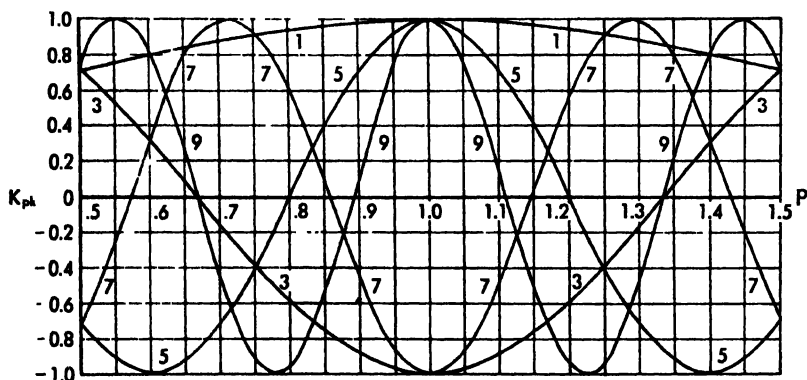


Fig. 12 Pitch factors

suppress, or even reverse a given harmonic. For example, let $p = 0.67$. Equation (7), or Fig. 12, shows that $K_1 = 0.87$, $K_3 = 0$, and $K_5 = -0.87$. Thus a $2/3$ pitch does not greatly alter the fundamental, but it suppresses the 3rd harmonic entirely and reverses the 5th harmonic. A $2/3$ pitch will

eliminate all multiple of 3 harmonics, and is often used for this purpose.

It will be remembered that the average value of a sine wave is $\frac{2}{\pi}$ times its amplitude, and the half-wavelength of a k th harmonic is τ/k (since by definition it has k wavelengths in a fundamental wavelength). Therefore the flux in a half-wavelength is

$$\phi_k = \frac{2}{\pi} B_k \frac{\tau}{k} l \quad (8)$$

Hence (6) may be rewritten

$$\phi = \sum K_{pk} \phi_k \sin k \left(\frac{\pi x_0'}{\tau} \pm \gamma_l \right) \quad (9)$$

It is possible also (Appendix IV) to take into account the effect of skewing the conductors an angle α , by introducing the *skew coefficient*

$$K_{sk} = \frac{\sin k\lambda \frac{2}{\tau}}{k\lambda \frac{2}{\tau}} \quad (10)$$

in which $\lambda = \frac{l \pi \tan \alpha}{\tau}$. This function is plotted in Fig. 13. It is evident

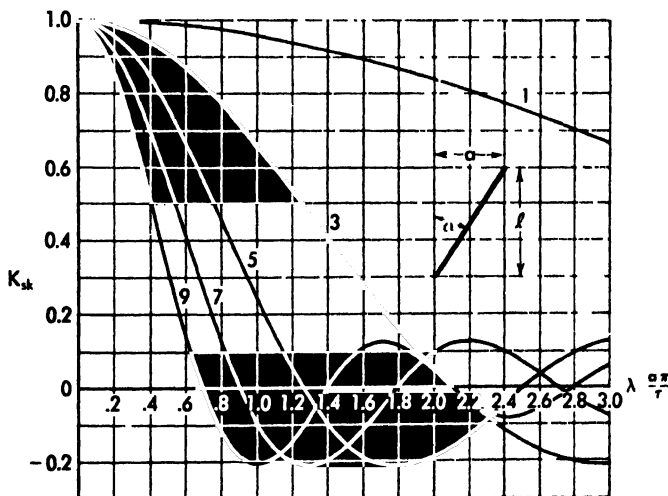


Fig. 13 Skew factor.

that a small amount of skew may be utilized to reduce the higher harmonics, such as cause telephone interference, but it is not practicable to use skew as a means of reducing the lower harmonics—say below the 11th. Skewing is usually resorted to in induction motors to obtain smoother running characteristics.

In (9) suppose ϕ_k , x'_0 and γ_k all to vary with time. Then by (1) the induced voltage is

$$e = -\frac{N}{10^8} \frac{d\phi}{dt} = -\sum \frac{N}{10^8} K_{pk} \left\{ \frac{\partial \phi_k}{\partial t} \sin k \left(\frac{\pi x'_0}{\tau} \pm \gamma_k \right) + k \phi_k \left(\frac{\pi}{\tau} \frac{dx'_0}{dt} \pm \frac{d\gamma_k}{dt} \right) \cos k \left(\frac{\pi x'_0}{\tau} \pm \gamma_k \right) \right\} \quad (11)$$

Here the three processes of voltage induction are easily identified with the three terms

$$\left. \begin{aligned} \frac{\partial \phi_k}{\partial t}, & \text{ variation of the flux} \\ \frac{dx'_0}{dt}, & \text{ movement of the conductors} \\ \frac{d\gamma_k}{dt}, & \text{ movement of the field} \end{aligned} \right\} \quad (12)$$

This equation and its extensions will be invoked and emphasized repeatedly hereafter in the explanation and analysis of different types of machines. Indeed, it is the central feature of the book, and it is mandatory that the student understand thoroughly its derivation and implications.

But armature windings consist of several coils in series, uniformly distributed along the armature. Figure 14 shows such a group of q coils, separated by the slot pitch σ . The center of the coil group is at x_0 , and there-

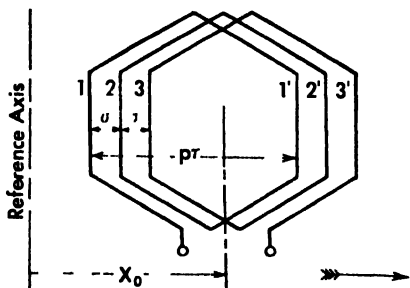


Fig. 14

fore the center of the h th coil from the end is at

$$x'_0 = x_0 - \frac{q+1}{2} \sigma + h\sigma \quad (13)$$

Suppose the voltage induced in this coil by a k th space harmonic of flux is

$$\begin{aligned} e_k &= E_k \left(\frac{\sin}{\cos} \right) k \left(\frac{\pi x'_0}{\tau} \pm \gamma_k \right) \\ &= E_k \left(\frac{\sin}{\cos} \right) \frac{k\pi}{\tau} \left(x_0 - \frac{q+1}{2} \sigma + h\sigma \pm \frac{\tau}{\pi} \gamma_k \right) \end{aligned} \quad (14)$$

In this equation the notation $\left(\frac{\sin}{\cos}\right)$ means that either or both may be used.

Then the voltage of the entire group of coils due to the k th space harmonic of flux is

$$\sum e_k = \sum_1^q E_l \left(\frac{\sin}{\cos}\right) \frac{k\pi}{\tau} \left(x_0 - q + \frac{1}{2} \sigma + h\sigma \pm \frac{\tau}{\pi} \gamma_l\right) \quad (15)$$

and this requires that q voltages of equal magnitude, but differing in phase by the angle $\alpha = k\pi\sigma/\tau$, be added. This may be done by the analytical method of Appendix I, but it is usually more instructive to do it geometrically, as shown in Fig. 15. Obviously, the several equal voltages form a polygon with equal exterior angles α and equal interior angles $(\pi - \alpha)$, and therefore are chords on a circle of radius

$$R = \frac{e}{2 \sin \frac{\alpha}{2}}$$

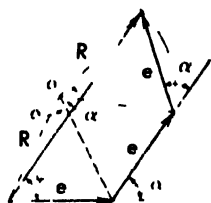


Fig. 15

and subtend at the center of the circle a total angle $(q\alpha)$. Therefore, the resultant voltage is

$$\sum e = 2R \sin \frac{q\alpha}{2} = \frac{\sin(q\alpha/2)}{\sin(\alpha/2)} e$$

or substituting for α

$$\sum e = \frac{\sin(k\pi q\sigma/2\tau)}{q \sin(k\pi\sigma/2\tau)} (q e) = K_{dk}(q e) \quad (16)$$

in which K_{dk} is the *distribution factor* of the phase belt.

Moreover, the resultant voltage is displaced ahead from the voltage in the first, $h = 1$, coil by the angle

$$\psi_{dk} = \frac{\pi - \alpha}{2} - \frac{\pi - q\alpha}{2} = \frac{q - 1}{2} \alpha = \frac{q - 1}{2} \frac{k\pi\sigma}{\tau}$$

so that the resultant voltage is

$$\begin{aligned} \sum e_k &= K_{dk} q E_l \left(\frac{\sin}{\cos}\right) \frac{k\pi}{\tau} \left(x_0 - q + \frac{1}{2} \sigma \pm \frac{\tau}{\pi} \gamma_l \pm \frac{\tau}{k\pi} \psi_{dk}\right) \\ &= K_{dk} q E_l \left(\frac{\sin}{\cos}\right) \left(\frac{k\pi x_0}{\tau} + k\gamma_l\right) \end{aligned} \quad (17)$$

Thus the effect of distribution is to reduce the voltage by the distribution factor K_{dk} and to displace it by the angle ψ_{dk} .

Hence by (17) and (11) the coil group voltage is

$$e_g = -\sum \frac{q_k V}{10^4} K_{pk} K_{dk} \left\{ \frac{\partial \phi_k}{\partial t} \sin k \left(\frac{\pi x_0}{\tau} \pm \gamma_k \right) + k \phi_k \left(\frac{\pi}{\tau} \frac{dx_0}{dt} + \frac{d\gamma_k}{dt} \right) \cos k \left(\frac{\pi x_0}{\tau} \pm \gamma_k \right) \right\} \quad (18)$$

The distribution factor K_{dk} is plotted in Fig. 16 for several harmonics for 3 phase machines with 60 degree phase belts, that is, $q\sigma = \tau/3$. The curves are valid for integer slots-per phase-per-pole only

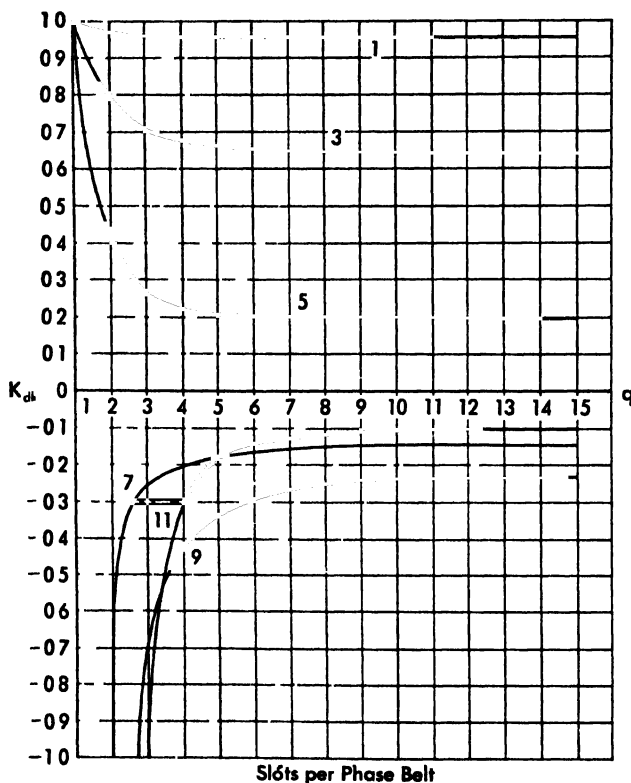


Fig. 16 Distribution factors

Finally, if several phases are interconnected, as in a star or zigzag, the resultant line voltage may have a different harmonic content than the phase voltages. If a harmonic voltage has the same magnitude E_k in each phase, but different phase angles $k\theta_r$, the resultant harmonic voltage for c phases connected in series is

$$E_k' = E_k \sum (\cos k\theta_r + j \sin k\theta_r) = K_{c,k}(E_k) \psi_{c,k} \quad (19)$$

in which

$$\left. \begin{aligned} K_{\phi} &= \frac{1}{c} \sqrt{(\sum \cos k\theta_i)^2 + (\sum \sin k\theta_i)^2} = \text{phase connection factor} \\ \psi_{\phi} &= \tan^{-1} \left(\frac{\sum \sin k\theta_i}{\sum \cos k\theta_i} \right) = \text{phase displacement angle} \end{aligned} \right\} \quad (20)$$

This factor and its associated displacement angle are tabulated for a few simple cases in the following table.

TABLE I
THE PHASE CONNECTION COEFFICIENT AND ANGLE

Connection k	1	3	5	7	9	11	13	15	17	19
ϕ Delta K_{ϕ}	1	1	1	1	1	1	1	1	1	1
ψ_{ϕ}	0	0	0	0	0	0	0	0	0	0
ϕ 1 K_{ϕ}	$\frac{\sqrt{3}}{2}$	0	$\frac{\sqrt{3}}{2}$	$\frac{\sqrt{3}}{2}$	0	$\frac{\sqrt{3}}{2}$	$\frac{\sqrt{3}}{2}$	0	$\frac{\sqrt{3}}{2}$	$\frac{\sqrt{3}}{2}$
ψ_{ϕ}	+30	0	+30	30	0	+30	0	0	+30	30
2 ϕ K_{ϕ}	1	1	1	1	1	1	1	1	1	1
ψ_{ϕ}	$\sqrt{2}$ +45	$\sqrt{2}$ 45	$\sqrt{2}$ +45	$\sqrt{2}$ 45	$\sqrt{2}$ +45	$\sqrt{2}$ 15	$\sqrt{2}$ +45	$\sqrt{2}$ 45	$\sqrt{2}$ +45	$\sqrt{2}$ 45
ϕ Star K_{ϕ}	$\frac{1}{2}$	1	$\frac{1}{2}$	$\frac{1}{2}$	1	$\frac{1}{2}$	$\frac{1}{2}$	1	$\frac{1}{2}$	$\frac{1}{2}$
ψ_{ϕ}	60	0	+60	60	0	+60	60	0	+60	60
ϕ Zigzag K_{ϕ}	$\frac{1}{2}$	0	$\frac{1}{2}$	$\frac{1}{2}$	0	$\frac{1}{2}$	$\frac{1}{2}$	0	$\frac{1}{2}$	$\frac{1}{2}$
ψ_{ϕ}	-60	0	+60	60	0	+60	60	0	+60	60

Four different harmonic reduction factors have been described—skew, pitch, distribution, and connection. While these reducing factors have different names, they are in fact due to the same essential cause

the arrangement of the winding so that the harmonic voltages produced in different parts are in partial or complete opposition, and thus tend to cancel out over the complete circuit. Figure 17 shows how this is accomplished in the case of the third harmonic.

If the conductor is skewed or spiralled so that half of it is cutting through a positive loop, and the other half through a negative loop of the harmonic of space distribution, then the voltage induced in the two halves of the conductor are always in direct opposition and therefore completely cancel within the conductor itself. The second simplest method of cancellation is to use a coil of fractional pitch so that both coil sides are cutting through positive loops of flux, but the voltages

generated thereby cancel in the coil. In this case the coil may be either of short or long pitch. The distribution of the winding in more than one slot per phase gives rise to a reduction of the harmonic voltages between the coils which make up the phase group. Finally, it is possible to eliminate those harmonics which are multiples of the number of machine phases, by connecting phases in series.

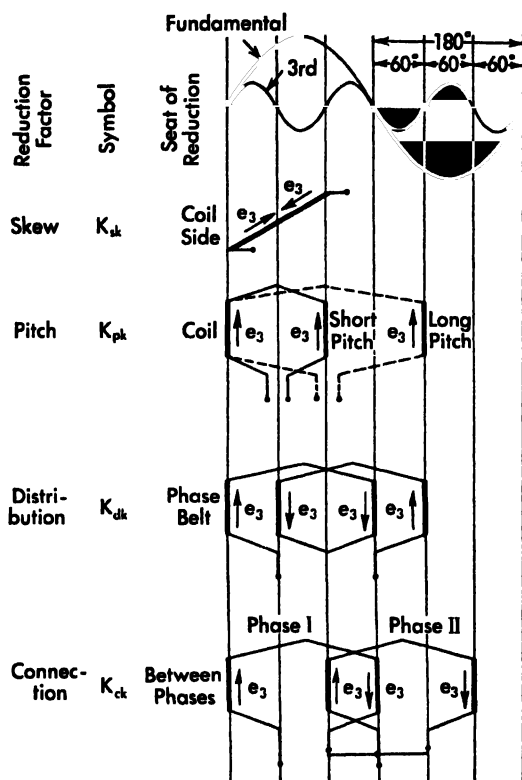


Fig. 17 Harmonic reduction.

As a rule it is desirable to suppress as many harmonics as possible at the least cost to the fundamental. For all harmonics are more or less objectionable, but when they are suppressed in such a way as to reduce materially the amplitude of the fundamental it means more flux in the air gap, more excitation, and possibly higher losses, or even a larger sized machine. It must be understood that other considerations than the relative efficiency have a decided bearing on the choice of a method of harmonic reduction. Thus if either skewing or fractional pitch is an

available method in a given case, the fractional pitch would undoubtedly be the choice; because it is less expensive to make straight slots and coils, there is considerable saving in copper and copper losses on account of shorter end windings, and for the same reason a possibly shorter machine with less windage loss.

The following Table II is a recapitulation of the several reduction factors:

TABLE II
THE HARMONIC REDUCTION FACTORS

	Reduction factor	Seat of the reduction
Skew factor	$K_s = \frac{\sin(k\lambda/2)}{k\lambda/2}$	In the coil side
Pitch factor	$K_{pk} = \sin \frac{kp\pi}{2}$	Between coil sides of the coil
Distribution factor of belt	$K_{dt} = \frac{\sin(k\pi q\sigma/2\tau)}{q \sin(k\pi\sigma/2\tau)}$	Between coils of the phase belt
Connection factor	$K_{cl} = \sqrt{(\sum \sin k\theta_i)^2 + (\sum \cos k\theta_i)^2}$	Between phases

Example: A 4-pole, 1800-rpm, synchronous machine has a double-layer winding and $Q = 72$ slots. The air-gap diameter is $d = 17.5$ inches and the effective length of the armature stacking is $l = 10.9$ inches. The slots are skewed $a = 1.75$ inches. The armature winding has $m = 6$ coil groups per pair of poles, each coil having $N = 8$ turns and $p = 0.833$ pitch. The coil groups are connected in series for 3-phase wye. The flux density distribution in kilolines per square inch, is given by

$$B = 47.2 \sin \frac{\pi x}{\tau} + 3.0 \sin \frac{3\pi x}{\tau} + 0.5 \sin 5\left(\frac{\pi x}{\tau} - 36^\circ\right) + 0.3 \sin 7\left(\frac{\pi x}{\tau} - 26^\circ\right)$$

$$\tau = \frac{\pi d}{p} = \frac{\pi 17.5}{4} = 13.75 \text{ pole pitch}$$

$$\sigma = \frac{\pi d}{Q} = \frac{\pi 17.5}{72} = 0.765 \text{ slot pitch}$$

$$q = \frac{2Q}{mP} = \frac{2 \times 72}{6 \times 4} = 6 \text{ slots phase belt} = 6 \text{ coils phase belt}$$

Then the flux components (kilolines) and harmonic reduction factors for the various harmonics are:

	Eq.	Fig.	Harmonic (k)			
			1	3	5	7
ϕ_k	(8)		4500	96	10	4
K_{sk}	(10)	3	0.99	0.94	0.84	0.70
K_{pk}	(7)	2	0.97	-0.71	0.26	0.26
K_{dk}	(16)	6	0.96	0.64	0.20	-0.15
K_k	$K_{sk} K_{pk} K_{dk}$		0.92	-0.43	0.043	-0.027

The field flux neither varies nor moves, and therefore the only term present in the voltage equation (18) is that due to the motion of the conductors. The angular velocity of the conductors is

$$\frac{\pi}{\tau} \frac{dv_n'}{dt} = \frac{\pi}{\tau} \pi d (rps) = \pi P \frac{rpm}{60} = \omega_n = 120\pi \text{ radians, sec.}$$

$$\therefore \frac{\pi}{\tau} \Delta v_n' = \omega_n t = 120 \pi t$$

Then by (18) the voltage induced in the coil group is

$$\begin{aligned} e &= - \frac{8 \times 6 \times 120\pi}{10^8} \left[0.92 \times 4500 \cos \omega_n t - 0.43 \times 288 \cos 3\omega_n t - 0.043 \right. \\ &\quad \left. \times 50 \cos 5(\omega_n t - 36^\circ) - 0.027 \times 28 \cos 7(\omega_n t - 26^\circ) \right] \\ &= -750 \cos \omega_n t + 22 \cos 3\omega_n t + 0.4 \cos 5(\omega_n t - 36^\circ) - 0 \end{aligned}$$

Thus the 5th and 7th harmonics are quite negligible.

A 3 phase, wye connection is obtained by connecting in series the coil groups occupying the same relative position under each pole (reversing the leads of alternate coil groups). The three phases thus formed are then connected in wye. The phase voltages are then four times the coil group voltages given above. According to (19) and Table I, the line voltages will be $\sqrt{3}$ times as great for the fundamental, the fifth and the seventh harmonic, but the third harmonic is eliminated completely. The final rms line to-line voltage therefore is

$$E = \frac{\sqrt{3}}{\sqrt{2}} 750 \times 4 = 3670$$

Problems

1. According to Equation (8), relative to the fundamental, the k th harmonic of flux is only $1/k$ th as important as the k th harmonic of flux density. What is the *physical* reason for this?

2. In the case of the coil of Fig. 11, suppose the flux is a rigid distribution pulsating in time, thereby inducing a transformer voltage in the coil. In the light of (11), would it be possible to move the coil at such a speed as to just nullify the transformer voltage by an equal and opposite speed voltage?
3. Confirm the geometry of Fig. 15 used in arriving at (16).
4. An alternator stator has 12 slots per pole. Compare its output if wound for single-phase, two-phase, three-phase, and six-phase. (Hint: The distribution factor will be different for each case.)
5. What attention would you pay to skew, pitch, or distribution factors if you wished to eliminate the 15th harmonic in the voltage of a wye-connected, three-phase generator? If you wished to eliminate a 3rd harmonic in a delta-connected machine?
6. Select a laboratory machine for which you can count the slots and determine dimensions. Calculate the skew, pitch and distribution coefficients of this machine for the fundamental and all harmonics up to the 21st
7. Compile tables of the distribution factor, K_{dk} , for 60°, 90°, 120°, and 180-degree phase belts having 2 to 8, as well as infinite, coils per belt, for all odd harmonics up to $k = 21$.
8. Draw curves of the skew factor, K_{sk} , such as shown in Fig. 13, for higher harmonics. What is the limiting value of the skew factor for very high harmonics?
9. How might the pitch factor, K_{pk} , be plotted, so that a single curve will suffice for all harmonics?
10. Suppose a machine has $2/3$ pitch and is delta-connected. By any means could it be made to deliver a 3rd-harmonic voltage?

4. Armature Reaction

The armature reaction of a distributed polyphase winding will be obtained in three steps. First, the magnetomotive force of a single fractional pitch coil will be found and expressed as a Fourier series. Then by vector addition an expression will be found for the magnetomotive force of a group of coils. And finally, the resultant armature reaction of all the phases will be developed. The same harmonic reduction factors encountered previously in the equations for the induced voltages will turn up again in the case of armature reaction. In the present discussion it will be assumed that no time harmonics are present. These are taken into consideration in the more general treatment given in Appendix II.

In Fig. 18 is shown a single coil of N -turns and pitch $p\tau$ carrying an instantaneous current i . The center of the coil is located at a distance x_0' from the arbitrary reference axis. Assuming the winding is of such a

nature that a similar coil a pole pitch away carries the same current (reversed), it is permissible to assume the magnetomotive force due to the two coils to be the blocked wave shown in Fig. 18. This wave has a magnetomotive force magnitude of $0.4\pi Ni$ and the magnetomotive force per coil, therefore, may be expressed by the Fourier series

$$F(x) = 0.8Ni \sum_1^{\infty} \frac{K_{pk}}{k} \cos \frac{k\pi}{\tau} (x - x_0') \quad (21)$$

in which K_{pk} is the pitch coefficient of (7). This equation shows that the space harmonics of armature reaction have magnitudes inversely proportional to their order, and in the case of fractional coil pitch they are further reduced by the pitch coefficients. The distribution is symmetrical about the mid-point of the coil, $x = x_0'$.

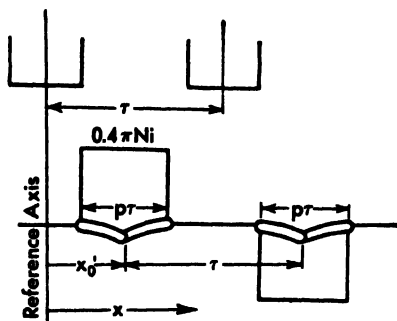


Fig. 18

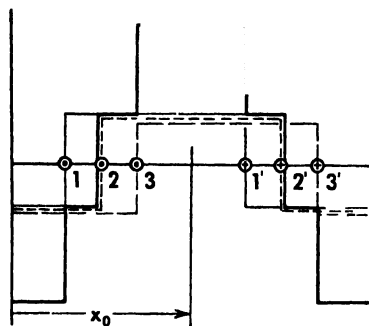


Fig. 19

Now consider a group of q coils displaced by the slot pitch σ and carrying equal currents i . Let the center of the group of coils be located at x_0 , as illustrated in Fig. 19 for the case of three full-pitch coils. The magnetomotive force of coil No. 1 is shown in light lines, that of No. 2 in dash lines and that of No. 3 in dotted lines. The resultant is shown in heavy lines. For any particular case the resultant blocked pyramid could be constructed as above and analyzed by Fourier's method to determine the harmonics. But it is easier and more general simply to add the Fourier series, (21), for each separate coil. For the h th coil, (13) holds, and the k th harmonic of magnetomotive force for the group of q coils therefore is

$$a_k(x) = 0.8Ni \frac{K_{pk}}{k} \sum_1^q \cos \frac{k\pi}{\tau} \left[x - x_0 + \frac{(q+1)\sigma}{2} - h\sigma \right] \quad (22)$$

But the addition of the q cosine terms leads to the distribution factor K_{dk} , and its displacement angle ψ_{dk} , just as in the case of the induced

voltages, (16). Therefore, the k th space harmonic of magnetomotive force for the group of coils is

$$a_k(x) = 0.8qNi \frac{K_{pk}K_{dk}}{k} \cos \frac{k\pi}{\tau} (x - x_0) \quad (23)$$

Thus distribution of the winding has further reduced each harmonic by its distribution factor K_{dk} .

Suppose, now, that the current is an alternating current

$$i = I_{\max} \sin (\omega t + \theta) \quad (24)$$

Substituting (24) in (23) and making an elementary trigonometric transformation, there results

$$\begin{aligned} a_k(x) &= 0.8q \frac{K_{pk}K_{dk}}{k} NI_{\max} \sin (\omega t + \theta) \cos \frac{k\pi}{\tau} (x - x_0) \\ &= 0.4q \frac{K_{pk}K_{dk}}{k} NI_{\max} \left\{ \sin \left[\omega t + \theta + \frac{k\pi}{\tau} (x - x_0) \right] \right. \\ &\quad \left. + \sin \left[\omega t + \theta - \frac{k\pi}{\tau} (x - x_0) \right] \right\} \quad (25) \end{aligned}$$

This equation may be interpreted as two equal sine waves travelling in opposite directions, because

$$\omega t + \theta \pm \frac{k\pi}{\tau} (x - x_0) = \text{constant} \quad (26)$$

defines a fixed point on the sine wave, and consequently the distance x from the reference axis at which (26) is satisfied progresses with time t . The velocity of progression is easily found by differentiating (26) with respect to t ,

$$\omega \pm \frac{k\pi}{\tau} \frac{dx}{dt} = 0$$

that is
$$\text{velocity} = \frac{dx}{dt} = \mp \frac{\omega\tau}{k\pi} \quad (27)$$

Thus one of the waves is travelling in the forward (positive) direction, and the other wave is travelling in the backward (negative) direction. Moreover, the velocity is inversely proportional to the order of the harmonic. For example, the 7th space harmonic travels only 1/7 as fast as the fundamental.

Referring to (25) and to Fig. 19, suppose the group of coils to be moving at some speed

$$\frac{\pi x_0}{\tau} = \omega_0 t \quad (28)$$

with respect to the reference axis. Then the arguments of the sine terms of (25) become

$$(\omega \mp k\omega_0)t \pm \frac{k\pi x}{\tau} + \theta$$

and the corresponding velocities of the harmonic magnetomotive forces, with respect to the reference axis, are

$$\frac{\pi}{\tau} \frac{dx}{dt} = \left(\omega_0 + \frac{\omega}{k} \right) \quad (29)$$

There are three special cases of this equation of importance in the analysis of rotating machines:

Reference Axis	ω_0	Velocity of Harmonic Waves
On the armature	0	$-\frac{\omega}{k}, \quad +\frac{\omega}{k}$
Stationary in space	ω	$\omega \frac{k-1}{k}, \quad \omega \frac{k+1}{k}$
Stationary in space	ω_0	$\omega_0 - \frac{\omega}{k}, \quad \omega_0 + \frac{\omega}{k}$

In the second case, when the armature is rotating at synchronous speed, it is seen that one component of the fundamental, $k = 1$, has zero velocity with respect to the reference axis, or is *stationary* in space.

It remains to determine the resultant armature reaction due to the entire polyphase winding. Consider a 3-phase machine for which the phase currents are

$$\left. \begin{aligned} i_1 &= I_{\max} \sin(\omega t + \theta) \\ i_2 &= I_{\max} \sin(\omega t + \theta - 120^\circ) \\ i_3 &= I_{\max} \sin(\omega t + \theta - 240^\circ) \end{aligned} \right\} \quad (30)$$

The current in phase-1 gives the armature reaction of (25). The current in phase-2 is lagging by 120 degrees in time, and this phase is 120 degrees behind in space. Therefore, if in (25) ωt is replaced by $(\omega t - 120^\circ)$, and $(\pi x_0 / \tau)$ is replaced by $(x_0 \pi / \tau - 120^\circ)$, that same equation will give the armature reaction of phase-2. Likewise, substituting $(\omega t - 240^\circ)$ and $(x_0 \pi / \tau - 240^\circ)$ in (25) will give the armature reaction for phase-3. Then for all three phases

$$A_A(x) = 0.4g \frac{K_{dl} K_{pt}}{k} N I_{\max} \left\{ \sin \left[\omega t + \theta \pm \frac{k\pi}{\tau} (x - x_0) \right] \right\}$$

$$\begin{aligned}
 & + \sin \left[\omega t + \theta - 120 + \frac{k\pi}{\tau} (x - x_0) + k120 \right] \\
 & + \sin \left[\omega t + \theta - 240 + \frac{k\pi}{\tau} (x - x_0) + k240 \right] \Big\} \\
 & \qquad \qquad \qquad (31)
 \end{aligned}$$

This is an equation of three sine waves distributed in *time* by the angle $(1 \mp k)120^\circ$, for which the sum is

$$\begin{aligned}
 & \sin (1 \mp k) 360^\circ \\
 & \sin (1 \pm k) 120^\circ
 \end{aligned}$$

It is zero unless $(1 \mp k)$ is zero or a multiple of 3 (the number of phases), in which case it is an indeterminate evaluating to 3. Hereby (31) may be written (putting $K_k = K_{dk}K_{pk}$ and $\pi x_0/\tau = \omega_0 t$)

$$\begin{aligned}
 A_k(x) &= 1.2q \frac{K_k}{k} NI_{max} \sin \left[\omega t + \theta + k \left(\frac{\pi x}{\tau} - \omega_0 t \right) \right] \Big\} \\
 & \qquad \qquad \qquad 1 \mp k = \text{multiple of 3 or zero.} \qquad \qquad \qquad (32)
 \end{aligned}$$

Therefore, the space harmonics of 3 phase armature reaction and their velocities with respect to the reference axis may be tabulated as follows:

k	Amplitude Factor	Velocity
1	$1.2qNK_1$	$(\omega_0 - \omega)$
3	(0)	
5	$1.2qNK_5$	$(\omega_0 + \omega/5)$
7	$1.2qNK_7$	$(\omega_0 - \omega/7)$
9	(0)	
11	$1.2qNK_{11}$	$(\omega_0 + \omega/11)$
13	$1.2qNK_{13}$	$(\omega_0 - \omega/13)$
15	(0)	
17	$1.2qNK_{17}$	$(\omega_0 + \omega/17)$
19	$1.2qNK_{19}$	$(\omega_0 - \omega/19)$

This table shows five interesting things about 3-phase armature reaction:

- (1) There are present no multiple of three space harmonics.
- (2) The amplitudes of the space harmonics rapidly diminish in importance due to the winding factors and to the factors k in the denominators. Consequently, for most purposes it is quite permissible to ignore them entirely, and to assume a sinusoidal distribution of armature reaction. Exceptions are in the calculation

of leakage reactance, and where certain harmonics must be avoided to prevent telephone interference or for other reasons.

- (3) The harmonics for which $(k - 1)$ is a multiple of 3 give rise to *backward* moving waves, while those for which $(k + 1)$ is a multiple of 3 give rise to *forward* moving waves with respect to a reference axis rigidly attached to the armature ($\omega_0 = 0$).
- (4) When the reference axis is fixed to the armature ($\omega_0 = 0$), the harmonic waves are going alternately in the negative and positive directions.
- (5) When the reference axis is stationary and the armature is moving in the forward direction at synchronous speed, $\omega_0 = \omega$, the armature reaction of the fundamental, $k = 1$, is constant and stationary in space, for by (32)

$$A_1(x) = 1.2qK_1 V I_{\max} \sin \left(\frac{\pi x}{\tau} + \theta \right) \quad (33)$$

If the armature is stationary and the field is revolving *backward* at synchronous speed, the reference axis may be taken on the field pole, and the same result is obtained, because the *relative* motion of the armature with respect to the field is then in the forward direction.

Equation (33) may be resolved into its *direct* and *quadrature* space components,

$$\begin{aligned} A_1(x) &= 1.2qK_1 V \left(I_{\max} \cos \theta \sin \frac{\pi x}{\tau} + I_{\max} \sin \theta \cos \frac{\pi x}{\tau} \right) \\ &= A_d \cos \frac{\pi x}{\tau} + A_q \sin \frac{\pi x}{\tau} \end{aligned} \quad (34)$$

the relative magnitudes depending on the power factor angle θ .

Problems

1. A 3-phase armature is wound with 120-degree phase belts, and has three 2 3 pitch coils per phase belt:
 - (a) Plot the magnetomotive force distribution for a single coil, assuming the areas of the positive and negative portions to be equal
 - (b) Plot the magnetomotive force distribution for a phase belt
 - (c) If the phases are excited by sinusoidal 3-phase currents, plot the resultant magnetomotive force at $\omega t = 0, 60, 120, 180, 240, 300$, and 360 .

Comment on: (1) any evidence of a *rotating field*, (2) any distortion in the magnetomotive force wave, (3) the average to the maximum magnetomotive force at different instants.

2. For the above machine, calculate the harmonics of armature reaction, with respect to the armature, by (32), after putting $\omega_d t = 0$.
 - (a) Compare the superposition of these harmonics of magnetomotive force with the block waves in the problem above.
 - (b) Explain the distortion shown by the block waves in terms of (32).
3. At what armature speed will the 7th harmonic magnetomotive force remain fixed in space with respect to the field pole? At what speed will the 5th harmonic magnetomotive force remain fixed in space with respect to the field pole?
4. According to (29), single-phase armature reaction possesses a forward and a backward travelling wave of fundamental wavelength. But according to (32), the space fundamental for 3-phase armature reaction is only a forward wave. What happened to the backward wave?

5. Reactances

The reactances of rotating machines are numerous, complicated, and often difficult to calculate. A considerable part of electrical machine design is given over to their evaluation; and operating characteristics are vitally dependent upon them. Some of these reactances (*i.e.* slot, end-turn, and air gap) are common to all rotating machines, while others (*i.e.* synchronous, direct and quadrature, transient and sub-transient, field leakage, and others) are peculiar to certain kinds of machines only. These reactances depend, too, on whether the machine is in the steady state or undergoing transients, and whether the load is balanced or unbalanced. Table III is a rough classification of the more important reactances.

Not all of these are independent, but rather depend upon different points of view. For example, of the total flux in the air gap, some links both field and armature and its fundamental space component is usually taken as the main useful flux. But certain harmonics in the air gap flux induce fundamental voltages which lag the main flux voltage by 90 degrees, and these may be considered either as a part of the armature reaction (see Appendix IV), or as a combination of reactances based on physical concepts (tooth-tip, zigzag, belt, and differential). The former point of view is the more rational, but the latter point of view is well established in text books and in design practice. In order to acquaint the student with the different prevalent ideas, this text provides a detailed analysis of harmonic air-gap fluxes and corresponding reactances in Appendix IV, but also offers a brief description of differential leakage reactance in Chapter 4 on the polyphase induction motor.

The present chapter is restricted to consideration of slot and end-turn leakage reactance. The other reactances are discussed either in the Appendices, or with respect to the machines to which they specifically apply.

TABLE III

Operating Condition	Leakage Reactance	Reactance of Armature Reaction	Synchronous Reactance
Steady state	Slot End-turn Differential tooth-tip zigzag belt Potier	Fundamental Harmonic	Direct Quadrature
Unbalanced load	Positive sequence Negative sequence Zero sequence	Positive sequence Negative sequence Zero sequence	Positive sequence Negative sequence Zero sequence
Transient	Field Armature Amortisseur		Transient Sub-transient

Slot leakage reactance is due to those flux linkages with the conductors in the slot by flux which crosses the slot, but which does not enter the air gap. This type of leakage reactance is common to all machines having conductors embedded in slots. In the case of double-layer windings,

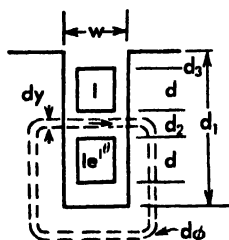


Fig. 20

there are two coil sides (belonging to different coils) in each slot, and every coil has one of its coil sides in the top of a slot and its other coil side in the bottom of a slot. The two coil sides in a slot may belong to the same phase or one may belong to one phase and the other to a different phase.

Figure 20 shows a slot having two coil sides of N -conductors each, carrying currents I and $I\theta$ respectively. The flux linkages may be calculated on the basis of the following assumptions:

1. The flux goes straight across the slot.
2. The iron part of the path is infinitely permeable.

3. The redistribution of currents in the conductor due to skin effect may be ignored.
4. The top and bottom coil sides are identical.
5. The winding arrangement is such that for every slot carrying I in the top and $I'\theta$ in the bottom conductor there will be another slot in which these are interchanged.

Referring to Fig. 20, there are four different regions to be considered. In each region the reluctance of an elementary path is w/dx , where l is the length of the slot, and the magnetomotive force acting on this path is 0.4π times the total current below it.

With I in the top of the slot and $I'\theta$ in the bottom of the slot, the interlinkages are

$$\begin{aligned}\lambda_1 &= 0.4\pi \frac{l}{w} N^2 \left[(I + I\epsilon^\theta)I d_3 + \int_0^d \left(\frac{y}{d} I + I\epsilon^\theta \right) \frac{y}{d} I dy \right] \\ &= 0.4\pi \frac{l}{w} N^2 I^2 \left[(1 + \epsilon^\theta) d_3 + \left(\frac{1}{3} + \frac{\epsilon^\theta}{2} \right) d \right]\end{aligned}$$

With I in the bottom of the slot and $I - \theta$ in the top of the slot, the interlinkages are

$$\begin{aligned}\lambda_2 &= 0.4\pi \frac{l}{w} N^2 \left[(I + I\epsilon^{-\theta})I d_3 + \int_0^d \left(\frac{y}{d} I\epsilon^{-\theta} + I \right) I dy \right. \\ &\quad \left. + I^2 d_2 + \int_0^d \left(\frac{y}{d} I \right)' dy \right] \\ &= 0.4\pi \frac{l}{w} N^2 I^2 \left[(1 + \epsilon^{-\theta}) d_3 + \left(\frac{4}{3} + \frac{\epsilon^{-\theta}}{2} \right) d + d_2 \right]\end{aligned}$$

The total interlinkages per ampere multiplied by 10^{-8} is the inductance

$$L = \frac{\lambda_1 + \lambda_2}{10^8 I^2} = \frac{0.4\pi l}{10^8 w} N^2 \left[2(1 + \cos \theta) d_3 + d_2 + \left(\frac{5}{3} + \cos \theta \right) d \right] \quad (35)$$

The above equation gives the reactance of a coil, one of whose coil sides is in the top of a slot shared by a coil side out of phase by an angle θ , and whose other coil side is in the bottom of a slot shared by a coil side out of phase by $-\theta$. It remains to identify the angle θ , and the portions of a coil belt to which they apply. Figure 21 indicates an m -phase winding (shown for $m = 6$), each phase belt spanning $2\pi/m$ radians. The phase belts in the tops of the slots are numbered $1, 2, 3, \dots$, while the return belts in the bottoms of the slots are numbered $1', 2', 3', \dots$. If the coil pitch is $p\pi$, it is clear that belt $1'$ will, in general, be covered

by two other phase belts (3 and 4 in the illustration). To find these belts, divide

$$\frac{2\pi/m + p\pi}{2\pi/m} = 1 + \frac{mp}{2} = \alpha + \beta$$

where

α is the integer part

β is the fractional part

Then the belts covering $1'$ in the tops of the slot are α and $(\alpha + 1)$.

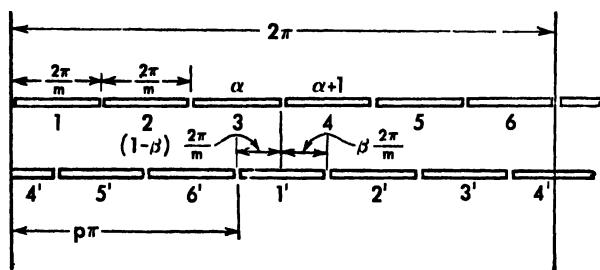


Fig. 21

The overlaps between $1'$ and α and between $1'$ and $(\alpha + 1)$ are respectively

$$\frac{2\pi}{m} (1 - \beta) \quad \text{and} \quad \beta \frac{2\pi}{m}$$

The phase angle of $1'$ is π and that of α and $\alpha + 1$ are $(\alpha - 1)2\pi/m$ and $\alpha 2\pi/m$ respectively; so that the angles between $1'$ and its mates are $(\alpha - 1)2\pi/m - \pi$ and $\alpha 2\pi/m - \pi$. A little consideration will show that the coil sides in the bottom of the slots occupied by 1 have the same overlaps as for $1'$, and are out of phase with 1 by $[\pi - (\alpha - 1)2\pi/m]$ and $[\pi - \alpha 2\pi/m]$ respectively.

Therefore, if there are q slots per phase per pole

$$\theta = \pi - (\alpha - 1) \frac{2\pi}{m} \quad \text{for } \beta q \text{ slots}$$

$$\theta = \pi - \alpha \frac{2\pi}{m} \quad \text{for } (1 - \beta)q \text{ slots}$$

and then by (35) the inductance per phase belt is (for N turns per coil)

$$L = \frac{0.4\pi}{10^8} \frac{l}{a} N^2 q \left\{ 2 \left[1 - \beta \cos \frac{(\alpha - 1)2\pi}{m} - (1 - \beta) \cos \frac{\alpha 2\pi}{m} \right] d_3 + d_2 \right. \\ \left. + \left[5 - \beta \cos \frac{(\alpha - 1)2\pi}{m} - (1 - \beta) \cos \frac{\alpha 2\pi}{m} \right] d_1 \right\}$$

$$= \frac{0.4\pi}{10^8} \frac{l}{\omega} N^2 q \left\{ 2Kd_3 + d_2 + \left(\frac{2}{3} + K \right) d \right\} \quad (36)$$

in which K is the coefficient of d_3 .

This factor K accounts for the out-of-phase currents in the slots occupied by a phase belt. It depends essentially on the pitch and on the number of phase belts per pair of poles. For typical constructions it reduces to the values given in the following table:

m	Pitch	K
6	$0.67 < p < 1.00$	$1.5p + 0.5$
6	$0.33 < p < 0.67$	$3.0p - 0.5$
6	$0.00 < p < 0.33$	$1.5p$
3	$0.67 < p < 1.00$	1.5
3	$0.00 < p < 0.67$	$2.25p$
4	$0.00 < p < 1.00$	$2p$
2	$0.00 < p < 1.00$	$2p$
∞	p	K_a^2

End turn leakage reactance is due to that flux linking the end turns which induces fundamental frequency voltages in the conductors. P. L. Alger* has analyzed this component of reactance as due to two sets of currents: (1) the axial currents flowing parallel to the shaft, and (2) the peripheral currents flowing circumferentially. The resolution of the current in an end conductor into these two space components is indicated in Fig. 22 as I_a and I_p respectively.

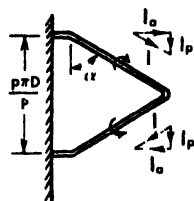


Fig. 22 End turn leakage.

Now as far as the axial components of current are concerned, they may be regarded as producing rotating fields of flux in exactly the same way as do the axial currents in the armature stacking, and these fields induce reactance voltages in the same way. There are, however, two major differences to be considered in comparing the voltages induced by axial currents in the stacking and in the end turns. First, in the case of the main winding the pitch factor K_p is constant for a given space harmonic; but in the case of the end winding it tapers from K_p at the iron to zero at the ends, and at any distance x from the ends it is $\sin p\pi x/2$. (The distribution factor, K_d , is the same for main windings or end turns.) But the winding factor enters

* Alger, P. L., "Calculation of the Armature Reactance of Synchronous Machines," *AIEE Trans.*, Vol. 47, 1928.

the reactance formula as the square — once because it appears in the magnetomotive force equation, and again because it appears in the electromotive force equation. Consequently, the proper pitch factor squared to use for the end turns is the average value:

$$K_p'^2 = \int_0^1 \sin^2 \frac{p\pi x}{2} dx = \frac{p\pi}{2p\pi} \frac{\sin p\pi}{2p\pi}$$

The second major difference to observe is that the end windings are in air, rather than embedded in the iron slots. It may be shown that a polyphase current sheet in air, of crest magnetomotive force A , will produce a sinusoidal flux per pole, per unit axial length, equal to the average of the magnetomotive force A_{av} . The span of a coil of pitch p on an armature of diameter D and number of poles P is $p\pi D/P$. If the end windings make an angle α with the iron of the core, they will project a distance $(p\pi D/P) \tan \alpha$ beyond the core for both ends. This is the effective length of the end turns for the axial components of current.

The armature reaction per pole of the end turns for an m -phase machine is, by (33),

$$A = 0.4mqNK_dK_p'I_{\max}$$

Therefore the end-turn flux per pole is

$$\phi_e = \frac{2}{\pi} (0.4mqNK_dK_p'I \sqrt{2}) \frac{p\pi D}{P} \tan \alpha$$

This flux will induce a reactance voltage in the $qNP/2$ turns,

$$\begin{aligned} E &= \frac{2\pi}{\sqrt{2} \cdot 10^8} f K_d K_p' q N \frac{P}{2} \phi_e \\ &= \frac{8\pi}{10^9} mf (K_d K_p' q N)^2 p D \tan \alpha I \end{aligned}$$

Alger takes the peripheral currents as concentrated in a ring located a distance from the iron equal to the center of gravity of the currents, and of circular cross-section having a diameter equal to half the axial projection of the end turns. Since this part of his analysis is rather arbitrary, it is omitted here. He finds the total end-turn reactance to be

$$x_e = \frac{8\pi}{10^9} mf (K_d q N)^2 \left[K_p'^2 D \tan \alpha + K_p'^2 D \frac{1 + 0.12p^2}{3} \right] \quad (37)$$

To compensate for the irregular peripheral space distribution of the end-turn magnetomotive force, he shows that the distribution factor K_d may be taken equal to unity.

Differential (or air gap) leakage reactance accounts for all fundamental-

frequency voltages induced by the space harmonics of armature reaction, but not including that due to the space fundamental. This latter is considered as armature reaction rather than as leakage reactance. A complete solution is rather involved, depending as it does on a general harmonic analysis of the air-gap fluxes. This is carried out in detail for a salient pole synchronous machine in Appendix IV and will not be repeated here. A somewhat similar analysis can be made for the induction motor.

In general, then, the total leakage reactance of a rotating machine (in the steady state) is

$$x_l = x_{\text{slot}} + x_{\text{ind}} + x_{\text{air gap}} \quad (38)$$

The first two terms are of the same form for most machines, but the air-gap term is different for different types of machines. General formulas will be found in this text for the synchronous generator and induction motor.

4 The Polyphase Induction Motor

1. Introduction

In the polyphase induction motor the energy is transferred electromagnetically from the primary (stator) windings to the secondary (rotor) windings, and the currents thus induced in the rotor react on the field of the stator to produce motor torque. There are no electrical interconnections between stator and rotor. The polyphase induction motor may have closed rotor windings, or be provided with slip rings and brushes for connection to an external circuit. In the latter case the machine has been called "the general alternating current transformer," since electrical energy of a given voltage, frequency, and number of phases in the primary windings may be converted in the rotor partly to mechanical and partly to electrical energy of a different voltage, frequency, and number of phases. Thus a single machine may be motor, transformer, frequency converter, and phase converter. The polyphase induction motor is the simplest and most rugged of all motors, and it can be designed with characteristics suitable for all except very special load requirements. Its efficiency and power factor are not as good as in some other types of motors, but it is cheaper to build, and is generally the most desirable and most extensively used for industrial applications, particularly for approximately constant speed loads.

2. Principles of Operation

The essential feature in the theory of polyphase induction motor is the revolving field produced by the stator, although the theory may be developed from other points of view. In this preliminary survey of the principles of operation of the motor, it will suffice to give a pictorial representation of the physics involved. The mathematical development will follow in a later section.

Figure 1 shows a stator core stacking V.S having a 3 phase winding consisting of coils 1-1', 2-2', and 3-3' displaced 120 degrees apart in space, and excited by polyphase currents 120 degrees apart in time. Actually, the winding would be made up of several coils for each phase but for our present purpose concentrated coils are assumed. The instantaneous phase currents are given in Fig. 2(a),

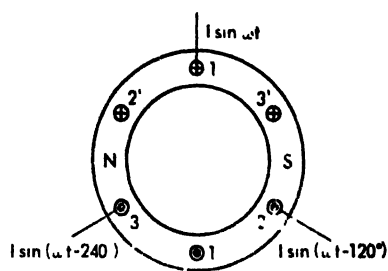


Fig. 1

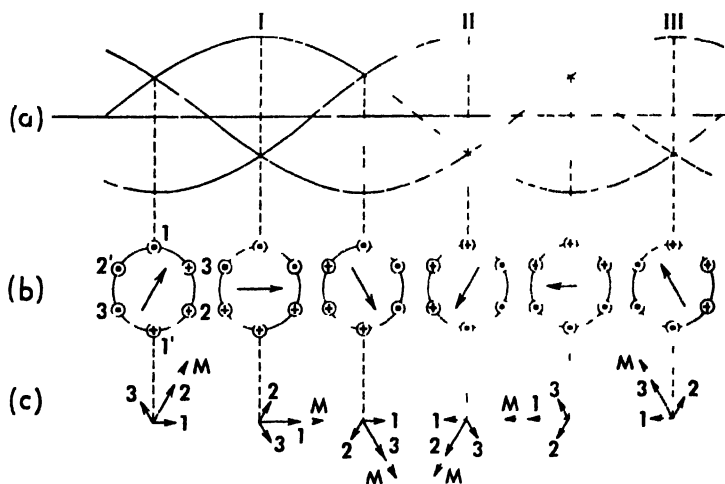


Fig. 2 Rotating field due to polyphase windings
(a) phase currents supplied to the windings
(b) instantaneous currents and mmf
(c) directions and magnitudes of mmf

and the current directions in the coils for different instants of time, are shown in Fig. 2(b). It is evident that the resultant magnetomotive force, represented by the arrow, is rotating synchronously in the clockwise

direction. The vectors for the instantaneous magnetomotive force of each coil are shown in Fig. 2(c). The resultant magnetomotive force is seen to be constant in magnitude, at least for the various instants selected. It will be proven later that it is constant in magnitude for all instants of time. The speed of the revolving field in rpm is given by

$$n_1 = \frac{120}{P} f$$

where P = number of poles and f_1 is the frequency.

The rotating magnetomotive force of constant magnitude, acting on the permeance of the air gap, produces a synchronously rotating field of flux; and this flux, sweeping by the conductors of stator and rotor, induces electromotive forces in them. As a result of this induced electromotive force, rotor currents flow, and these currents react on the field causing the rotor to revolve. If the rotor is stationary, the rotating field cuts its conductors at synchronous speed, inducing a voltage E_2 and rotor currents are of line frequency. But if the rotor is revolving at speed n_2 , the rotating field is cutting the rotor conductors at a relative speed of $n_1 - n_2 = sn_1$, where the fraction $s = 1 - n_2/n_1$ is called the *slip*. The rotor voltage is then only sE_2 of that at standstill, and the frequency is only $f_2 = sf_1$, thus approaching d-c conditions as the speed nears synchronism ($s = 0$). If the rotor were to reach synchronous speed, $n_2 = n_1$, the relative speed between rotating field and rotor would be zero, and consequently no voltages would be induced, nor could any rotor currents flow to produce torque. Consequently, the rotor must always revolve at less than synchronous speed in order to produce torque. At synchronous speed its power and torque are zero.

The rotor itself is a polyphase winding, and the polyphase currents induced in it produce a rotating field revolving at slip speed with respect to the rotor. However, the rotor is revolving at $(1 - s)$ speed, so that the rotor field is actually revolving at synchronous speed relative to the stator, and the two fields may be superimposed.

The rotor currents of slip frequency are determined by the rotor voltage and the rotor impedance. Rotor reactance at normal speed is relatively small compared with its resistance, since the frequency is low (running slip is of the order of one or two per cent and slip frequency is only a cycle or two). Thus at normal speed it is the rotor resistance, rather than the reactance, which determines the rotor current, and this current is of high power factor. But during starting, when the frequency of the rotor currents is high, the reactance ($2\pi f_2 L$) dominates, and the rotor current then has a low power factor.

The rotating flux is the resultant of the stator and rotor currents, and the relative magnitude and phase of these two currents must be such as to provide the necessary excitation at all times, just as in the transformer. However, the existence of an air gap in the induction motor requires a relatively higher magnetizing component of current in the motor than in the transformer. The bulk of the hysteresis and eddy-current losses (proportional to $f^{1.6}$ and f^2 respectively) are found in the stator of the motor, since the rotor slip frequency is very low. But an additional component of core loss is introduced by the high-frequency pulsation of the flux in the rotor teeth as they pass the stator teeth. The exciting current of the induction motor may be 20 to 40 per cent of the rated current, as compared to 2 to 10 per cent in a transformer.

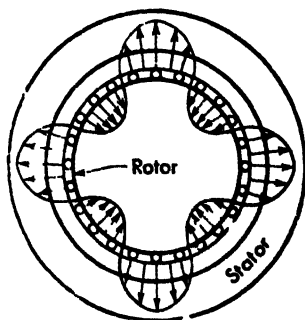


Fig. 3 Stator and rotor poles in cage

It is clear from Fig. 3 that the stator magnetomotive force induces the same number of poles on the rotor as on the stator.

3. Construction

Structurally, the induction motor consists of a laminated stator core in the slots of which are embedded the polyphase winding, a laminated rotor core in the slots of which are embedded the rotor conductors, and the frame with its end bells, shaft bearings, and foundation plate.

Induction motors are classified with respect to their rotor construction as *squirrel cage*, *double squirrel cage*, and *wound rotor*. The squirrel cage motors are further classified with respect to their characteristics and duty as follows:

Class	Torque	Starting Current	Slip	Method of Starting
A	Normal	Normal	Low	Compensator or full voltage
B	Normal	Low	Low	Full voltage
C	High	Low	Low	Full voltage
D	High	Low	High	Full voltage
E	Low	Normal	Low	Compensator
F	Low	Low	Low	Full voltage

Induction motors are also classified with respect to the kind of service which they are to perform *dustproof*, *splashproof*, *totally enclosed*, *explosion-proof*, etc.

Figure 4 is a photograph of a standard line of semi-enclosed, poly-phase, squirrel-cage induction motors. The enclosed upper portion offers protection from drips, while openings in the lower parts of the end bells and casing provide for ventilation.

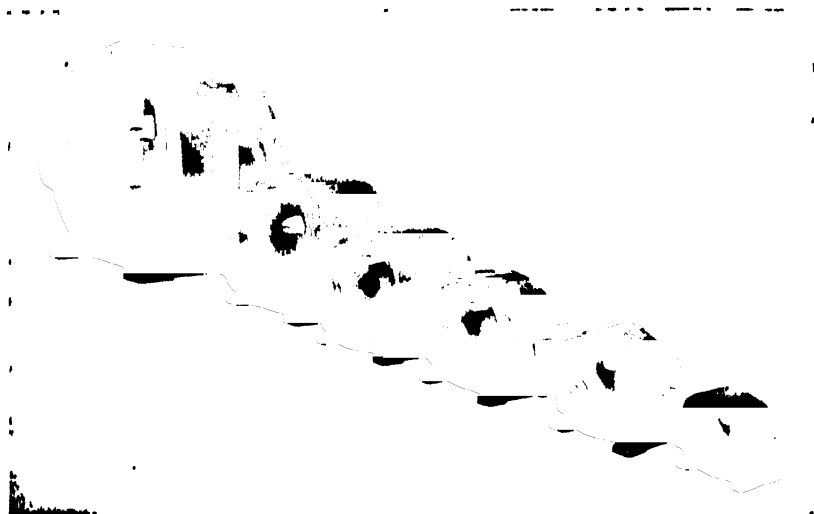


Fig. 4 Standard line of polyphase squirrel cage induction motors. (General Electric Company)

Figure 5 is a cutaway view of a wound rotor motor, showing the stator and rotor coils projecting from the stator and rotor punchings, and the method of securing the laminations in place by bolts and clamps. The rotor slip rings and brush rigging, shaft, ventilating fan, frame, end bells, bearings and other mechanical details should be noted.

Figure 6a shows an assembled stator with form-wound coils held in place in the stator slots by fiber wedges. Both form-wound and skein windings are used in induction motors but the latter are for small machines. Either lap or wave windings may be used, and are the same type as in alternators. The details of the end turns and connections should be noted. The radial ventilating ducts spaced along the length of the core, usually two to three inches apart, may be seen in the illustration. Figure 6b is a close-up of the stator windings and phase connections, showing the binding together of the coils. The fingers of the clamping structure which support the stator teeth may be seen between

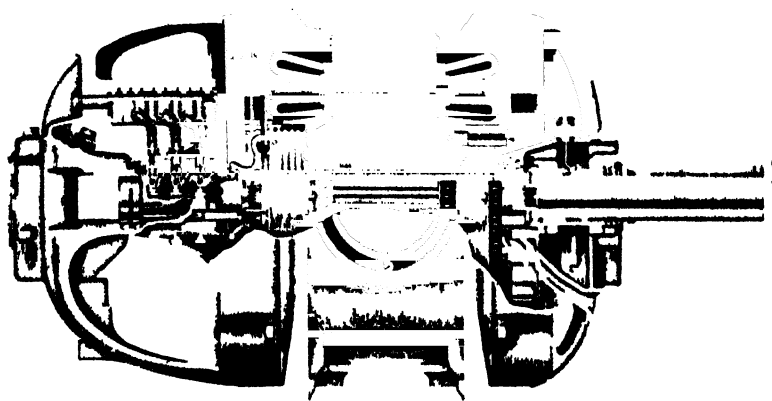


Fig 5 Cutaway view of a wound rotor polyphase induction motor (Westinghouse Electric Corporation)

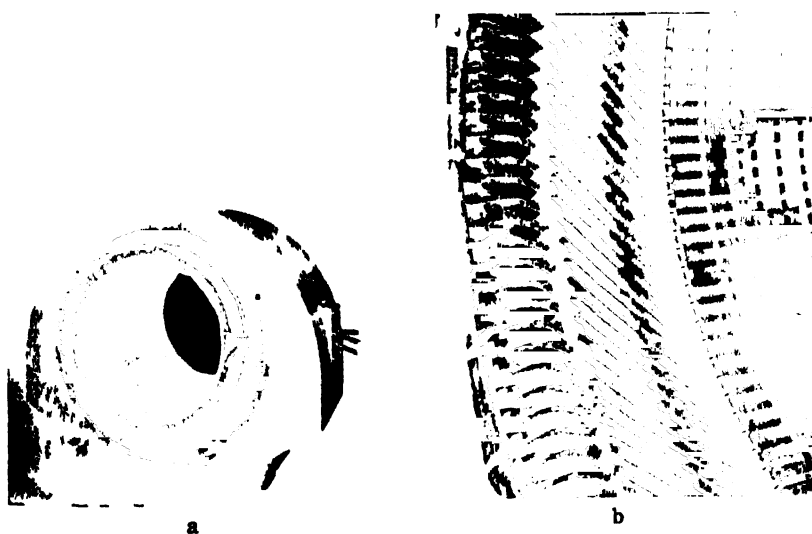


Fig 6 Stator and stator windings of a polyphase induction motor (General Electric Company)



Fig. 7 *a* Frame with stator laminations in place (*General Electric Company*)
b Showing method of securing stator punchings by means of clamping rings and bolts (*Westinghouse Electric Corporation*)

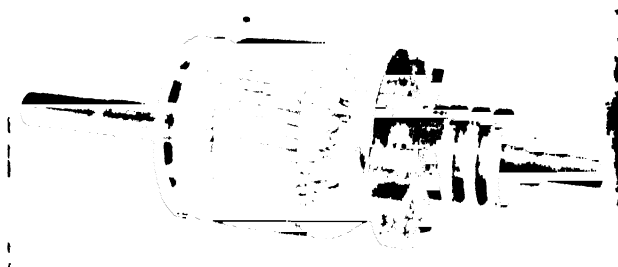


Fig. 8 Wound rotor of an induction motor, showing rotor windings, slip rings and fans (*General Electric Company*)

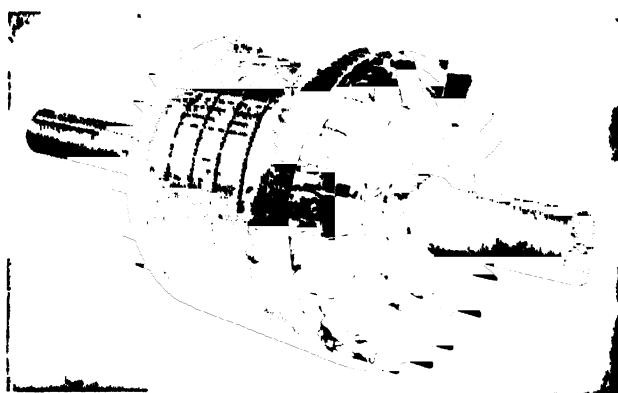


Fig. 9 Squirrel cage rotor with brazed bars (*General Electric Company*)

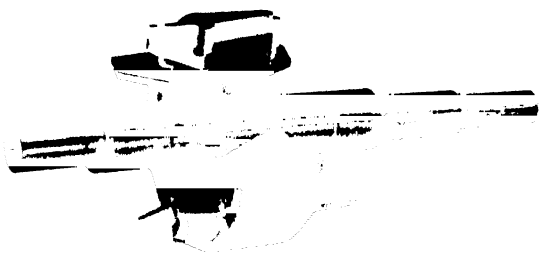


Fig. 10 Squirrel cage rotor (one third cutaway) with cast aluminum skewed bars (*General Electric Company*)

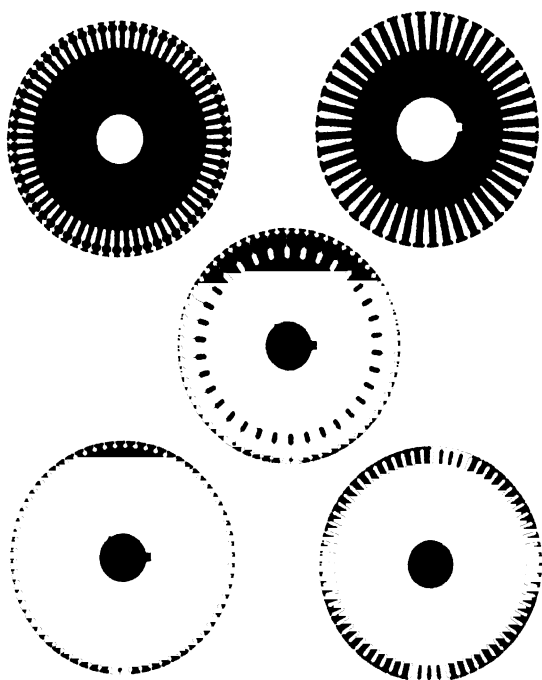


Fig. 11 Some typical rotor laminations (*General Electric Company*)

the coils, as well as the fiber slot wedges and the radial ventilating ducts.

Figure 7a shows the stator punchings in the frame. The punchings are usually riveted together in small machines, but in larger sizes are either bolted or else held by end rings and bolts as indicated in Fig. 7b. These illustrations show standard semi-open slots to accommodate skein or hand-wound coils.

Rotors are of two general types—wound rotor and squirrel cage. In the former, a polyphase winding is placed in the rotor slots and its connections brought out to slip rings. Figure 8 shows such a rotor with hand wound coils and skewed coil sides. Note the slot insulating channels projecting beyond the stacking. Why are the fans at the two ends of the rotor of different construction? Rotors may be wound for any number of phases, but are usually 3 phase. Of course, they must be wound for the same number of poles as the stator. The rotor laminations are usually thicker than for the stator, since the rotor frequency is much lower.

In the squirrel cage rotor the conductors are embedded in the slots and joined to common end rings at the two ends of the stacking. The bars may be round or rectangular, copper or brass, bolted, welded, or brazed to the end rings as in Fig. 9. This illustration shows the bars, end rings, radial ventilating ducts and spacers, clamping bolts, fans, spider, shaft and keyway. Figure 10 shows a cutaway view of a modern rotor with aluminum conductors of any desired shape cast integral with the end rings and fan blades.

The rotor slots take a variety of shapes—open, rectangular, semi-closed, inverted T, etc. Some

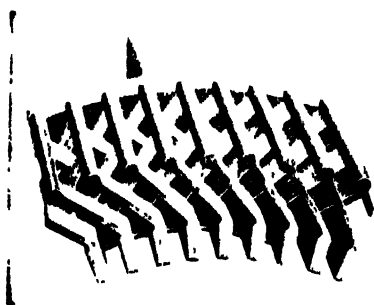


Fig. 12 The "Valv amp" double squirrel cage rotor (General Electric Company)

typical rotor laminations are shown in Fig. 11. Number 1 is for a double squirrel cage motor designed to give normal torque and low starting current. The inner rectangular portion of the slot carries a low resistance copper or aluminum bar, and the outer oval portion of the slot is filled with a high resistance brass or aluminum bar. Number 2 is for a wound rotor. Number 3 is an-

other double squirrel cage designed for high torque and low starting current. Number 4 is for a high torque and high slip motor. Number 5 is a normal torque and normal starting current design. The number

of rotor slots must not be a multiple of the number of stator slots, if the possibility of locking and subsynchronous crawling is to be avoided.

Figure 12 shows a cutaway view of an interesting recent modification of the double squirrel cage principle, in which the narrow neck connecting the upper and lower portions of the slot is interrupted at intervals over the core length in order to increase the effective impedance of the top bar. Also, the interrupted neck increases the heat capacity of the top bar so that it will not become too hot at starting.

4. The Rotating Field

A full-pitch single coil of N -turns excited by I amperes will develop a rectangular space distribution of magnetomotive force of magnitude $0.2\pi NI$, the fundamental of which will have a crest value $4/\pi$ times as great, Fig. 13. But in a distributed winding made up of fractional pitch, skewed coils, the magnetomotive force is reduced by the skew pitch, and distribution factors, so that the fundamental of magnetomotive force becomes $0.8K_s K_p K_d NI = 0.8K NI$, where $K = K_s K_p K_d$ is the combined reduction factor (see Sec. 3, Chap. 3).

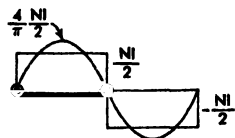


Fig. 13

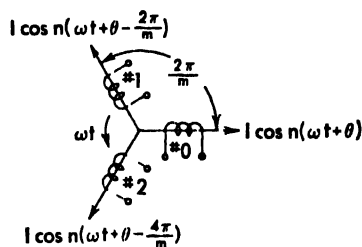


Fig. 14

Now consider a polyphase induction motor, Fig. 14, in which the m phase windings are distributed uniformly around the stator with an angle of $2\pi/m$ electrical radians between the centers of adjacent phases, and let the phases be numbered $k = 0, 1, \dots, m-1$. The magnetomotive force of phase k is centered on, or directed at, an angle $2\pi k/m$ in space, and this direction may be specified by the unit vector $e^{j2\pi k/m}$, in which the j - $\sqrt{-1}$ refers to a *space*, and not a time vector. If phase k is excited by an n th harmonic current $I \cos n(\omega t + \theta - 2\pi k/m)$, that is displaced in time by an angle $n2\pi k/m$ from the excitation of the reference phase $k = 0$, then the space fundamental of magnetomotive force for the k th phase is

$$M_k = 0.8 K NI \cos n\left(\omega t + \theta - \frac{2\pi k}{m}\right) e^{j2\pi k/m}$$

$$\begin{aligned}
&= 0.8 KNI \left\{ \cos n \left(\omega t + \theta - \frac{2\pi k}{m} \right) \left(\cos \frac{2\pi k}{m} + j \sin \frac{2\pi k}{m} \right) \right\} \\
&= 0.4 KNI \left\{ \cos \left[n\omega t + n\theta - (n+1) \frac{2\pi k}{m} \right] - \right. \\
&\quad \left. j \sin \left[n\omega t + n\theta - (n+1) \frac{2\pi k}{m} \right] + \cos \left[n\omega t + n\theta - (n-1) \frac{2\pi k}{m} \right] \right. \\
&\quad \left. + j \sin \left[n\omega t + n\theta - (n-1) \frac{2\pi k}{m} \right] \right\} \\
&= 0.4 KNI \left\{ e^{-jn\omega t + jn\theta} e^{j(n+1)\frac{2\pi k}{m}} + e^{jn\omega t - jn\theta} e^{-j(n-1)\frac{2\pi k}{m}} \right\} \quad (1)
\end{aligned}$$

The two terms $e^{jn\omega t + jn\theta}$ and $e^{-jn\omega t - jn\theta}$ obviously represent forward and backward rotating vectors in space, revolving at n times synchronous speed.

The total magnetomotive force for all m phases is the sum $\sum M_k$. The summation may be effected with the help of the geometric series

$$\sum_{\alpha=0}^{m-1} x^\alpha = 1 + x + x^2 + \cdots + x^{m-1} = \frac{x^m - 1}{x - 1}$$

whereupon, if α is any integer (including zero),

$$\sum_{\alpha=0}^{m-1} e^{j(n+1)\frac{2\pi k}{m} \alpha} = \frac{e^{j(n+1)\frac{2\pi k}{m} m} - 1}{e^{j(n+1)\frac{2\pi k}{m}} - 1} = \begin{cases} m & \text{if } (n+1) = \alpha m \\ 0 & \text{if } (n+1) \neq \alpha m \end{cases} \quad (2)$$

$$\sum_{\alpha=0}^{m-1} e^{-j(n-1)\frac{2\pi k}{m} \alpha} = \frac{e^{-j(n-1)\frac{2\pi k}{m} m} - 1}{e^{-j(n-1)\frac{2\pi k}{m}} - 1} = \begin{cases} m & \text{if } (n-1) = \alpha m \\ 0 & \text{if } (n-1) \neq \alpha m \end{cases} \quad (3)$$

Therefore, the magnetomotive force for all phases is

$$\begin{aligned}
M = 0.4 KNI \left[\begin{cases} m & \text{if } (n+1) = \alpha m \\ 0 & \text{if } (n+1) \neq \alpha m \end{cases} e^{-jn\omega t + jn\theta} \right. \\
\left. + \begin{cases} m & \text{if } (n-1) = \alpha m \\ 0 & \text{if } (n-1) \neq \alpha m \end{cases} e^{jn\omega t - jn\theta} \right] \quad (4)
\end{aligned}$$

This is an extremely interesting result, for it shows that harmonic excitation of a polyphase winding may give rise to a magnetomotive force of constant magnitude revolving either forward, or backward, or to no resultant field at all. For example, using +, -, 0 to indicate forward, backward, and null fields, we have for a three phase ($m = 3$) winding excited by different time harmonics

Time harmonic (n)	1	3	5	7	9	11	13
Rotating field	+	0	-	+	0	-	+

We shall return at a later time to a consideration of the effect of these harmonics on the torque of the induction motor. For the present, consider the fundamental of excitation ($n = 1$) and let us write subscript 1 for stator quantities. Then (4) gives

$$\mathbf{M}_1 = 0.4K_1N_1I_1m_1e^{j\omega t + \theta_1} = 0.4\sqrt{2}K_1N_1m_1I_1e^{j\omega t} \quad (5)$$

in which $I_1 = I_1e^{j\theta} / \sqrt{2}$ is the rms value of the vector current. This is a forward revolving field of constant magnitude, and it will cause a flux to rotate around the air gap of the motor in the same way as with revolving field poles

Suppose, now, that the rotor, having the same number of poles as the stator, is wound for m_2 phases, with N_2 turns per phase and a winding reduction factor K_2 . As the stator field cuts the conductors of the rotor, it will induce currents I_2 in them, and since the rotor phases are uniformly distributed around the rotor, the induced currents in adjacent phases will differ in time by the angle $2\pi/m_2$. The rotor itself, being a polyphase winding, will have a resultant magnetomotive force which will react on the stator field, causing the rotor to rotate in the same direction. If there were no load or windage and friction, and no losses in the machine, the rotor would revolve synchronously, for then there would be no relative motion between stator field and rotor conductors, and therefore no voltages induced in the latter. However, the rotor speed will be less than synchronous by a fraction

$$s = \frac{(\text{synchronous speed}) - (\text{rotor speed})}{(\text{synchronous speed})} \quad (6)$$

called the *slip*. Thus the stator field, revolving at synchronous speed ωt with respect to the stator, induces a voltage of normal frequency f_1 in the stator coils. But with respect to the rotor the stator field is revolving at a relative speed (see Fig. 15)

$$\omega - (1 - s)\omega = s\omega \quad (7)$$

and consequently the currents induced in the rotor are of slip frequency $f_2 = sf_1$. Therefore, the rotor magnetomotive force relative to the rotor is

$$\mathbf{M}_2 = 0.4\sqrt{2}K_2N_2m_2I_2e^{j\omega t} \quad (\text{with respect to rotor}) \quad (8)$$

But since the rotor is moving at a speed $(1 - s)\omega$ relative to the stator, the field due to (8) is moving at a speed $s\omega + (1 - s)\omega = \omega$, or syn-

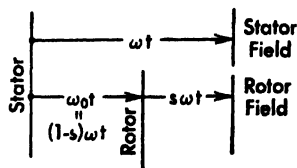


Fig. 15

chronously, with respect to the stator. Hence the stator and rotor magnetomotive forces superimpose to give a resultant

$$\begin{aligned} \mathbf{M} &= \mathbf{M}_1 + \mathbf{M}_2 = 0.4 \sqrt{2} (K_1 N_1 m_1 I_1 + K_2 N_2 m_2 I_2) e^{j\omega t} \\ &= 0.4 \sqrt{2} K_1 N_1 m_1 \left(I_1 + \frac{K_2 N_2 m_2}{K_1 N_1 m_1} I_2 \right) e^{j\omega t} \\ &= 0.4 \sqrt{2} K_1 N_1 m_1 I_0 e^{j\omega t} \end{aligned} \quad (9)$$

in which the rotor current I_2 has been referred to the stator by the ratio $(K_2 N_2 m_2) / (K_1 N_1 m_1)$ in the same way that the secondary current of the transformer is referred to the primary by the turn ratio. In the induction motor the effective turns must be used, and in addition the number of phases.

The resultant magnetomotive force, acting on the permeance P_0 of the air gap, produces the rotating field

$$\phi_0 = \mathbf{M} P_0 = 0.4 \sqrt{2} K_1 N_1 m_1 P_0 I_0 e^{j\omega t} = \Phi_0 e^{j\omega t} \quad (10)$$

This flux induces in the stator a voltage

$$e_1 = - \frac{K_1 N_1}{10^8} \frac{d\Phi_0 e^{j\omega t}}{dt} = -j \frac{\omega}{10^8} V_1 K_1 \Phi_0 e^{j\omega t} \quad (11)$$

The flux has a velocity of $s\omega t$ with respect to the rotor, so that the voltage induced in the rotor is the slip frequency voltage

$$e_2 = - \frac{K_2 N_2}{10^8} \frac{d\Phi_0 e^{js\omega t}}{dt} = -js \frac{\omega}{10^8} K_2 N_2 \Phi_0 e^{j\omega t} \quad (12)$$

When the rotor is at standstill ($s = 1$), the rotor voltage is at stator frequency, and the voltages are in effective turn ratio

$$\frac{E_2}{E_1} = \frac{K_2 N_2}{K_1 N_1} = \frac{1}{a} \quad (13)$$

5. The Vector Diagram and Equivalent Circuit

Equations (11) and (12) in rms vector form become

$$\mathbf{E}_1 = -j4.44 f_1 K_1 N_1 \Phi_0 10^{-8} \quad (14)$$

$$s\mathbf{E}_2 = -js4.44 f_1 K_2 N_2 \Phi_0 10^{-8} \quad (15)$$

If the voltage applied to the stator is V_1 and the stator impedance is $\mathbf{Z}_1 = R_1 + jX_1$, then calling $\mathbf{E}_0 = -\mathbf{E}_1$ the voltage necessary to overcome the induced voltage, we have

$$\mathbf{V}_1 = -\mathbf{E}_1 + \mathbf{Z}_1 \mathbf{I}_1 = \mathbf{E}_0 + \mathbf{Z}_1 \mathbf{I}_1 \quad (16)$$

If the voltage applied to the rotor slip rings (assuming a wound-rotor

induction motor and an external source of voltage of proper frequency) is V_2 , and the rotor impedance at frequency f_1 is $Z_2 = R_2 + jX_2$ (or $R_2 + jsX_2$ at frequency $f_2 = sf_1$), then

$$V_2 = -sE_2 + (R_2 + jsX_2)I_2 \quad (17)$$

The exciting current, by (9),

$$I_0 = \left(I_1 + \frac{K_2 N_2 m_2}{K_1 N_1 m_1} I_2 \right) = \left(I_1 + \frac{m_2}{m_1} \frac{I_2}{a} \right) = (I_1 + I_2') \quad (18)$$

may be accounted for, as in transformer theory, by an exciting admittance ($Y_0 = G_0 - jB_0$), thus

$$I_0 = Y_0 E_0 = (G_0 - jB_0)E_0 \quad (19)$$

Equations (16), (17), (18), and (19) are the equations of the induction motor. In order to interpret them in terms of a vector diagram and equivalent circuit, it is necessary to reduce (17) to stator terms:

$$\begin{aligned} V_2' &= \frac{a}{s} V_2 = -E_2 a + \frac{a}{s} (R_2 + jsX_2) I_2 \\ &= -E_1 + \frac{m_1 a^2}{m_2} \left(\frac{R_2}{s} + jX_2 \right) \left(\frac{m_2}{m_1} \frac{I_2}{a} \right) \\ &= E_0 + \left(\frac{R_2'}{s} + jX_2' \right) I_2' \\ &= E_0 + Z_2' I_2' \end{aligned} \quad (20)$$

where $I_2' = \frac{m_2}{m_1} \frac{I_2}{a}$ now agrees with the I_2' of (18), and the referred values

of impedance are $R_2' = \frac{m_1 a^2}{m_2} R_2$ and $X_2' = \frac{m_1}{m_2} a^2 X_2$. The interpretation

is then given in Fig. 16. The equivalent circuits for each part, corresponding to air gap, stator, and rotor, may be joined together as a composite circuit, since the conditions of voltage equality and current continuity are satisfied at the junction. The composite circuit may be confirmed by showing that its driving point and transfer impedances agree with the foregoing equations, or by showing that the circuit holds under the limiting conditions of open- and short circuited terminals. For example, from (20)

$$I_2' = \frac{V_2' - E_0}{Z_2'}$$

and substituting this and (19) in (18)

$$Y_0 E_0 = I_1 + \frac{V_2' - E_0}{Z_2'}$$

from which E_0 may be found and substituted in (16) to give

$$V_1 = \left(Z_1 + \frac{1}{Y_0 + \frac{1}{Z_2'}} \right) I_1 + \frac{V_2'}{1 + Y_0 Z_2'} \quad (21)$$

If the rotor is short-circuited ($V_2' = 0$), the coefficient of I_1 is seen to be the impedance Z_1 of the equivalent circuit. On the other hand, if the stator is open-circuited ($I_1 = 0$), and a voltage V_2' applied to the rotor, the second term of (21) is seen to agree with the voltage E_0 of the equivalent circuit.

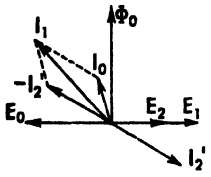
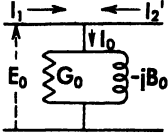
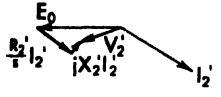
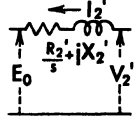
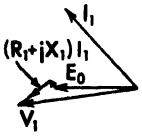
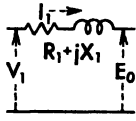
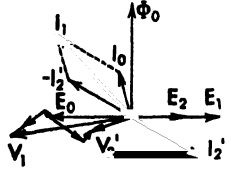
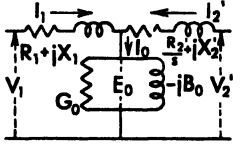
VECTOR DIAGRAM	EQUATIONS	EQUIVALENT CIRCUIT
	$E_1 = -j 4.44 f_1 K_1 N_1 \Phi_0 10^{-8}$ $E_2 = -j 4.44 f_1 K_2 N_2 \Phi_0 10^{-8}$ $E_0 = -E_1 = -\alpha E_2$ $I_2' = \frac{m_2}{m_1} \frac{I_2}{s}$ $I_0 = I_1 + I_2' = Y_0 E_0$	
	$V_2' = E_0 + \left(\frac{R_2'}{s} + jX_2' \right) I_2'$ $= \frac{\alpha}{s} V_2$ $R_2' = \frac{m_1}{m_2} \alpha^2 R_2, X_2' = \frac{m_1}{m_2} \alpha^2 X_2$	
	$V_1 = E_0 + (R_1 + jX_1) I_1$	
	$V_1 = \left(Z_1 + \frac{1}{Y_0 + \frac{1}{Z_2'}} \right) I_1 + \frac{V_2'}{1 + Y_0 Z_2'}$ $= Z_0 I_1 + \frac{V_2'}{1 + Y_0 Z_2'}$	

Fig. 16

6. Power Equations

The exciting current I_0 of an induction motor is relatively greater than in a transformer, since the flux must be forced across an air gap. Never-

theless, no great error is committed if the exciting admittance Y_0 of the equivalent circuit is moved to the line terminals, as in Fig. 17. The

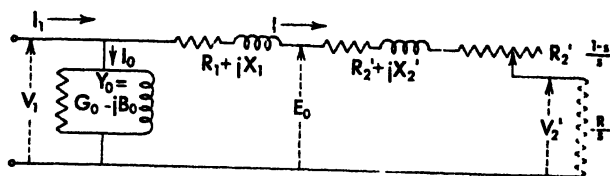


Fig. 17 Approximate equivalent circuit of the polyphase induction motor.

analysis is greatly simplified by this artifice. Under this condition

$$I_0 = Y_0 V_1 = (G_0 - jB_0) V_1 = \text{exciting current} \quad (22)$$

$$I = \frac{V_1 - V_2'}{R_1 + R_2' s + j(\lambda_1 + \lambda_2')} = \text{load current} \quad (23)$$

$$I_1 = I_0 + I = V_1 \left[G_0 - jB_0 + \frac{1}{R_1 + R_2' s + j(\lambda_1 + \lambda_2')} \right] - \frac{V_2'}{R_1 + R_2' s + j(\lambda_1 + \lambda_2')} \quad (24)$$

$$\cos \theta_0 = \frac{G_0}{\sqrt{G_0^2 + B_0^2}} = \text{power factor of exciting current} \quad (25)$$

$$\cos \theta = \frac{R_1 + R_2' s}{\sqrt{(R_1 + R_2' s)^2 + (\lambda_1 + \lambda_2')^2}} = \text{pf of load current} \quad (26)$$

$$\cos \theta_1 = \frac{G_0 + (R_1 + R_2' s) / Z'^2}{\sqrt{\left(G_0 + \frac{R_1 + R_2' s}{Z'^2} \right)^2 + \left(B_0 + \frac{\lambda_1 + \lambda_2'}{Z'^2} \right)^2}} = \text{pf of stator current } (V_2' = 0) \quad (26a)$$

It has been noticed that the resistance component of the rotor part of the equivalent circuit is $R_2' s$, and thus changes with the slip. Since the normal slip of an induction motor is only a few per cent, it is evident that $R_2' s$ is the dominant term in the rotor impedance, even though X_2' be, say, ten times as large as R_2' . However, the rotor copper loss is $R_2' I_2^2 = R_2' I^2 s$, while the total energy consumed by the resistance $R_2' s$ is $R_2' I^2 s$. It is, therefore, desirable to separate the equivalent circuit resistance into two parts

$$\frac{R_2'}{s} = R_2' + R_2' \frac{1-s}{s}$$

as shown in Fig. 17, so that the first term R_2' will represent true rotor copper loss.

The electrical energy transmitted to the external rotor circuit is $V_2 I_2 \cos \theta_2$ where V_2 and I_2 are the actual voltage and current of the motor itself (*not* the equivalent circuit), and $\cos \theta_2$ is the power factor at the rotor terminals.

Now by the conservation of energy:

$$\left\{ \begin{array}{l} \text{Input} \\ \text{to} \\ \text{stator} \end{array} \right\} - \left\{ \begin{array}{l} \text{Gross} \\ \text{mechanical} \\ \text{power} \end{array} \right\} = \left\{ \begin{array}{l} \text{Electrical energy} \\ \text{transmitted to} \\ \text{external circuit} \end{array} \right\} + \left\{ \begin{array}{l} \text{Core} \\ \text{loss} \end{array} \right\} + \left\{ \begin{array}{l} \text{Stator} \\ \text{copper} \\ \text{loss} \end{array} \right\} + \left\{ \begin{array}{l} \text{Rotor} \\ \text{copper} \\ \text{loss} \end{array} \right\} \quad (27)$$

Remembering that there are m_1 stator phases and m_2 rotor phases, and that all previous equations were set up on a "per phase" basis, (27) may be written explicitly

$$m_1 V_1 I_1 \cos \theta_1 = P + m_2 V_2 I_2 \cos \theta_2 + m_1 G_0 V_1^2 + m_1 R_1 I_1^2 + m_2 R_2 I_2^2 \quad (28)$$

But in the equivalent circuit, the input per phase is

$$V_1 I_1 \cos \theta_1 = G_0 V_1^2 + R_1 I^2 + \frac{R_2'}{s} I^2 + V_2' I \cos \theta_2 \quad (29)$$

Equating m_1 times (29) to (28), and putting $V_2 = \frac{s}{a} V_2'$, $I_2 = \frac{m_1 a}{m_2} I_2'$,

$I \cong I_1 \cong I_2'$ and rearranging, there results

$$P = m_1 R_2' I^2 \left(\frac{1-s}{s} \right) + m_1 V_2' I \cos \theta_2 (1-s) \quad (30)$$

The *net* mechanical power is less than this by the windage and friction losses. It is sometimes customary to include windage and friction with the core loss $G_0 V_1^2$, if the voltage is constant and the speed substantially constant. But the approximation is poor in wound-rotor induction motors having an appreciable speed range.

Making use of (23), there is

$$P = m_1 R_2' \left(\frac{1-s}{s} \right) \left(\frac{V_1 - V_2'}{\left(R_1 + \frac{R_2'}{s} \right)^2 + (X_1 + X_2')^2} + \frac{m_1 V_2' |V_1 - V_2'| \cos \theta_2 (1-s)}{\left(R_1 + \frac{R_2'}{s} \right)^2 + (X_1 + X_2')^2} \right) \quad (31)$$

There are a number of special cases of practical importance. The general case, (31), is itself of practical importance in connection with cascade

induction motors, and motors in which rotor voltages are introduced by Kramer or Scherbius controls.

Case I: Rotor short-circuited

In this case $V_2' = 0$ and (31) reduces to the usual equation given in most textbooks for the mechanical (gross) output of an induction motor

$$P = m_1 R_2' \left(\frac{1-s}{s} \right) \frac{V_1^2}{\left(R_1 + \frac{R_2'}{s} \right)^2 + (X_1 + X_2')^2} = m_1 R_2' \left(\frac{1-s}{s} \right) I^2 \quad (32)$$

Now since
$$I = \frac{E_0}{\sqrt{(R_2' / s)^2 + (X_2')^2}}$$

(32) becomes

$$\begin{aligned} P &= m_1 \frac{R_2'}{s} (1-s) \frac{E_0 I}{\sqrt{(R_2' / s)^2 + (X_2')^2}} = m_1 E_0 I \frac{R_2' s}{\sqrt{(R_2' / s)^2 + (X_2')^2}} (1-s) \\ &= m_1 E_0 I \cos \theta_2 (1-s) \\ &= m_1 E_0 I \cos \theta_2 - m_1 s E_0 I \cos \theta_2 \end{aligned} \quad (33)$$

Now E_0 is the voltage due to the air gap flux, and sE_0 is the voltage actually consumed by the rotor, so that their difference $E_0(1-s)$ is of the nature of a counter electromotive force.

Equation (32) shows that the power is zero at standstill ($s = 1$) and at synchronous speed ($s = 0$). For values of slip in the range $(0 < s < 1)$ the power is positive and the machine behaves as a motor. When the machine is driven above synchronous speed ($s < 0$), the power is negative and the machine becomes a generator. Finally, if the motor is reversed ($s > 1$), the power is negative and the machine is acting as an electrical brake.

Case II: Rotor circuit closed through an external resistance

If the external resistor is R ohms per phase, then referred to the stator,

it is $\frac{R'}{s} = \frac{m_1}{m_2} a^2 \frac{R}{s}$ and $V_2' = \frac{R'}{s} I$. Then by (30)

$$P = m_1 R_2' \left(\frac{1-s}{s} \right) I^2 + m_1 \frac{R'}{s} I^2 (1-s) = m_1 (R_2' + R') \left(\frac{1-s}{s} \right) I^2 \quad (34)$$

and the effect is the same as increasing the rotor resistance by R' .

Case III: Operation at synchronous speed

As the slip approaches zero in (31), the term $V_2' = aV_2 s$ dominates the numerators and $R_2' s$ dominates the denominators, and the current

in the rotor becomes d-c so that $\theta_2 \rightarrow 0$. Then (31) reduces to an indeterminate:

$$P = \left[m_1 \frac{a^2 V_2'^2}{s R_2'} - m_1 \frac{a^2 V_2'^2}{s R_2'} \right]_{s=0} = 0 \quad (35)$$

which tells us nothing about what occurs at synchronous speed. Actually, however, if a direct voltage is applied to the rotor so that a direct current flows from one terminal to the others, the machine will behave as a synchronous motor. The practical application of this principle will be discussed in a subsequent section.

Case IV: Negative slip

If in (31) the slip is negative, $s = -\sigma$, we have

$$P = -m_1 R_2' \frac{1 + \sigma}{\sigma} \frac{V_1 - V_2'^2}{\left(R_1 - \frac{R_2'}{\sigma} \right)^2 + (X_1 + X_2')^2} + \frac{m_1 V_2' V_1 - V_2' \cos \theta_2 (1 + \sigma)}{\left(R_1 - \frac{R_2'}{\sigma} \right)^2 + (X_1 + X_2')^2} \quad (36)$$

The first term is always negative, representing generator action, but the second term is positive if $\theta_2 < \pi/2$, and therefore the machine may continue to act as a motor if the rotor applied voltage is of proper magnitude and phase. Thus the motor range of an induction machine may be extended through and beyond synchronism by introducing appropriate rotor applied voltages.

7. Torque

If synchronous speed of the motor in rpm is n_1 , the rotor speed at slip s is $n_2 = (1 - s)n_1$ and the torque in pound feet is related to the mechanical power by

$$T = \frac{33000}{746} \frac{P}{2\pi n_2} = \frac{33000}{746} \frac{P}{2\pi n_1(1 - s)} \quad (37)$$

in which the power is given by (30) or (31). For a motor with no external rotor voltage, equation (32) applies, and the torque is

$$T = \frac{33000}{2\pi n_1 746} \frac{m_1 V_1^2 R_2' s}{(R_1 + R_2' s)^2 + (X_1 + X_2')^2} \quad (38)$$

The torque has a maximum value when $dT/ds = 0$ of

$$T_{\max} = \frac{33000}{2\pi n_1 746} \frac{m_1 V_1^2}{2 \left[(R_1 + \sqrt{R_1^2 + (X_1 + X_2')^2}) \right]} \quad (39)$$

$$\text{for } s = \frac{\pm R_2'}{\sqrt{R_1^2 + (X_1 + X_2')^2}} \quad (40)$$

The + sign is used for motor torque and the - sign for generator torque, Fig. 18. Equations (39) and (40) clearly show that maximum torque is independent of the rotor resistance, but the slip at which it occurs is directly proportional to the rotor resistance. Thus by adding external resistance to the rotor circuit it is possible to shift the maximum torque point further back from synchronous speed, as shown in

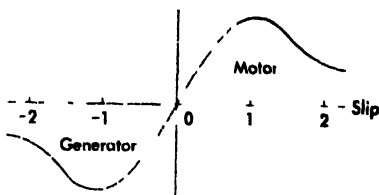


Fig. 18

Fig. 19. If the rotor resistance is made equal to $\sqrt{R_1^2 + (X_1 + X_2')^2}$,

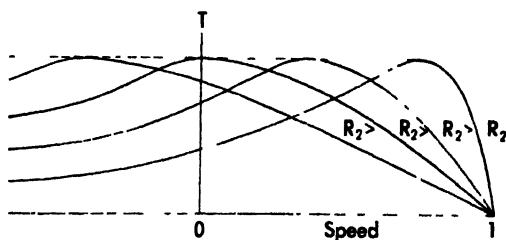


Fig. 19 Effect of rotor resistance on the torque-speed characteristic

then according to (40) maximum torque will occur at standstill. A still greater value of rotor resistance will move the maximum torque to the region of reverse speed.

8. Determination of Constants

The complete performance of the polyphase induction motor may be specified in terms of the applied voltage V_1 , the slip s , and the six constants G_0 , B_0 , R_1 , X_1 , R_2' , X_2' . These six constants may be obtained from the design sheet, or from *running light* and *blocked rotor* tests, corresponding to the open and short-circuit tests on transformers. Referring to the approximate equivalent circuit of the induction motor, Fig. 20(a), it is evident that at or near synchronism, $s = 0$, the impedance of the rotor circuit is very high, and is essentially a resistance R_2' . (If the induction motor were driven at exactly synchronous speed, $s = 0$, no current would flow in the rotor circuit, and the entire input would be consumed as core loss and the stator copper loss of the exciting current.)

At standstill, $s = 1$, the input current is practically entirely reflected in the rotor, and the bulk of the power input is consumed by the resistances $R_1 + R_2'$. The stator resistance R_1 is 20 per cent to 60 per cent greater than its d-c measured value, because of the eddy-current losses in the conductors. These losses can be reduced by stranding the conductor and transposing the strands. At normal speed the rotor resistance R_2' is practically the same as its d-c resistance, since the rotor frequency is low,

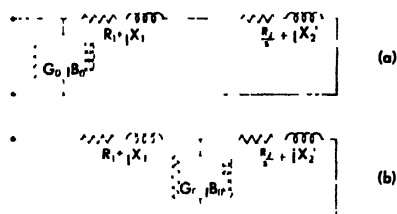


Fig. 20

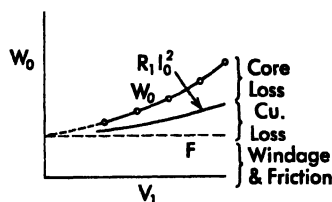


Fig. 21

but at standstill the rotor frequency is the same as the stator frequency, and the rotor resistance is increased in the same proportion. For the same reason, the rotor core loss is much greater at standstill than at normal speed. But windage and friction are smaller at lower speeds, and vanish at standstill. Thus rotor core loss and windage and friction compensate each other to a certain extent, and both are usually included in $G_0 V_1^2$.

To a first approximation, then, the two tests yield:

Running light test ($s \approx 0$)	$V_2 = 0$	Blocked rotor test ($s = 1$)
V_1, I_0, W_0	Stator input phase	V_b, I_b, W_b
$Z = V_1 / I_0$	$R_1 = (1.2 \text{ to } 1.6) R_M$	$Z = V_b / I_b$
$G_0 = W_0 / V_1^2$	$R_2' = (R_1 + R_2') - 1.4 R_M$	$R_1 + R_2' = W_b / I_b^2$
$B_0 = \sqrt{1 - G_0^2 Z^2}$	$R_2' \approx (R_1 + R_2') - 1.4 R_M$	$V_1 + X_2' = \sqrt{Z^2 - (R_1 + R_2')^2}$
$\cos \theta_0 = W_0 / V_1 I_0$	$V_2' = V_1$ (assumed)	$\cos \theta_b = W_b / V_b I_b$

The approximations given in the table ignore the resistance losses in stator and rotor due to the small current necessary to overcome windage and friction, in calculating V_0 ; while core loss and magnetizing susceptance are ignored in calculating Z . Many methods have been devised for obtaining better approximations. Sometimes the windage and friction loss can be determined by driving the motor with another machine and measuring the power required. The loss can also be segregated by taking

running-light input measurements at several different applied voltages, including the lowest voltage sufficient to rotate the motor near normal speed, Fig. 21, and extrapolating the curve of watts-input to zero voltage. The intercept must then be the windage and friction loss, since the core loss at zero voltage is zero. Then if the windage and friction loss of F watts per phase is *not* to be included by G_0 , there is very closely

$$G_0 = \frac{W_0 - F}{V_0^2} \quad (41)$$

$$B_0 = \frac{I_0}{V_0} \sin \theta_0 = \frac{I_0}{V_0} \left[1 - \left(\frac{W_0}{V_0 I_0} \right)^2 \right] \quad (42)$$

The resistance, as corrected for core loss, becomes

$$R_1 + R_2' = \frac{W_b - G_0 V_b^2}{I_b^2} \quad (43)$$

and if $\cos \theta_b = W_b / V_b I_b$ we have $Z = V_b / I = V_b (I_b - I_0)$, or

$$(R_1 + R_2') + j(X_1 + X_2') = \frac{1}{I_b (\cos \theta_b - j \sin \theta_b) - (G_0 - jB_0) V_b}$$

from which

$$X_1 + X_2' = \frac{1}{(I_b \cos \theta_b - G_0 V_b)^2 + (I_b \sin \theta_b - B_0 V_b)^2} (R_1 + R_2')^2 \quad (44)$$

Equations (41) to (44) contain the corrections for the constants of the approximate equivalent circuit, Fig. 20(a).

The determination of the corrected constants for the exact equivalent circuit is a bit more involved. Referring to Fig. 20(b), and noting that $X_1 \gg R_1$ and $\theta_0 \cong 90^\circ$, we find (taking V_1 as reference vector) for the running light test,

$$\begin{aligned} E_0 &= V_1 - (R_1 + jX_1)I_0 = V_1 - (R_1 + jX_1)I_0(\cos \theta_0 - j \sin \theta_0) \\ &\cong V_1 - X_1 I_0 \end{aligned}$$

The power input per phase is

$$W_0 = G_0 E_0^2 + R_1 I_0^2 + F$$

and therefore

$$G_0 = \frac{W_0 - F - R_1 I_0^2}{(V_1 - X_1 I_0)^2} \cong \frac{W_0 - F - R_1 I_0^2}{V_1^2} \quad (45)$$

The windage and friction loss is to be determined as in Fig. 21, or by driving the motor with another machine. If the input losses are taken with the motor driven at exactly synchronous speed, then F is not entered

in (45). We also have

$$V_0 = \frac{I_0}{E_0} = \frac{I_0}{V_1 - X_1 I_0} \cong \frac{I_0}{V_1} \quad (46)$$

$$B_0 = \sqrt{V_0^2 - G_0^2} \quad (47)$$

During blocked rotor test

$$\frac{V_b}{I_b} = Z_1 + \frac{Z_2'}{1 + Z_2' Y_0} = Z_1 + Z_2' (1 - Z_2' Y_0 + Z_2'^2 Y_0^2 - \dots)$$

Dropping all terms beyond the second in the series, and rearranging, we get

$$Z_1 + Z_2' = \frac{V_b}{I_b} (\cos \theta_b + j \sin \theta_b) + (R_2' + jX_2')^2 (G_0 - jB_0)$$

from which

$$R_1 + R_2' = \frac{V_b}{I_b} \cos \theta_b + 2R_2' X_2' B_0 + (R_2'^2 - X_2'^2) G_0 \cong \frac{V_b}{I_b} \cos \theta_b \quad (48)$$

$$X_1 + X_2' = \frac{V_b}{I_b} \sin \theta_b + 2R_2' X_2' G_0 - (R_2'^2 - X_2'^2) B_0 \cong \frac{V_b}{I_b} \sin \theta_b \quad (49)$$

By successive approximations, equations (45) to (49) may be quickly solved. First, the approximate values as given by the second forms in each equation are calculated. Then using those approximate values the more exact values are found by substitution.

Example A 3 phase, wye-connected, 60-cycle, 220 volt, 5-hp, 1800 rpm induction motor has the following test data

Running light		Blocked rotor
220 (127 phase)	voltage	68 (39.3 phase)
4.35	current	20
244 (81.3 phase)	watts	1265 (422 phase)
65 (21.7 phase)	windage and friction	

Stator resistance at 75 C and including skin effect, $R_1 = 0.545$ ohms per phase. For the approximate equivalent circuit, by (41), (42), (43) and (44)

$$G_0 = \frac{81.3 - 21.7}{127^2} = 0.0037,$$

$$B = \frac{4.35}{127} \left[1 - \left(\frac{81.3}{127 \times 4.35} \right)^2 \right] = 0.0339$$

$$\cos \theta_b = \frac{422}{39.3 \times 20} = 0.537, \quad \sin \theta_b = 0.843$$

$$R_1 + R_2' = \frac{422 - 0.0037 \times 39.3^2}{2.0^2} = 1.040 \text{ ohms, } \therefore R_2' = 1.040 - 0.545 = 0.495$$

$$X_1 + X_2' = \left[\frac{20 \times 0.537 - 0.0037 \times 39.3^2}{20 \times 0.843 - 0.0339 \times 39.3} - 1.040 \right] = 1.816$$

For the exact equivalent circuit, by (45) to (49) inclusive, and using previous values of the constants in the "correction terms,"

$$G_1 = \frac{81.3 - 21.7 - 0.545 \times 4.35^2}{(127 - 0.908 \times 4.35)^2} = 0.0033$$

$$Y_0 = \frac{4.35}{127 - 0.908 \times 4.35} = 0.0353$$

$$B_0 = \sqrt{0.0353^2 - 0.0033^2} = 0.0352$$

$$R_1 + R_2' = \frac{39.3}{20} \times 0.537 + 2 \times 0.495 \times 0.908 \times 0.0352 + (0.495^2 - 0.908^2 \times 0.0033) = 1.085$$

$$X_1 + X_2' = \frac{39.3}{20} \times 0.843 + 2 \times 0.495 \times 0.908 \times 0.0033 + (0.495^2 - 0.908^2 \times 0.0352) = 1.671$$

Recapitulating, we have for the different assumptions

Constants	Approx equiv circuit		Exact equiv circuit	
	1st approx.	corrected	1st approx	corrected
G_1	0.0050	0.0037	0.0031	0.0033
B_0	0.0339	0.0339	0.0341	0.0352
$R_1 + R_2'$	1.054	1.040	1.054	1.085
$X_1 + X_2'$	1.656	1.816	1.656	1.671

These comparisons show rather conclusively that the approximate values are sufficiently exact, particularly since the equivalent circuit is itself an approximation—in setting it up, time and space harmonics were neglected, conductor skin-effect correction guessed at, rotor and stator core loss taken to be proportional to the main flux only, saturation effects ignored, etc. Therefore, there is little practical justification for using other than the approximate equivalent circuit, or in calculating the constants by other than the so-called first approximation method. As a matter of experience, the performance characteristics of a given motor, calculated from the approximate equivalent circuit, are just as likely as

not to agree more closely with the test results than calculations based on the so-called exact equivalent circuit. G_0 varies with the saturation, rotor-core loss (a function of f_2), and speed (windage and friction). R_2' varies with the speed, since skin effect is proportional to f_2^2 . X_1 and X_2' change with load, due to saturation in the teeth.

9. The Circle Diagram

The current vector for a simple $R - X$ circuit, Fig. 22, follows a circular locus of diameter V/X as the resistance is varied, since

$$I = \frac{V}{Z} = \frac{V}{X} \frac{X}{Z} = \frac{V}{X} \sin \theta$$

From a circle diagram constructed on this principle, corresponding values of current I and power-factor angle θ may be taken.

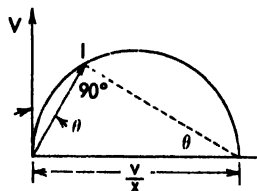
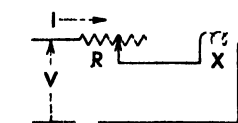


Fig. 22

Over half a century ago, Alexander Heyland (Elektrotech. Zeitsch., 41, p. 561, 1894) applied this idea to the performance calculations of the induction motor. Since then, numerous forms and variations of the circle diagram, for both the approximate and the exact equivalent circuits of the induction motor, have appeared in the literature, but the only one which has survived in general use is the one illustrated in Fig. 23 for the approximate equivalent circuit. The current I in the series part of the circuit, $(R_1 + R_2' s) + j(X_1 + X_2')$, obviously follows the circular path $O'PD$, on diameter $O'D$ equal to $V_1/(X_1 + X_2')$, as the resistance

varies with the slip. However, since the resistance is never less than $R_1 + R_2'$, corresponding to standstill at $s = 1$, the motor operating range of the circle is confined to the arc $O'PB$, where O' is the no-load or running light point, and B is the blocked-rotor point. Input current I_1 and exciting current I_0 readily appear on the same diagram by shifting the origin to O so that $I_1 = I_0 + I$. Then for any point P the magnitudes of the currents I_1 , I_0 , I and their phase angles θ_1 , θ_0 , θ are found. The projections of these currents on the voltage axis V_1 give the in-phase or power components,

$$I_1 \cos \theta_1 = \frac{V_1 I_1 \cos \theta_1}{V_1} = \frac{P_1}{V_1}$$

$$I_0 \cos \theta_0 = G_0 V_1 = \frac{G_0 V_1^2}{V_1}$$

$$I \cos \theta = \frac{R}{Z} I = \frac{R}{V_1} \frac{V_1}{Z} I = \frac{RI^2}{V_1}$$

and thus multiplication by V_1 gives the power and energy losses.

Under blocked-rotor conditions, point P moves to B so that $\theta = \theta_B$, $I = I_B$, and then $V_1 \cdot \vec{AC} = V_1 I_0 \cos \theta_0 = G_0 V_1^2$ is the core loss, while $V_1 \cdot \vec{BC} = (R_1 + R_2') I_B^2$ is the resistance loss. If the line BC is divided so that $\vec{BT} : \vec{TC} :: R_2' : R_1$ then BT and TC are proportional, respectively, to the rotor and stator copper losses.

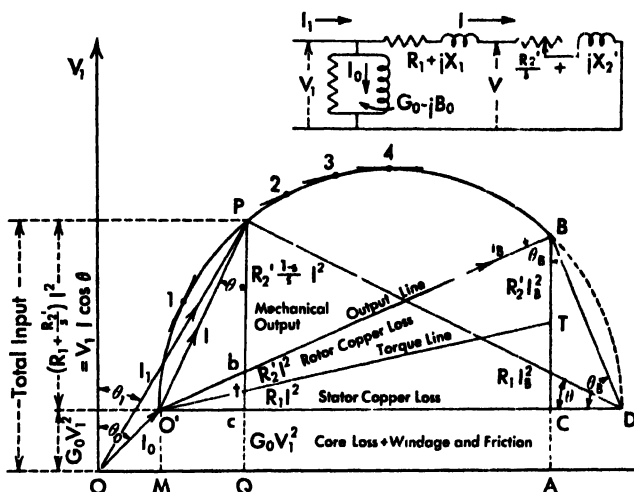


Fig. 23 Circle diagram of the polyphase induction motor.

Now draw the lines $O'B$ and $O'T$ cutting the perpendicular at points b, t, c . Then from the geometry of the figure

$$\begin{aligned} V_1 \cdot \vec{bc} &= V_1 \frac{\vec{BC}}{\vec{OC}} \cdot O'C = V_1 \cot \theta_B I \sin \theta \\ &= V_1 \frac{R_1}{X_1 + \frac{R_2'}{s}} I \frac{X_1 + \frac{X_2'}{s}}{Z} = (R_1 + R_2') I^2 \end{aligned}$$

and therefore \vec{bt} and \vec{tc} are proportional to the rotor and stator copper losses at current I . The rotor mechanical output must then be $V_1 \cdot \vec{Pb}$. The total input to the rotor is $V_1 \cdot \vec{Pi}$, and by (38) this is equal to the torque when multiplied by $33,000/2\pi n_1 746$. The slip is given by the ratio

$$s = \frac{\frac{R_2'}{s} I^2}{\frac{R_2'}{s} I^2} = \frac{\vec{bt}}{\vec{Pi}}$$

The efficiency is

$$\eta = \frac{\text{output}}{\text{input}} = \frac{\overline{Pb}}{\overline{PQ}}$$

Maximum power factor occurs when the current vector I_1 is tangent to the circle at point 1. Maximum output occurs when the tangent to the circle is parallel to the output line $O'B$ at point 2. Maximum torque occurs when the tangent to the circle is parallel to the torque line $O'T$ at point 3. And maximum input occurs when the circle reaches its crest at point 4.

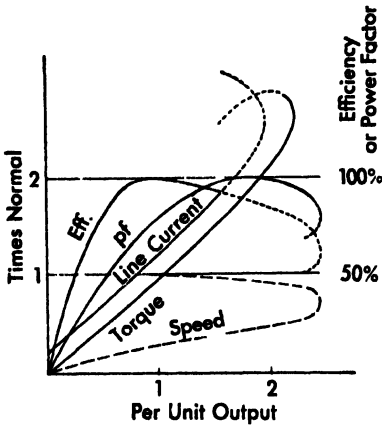


Fig. 24 Performance characteristics.

It is possible to employ geometric constructions leading to graduated line segments on which slip, efficiency, or other variables may be read directly. But unless a great many points are to be computed, or a slide rule is not at hand, there appears to be little

need for elaborating on the simple circle diagram.

Recapitulating, if the circle diagram has been laid out on a current scale, we have

	Input	Load Circuit	Exciting Circuit
Current	$I_1 = OP$	$I = O'P$	$I_0 = OX'$
Pf angle	θ_1	θ	θ_0
Watts	$m_1 V_1 P \zeta$	$m_1 V_1 P_t$	$m_1 V_1 \zeta'$
Vars input	$m_1 V_1 OX$	$m_1 V_1 O'c$	$m_1 V_1 OM$
Volt amp input	$m_1 V_1 OP$	$m_1 V_1 O'P$	$m_1 V_1 OX'$
Watts output		$m_1 V_1 \bar{P}b$	
Core loss			$m_1 V_1 \zeta Q$
Copper loss	$m_1 V_1 ct$ (stator)	$m_1 V_1 tb$ (rotor)	
Total loss	$m_1 V_1 b\bar{Q}$		
Efficiency	$\eta = \frac{\bar{Pb}}{P \zeta}$		
Torque		$\frac{33000}{2\pi n_s 746} m_1 V_1 P_t$	
Slip		$s = \frac{bt}{\bar{P}t}$	
Speed		$1 - s = \frac{\bar{P}b}{P_t}$	

Typical performance characteristics calculated from the circle diagram are shown in Fig. 24. The dotted portions of the curves represent regions

of instability. Reasonable accuracy requires that the circle be drawn with a diameter of, say, 10 inches. It may be constructed in terms of the six design constants G_0 , B_0 , R_1 , X_1 , R_2' , X_2' if known, or from test data. Thus the running-light test data give I_0 and θ_0 from which point O' is located, and the blocked-rotor test data give I_R and θ_R from which point B is located. The center of the circle is then at the point where the perpendicular bisector of $O'B$ cuts the line $O'D$.

10. Analytical Derivation of Exact Circle Diagram

Referring to Fig. 20b for the exact equivalent circuit, the over-all admittance is

$$Y = G - jB = \frac{1}{Z_1 + \frac{Z_2'}{1 + Z_2'Y_0}} = \frac{1 + Z_2'Y_0}{Z + Z_2' + Z_1Z_2'Y_0} \quad (50)$$

Solving for Z_2' , and substituting orthogonal components, there is

$$Z_2' = \frac{R_2'}{s} + jX_2' = \frac{1 - (G - jB)(R_1 + jX_1)}{(G - jB) - (G_0 - jB_0) + (G - jB)(G_0 - jB_0)(R_1 + jX_1)}$$

Now if the right-hand member is rationalized and its imaginary component equated to jX_2' on the left, there results

$$X_2' = \frac{-G^2(X_1 + B_0Z_1^2) - B^2(X_1 + B_0Z_1^2) + 2GB_0R_1 + (2B/X_1 + 1)B - B_1}{(G^2 + B^2)(1 + 1/s^2Z_1^2 + 2G_0R_1 + 2B_0X_1) - 2G(G_1 + 1/s^2R_1) - 2B(B_1 + 1/s^2X_1) + 1/s^2}$$

and this expression may be rearranged in the form

$$\left(G - \frac{J}{L}\right)^2 + \left(B - \frac{K}{L}\right)^2 = \left(\frac{1}{2L}\right)^2 \quad (51)$$

where $J = R_1X_2'Y_0^2 + R_1B_0 + X_2'G_0$

$$K = X_1X_2'Y_0^2 + X_1B_0 + X_2'B_0 + \frac{1}{s}$$

$$L = X_2'(1 + Z_1^2Y_0^2 + 2R_1G_0 + 2X_1B_0) + X_1 + Z_1^2B_0$$

which is the equation of a circle of radius $1/2L$ and center at J/L and K/L . If Equation (51) is multiplied through by V_1 , then GV_1 and BV_1 are the components of the stator current, $I_1 = (G - jB)V_1$. It is to be noted that rotor resistance R_2' and slip s do not appear in (51), but R_2'/s does fix specific points on the circle, as is evident from (50). The standstill point, $s = 1$, follows from (50) upon substituting $Z_2' = (R_2' + jX_2')$. The synchronous speed point, $s = 0$, follows from (50)

upon substituting $Z_2' = \infty$, which gives

$$[G - jB]_{\infty} = \frac{(G_0 + R_1 I_0^2) - j(B_0 + X_1 Y_0^2)}{1 + Z_1^2 Y_0^2 + 2(R_1 G_0 + X_1 B_0)} \quad (52)$$

In practical cases this can hardly be distinguished from $(G_0 - jB_0)$, and in fact the circle of (51) differs very little from the circle for the approximate equivalent circuit. (See Problems 8 and 10.)

11. The Design Constants

The six design constants of the induction motor, which together with the type of windings, number of poles, voltage and frequency, determine its performance characteristics, are G_0 , B_0 , R_1 , X_1 , R_2 , X_2 . The manufacturers possess an abundance of design data, of both a theoretical and empirical nature, for computing these parameters to a high degree of accuracy, but design calculations and procedures differ considerably among the different manufacturers. In this text consideration of these design constants will be limited to a discussion of basic principles.

12. The Core Loss (G_0)

In accordance with the theory of the induction motor developed in the foregoing pages, the core loss is accounted for by the parameter G_0 as $m_1 G_0 V_1^2$, although this same factor may include the windage and friction losses. Core-loss curves (which include both eddy-current and hysteresis loss) as functions of flux density and frequency, and which include test corrections for nonuniform flux distributions due to irregular shapes and saturation of parts, permit the loss in different portions of the magnetic circuit to be computed. Since core loss varies approximately as the volume of iron and square of the flux density, it is evident that for the same total flux a reduction in core loss can be secured by increasing the areas and operating at reduced flux densities

$$P_0 \propto B^2 v = \left(\frac{\phi}{A}\right)^2 (Al) = \frac{\phi^2 l}{A}$$

But this adds to the cost of the motor.

13. The Magnetizing Current (B_0)

The magnetizing current depends on the flux densities in the different parts of the motor, and due to saturation increases greatly with higher flux densities. This current, which in standard designs may be as high

as 40 per cent of the load current, not only depresses the power factor, but increases the stator copper loss. It can be reduced by operating at lower flux densities, but then the size and cost of the motor is increased. It is limited by using the smallest air gaps which are feasible from a mechanical point of view, and by using teeth having thin overhangs that almost close the slot. In small motors it can be compensated by shunt capacitors supplied as part of the motor.

14. The Winding Resistances (R_1 , R_2)

The ordinary d-c resistance of a conductor is given by

$$R = \frac{l}{A} \rho_0 [1 + \alpha_0(T - T_0)] \quad (53)$$

in which l is its length, A its cross-section, ρ_0 the resistivity at temperature T_0 , T any other temperature, and α_0 the temperature coefficient at 0°C. But the conductors of the motor are embedded in iron and linked by considerable leakage flux across the slot and from tooth tip to tooth tip in the air gap. This flux causes a very uneven distribution of current in the stator conductors at all times and increases the effective stator resistance by as much as 50 per cent. The same is true of the rotor resistance during the starting period when its frequency is high, but under running conditions the skin effect is negligible, since the frequency is only a few cycles. Skin effect calculations are involved, and cannot be separated from consideration of slot leakage reactance.* Stranding of conductors and transposition of the strands reduces the eddy-current loss in the conductors. Skewing a conductor increases the length slightly, and adds to its resistance. High-frequency flux pulsation, due to the passage of rotor teeth by the stator teeth, add to the conductor eddy-current losses.

15. The Leakage Reactances (X_1 , X_2)

The leakage reactance of an induction motor is usually calculated in several separate parts as *slot*, *end-connection*, *tooth-tip* or *zigzag*, and *belt* or *differential* leakage flux reactances. The slot leakage flux may be calculated in the same way as for synchronous machines. It is sufficient to assume the flux to go straight across the slot, Fig. 25, and uniform current distribution, although exact determination of the flux and current distributions are possible.* On these assumptions the stator leakage

* Bewley, L. V., *Two-dimensional Fields in Electrical Engineering*, New York, The Macmillan Co., 1948.

flux for an open slot is (see Sec. 5, Chap. 3) proportional to

$$\phi_{s1} = \frac{K}{w'} \left(\frac{d_1}{3} + d_s \right) + (1 - K) \frac{d_1}{12w'} - \frac{d_2}{4w'} \left(K - \frac{2}{3} \right) \quad (54)$$

in which the dimensions refer to Fig. 25, and K is a factor accounting for the fact that the two conductors in the top and bottom of the slot

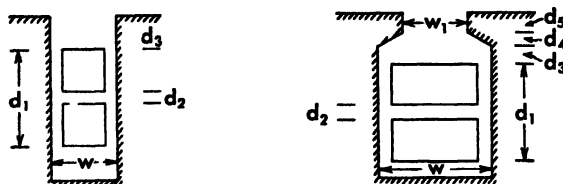


Fig. 25 Slot dimensions

do not carry in-phase currents unless the coils are full pitch. Values of K are given in the following table:

	1 > pitch > 2 3	2 3 > pitch > 1 3	1 3 > pitch > 0
1 ϕ - 180° belt	pitch	pitch	pitch
2 ϕ - 90° belt	pitch	pitch	pitch
3 ϕ - 60° belt	0.75 pitch + 0.25	1.50 pitch - 0.25	0.75 pitch
3 ϕ - 120° belt	0.75	1.125 pitch	1.125 pitch
$\infty \phi$ - 0° belt	K_p'	K_p''	K_p''

The leakage flux for the rotor (referred to the stator) is proportional to

$$\phi_{2s} = \frac{K_{p1}^2 K_{d1}^2 S_1}{K_{p2}^2 K_{d2}^2 K_{p2}^2 S_2} \left[K \left(\frac{d_s}{w'} + \frac{2d_1}{w'} + \frac{d_1}{w'} + \frac{d_1}{3w'} \right) + \frac{d_1}{12w'} (1 - K) \right] \quad (55)$$

where S_1 and S_2 are the total stator and rotor slots respectively, and K_{p1} , K_{p2} , K_{d1} , etc. are the skew, pitch and distribution coefficients. These are each equal to unity for a squirrel-cage winding. The terms enclosed by the horizontal brace ~ are replaced by 0.60 for a squirrel cage.

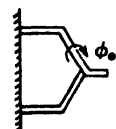


Fig. 26
End turn
leakage flux.

The end-connection leakage flux, Fig. 26, cannot be calculated precisely, but a good estimate is given by C. A. Adam's formula

$$\phi_r = \frac{K D S_1}{2 P l} \times \begin{cases} 0.9 & \text{for 2 pole motors} \\ 1.2 & \text{for 6600 volt motors} \\ 1.5 & \text{for two conductors per slot} \end{cases} \quad (56)$$

where P = number of poles
 D = diameter of air gap in inches
 l = core length (less ducts) in inches
 K = out-of-phase correction factor (table above)

In addition to the discrete leakage fluxes discussed above, there are space harmonic fluxes in the air gap which induce fundamental voltages in the stator, but do not contribute to the power output. They are, therefore, properly classified as reactance voltages. Their determination rests on the general harmonic analysis given in the Appendices. When such an analysis is made, the total *differential leakage reactance* may be split into *belt* and *zigzag* leakage reactance. To the latter are attributed those harmonics due to the teeth, and then belt reactance is calculated as the difference between the total differential and zigzag reactances. Physically, zigzag leakage fluxes are those which zigzag back and forth between stator and rotor teeth, as indicated in Fig. 27.

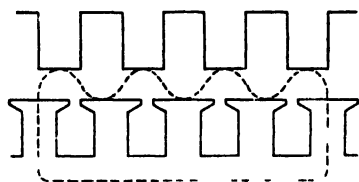


Fig. 27 Zigzag leakage flux

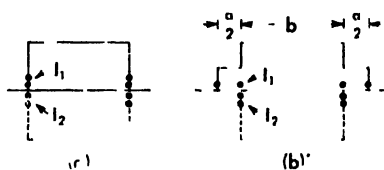


Fig. 28 Belt differential leakage reactance

The physical explanation of belt leakage fluxes has been given by Hellmund and Veinott* in terms of Fig. 28. Suppose for the sake of simplicity that stator and rotor have the same number of turns and carry equal currents. Then if both windings have the same distribution, Fig. 28(a), equal voltages are induced in each, and there is no "leakage" flux between them. Now suppose the distributions to be as in Fig. 28(b), in which the two winding distributions no longer match. Neglecting the resistance and reactance of the secondary, its total flux linkages must be zero, since its voltage must then be zero. The flux linkages of the secondary are proportional to

$$\lambda_2 = 2(b2I_1 + b2I_2) = 0 \quad \text{or} \quad I_2 = -I_1$$

while the flux linkages of the primary are

$$\lambda_1 = (2b2I_1 + aI_1 + 2b2I_2) = aI_1$$

* Hellmund and Veinott, "Transformer Ratio and Differential Leakage of Distributed Windings," *IEEE Trans.* Vol. 49, 1930

Thus it is seen that even though the currents are equal and opposite and there are no flux linkages with the secondary, nevertheless there are flux linkages with the primary, and these constitute the *belt differential leakage reactance*. The above example has been made as simple as possible in order to illustrate the principles, but it is clear that in any case in which the two windings are dissimilarly arranged, there may be differential leakage flux. The method of calculating differential leakage is given in Chap. 3.

The total leakage reactance of the induction motor is (dimensions in inches)

$$X = \frac{2fm_1LN_1^2}{10^7S_1} (\phi_{s1} + \phi_{s2} + \phi_r) + X_{zz} + X_B \text{ ohms per phase} \quad (57)$$

in which X_{zz} is the zigzag and X_B the belt reactance.

16. Performance Calculations

The ultimate purpose of any method of analysis is the determination of the principal characteristics of the motor—speed, torque, power output, power factor, current, losses, and efficiency—as well as to study the effects of variation in voltages and frequency, and changes in the design constants.

In the previous sections three different methods—general equations, equivalent circuits (exact and approximate), vector and circle diagrams (exact and approximate)—have been presented for analyzing the polyphase induction motor. In addition, there are other types of circle diagrams, and the cross-field theory. The latter will be developed in detail for the single-phase induction motor in the next chapter. Each method of analysis has certain advantages. The general equations are, of course, the basis for all methods.

The equivalent circuit (originally proposed by C. P. Steinmetz) and its approximations show the intimate relationship of the induction motor to the transformer. It is well adapted to the formulation of design equations, particularly in series form. P. L. Alger has given such an analysis,* in which the reciprocals of complex constants are expanded in infinite series, and only the dominate terms retained, as the circuit is successively reduced to a final over-all impedance. Calculations based on the approximate equivalent circuit appear to be sufficiently accurate for ordinary purposes. Indeed, it is questionable if the additional refinement of the so-called exact equivalent circuit leads to more accurate results.

* Alger, P. L. "Induction Motor Performance Calculation," *AIEE Trans*, Vol. 49, 1930.

The circle diagram not only offers a visual picture of the way in which the different characteristics vary with respect to each other, but is also the best adapted to the calculation of mass data for complete characteristic curves. However, accuracy demands that the circle diagram be made with care and of reasonable size - say 10-inch diameter.

Characteristics are plotted in different ways, but usually against *output*, as in Fig. 24 or against *speed* or *slip* as in Fig. 29. The latter is preferable for determining the acceleration of a load, or for seeing the effects of load changes on speed regulation.

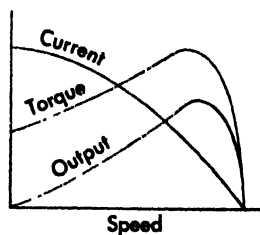


Fig. 29

17. Effect of Harmonics

Time harmonics may exist in the applied voltage, or be introduced by magnetic saturation, or result from pulsating space harmonics of flux due to the passage of the teeth of the rotor by those of the stator. If polyphase time harmonics of current are permitted to flow, they give rise to rotating fields which, according to (4), may be null, forward or backward, and which produce corresponding torques. The speed of a rotating n th harmonic field is n -times that of the fundamental field, and therefore synchronous rotor speed with respect to the fundamental

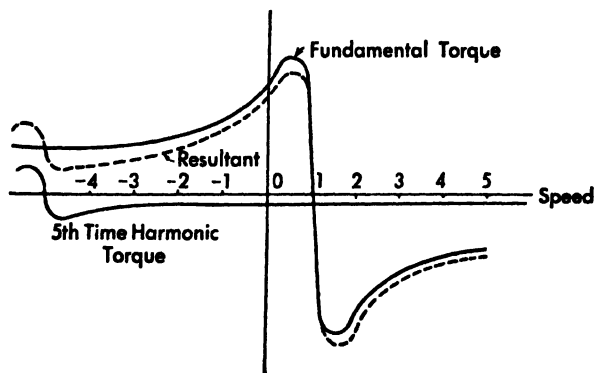


Fig. 30 Effect of time harmonics on the torque speed characteristic.

is only $1/n$ th synchronous speed with respect to the n th harmonic. Figure 30 shows a 5th time harmonic torque (greatly exaggerated) superimposed on the fundamental torque. The harmonic-torque curve is stretched out five times as long as the fundamental-torque curve, and since a 5th time

harmonic produces a backward rotating field, its torque-speed curve passes through zero at five times synchronous speed backward. Thus the net torque is reduced by the presence of a 5th time harmonic. On the other hand, a 7th time harmonic would augment the net torque, while any 3rd harmonic or its multiple would have no effect on the torque. In practice, the time harmonics are always small and may be ignored.

Space harmonics may exist in the flux depending upon the skew, pitch and distribution of the windings and the slot and teeth combinations. A complete harmonic analysis will not be carried out here, but reference may be made to the Appendices where it is shown that space harmonics may be of any order

$$k = \begin{cases} (2\alpha m + 1) & \text{for forward rotating fields} \\ (2\alpha m - 1) & \text{for backward rotating fields} \end{cases}$$

where: k = order of the space harmonic

α = any positive integer

m = number of phases

Now a k th space harmonic of flux has k times as many poles as the fundamental, and therefore its torque-speed curve passes through zero at $1/k$ synchronous speed, positive or negative, depending on whether its field is forward or backward. Figure 31 shows the torque-speed curves for the fundamental, fifth, and seventh space harmonics, and their resultant. It is evident that such space-harmonic torque cusps may cause dips in the torque-speed curve which will not permit the motor to bring its load up to full speed.

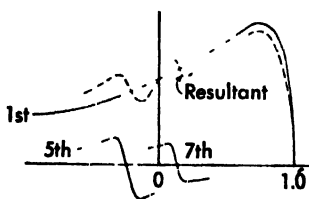


Fig. 31 Effect of space harmonics

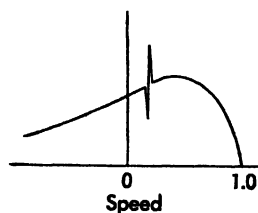


Fig. 32 Cusp in the torque-speed characteristic.

There is still another effect due to space harmonics, called *subsynchronous locking*. It is possible for certain rotor harmonics to produce rotating fields which revolve in synchronism with certain stator harmonic fields (of a different order) for one particular rotor speed. When the rotor reaches this critical speed the two fields lock in synchronism, and may

cause a pronounced cusp as shown in Fig. 32, and the motor may not be able to "pull out of synchronism" at this speed.

The theory of parasitic torques in induction motors is not complete. Designers rely to a large extent on empirical rules and design records to avoid stator-rotor slot combinations which will cause subsynchronous locking, crawling, and excessive noise. Skewing of the rotor bars will smooth out the torque-speed curves and reduce the noise, but skewing adds to the cost and increases the leakage reactance.

Space harmonics also increase the core loss, since the frequency of the rotor harmonic currents due to them is high. If synchronous (fundamental) speed is n_1 , then for the k th space harmonic (which has k times as many poles) synchronous speed is $\pm n_1/k$ and therefore the slip with respect to the k th harmonic is

$$s_k = \frac{\pm n_1/k - n_2}{\pm n_1/k} = 1 + \frac{n_2}{n_1}k = 1 + k(1 - s)$$

and the rotor frequency for this harmonic is

$$s_k f_1 = [1 + k(1 - s)]f_1$$

or high when the motor is running at normal speed.

18. Starting of Polyphase Induction Motors

The starting torque of an ordinary polyphase induction motor is usually between 100 and 200 per cent of its running torque, whereas its low power factor starting current may be 5 or 10 times normal running current. High starting currents are not only objectionable on the power system, but require oversize fuses and abnormally high settings for the relays and circuit breakers, militating against their protective functions. There are three common methods for reducing the starting current: (1) reduced voltage starting, (2) wound rotor motors with external resistors, and (3) special designs. The problem is to reduce the starting current to tolerable values without reducing the torque below that necessary to start and accelerate the load, and without jeopardizing good running characteristics. It will be sufficient for our purposes to investigate the possibilities in terms of the approximate equivalent circuit, and neglecting the exciting current. The torque (in synchronous watts) and current equations then are, putting $X = X_1 + X_2'$,

$$I = \frac{V_1}{\sqrt{(R_1 + R_2'/s)^2 + X^2}} \quad (58)$$

$$I = \frac{V_1}{\sqrt{(R_1 + R_2')^2 + X^2}} \text{ for } s = 1 \quad (58a)$$

$$T = \frac{R_2}{s} \frac{m_1 V_1^2}{(R_1 + R_2'/s)^2 + X^2} \quad (59)$$

$$= R_2' - \frac{m_1 V_1^2}{(R_1 + R_2')^2 + X^2} \text{ for } s = 1 \quad (59a)$$

$$T_{\max} = \frac{m_1 V_1^2}{2(R_1 + \sqrt{R_1^2 + X^2})} \text{ for } s = \frac{R_2'}{\sqrt{R_1^2 + X^2}} \quad (60)$$

It is evident from (58a) that the starting current may be reduced by reducing the applied voltage, but in so doing the starting torque is reduced as the square of the voltage, according to (59a). Nevertheless, this is the most universal method of starting induction motors of moderate size. It is also clear from (58a) that the starting current may be reduced by increasing R_2' , and from (59a) it is seen that this may result in an actual increase in the starting torque, although a permanent material increase in R_2' would result in a motor with high slip, excessive running losses ($R_2'I^2$), and low efficiency. High starting and moderate running rotor resistance is possible with wound rotor and double squirrel cage motors.

19. Line Start Motors

It is not necessary or feasible to provide auxiliary starting devices for small motors, and they are usually designed to start at full line voltage. They accelerate rapidly and the over current period is of short duration. Also, such motors usually have high rotor resistance to yield high starting torques, and the resulting lower running efficiency is not of great importance.

20. Autotransformer or Compensator Starting

Autotransformers with one or more taps provide a simple and effective way of reducing the voltage applied to the motor during starting. Figure 33 shows a diagram of connections of two autotransformers operating open-delta on a 3-phase system for starting an induction motor. The open-delta arrangement is satisfactory for starting, as the autotransformers carry load for only a short period. Assuming perfect transformation of voltage ratio a , the motor voltage becomes V_1/a , and the corresponding motor current, by (58), is reduced in the same ratio. But line current is, by transformer ratio, $1/a$ times motor current, or $1/a^2$ the starting

current at full line voltage. The lowest tap is fixed by the smallest voltage which will yield sufficient starting torque. Taps are then changed automatically by a relay at definite current values until the motor is brought up to full speed.

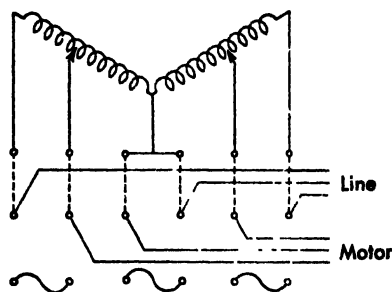


Fig. 33 Compensator starting.

Let the permissible maximum line current be I'_{\max} and suppose the transformer is on tap k with transformation ratio a_k . When contact is first made with tap k the motor current is $a_k I'_{\max}$. When the motor current has fallen to the permissible minimum value $I_{\min(k)}$ (fixed by the minimum torque requirement) the slip will be given by

$$I_{\min(k)} = \frac{V_1}{a_k \sqrt{(R_1 + R_2' s_k)^2 + (X_1 + X_2')^2}} \quad (61)$$

At this instant let the voltage be increased to $V_1' a_{k+1}$ such that the line current is again I'_{\max} , or the motor current $a_{k+1} I'_{\max}$. Then

$$a_{k+1} I'_{\max} = \frac{V_1'}{a_{k+1} \sqrt{(R_1 + R_2' s_k)^2 + (X_1 + X_2')^2}} \quad (62)$$

and comparing (61) and (62) there results

$$a_{k+1} = \sqrt{\frac{I'_{\max}}{I_{\min(k)}}} \quad (63)$$

The initial transformer tap at start ($s_0 = 1$) is, by (62),

$$a_1 = \sqrt{\frac{1}{(R_1 + R_2')^2 + (X_1 + X_2')^2}} \sqrt{\frac{V_1'}{I'_{\max}}} \quad (64)$$

If the load torque (including torque for acceleration), as function of the slip, is $T(s)$, then the slip s_k at which minimum current occurs must satisfy the equality

$$T(s_k) = \frac{33000 m_1}{2\pi n_1 746} \frac{R_2'}{s_k} \frac{(V_1' a_k)^2}{(R_1 + R_2'/s_k)^2 + (X_1 + X_2')^2} \quad (65)$$

Since the load torque $T(s_k)$ is usually given as a curve, this is best solved by plotting the two sides of the equation against slip and determining s_k from their intersection.

Starting compensators are built as complete units including the auto-transformer, relays, undervoltage releases, and contactors all enclosed in a cabinet. The relays operate automatically to change taps on the auto-transformer at predetermined values of current.

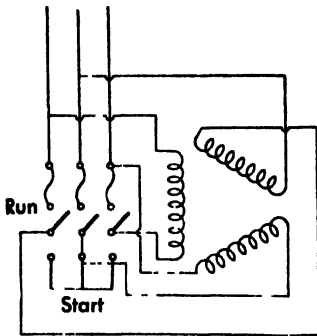


Fig. 34 Wye delta starting

21. Wye-delta Starting

Figure 34 shows a 3-phase motor with all leads brought out and connected to a triple-pole, double-throw switch so that the windings may be connected wye for starting and delta for running. When connected wye the volts per phase are reduced to $1/\sqrt{3}$ of normal with a corresponding reduction of $1/\sqrt{3}$ in starting current per phase, or one-third as much line starting current as for the delta connection. The torque, being proportional to the square of the current, is reduced to one-third.

22. Wound-rotor Motor with External Resistor

The wound rotor motor with adjustable external resistor offers the best, but most expensive method of starting, since, as has already been pointed out, maximum starting torque may be obtained with moderate current. As the motor comes up to speed the resistor is cut out in steps until the rotor is short circuited under normal running conditions. Thus optimum starting conditions do not vitiate good running characteristics. Suppose the resistor to be cut out in steps so that the current will vary between I_{\max} and I_{\min} , and let the total resistance in the rotor for any stage k be r_k . Then by (58) the current decreases from a maximum, (66), at slip s_{k-1} to a minimum, (67), at slip s_k .

$$I_{\max} = \frac{V_1}{\sqrt{(R_1 + r_k/s_{k-1})^2 + X^2}} \quad (66)$$

$$I_{\min} = \frac{V_1}{\sqrt{(R_1 + r_k/s_k)^2 + X^2}} \quad (67)$$

Now by (66), since the maximum current is the same for every stage,

$$\frac{r_{k+1}}{s_k} = \frac{r_l}{s_{l-1}} \quad (68)$$

By (66), (67), and (68)

$$\frac{r_{l+1}}{r_l} = \frac{\sqrt{(I_1 I_{\max})^2 - \lambda^2 - R_1}}{\sqrt{(I_1 I_{\max})^2 - \lambda^2 - R_1}} = \text{constant} \quad (69)$$

Thus there is a fixed ratio between successive resistances, and the slip s_l at any transition point may be calculated from (68) starting with $s_0 = 1$. Now either the starting current can be specified as I_{\max} and the final current peak allowed to be what it may, or the final current peak can be specified and the starting current allowed to be what it will, but both specifications simultaneously are, in general, incompatible.

In the case, Fig. 35, where the starting current is to be limited to I_{\max} for $s_0 = 1$, (66) gives the necessary resistance r_1 and (67) then gives the slip s_1 at which the current becomes I_{\min} . Successive values of r_{l+1} follow from (69), and corresponding slips from (68), until the rotor is finally short-circuited, and the current peak goes to a value determined by (66).

In the case where the final current peak is to be held to a limit I_{\max} , the slip at which this occurs is found from (66), and the resistance steps are given by (69). The starting current may be larger or smaller than I_{\max} .

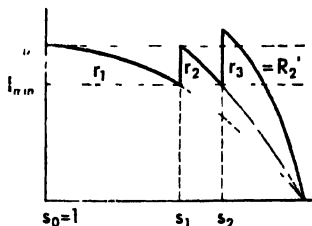


Fig. 35 Starting cycle with limit on initial current

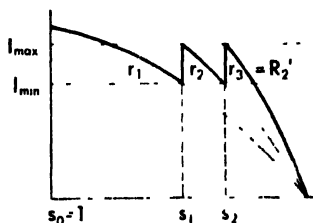


Fig. 36 Starting cycle with limit on current

Current diagrams may also be constructed on the basis of a fixed number of steps, or on other assumptions, but the general procedure is along the lines outlined above.

It is sometimes required to determine a starting cycle in which the torque is not to fall below a minimum value T_{\min} , and maximum torque T_{\max} is to be available at start, Fig. 37. This cycle yields fastest acceleration. The rotor resistance to give maximum torque at standstill must be

$$r_1 = \sqrt{R_1^2 + \lambda^2}$$

and this is reduced in steps as the motor comes up to speed. By (60) and (59)

$$\frac{T'_{\min}}{T_{\min}} = \frac{(R_1 + r_1/s_1)^2 + X^2}{2(R_1 + \sqrt{R_1^2 + X^2})(r_1/s_1)} \quad (70)$$

and solving for s_1 , one can determine the slip at which the resistance is to be reduced from r_1 to a value r_2 which satisfies the condition

$$T_{\min} = \frac{r_2}{s_1 (R_1 + r_2/s_1)^2 + X^2} = \frac{r_1}{s_1 (R_1 + r_1/s_1)^2 + X^2}$$

which yields

$$r_2 = r_1 s_1^2 \quad (71)$$

With this new value of rotor resistance the motor accelerates to a slip

$$s_2 = \frac{r_2}{r_1} s_1 = s_1^3 \quad (72)$$

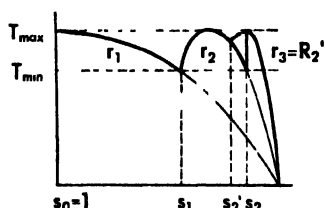


Fig. 37 Starting cycle with limit on torque

when the rotor resistance is changed to $r_3 = r_2 s_1^2$. The process is continued until at the final step the rotor is short-circuited. At the final short-circuiting of the rotor (s_2 in Fig. 37) the torque may jump abruptly, since the rotor resistance is not necessarily the value required by

(71) for smooth transition. To avoid this torque jump, the short-circuiting can be made at a slip s' which satisfies the condition

$$\frac{r}{s'} (R_1 + r/s')^2 + X^2 = \frac{R_2'}{s'} (R_1 + R_2'/s')^2 + X^2$$

from which

$$s' = \sqrt{\frac{r R_2'}{R_1^2 + X^2}} \quad (73)$$

Example: A 3-phase, Y-connected, 60-cycle, 220-volt, 5-hp, 1800-rpm, wound rotor induction motor has the following constants: $R_1 = 0.545$, $R_2' = 0.541$, $X_1 + X_2' = 1.68$. The slip at full load is $s = 0.05$. The line current during the starting cycle is not to exceed 3 times normal current. The load torque equation is $T(s) = 10 + 6.1(1 - s)^2$ lb-ft. Investigate the different starting methods, neglecting the exciting current.

1. Line start

$$\text{Normal current } I = \frac{127}{\sqrt{(0.545 + 0.541/0.05)^2 + 1.68^2}} = 11.07$$

$$\text{Normal torque } T = \frac{33000 \times 3}{2\pi 1800 \times 746} \frac{0.541}{0.05} 11.07^2 = 15.6 \text{ lb-ft}$$

$$\text{Starting current } I_{(0)} = \frac{127}{\sqrt{(0.545 + 0.541)^2 + 1.68^2}} = 63.5$$

$$\text{Starting torque } T_{(0)} = 0.01175 \times 0.541 \times 63.5^2 = 25.6 \text{ lb-ft}$$

The starting current is nearly twice the allowable line current, which precludes this method of starting.

2. Compensator starting

The maximum permissible line starting current is $I'_{\max} = 3 \times 11.07 = 33.2$ amperes. By (64), the initial transformer tap is

$$a_1 = \left(\frac{127}{33.2} \right)^{1/2} \frac{1}{[(0.545 + 0.541)^2 + 1.68^2]^{1/4}} = 1.38$$

giving an initial motor current of $1.38 \times 33.2 = 45.8$ amperes and a starting torque of

$$T_{(0)} = 0.01175 \times 0.541 \times 45.8^2 = 13.4 \text{ lb-ft}$$

By (65), the slip at which the tap is changed satisfies the equation,

$$10 + 6.1(1 - s_1)^2 = 0.01175 \frac{(0.541 + 0.541 s_1 + 1.38)^2}{s_1 [0.545 + 0.541 s_1 + 1.68^2]}$$

from which it is found that $s_1 = 0.108$, and the minimum current, by (61), is

$$I_{\min} = \frac{127 \cdot 1.38}{\sqrt{(0.545 + 0.541 \cdot 0.108)^2 + 1.68^2}} = 15.80$$

Hence by (63) the new transformer ratio is

$$a_2 = \left| 1.38 \frac{15.80}{33.20} \right| = 0.81$$

which, being less than unity, means that the motor would be thrown directly on the line at this instant. The line current at the instant after change-over is

$$I = 1.38 \times I_{\min} = 21.80$$

and the torque jumps to

$$T_{(1)}' = 0.01175 \times \frac{0.541}{0.108} \cdot 21.80^2 = 28 \text{ lb-ft}$$

3. Wye-delta starting

Suppose that a motor drawing the same line current and with the same torque characteristics as specified in the example can be designed for a delta running connection, but may be started wye-connected. The starting current per phase in delta with 220 volts across the winding is $63.5 / 1.73 = 36.6$ amperes. If connected in wye, the voltage across each phase is reduced by the $\sqrt{3}$, and the new phase and line current is $36.6 / 1.73 = 21.2$. This is below the per-

missible maximum line current. The torque, however, being proportional to the square of the current is one-third of the delta starting torque, or 25.6 \times 8.5 lb-ft. This is below that required by the load, and therefore wye-delta starting is not suitable for this case.

4. Wound rotor (current limitations)

Maximum starting current is 33.2 amperes. This will require a total rotor resistance (referred to the stator) such that

$$33.2 = \frac{127}{\sqrt{(0.545 + r_1)^2 + 1.68^2}} \text{ or } r_1 = 2.88 \text{ ohms}$$

At this current and resistance the starting torque is

$$T_{01} = 0.01175 \times 2.88 \times 33.2^2 = 37.3 \text{ lb-ft}$$

which is several times that required by the load.

If it is desired to have the fewest possible steps in the external resistance, then minimum current may be determined by finding the slip at which the torque with $r_1 = 2.88$ ohms in the rotor is just equal to the load torque. However, by taking a higher value for the minimum current more steps, but faster acceleration and smoother starting are possible. In the present case, try $I_{min} = 20$ amperes. Then by (69),

$$\frac{r_1}{r_k} = \frac{\sqrt{(127/33.2)^2 - 1.68^2} - 0.545}{\sqrt{(127/20)^2 - 1.68^2} - 0.545} = 0.52$$

And by (68), starting with $s_0 = 1$, the slip at which the current reaches a minimum is

$$s_1 = 0.52 \times 1 = 0.52$$

At this slip the torque is

$$T_{01} = 0.01175 \times \frac{2.88}{0.52} \times 20^2 = 26 \text{ lb-ft}$$

Repeated use of (68) and (69) and the torque equation yield in succession

k	0	1	2	3	4	
r_1	2.88	2.88	1.50	0.78	0.541	(rotor resistance)
s_k	1.00	0.52	0.27	0.14	0.05	(full load slip)
T_k		26	26	26	15.6	(full load torque)
T_k'	37.3	37.3	37.3	33.2		(peak torque)

At the third step, when the rotor is short-circuited, the current jumps to

$$I_{03} = \frac{127}{\sqrt{(0.545 + 0.541/0.14)^2 + 1.68^2}} = 26.9$$

and the torque to $T_{03} = 0.01175 \frac{0.545}{0.14} 26.9^2 = 33.2$

Wound-rotor (maximum torque at start)

The rotor resistance for maximum torque at start is

$$r_1 = \sqrt{0.545 + 1.68^2} = 1.76 \text{ ohms}$$

and starting current is

$$\frac{127}{\sqrt{(0.545 + 1.76)^2 + 1.68^2}} = 44.7 \text{ amperes}$$

This exceeds the allowable starting current of 33.2 amperes. Nevertheless, the calculations will be completed. Maximum torque is, by (60),

$$T_{\max} = 0.01175 \times \frac{127}{2(0.545 + \sqrt{0.545^2 + 1.68^2})} = 41 \text{ lb ft}$$

Let minimum torque be taken as $T_{\min} = 30 \text{ lb ft}$. Then by (70)

$$\frac{41}{30} = \frac{(0.545 + 1.76 s_1)^2 + 1.68^2}{2(0.545 + \sqrt{0.545^2 + 1.68^2 (1.76 s_1)^2})}$$

which is satisfied by $s_1 = 0.39$. The new resistance for the rotor at this slip is, by (71),

$$r = 1.76 \times 0.39 = 0.696 \text{ ohms}$$

Since this is less than the rotor resistance of 0.541 ohms, the rotor would be short-circuited at this slip, and the torque jumps to

$$T_1' = 0.01175 \times \frac{0.541}{0.39} \times \frac{127}{(0.545 + 0.541/0.39)^2 + 1.68^2} = 40.2 \text{ lb ft}$$

The abrupt jump in torque could have been avoided, according to (73), by short-circuiting the rotor at a slip

$$s' = \frac{1.76 \times 0.541}{0.545 + 1.68} = 0.552$$

23. The Double Squirrel-cage Induction Motor

Good running characteristics—high efficiency, high power factor, and close speed regulation—call for low rotor resistance and small exciting admittance. On the other hand, good starting characteristics

high torque and moderate starting current require a high rotor resistance and low reactances. These apparently incompatible requirements for good running and good starting characteristics in the same

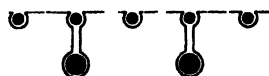


Fig. 38

machine are reconciled in the double squirrel-cage motor, Fig. 38. The outer cage consists of high-resistance bars

of small cross-section, sometimes made of brass. The inner cage consists of low resistance bars of large cross-section. The rotor frequency is high at starting, and the consequent high reactance excludes current from the deep conductors and thus the inner cage contributes only moderate starting torque. The outer cage with its high resistance and relatively small reactance contributes a major share of the starting torque. As the motor speeds up the reactance decreases and the rotor resistances become the principal components of the impedance, and thus near synchronous speed the low-resistance inner cage carries the bulk of the current and furnishes the major portion of the torque. The resultant torque may be thought of as the combination of the torque-speed curves of the high- and low-resistance cages respectively, as shown in Fig. 39. The relative behaviors of the two cages may be summarized in the following table, in which primed quantities refer to the outer high-resistance cage and double primed quantities to the inner low-resistance cage:

	High	Low
Start	$R_2', V_2'', I_2', Pf', T'$	$R_2'', V_2', I_2'', Pf'', T''$
Run	$R_2', I_2'', Pf', T'', \text{Eff.}', \text{Reg.}'$	$R_2'', X_2', X_2'', I_2', Pf'', T', \text{Eff.}', \text{Reg.}''$

A considerable range in resultant characteristics is obtainable through a judicious selection of the design constants of motors of this type. The NEMA Standards specify 6 classifications.

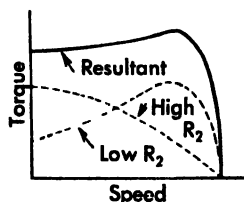


Fig. 39 Torque speed characteristic of a double squirrel cage induction motor.

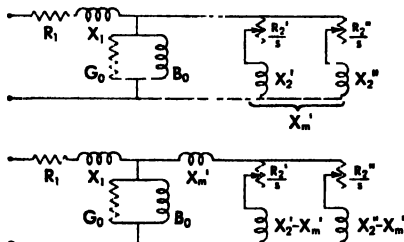


Fig. 40 Equivalent circuit of the double squirrel cage induction motor.

The equivalent circuit of the double squirrel-cage motor is shown in Fig. 40a. The mutual reactance between the two windings is $X_m \cong X_2'$ for a high- and a low-resistance bar in each slot, since any slot or tooth-tip flux caused by the upper bar current links the lower bar. However, when the two cages do not have the same number of slots, $X_m < X_2'$. The equivalent circuit may be reduced to Fig. 40b.

24. Speed Control

The speed of an induction motor may be regulated in five practicable ways: (1) by changing the number of poles, (2) by changing the applied frequency, (3) by rheostatic control in the rotor, (4) by introducing applied voltages of proper frequency to the rotor, and (5) by mounting the stator in bearings and driving it with an auxiliary motor. The induction motor is essentially a constant-speed motor and is not sensitive to speed control by variation of the stator voltage.

25. Changing the Number of Poles

The synchronous speed of an induction motor is

$$n = 120 \frac{f}{p}$$

thus inversely as the number of poles. If the winding is regrouped to provide a different number of poles (usually 2 : 1), or if the motor is constructed with two or more independent windings having different number of poles, several discrete speeds may be obtained. However, as the number of poles is increased the flux per pole (for the same flux density) is decreased proportionately. Moreover, a regrouping of the winding results in different pitch factors. Therefore, the applied voltage must be changed for the different speeds, if the motor is to operate efficiently, and this calls for a variable voltage source of power, such as is feasible in electric ship propulsion. Multiple pole motors usually have squirrel cage rotors, since the number of rotor poles is then automatically the same as the number of stator poles. Otherwise a wound rotor would have to be wound for the same pole combinations as the stator, and changed coincidentally.

26. Changing the Applied Frequency

The speed of an induction motor varies directly as the frequency, but speed regulation by this means is not feasible unless a separate prime mover is used to supply the power, as in electric propulsion on ships. Multiple-pole induction motors are often used to drive ship propellers, and are supplied with power from turbogenerators having a speed range sufficient to permit smooth speed control between the definite speeds corresponding to the different number of motor poles.

27. Rotor Rheostatic Control

For a given torque the slip increases directly as the rotor resistance (see Eq. 38). But the rotor loss also increases proportional to the rotor resistance, and for large values of slip this loss constitutes the bulk of the total motor losses. For this reason rotor rheostatic speed control is not economical. Nevertheless, for loads having intermittent duty cycles consisting largely of accelerating and decelerating periods, as for steel mills and hoists, and where large peaks in the power drawn from the line will not be tolerated, the Ward-Leonard system employing wound-rotor induction motors with rheostatic control, driving d-c generators which in turn supply the main d-c motor, are much used. In such cases, Fig. 41,

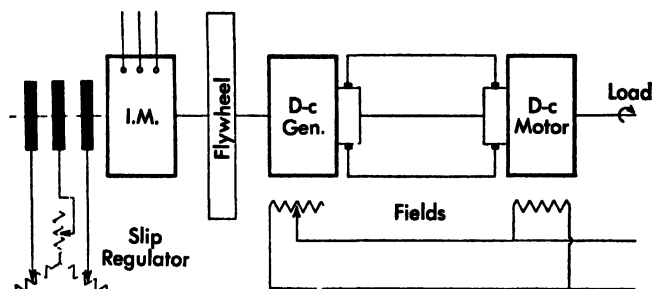


Fig. 41 The Ward-Leonard system.

the motor generator set is provided with a flywheel which yields its kinetic energy as the speed decreases, and absorbs energy as the speed increases, and in this way equalizes the power taken by the induction motor from the supply lines. The rheostat, called a *slip regulator*, is usually a water resistor which is adjusted automatically by relay control so as to regulate the motor input at a constant value.

28. Concatenation

Two wound rotor induction motors on the same shaft and connected so that the stator of the second motor receives its input from the rotor of the first motor constitute a concatenated or cascade arrangement, Fig. 42. If the first motor has p_1 and the second p_2 poles, synchronous speed for the two motors at frequency f_1 are

$$n_1 = 120 \frac{f_1}{p_1} \quad (74)$$

$$n_2 = 120 \frac{f_1}{p_2} \quad (75)$$

Calling the slips for the two motors s_1 and s_2 respectively the common shaft speed is

$$n = 120 \frac{f_1}{p_1} (1 - s_1) = 120 \frac{f}{p} (1 - s_1) = 120 \frac{f_1 s_1}{p} (1 - s_1) \quad (76)$$

from which
$$s_1 = \frac{p}{p_1 + p} - s_2 \frac{p}{p_1 + p} \quad (77)$$

and therefore the synchronous speed of the set is

$$n_1 = \frac{120 f_1}{p_1 + p} \quad (78)$$

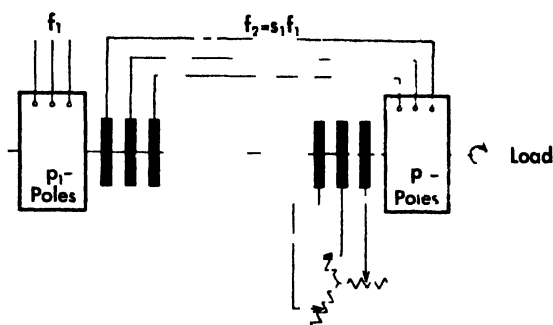


Fig 42 Induction motors in cascade

In terms of the synchronous speed n of the set in cascade the slip is

$$s = \frac{n - n_1}{n} = 1 - \frac{n_1}{n} = \frac{p + p_1}{p_1} s_1 \quad (79)$$

while from (76) and comparison with (79)

$$s_1 s = \frac{p + (p_1 + p) s_1}{p_1} s \quad (80)$$

$$s_1 = \frac{p + p_1 s}{p + p_1} = a + b s \quad (81)$$

$$s = \frac{(p + p_1) s}{p + p_1 s} = \frac{s}{a + b s} \quad (82)$$

Note that
$$a + b = \frac{p}{p + p_1} + \frac{p_1}{p + p_1} = 1 \quad (83)$$

$$\frac{n_0}{n_1} = b \frac{n_1}{n_2} - a \quad (84)$$

It is thus possible to obtain three basic speeds from a pair of induction motors, corresponding to No 1 motor connected to the line (74), No 2

motor connected to the line (75), and the two motors in cascade (78). Furthermore, if the rotor of the second motor is connected to an external resistor, the speed can be adjusted over a considerable range.

The rotor frequency of the first motor is $f_2 = s_1 f_1$ and this is the stator frequency for the second motor. The rotor frequency of the second motor is $s_2 f_2 = s_1 s_2 f_1$. All reactances are proportional to the frequencies.

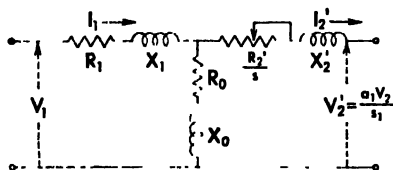
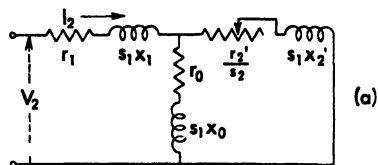


Fig. 43

Fig. 44

The equivalent circuit of the first motor, Fig. 43, is the same as shown in Fig. 16, and recalls that the actual rotor terminal voltage V_2 is related to the equivalent circuit voltage by the relationship $V_2' = a_1 V_2 / s_1$, and also

$$I_2' = \frac{m_2 I_2}{m_1 a_1}.$$

The equivalent circuit of the second motor is shown in Fig. 44a. Since the reactances are in terms of line frequency f_1 it is necessary to multiply them by s_1 when referred to the stator frequency $f_2 = s_1 f_1$. Now for this equivalent circuit

$$V_2 = z I_2$$

and before it can be joined to the equivalent circuit shown in Fig. 43, the voltage must be changed to V_2' and the current to I_2' , thus

$$V_2' = \frac{a_1}{s_1} V_2 = \frac{a_1}{s_1} z \frac{m_1 I_2' a_1}{m_2} = \left(\frac{a_1^2 m_1}{s_1 m_2} z \right) I_2' = \frac{z''}{s_1} I_2'$$

The new equivalent circuit is Fig. 44b, and this may now be connected to that of Fig. 43 to form the equivalent circuit, Fig. 45, for the two motors in cascade. Since $s_1 s_2$ may be replaced by s in accordance with (80), and s_1 by $a + bs$ according to (81), the behavior of the set is seen to be a function of the single parameter s . To a first approximation the exciting

admittances may be moved to the line terminals, and the load current then is

$$I = \frac{V_1}{\left(R_1 + \frac{R_2' + r_1''}{a + bs} + \frac{r_2''}{s} \right)^2 + (X_1 + X_2' + x_1'' + x_2'')^2} \quad (85)$$

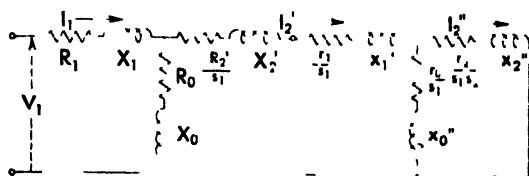


Fig. 45 Per-unit circuit for concatenated motors

The power input to the load circuit becomes

$$P_0 = m_1 \left(R_1 + \frac{R_2' + r_1''}{a + bs} + \frac{r_2''}{s} \right) I^2 \quad (86)$$

and subtracting the copper loss

$$m_1 (R_1 + R_2' + r_1'' + r_2'') I^2 \quad (87)$$

leaves for the mechanical power output

$$P = m_1 \left[(R_2' + r_1'') \frac{bs(1-s)}{a + bs} + r_2'' \frac{1-s}{s} \right] I^2 \quad (88)$$

The torque is

$$T = \frac{44.25P}{2\pi n_0(1-s)} = \frac{44.25m_1}{2\pi n_0} \left[(R_2' + r_1'') \frac{b}{a + bs} + \frac{r_2''}{s} \right] I^2 \quad (89)$$

This equation does not, however, show the proper division of total torque between the two motors. Referring to Fig. 45 the effective resistance in the rotor circuit of the first motor may be written

$$\frac{R}{s_1} = \left(R_2' + r_1'' + \frac{r_2''}{s} \right) \frac{1}{s_1}$$

and since the torque of a motor is proportional to the total resistance in its rotor circuit divided by its slip

$$I_1 = 44.25 \frac{m_1}{2\pi n_1} \frac{R}{s_1} I = 44.25 \frac{m_1}{2\pi n_0} \frac{n_0}{n} \frac{R}{s_1} I$$

$$= 44.25 \frac{m_1}{2\pi n_0} \frac{b}{a + bs} \left(R_2' + r_1'' + \frac{r_2''}{s} \right) I^2 \quad (90)$$

Likewise for the second motor, whose synchronous speed at frequency f_1 is n_2 ,

$$T_2 = 44.25 \frac{m_1}{2\pi n_2} \frac{r_2''}{s} I^2 = 44.25 \frac{m_1}{2\pi n_0} \frac{n_0}{n_2} \frac{r_2''}{s} I^2 = 44.25 \frac{m_1}{2\pi n_0} a \frac{r_2''}{s} I^2 \quad (91)$$

Hence for small slips ($s \rightarrow 0$)

$$\frac{T_1}{T_2} = \frac{b}{a} = \frac{p_1}{p_2} \quad (92)$$

and the torque is divided in the ratio of the number of poles.

29. Speed Control by Applied Rotor Voltage

The general equations (14) to (40) for the induction motor, and the resulting equivalent circuit, Fig. 16, were set up on the assumption that a voltage V_2 was applied to the rotor, as well as a voltage V_1 applied to the stator. It is evident from (31) that the torque depends not only on the magnitude of V_2 , but also on its phase angle θ_2 , so that the applied voltage V_2 may feed power to, or take power from, the rotor. Now if speed control is to be secured by means of a voltage applied to the rotor, that voltage must have the same frequency as the rotor induced voltage at all values of slip, that is $f_2 = sf_1$. Moreover, it must be possible to vary both the magnitude and phase angle of the rotor applied voltage, and the electrical power taken from the rotor should be returnable to the line as electrical power (the constant torque drives), or returnable to the shaft as mechanical power (the constant horsepower drives). There are several

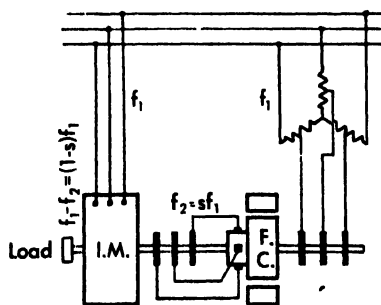


Fig. 46 The Leblanc system.

systems in common use for accomplishing these requirements, and they all make use of an auxiliary commutating machine which functions as a frequency converter and in some cases as an auxiliary motor or generator.

30. The Leblanc Control System

The Leblanc control system is shown in Fig. 46. The frequency converter (F.C.) is mounted on the same shaft as the wound rotor induction motor (I.M.). This frequency converter has an armature winding with slip rings at one end and a commutator at the other, just as in a rotary converter, and there are three brushes, 120 electrical degrees apart, bearing on the commutator. The stator of the frequency converter consists only of a magnetic core there are no stator windings. An autotransformer with tap adjustments

permits the voltage applied to the slip rings of the converter to be varied. When the set is running at slip s the frequency induced in the motor rotor is $f_2 = sf_1$, and it will suffice to show that the frequency is the same at the brushes of the converter. When frequency f_1 is applied to the slip rings of the converter, a rotating field of this frequency is set up *with respect to the armature* by the polyphase winding. But the armature is rotating at frequency $f_1(1 - s)$, and therefore the field is rotating at frequency $f_1 - f_1(1 - s) = sf_1 = f_2$ with respect to the stator or brushes, and this is the frequency picked off by the brushes. Thus a voltage of proper frequency is available for insertion in the rotor circuit of the induction motor, and the magnitude of this voltage can be adjusted by means of the autotransformer. Moreover, by shifting the brushes, the phase of the voltage can be adjusted and the power factor of the motor improved. However, the frequency converter does not act as an auxiliary motor, it merely serves as an adjustable connecting link between the motor rotor and the line. Thus speed control is possible without the high losses incurred by rheostatic control

31. The Kramer Control System

The Kramer control system and its modifications are shown in Fig. 47. The simplest system, Fig. 47a, has an a c commutating machine on the

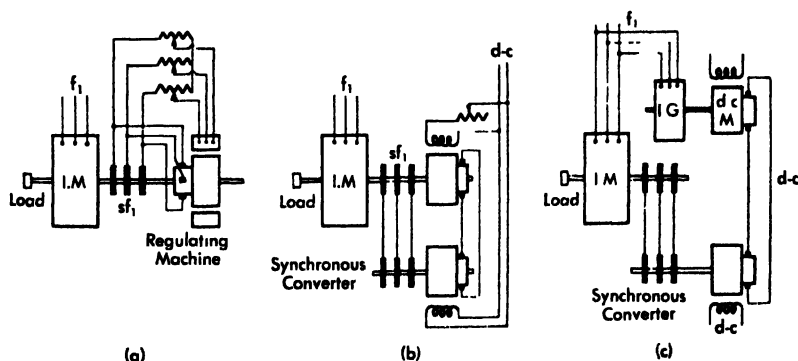


Fig. 47 The Kramer systems.

- (a) constant horsepower drive
- (b) constant horsepower drive
- (c) constant torque drive.

shaft of the main motor, the stator of which is excited by the rotor voltage of slip frequency $f_2 = sf_1$. This is also the voltage from the commutator. By varying the autotransformer, the regulating machine can be made to

deliver voltages of different magnitude to the rotor of the induction motor, thereby effecting speed control; and by shifting the brushes the power factor may be corrected. The regulating machine acting as a motor converts the power, taken from the induction-motor rotor, to mechanical power on the shaft. If the maximum slip is to be s_m then approximately

$$\frac{\text{size of regulating machine}}{\text{size of induction motor}} \cong \frac{RI^2}{RI^2 s_m} = s_m$$

and therefore wide-speed adjustment requires a large and expensive auxiliary machine. For low-speed drives the auxiliary machine is particularly large, while for high-speed drives design difficulties are encountered. These disadvantages may be circumscribed in the modified Kramer drive shown in Fig. 47b. Here the a-c commutating machine is a separate machine in fact a rotary converter receiving power from the slip rings of the induction motor and converting it to direct current, which is used either to drive a d-c motor on the main shaft, Fig. 47b, or to return power to the line, Fig. 47c. The former is called a *constant horsepower drive*, and the latter a *constant torque drive*. The Kramer system permits speed above as well as below synchronism.

It is clear that the commutator voltage is determined by the field excitation of the d-c machine, and this in turn is converted to alternating current at a fixed ratio by the synchronous converter and fed into the rotor of the main motor. The converter will run at such a speed that the frequency at its slip rings will match that at the slip rings of the main induction motor. If the excitation of the d-c machine is increased, its commutator voltage increases and the electromotive force fed into the rotor of the main motor likewise increases, thereby causing the speed to decrease. The d-c machine is then acting as a motor, and its output may be utilized on the main shaft (constant horsepower drive) or returned to the power system (constant torque drive). Suppose that the excitation of the d-c machine is weakened. Its commutator voltage is reduced, and the voltage injected into the rotor of the main motor likewise decreases, thereby causing the speed to increase. If the excitation of the d-c machine is reduced to zero, the only external voltage across the rotor of the main motor will be the drop through the armature impedance of the synchronous converter and the speed will be close to synchronous. If, now, the field of the d-c machine is reversed, the voltage injected into the main motor rotor can be made sufficient to cause the main motor to speed up above synchronism; or for that matter operate at exactly synchronous speed (in which case the synchronous converter is not rotating and is

simply transferring direct voltage from the d-c machine to the induction motor rotor). Thus by field control of the auxiliary d-c machine the speed can be adjusted over a range below to above synchronism.

Problems

1. If the main motor is 1200-hp, 60-cycles, and a plus or minus 30 per cent speed regulation is desired, what should be the standard frequency and power rating of the synchronous converter and of the d-c machine?
2. In the constant torque drive, Fig. 47(c), why is an induction generator used, rather than a synchronous generator?
3. The constant horsepower Kramer drive is usually more expensive than the constant torque drive, in spite of the fact that it has one less machine. Explain why this is so.
4. Consult other sources and prepare a report, accompanied by complete diagrams, describing how a Kramer system is started.

32. The Scherbius System

In the Scherbius system, an a.c. commutating machine, Fig. 48, is directly connected to an induction machine. Both the commutator and field of the special motor are fed from the slip rings of the main induction

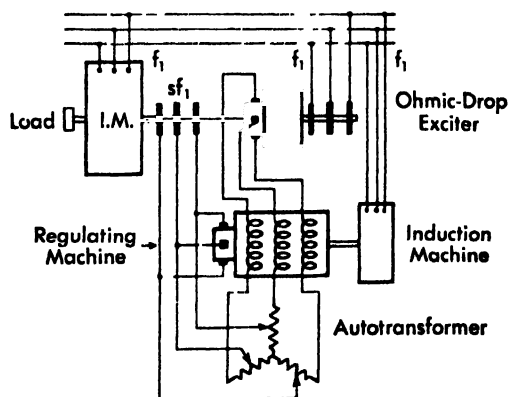


Fig. 48 The Scherhaus system

motor, and therefore supplied with slip frequency power. Such an arrangement will operate below or above synchronism but will not operate at, nor pass through, synchronism, because the slip-ring voltage would then be zero. In order to circumvent this deficiency, a variable frequency converter, called an *ohmic drop exciter*, driven by the main motor, is in

series with the auxiliary machine field. This machine is essentially a synchronous converter armature whose commutator voltage bears a fixed ratio to its slip-ring voltage, regardless of speed. Its connections are such that the rotating field established by the alternating currents is in an opposite direction to the mechanical rotation; so that at synchronous speed the field is stationary in space and the commutator voltage is direct current. The ohmic-drop exciter will therefore furnish d-c excitation at the synchronous speed. The a-c commutating machine operates more or less at constant speed, and therefore its commutator voltage is directly proportional to its excitation. By changing taps on the auto transformer supplying its stator, this excitation may be changed, and thus bring about a change in commutator voltage and consequent change in speed of the main motor.

33. Mechanical Speed Control

The rotor of an induction motor rotates at $(1 - s)$ synchronous speed with respect to the stator, and in an efficient motor the slip s is very small.

If the stator itself is rotated at a speed $\pm \Delta n$, the rotor speed must change by this amount, that is

$$n_2 = (1 - s)n_1 + \Delta n$$

It is immaterial by what means the stator is driven. In the Rossman drive, Fig. 49, the stator of the main induction motor is mounted in bearings and can be driven in either direction by an auxiliary d-c motor which receives its power from a separate motor-generator

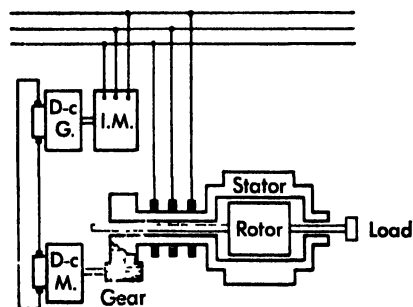


Fig. 49 The Rossman drive

set. The power supplied (or received) by the auxiliary motor is $\pm T\Delta n_1$, and thus this motor must be $\Delta n_1 n_1$ as large as the main motor. This is a constant torque drive.

34. The Induction Generator

The power and torque equations of a polyphase induction machine, as given by (32) and (38), are respectively

$$P = m_1 R_2' \frac{1-s}{s} \frac{V_1^2}{\left(R_1 + \frac{R_2'}{s}\right)^2 + (X_1 + X_2')^2} \dots = m_1 \frac{1-s}{s} R_2' I_2'^2 \quad (93)$$

$$T = \frac{33000m_1}{2\pi n_1 746} \frac{R_2'}{s} \cdot \frac{V_1^2}{\left(R_1 + \frac{R_2'}{s}\right)^2 + (X_1 + X_2')^2} \quad (94)$$

Then depending on the value of the slip, s , there are the three possible operating ranges for the induction machine:

slip	$s < 0$	$0 < s < 1$	$s > 1$
power	negative	positive	negative
torque	negative	positive	positive
action	generator	motor	brake

Thus by driving the motor backward (slip greater than unity) the machine acts as a brake, returning power to the supply lines. This possibility is sometimes made use of in electric locomotives, where it is called *regenerative braking*. It is also sometimes used with hoists and cranes.

If the motor is driven above synchronous speed (negative slip), both the torque and the power are seen to become negative, that is, the machine is a generator. However, the induction machine is not self-exciting, nor can it maintain a fixed frequency independent of load and speed. For these reasons it must be operated in parallel with synchronous generators of sufficient capacity to provide its exciting current and to maintain constant voltage and frequency. (It is possible to provide magnetizing current from a capacitor bank once the machine is in operation, but even in that case a synchronous generator must be available for starting, and after the synchronous machine is disconnected the frequency will vary with the load.)

The performance characteristics of the induction generator, operating on a bus of constant voltage and frequency, may be analyzed either by the equivalent circuit or the circle diagram. In the former case, the currents, torques, and power are calculated exactly as for an induction motor, but using negative values of slip. The vector diagram is easily constructed by reversing the currents in the motor diagram. In the latter case the circle of Fig. 23 must be completed on the under side of the diameter OD and the operating point taken on this lower semicircle. The operating range, as in the case of the motor, is restricted to a narrow range in values of negative slip—usually to less than 5 per cent. Over this range, as is clear from the circle diagram, the quadrature component of current is practically constant, and therefore the induction generator requires a lagging component of exciting current (or delivers a leading

component of current) independent of the load. Thus a capacitor may be used to absorb this current, thereby furnishing excitation to the induction machine.

Induction generators find an application in small unattended hydro-plants operating in parallel with large systems. Such installations are extremely simple and foolproof—no governors (except for over-speed), no exciters, no synchronizing, no hunting, and no loss of stability. Induction generators are also used as auxiliary machines in connection with speed control systems for large motors. But in general, due to their low power-factor and poor efficiency, they cannot compete with synchronous generators in major power developments.

Problems

1. Show that the middle expressions in Eqs. (2) and (3) actually reduce to the final expressions for the conditions indicated.
2. If the phase angles $2\pi k/m$ in (1) are reversed, what form does (4) take and what then is the physical significance of its terms?
3. Write down in parallel columns the corresponding equations and definitions for the transformer and for the polyphase induction motor, noting carefully the similarities and differences. Show also the equivalent circuits and vector diagrams for the two.
4. A 3-phase, 60-cycle, 440-volt, 15 hp, 1800-rpm induction motor has the following data:
 Stator: wye-connected, 112-turns per phase, 2 coil sides per slot, 4 slots per phase per pole, coil pitch 12 slots, resistance per phase at 75 C 0.33 ohm.
 Rotor: squirrel cage, 57 bars, skew one slot.
 - (a) What are the skew, pitch, and distribution factors for the stator and rotor respectively?
 - (b) What is the voltage transformation ratio between stator and rotor?
 - (c) What is the current transformation ratio between stator and rotor?
 - (d) What is the rotor induced voltage at standstill?
 - (e) What is the rotor induced voltage and frequency at 0.015 slip?
5. Derive (39) and (40) from (38).
6. A 3-phase, wye-connected, 60-cycle, 220-volt, 10-hp, 1800-rpm induction motor has the following test data:

Running light

220	voltage
6.4	current
239	watts
1.30	friction and windage

Blocked rotor

64
62
1922

Stator d-c resistance at 75 C is $R_1 = 0.242$ ohm per phase (increase 25 per cent for skin effect)

- (a) Determine the six motor constants for
 - (1) the approximate equivalent circuit
 - (2) the exact equivalent circuit
 - (b) What is the slip corresponding to rated power output?
 - (c) What is the slip corresponding to maximum torque?
 - (d) What is the maximum torque?
7. Using the approximate equivalent circuit, calculate and plot against speed the following characteristics for the motor of Prob. 6: (1) stator current, (2) stator pf, (3) core loss, (4) stator copper loss, (5) rotor copper loss, (6) total loss, (7) power output, (8) power input, (9) efficiency, (10) torque.
8. Construct the circle diagram for the motor of Prob. 6 and from it plot against output the following characteristics: (1) stator current, (2) stator pf, (3) losses, (4) input, (5) efficiency, (6) torque, (7) speed.
9. Compare the calculations of Probs. 7 and 8 with respect to (1) accuracy, (2) time, (3) information conveyed.
10. Superimpose the *exact* circle diagram of Sec. 10 on the approximate circle diagram of Prob. 8. Locate the zero and unit slip points on the exact circle.
11. The motor of Prob. 6 is used to drive a load having a torque requirement of $T = 15 + (rpm)^2 \cdot 5 \times 10^{-6}$. Investigate the possibilities and draw curves of current and torque for:
- (a) Line starting
 - (b) Compensator starting
 - (c) Wye-delta starting
 - (d) Wound rotor, limit on starting current to 3 times normal
 - (e) Wound rotor, maximum torque at start
12. Two 60-cycle induction motors of 6 and 10 poles, respectively, are arranged for operation in cascade. What combinations of speed are possible? If the total rating of the set is 120-hp, how should each of the two machines be rated?

5 The Single Phase Induction Motor

1. Introduction

Single-phase induction motors are employed where polyphase power is not available. Their use is generally restricted to small sizes because of their poor speed regulation, low efficiency and power factor, the absence of starting torque without auxiliary means, and the reduced output in a given frame size as compared with polyphase motors. Single-phase motors are invariably the squirrel cage type, and are usually standard three-phase, wye-connected designs in which one phase winding has either been left out or is idle. Thus only two-thirds of the slots are active and the output is reduced accordingly. The presence of dissymmetry and single-phase forces result in unbalanced conditions leading to vibration and noise. Nevertheless, because of the great number of fractional horsepower applications in both the domestic and industrial fields, the value of sales of single-phase motors is very great.

2. Principles of Operation

The single-phase stator winding causes a flux stationary in space and pulsating in time. When the rotor is at standstill, the pulsating stator flux by transformer action induces rotor currents, Fig. 1a, which oppose the stator flux, but produce no torque with it, and therefore the motor will not start. But if the motor is once started by any of the means here-

inafter described, the moving conductors will cut through the stator flux and have generated in them by rotation a set of currents, Fig. 1b, orthogonal in space to the stator flux, and which are then properly disposed in time and space to react on the stator flux and produce torque. Furthermore, the cross-field set up by the rotational generated currents reacts with the transformer induced currents to produce torque. This conception is known as the *cross-field theory* of the single-phase induction motor, and will be enlarged upon in Sec. 8.

There is, however, another point of view, called the *double-revolving field theory*, from which the characteristics of the single-phase induction motor may be developed. This theory makes use of the fact that a pulsating field is equivalent to two equal and oppositely rotating fields, each of which develops its own torque on the rotor. At standstill the two torques are equal and opposite; but for any rotor speed, one of the torques dominates, because the slips are different.

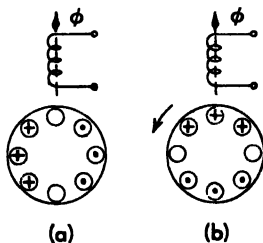


Fig. 1 Rotor voltages of the single phase induction motor.
 a. due to transformer action
 b. due to cutting action

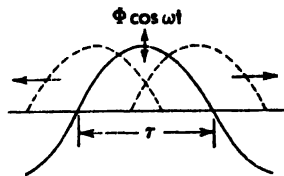


Fig. 2

3. The Double-Revolving Field Theory

Assume the single-phase stator flux to be sinusoidally distributed in space, and varying sinusoidally in time. Then if 2τ is the wavelength of the space distribution, the flux may be represented by

$$\phi = \Phi \sin \frac{\pi x}{\tau} \cos \omega t \quad (1a)$$

$$= \frac{\Phi}{2} \left[\sin \left(\frac{\pi x}{\tau} - \omega t \right) + \sin \left(\frac{\pi x}{\tau} + \omega t \right) \right] \quad (1b)$$

$$= (\text{forward wave}) + (\text{backward wave}) \quad (1c)$$

That any function $f(\lambda x \pm \omega t)$ is a traveling wave of fixed shape and magnitude is easily seen by putting

$$\lambda x \pm \omega t = \text{constant} \quad (2)$$

which then defines a particular value of, or point on, the function, and for any instant of time t there is a corresponding x for which the function has this same value. Indeed, the velocity with which the point travels is found by differentiating (2),

$$\frac{dx}{dt} = \pm \frac{\omega}{\lambda} = \pm v \quad (3)$$

the (+) sign representing a forward traveling wave and the (−) sign a backward traveling wave. Thus the pulsating flux is expressible as a pair of oppositely rotating fields of equal magnitude.*

If the motor speed is ω_0 and synchronous speed is ω , then the slips with respect to the forward and backward fields are

$$s = \frac{\omega - \omega_0}{\omega} = 1 - \frac{\omega_0}{\omega} = 1 - \frac{f_0}{f} \quad (4)$$

$$s_b = \frac{\omega - (-\omega_0)}{\omega} = 1 + \frac{\omega_0}{\omega} = 1 + \frac{f_0}{f} = 2 - s \quad (5)$$

It is convenient to consider the single phase motor as two superimposed 2-phase motors, having forward and backward rotating fields respectively.

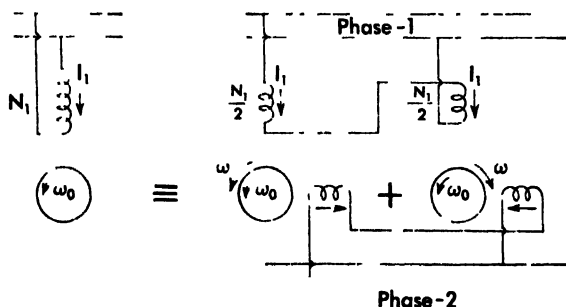


Fig. 3 Single phase motor equivalent to two 2 phase motors.

as indicated in Fig. 3. The actual stator winding of N_1 turns contributes

* The exposition sometimes found in textbooks of putting $\cos \omega t = \frac{e^{j\omega t}}{2} + \frac{e^{-j\omega t}}{2}$ and concluding that the pulsating field has thereby been expressed as a pair of oppositely rotating fields is hardly acceptable. The notion of a traveling wave or rotating field connotes something happening in *space* and in *time*. There is nothing about space in $e^{j\omega t}$, it refers only to a time diagram.

$N_1/2$ turns to each 2-phase motor, and the stator currents are the same in each, so that the phase-1 ampere-turns balance is

$$\frac{N_1 I_1}{2} + \frac{N_1 I_1}{2} = N_1 I_1$$

But the currents in the phase-2 coils must be opposed in order to develop rotating fields of opposite direction, and their superimposed ampere-turns therefore cancel. Thus the two fictitious polyphase machines superimpose to form the actual single-phase motor.

Each 2-phase motor has a stator resistance of r_1 ohms per phase and a reactance of x_1 ohms per phase, and since the stators are in series, there must be $2r_1 = R_1$ and $2x_1 = X_1$ to satisfy the single phase stator impedance.*

Rotor quantities are referred to the stator as (since $m_1 = 2$)

$$E_2' = \frac{K_1 V_1}{K_2 N_2} E_2 = \frac{a}{2} E_2 \quad (6)$$

$$I_2' = \frac{m_2 K_2 V_2}{m_1 K_1 N_1} I_2 = \frac{m_2}{a} I_2 \quad (7)$$

$$s_2' = \frac{1}{2m_2} \left(\frac{K_1 N_1}{K_2 N_2} \right)^2 s_2 = \frac{a^2}{2m_2} s_2 \quad (8)$$

4. General Equations from the Revolving Field Theory

Now using subscripts f and b to distinguish the forward and backward field 2-phase motors of Fig. 3, but otherwise adhering to the conventions used in the analysis of the polyphase motor in Chapter 4, we can write the general equations for the motor. The stator voltage equation is

$$\begin{aligned} V_1 &= V_{1f} + V_{1b} = z_1 I_{1f} + E_{0f} + z_1 I_{1b} + E_{0b} \\ &= 2z_1 I_1 + E_{0f} + E_{0b} \\ &= Z_1 I_1 + E_{0f} + E_{0b} \end{aligned} \quad (9)$$

in which E_{0f} and E_{0b} are the voltages to overcome those induced in the stator by the forward and backward rotating fields, and $Z_1 = 2z_1$.

* It will be noticed upon superposition of the two motors with their stator coils coinciding, that the mutual reactance between them must be the same as their self reactances, and since reactance varies as the square of the number of turns the over all reactance is

$$x_1 + x_1 = \frac{X_1}{4} + \frac{X_1}{4} + 2 \frac{X_1}{4} = X_1$$

from which $x_1 = X_1/2$ as before.

The two rotor voltage equations, referred to the stator, are

$$0 = E_{0f} + \left(\frac{r_2'}{s} + jx_2' \right) I_{2f}' \quad (10)$$

$$0 = E_{0b} + \left(\frac{r_2''}{2-s} + jx_2' \right) I_{2b}' \quad (11)$$

In (10) and (11) a distinction has been made between the rotor (referred) resistance for the forward field r_2' , and that for the backward field r_2'' . In the former case the rotor frequency is very small and skin effect is negligible, while in the latter case the frequency is about twice the stator frequency and the skin effect very high.

For each polyphase motor the sum of the stator and rotor currents (referred) is the exciting current responsible for the main flux and for the core loss, as accounted for by the exciting admittances (or impedances)

$$I_{0f} = I_1 + I_{2f}' = Y_0 E_{0f} = \frac{E_{0f}}{Z_0} \quad (12)$$

$$I_{0b} = I_1 + I_{2b}' = Y_0 E_{0b} = \frac{E_{0b}}{Z_0} \quad (13)$$

5. The Equivalent Circuit of the Revolving Field Theory

Equations (9) to (13) inclusive are interpreted in terms of the equivalent circuit of Fig. 4.

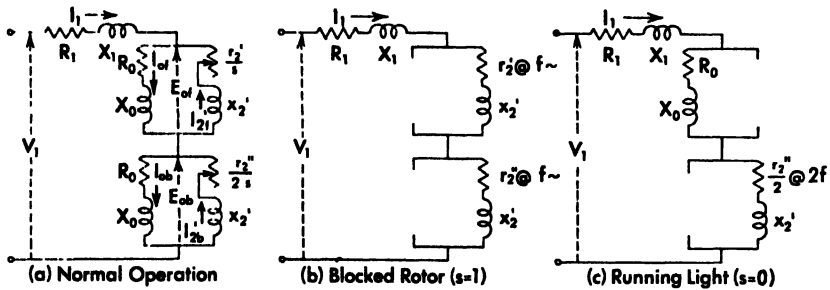


Fig. 4 Equivalent circuit (revolving field theory).

On *blocked rotor test*, $s = 1$, the impedance through the rotor circuits is small compared with the exciting impedances, and the circuit reduces, approximately, to Fig. 4b, and

$$\begin{aligned} V_1 &\cong [R_1 + jX_1 + (r_2' + r_2'') + j2x_2'] I_1 \\ &= [R_1 + jX_1 + R_2' + jX_2'] I_1 \end{aligned} \quad (14)$$

from which it is clear that the measured test values of the rotor impedance are double the equivalent circuit values, that is, $R_2' = (r_2' + r_2'')$ and $X_2' = 2x_2'$, thus confirming the previous analysis.

On *running light test*, $s = 0$, the impedance through the r_2' branch is infinite and that part of the circuit is open, but the impedance through the r_2'' branch is small compared to the exciting impedance, Fig. 4c, and so

$$\begin{aligned} V_1 &= \left(R_1 + jX_1 + R_0 + jX_0 + \frac{r_2''}{2} + jx_2' \right) I_1 \\ &\cong (R_0 + jX_0) I_1 \end{aligned} \quad (15)$$

Hence $Z_0 = R_0 + jX_0$ may be determined from volt, current, and power measurements under running light conditions.

Solution of the equivalent circuit, Fig. 4, for the currents I_{21}' and I_{2b}' gives the power input to the rotor

$$P_0 = \left(\frac{r_2'}{s} I_{21}'^2 + \frac{r_2''}{2-s} I_{2b}'^2 \right) \quad (16)$$

and subtracting the copper losses $(r_2' I_{21}'^2 + r_2'' I_{2b}'^2)$ leaves for the mechanical power output

$$P = \left[r_2' \left(\frac{1-s}{s} \right) I_{21}'^2 + r_2'' \frac{s}{2-s} I_{2b}'^2 \right] \quad (17)$$

The torque then is (in synchronous watts)

$$T = \frac{P}{(1-s)} = \left(\frac{r_2'}{s} I_{21}'^2 - \frac{r_2''}{2-s} I_{2b}'^2 \right) \quad (18)$$

which shows that the torque due to the backward field opposes that due to the forward field. The two torque curves and their resultant are plotted in Fig. 5. It is clear that the torque passes through zero a little prior to $s = 0$.

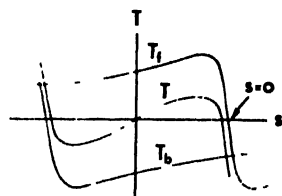


Fig. 5

6. Single-phase Constants from Three-phase Measurements

Any 3-phase induction motor may be converted into a single-phase motor merely by opening one phase. In fact, many single-phase motors are built on 3-phase motor frames and stators simply by leaving one stator phase winding out or idle. It may be shown that there is a definite relationship between the single-phase and 3-phase constants of such motors. While this is most readily done by means of symmetrical components, the same results will be obtained here from the double revolving field idea and superposition.

Referring to Fig. 6, there is shown a 3-phase stator winding with phase a left open and phases b and c connected in series to a single-phase source. The currents I_{nb} and I_{nc} are in time opposition. But as shown

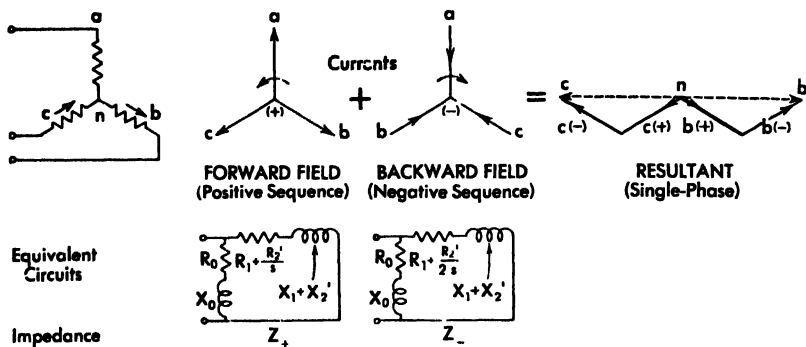


Fig. 6

by the time vector diagrams of Fig. 6, superposition of the forward (+) and backward (-) phase sequence diagrams ($a - b - c$) and ($a - c - b$), yield the resultant single phase current $I_{cn} = I_{nb}$ since the sequence currents I_{a+} and I_{a-} cancel. Now the two 3-phase sequences develop fields rotating in opposite directions, and their respective equivalent circuits are as shown, having total impedances Z_+ and Z_- . Then the phase voltages are

$$E_{bn} = Z_+ I_{b+} + Z_- I_{b-} \quad (19)$$

$$E_{cn} = Z_+ I_{c+} + Z_- I_{c-} \quad (20)$$

and from these equations, and reference to Fig. 7,

$$\begin{aligned} E_{bn} &= E_{b+} - E_{cn} \\ &= Z_+ (I_{b+} - I_{c-}) + Z_- (I_{b-} - I_{c+}) \\ &= Z_+ (-j\sqrt{3} I_{a+}) + Z_- (-j\sqrt{3} I_{a+}) \\ &= -j\sqrt{3} (Z_+ + Z_-) I_{a+} \end{aligned} \quad (21)$$

Hence

$$I_{a+} = \frac{-E_{bn}}{j\sqrt{3} (Z_+ + Z_-)} \quad (22)$$

$$I_{b+} = -j\sqrt{3} I_{a+} = \frac{-E_{bn}}{Z_+ + Z_-} \quad (23)$$

The equivalent circuits of Fig. 6 may be considered to refer to phase a . If their solutions show that the load components of I_a in the two circuits are I_{2+} and I_{2-} respectively, then the power output is

$$P = 3 \left[R_2' \left(\frac{1-s}{s} \right) I_{2+}^2 + R_2' \left(\frac{1-s}{s-2} \right) I_{2-}^2 \right] \quad (24)$$

which agrees with (17).

It is clear from (23) that the single-phase impedances are the sums of the positive and negative sequence 3-phase impedances; and at stand-still, $s = 1$, the reactances and resistances single-phase are seen to be just double the 3-phase values per phase. In other words, the constants per leg are the same, whether single-phase or three phase.

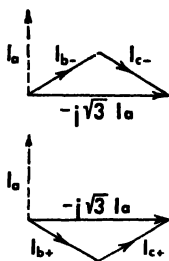


Fig. 7

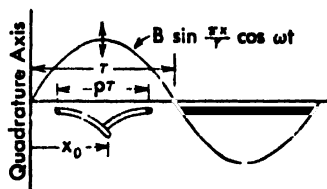


Fig. 8 Coil moving through a pulsating flux.

7. Transformer and Speed Voltages

Voltage may be induced in a coil by two different means: (1) by *transformer action*, in which the coil is stationary and the flux linking it is varied, or (2) by *cutting action*, in which the moving coil cuts through the flux. These are the familiar $d\phi/dt$ and Blv terms encountered in the transformer and generator respectively. The latter voltage is variously referred to as a generator, or speed voltage. Both actions may occur simultaneously.

Referring to Fig. 8, consider a coil of pitch $p\tau$ moving through a sinusoidal flux density distribution

$$B \sin \frac{\pi x}{\tau} \cos \omega t \quad (25)$$

in which

$$\omega = 2\pi f$$

$$2\tau = \text{wavelength of the flux density}$$

The flux linked by the coil of axial length l , when its center is at x_0 , is

$$\begin{aligned} \phi &= \int_{x_0 - p\tau/2}^{x_0 + p\tau/2} lB \cos \omega t \sin \frac{\pi x}{\tau} dx \\ &= lB \frac{\tau}{\pi} \left[\cos \frac{\pi}{\tau} \left(x_0 - \frac{p\tau}{2} \right) - \cos \frac{\pi}{\tau} \left(x_0 + \frac{p\tau}{2} \right) \right] \cos \omega t \end{aligned}$$

$$\begin{aligned}\phi &= \frac{2}{\pi} \tau l B \sin \frac{p\pi}{2} \sin \frac{\pi x_0}{\tau} \cos \omega t \\ &= \Phi K_p \sin \frac{\pi x_0}{\tau} \cos \omega t\end{aligned}\quad (26)$$

where Φ is the total flux per half wavelength, and K_p is the pitch factor. Then by Faraday's law the induced voltage in the coil, due both to the variation of the flux and to movement of the coil through the flux, is

$$\begin{aligned}e &= -\frac{N}{10^8} \frac{d\phi}{dt} = -\frac{N}{10^8} \left(\frac{\partial \phi}{\partial x_0} \frac{dx_0}{dt} + \frac{\partial \phi}{\partial t} \right) \\ &= -\frac{K_p N \Phi}{10^8} \left[\frac{\pi}{\tau} \frac{dx_0}{dt} \cos \frac{\pi x_0}{\tau} \cos \omega t - \omega \sin \frac{\pi x_0}{\tau} \sin \omega t \right]\end{aligned}\quad (27)$$

But the position of the coil, as function of time, may be expressed as

$$\frac{x_0 \pi}{\tau} = \omega_0 t \quad \text{hence} \quad \frac{\pi}{\tau} \frac{dx_0}{dt} = \omega_0 \quad (28)$$

so that (27) becomes

$$e = \frac{K_p N \Phi \omega}{10^8} \left(\sin \omega t \sin \frac{\pi x_0}{\tau} - \frac{\omega_0}{\omega} \cos \omega t \cos \frac{\pi x_0}{\tau} \right) = e_t + e_v \quad (29)$$

The first term is independent of the velocity of the coil and is obviously a *transformer* voltage e_t , while the second term depends directly on the velocity and is a *velocity* voltage e_v . It will be noticed that the velocity voltage is proportional to the velocity and changes sign when the direction of motion is reversed. This is taken care of in the equation by the sign of ω_0 . Note also that

$$\left| e_v \right| = \frac{\omega_0}{\omega} \left| e_t \right|$$

Now it is of the utmost importance to recognize that the above equations are functions of both time t and space x_0 , and they may appear quite different when plotted as functions of t with x_0 constant than when plotted as functions of x_0 with t constant. If the $(-)$ sign in front of the second term of (29) be associated with the time function $(-\omega_0/\omega) \cos \omega t$, then the space and time diagrams of (26) and (29) are as shown in Fig. 9.

It will be observed that there is a radical difference in point of view in constructing space and time vector diagrams. In the *time* diagram the vectors are conceived of as *rotating* in the counterclockwise direction, and one vector is considered ahead of, or leading, another vector if it arrives at a reference line first. Thus in Fig. 9 the flux ϕ is 90 degrees in time ahead of the voltage e_t , because it reaches the vertical position

first. But in constructing a *space* vector diagram, the vectors are conceived of as fixed - not rotating - and one vector is considered ahead of another if it is further along the positive direction in space. Positive direction is arbitrary and may be taken either way. Thus in Fig. 9 direction is measured positive in going from the quadrature to the direct axis, and thus the *d*-axis is shown 90 degrees in space ahead of the *q*-axis. The flux ϕ is a maximum in the *d*-axis, and is therefore shown 90 degrees in space ahead of the voltage e_i , which is a maximum in the *q*-axis.

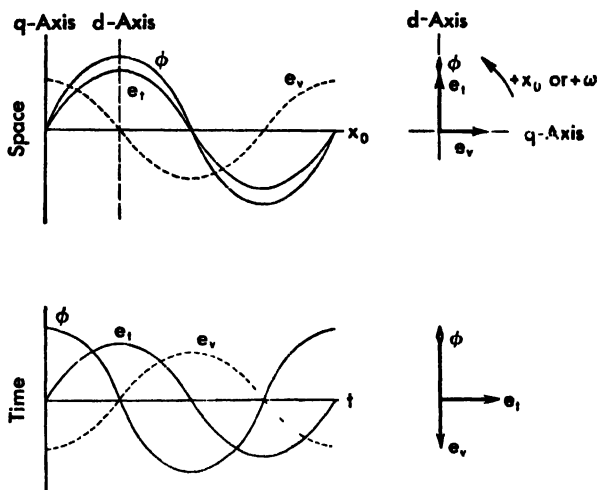


Fig. 9 Space and time diagrams of the flux and voltages when both transformer and cutting actions are present

Equation (29) gives the voltages as functions of t in any axis x_0 , and the frequency of these voltages, whether due to transformer or cutting action, is the same as the stator frequency f . However, this is not the frequency in the individual conductors. Substituting $x_0 \pi \tau = \omega_0 t$ in (29) and performing an elementary transformation, it becomes

$$e = \frac{K_p N \Phi \omega}{2 \times 10^8} \left\{ [\cos (\omega - \omega_0) t - \cos (\omega + \omega_0) t] - \frac{\omega_0}{\omega} [\cos (\omega - \omega_0) t + \cos (\omega + \omega_0) t] \right\} \quad (29a)$$

This equation shows that there are two frequencies $(f - f_0)$ and $(f + f_0)$ in the moving conductors; that is, the slip frequencies of the double revolving field theory.

The speed voltage in the quadrature axis is opposite in time-phase to

the flux. Neglecting resistance, it will cause a current through the inductance L of the coil

$$\begin{aligned} i_c &= \frac{1}{L} \int e_c dt = -\frac{K_p V \Phi \omega_0}{L 10^8} \cos \frac{\pi x_0}{\tau} \int \cos \omega t dt \\ &= -\frac{K_p V \Phi}{L 10^8} \cdot \frac{\omega_0}{\omega} \cos \frac{\pi x_0}{\tau} \sin \omega t \end{aligned} \quad (30)$$

This current will produce a cross-flux in space and time phase with itself, that is in the positive quadrature axis and leading the main flux ϕ by 90 degrees in time (assuming the $-$ sign to belong to the time function).

A thorough understanding of Fig. 9 and the equations on which it is based is essential to what follows.

8. Cross-field Theory of the Single-phase Induction Motor

Figure 10 represents a single-phase induction motor with a squirrel-cage rotor. The stator winding is shown as a concentrated coil, although actually it would be a conventional lap or wave winding. The direct axis is centered on the stator coil, while the quadrature axis is drawn to the right. Positive direction of rotation is taken as counterclockwise. It is also customary to refer to the *main flux* (d -axis) and the *cross-flux* (q axis). In what follows it is necessary to distinguish: *what* fluxes (main or cross) are responsible for a voltage, *how* the voltage is generated (transformer or cutting action), and *where* it appears (direct or quadrature axis). For this purpose a triple index notation will be adopted, in which

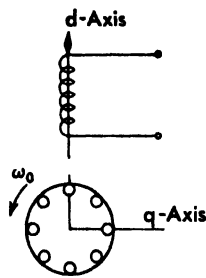


Fig. 10

m, c refer to main and cross flux, respectively

t, τ refer to transformer and cutting action, respectively

d, q refer to direct and quadrature axis, respectively

Thus the voltage E_{mtd} is caused by the transformer action of the main flux and it exists in the direct axis, whereas the voltage E_{ctd} is caused by the cutting of the cross flux and it exists in the direct axis.

In Fig. 11 the first two columns show the effects of the main flux and the last two columns the effects of the cross flux, due to both transformer and cutting action. The space diagrams show the space location of the vector, and the time diagrams the phase. It is immaterial whether a $(-)$ sign in the equations be considered as associated with the space or with the time diagrams. Thus the position in space of E_{ctd} may be reversed

if it also be reversed on the time diagram. Beginning with the first column of Fig. 11, there is shown the main flux ϕ_m in the direct axis as reference vector. This flux results from the exciting current I_0 , the in phase component of which produces the flux, and the orthogonal component of which accounts for the core loss in the direct axis. The main flux induces the direct axis voltage E_{mtd} by transformer action, and the quadrature axis voltage E_{mvq} by cutting action. The latter voltage causes the quadrature axis lagging current I_q . One component of I_q produces a cross flux ϕ_c , while an orthogonal component accounts for the core loss due to the quadrature flux. The cross flux ϕ_c induces the voltage E_{ctq} by transformer action, and the voltage E_{cld} by cutting action.

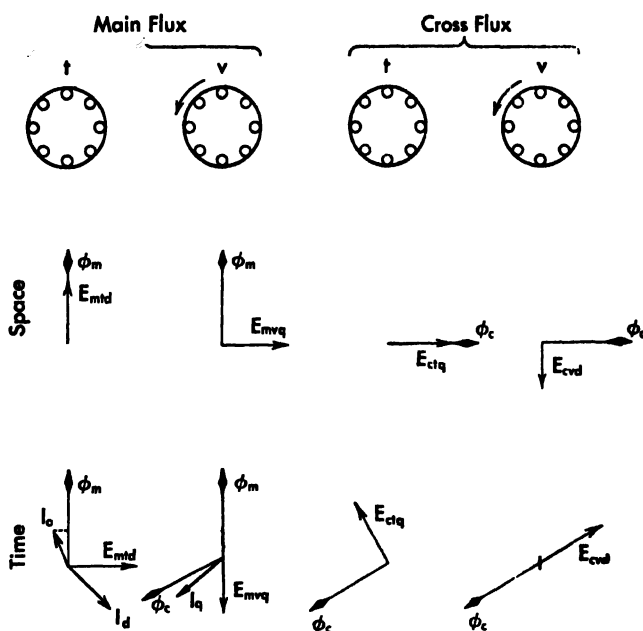


Fig. 11 Space and time diagrams of the main and cross fluxes, and the transformer and speed voltages of the single phase in induction motor, according to the cross-field theory.

Now the speed voltages are (ω_0/ω) times the corresponding transformer voltages, and the induced voltages may be accounted for by their magnetizing impedances. Also, the rotor may be assumed to cut the direct axis and quadrature axis leakage fluxes $X_2 I_d$ and $X_2 I_q$ as well as the fluxes ϕ_m and ϕ_c . Then

$$E'_{mtd} = -Z'_0 I_0 \text{ (referred to the stator)} \quad (31)$$

$$E_{mvq} = -j \frac{\omega_0}{\omega} E_{mtd} - \frac{\omega_0}{\omega} X_2 I_d \quad (32)$$

$$E_{ctq} = -Z_0 I_q \quad (33)$$

$$E_{crd} = -j \frac{\omega_0}{\omega} E_{ctq} - \frac{\omega_0}{\omega} X_2 I_q = \frac{\omega_0}{\omega} j(Z_0 + jX_2) I_q \quad (34)$$

The stator current is the difference between the stator exciting current I_0 and the rotor direct axis current I_d' (referred to the stator)

$$I_1 = I_0 - I_d' \quad (35)$$

The voltage equation for the stator, in terms of its leakage impedance Z_1 , then is (putting $E_0 = -E'_{mtd}$),

$$V_1 = Z_1 I_1 - E'_{mtd} = Z_1 I_1 + E_0 \quad (36)$$

and the stator time vector diagram, as the interpretation of Fig. 11 and equations (35) and (36), is Fig. 12. This diagram is similar in all respects to that for a transformer or polyphase induction motor.

The voltage equation for the rotor direct axis includes the transformer voltage E_{mtd} and the speed voltage E_{crd} . Now Fig. 11 shows that the speed voltage is opposite in space to the transformer voltage, that is their effects are opposed. Therefore, in the composite *time* diagram, Fig. 13, E_{crd} must be reversed from its position on the time diagram of Fig. 11. The total voltage in the rotor is consumed by the rotor impedance Z_2 or

$$E_{mtd} - E_{crd} + Z_2 I_d = j \frac{\omega_0}{\omega} (Z_0 + jX_2) I_d + Z_2 I_d \quad (37)$$

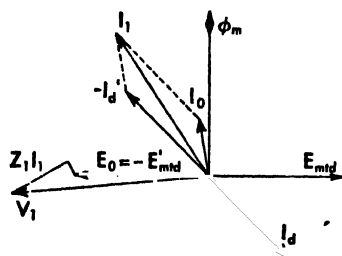


Fig. 12

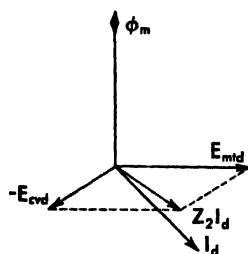


Fig. 13

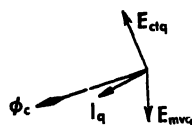


Fig. 14

The total voltage in the quadrature axis, Fig. 14, is made up of the components E_{mvq} and E_{ctq} , and this voltage is consumed by the rotor impedance Z_2 , or

$$E_{mvq} + E_{ctq} = Z_2 I_q \quad (38)$$

hence by (32) and (33)

$$-j \frac{\omega_0}{\omega} E_{mtd} = \frac{\omega_0}{\omega} X_2 I_d + (Z_0 + Z_2) I_q \quad (39)$$

Solving (37) and (39) simultaneously for the rotor currents, there results

$$I_d = \frac{(1 - S^2)(Z_0 + Z_2) + S^2 R_2}{(Z_0 + Z_2)(Z_2 - jX_2 S^2) + jX_2 S^2 R_2} E_{mtd} \quad (40)$$

$$I_q = \frac{-jSR_2}{(Z_0 + Z_2)(Z_2 - jX_2 S^2) + jX_2 S^2 R_2} E_{mtd} \quad (41)$$

in which $S = \omega_0 / \omega$ is the per unit speed.

The impedance in the d -axis is

$$\begin{aligned} Z_d = \frac{E_{mtd}}{I_d} &= \frac{(Z_0 + Z_2)(Z_2 - jX_2 S^2) + jX_2 S^2 R_2}{(1 - S^2)(Z_0 + Z_2) + S^2 R_2} \\ &= jX_2 + \frac{(Z_0 + Z_2)}{S^2} \cdot \frac{1 - S^2}{1 - S^2} \\ &\quad + \frac{R_2}{S^2} + \frac{R_2}{1 - S^2} \end{aligned} \quad (42)$$

If all impedances are referred to the stator, from (36) and (42) the equivalent circuit is as shown in Fig. 15. Since slip $s = (1 - \omega_0 / \omega)$ is

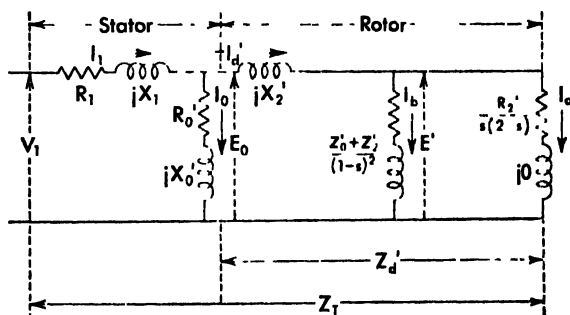


Fig. 15 Equivalent circuit corresponding to the cross field theory of the single phase induction motor

related to the per unit speed S by $S = 1 - s$, it follows that $S^2 = (1 - s)^2$ and $(1 - S^2) = s(2 - s)$. The essential characteristics of the motor may be obtained from the solution of this equivalent circuit. The calculations are expedited by the following tabular procedure:

	Stator	Rotor	
	$I_1 = V_1 / Z_T$ $E_0 = V_1 - Z_1 I_1$ $I_0 = E_0 / Z_0'$ $I_d' = I_1 - I_0$ (check)	$-I_d' = E_0 / Z_d'$ $E' = E_1 - j X_2' I_d'$ $I_a = (1 - S^2) E' / R_2'$ $R_2' I_a^2$ $V_1 I_1 \cos \theta_1 - R_0' I_0'^2 - R_1 I_1^2$ $E_a I_d' \cos \theta_d' = E_a I_d'$	$I_0' = \frac{-j R_2' S I_d'}{(1 - S^2)(Z_0' + Z_2') + k_2' S}$ $I_b = S^2 E' / (Z_0' + Z_2')$ $R_0' I_b^2$ $R_2' I_b^2$ $(V_1 I_1 \cos \theta_1 - R_0' I_0'^2 - R_1 I_1^2 - R_2' I_a^2 - R_2' I_b^2 - R_0' I_0'^2)$ (Gross output) (windage and friction) (Net output) (stator input)
Core loss			
Copper loss			
Input			
Gross output (elec.)			
Net output (mech.)			
Efficiency			
Power factor	R_T / Z_T		
Torque			(Gross output) S

9. Starting of Single-phase Induction Motors

It has already been pointed out, Fig. 5, that the starting torque of a pure single-phase induction motor is zero, but once started in either direction it will accelerate to whatever speed the load permits. Numerous methods have been developed for starting these motors, of which there are three general categories:

- 1. Starting by external means
 - a. rotating the rotor by hand (small and medium size motors)
 - b. separate starting motors (motor-generator sets, phase converters)
- 2. Starting as polyphase motors by means of auxiliary windings
 - a. shaded pole motors
 - b. split phase motors (resistor and capacitor start)
 - c. capacitor motors
- 3. Starting as an alternating current commutator motor (see Chap. 6)
 - a. repulsion start motor

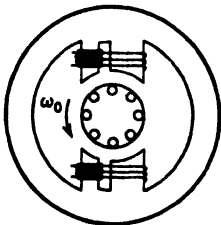


Fig. 16 Shaded pole motor.

Single-phase motors driving direct current or polyphase generators connected to power sources may be started from the generator end.

10. Shaded-pole Motors

Shaded pole motors are built in small sizes where the starting torque need not be great, and where efficiency is not of much concern. They are of the salient split-pole type, Fig. 16. The

pole is in two sections, the stator winding surrounding both sections, and a low-resistance copper band surrounding the forward section in the direction of rotation. Let

X_1 = self-inductive reactance of the stator winding

X_3 = self-inductive reactance of the shading band

X_m = mutual-inductive reactance between winding and band

R_3 = resistance of the shading band

E = induced voltage in the stator winding

Then ignoring the rotor currents

$$E = jX_1 I_1 + jX_m I_3 \quad (43)$$

$$0 = jX_m I_1 + (R_3 + jX_3) I_3 \quad (44)$$

from which
$$I_1 = \frac{Z_3 E}{jX_1 Z_3 + X_m^2} \quad (45)$$

$$I_3 = \frac{-jX_m E}{jX_1 Z_3 + X_m^2} \quad (46)$$

The flux in the shaded pole section is

$$\frac{\omega N}{10^8} \phi_3 = X_m I_1 + X_3 I_3 = E \frac{X_m Z_3 - jX_m X_3}{jX_1 Z_3 + X_m^2} - E \frac{R_3 X_m}{jX_1 Z_3 + X_m^2} \quad (47)$$

The flux in the unshaded pole section is

$$\begin{aligned} \frac{\omega N \phi_1}{10^8} &= X_1 I_1 + X_m I_3 = \frac{\omega N \phi_3}{10^8} \\ &= E \frac{X_1 Z_3 - jX_m^2 - R_3 X_m}{jX_1 Z_3 + X_m^2} = E \frac{(X_1 - X_m)R_3 + j(X_1 X_3 - X_m^2)}{jX_1 Z_3 + X_m^2} \end{aligned} \quad (48)$$

Comparison of (47) and (48) shows that the flux in the shaded pole section lags that in the unshaded pole section by an angle

$$\theta = \tan^{-1} \frac{X_1 X_3 - X_m^2}{(X_1 - X_m)R_3} \cong \tan^{-1} \frac{X_1}{R_3} \rightarrow 90^\circ \quad (49)$$

where the approximation results by taking $X_m = X_3$ and a 1 : 1 turn ratio; and if the reactance X_3 is large compared to the resistance R_3 , the angle approaches 90 degrees. The two fields are of unequal strength, so that the pole may be looked on as producing a weak 2 phase field superimposed on a single-phase field. But the 2-phase flux results in a rotating field (in the direction toward the shaded pole section) and thus pro-

vides the desired starting torque. The shading coil remains permanently in circuit, and consequently there is always some 2-phase effect in the performance of a single-phase induction motor utilizing this method of starting. The short-circuited shading coil adds to the losses in the machine. The simplicity and low cost of this type motor are its principal advantages.

11. Split-phase Motors

The split-phase motor, Fig. 17, has a 2-phase stator winding consisting of a main winding M and an auxiliary winding A in space quadrature with M . If the currents supplied to those two windings are equal in magnitude and out of phase by exactly 90 degrees, the motor will behave as a 2-phase induction motor. If the currents are unequal and not exactly 90 degrees out of phase, the motor behaves as though a 2-phase field were superimposed on a single-phase field, the former producing a rotating field which results in starting torque. Fig. 17(a) shows a *resistor-start* motor in which resistance R in the auxiliary winding circuit is used to bring about the differences in phase between the currents. Sometimes the resistor is placed in the main winding circuit and is cut out as the motor comes up to speed, and an external reactor is placed in the circuit of the auxiliary winding, so that the two currents are as much out of phase as possible by this method. Figure 17(b) shows a *capacitor-start* motor in which a capacitor C in the auxiliary winding circuit is used to provide the desired phase displacement. When the motor attains full speed, the starting winding is usually disconnected by a centrifugal switch.

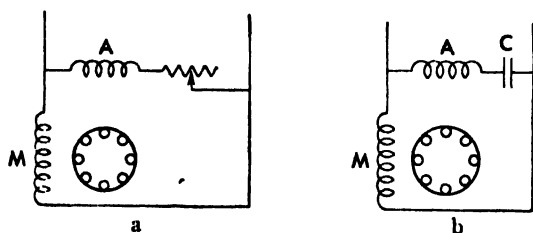


Fig. 17 Split phase motors.
(a) Resistor start
(b) Capacitor start.

12. The Capacitor Motor

The capacitor motor is a split-phase machine in which the auxiliary winding remains permanently in circuit, and the motor is intended to

have the running characteristics of a 2-phase motor. Because it can be designed to have high starting torque, as well as good running characteristics (including leading power-factor), and because its speed can be controlled rather easily, this motor seems destined to supplant some of the other types of single-phase motors. Figure 18 shows two popular connections. Since the voltage across the auxiliary winding varies with the current (due to the drop in the capacitor), it is desirable to cut out some of the capacitance after the motor comes up to speed. In (a) this is done by opening switch S_1 ; in (b) the same result is accomplished by using an autotransformer.

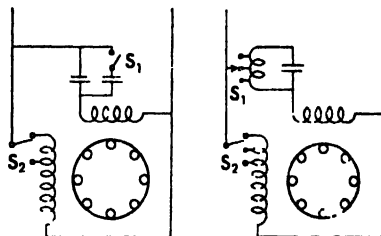


Fig. 18 The capacitor motor.

Example: A 3-phase, Y-connected, 60-cycle, 220-volt, 5-hp, 1800-rpm induction motor has the following per-phase constants: $G_0 = 0.00324$, $B_0 = 0.0351$, $R_1 = 0.545$, $R_2' = 0.538$, $X_1 = X_2' = 0.84$. Windage and friction is 65 watts. This motor is to be operated as a single-phase motor at 220 volts and 60 cycles by leaving one phase open. Calculate its characteristics at 4.9 per cent slip by both the double-revolving-field and the cross-field methods, compare the results, and discuss the two methods of solution from the point of view of work involved, accuracy, and design. Assume 60-cycle skin effect to increase the resistance by 50 per cent, and 120 cycles to increase it by 70 per cent.

1. Double-revolving field theory

According to Sec. 6, the blocked rotor impedance of the motor on single-phase is twice that per phase of the motor on three-phase. Hence the blocked-rotor, single-phase values are

$$R_1 + jX_1 = 2(0.545 + j0.84) = 1.090 + j1.68 = 2.04, 57.1^\circ$$

$$r_2' + r_2'' + j2X_2' = 2(0.538 + j0.84) = 1.076 + j1.68 = 1.994, 57.3^\circ$$

It is pertinent to note that under blocked rotor conditions both forward and backward revolving fields induce 60-cycle currents in the rotor. Hence

$$r_2'(60 \sim) = r_2''(60 \sim) = 0.538$$

But under running conditions, r_2' is at only 3 cycles, or practically direct current, while r_2'' is at 117 cycles, or practically double frequency. Hence

$$r_2' = \frac{0.538}{1.50} = 0.359$$

$$r_2'' = 1.70 \times 0.359 = 0.610$$

$$x_2' = 0.84$$

Now under running light conditions the single-phase core loss and magnetizing current, according to Fig. 4(c) are accounted for by $R_0 + jX_0$, and this impedance by Sec. 6 is twice the three-phase value per phase. Hence

$$R_0 = 2 \frac{0.00324}{0.0032^2 + 0.0351^2} = 5.23$$

$$X_0 = 2 \frac{0.0351}{0.0032^2 + 0.0351^2} = 56.6$$

Then we have

$$Z_0 = 5.23 + j56.6 = 56.8 \angle 84.7^\circ$$

$$Z_1 = 1.090 + j1.680 = 2.04 \angle 57.1^\circ$$

$$Z_f = \frac{(5.23 + j56.6)(7.33 + j0.84)}{12.56 + j57.44} = 6.93 + j1.67 = 7.13 \angle 13.5^\circ$$

$$Z_b = \frac{(5.23 + j56.6)(0.31 + j0.84)}{5.54 + j57.44} = 0.306 + j0.826 = 0.88 \angle 69.7^\circ$$

$$Z_T = Z_1 + Z_f + Z_b = 8.326 + j4.170 = 9.31 \angle 26.6^\circ$$

$$I_1 = \frac{220 \angle 0^\circ}{9.31 \angle 26.6^\circ} = 21.13 - j10.60 = 23.62 \angle -26.6^\circ$$

$$\cos \theta_1 = \cos 26.6^\circ = 0.894$$

$$E_{10} = (7.13 \angle 13.5^\circ)(23.62 \angle -26.6^\circ) = 163.6 - j38.1 = 168.5 \angle -13.1^\circ$$

$$I_{10} = \frac{168.5 \angle -13.1^\circ}{56.8 \angle 84.7^\circ} = -0.40 - j2.94 = 2.97 \angle -97.8^\circ$$

$$I_{2f}' = \frac{168.5 \angle 166.9^\circ}{7.38 \angle 6.5^\circ} = -21.53 + j7.66 = 22.82 \angle 160.4^\circ$$

$$E_{1b} = (0.88 \angle 69.7^\circ)(23.62 \angle -26.6^\circ) = 15.18 + j13.28 = 20.8 \angle 43.1^\circ$$

$$I_{1b} = \frac{20.8 \angle 43.1^\circ}{56.83 \angle 84.7^\circ} = 0.27 - j0.24 = 0.37 \angle -41.6^\circ$$

$$I_{2b}' = \frac{20.8 \angle 223.1^\circ}{0.88 \angle 69.7^\circ} = -20.85 + j10.35 = 23.27 \angle 153.6^\circ$$

$$\text{Core loss} = 5.23 \times 2.97^2 + 5.23 \times 0.37^2 = 47$$

$$\text{Copper loss} = 1.09 \times 23.62^2 + 0.359 \times 22.82^2 + 0.610 \times 23.27^2 = 1127$$

$$\text{Windage and friction} = 65$$

$$\text{Total losses} = 1239$$

$$\text{Input to stator} = 220 \times 23.62 \times 0.894 = 4650$$

$$\begin{aligned} \text{Gross output} &= \frac{1-s}{s} r_2' I_{2f}'^2 - \frac{1-s}{2-s} r_2'' I_{2b}''^2 \\ &= \frac{0.951}{0.049} 187^2 - \frac{0.951}{1.951} 331^2 = 3469 \end{aligned}$$

$$\text{Net output} = 3469 - 65 = 3404$$

$$(\text{check}) = 4650 - 1239 = 3411$$

$$\text{Efficiency} = \frac{3405}{4650} = 0.732$$

$$\text{Torque} = \frac{33000}{746(2\pi 1800)} \frac{3405}{1 - 0.049} = 14.6 \text{ lb-ft}$$

2. Cross-field theory

Under running-light conditions, $s = 0$, the cross-field equivalent circuit of the single-phase induction motor, Fig. 15, reduces to that shown in Fig. 19(a);

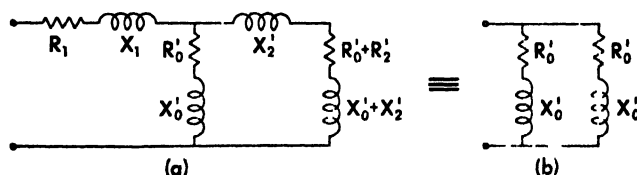


Fig. 19 Equivalent circuit of the single phase induction motor under running light conditions

and to a first approximation this in turn reduces to Fig. 19(b). That is, the exciting impedance under running-light conditions is $0.5(R_0' + jX_0')$. But according to Sec. 6, the single-phase impedance is twice the three-phase values per phase. Hence,

$$Z_0' = R_0' + jX_0' = 4(2.615 + j28.3) = 10.46 + j113.2 = 113.7 \angle 84.7^\circ$$

$$Z_1 = 2(0.545 + j0.84) = 1.090 + j1.68 = 2.0 \angle 56.9^\circ$$

Now according to (29a) there are two frequencies of 3 and 117 cycles in each conductor. But unlike the double-revolving field theory, the cross-field theory does not yield an equivalent circuit in which it is possible to state that skin effects corresponding to certain frequencies should be used in certain branches. Actually, the equivalent circuit was derived for the d -axis, in which axis the frequency is 60 cycles. But resistance is in a conductor, not in an axis, and the

conductor has two frequencies. However, as seen from double-revolving-field theory, the slip frequency current is principally responsible for the torque. Therefore, in the cross-field theory the slip frequency rotor resistance should be used to secure closest agreement with the numerical values of the revolving-field theory. Hence,

$$Z_2' = 2(0.359 + j0.84) = 0.718 + j1.68 = 1.825/66.5^\circ$$

$$Z_d' = \frac{\left(\frac{10.46 + j113.2 + 0.72 + j1.68}{0.951^2} \right) \left(\frac{0.718}{1.951 \times 0.049} \right)}{19.89 + j127.2} + j1.68$$

$$= 7.41 + j2.11 = 7.72/15.9^\circ$$

$$Z_T = (1.09 + j1.68) + \frac{(113.7/84.7^\circ)(7.72/15.9^\circ)}{116.7/81.2^\circ}$$

$$= 8.18 + j4.17 = 9.18/27^\circ$$

$$I_1 = \frac{220/0^\circ}{9.18/27^\circ} = 21.35 - j10.88 = 23.95/-27^\circ$$

$$E = 220 - (2.0/56.9^\circ)(23.95/-27^\circ) = 178.5 - j23.8 = 180.2/-7.6^\circ$$

$$I_0 = \frac{180.2/-7.6^\circ}{113.7/84.7^\circ} = -0.064 - j1.584 = 1.59/-92.3^\circ$$

$$-I_d' = I_1 - I_0 = 21.414 - j9.296 = 23.35/-23.45^\circ$$

$$E' = (178.5 - j23.8) - j1.68 \times 23.35/-23.45^\circ = 162.92 - j59.6 = 173.4/-20.1^\circ$$

$$I_a = (1 - 0.951') \frac{173.4/-20.1^\circ}{0.718} = 21.67 - j7.93 = 23.07/-20.1^\circ$$

$$I_b = \frac{0.951' \times 173.4/-20.1^\circ}{(10.46 + j113.2) + (0.72 + j1.68)} = -0.34 - j1.32 = 1.36/-104.3^\circ$$

$$\text{Core loss } 10.46 \times 1.59^2 + 10.46 \times 1.36^2 = 46$$

$$\text{Copper loss } 1.09 \times 23.95^2 + 0.718 \times 23.07^2 + 0.718 \times 1.36^2 = 1008$$

$$\text{Windage and friction} = 65$$

$$\text{Total losses} = 1119$$

$$\text{Input to stator } 220 \times 23.95 \times 0.891 = 4700$$

$$\text{Net output } 4700 - 1119 = 3581$$

$$\text{Efficiency } \frac{3581}{4700} = 0.762$$

$$\text{Torque } \frac{33000}{746(2\pi 1800)} \frac{3581}{0.951} = 14.72 \text{ lb-ft}$$

3. *Comparison of calculations*

From the point of view of length and time of computation, there is little to choose between the two methods of calculation. There are a few more items in the revolving-field theory, but this is compensated by the greater complexity of some of the items in the cross-field theory.

The revolving-field theory is explicit about the frequencies and corresponding skin-effect corrections to use in its various branches; whereas the 60-cycle frequency required in all branches by the cross-field theory is obviously not appropriate for skin-effect calculations, and it is necessary to arbitrarily use slip frequency for the rotor resistance in order to secure accurate results. In fact, even better numerical agreement between the two theories can be obtained (comparing the equivalent circuits) by putting

$$\begin{array}{ccc} \text{Revolving-field} & & \text{Cross-field} \\ \frac{r_2'}{s} + \frac{r_2''}{2-s} & = & \frac{R_2'}{s(1-\frac{s}{2}) - s} \end{array}$$

from which

$$R_2' = (2-s)r_2' + sr_2'' = 1.951 \times 0.359 + 0.040 \times 0.610 = 0.730$$

From the point of view of the designer who must juggle design constants to obtain specified or desired characteristics, the revolving-field equivalent circuit is perhaps superior, since it is more symmetrical and the physical significance of its parts easier to see. Also, its derivation is much less involved.

The numerical results of the two methods agree reasonably well, particularly in view of the arbitrary inclusion of skin effect in the cross-field theory. A comparison is

<i>Revolving-field</i>		<i>Cross field</i>
47	Core loss	46
1127	Copper loss	1008
65	Windage and friction	65
1239	Total losses	1119
4650	Input	4700
3405	Net output	3581
0.732	Efficiency	0.762
0.894	Power factor	0.891
14.00	Torque	14.72

Problems

1. Plot the resultants and traveling wave components of a pulsating sinusoid, Eq. (1), at the following instants: $\omega t = 0, 45^\circ, 90^\circ, 180^\circ, 225^\circ, 270^\circ, 315^\circ, 360^\circ$.
2. If a 60-cycle motor has a pole pitch of $\tau = 6$ in ches, what is the velocity in inches per second of its traveling wave components?

3. If the mechanical speed of rotation of a 60-cycle motor is 95 per cent of synchronous speed, what is the frequency of mechanical rotation, and what are the slips of its forward and backward revolving fields?
4. The winding factors for a single-phase squirrel-cage motor are $K_1 = 0.9$ and $K_2 = 0.92$, the stator has 37 turns and the squirrel-cage has 25 bars. What is the factor for referring the rotor resistance to the stator?
5. A 3-phase, wye-connected, 60-cycle, 220-volt, 10-hp, 1800-rpm induction motor has the following test data:

<i>Running light</i>		<i>Blocked motor</i>
220	volts	64
6.4	amperes	62
239	watts	1922
1.30	friction and windage loss	

Stator d-c resistance at 75 C is $R_1 = 0.242$ ohms per phase.

This motor is to be operated as a single-phase motor. Calculate its performance at 5 per cent slip by

- the double revolving field theory, and
- by the cross-field theory. Neglect skin effect.

6 Alternating Current Commutator Machines

1. Introduction

There is a great variety of alternating current commutating machines which may be classified under three principal groups as:

- (1) Single-phase motors
 - a. series motors (simple, compensated, doubly fed)
 - b. repulsion motors (brush shifting, double brush set)
- (2) Polyphase motors
 - a. series motor (adjustable speed)
 - b. shunt motor (adjustable speed)
 - c. Schrage brush-shift motor
 - d. Heyland motor
- (3) Converters
 - a. rotary (or synchronous) converter
 - b. frequency converters

The analysis for a-c commutating machines is in a much less developed state than for synchronous machines, or for polyphase and single-phase induction motors. First of all, the phenomenon of commutation adds greatly to the complexity of the problem—in fact, a thoroughly satisfactory analysis does not exist. And secondly, the bulk of a-c

commutating machines are built in small sizes whose design can be tested quickly and cheaply and modified accordingly, and whose characteristics are of no great concern to the user. The relatively small number of larger machines, such as railway motors, has not been sufficient to attract the engineering interest and talent that power equipment has. All this is economically unfortunate, as the potential savings that would ensue from increased efficiency and better characteristics for a-c commutating machines are enormous.

2. General Principles

Before passing to the detailed consideration of specific machines, it will be profitable to review a few general principles. In Chapter 3 it was shown that there are three ways in which a voltage may be induced in a winding:

- (1) *Transformer action*, in which a distribution of flux fixed in space is varied in time (usually sinusoidally) and thereby induces a voltage in a stationary coil or winding (*i.e.* the transformer).
- (2) *Rotating field*, in which a field of constant magnitude revolves in space, cutting the conductors of a stationary coil or winding and generating a voltage therein (*i.e.* the rotating field of a polyphase induction motor, or the revolving field poles of an alternator).
- (3) *Moving conductors*, which sweep through a stationary unvarying field, and generate a voltage (*i.e.* the armature of a d-c machine, or a revolving armature synchronous generator).

All three processes may occur simultaneously in any particular machine, and at least two of them are identifiable in a-c commutating machines. The general equation, including the effects of time and space harmonics, is given as Eq. (18) of Chapter 3. Considering only the fundamental in the space distribution of the flux, and assuming it to be a simple harmonic time function $\phi = \Phi \cos \omega t$, the voltage equation reduces to

$$\begin{aligned}
 e &= - \frac{KN}{10^8} \left[\frac{\partial \phi}{\partial t} \sin \left(\frac{\pi x_0}{\tau} - \gamma \right) - \left(\frac{d\gamma}{dt} - \frac{\pi}{\tau} \frac{dx_0}{dt} \right) \phi \cos \left(\frac{\pi x_0}{\tau} - \gamma \right) \right] \\
 &= \frac{KN\Phi}{10^8} \left[\omega \sin \omega t \sin \left(\frac{\pi x_0}{\tau} - \gamma \right) \right. \\
 &\quad \left. + \left(\frac{d\gamma}{dt} - \frac{\pi}{\tau} \frac{dx_0}{dt} \right) \cos \omega t \cos \left(\frac{\pi x_0}{\tau} - \gamma \right) \right] \quad (1)
 \end{aligned}$$

in which

$K = K_d K_p K_s =$ distribution, pitch, and skew factor

$N =$ total number of turns in the coil belt

$\Phi =$ flux per pole

$f =$ frequency of the flux pulsation

$\omega = 2\pi f$

$x_0 =$ position of the center of the coil belt from the q -axis

$\tau =$ pole pitch

$\gamma =$ displacement angle of the flux, measured from the q -axis

Consider, now, the case of an a-c commutating machine, Fig. 1, having a field which not only is pulsating in time at frequency f , but which field is also rotating at an angular velocity $d\gamma/dt = \omega_1$. Suppose further, that the brushes of this machine have been shifted an angle α from the q -axis, so that the belt of conductors between brushes have their coil group center at πx_0 $\tau = \alpha$. The rotating

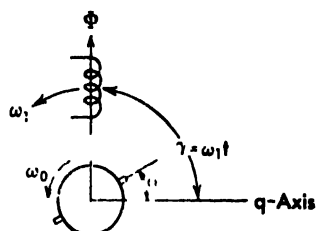


Fig. 1 General a-c commutating machine with rotating field and armature.

conductors have a velocity $\frac{\pi dx_0}{\tau dt} = \omega_0$. Inserting these conditions in

(1), there results

$$\begin{aligned}
 e &= \frac{KN\Phi}{10^8} [-\omega \sin \omega t \sin (\omega_1 t - \alpha) + (\omega_1 - \omega_0) \cos \omega t \cos (\omega_1 t - \alpha)] \\
 &= \frac{KN\Phi}{2 \cdot 10^8} [(\omega + \omega_1 - \omega_0) \cos \{(\omega + \omega_1)t - \alpha\} \\
 &\quad - (\omega - \omega_1 + \omega_0) \cos \{(\omega - \omega_1)t + \alpha\}] \quad (2)
 \end{aligned}$$

This equation shows that in the general case there will be two distinct frequencies at the brushes, corresponding to the sum and difference of the frequencies of pulsation and rotation of the field. But the frequency at the brushes is independent of the speed of rotation of the armature. If the field is stationary ($\omega_1 = 0$), or is of constant magnitude ($\omega = 0$), only one frequency will appear at the brushes. If the armature rotates synchronously with the field ($\omega_0 = \omega_1$), and the field is constant ($\omega = 0$), there will be no induced voltage. As special cases of this general case, there are:

Case I: field and conductors stationary ($\omega_1 = 0$, $\omega_0 = 0$).

$$e = \frac{KN\Phi}{10^8} \omega \sin \omega t \sin \alpha \quad (3)$$

The brush voltage is due entirely to transformer action, and is a maximum when the brush shift is $\alpha = 90$ degrees, that is with the brushes centered on the main flux axis. The voltage vanishes when the brushes are on the quadrature axis. The frequency at the brushes is the same as that of the main flux, and the voltage is proportional to that frequency.

Case II: constant ($\omega = 0$) rotating field, stationary conductors ($\omega_0 = 0$).

$$e = \frac{KN\Phi}{10^8} \omega_1 \cos (\omega_1 t - \alpha) \quad (4)$$

The brush voltage is of stator frequency, and is proportional to that frequency.

Case III: field constant ($\omega = 0$) and stationary ($\omega_1 = 0$), conductors rotating.

$$e = - \frac{KN\Phi}{10^8} \omega_0 \cos \alpha \quad (5)$$

The brush voltage is direct voltage, proportional to the speed, and a maximum when the brush shift is $\alpha = 0$, that is with the brushes centered on the quadrature axis.

3. The Series Motor

The a-c series motor is used in the larger sizes – up to several thousand horsepower – for electric traction, in which field it enjoys the same advantages as the d-c series motor. Railway motors can be designed to operate satisfactorily at 25 cycles, but have not been successful at 60 cycles because of commutation difficulties. In the fractional horsepower class series motors find a wide field of application for industrial (portable tools) and domestic use at 60 cycles. The bulk of the motors found on household appliances are of this type. Commutation difficulties are of no great concern because the currents are small and the speeds very high (up to 8000 rpm normally, and even 16,000 at no-load).

Structurally, the simple a-c series motor, Fig. 2a resembles the d-c series motor; except that both the field and armature magnetic circuits of the a-c motor must be laminated to reduce the core loss. It may have either salient or non-salient poles. But a simple series motor of this type has high reactance and low power factor, and very poor commutation

if the speed is not high. It will run just as well, or better, on direct current as on alternating current, for which reason, in fractional horsepower sizes, it is called a *universal* motor. However, commutation difficulties and low power factor exclude it from applications beyond fractional horsepower. The high reactance is due to the sum of the field and armature reactances. Since the brushes are on the quadrature axis it is evident that the brush voltage is entirely a speed voltage in that axis, and the series current armature reaction is along that axis.

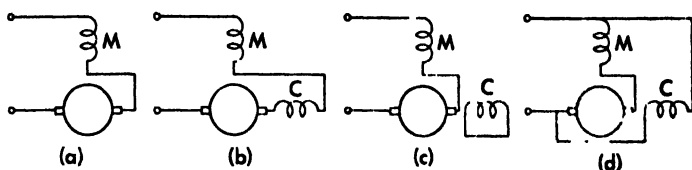


Fig. 2 Types of a-c series motors.

- (a) simple series
- (b) conductively connected
- (c) inductively connected
- (d) doubly fed

This armature magnetomotive force not only causes leakage fluxes in the slots, air gap, and end turns, but also produces a heavy cross flux in the quadrature axis which induced a large electromotive force in the brush axis by transformer action.

The excessive reactance of the simple series motor is reduced by low frequency (16-23 and 25 cycles are usually used for a c electric railways), by small air gaps and short magnetic circuits, and by multiple poles.

The torque of the series motor is always in the same direction, since field and armature current reverse simultaneously, and the torque is proportional to the product of the field and armature ampere turns. In order to secure the desired torque without excessive reactance, the field winding is usually designed with only a few turns, and the armature with many turns. The large armature magnetomotive force along the quadrature or brush axis is then neutralized by means of a distributed compensating winding. Such a winding cannot neutralize the cross flux completely, nor can it affect the slot and zigzag leakage reactance of the rotor. There are several ways by which the compensating winding may be excited. In Fig. 2b it is shown connected conductively in series with the armature. In Fig. 2c it is shown as a short-circuited secondary winding, or inductively connected. In this case the neutralization is only partial, since the ampere-turns of the secondary winding are less than those of the armature by the amount of the magnetizing ampere-

turns. In Fig. 2c the compensating winding is shown connected in shunt across the line. In some cases it is connected to an autotransformer with a choice of taps, so that the compensation can be adjusted to the load. Compensating windings are invariably distributed, so as to match the distribution of the armature ampere-turns as nearly as possible.

During commutation the short-circuited armature coil is centered on the direct axis, and the main flux by transformer action induces in it a voltage lagging by 90 degrees. Thus, not only must the current in the coil be reversed as in a d-c machine, but the voltage induced by transformer action of the main flux must be overcome to secure good commutation. A simple interpole will assist in reversal of the current but does not neutralize the transformer voltage, because, as seen in the vector diagram of Fig. 3a, the speed voltage e_s , due to rotation of the coil through the interpole flux, is at right angles to the transformer voltage e_t ; and the resultant voltage e is greater than e_t . However,

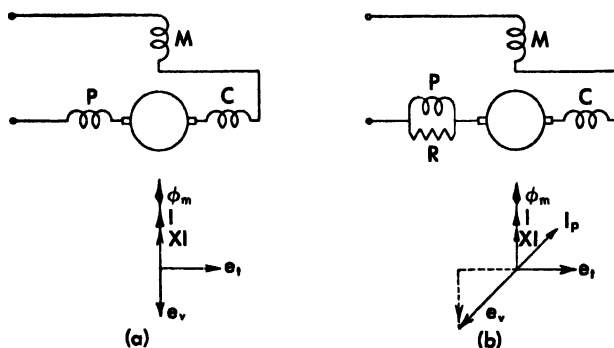


Fig. 3 AC series motors with commutating and interpole windings.

if the interpole winding is shunted by a resistor, as in Fig. 3b, the current through the interpole winding can be made to lag the main current by any angle $\theta_p = \tan^{-1}(X_p R)$, and its ampere turns can be made sufficient so that both the transformer voltage e_t and the self-inductive voltage IX of the commutating coil are neutralized. The resistance shunt must be adjusted if the speed changes materially, since e_s is proportional to the speed.

In the doubly-fed motor of Fig. 2d, the flux in the compensating winding lags the line voltage by approximately 90 degrees, and by speed action generates in the coil undergoing commutation a voltage partly in phase opposition to the transformer voltage e_t . This scheme is used

on many railway motors. Other methods for adjusting the phase of the interpole current have been devised, but they will not be described here.

Commutation also can be improved by using high-resistance carbon brushes, or by using high-resistance leads as in Fig. 4. These resistance leads are in parallel to the load current and in series to the short-circuit current. At standstill the leads may burn out.

The commutation problem in an a-c series motor necessitates operating at low volts per turn and only a few (usually one) turns per coil, and this restricts such motors to the low voltage field, rarely exceeding 300 volts. Since only one coil may be commutated at a time, the brush width is one commutator segment, and therefore in the larger machines the commutator is longer than in d-c machines.

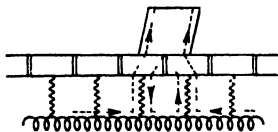


Fig. 4 High resistance leads.

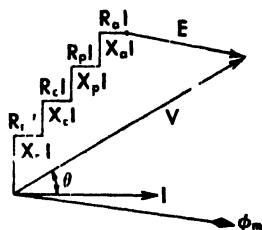


Fig. 5 A-c series motor.

The vector diagram for a series motor with compensating winding and interpole is shown in Fig. 5. The series current I has been taken as the reference vector. The main field flux ϕ lags the current by the hysteretic angle. Each field winding and the armature has a resistance and a reactance accounting for both the leakage and transformer fluxes. The counter electromotive force of the motor is a speed voltage in the brush axis proportional to the speed. If the transformer voltage induced in the armature (direct axis) by the main flux is E_{mtd} , and if this be accounted for in the usual fashion as $E_{mtd} = -Z_0 I$, where Z_0 is the exciting impedance, then the voltage to overcome the counter electromotive force of the motor is

$$E = -j \frac{\omega_0}{\omega} Z_0 I = \frac{\omega_0}{\omega} (X_0 - jR_0) I = S(X_0 - jR_0) I \quad (6)$$

in which $S = \omega_0 / \omega$ is the speed as fraction of synchronous speed, and this voltage, plus the sum of the impedance drops, is the applied voltage of the motor,

$$\begin{aligned} V &= E + (Z_m + Z_c + Z_p + Z_a) I \\ &= [(R + SX_0) + j(X - SR_0)] I \end{aligned} \quad (7)$$

The voltage E is in time-phase with the main flux, as shown in Fig. 5. From (7)

$$I = \frac{V}{\sqrt{(R + SX_0)^2 + (X - SR_0)^2}} \quad (8)$$

$$\text{and } \cos \theta = \frac{R + SX_0}{\sqrt{(R + SX_0)^2 + (X - SR_0)^2}} \rightarrow \begin{cases} R/Z & \text{as } S \rightarrow 0 \\ X_0/Z_0 & \text{as } S \rightarrow \infty \end{cases} \quad (9)$$

The power input is

$$P = VI \cos \theta = \frac{V^2(R + SX_0)}{(R + SX_0)^2 + (X - SR_0)^2} \quad (10)$$

and the gross power output is

$$P = SX_0 I^2 = \frac{V^2 SX_0}{(R + SX_0)^2 + (X - SR_0)^2} \quad (11)$$

The torque then is

$$T = \frac{P}{S} = \frac{V^2 X_0}{(R + SX_0)^2 + (X - SR_0)^2} \rightarrow \begin{cases} V^2 X_0 / Z^2 & \text{as } S \rightarrow 0 \\ V^2 X_0 / S^2 Z_0^2 & \text{as } S \rightarrow \infty \end{cases} \quad (12)$$

The torque is a maximum at standstill—usually 2 or 3 times normal running torque—but decreases inversely as the square of the speed at high speeds.

The previous analysis ignored the effect of the short-circuited coil undergoing commutation. The effect can be taken into account by the cross field theory.* Saturation and space harmonics also play an important part in the characteristics of a-c commuting motors, so that

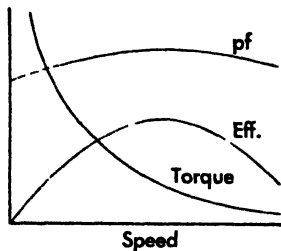


Fig. 6 Performance characteristics of the a-c series motor.

the foregoing simple analysis oftentimes fails to give reasonably accurate results. It is also very difficult to obtain reliable test results on small motors, because of meter inaccuracies, and because the loads they impose on the circuit are an appreciable part of the quantities being measured.

Typical characteristics for an a-c series motor are shown in Fig. 6. The torque characteristic is similar to that of a d-c series motor, and is well adapted to loads requiring a heavy starting torque. The power factor is considerably better than that of an induction motor.

Table I lists some of the salient features of large and small a-c series motors.

* West, H. R. "The Cross-field Theory of Alternating-Current Machines," *Trans. AIEE*, February, 1926.

TABLE I
A C SERIES COMMUTATING MOTORS

Large size		Small size
railway traction	Type of service	portable tools and domestic appliances
up to 2200 hp	Horsepower rating	up to 3 4-hp
200 to 400	Voltage rating	115 to 230
15 to 25 cycle	Frequency	up to 60 cycle
	Speed	3500 to 16,000
lower than for d-c	Power Wt. ratio	high
	Efficiency, full load	50 to 60%
	Power factor, full load	80 to 90%
non-salient, distributed	Type of field pole	salient or non-salient
many	Number of poles	2 to 6
few	Turns pole	few
shunted, or line excited	Interpoles	not generally
in slots in pole face	Compensating winding	not generally necessary
many	Armature coils	many
few	Turns coil	few
small	Volts turn	small
higher than for d-c	Commutator speed	
longer than for d-c	axial length	
larger than for d-c	diameter	
many	segments	
short and laminated	Magnetic circuit	short and laminated
short	Air gap	
yes	High-resistance brushes	yes
sometimes	High-resistance leads	no

4. The Repulsion Motor

The modern repulsion motor, Fig. 7, consists of a single phase field winding, and an armature with a commutator having one or more pairs of short-circuited brushes. The brush axis is shifted α degrees from the field axis. The motor will develop torque in the direction of brush shift. Motors of this type in fractional horsepower and moderate sizes are in competition with the a-c series commutating motor and with the capacitor motor, but in recent years have been yielding to the latter because of the absence of a commutator, resulting in radio interference.

It is clear from Fig. 7 that the field turns N , assumed to be distributed sinusoidally around the stator, may be resolved into components $N \cos \alpha$

in line with the brushes (the q -axis) and $N \sin \alpha$ in quadrature with the brushes (the d -axis).^{*} Since the brushes are short-circuited, the armature current and its magnetomotive force are constrained to the brush axis,

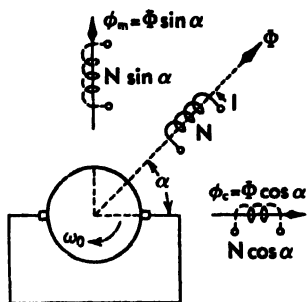


Fig. 7 The repulsion motor.

and the torque results from the interaction between the armature current and the orthogonal (d -axis) component of the field flux. The armature current itself flows in response to two voltage components in the brush axis: (1) a speed voltage E_{mrq} due to the armature conductors cutting the flux $\phi_m = \Phi \sin \alpha$, and (2) a transformer voltage E_{td} due to the transformer action of the flux $\phi = \Phi \cos \alpha$. In addition, the short-circuited armature coil undergoing commutation has a transformer voltage

induced in it by the flux ϕ_m , a speed voltage generated by rotation through the cross flux ϕ , and an electromotive force of self induction due to the reversal of its current. Its resulting current reacts on the cross flux ϕ , to produce a torque in opposition to the principal torque. Since the armature voltages and currents, whether due to transformer or cutting action, are proportional to the field current, it is evident that the repulsion motor possesses series characteristics, the speed decreasing with the load. Indeed, the equations for the repulsion motor can be shown to be identical in form to those derived for the series motor.

In the following equations it is assumed that the armature and field each have N turns, or that all armature quantities have been referred to the stator. All impedances are based on N -turns.

If Z_0 is the exciting admittance for N -turns, then the voltage induced in the rotor d -axis by the flux ϕ_m (remembering that an impedance varies as the square of the turns) is

$$-E_{md} = \frac{N}{N \sin \alpha} (Z_0 \sin^2 \alpha) I_1 = (R_0 + jX_0) I_1 \sin \alpha \quad (13)$$

which is the same as though there were N -turns in the stator d -axis traversed by a current $I_1 \sin \alpha$. The flux ϕ_m also generates in the q -axis a speed voltage

$$E_{mrq} = jSE_{md} = S(X_0 - jR_0)I_1 \sin \alpha \quad (14)$$

^{*} In the Atkinson repulsion motor (1898), two separate field windings were actually provided. Separation into two separate windings does not increase the reactance, since $(N \cos \alpha)^2 + (N \sin \alpha)^2 = N^2$, but does increase the resistance and stator copper loss since $(N \cos \alpha + N \sin \alpha) > N$.

The cross-flux ϕ_c may be accounted for by the q -axis impedance $Z_0 \cos^2 \alpha$ and an exciting current

$$I_0 = I_1 + \frac{I_2}{\cos \alpha} \quad (15)$$

in which the rotor current I_2 has been referred to the stator by the turn-ratio $\cos \alpha$. The flux ϕ_c induces in the rotor q -axis a voltage

$$-E_{ctq} = \frac{N}{N \cos \alpha} (Z_0 \cos^2 \alpha) I_0 = Z_0 \left(I_1 + \frac{I_2}{\cos \alpha} \right) \cos \alpha \quad (16)$$

The total voltage in the brush axis of the armature is consumed by the armature leakage impedance,

$$E_{mrq} + E_{ctq} = Z_2 I_2 \quad (17)$$

From (14), (16), and (17)

$$-E_{ctq} = \frac{Z_0}{Z_2 + Z_0} [S(X_0 - jR_0) \sin \alpha + Z_2 \cos \alpha] I_1 \quad (18)$$

The stator applied voltage is the sum of the voltages induced by the fluxes ϕ_m and ϕ_c in the stator windings, and the stator leakage impedance drops, that is

$$V = -E_{mtd} \sin \alpha - E_{ctq} \cos \alpha + (Z_1 \sin^2 \alpha) I_1 + (Z_1 \cos^2 \alpha) I_1 \quad (19)$$

Substituting (13) and (18) this becomes

$$\begin{aligned} V &= Z_0 \sin^2 \alpha I_1 + \frac{Z_0 \cos \alpha}{Z_2 + Z_0} [S(X_0 - jR_0) \sin \alpha + Z_2 \cos \alpha] I_1 + Z_1 I_1 \\ &= \left[Z_0 \sin^2 \alpha + Z_1 + \frac{Z_2 Z_0 \cos^2 \alpha}{Z_2 + Z_0} + \frac{Z_0 S(X_0 - jR_0) \sin \alpha \cos \alpha}{Z_2 + Z_0} \right] I_1 \\ &= \left[Z + \frac{Z_0 S(X_0 - jR_0) \sin \alpha \cos \alpha}{Z_2 + Z_0} \right] I_1 \end{aligned} \quad (20)$$

which is identical in form with (7) for the series motor. This analysis neglects the short-circuited commutating coil.

If Z_2 is ignored in comparison with Z_0 , then by (13) and (18)

$$\frac{E_{ctq}}{E_{mtd}} = \frac{\phi_c}{\phi_m} = -jS \quad (21)$$

At synchronous speed the two fields are equal in magnitude as in a two-phase induction motor, and being in time and space quadrature are equivalent to a uniform rotating field. When the speed is not synchronous the two orthogonal fields are unequal and the resultant field is elliptical.

In the short-circuited coil there is a transformer voltage due to ϕ_m

and a speed voltage due to ϕ_c , and the total coil voltage is, making use of (21),

$$e = e_t + e_r = j\omega\phi_m + \omega_0\phi_c = \left(1 - j\frac{\omega_0}{\omega}\frac{\phi_c}{\phi_m}\right)e_t = (1 - S^2)e_t \quad (22)$$

At synchronous speed, $S = 1$, this voltage is zero, and the commutation is good. At standstill, $S = 0$, the voltage is equal to the transformer voltage, e_t . At $S = \sqrt{2}$ the voltage is again $-e_t$ and thereafter becomes greater, impairing commutation. The commutation of the repulsion motor is better than that of the series motor at synchronism, about equal at standstill, and much worse at speeds greater than double synchronous speeds.

Equation (20) defines the total impedance Z_T of the motor for any speed S , and thus the stator current is

$$I_1 = \frac{V}{Z_T} \quad (23)$$

The rotor current follows from (17) upon substituting (14), (18) and (23)

$$I_2 = \left[\frac{S(X_0 - jR_0) \sin \alpha - Z_0 \cos \alpha}{Z_2 + Z_0} \right] \frac{V}{Z_T} \quad (24)$$

The losses then may be computed as:

$$\begin{aligned} \text{Stator copper loss} & R_1 I_1^2 \\ \text{Rotor copper loss} & R_2 I_2^2 \\ \text{Core loss} & \end{aligned} \quad (25)$$

$$R_0(I_1 \sin \alpha)^2 + R_0(I_1 \cos \alpha + I_2)^2 = R_0(I_1^2 + 2I_1 I_2 \cos \alpha + I_2^2)$$

$$\text{The stator input is} \quad V I_1 \cos \theta_1 = \frac{R_1 V^2}{Z_1^2} = R_1 I_1^2 \quad (26)$$

The gross mechanical output is the input less the losses

$$(R_T - R_1 - R_0)I_1^2 - (R_2 + R_0)I_2^2 - 2R_0 I_1 I_2 \cos \alpha \quad (27)$$

and the torque is the gross output divided by the speed

$$T = \frac{(R_T - R_1 - R_0)I_1^2 - (R_2 + R_0)I_2^2 - 2R_0 I_1 I_2 \cos \alpha}{S} \quad (28)$$

It is also possible to find the torque as the product of the current and the in-phase component of the speed term in the voltage Equation (20) divided by the speed, that is

$$T = \left\{ \text{real of } \frac{Z_0(X_0 - jR_0) \sin \alpha \cos \alpha}{Z_2 + Z_0} \right\} I_1^2 \quad (29)$$

If Z_2 be neglected in comparison with Z_0 this becomes

$$T \cong X_0 I_1^2 \quad (30)$$

and with the additional assumption that R_0 may be neglected in (20)

$$I_1 \cong \frac{V}{R_1 + jX_1 + jX_0 \sin^2 \alpha + (R_2 + jX_2) \cos^2 \alpha + SX_0 \sin \alpha \cos \alpha} \quad (31)$$

the equivalent circuit for which is a simple series circuit.

7 The Synchronous Generator and Motor

1. Introduction

The synchronous generator is a rotating machine for converting mechanical power into alternating current electrical power. It may be single or polyphase, but by far the majority are 3-phase machines. If 3 phase, it may be either delta or (more usually) wye-connected. It consists essentially of an alternating current armature winding embedded in the slots of the armature magnetic core, and direct current windings on the field poles. Either armature or field may be the rotating element, although in most cases the field is the rotor. The field may be the round rotor type (as in large high speed turbo-generators), or the salient-pole type (as in hydraulic or engine-driven units).

The synchronous generator is the most important of all electrical machines, not only because it is the principal source of electrical power, but also because it is built in far larger sizes (up to 165,000 kw in a single unit). It is the principal element in the power system from the point of view of balanced operation, fault currents, and system stability. For these reasons its theory has been worked out more thoroughly, and with a greater degree of refinement, than that of any other machine.

However the synchronous machine possesses much in common, both structurally and in theory, with other electrical machines. Its armature construction and armature windings resemble closely those of a polyphase induction motor or any other type of a-c motor. Such differences as exist are dictated by size or speed rather than by type of machine. The process

of voltage induction in such windings — and its modification by skew, pitch, distribution and phase connection factors — presents nothing new. The development of armature reaction in such windings — and its modification by the harmonic reduction factors — presents nothing new. Even the same kinds of leakage fluxes — slot, end turn, and air gap — are encountered in the alternator as in, say, the induction motor. These things already have been considered in Chapter 3, and in greater detail in the Appendices, and need not be repeated again.

But the synchronous generator, motor, and converter are unique among alternating current machines in two respects: (1) they run at constant synchronous speeds, and (2) their field flux is furnished by d-c excitation. These two factors are responsible for their distinguishing features of construction and special analytical treatment

2. Principles of Operation

An elementary single-phase, 2-pole alternator is shown in Fig. 1a. The field poles are stationary and the coil is assumed to rotate in the clockwise direction. The reference axis is taken as the pole axis.

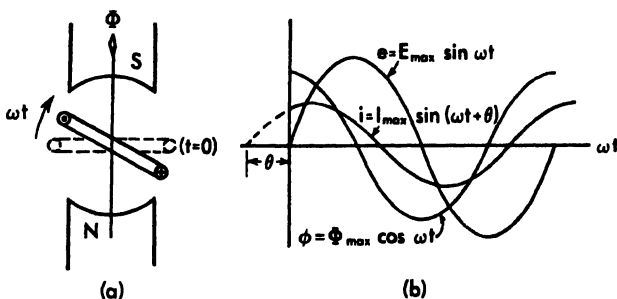


Fig. 1 Elementary alternator

When the coil axis is along the pole axis, at $t = 0$, the flux, Φ_{\max} , linked therewith is a maximum. Assuming the flux to be sinusoidally distributed in space, the flux linked with the coil at any instant t is

$$\phi = \Phi_{\max} \cos \omega t \quad (1)$$

which is plotted in Fig. 1b. The voltage induced in the coil is, by Faraday's law,

$$\begin{aligned} e &= - \frac{N}{10^8} \frac{d\phi}{dt} \\ &= + \frac{\omega N \Phi_{\max}}{10^8} \sin \omega t \\ &= E_{\max} \sin \omega t \end{aligned} \quad (2)$$

This voltage is also plotted in Fig. 1b, showing that it lags the flux by 90 degrees in *time* as well as in *space*, since in the synchronous machine time and space angles are identical.

The *effective value* of the induced voltage is

$$E = \frac{E_{\max}}{\sqrt{2}} = \frac{\sqrt{2}\pi f N \Phi_{\max}}{10^8} = \frac{4.44 f N \Phi_{\max}}{10^8} \quad (3)$$

Suppose, now, that the impedance of the coil and its external circuit is

$$Z = R \pm jX$$

Then the current will be

$$I = \frac{E}{Z} = \frac{E}{Z} \angle \theta \quad (4)$$

in which θ will be taken as positive for a leading current. The current does not reach its maximum until the coil has moved through an angle $\omega t = (\pi/2 - \theta)$, as shown in Fig. 1b.

Consider next the magnetomotive force of armature reaction due to this current. It has a magnitude, per pole,

$$A = \frac{0.4\pi N i}{2} = 0.2\pi N I_{\max} \sin(\omega t + \theta) \quad (5)$$

and is directed perpendicular to the plane of the coil.*

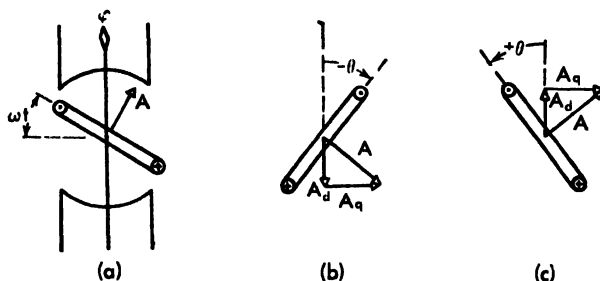


Fig. 2 Direct and quadrature components of armature reaction of a single coil

As shown in Fig. 2 it may be resolved into *direct* (in line with the pole axis) and *quadrature* (perpendicular to the pole axis) components $A_d = A \cos \omega t$ and $A_q = A \sin \omega t$. Or expressed in (space) vector form

$$A = A_d + jA_q$$

* This is, of course, a rectangular space wave whose space fundamental has a magnitude of $\frac{4}{\pi}A$. The $\frac{4}{\pi}$ is incorporated in the following equations.

$$\begin{aligned}
&= A(\cos \omega t + j \sin \omega t) \\
&= 0.8NI_{\max}(\cos \omega t + j \sin \omega t) \sin (\omega t + \theta) \\
&= 0.4NI_{\max}\{\sin \theta + \sin (2\omega t + \theta)\} + j[\cos \theta - \cos (2\omega t + \theta)] \quad (6)
\end{aligned}$$

Thus the single-phase armature reaction consists of constant and double-frequency components of equal magnitude. Ignoring the latter for the moment, it is clear that the constant term of the direct component of armature reaction, being proportional to $\sin \theta$, will *oppose* the main field when the power factor is lagging, and *assist* the main field when the power factor is leading. At unity power factor it vanishes.

On the other hand, the constant term of the quadrature component of armature reaction, being proportional to $\cos \theta$ sets up a cross field for lagging, leading or unity power factor which is always in the same direction, and which *opposes* the motion. It is this component which is responsible for the torque of the machine. Only in the case of zero power factor, when A is in line with the poles, does it vanish entirely.

The following table indicates the effect of power factor on the constant terms of armature reaction.

Power factor	θ	A_d	A_q
zero, lagging	-90°	$0.4 NI_{\max}$ (opposes)	0
lagging	$-\theta$	$-0.4 NI_{\max} \sin \theta$ (opposes)	$+0.4 NI_{\max} \cos \theta$
unity	0	0	$+0.4 NI_{\max}$
leading	$+\theta$	$+0.4 NI_{\max} \sin \theta$ (assists)	$+0.4 NI_{\max} \cos \theta$
zero, leading	$+90^\circ$	$+0.4 NI_{\max}$ (assists)	0

The instantaneous electrical power generated is

$$\begin{aligned}
p &= ei = E_{\max} \sin \omega t I_{\max} \sin (\omega t + \theta) \\
&= \frac{E_{\max} I_{\max}}{2} [\cos \theta - \cos (2\omega t + \theta)] \\
&= EI [\cos \theta - \cos (2\omega t + \theta)] \quad (7)
\end{aligned}$$

and thus consists of an average component $EI \cos \theta$ and a double frequency component $EI \cos (2\omega t + \theta)$, in which θ is the power factor angle.

The torque, in synchronous watts, is

$$T_{\phi} = \frac{p}{\omega} = \frac{EI \cos \theta}{\omega} - \frac{EI \cos (2\omega t + \theta)}{\omega} \quad (8)$$

Thus the single-phase alternator has an undesirable *double-frequency* component of torque.

Now consider a 3-phase machine having three separate coils $a - a'$, $b - b'$, $c - c'$, displaced in space by 120 degrees, as shown in Fig. 3a. The voltage induced in the three separate coils (or phases) will reach their

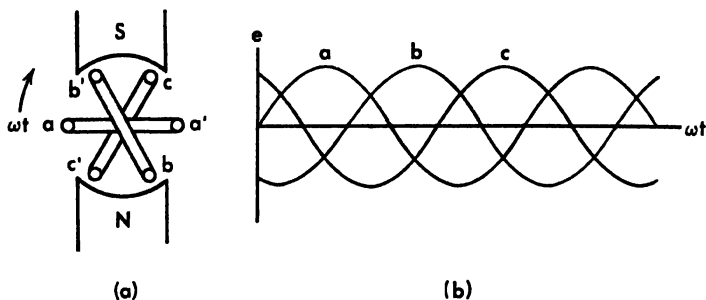


Fig. 3 Elementary three phase alternator

maximum 120 degrees apart in time, as indicated in Fig. 3b. If the loads are balanced, the phase currents will be equal in magnitude, and differ by 120 degrees in time,

$$\left. \begin{aligned} i_a &= I_{\max} \sin (\omega t + \theta) \\ i_b &= I_{\max} \sin (\omega t - 120^\circ + \theta) \\ i_c &= I_{\max} \sin (\omega t - 240^\circ + \theta) \end{aligned} \right\} \quad (9)$$

The current of phase a produces armature reaction in accordance with (6), and this same equation holds for phases b and c if ωt therein is replaced by $(\omega t - 120)$ and $(\omega t - 240)$ respectively. Then the resultant armature reaction is (per pole)

$$\begin{aligned} A &= A_a + A_b + A_c \\ &= 0.4 V I_{\max} \{ 3 \sin \theta + j 3 \cos \theta \} \\ &\quad + [\sin (2\omega t + \theta) + \sin (2\omega t - 240^\circ + \theta) + \sin (2\omega t - 480^\circ + \theta)] \\ &\quad + j [\cos (2\omega t + \theta) + \cos (2\omega t - 240^\circ + \theta) + \cos (2\omega t - 480^\circ + \theta)] \} \\ &= 1.2 V I_{\max} (\sin \theta + j \cos \theta) = A_a + j A_q \end{aligned} \quad (10)$$

since the double frequency terms cancel. This result shows that three-phase armature reaction consists only of constant terms, having three times the magnitude but the *same direction* as for the single-phase machine. Therefore, the above table is equally valid for the three-phase machine if its values are multiplied by 3.

Writing the power Equation (7) for each phase and adding for the total generated power of the machine there results,

$$p = p_a + p_b + p_c$$

$$\begin{aligned}
 P &= EI[\cos \theta - \cos (2\omega t + \theta)] \\
 &\quad + EI[\cos \theta - \cos (2\omega t - 240^\circ + \theta)] \\
 &\quad + EI[\cos \theta - \cos (2\omega t - 480^\circ + \theta)] \\
 &= 3EI \cos \theta
 \end{aligned} \tag{11}$$

since the sum of the double-frequency quantity is zero. Hence the power of a 3-phase alternator, unlike that of the single-phase machine, is constant. Its torque is also constant,

$$T_{3\phi} = \frac{p}{\omega} = \frac{3EI \cos \theta}{\omega} \tag{12}$$

So far only 2-pole machines have been considered. But it is clear that if there are P -poles there will be $P/2$ cycles of voltage or current for each revolution of the armature, and the frequency (alternations per second) will be

$$f = \frac{P}{2} \frac{\text{rpm}}{60} = \frac{P}{2} (\text{rps}) \tag{13}$$

Since there is one complete cycle per pair of poles, it is evident that

$$(\text{electrical angle}) = \frac{P}{2} (\text{mechanical angle}) \tag{14}$$

It remains to develop the vector diagrams for the two cases of non-salient and salient pole machines, as shown in Fig. 4a and 4b respectively.

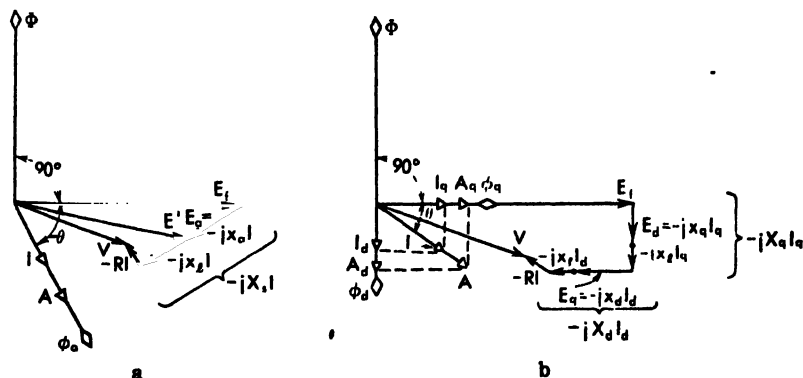


Fig. 4 Vector diagrams of synchronous machines.
(a) round rotor
(b) salient pole

In the case of the non-salient pole machine, the reluctance of the magnetic paths is substantially the same in the direct or quadrature axis.

Referring to Fig. 4a, let the field flux, Φ , Eq. (1), be selected as reference vector and drawn vertically. Then by (2) the induced voltage, E_f , lags the flux by 90 degrees. The current, I , Eq. (4), lags the induced voltage E_f by the angle θ , and in a three-phase machine, Eq. (10), causes a constant magnetomotive force of armature reaction in phase with itself. This magnetomotive-force of armature reaction causes a flux ϕ_a , stationary in space with respect to the field poles, which in turn induces a voltage E_a lagging it by 90 degrees. The two induced voltages E_f (due to the field excitation) and E_a (due to armature reaction) combine vectorially to give the voltage E' . But the terminal voltage of the machine is less than this by the resistance and reactance drops in the winding. The latter is due to the leakage fluxes in the slots, around the end connections, and elsewhere.

$$V = E' - (R + jx_l)I \quad (15)$$

Now the leakage reactance drop $-jx_l I$ is at right angles to the current and proportional thereto, as is the voltage E_a due to armature reaction. It is accordingly customary to introduce a fictitious *reactance of armature reaction*, x_a , such that

$$E_a = -jx_a I \quad (16)$$

and it is perfectly obvious from Fig. 4a that this reactance drop may be combined with the leakage reactance $-jx_l I$ to define a total or *synchronous reactance*

$$X_s = x_l + x_a \quad (17)$$

Now for the salient pole machine the reluctance in the quadrature path is considerably higher than that of the direct path. Therefore, the direct component of armature reaction, $A_d = A \sin \theta$, in line with the poles, causes more flux per ampere than does the quadrature component $A_q = A \cos \theta$. The diagram of Fig. 4b then applies. As before, the field flux Φ induces a voltage E_f lagging it by 90 degrees. The current, I , lagging E_f by an angle θ , produces in phase with itself the armature reaction A . But A has direct and quadrature components A_d and A_q in line and perpendicular to the field poles, and these cause the fluxes ϕ_d and ϕ_q respectively. The corresponding induced voltages E_d and E_q lag ϕ_d and ϕ_q by 90 degrees, and may be accounted for by fictitious *reactances of armature reaction*, x_d and x_q respectively, as

$$\left. \begin{aligned} E_q &= -jx_d I_d \text{ (a quadrature axis voltage)} \\ E_d &= -jx_q I_q \text{ (a direct axis voltage)} \end{aligned} \right\} \quad (18)$$

The leakage reactance drop in the winding is

$$-jx_l I = -jx_l(I_d + I_q) = -jx_l I_d - jx_l I_q \quad (19)$$

hence may be combined with the armature reaction drops to define the *direct* and *quadrature* components of *synchronous reactance*

$$X_d = x_d + x_l$$

$$X_q = x_q + x_l \quad (20)$$

The foregoing analysis of this section has deliberately ignored many refinements in order to present an over-all picture of the principles involved, unencumbered by a mass of details. In subsequent sections of this chapter the analysis will go deeper, but Chapter 3 should be reviewed carefully before proceeding. Finally, in the Appendices, a general harmonic analysis is presented.

Problems

1. Show that I_q is in such a direction as to *oppose* the motion.
2. What trigonometric identities were employed in obtaining the final results in equations (6), (7), (10), and (11)?
3. What would be the effect on the prime mover of the double frequency torque term in (8)? What happened to this term in the case of the three phase generator, (12)?
4. Write equations for a 2-phase machine (two armature coils 90 degrees apart) corresponding to (9), (10), (11), and (12).
5. Write equations for a 6-phase machine (six armature coils 60 degrees apart) corresponding to (9), (10), (11), and (12).
6. Suppose the direction of rotation is reversed (counterclockwise). What, if any, modification would this entail in equations (1) to (12) inclusive, and in Figs. 1 and 2?
7. Suppose an alternator has some residual magnetism in its field, but on exciter. How could this machine be made to provide normal terminal voltage at rated speed? Explain in terms of (a) diagrams, (b) equations.
8. The equations of torque, (8) and (12), were given in terms of *synchronous watts*. Convert them to *lb-ft*.
9. List the rpm of 60-cycle synchronous machines up to 24 poles.
10. Show by means of the equations developed in the text that the vector diagram for the salient pole machine, Fig. 4b, reverts to that for the round rotor, Fig. 4a, if the direct and quadrature components of synchronous reactance are equal.

11 Redraw the vector diagrams of Fig 4 for the case of a leading current

12 A round rotor generator has a leakage reactance of $x_l = 0.15$, an armature reaction reactance of $x_a = 0.75$ and a resistance of $R = 0.05$. The terminal voltage is $V = 1.0$, and the current is $I = 0.80$ at a terminal power factor of $\cos \phi = 0.80$ lagging. All values are in *per unit*. Construct its vector diagram to scale.

13 A salient pole generator has a leakage reactance of $x_l = 0.15$, armature reaction reactances of $x_d = 0.95$ and $x_q = 0.50$ and a resistance of $R = 0.05$. The induced voltage is $E_f = 1.40$ and the angle between the induced voltage and the lagging current $I = 0.80$ is $\theta = 60^\circ$. All values are in *per unit*. Construct the vector diagram. (Note: Had we started with the terminal voltage V , instead of the induced voltage E_f , we would have reached an impasse since the current needs to be resolved into direct and quadrature components with respect to I , whose direction is unknown. The way in which this dilemma is easily resolved will be developed in a subsequent section.)

3 Construction

Synchronous machines may be either the revolving armature (as in d.c. machines) or the revolving field type. The former construction requires the use of slip rings for bringing out the high voltage high current leads and presents a more difficult insulation and mechanical bracing problem. For these reasons it is rarely used except in rotary converters.

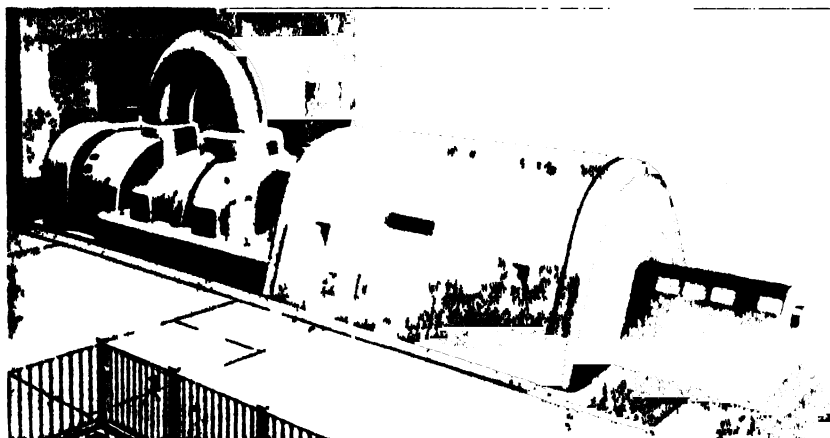


Fig 51: Modern turbo generator showing compound turbine generator and exciter. (Westinghouse Electric Corporation)

There are two types of revolving field synchronous machines: (1) the round rotor and (2) the salient pole.

Round rotor construction is used in turbo alternators and in large

power high speed motors where the diameter of the rotor must be kept small in order to avoid excessive centrifugal forces. Since the diameter is small, the length must be comparatively long to yield the larger outputs. A typical turbo-alternator, in various stages of completion, is shown by the series of illustrations of Fig. 5. Figure 5a shows a moderately large turbo-generator of modern construction with a compound turbine, generator, and exciter. In recent years considerable attention has been devoted to streamlining the exterior of these large machines in an effort to improve their appearance. A cross-section through such a generator is shown in Fig. 5b, which depicts the frame, laminations and the cooling ducts between them, the ends of the armature coils with their leads, rotor with the fan and the slip rings, the water cooling coils,



Fig. 5b Cutaway view of the generator and exciter (Westinghouse Electric Corporation)

and other structural details. It is interesting to note that the active material of such a machine is considerably less than would be surmised from its outside dimensions, the additional space being required for the frame and the cooling ducts. Figure 5c shows the frame and armature stacking of a hydrogen cooled generator. The fabricated construction of the frame should be noted, as contrasted with the cast iron frames of a few years ago. The illustration also shows the radial cooling ducts at intervals along the stacking, and the finger clamps pressing against the teeth at the end of the stacking. A cross section through the arma



Fig. 5c Stator frame and laminations of a hydro gen cooled turbo generator (General Electric Company)

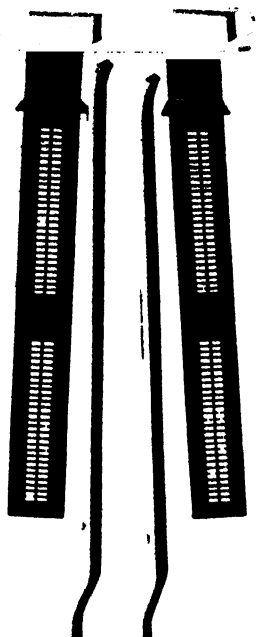


Fig. 5d Cross section through the armature winding showing conductors, slots, slot wedges and spacers for the radial cooling ducts. (Westinghouse Electric Corporation)

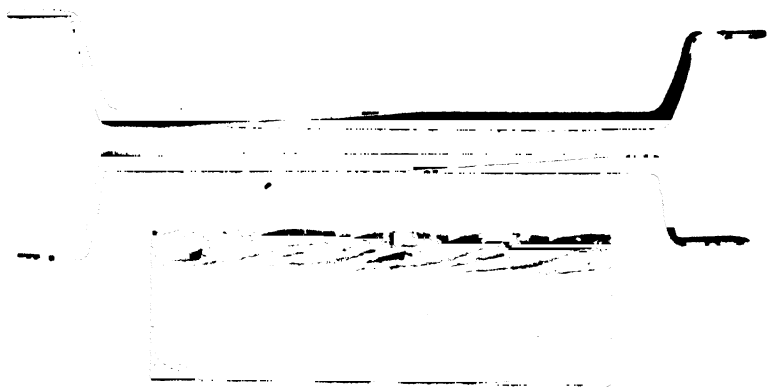


Fig. 5e Insulated armature bars showing transposed conductors (white chalk line shows path of a single conductor) (General Electric Company)



Fig. 51 Completed two pole rotor showing cooling fans, slip rings, and retaining rings. (Westinghouse Electric Corporation)



Fig. 52 Detail of the field winding at the end of the rotor showing one of the leads which goes through the hollow shaft to the slip ring. (Westinghouse Electric Corporation)

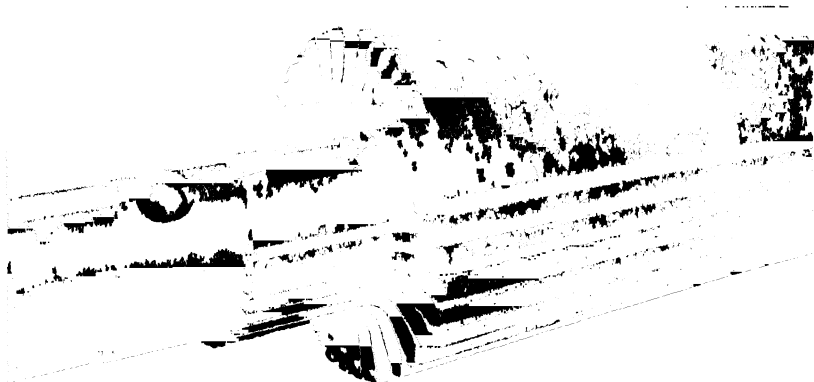


Fig 5h Rotor forging showing slots and ventilating holes (Westinghouse Electric Corporation)

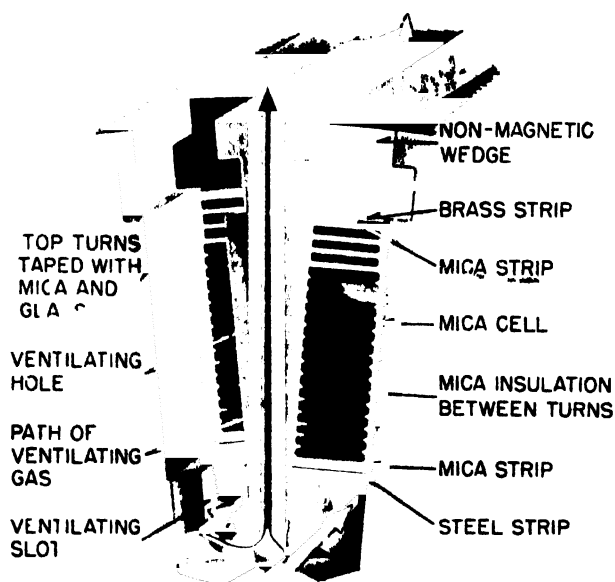


Fig 5i Cross section through the field windings (Westinghouse Electric Corporation)

ture winding, showing the insulated conductors, slots, fiber-slot wedges, and the radial cooling duct separators is shown in Fig. 5d. Figure 5e shows an insulated armature bar with transposed conductors. Large conductors are always made up of a number of strands, insulated from each other, to reduce the eddy-current loss, as well as to permit easy bending. Figure 5f shows a completed 2-pole rotor. The leads connecting the field coils to the slip rings pass through the hollow shaft and are brought out through insulated stubs as shown at the slip ring end of the shaft. The numerous round holes shown in the rotor casing are ventilating ducts. The end windings of the field coils are held in place by retaining rings. Figure 5g shows the retaining ring removed and the manner in which the end turns are arranged. This illustration shows a strap lead disconnected from the radial insulated stub which enters the hollow shaft. The rotor forging is shown in Fig. 5h. Sometimes rotors are built up of steel plates (about 2-inches thick) bolted together, and either bolted to the shaft flanges or keyed to a through shaft. The field windings consist of form-wound bar copper, or strap, insulated by mica tape. A cross-section through a field winding is shown in Fig. 5i. Note the longitudinal ventilating slots and the radial ventilating holes. The windings are held in place in the slots by nonmagnetic wedges.

Salient pole construction is used in waterwheel and engine driven generators, in low speed motors, and in high speed motors of moderate output. The various features of salient pole construction are shown in the series of illustrations of Fig. 6. A cutaway view of a large vertical hydro-electric generator is shown in Fig. 6a. The weight of the rotor is supported by a thrust-bearing mounted on the bracket over the generator, and the shaft is kept centered by the guide bearing just beneath the rotor spider. This machine has both a main and a pilot exciter mounted on the shaft extension above the thrust-bearing. A somewhat different type of construction is used where head space is at a premium. This is the so-called umbrella type construction, shown in Fig. 6b. Here the thrust-bearing is mounted below the spider and the guide bearing is at the top. The arms of the rotor spider slant downward from the hub, hence the name "umbrella type." A typical synchronous motor with salient poles is shown in Fig. 6c. Note the use of structural steel and welding. Only the bearing pedestals are cast. Figure 6d shows the armature of such a machine. Note the clamping plates and the radial cooling ducts along the stacking. Figure 6e shows the armature stacking assembled in the frame. Figure 6f shows the armature coils in the slots, and the manner in which they are assembled. The slot-wedges, which

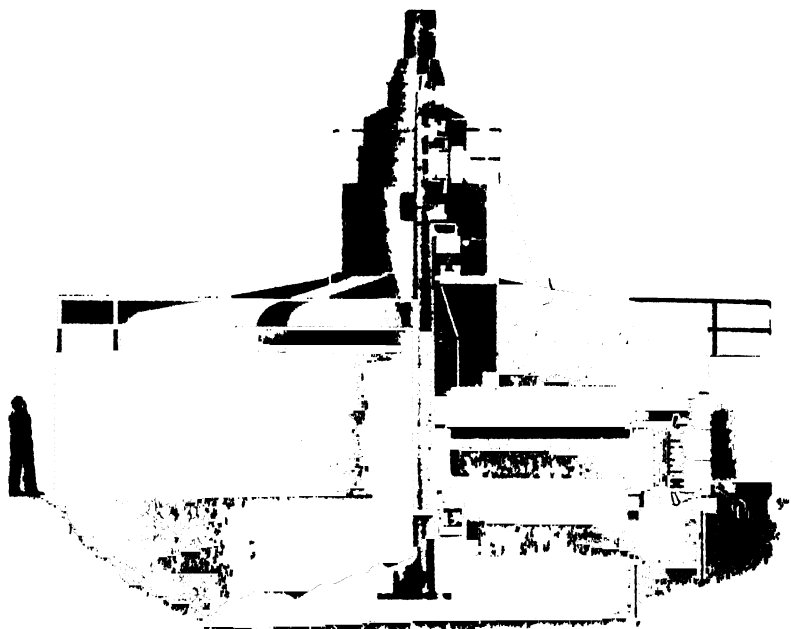


Fig. 6a Cutaway view of a large vertical hydroelectric generator with main and pilot exciter mounted above the thrust bearing. (Westinghouse Electric Corporation)



Fig. 6b Cutaway view of an umbrella type generator. (Westinghouse Electric Corporation)

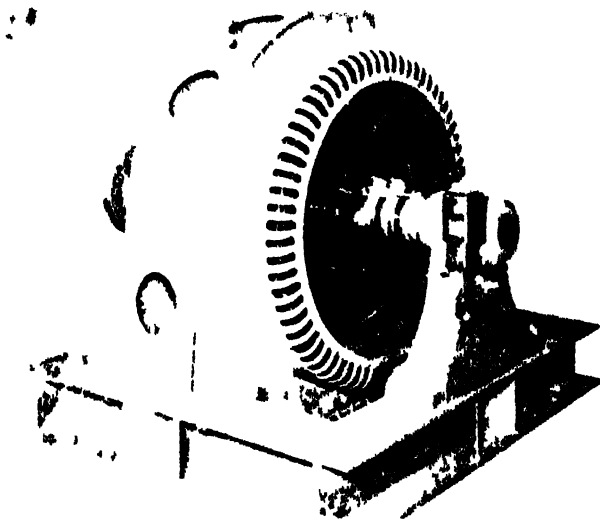


Fig 6/ Synchronous motor 1000113 GE (General Electric Company)

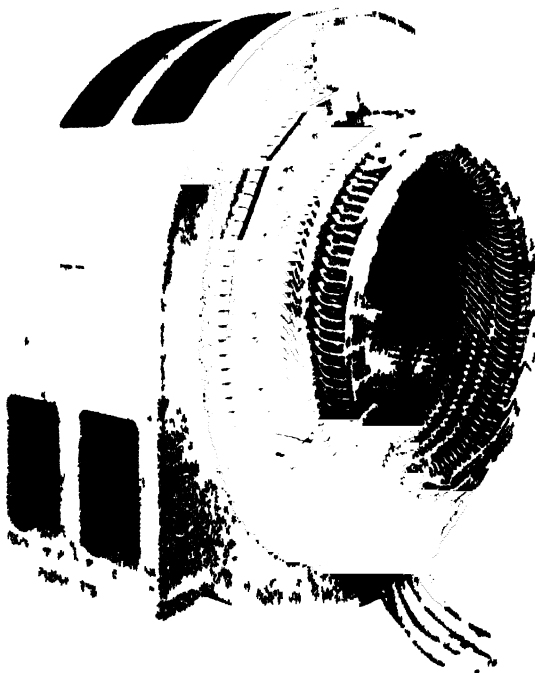


Fig 6/ Synchronous motor 1000113 GE (General Electric Company)



Fig 6a Armature stacking assembled in the frame (Westinghouse Electric Corporation)



Fig 6b Synchronous motor stator windings (General Electric Company)

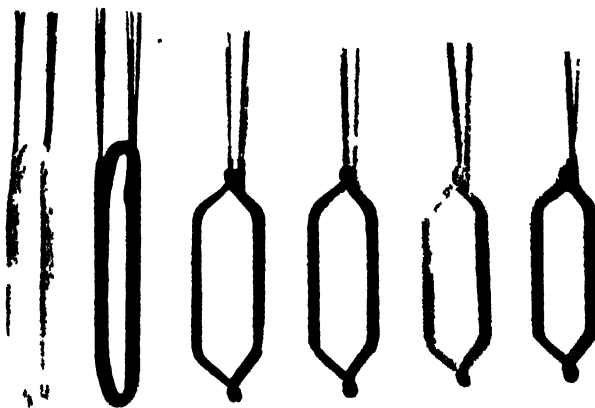


Fig. 6g Steps in winding armature coils (*General Electric Company*)

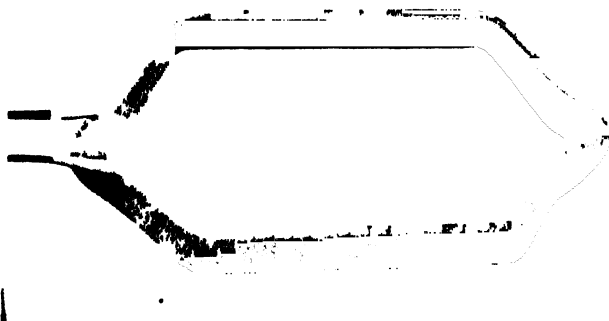


Fig. 6h Completed armature coil (*Westinghouse Electric Corporation*)



Fig. 6f Synchronous motor revolving field showing field poles, keyed starting winding collector rings and shaft. (General Electric Company)

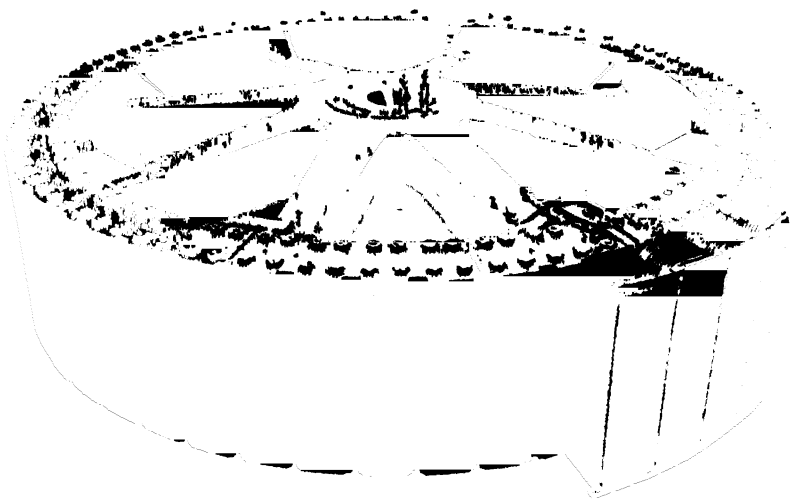


Fig. 6g A large rotor with pole-keyed core stacking (Westinghouse Electric Corporation)

hold the coils in place, are clearly shown. Various steps in the winding of armature coils are depicted in Fig. 6g. This is done, of course, on suitable forms. A completed armature coil is shown in Fig. 6h, which brings out the manner in which the strands are taped and protected by the slot wrappings. Figure 6i shows the revolving field of a synchronous

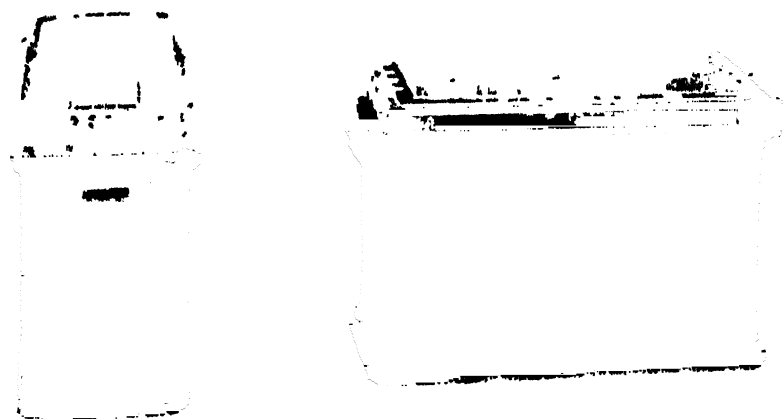


Fig. 6. Field pole with starting winding (General Electric Company)

motor. The field poles are bolted to a ring spider, which in turn is keyed to the shaft. In this machine a squirrel cage starting winding is embedded in the pole faces. For ease of construction the end rings of the starting winding are made up of segments bolted together. Figure 6j illustrates the manner in which the field poles are sometimes keyed to the rotor core, which in turn is keyed to the arms of the rotor spider. The details of a field pole are shown in Fig. 6k, along with the starting winding.

4. Analysis of Synchronous Machines

Under Sec. 2, *Principles of Operation* equations of flux, voltage, current, armature reaction, power, and torque were developed for a simple alternator having full pitch concentrated coils and sinusoidally distributed field flux and components of armature reaction. These equations culminated in the vector diagrams, Fig. 4 for the non salient and salient pole machines. But in actual alternators having fractional pitch distributed windings, and nonsinusoidal distributions of flux, certain modifications must be made in the equations. Identical vector diagrams will result, although some of the constants involved have somewhat different values. The more detailed analysis is based on the general

equations of induced voltage, armature reaction, and reactances given in Chapter 3 and in the Appendices. The analysis will follow the outline:

- (a) Flux distribution due to the field pole excitation
- (b) Armature reaction
- (c) Air gap flux
- (d) Induced voltage
- (e) Reactances
- (f) Vector diagrams
- (g) Excitation and regulation
- (h) Power and torque
- (i) Stability limits
- (j) Mechanical oscillations
- (k) Starting and synchronizing
- (l) Parallel operation
- (m) Circle diagram
- (n) Losses and efficiency

5. Flux Distribution Due to Field Pole Excitation

Figure 7 shows the developed view of a pair of field poles and a slotted armature. The poles are excited by currents in the field coils, F , resulting

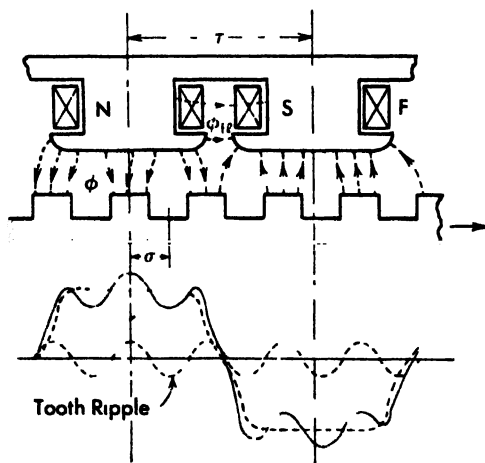


Fig. 7

in a flux distribution such as indicated by the dotted lines and arrow heads

Some of the flux, ϕ_l , called the *field leakage flux*, goes from pole to

pole without entering the armature. Obviously, such field leakage flux is not useful in generating an electromotive force in the armature conductors, but does contribute to the saturation in the pole body, and is therefore undesirable. This flux is also of importance under transient conditions.

The useful flux, ϕ , crosses the air gap and enters the armature. If the armature surface were smooth, the flux density distribution along that surface would also be a smooth curve, determined by the amount of pole tip chamfer and the ratio of pole arc to air gap. It would be symmetrical about the pole axes, and could be represented by the Fourier series

$$\sum \beta_k \cos (2k - 1) \frac{\pi x}{\tau} \quad (21)$$

This distribution is generally flat-top and contains appreciable harmonics besides the fundamental. It is theoretically possible to obtain a pure sinusoid of flux density by the shape and dimensions of the pole face, but it is not practicable to do so.

But the presence of the teeth and slots causes a *tooth ripple* to appear in the flux density wave. If the field were a solid continuous surface, the ripple would simply move along with the armature and not induce any voltage, since it would move with the same speed as the conductors and would not cut them. But the field poles do not present a continuous surface, and as each tooth passes a pole tip its flux is transferred to the next pole, so that the total flux per pole is pulsating at the tooth frequency ($2f_\tau$), where τ is the pole pitch and σ is the tooth pitch. The amount of this pulsation may be determined by making a series of flux plots for different positions of the armature and finding the total flux for each position. The tooth pulsation may be represented by

$$\Delta \beta \cos \left(\frac{2\tau}{\sigma} \omega t \right) = \Delta \beta \cos \omega' t \quad (22)$$

6. Armature Reaction

Equation (32), Sec. 4, Chap. 3, gives the k th space harmonic of armature reaction for a 3-phase (120-degree phase belts) fractional pitch, distributed winding supplied with balanced 3 phase currents and running at any speed ω_n . For a synchronous machine, $\omega_n = \omega$.

If the armature currents are given by (9), the k th harmonic of armature reaction is (per pole)

$$A_k(x) = 1.2 \frac{K_A}{k} q N I_{\max} \left\{ \sin \left[(1 - k') \omega t + \theta + \frac{k' \pi x}{\tau} \right] + \sin \left[(1 + k'') \omega t + \theta - \frac{k'' \pi x}{\tau} \right] \right\} \quad (23)$$

in which

k' is any harmonic for which $(k' - 1)$ is a multiple of 3

k'' is any harmonic for which $(k'' + 1)$ is a multiple of 3

Space harmonics are important in determining the air-gap reactance (see Appendix IV); but otherwise are relatively unimportant and do not influence the characteristics of the machine appreciably. Thus the k th harmonic is only $1/k$ th the magnitude of the fundamental, for a full pitch concentrated winding, and is further reduced by the winding harmonic reduction factor K_f . For our present purposes only the fundamental of (23) need be considered. Putting $k = 1$

$$A_1(x) = 1.2K_f q N I_{max} \sin \left(\theta + \frac{\pi x}{\tau} \right) \quad (24)$$

in which x is measured from an arbitrary stationary reference axis (with respect to the field). Let this reference axis be taken as the center line of the S pole.

Expanding this expression and putting

$$\begin{aligned} I_d &= I_{max} \sin \theta = \text{direct component of current} \\ I_q &= I_{max} \cos \theta = \text{quadrature component of current} \end{aligned} \quad (25)$$

there results

$$A_1(x) = 1.2qK_f N \left(I_d \cos \frac{\pi x}{\tau} + I_q \sin \frac{\pi x}{\tau} \right) = A_d \cos \frac{\pi x}{\tau} + A_q \sin \frac{\pi x}{\tau} \quad (26)$$

Except for the winding factor K_f this equation is the same as the previously derived (10). It shows that the armature reaction due to the *direct* component of current, I_d , is sinusoidally distributed in space, centered on the polar or direct axis, and *opposes* the field magnetomotive force (for $-\theta$), Fig. 8. On the other hand, the armature reaction due to the quadrature component of current, I_q , is sinusoidally distributed in space and is centered on the interpolar or quadrature axis.

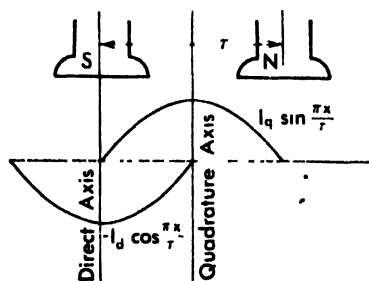


Fig. 8

This quadrature component of armature reaction thus will build up flux in the quadrature axis.

The resolution of the armature reaction into two components in line and quadrature with the field poles, and an analysis of the consequences,

was first proposed by the French engineer Blondel. Subsequently the idea was extended by Doherty and Nickle to include the effects of space harmonics. Their rigorous analysis leads to precise definitions of direct and quadrature synchronous reactances and to specific directions for resolving these synchronous reactances into armature reaction and leakage reactance components. A somewhat more compact analysis, based on the Doherty and Nickle analysis, but relying entirely on mathematical procedure rather than physical concepts, and including both space and time harmonics, is given in the Appendices.

At unity power factor, $\theta = 0$, there is by (25) only a quadrature component, I_q , of armature current, and by (26) the armature reaction is entirely in the quadrature axis. At zero power factor lagging, $\theta = -90$ degrees, there is by (25) only a direct component, I_d , of armature current, and by (26) the armature reaction is entirely in the direct axis and *opposing* the field flux. At zero power factor leading, $\theta = +90$ degrees, there is by (25) only a direct component, I_d , of armature current, and by (26) the armature reaction is entirely in the direct axis and *assisting* the field flux.

These three cases and space vector diagrams are illustrated in Fig. 9.

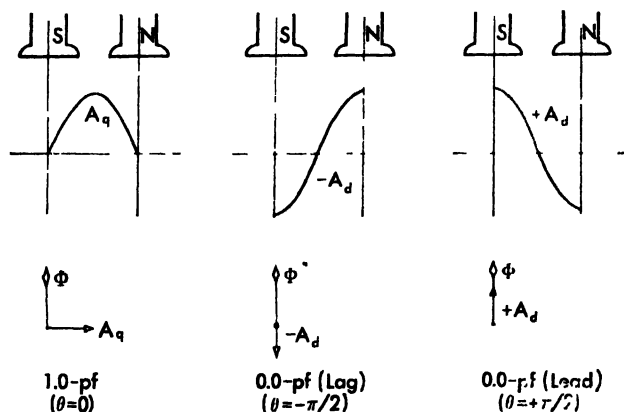


Fig. 9 Effect of power factor on armature reaction

Problems

1. List all the space harmonics up to the 21st which contribute to 3-phase armature reaction, and give their magnitudes, velocities, and direction of rotation with respect to both the armature and the field.
2. Write the equation for the fundamental of armature reaction for an alter-

nator on short circuit (neglecting its resistance). Draw the vector diagram showing relationship, in both phase and magnitude, of the armature reaction with respect to the field magnetomotive force.

3. A 3-phase alternator, with 120-degree phase belts, has 3 slots per phase belt, 8 turns per coil, 0.889 coil pitch, and is carrying a current of 120 amperes per coil at a lagging angle $\theta = -60$ degrees. What are its direct and quadrature components of armature reaction? Show a vector diagram.

4. In the above machine, what are the 3rd, 5th, and 7th space harmonics of armature reaction?

7. Flux Distribution Due to Armature Reaction

The flux distribution due to the field pole excitation is given in Sec. 5. Armature reaction by itself will also produce flux in the air gap, and in general this flux distribution will be different, depending on whether a

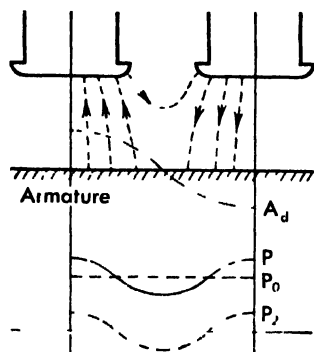


Fig. 10

direct or quadrature component of armature reaction is responsible for it. Figure 10 shows a direct axis, fundamental component of armature reaction producing flux in the air gap. It is possible to make a field flux plot* and determine the flux density at each point along the armature surface. The density at any point divided by the armature magnetomotive force at that point is the permeance there. Thus a permeance curve, Fig. 10, can be plotted. Such curves consist of a constant term

and even harmonics, of which the second dominates. Furthermore, the permeance curve is essentially the same for either a direct or quadrature component of armature reaction. To a good approximation it may be represented by only the first two terms of its Fourier series,

$$P(x) = P_0 + P_2 \cos \frac{2\pi x}{\tau} \quad (27)$$

Then if the armature reaction is

$$A_1(x) = A_d \cos \frac{\pi x}{\tau} + A_q \sin \frac{\pi x}{\tau} \quad (28)$$

* Bewley, L. V., *Two dimensional Fields in Electrical Engineering*, The Macmillan Co., 1948.

the flux density is

$$\begin{aligned} \beta_a &= \left(P_0 + P_2 \cos \frac{2\pi x}{\tau} \right) \left(A_d \cos \frac{\pi x}{\tau} + A_q \sin \frac{\pi x}{\tau} \right) \\ &= \left(P_0 + \frac{P_2}{2} \right) A_d \cos \frac{\pi x}{\tau} + \left(P_0 - \frac{P_2}{2} \right) A_q \sin \frac{\pi x}{\tau} \\ &\quad + \frac{P_2}{2} \left(A_d \cos \frac{3\pi x}{\tau} + A_q \sin \frac{3\pi x}{\tau} \right) \end{aligned} \quad (29)$$

Thus the second harmonic in the permeance causes a third harmonic in the flux density. The fundamental permeance of the direct path is $P_2/2$ greater than the average permeance P_0 , while that in the quadrature path is $P_2/2$ less than the average. For a uniform air gap $P_2 = 0$. (See the Appendices for a more general analysis.)

In an unsaturated machine, the field flux density, (21), and the armature reaction flux density, (29), may be added. But this is not possible in a saturated machine. In that case it is first necessary to combine the field and direct (fundamental) component of armature reaction to find the resultant magnetomotive force and from this resultant determine the flux from the saturation curve. However, except in the teeth, there is little saturation in the quadrature axis, and it is customary to assume no saturation in that axis.

The space vector diagram for lagging power factor is shown in Fig. 11. The current I is at an angle $-\theta$ from the quadrature axis, and has direct and quadrature components $-I_d$ and I_q respectively. These currents produce fundamentals of armature reaction $-A_d$ and A_q , respectively. The former opposes the field magnetomotive force, F , and the resultant $(F - A_d)$ is responsible for the direct axis pole flux ϕ_d . The quadrature component A_q , acting on the interpolar path, produces the quadrature axis flux ϕ_q .

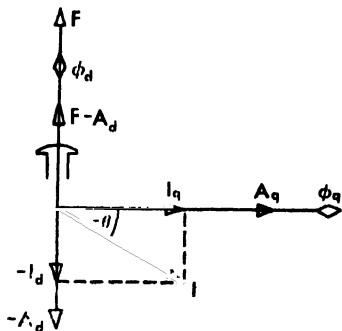


Fig. 11

Problems

1. For $F = 1$ and $A = 0.50$ draw to scale the vector diagrams for the following cases:

- (a) $\theta = 0$, (b) $\theta = 90^\circ$, (c) $\theta = -90^\circ$, (d) $\theta = 45^\circ$, (e) $\theta = -45^\circ$

In each case note whether armature reaction opposes or assists the field.

2. Draw a curve showing the ratio of the quadrature to the direct permeance, as the second harmonic varies from zero to 50 per cent of the constant term

8. Induced Voltage

The total fundamental flux density in an unsaturated machine is the sum of that due to the field, (21), and that due to armature reaction, (29). With respect to the center line through the S -pole, this is

$$\begin{aligned}\beta(x) &= \beta_1 \cos \frac{\pi x}{\tau} + \left(P_0 + \frac{P_2}{2}\right) A_d \cos \frac{\pi x}{\tau} + \left(P_0 - \frac{P_2}{2}\right) A_q \sin \frac{\pi x}{\tau} \\ &= \beta_1 \sin \left(\frac{\pi x}{\tau} + \frac{\pi}{2}\right) + \left(P_0 + \frac{P_2}{2}\right) A_d \sin \left(\frac{\pi x}{\tau} + \frac{\pi}{2}\right) \\ &\quad + \left(P_0 - \frac{P_2}{2}\right) A_q \sin \frac{\pi x}{\tau} \quad (30)\end{aligned}$$

Now each of the three terms of (30) is in the same form as (Chap. 3, Eq. 2), and since neither their amplitudes nor their phase angles are functions of time, it follows that (Chap. 3, Eq. 18) will contain induced voltage terms due only to the synchronous speed of the conductors,

$$\frac{\pi}{\tau} \frac{dx_0}{dt} = \omega$$

For a coil group of q coils whose center is at

$$\frac{\pi}{\tau} x_0 = \omega t$$

and taking skew, (Chap. 3, Sec. 10), and distribution, (Chap. 3, Eq. 17), into account, the fundamental induced voltage of the coil group becomes (Chap. 3, Eq. 18)

$$e_1 = \frac{qN}{10^8} K_{s1} K_{p1} K_{d1} \omega [\phi_1 \sin \omega t + \phi_d \sin \omega t - \phi_q \cos \omega t] \quad (31)$$

in which

q = coils per group

N = turns per coil

K_{s1} = skew factor for the fundamental

K_{p1} = pitch factor for the fundamental

K_{d1} = distribution factor for the fundamental

$\phi_1 = \frac{2}{\pi} \tau l \beta_1$ = field flux per pole

$\phi_d = \frac{2}{\pi} \tau l \left(P_0 + \frac{P_2}{2}\right) A_d$ = direct axis armature reaction flux

$$\phi_q = \frac{2}{\pi} \tau l \left(P_0 - \frac{P_2}{2} \right) A_q = \text{quadrature axis armature reaction flux}$$

$$\omega = 2\pi f = \text{synchronous speed}$$

This equation, together with (30), clearly shows:

- (1) The induced voltage due to the field flux reaches a maximum at $\omega t = \pi/2$, that is 90 degrees later in time than when the coil group was centered on the pole.
- (2) The direct component of armature reaction develops a flux in space phase with the field flux (assisting or opposing it, depending on whether the power factor angle is leading or lagging), and its induced voltage is 90 degrees later in time than when the coil is centered on this flux.
- (3) The quadrature component of armature reaction develops a flux ahead of the field flux by 90 degrees in space, and its induced voltage does not reach a maximum until $\omega t = \pi$.

Now ϕ_d is proportional to I_d and ϕ_q is proportional to I_q , and the voltage due to them may be accounted for by proportionality factors x_d and x_q , so that (31) may be contracted to

$$e_1 = E_f \sin \omega t + x_d I_d \sin \omega t - x_q I_q \cos \omega t \quad (32)$$

This equation gives the fundamental induced voltage due to the space fundamentals of flux. It shows that the field voltage and direct component of armature reaction voltage are in phase, and that the quad-

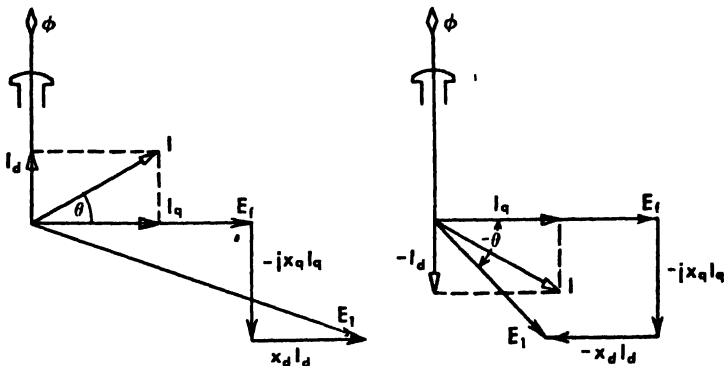


Fig. 12

ature component of armature reaction voltage is lagging by 90 degrees. These voltages may therefore be superimposed on the vector diagram of Fig. 11 as shown in Fig. 12 for $+\theta$ and $-\theta$.

Taking the quadrature axis as reference vector, and using rms values, the vector equations are

$$I = I_q + jI_d \quad (33)$$

$$E_1 = E_f + x_d I_d - jx_q I_q \quad (34)$$

9. Reactances

The reactances of rotating machines in general have been discussed in Chapter 3. The slot leakage and end turn reactance of a synchronous machine presents nothing new. But the air gap reactances of synchronous machines, particularly those with salient poles, needs further discussion. A complete harmonic analysis of the air gap fluxes and the voltages which they induce is very involved (see Appendix IV). From such an analysis it is possible to segregate out all those space harmonics of flux which induce time fundamentals of voltage, and the total voltage thus induced may be attributed to armature reaction. However, designers prefer to make a further subdivision which will segregate the slot harmonics from the others, so that the effects of design changes can be detected more easily. From a harmonic analysis point of view, this amounts to:

- (1) Designating the fundamental induced voltage due to the space fundamentals of armature reaction as *armature reaction reluctance voltages*.
- (2) Designating the fundamental induced voltage due to all other space harmonics of armature reaction as *differential leakage reluctance voltage*.

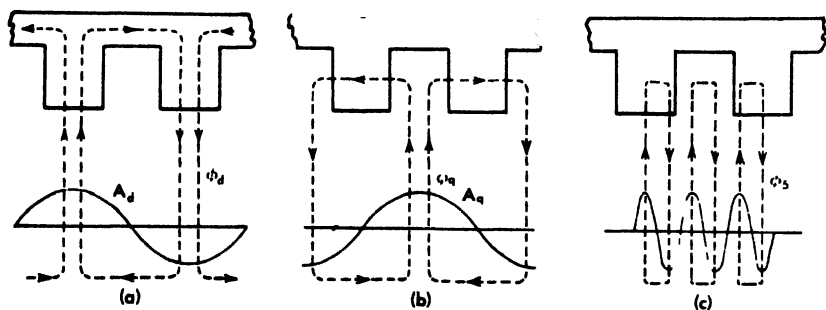


Fig. 13 Flux distribution due to direct, quadrature, and 5th harmonic of armature reaction.

A physical idea of the significance of the above segregation may be obtained from Fig. 13.

In Fig. 13(a) there is shown a space fundamental of direct armature reaction producing a flux ϕ_d which links the field coils, and which is therefore pure armature reaction; and the voltage which it induces is appropriately armature reaction voltage.

In Fig. 13(b) is shown a space fundamental of quadrature armature reaction producing a flux ϕ_q , which in effect establishes a set of quadrature field poles; and therefore the voltage which it induces is appropriately armature reaction voltage.

In Fig. 13(c) is shown a 5th space harmonic of armature reaction. But as shown in Appendix II, this 5th space harmonic does not remain stationary, but revolves at 1.5 synchronous speed (with respect to the armature) and induces a fundamental voltage. It is clear from Fig. 13(c) that its flux does not link with the field coils; and the voltages due to it are therefore appropriately leakage reactance voltages. The same argument applies to any other space harmonic which induces a fundamental voltage.

There are still other space harmonics of armature reaction which induce time harmonics of voltage, but these are not fundamental frequency effects and contribute nothing to normal frequency reactances.

The flux ϕ_q must be less per ampere-turn of armature reaction than ϕ_d , since the reluctance of the quadrature axis path is more than that of the direct axis path. Therefore $x_q < x_d$. In an unsaturated salient pole machine the range is approximately ($0.30 < x_q/x_d < 1.00$). But these synchronous reactances include both armature reaction and leakage reactances.

The leakage reactances in the two paths are not much different, and are usually taken as equal. The leakage reactance is

$$x_l = x_{\text{slot}} + x_{\text{end turns}} + x_{\text{differential}} \quad (35)$$

and what little difference exists is due to difference in the last term. The voltage due to it is

$$-jx_l I = -jx_l(I_q + jI_d) = x_l I_d - jx_l I_q \quad (36)$$

The unsaturated synchronous reactance X_d could be obtained by operating the machine at low voltage and 0-pf (hence $I = I_d$), and measuring phase voltages and currents. The saturated values require a more involved procedure which is discussed in Sec. 11 of this chapter.

A method of obtaining the unsaturated synchronous reactances is to drive the machine at slightly less than synchronous speed, with the field circuit open, and reduced balanced polyphase voltage applied to the

armature, and measure the armature voltage and current and the field voltage, Fig. 14. As the armature revolves at slip frequency with respect to the poles, the phase being measured is centered alternately on the direct and quadrature axis, and the reactance is therefore varying between the two extremes

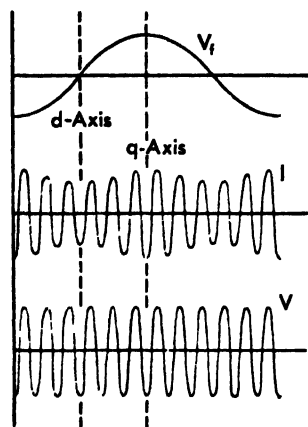


Fig. 14

$$X_d = \frac{\text{maximum voltage}}{\text{minimum current}}$$

$$X_q = \frac{\text{minimum voltage}}{\text{maximum current}}$$

The field voltage serves as an additional check, since it is zero for the X_d measurement. If the applied voltage is not constant (being influenced by the current), it is better to take oscillograms, as shown in Fig. 14.

Fig. 14.

10. Vector Diagrams of Synchronous Machines

The previously derived equations from which the complete vector diagram of the salient pole synchronous machine may be constructed (with the quadrature axis as reference vector) are:

$$I = I_q + jI_d \text{ armature current} \quad (37)$$

$$A = A_q + jA_d \text{ armature reaction} \quad (38)$$

$$F = 0 + jF \text{ field mmf} \quad (39)$$

$$\phi = 0 + j\phi \text{ flux in direct axis} \quad (40)$$

$$E_1 = E_f + x_d I_d - jx_q I_q \text{ induced voltage} \quad (41)$$

$$jx_l I = jx_l(I_q + jI_d) \text{ leakage reactance drops} \quad (42)$$

The terminal voltage, V , is the induced voltage less the leakage reactance and the armature resistance drops

$$\begin{aligned} V &= E_1 - jx_l I - RI \\ &= E_f + (x_d + x_l)I_d - j(x_q + x_l)I_q - RI \\ &= E_f + X_d I_d - jX_q I_q - R(I_q + jI_d) \end{aligned} \quad (43)$$

in which the exactly similar roles of the armature reaction coefficients and the leakage reactances allow us to define

$$\left. \begin{aligned} X_d &= x_d + x_l = \text{direct axis synchronous reactance} \\ X_q &= x_q + x_l = \text{quadrature axis synchronous reactance} \end{aligned} \right\} \quad (44)$$

For a round rotor machine $X_s = X_d = X_q$ and (43) reduces to

$$V = E_f - jX_s(I_q + jI_d) - RI = E_f - (R + jX_s)I \quad (45)$$

The vector diagrams for the salient pole and round rotor machines are then constructed as shown in Fig. 15(a) and (b) respectively for a lagging current ($\theta = -45^\circ$ and therefore I_d is negative).

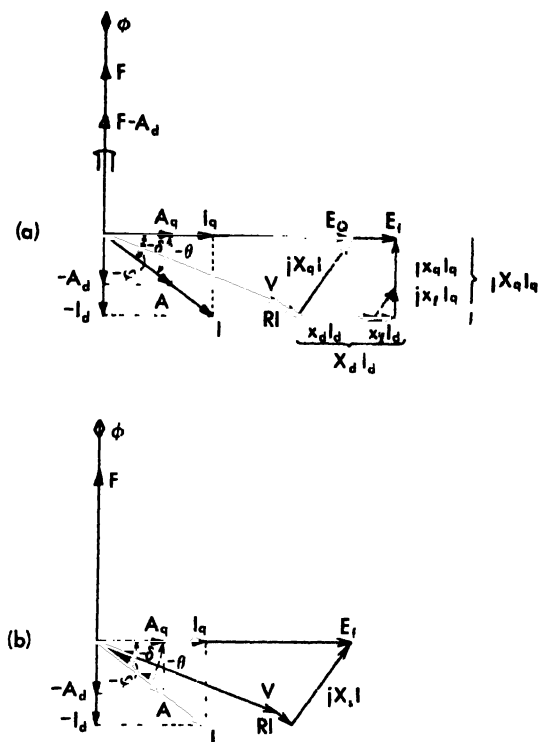


Fig. 15 Vector diagrams for
a. salient poles
b. round rotor

In the salient pole machine diagram the direct axis is symbolized by a field pole with magnetomotive force F . The direct axis component of current, I_d , opposes the field magnetomotive force, so that the resultant direct axis magnetomotive force is $(F - A_d)$ producing the main flux ϕ . This flux induces a voltage E_f which reaches its maximum when the phase is centered on the quadrature axis, that is 90 degrees later in time. This voltage, therefore, appears on the vector diagram lagging the flux by 90 degrees. The armature current, I , is shown lagging E_f by the angle

$\theta = 45$ degrees, and having components I_d and I_q in the direct and quadrature axis. Each of these currents produces a corresponding component of armature reaction, A_d and A_q respectively. The terminal voltage, V , is less than the induced voltage by the resistance drop RI and the synchronous reactance drops $jX_q I_q$ and $X_d I_d$, in accordance with (43). If desired, the resistance drop may be resolved into components RI_q and jRI_d , and the synchronous reactance drops split into their armature reaction and leakage reactance portions, as indicated on the diagram.

But usually it is required to construct the diagram given the terminal voltage V , armature current I , and power factor angle ϕ . The procedure then is:

- (1) Use $V = V + j0$ as reference vector (horizontal)
- (2) Construct $I = I \angle \phi$ at an angle ϕ from V
- (3) Add the RI drop in phase with I
- (4) Add the drop $jX_q I$ leading I by 90 degrees, thus locating the voltage E_q on the quadrature axis. That this construction locates the quadrature axis is easily seen by noting that the component of $jX_q I$ orthogonal to the quadrature axis is $jX_q I_q$, since the former is perpendicular to I and the latter to I_q .
- (5) With the quadrature axis located, find the current projections I_q and I_d .
- (6) Complete the diagram with the $X_d I_d$ and $jX_q I_q$ voltage drops.

$$\text{The voltage} \quad E_t = V + (R + jx_l)I \quad (46)$$

is called the voltage behind the leakage impedance.

$$\begin{aligned} \text{The voltage} \quad E_q &= V + (R + jX_q)I \\ &= V + RI + jx_l I + jx_q I \\ &= E_t + jx_q I \end{aligned} \quad (47)$$

is called the *voltage behind the quadrature impedance*. It is of importance in calculating the transfer of power, as well as in the construction of the vector diagram.

From (43) and (47)

$$\begin{aligned} E_t - E_q &= (V - X_d I_d + jX_q I_q + RI) - (V + RI + jX_q I) \\ &= -X_d I_d + jX_q I_q - jX_q (I_q + jI_d) \\ &= -(X_d - X_q)I_d \end{aligned} \quad (48)$$

The reader should verify this geometrically from the vector diagram. For a round rotor machine $X_d = X_q$ and this term vanishes.

The angle δ between the terminal voltage and the quadrature axis is called the *torque angle*. It is of great importance in connection with the power transfer, stability, hunting, and other characteristics of machines. From the vector diagram of Fig. 15

$$\delta = \theta - \phi \quad (49)$$

$$I_d = I \sin (\delta + \phi) \quad (50)$$

$$I_q = I \cos (\delta + \phi) \quad (51)$$

$$V \sin \delta = X_q I_q - R I_d \quad (52)$$

Substituting (50) and (51) in (52)

$$\begin{aligned} V \sin \delta &= X_q I \cos (\delta + \phi) - R I \sin (\delta + \phi) \\ &= (X_q I \cos \phi - R I \sin \phi) \cos \delta - (X_q I \sin \phi + R I \cos \phi) \sin \delta \end{aligned}$$

from which, upon dividing through by $\cos \delta$ and rearranging

$$\tan \delta = \frac{(X_q \cos \phi - R \sin \phi) I}{V + (X_q \sin \phi + R \cos \phi) I} \quad (53)$$

This equation gives the torque angle for any load current, I , and power factor angle, ϕ . The angle is independent of the direct axis synchronous impedance.

Also from the vector diagram

$$\begin{aligned} E_f &= V \cos \delta + R I_q + X_d I_d \\ &= V \cos \delta + R I \cos (\delta + \phi) + X_d I \sin (\delta + \phi) \end{aligned} \quad (54)$$

Thus with δ known from (53) the induced voltage for an unsaturated machine may be found from (54).

The vector diagram for the round rotor machine, Fig. 15b, is considerably simpler. It can be constructed directly from (45), or reduced from the salient pole diagram by making $X_q = X_d = X_s$. The construction procedure is completed by the first four items of those listed for a salient pole machine.

A synchronous machine may operate as:

1. A generator, if the torque angle is positive
2. A motor, if the torque angle is negative
3. A synchronous condenser, if the torque angle is zero.

Thus the same identical machine may be generator, motor, or condenser, depending upon whether it is delivering power to the line, taking power from the line, or merely floating on the line and providing only reactive (lagging or leading) kva. Moreover, by changing the excitation of

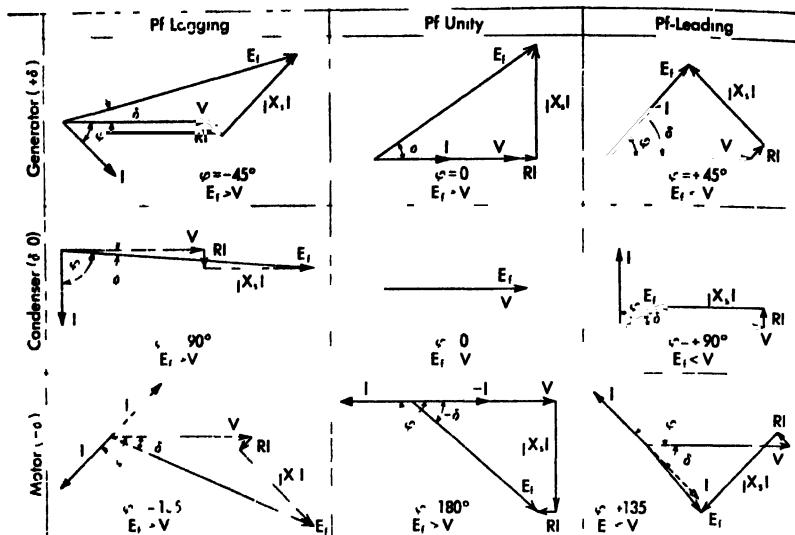


Fig. 16 Vector diagrams for round rotor machine

a motor or condenser it can be made to take a leading or lagging current. These possibilities are shown in Fig. 16 for a round rotor machine and in Fig. 17 for a salient pole machine, where power factor angles are shown at 45 degree intervals. In these diagrams the current is

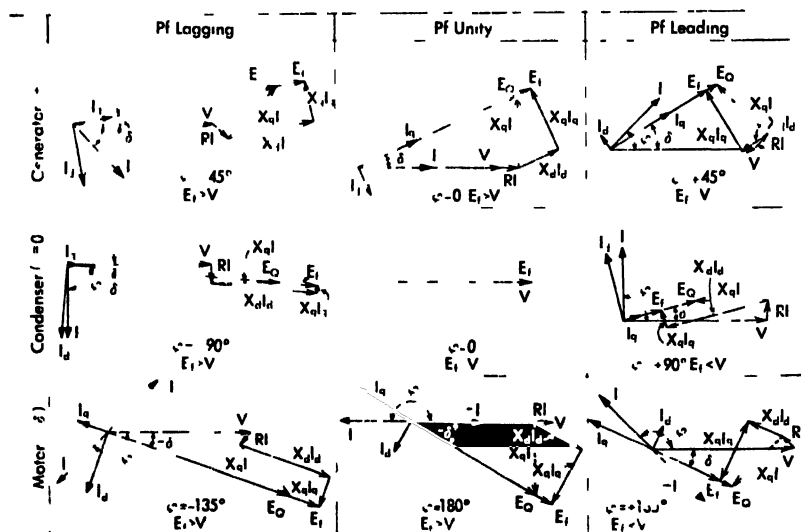


Fig. 17 Vector diagrams for salient pole machine

output current from the machine to the bus. *Input* current is the negative of output current, as indicated in the motor diagrams. (The student will do well to construct the diagrams of Fig. 16 and Fig. 17 without recourse to the text; for when he can do this he is approaching a real understanding of synchronous machines.) It is important to note that there need not be separate theories for generator, motor, and condenser. Positive torque angle means generator action; negative torque angle means motor action; and zero torque angle means synchronous condenser action. An over excited machine operating on a fixed voltage bus will supply a lagging current as a generator or draw a leading current as a motor.

Synchronous condensers are simply synchronous machines not intended for power purposes, but specially designed so as to be able to deliver large amounts of lagging or leading reactive kva for the regulation of transmission lines. During periods of light loads on the transmission line the receiver voltage tends to rise above normal due to the leading current taken by the shunt capacitance of the line. At such periods the synchronous condenser is operated under excited and draws lagging kva sufficient to reduce the line voltage to normal. Conversely, during periods of heavy load the synchronous condenser is operated over excited and draws leading kva sufficient to maintain the line voltage. Synchronous condensers must, therefore, be designed to have a much wider operating range of reactive kva than generators or motors, and this calls for a more liberal field design. The direct component of synchronous reactance, X_d , of a synchronous condenser is usually from 50 to 100 per cent higher than for motors or generators. Sometimes a turbo generator, when not required to deliver power, is kept floating on the line and operated as a synchronous condenser for the purpose of supplying reactive kva for line regulation or power factor correction.

In many industrial applications synchronous motors are selected in preference to induction motors because they can supply corrective (leading) kva to compensate for the poor power factor of other apparatus in the plant.

Problems

1. The current and voltage equations for Fig. 15 may be written:

$$I = I_q + I_d$$

$$E_f = V + RI + jX_d I_d + jX_q I_q$$

Rearrange the voltage equation in the two forms

$$\begin{aligned} E_f &= V + RI + j(X_d - X_q)I_d + jX_q I \\ &= V + RI + jX_d I - j(X_d - X_q)I_q \end{aligned}$$

and interpret each of these on the vector diagram. Verify the equations from the geometry of the diagram.

2. Since the voltage equation for a generator is applicable to a motor by reversing the current, show that the motor equation may be written as

$$V = E_f + RI + jX_d I_d + jX_q I_q$$

which is identical with the generator equation if the roles of V and E_f are interchanged. From this point of view, what changes should be made in the motor diagrams of Fig. 17?

3. A synchronous machine has the following constants (on a per-unit basis): $V = 1$, $I = 0.8$ at 0.80 pf (lagging), $x_d = 0.70$, $x_q = 0.40$, $x_l = 0.15$, $R = 0.05$.

(a) What is the torque angle, δ ? (b) Construct the vector diagram with E_f as reference vector (horizontal), without making use of the procedure described in the text. (c) Construct the vector diagram with V as reference vector (horizontal), making use of the procedure described in the text. (d) Repeat the above for 0.8 pf (leading).

4. The constants of a round rotor and of a salient pole machine are identical except that for the latter $X_q < X_d$. Which will have the greater torque angle for given terminal conditions?

5. Prove that the equations and vector diagrams for the salient pole machine reduce to those for the round rotor machine when $X_q = X_d$.

11. Regulation and Excitation of an Alternator

Regulation is defined as the per cent increase in voltage when the load is removed, speed and field excitation remaining constant, that is

$$\text{Per cent Regulation} = 100 \frac{E_f - V}{V} \quad (55)$$

in which V is the rated terminal voltage and E_f the no-load voltage at the same speed and excitation. The difference in voltage is due to the internal impedances of the machine, and these comprise: (a) armature resistance as modified by skin effect and stray loss, (b) the true leakage reactances due to flux in the slots, around the end turns and harmonic fluxes in the air gap, and (c) armature reaction. The calculation of the excitation voltage from the terminal conditions is greatly complicated by saturation effects. The problem is further aggravated by the fact that the degree of saturation in some parts of the magnetic circuit (*i.e.*, the field pole) is not the same as in other parts (*i.e.*, the armature), because the fluxes in the two parts differ by the amount of certain leakage fluxes. Moreover, in salient pole construction, the degree of saturation in the direct and quadrature paths is quite different.

There are three basic methods (with numerous minor variations) for computing the excitation voltage from the terminal conditions:

1. The *electromotive force method*, in which armature reaction is accounted for in the fictitious synchronous impedance voltage drops. This method gives results which are invariably too high, hence is often called the *pessimistic method*. It has the advantage of simplicity and of requiring a minimum of test data. The old (prior to 1936) AIEE standard was a modification of this method.

2. The *magnetomotive force method* in which the leakage reactance effects are lumped with the armature reaction. This method gives results which are invariably too low, hence is often called the *optimistic method*. It is more complicated than the electromotive force method. The present ASA standard is a modification of this method.

3. The *general method* in which leakage reactance drops are treated as voltages, and armature reactions as magnetomotive forces. It is the most rational and reliable of the three methods, but requires additional test or design data. Extensions of this method take into account the different degrees of saturation found in different parts of the machine. It is the only feasible method for use with salient pole machines.

Load Characteristics

As a preliminary to the detailed discussion of the above methods it is advisable to define the several kinds of characteristics which enter into the computations. These are shown on Fig. 18. The curve OC is the *open circuit saturation curve*, and shows how the voltage varies with the field current. Its lower portion is practically straight, so that at low saturation the voltage is a linear function of the field current. The continuation of this straight portion is the *air gap line*, OG . At zero power factor and a fixed armature current the characteristic becomes the *zero power factor curve*, AB . Under this condition a field current OA is required to circulate the prescribed armature current when

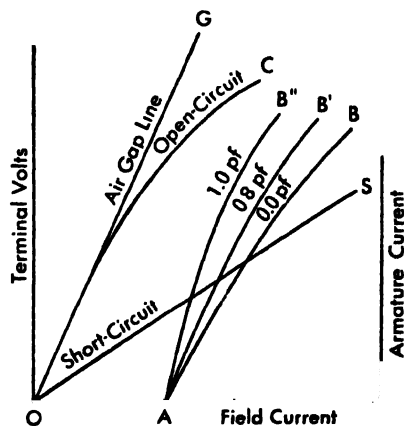


Fig. 18

the voltage reduces to zero (short-circuit). At any other power factor and armature current the characteristic takes up some position AB' , AB'' , etc. intermediate between the open-circuit and zero power characteristic, but

all such characteristics originate at a field current OA when the voltage is zero, since then the machine is short-circuited. The line OS is the *short-circuit* characteristic, and shows how the short-circuited armature current varies with the field excitation. Under short-circuit the whole of the induced voltage is consumed by the armature resistance and leakage reactance, and since this impedance is small, its voltage drop is only a fraction of the rated voltage; so that the net flux in the machine is below normal even at several times rated armature current. This means that there is little or no saturation, and consequently the characteristic is a straight line. Of course, if tests were made at many times normal armature current, saturation would set in and the curve would droop, as for any saturation curve.

12. The Potier Diagram

By an ingenious process due to Potier it is possible to determine both the leakage reactance and the armature reaction (in terms of field current) from the open circuit and the zero pf characteristics. Referring to Fig. 19(a), at zero pf the current lags the terminal voltage by 90 degrees.

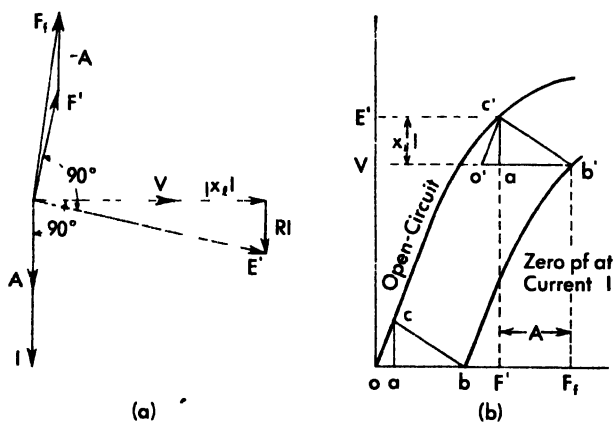


Fig. 19 Potier triangles.

The leakage reactance drop, $jx_l I$, is in phase with the terminal voltage, V , while the (to be assumed negligible) resistance drop, RI , is at right angles to V . The voltage behind the leakage impedance is then E' , and to induce this voltage requires that a corresponding flux, ϕ' , cross the air gap. The flux in the field poles will exceed ϕ' by the field pole leakage flux which passes between adjacent poles without crossing the air gap

to the armature. Ignoring this field pole leakage, the saturation in the poles must correspond to ϕ' , or to its induced voltage E' . Now the armature reaction, A , due to the zero pf current is in phase therewith. The field ampere turns must then be sufficient to neutralize A and provide a net excitation F' , that is

$$F_f = F' + A$$

It is evident from Fig. 19(a) that *if the relatively small resistance drop RI be neglected*, then F' , A , and F_f will be in phase and can be combined arithmetically, and likewise E' , V and $a_d I$ will be in phase and can be combined arithmetically. These relationships are defined in Fig. 19(b) by the triangle $a'b'c'$, $V = E' - a_d I$, and $F_f = F' + A$. Therefore, given the open-circuit and the zero pf characteristics, the problem is to determine the triangle $a'b'c'$, for once this is accomplished the leakage reactance is $x_d I = a'd'$ and the armature reaction is $A = a'b'$. It is clear that the two curves must be parallel in the sense that if $a'b'c'$ is moved parallel to itself with c' on the open-circuit characteristic, then b' must follow the zero pf characteristic, for since the armature current I is constant, both the leakage reactance drop and the armature reaction must be constant for any field excitation. But at zero terminal voltage, $V = 0$, the triangle is at abc , and here it is seen to be a part of the larger (Potier) triangle obc . Therefore, to construct the triangle $a'a'b'c'$ at any level:

1. draw $a'b'$ parallel and equal to ab
2. draw $a'c'$ parallel to ac intersecting the open circuit characteristic at c'
3. complete the triangle by adding $c'b'$

As a matter of fact, it is not necessary to have a complete zero pf characteristic. If the short circuit point b and any other point b' are given, the Potier triangle can be constructed, and by moving it parallel to itself the whole zero pf characteristic may be constructed. Conversely, given the zero pf characteristic and one point on the open circuit curve, the latter may be completed.

13. The Electromotive Force (Emf) Method (round rotor)

The only test data required for this method are the open circuit and short-circuit characteristics, Fig. 20(a). The armature reaction and leakage reactances together are included in the synchronous reactance, X_s , and the vector diagram of Fig. 20(b) is assumed to apply. On short-circuit, Fig. 20(c), the terminal voltage V reduces to zero and the whole of the voltage E , is consumed by $(R + jX_s)I$. Since the resistance

drop is small compared with the reactance drop, as well as orthogonal to it, no great error is committed by taking $E_f = Z_s I_{sc} \cong jX_s I_{sc}$. Then the X_s curve can be plotted on Fig. 20(a) as the ratio E_f/I_{sc} . Since the

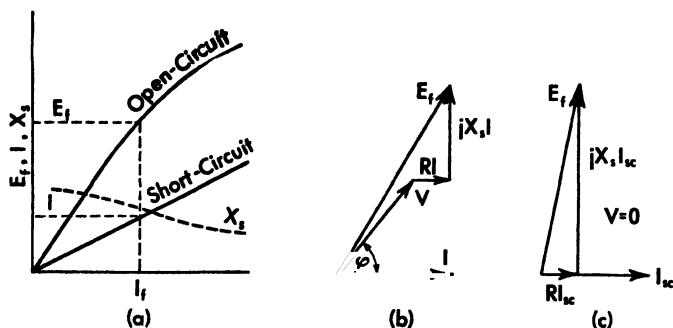


Fig. 20 The EMF method.

short circuit characteristic is taken under conditions of low flux, and therefore no saturation, it is evident that the value of X_s at any field current, as given above, will be too large. For this reason, it is customary to use the X_s corresponding to the largest armature current tested (usually limited by heating to about twice normal rated current). From Fig. 20(b) the induced voltage is (taking I as reference vector),

$$\begin{aligned} E_f &= V + (R + jX_s)I \\ &= V(\cos \phi + j \sin \phi) + RI + jX_s I \\ &= (V \cos \phi + RI) + j(V \sin \phi + X_s I) \end{aligned} \quad (56)$$

Therefore, the induced voltage has a magnitude

$$E_f = \sqrt{(V \cos \phi + RI)^2 + (V \sin \phi + X_s I)^2} \quad (57)$$

Problem: Show that the short-circuit current of an alternator is independent of speed, except at very low speeds.

14. The Old AIEE Method (round rotor)

Referring to Fig. 21(a) it is evident that at zero pf the difference between the excitation voltage, E_f , and the terminal voltage, V , is substantially the synchronous impedance drop $jX_s I$. Hence if both an open-circuit and a zero pf characteristic are available, Fig. 21(b), the difference between them is the synchronous impedance drop. This method has the advantage over the electromotive force method of taking into account the saturation which exists for armature current I

at terminal voltage V . However, additional test data in the way of a zero pf characteristic are required. Moreover, as will be shown later, it yields an erroneous angle between V and E , and cannot be used in

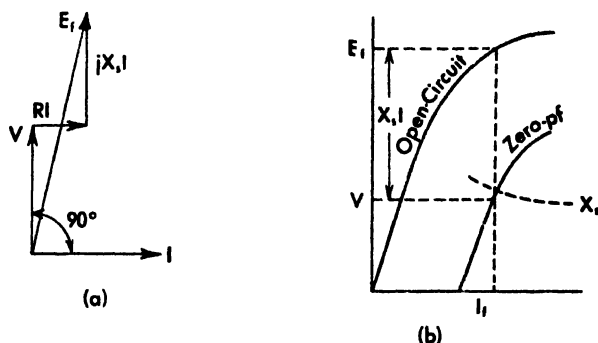


Fig. 21 The old AIEE method.

stability studies. In applying this method, corresponding values of E_f and $X_s I$ are read from the characteristic curves and the value of V found from the following equation,

$$V = \sqrt{E_f^2 - (RI \sin \varphi - X_s I \cos \varphi)^2} - (RI \cos \varphi + X_s I \sin \varphi) \quad (58)$$

Problem: Devise a graphical method for finding V for any load and power factor when values of E_f and X_s corresponding to a given field current are taken from the characteristics.

15. The Magnetomotive Force (Mmf) Method (round rotor)

This method, like the electromotive force method, requires only the open-circuit and short-circuit characteristics. The effects of leakage reactance and of armature reaction are both included in the armature magnetomotive force. Referring to Fig. 22(a), the resistance drop is added to the terminal voltage, V , to give the voltage V' induced in the conductor by main and leakage fluxes. This voltage V' requires a field excitation F' , as given by the open circuit characteristic, Fig. 22(b). On short-circuit, the excitation, A in Fig. 22(b), is consumed in overcoming the armature reaction and the leakage impedance. But the latter is sensibly equal to the Potier reactance. The total field excitation is then the vector sum

$$F_t = F' - A$$

and the corresponding voltage on open-circuit, Fig. 22(b), is E_f . Since the armature magnetomotive force is taken from the short-circuit characteristic under conditions of no saturation, it will be smaller than

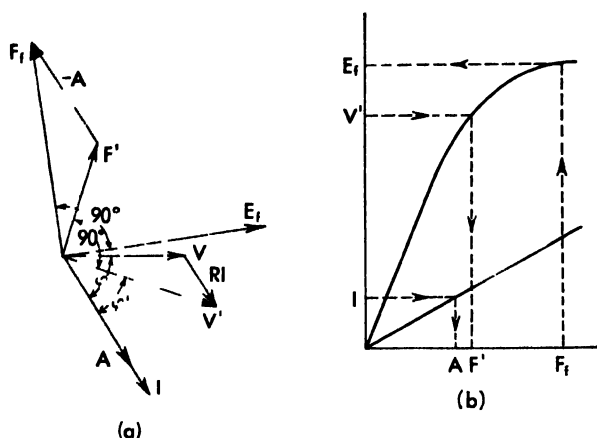


Fig. 22 The MMF method

actually required under saturated operating conditions, and F_f as thus computed will be too small. The method is accordingly sometimes called the *optimistic* method.

16. The ASA Method (round rotor)

This is essentially a magnetomotive force method in which an adjusted value of magnetomotive force is used to correct for saturation. It requires

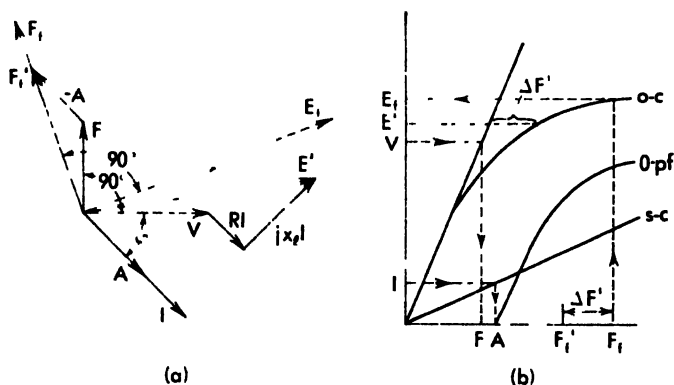


Fig. 23 The ASA method

three characteristics: the open circuit; the air gap line; and the short circuit (for the full load zero p.f.). Referring to Fig. 23(a), the field ampere-

turns, F , corresponding to the terminal voltage V are found from the air gap line of Fig. 23(b). The armature ampere-turns, A , required to circulate full load current are taken from the short-circuit characteristic (or from the zero pf characteristic), and combined, Fig. 23(a), to yield the resultant magnetomotive force

$$F_1' = F - A \quad (59)$$

Now the voltage behind the leakage impedance E' is the best measure of the flux in the field poles, where most of the saturation occurs. At this voltage Fig. 23(b) shows that the difference between the unsaturated (air-gap line) and saturated (open circuit characteristic) field ampere-turns is $\Delta F'$. Therefore, this amount should be added to the unsaturated ampere turns to determine the total required, that is

$$F_1 = F_1' + \Delta F' \quad (60)$$

17. The General Method (round rotor)

In all of the previously described methods there are involved either obvious approximations, or semi empirical corrections. The so called general method is more rational, because it treats electromotive forces as voltages and magnetomotive forces as ampere turns, and results based on it are in much closer agreement with test data. It requires the open circuit and zero pf characteristics.

Referring to Fig. 24(a), the voltage E' behind the leakage impedance,

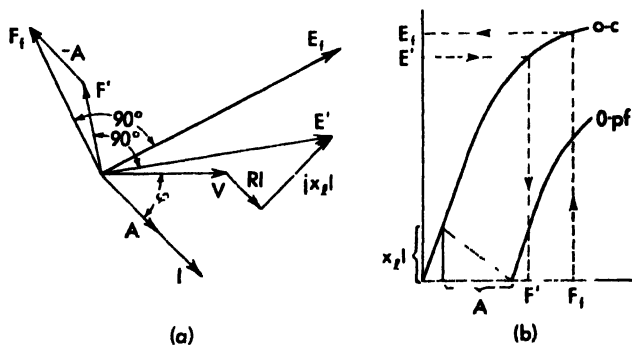


Fig. 24 The general method

corresponding to the main flux, is determined from the equation

$$E' = V + (R + jX_L)I(\cos \varphi - j \sin \varphi) \quad (61)$$

and the corresponding ampere turns, F' , taken from the open-circuit

characteristic, Fig. 24(b). The armature reaction, A , is determined from the Potier triangle and combined with F' ,

$$F_1 = F' - A \quad (62)$$

The induced voltage E_f corresponding to F_1 is then read from the open circuit characteristic and placed 90 degrees behind F_1 in the vector diagram.

If the zero pf characteristic is available, this is the most reliable method to use.

18. Salient Pole Machines

The two-reaction theory of salient pole machines is based on the resolution of the armature magnetomotive force into direct and quadrature components in line with the field pole and interpolar axes respectively. The direct axis component adds directly to the field pole magnetomotive force to produce a resultant main flux which crosses the air gap and induces the quadrature component of voltage. This component of flux is subject to saturation in the field poles and in the armature core. The open circuit characteristic is a fair measure of this saturation. But the quadrature component of armature reaction, acting on the relatively smaller permeance of the quadrature path, produces a flux of low density and negligible saturation. Therefore, its induced voltage may be accounted for by a constant quadrature synchronous reactance X_q .

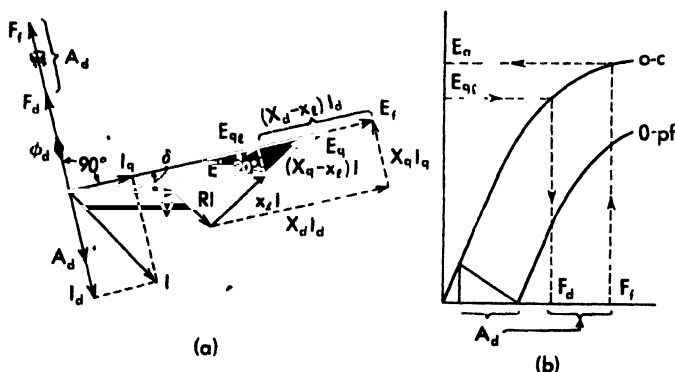


Fig. 25 Excitation of a salient pole machine.

The vector diagram for the salient pole machine is shown in Fig. 25(a), the dotted portions applying to an unsaturated machine. The quadrature component of voltage behind the leakage reactance is

$$E_{q1} = V + RI + jx_l I + j(X_q - x_l)I_a \quad (63)$$

Neglecting the resistance R , this has a magnitude

$$E_{qt} \cong V \cos \delta + x_l I_a \quad (64)$$

If the machine is unsaturated, the quadrature component of induced voltage has a magnitude

$$E_r \cong V \cos \delta + N_d I_a \quad (65)$$

But the induced voltage E_{qt} requires a flux ϕ_d which crosses the air gap and saturates the poles. Referring to the open-circuit characteristic of Fig. 25(b), it is seen that a net field excitation F_d is necessary to supply the flux ϕ_d . From the Potier diagram it is also evident that the direct component of armature reaction (in field current terms) is A_d , and this combines directly with the field current to give the resultant magnetomotive force

$$F_d = F_f + A_d \quad (66)$$

From the open-circuit characteristic, it is seen that the corresponding open-circuit voltage E_q is less than the E_r found from the conventional diagram with constant N_d .

Additional refinements are possible, such as allowing for saturation in the quadrature path, or distinguishing between the saturation in the field poles (based on E_{qt}) and that in the armature core and teeth (based on E_f). In view of the difficulty of obtaining sufficient data to sustain such refinements, and the minor corrections which they represent, it is not believed worthwhile to pursue them further.

19. Comparison of the Different Methods

Six different methods of calculating the excitation voltage, and therefore the regulation, of an alternator have been given on the previous pages. (There are many more!) Comparing the electromotive force, magnetomotive force, and general methods for a round rotor machine, in the light of the derived zero-power factor characteristic, Fig. 26, it is clear that the vertical subtraction of a constant $X_s I$ (the electromotive force method) leads to a much lower curve than does the

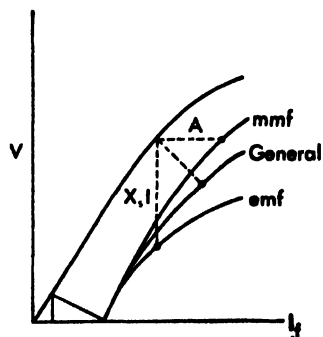


Fig. 26

horizontal addition (magnetomotive force method) of a constant armature reaction; while the Potier triangle of the general method describes an in-

intermediate curve. But to bring out more clearly the differences, a numerical example will be worked out by all six methods for the same machine under identical terminal conditions.

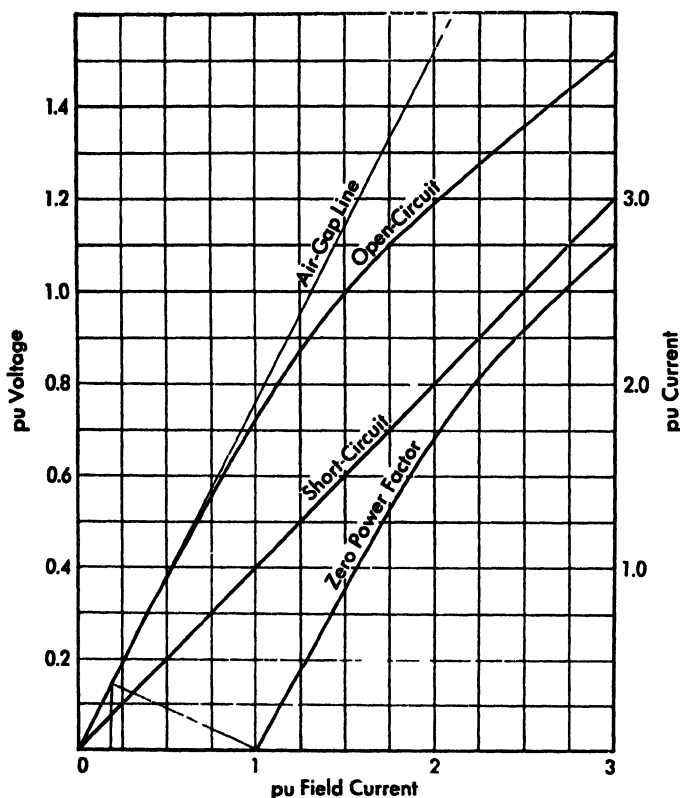


Fig. 27

Example: The open-circuit and full load zero power factor characteristics of a salient pole alternator are given in Fig. 27 in *per unit* values. The armature resistance is $R = 0.01$ and the quadrature synchronous reactance is $X_q = 0.40$. Calculate the open-circuit voltage for 0.8 pf (lag) by all methods. (In all except the last method disregard the salient poles.)

As preliminaries: (1) construct the short-circuit characteristic by drawing a straight line from the origin through $I = 1$, $I_f = 1$ (the intercept of zero pf characteristic); (2) construct the Potier triangle as previously described, noting that $x_f I = 0.15$ and $A_d = 0.82$; (3) draw the air gap line tangent to the open-circuit characteristic at the origin.

Electromotive Force Method

Corresponding values of V and I , taken from the open-circuit and short-circuit characteristics respectively, are

E_c	0.20	0.40	0.60	0.80	1.00	1.10	1.50
I	0.25	0.53	0.80	1.12	1.50	1.74	2.94
$X_s = E/I$	0.80	0.75	0.75	0.72	0.67	0.63	0.51

Taking the smallest value of $X_s = 0.51$, Eq. (57) gives

$$E_c = \sqrt{(0.80 + 0.01)^2 + (0.60 + 0.51)^2} = 1.37$$

Old AIEE Method

Assume several values of E_c , find the corresponding X_s from the o-c and s-c curves, and calculate V by (58).

E_c	1.20	1.35	1.40
X	0.53	0.44	0.41
V	0.74	0.98	1.05

A plot of these data indicates $E_c = 1.37$ for $V = 1.00$

Magnetomotive Force Method

The voltage behind the resistance is

$$V' = V + RI = 1.00 + 0.01(0.8 - j0.6) = 1.008 - j0.006$$

having a magnitude of $V' = 1.01$. The corresponding field excitation is $F' = 1.50$. The field excitation to circulate unit short-circuit current is $A = 1.00$. Adding this graphically to F' gives $F_f = 2.24$. The corresponding open-circuit voltage is $E_o = 1.30$.

The ASA Method

The leakage reactance as measured from the Potier diagram is $x_l = 0.15$. The voltage behind leakage impedance is

$$E' = V + Z_l I = 1.00 + (0.01 + j0.15)(0.8 - j0.6) = 1.098 + j0.114$$

This has a magnitude of $E' = 1.103$. At this voltage the difference in field current between the open-circuit and air gap lines is $\Delta F' = 0.28$.

The field current on the air gap line corresponding to $V = 1$ is $F = 1.32$. Combining this (graphically) with the field current $A = 1.00$ to circulate unit short-circuit current gives $F_f' = 2.08$, and adding the saturation effect $\Delta F' = 0.28$ gives $F_f = 2.36$. The corresponding open-circuit voltage is $E_o = 1.34$.

The General Method

From the previous case, the voltage behind the leakage impedance is $E' = 1.10$ and the corresponding field current is $F' = 1.73$. The armature reaction (in field current terms) from the Potier triangle is $A = 0.82$. Combining graphically with F' gives $F_f = 2.36$. The corresponding open-circuit voltage is $E_f = 1.34$.

Salient Pole Method

This method is best applied graphically in accordance with the diagram of Fig. 25. The student should carry out the construction, and verify that $E_{q1} = 1.06$, for which $F_d = 1.63$ on the open-circuit characteristic. The armature current $I = 1.0$ has components $I_d = 0.85$ and $I_q = 0.53$. The Potier triangle shows an armature reaction (in field current terms) of 0.82 for $I_d = 1.0$, hence in the present case $.I_d = 0.85 \times 0.82 = 0.70$. Therefore the field current must be $F_f = 1.63 + 0.70 = 2.33$, and the corresponding open-circuit voltage is $E_q = 1.33$.

Recapitulation

The several methods give the following comparative results

Emf	1.37	obviously too high
AIEE	1.37	takes too long to calculate
Mmf	1.30	obviously too low
ASA	1.34	method is long and cumbersome
General	1.34	} most reliable results
Salient Pole	1.33	

In other cases the relative values may be quite different. But the general and salient pole methods are the best to use.

Problems

1. The zero-pf characteristic for unit current is given in Fig. 27. Construct, by means of Potier triangles, the zero-pf characteristics for 0.75, 0.50, and 0.25 per-unit currents.
2. Is the leakage reactance as found by the Potier diagram equal to, less than, or greater than the true armature leakage reactance? Why?
3. Given the open-circuit and zero-pf characteristics, how would you determine the synchronous impedance for field currents smaller than that at which the zero-pf curve is zero?
4. The vector diagrams used in the text to illustrate the six different methods of calculating the excitation, were all drawn for *lagging* power factors. Prepare a chart with four columns labelled *Lagging Pf*, *Unity Pf*, *Leading Pf*, and *Short-Circuit*; and then for *each* method drawn the appropriate vector diagram in its column (a total of 24 vector diagrams).

5. For the data of Fig. 27 plot the synchronous reactance as obtained from the short-circuit and from the zero-pf characteristics. Why do they differ?
6. Perform tests on one of the laboratory machines to obtain its open-circuit and zero-pf characteristics, and determine its regulation at some load and power factor. Check by each of the six methods given in the text.
7. For the machine having the characteristics of Fig. 27 construct the 0.80 lagging, 1.00, and 0.80 leading power factor, 0.50 load characteristics by: (a) the emf method, (b) the AIEE method, (c) the mmf method, (d) the ASA method, (e) the general method, and (f) the general method for salient pole machines.
8. For the machine having the characteristics of Fig. 27, calculate and plot curves of terminal volts, V , versus armature current, I , for 0.80 lagging, 1.00, and 0.80 leading power factors by each of the methods mentioned in problem 7 above.

20. Power Transfer Between Two Voltage Sources

The problem of power transfer between two synchronous machines is of great importance in the parallel operation of alternators and in system stability studies. Indeed, a considerable portion of the subject of system stability is concerned with just this problem. Three cases will be considered in this text: (1) round rotor machines without saturation, (2) salient pole machines without saturation, and (3) salient pole machines with saturation. As a preliminary, before taking up these specific cases, a general equation for power transfer between two voltage sources will be derived.

Figure 28(a) shows an impedance Z , θ connecting two voltage sources having phase angles δ_1 and δ_2 with respect to an arbitrary reference axis.

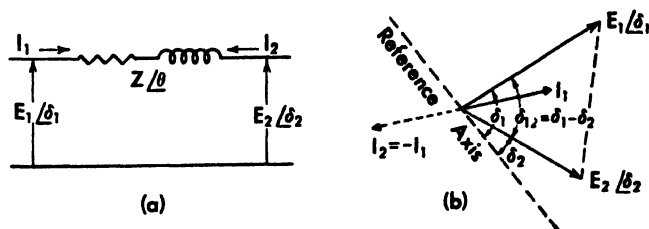


Fig. 28 Power transfer between two sources.

This impedance constitutes the *system* into which flow the currents I_1 and I_2 from the two voltage sources. The corresponding vector diagram is shown in Fig. 28(b). In this simple series circuit

$$I_1 = -I_2 = \frac{E_1 - E_2}{Z} = \frac{E_1}{Z} \angle \delta_1 - \theta - \frac{E_2}{Z} \angle \delta_2 - \theta \quad (67)$$

The two parts of this current make angles of $(\delta_1 - \delta_1 + \theta)$ and $(\delta_1 - \delta_2 + \theta)$ with respect to the voltage E_1 , and angles $(\delta_2 - \delta_1 + \theta)$ and $(\delta_2 - \delta_2 + \theta)$ with respect to the voltage E_2 . Therefore, projecting the current onto the voltages by the cosines of these angles, the power supplied by each machine is seen to be the scalar (dot) product

$$P_1 = E_1 \cdot I_1 = \frac{E_1^2}{Z} \cos \theta - \frac{E_1 E_2}{Z} \cos (\delta_{12} + \theta) \quad (68)$$

$$P_2 = E_2 \cdot I_2 = \frac{E_2^2}{Z} \cos \theta - \frac{E_2 E_1}{Z} \cos (\delta_{21} + \theta) \quad (69)$$

in which $\delta_{12} = -\delta_{21} = (\delta_1 - \delta_2)$ is the displacement angle between the two voltages. These powers are a maximum, for power transferred from E_1 to E_2 , for $\delta_{12} + \theta = \pi$ and $\delta_{21} + \theta = 0$ respectively, which give

$$P_{1(\max)} = \frac{E_1^2}{Z} \cos \theta + \frac{E_1 E_2}{Z} = \frac{E_1^2}{Z^2} r + \frac{E_1 E_2}{Z} \quad (70)$$

$$P_{2(\max)} = \frac{E_2^2}{Z} \cos \theta - \frac{E_1 E_2}{Z} = \frac{E_2^2}{Z^2} r - \frac{E_1 E_2}{Z} \quad (71)$$

The negative sign shows the second machine to be a motor. These two maxima do not occur at the same displacement angle, unless there is no resistance in the circuit. In that case $r = 0$ and

$$P_{1(\max)} = \frac{E_1 E_2}{x} = -P_{2(\max)} \quad (72)$$

It is not difficult to prove by (67), (68), and (69) that

$$P_1 + P_2 = r I_1^2 \quad (73)$$

Problems

1. Prove (73).

2. If $E_1 = E_2$ show that $P_{2(\max)}$ is a grand maximum for $x = \sqrt{3}r$.

3. In per-unit values $E_1 = 1.2$, $E_2 = 1.0$, and $Z = r + jx = 0.10 + j0.80$. Plot curves of P_1 , P_2 and the resistance loss against δ_{12} up to 180 degrees. Check the plotted maxima against those calculated by (70) and (71). Note where the maxima fall.

4. Repeat the above problem when $r = 0$.

21. Power Transfer Between Round Rotor Machines (unsaturated)

This problem is not only important with respect to round rotor machines, but also is usually a sufficiently good approximation for salient pole machines under saturated conditions (when $x_d \cong x_q$), or for stability studies.

The equivalent circuit of the round rotor machine is simply an induced voltage E , a series (synchronous) impedance z , and a terminal voltage V . Suppose we have two round rotor machines connected by a series impedance z . Then the equivalent circuit and vector diagram are as shown in Fig. 29. The usual requirement is first to determine the excitations of

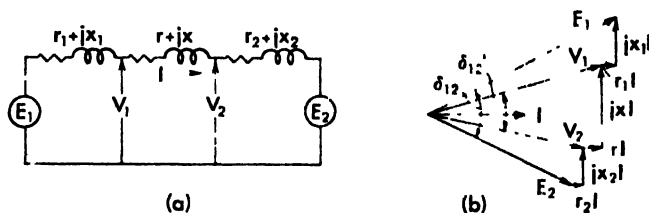


Fig. 29 Power transfer between round rotor machines

the two machines corresponding to specified terminal voltages V_1 and V_2 and load; and then with these excitations held constant to plot the power transfer as function of the angle δ , and in particular to find maximum power. An example will clarify the procedure.

Example: A round rotor generator having a per unit synchronous reactance of $x_1 = 0.80$ supplies a round rotor motor having a synchronous reactance of $x_2 = 0.60$ over a transmission line of impedance $Z = 0.10 + j0.50 = 0.51 \angle 78.7^\circ$. The system is operating with terminal voltages $V_1 = 1.1$ and $V_2 = 1.0$ at a receiver power load of $P_2 = -0.75$. (a) Determine the excitation on the generator and motor. (b) Find the power transfer for constant excitation as function of the torque angle between machines. The total impedance is $(jx_1 + Z + jx_2) = 0.10 + j1.9 = 1.90 \angle 87.0^\circ$.

Equation (69) may be used to find the angle δ'_{12} between the terminal voltages V_1 and V_2 , thus

$$-0.75 = \frac{1.0}{0.51} \cos 78.7^\circ - \frac{1.0 \times 1.1}{0.51} \cos (\delta'_{12} + 78.7^\circ)$$

from which $\delta'_{12} = 20.5^\circ$. Then using V_2 as reference vector

$$I = \frac{V_1 - V_2}{Z} = \frac{1.1 \angle 20.5^\circ - 1.0 \angle 0^\circ}{0.51 \angle 78.7^\circ} = 0.757 \angle -6.6^\circ$$

$$E_1 = V_1 + jv_1 I = 1.1 \angle 20.5^\circ + j0.80 \times 0.757 \angle 6.6^\circ = 1.381 \angle 45.8^\circ$$

$$E_2 = V_2 - jv_2 I = 1.0 \angle 0^\circ - j0.60 \times 0.757 \angle 6.6^\circ = 1.145 \angle -23.2^\circ$$

These values can be verified graphically.

Now keeping the excitations E_1 and E_2 constant, the machine powers follow from (68) and (69),

$$P_1 = \frac{1.381^2}{1.90} \cos 87^\circ - \frac{1.381 \times 1.145}{1.90} \cos (\delta_{12} + 87^\circ)$$

$$= 0.053 - 0.833 \cos (\delta_{12} + 87^\circ)$$

$$P_2 = \frac{1.145^2}{1.90} \cos 87^\circ - \frac{1.381 \times 1.145}{1.90} \cos (87^\circ - \delta_{12})$$

$$= 0.036 - 0.833 \cos (87^\circ - \delta_{12})$$

Under the initial operating conditions $\delta_{12} = 45.8^\circ + 23.2^\circ = 69^\circ$ and $P_1 = 0.81$ and $P_2 = -0.75$ and the sum of these powers, 0.06, is the resistance loss in the circuit.

22. Power Transfer Between Salient Pole Machines (unsaturated)

A salient pole synchronous generator supplying a salient pole synchronous motor over a transmission line of impedance $z = r + jx$ is shown in Fig. 30(a). The machines are assumed to be unsaturated

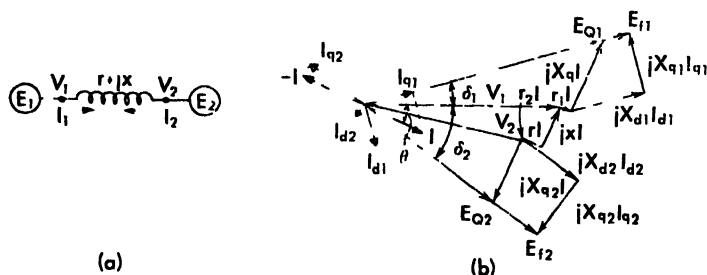


Fig. 30 Power transfer between salient pole machines

The generator terminal voltage (selected as reference vector) is V_1 and the current I is taken as lagging this voltage by an angle θ , as shown in Fig. 30(b). The generator vector diagram is then constructed in the usual way. The motor terminal voltage is

$$V_2 = V_1 - (r + jx)I \quad (74)$$

The motor may be regarded as a generator having an output current $-I$, and its vector diagram constructed on V_2 in the usual way. There is,

however, a simpler way. We have $-I = I_{d2} + I_{q2}$ and therefore

$$\begin{aligned} E_2 &= V_2 - r_2 I + jX_{d2}I_{d2} + jX_{q2}I_{q2} \\ &= V_1 - rI - jxI - r_2 I + jX_{d2}I_{d2} + jX_{q2}I_{q2} \\ &= V_1 - (r + r_2)I + jx(I_{d2} + I_{q2}) + jX_{d2}I_{d2} + jX_{q2}I_{q2} \\ &= V_1 - (r + r_2)I + j(x + X_{d2})I_{d2} + j(x + X_{q2})I_{q2} \end{aligned} \quad (75)$$

This equation shows that the motor vector diagram may be constructed directly on V_1 by adding r to r_2 and x to both X_{d2} and X_{q2} .

The power output of the generator is

$$\begin{aligned} P_1 &= VI \cos \theta \\ &= I_{q1}V_1 \cos \alpha_1 + I_{d1}V_1 \sin \delta_1 \end{aligned} \quad (76)$$

From the vector diagram

$$I^2 = I_{d1}^2 + I_{q1}^2 \quad (77)$$

$$E_1 = V_1 \cos \delta_1 + r_1 I \cos (\delta_1 + \theta) + X_{d1}I_{d1} \quad (78)$$

$$0 = V_1 \sin \delta_1 + r_1 I \sin (\delta_1 + \theta) - X_{q1}I_{q1} \quad (79)$$

Equations (77), (78), and (79) may be solved simultaneously for I_{d1} and I_{q1} and these values substituted in (76) to determine the power output. Analytically this leads to long and awkward expressions. It is generally sufficient to neglect the generator resistance r_1 , in which case (78) and (79) give

$$I_{d1} = \frac{E_1 - V_1 \cos \delta_1}{X_{d1}} \quad (80)$$

$$I_{q1} = \frac{V_1 \sin \delta_1}{X_{q1}} \quad (81)$$

which substituted in (76) yields

$$\begin{aligned} P_1 &= \frac{V_1^2 \sin \delta_1 \cos \delta_1}{X_{q1}} + \frac{(E_1 - V_1 \cos \delta_1)V_1 \sin \delta_1}{X_{d1}} \\ &= \frac{E_1 V_1}{X_{d1}} \sin \delta_1 + V_1^2 \frac{(X_{d1} - X_{q1})}{2X_{d1}X_{q1}} \sin 2\delta_1 \end{aligned} \quad (82)$$

This equation shows that the power output of a salient pole machine consists of a principal term varying as the sine of the torque angle δ_1 and a secondary term varying as the second harmonic of the torque angle. For a round rotor machine $X_q = X_d$ and the second harmonic term vanishes.

The equation is plotted in Fig. 31 for the case $E_1 = V_1 = 1.0$, $X_{d1} = 1.0$ and $X_{q1} = 0.60$, for both a salient pole and round rotor machine. It is

clear that maximum power (for E_1 and V_1 held constant) occurs at 90 degrees for the round rotor machine, but at less than this for the salient pole machine.

Returning to the vector diagram, Fig. 30(b),

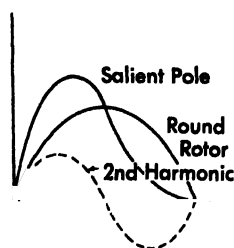


Fig. 31

$$\begin{aligned}
 I &= \frac{E_{Q1} - E_{Q2}}{(r_1 + r + r_2) + j(X_{q1} + x + X_{q2})} \\
 &= \frac{E_{Q1} \delta_1 - E_{Q2} \delta_2}{Z_{12} \theta_{12}} \\
 &= \frac{E_{Q1}}{Z_{12}} \delta_1 - \theta_{12} - \frac{E_{Q2}}{Z_{12}} \delta_2 - \theta_{12} \quad (83)
 \end{aligned}$$

in which $Z_{12} \theta_{12} = (r_1 + r + r_2) + j(X_{q1} + x + X_{q2})$ is the transfer impedance between machine voltages E_{Q1} and E_{Q2} .

The components of (83) make angles $(\delta_1 - \delta_1 + \theta_{12})$ and $(\delta_1 - \delta_2 + \theta_{12})$ with E_{Q1} and therefore

$$I_{d1} = \frac{E_{Q1}}{Z_{12}} \sin \theta_{12} - \frac{E_{Q2}}{Z_{12}} \sin (\delta_{12} + \theta_{12}) \quad (84)$$

Then

$$\begin{aligned}
 E_1 &= E_{Q1} + (X_{d1} - X_{q1})I_{d1} \\
 &= \left[1 + \frac{(X_{d1} - X_{q1})}{Z_{12}} \sin \theta_{12} \right] E_{Q1} - \left[\frac{X_{d1} - X_{q1}}{Z_{12}} \sin (\delta_{12} + \theta_{12}) \right] E_{Q2} \quad (85)
 \end{aligned}$$

Likewise

$$E_2 = \left[1 + \frac{(X_{d2} - X_{q2})}{Z_{12}} \sin \theta_{12} \right] E_{Q2} - \left[\frac{X_{d2} - X_{q2}}{Z_{12}} \sin (\delta_{21} + \theta_{12}) \right] E_{Q1} \quad (86)$$

For given excitations E_1 and E_2 and displacement angle δ_{12} , these two equations may be solved simultaneously for E_{Q1} and E_{Q2} . The power transferred may then be calculated by (68) and (69) with an appropriate change of nomenclature, that is

$$P_1 = \frac{E_{Q1}^2}{Z_{12}} \cos \theta_{12} - \frac{E_{Q1}E_{Q2}}{Z_{12}} \cos (\delta_{12} + \theta_{12}) \quad (87)$$

$$P_2 = \frac{E_{Q2}^2}{Z_{12}} \cos \theta_{12} - \frac{E_{Q1}E_{Q2}}{Z_{12}} \cos (-\delta_{12} + \theta_{12}) \quad (88)$$

The usual requirement is first to determine the excitations for given initial conditions of terminal voltage, load current and power factor; and then holding the excitations constant to find the power outputs by (87) and (88) after having found E_{Q1} and E_{Q2} from (85) and (86). A

numerical example, including the effect of saturation, is worked out in the next section.

Problems

1. If resistance is included, show from equations (76), (77), (78), and (79) that the power output of a salient pole synchronous generator is

$$P = \frac{EV(X_d \sin \delta + r \cos \delta)}{r^2 + X_d X_q} + \frac{V^2[(X_d - X_q) \sin 2\delta - 2r]}{2(r^2 + X_d X_q)}$$

2. The per unit values for a salient pole machine are $E = 1.4$, $V = 1.0$, $X_d = 1.0$, $X_q = 0.6$ and $r = 0.1$. Plot on a common graph sheet the P vs δ curves for the following conditions:

- (a) All constants included
- (b) Resistance neglected
- (c) X_q taken equal to $X_d = 1.0$

23. Power Transfer Between Salient Pole Machines (saturated)*

The equations of the previous section apply also to saturated machines if the excitation voltages are calculated by the method of Sec. 18 and if appropriate saturated values are used for the direct axis synchronous impedances. The procedure will be carried out in detail for a numerical case.

Example: Two identical laboratory synchronous machines mounted on the same shaft and driven by a d.c. motor are arranged so that the cradle-mounted stator of one of the machines may be turned to any displacement angle δ between the two stators. The open circuit and zero pf ($I_d = 10$) characteristics, as found by test, are given in Fig. 32, and the Potier triangle constructed in the usual manner. The leakage reactance drop ΔI_d and the armature reaction (in field current terms) are then known for $I_d = 10$. For any other current a new Potier triangle is constructed by proportion (for example, at $I_d = 7.5$ amperes, it is 75 per cent as large as for $I_d = 10$). Then other zero pf characteristics ($I_d = 7.5$, 5.0, and 2.5) may be constructed. Then for any field current I_f and armature current I_a the difference in voltage between the open-circuit and appropriate zero-pf curve is the $X_d I_d$ drop, or

$$X_d = \frac{\Delta V}{I_d} \quad (89)$$

Obviously, X_d is a function of both I_f and I_a . Values of X_d plotted against armature current, with field current as parameter, are shown in Fig. 33.

* The author is indebted to his colleague, Professor A. R. Miller, for the method given in this section of taking saturation into account.

The quadrature reactance, X_q , is shown as a dotted line. It is assumed to be constant and unaffected by saturation. The greater the degree of saturation the smaller X_d , and at high saturation X_d approaches X_q . Thus a highly saturated salient pole machine has the characteristics of a round rotor machine. The values of X_d are asymptotic to the unsaturated values.

The circuit constants per phase are:

$$\left. \begin{aligned} r_a &= 0.3 \text{ ohms (measured)} \\ x_l &= 1.8 \text{ ohms (Potier diagram)} \\ X_q &= 4.5 \text{ ohms (measured)} \\ X_d &\text{ from Fig. 33} \\ Z &= r + jx = 0.45 + j10.5 \text{ ohms} \\ A_d &= 0.08 I_d \text{ (in terms of field amperes)} \end{aligned} \right\} \begin{array}{l} \text{each} \\ \text{machine} \end{array}$$

The initial conditions are:

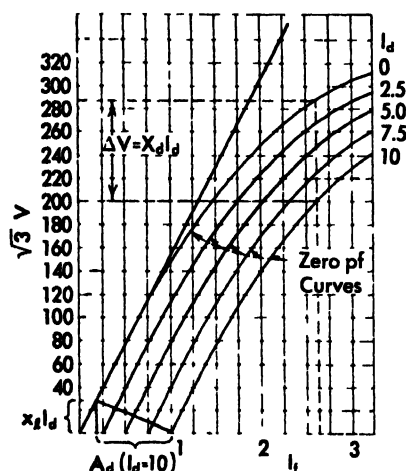


Fig. 32 Zero power factor characteristics

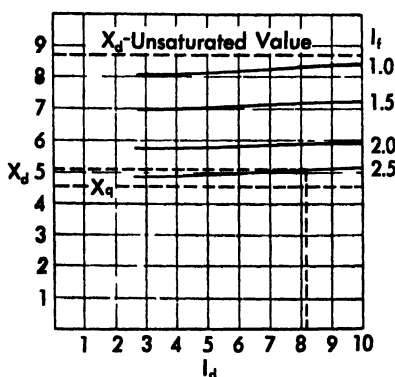


Fig. 33

$$\begin{aligned} \delta &= 60^\circ \text{ (displacement between stators)} \\ I_f &= 2.5 \text{ amperes (field excitation)} \\ V &= 250 \text{ volts (line-to-line) at motor terminals} \\ I &= 8.2 \text{ amperes} \\ W &= 3,300 \text{ watts input at motor terminals} \\ \cos \theta &= \frac{3,300}{\sqrt{3} \times 250 \times 8.2} = 0.932 \text{ (leading)} \end{aligned}$$

The vector diagram for the initial conditions is laid out to scale in Fig. 34, starting with the motor terminal voltage $V = 250 \sqrt{3} = 433$ and the cur-

rent $I = 8.2$ leading the voltage by $\theta = 21.6^\circ$. The external impedance has been combined with the machine impedance in laying out the generator part of the diagram. The diagram is constructed in the usual manner and shows voltages $E_{q1} = 156$ and $E_{q2} = 161$ for the generator and motor respectively. The angle on the vector diagram is $\delta_{12} = 61.5$ degrees as compared with the test angle of 60 degrees. The current components are $I_{d1} = 3.6$, $I_{q1} = 7.4$, $I_{d2} = 4.7$, $I_{q2} = 6.8$.

The excitations are calculated as follows:

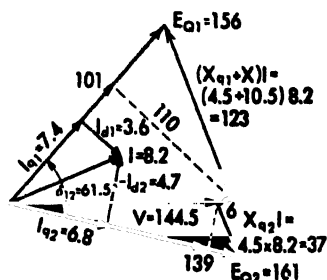


Fig. 34

$$\begin{aligned}
 E_{q1} &= V + (r_a + jX_d)I + j(X_{q1} - X_d)I_{q1} + j(X_d - X_{q1})I_{d1} \\
 E_{q1} &= 101 + (1.8 + j10.5)3.6 = 145 \text{ (250-3 phase) volts} \\
 I_{d1} &\text{ (from open-circuit curve) } = 2.13 \text{ amps} \\
 A_{d1} &= 0.08 \times 3.6 = 0.29 \\
 \text{Total generator excitation} &= 2.12 \text{ (test 2.50)} \\
 \text{Generator open-circuit voltage} &= 71 \text{ (3}\phi \text{) test 275)} \\
 E_{q2} &= V - r_a I + jX_{d2}I_{d2} + jX_d I_{q2} \\
 E_{q2} &= 139 + 1.8 \times 4.7 = 148 \text{ (256-3 phase)} \\
 I_{d2} &\text{ (from open-circuit curve) } = 2.20 \\
 A_{d2} &= 0.08 \times 4.7 = 0.38 \\
 \text{Total motor excitation} &= 2.58 \text{ (test 2.50)} \\
 \text{Motor open-circuit voltage} &= 280 \text{ (3}\phi \text{) (test 275)}
 \end{aligned}$$

There is a 4.3 per cent error in the calculation of the excitations, and about the same error in the calculated torque angle between machines.

The second part of the problem is to calculate the maximum power, using equations (87) and (88). The impedances between the voltages E_{q1} and E_{q2} is

$$Z_{12} = (r + 2r_a) + j(X_d + X_{q1} + X_{q2}) = 1.05 + j19.5 = 19.5 \angle 86.9^\circ$$

The machines will be saturated, and as a first approximation take $X_d = X_{q1}$, neglect resistance, and put $\delta_{12} = 90$ degrees. Then by (85) and (86)

$$E_{q1} = E_1 = \frac{271}{\sqrt{3}} = 157$$

$$E_{q2} = E_2 = \frac{280}{\sqrt{3}} = 162$$

$$I = \frac{E_1 \angle 90^\circ - E_2}{jX_{12}} = \frac{j157 - 162}{j19.5} = 8.05 + j8.30 = 11.91 \angle 45.9^\circ$$

$$I_{d1} = 11.91 \sin (90-45.9) = 8.05$$

$$I_{d2} = 11.91 \sin 45.9 = 8.30$$

$$P = \frac{E_1 E_2}{X_{12}} \sin \delta_{12} = \frac{157 \times 162}{19.5} \sin 90^\circ = 1305 \text{ Test (1220)}$$

The values of I_{d1} and I_{d2} correspond on Fig. 33 to values of $X_{d1} = 5.1$ and $X_{d2} = 5.1$. Then as a second approximation, (85) and (86) become

$$\begin{aligned} 157 &= \left[1 + \left(\frac{5.1 - 4.5}{19.5} \right) \sin 86.9^\circ \right] E_{Q1} - \left[\left(\frac{5.1 - 4.5}{19.5} \right) \sin (\delta_{12} + 86.9^\circ) \right] E_{Q2} \\ &= 1.03 E_{Q1} - 0.03 \sin (\delta_{12} + 86.9^\circ) E_{Q2} \end{aligned}$$

$$\begin{aligned} 162 &= \left[1 + \left(\frac{5.1 - 4.5}{19.5} \right) \sin 86.9^\circ \right] E_{Q2} - \left[\left(\frac{5.1 - 4.5}{19.5} \right) \sin (86.9^\circ - \delta_{12}) \right] E_{Q1} \\ &= 1.03 E_{Q2} - 0.03 \sin (86.9^\circ - \delta_{12}) E_{Q1} \end{aligned}$$

These equations may be solved simultaneously and a curve plotted of E_{Q1} and E_{Q2} as functions of δ_{12} . In the neighborhood of $\delta_{12} = 90$ degrees the values do not vary appreciably from $E_{Q1} = 152$ and $E_{Q2} = 158$. Hence by (87) and (88)

$$P_1 = \frac{152^2}{19.5} \cos 86.9^\circ - \frac{152 \times 158}{19.5} \cos (\delta_{12} + 86.9^\circ) = 64 - 1230 \cos (86.9^\circ + \delta_{12})$$

$$P_2 = \frac{158^2}{19.5} \cos 86.9^\circ - \frac{152 \times 158}{19.5} \cos (86.9^\circ - \delta_{12}) = 69 - 1230 \cos (86.9^\circ - \delta_{12})$$

The maximum powers are

$$P_{1(\max)} = +1294 \text{ at } \delta_{12} = 93.1^\circ$$

$$P_{2(\max)} = -1161 \text{ at } \delta_{12} = 86.9^\circ$$

24. Power Equation (round rotor)

The voltage equation for the round rotor generator is

$$\mathbf{E} = \mathbf{V} + (R + jX_s)\mathbf{I} \quad (90)$$

and the motor equation is given by substituting $-\mathbf{I}$ for \mathbf{I} .

Taking \mathbf{V} as reference vector, and putting $\mathbf{E} = E \angle \delta$, the current is

$$\mathbf{I} = \frac{\mathbf{E} - \mathbf{V}}{R + jX_s} = \frac{(E \cos \delta - V) + jE \sin \delta}{R + jX_s} \quad (91)$$

The terminal output of a generator is the product of the *conjugate* of its terminal voltage by its current, hence by (90)

$$\begin{aligned} P + jQ &= \hat{\mathbf{V}}\mathbf{I} = [\mathbf{E} - (R - jX_s)\mathbf{I}]\mathbf{I} \\ &= \mathbf{E}\mathbf{I} - R\mathbf{I}^2 + jX_s\mathbf{I}^2 \end{aligned} \quad (92)$$

The term (EI) is the input to the generator, the term (RI^2) its copper loss, and the term (XI^2) its reactive volt-amperes. An equation independent of I is obtained from (91),

$$\begin{aligned} P + jQ = \hat{V}I - V(E \cos \delta - V + jE \sin \delta) \frac{R}{Z_s^2} - \frac{jX_s}{Z_s^2} \\ = \frac{R(V'E \cos \delta - V^2) + X_s V'E \sin \delta}{Z_s^2} \\ + j \frac{RVE \sin \delta - X_s(V'E \cos \delta - V^2)}{Z_s^2} \quad (93) \end{aligned}$$

and putting $\alpha = \tan^{-1} \frac{R}{X_s}$ this becomes

$$P + jQ = \left[\frac{VE}{Z_s} \sin(\delta + \alpha) - \frac{RV^2}{Z_s^2} \right] + j \left[\frac{X_s V^2}{Z_s^2} - \frac{VE}{Z_s} \cos(\delta + \alpha) \right] \quad (94)$$

For negative δ the power output becomes negative (meaning that the machine is taking power *from* the line, that is a motor).

The generator *input* is greater than (93) by the $(R - jX_s)I^2$ terms of (92). By (91)

$$I^2 = \frac{(E \cos \delta - V)^2 + E^2 \sin^2 \delta}{Z_s^2} = \frac{E^2 + V^2 - 2VE \cos \delta}{Z_s^2} \quad (95)$$

Hence the generator input is, by (94) and (95),

$$\begin{aligned} P_u + jQ_u = P + jQ + RI^2 - jX_s I^2 \\ \left[\frac{VE}{Z_s} \sin(\delta + \alpha) + \frac{RE^2}{Z_s^2} \right] + j \left[\frac{VE}{Z_s} \cos(\delta + \alpha) - \frac{X_s E^2}{Z_s^2} \right] \quad (96) \end{aligned}$$

For negative δ the machine is a motor, and its power input becomes negative. The motor (gross) power output therefore is

$$P_m = \frac{VE}{Z_s} \sin(\delta + \alpha) - \frac{RE^2}{Z_s^2} \cong \frac{VE}{X_s} \sin \delta \quad (97)$$

Net mechanical power output is less than this by the friction and windage.

The *stiffness coefficient* of the motor is

$$\frac{dP}{d\delta} = \frac{VE}{Z_s} \cos(\delta + \alpha) \cong \frac{VE}{Z_s} \cos \delta \quad (98)$$

This is zero for $\delta = 90^\circ - \alpha$, at which value the motor output reaches a maximum of

$$P_{m(\max)} = \frac{VE}{Z_s} - \frac{RE^2}{Z_s^2} \cong \frac{VE}{X_s} \quad (99)$$

A low impedance machine is *stiffer*, and has a higher pull-out power, than

a high impedance machine. Increasing the excitation, E , increases the stiffness and pull-out power, not only because E itself is increased, but also because X_s decreases on account of saturation.

Solving (99) for E , we find

$$E = \frac{Z_s}{2R} [V \pm \sqrt{V^2 - 4RP_{m(\max)}}] \quad (100)$$

as the two limiting excitations for a power output P_m .

Maximum power with respect to E or X_s may be found from the power equation (99), but the results are of little practical importance. The value of E so found is far into the region of saturation, and the value of X_s so found is much too small for a practical machine. In both cases the currents are excessive. The foregoing equations assume an *unsaturated* machine, and they do not apply under conditions of marked saturation.

25. Power Equations (salient pole)

The terminal power for a salient pole synchronous generator has been shown to be (neglecting resistance)

$$P = VI \cos \varphi = \frac{E_f V}{X_d} \sin \delta + V^2 \frac{X_d - X_q}{2X_d X_q} \sin 2\delta \quad (101)$$

This equation applies equally well to a motor if $-I$ is substituted for I . The round rotor machine equation is given by the special case $X_d = X_q = X_s$.

The power or torque of a salient pole machine contains a term

$$V^2 \frac{X_d - X_q}{2X_d X_q} \sin 2\delta \quad (102)$$

independent of the excitation E . This is the so-called *reluctance torque*, and is due to the variation of reluctance in the air gap. The rotating field of armature reaction has maximum flux linkages when the magnetomotive force is centered on a pole, and consequently the field pole will follow the magnetomotive force so as to insure these maximum flux linkages. This reluctance torque will allow the machine to operate synchronously and carry some load—sometimes as high as half the total load. Reluctance torque is of assistance in pulling a machine into step during synchronizing. Reluctance torque also occurs in the induction motor, because of the permeance variation between the stator and rotor teeth, and is responsible for sub-synchronous locking.

The rate at which the power varies with the torque angle has been

variously called *synchronizing power*, *stiffness of coupling*, *rigidity factor*, and *stability factor*. It is, from (101),

$$\frac{dP}{d\delta} = \frac{E_f V}{X_d} \cos \delta + 1^2 \frac{X_d - X_q}{X_d X_q} \cos 2\delta \quad (103)$$

Thus the increment of power for an increment of displacement is, to a first approximation,

$$\Delta P = \frac{dP}{d\delta} \Delta \delta \quad (104)$$

This is greater for a salient pole than for a round rotor machine, by the contribution of the reluctance torque. Thus salient pole machines are *stiffer* than round rotor machines.

At light loads, when δ is small, $\sin \delta \cong \delta$, and

$$P \cong \frac{E_f V}{X_d} \delta + 1^2 \frac{X_d - X_q}{X_d X_q} \delta^2 \quad (105)$$

$$\frac{dP}{d\delta} \cong \frac{E_f V}{X_d} + 1^2 \frac{X_d - X_q}{X_d X_q} \delta \quad (106)$$

The machine has maximum stiffness at small loads.

Equating (103) to zero yields as the condition for maximum power (with respect to torque angle at constant terminal and excitation voltages)

$$\begin{aligned} -E_f \cos \delta &= \frac{V}{X_q} (X_d - X_q) \cos 2\delta \\ &= \frac{V}{X_q} (X_d - X_q) (2 \cos^2 \delta - 1) \end{aligned} \quad (107)$$

from which

$$\cos \delta = \frac{-X_q E_f}{4V(X_d - X_q)} \pm \sqrt{\frac{1}{2} + \left[\frac{X_q E_f}{4V(X_d - X_q)} \right]^2} \quad (108)$$

(The negative sign before the radical does not yield reasonable results.) For a round rotor machine, $X_d = X_q = X_s$, (108) gives $\cos \delta = 0$ or $\delta = 90^\circ$. Maximum power for the salient pole machine occurs at a smaller angle, $\delta < 90^\circ$.

The insertion of the angle determined from (108) in (101) gives the maximum power. For greater values of δ the stability factor, $dP/d\delta$, of (103) becomes negative; that is in (104) ΔP is negative for positive $\Delta \delta$ and the machine will pull out of step. Maximum power is sometimes called *pull-out power* or the *limit of stability*, because if the motor is operating at maximum power and a small increment, ΔP , of load is added, the torque angle δ will increase, but at this new value of torque angle the motor can no longer carry the load and will drop out of synchronism.

26. Excitation Characteristics (round rotor)

The so-called *V-curves*, Fig. 35, of a synchronous motor are curves of armature current plotted against field current (or induced voltage) with constant power output as parameter. These characteristics take their

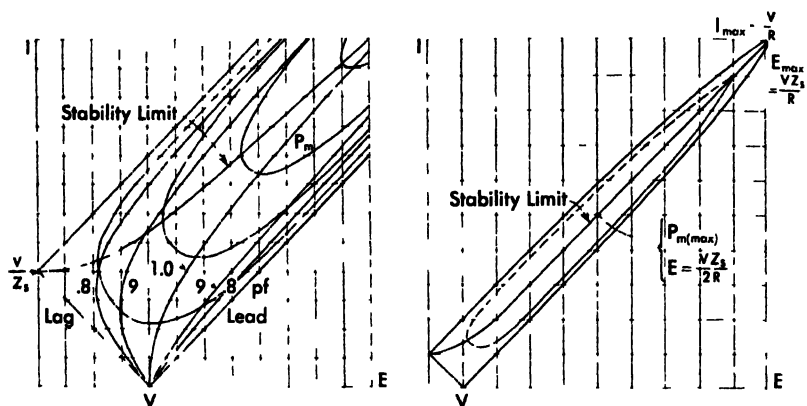


Fig. 35 Excitation characteristics.

name from the shape of the operating portions of the curves. If continued theoretically (into regions of instability) they become oval-shaped closed curves, and are sometimes referred to as *O-curves*. Since these characteristics depend on the degree of saturation in the machine, the exact field current should be calculated by one of the appropriate methods given in previous sections. Before carrying out such a calculation in an example, it will be instructive to study the general nature of *V-curves* by ignoring saturation.

By (91), the current squared is

$$I^2 = \frac{E^2 + V^2 - 2VE \cos \delta}{Z_s^2} \quad (109)$$

from which
$$\cos \delta = \frac{E^2 + V^2 - Z_s^2 I^2}{2VE} \quad (110)$$

and therefore
$$\sin \delta = \sqrt{1 - \left(\frac{E^2 + V^2 - Z_s^2 I^2}{2VE} \right)^2} \quad (111)$$

Expanding (97) and substituting (110) and (111)

$$P_m = \frac{VE}{Z_s} \sin \delta \cos \alpha + \frac{VE}{Z_s} \cos \delta \sin \alpha - \frac{RE^2}{Z_s^2}$$

$$= \frac{X_s}{2Z_s^2} \sqrt{4V^2E^2 - (E^2 + V^2 - Z_s^2I^2)^2} \\ + \frac{R}{2Z_s} (E^2 + V^2 - Z_s^2I^2) - \frac{RE^2}{Z_s^2}$$

Transposing and squaring to eliminate the radical, and rearranging, there results the quadratic equation in I^2 ,

$$Z_s^4I^4 + [2Z_s^2(E^2 - V^2) - 4X_s^2E^2 + 4RZ_s^2P_m]I^2 \\ + [(E^2 - V^2)^2 + 4RP_m(E^2 - V^2) + 4Z_s^2P_m^2] = 0 \quad (112)$$

Plots of I versus E with P_m as parameter are the (unsaturated, round rotor) O -curves.

The apexes of the V -curves are for unity power factor, because the current for a given power is then a minimum. The left-hand branches of the V -curves are for lagging power-factor, since a synchronous motor draws a lagging current for low excitations. The right hand branches are for leading power factor, as an over excited motor draws a leading current.

The *zero-output* characteristic may be found from (112) by putting $P_m = 0$. It reduces to

$$(Z_s^2I^2 + 2X_sEI + E^2 - V^2)(Z_s^2I^2 - 2X_sEI + E^2 - V^2) = 0 \quad (113)$$

This pair of ellipses specifies the outside boundary of the V -curves.

The *stability limit* is defined by substituting (99) in (112). After some rearrangement there results

$$Z_s^2I^2 - \left(E - \frac{R}{Z_s}V\right)^2 - \left(\frac{X_s}{Z_s}V\right)^2 = 0 \quad (114)$$

This hyperbola, plotted in Fig. 35, shows the maximum power, or stability limit, for a given excitation. Portions of the O -curves above this limit must therefore depict operation beyond the limit of stability, and are consequently not realizable. They are shown dotted. The excitation limits for a fixed power output are where the O curve intersects the stability limit curve. These points may be checked by (100).

The condition for maximum power with respect to excitation is, from (99),

$$\frac{dP_{m(\max)}}{dE} = \frac{V}{Z_s} - 2 \frac{R}{Z_s^2} E = 0$$

or

$$E = \frac{VZ_s}{2R} \quad (115)$$

On the stability limit curve this point is the center of the O -curves.

It is convenient to superimpose on the *O*-curves, the motor *compounding curves*. These are curves of armature current *vers* excitation (*E* or *I_f*), with pf as parameter. For a motor, putting $I = -I/\phi$ and $V = V/(1)$ in (90),

$$\begin{aligned} E &= V - (R + jX_s)I(\cos \phi + j \sin \phi) \\ &= (V - RI \cos \phi + X_s I \sin \phi) - j(RI \sin \phi + X_s I \cos \phi) \end{aligned}$$

Taking the sum of the squares of the real and imaginary components, there results, after some simplification,

$$E^2 = V^2 + X_s^2 I^2 + 2VI(X_s \sin \phi - R \cos \phi) \quad (116)$$

This hyperbola defines a set of constant power-factor curves. The unity-pf curve is given by $\phi = 0$. Positive values of ϕ are for leading pf and negative values of ϕ for lagging pf. Every pf curve originates in Fig. 35 at $I = 0$ and $E = V$.

27. Excitation Characteristics (salient pole motor)

If resistance is neglected, the torque angle of a salient pole motor may be found from (53) upon putting $R = 0$, and reversing the current by adding π to ϕ ,

$$\tan \delta = \frac{X_q I \cos \phi}{V - X_q I \sin \phi} \quad (117)$$

From this expression there are readily found

$$\sin \delta = \frac{X_q I \cos \phi}{\sqrt{V^2 - 2X_q V I \sin \phi + X_q^2 I^2}} \quad (118)$$

$$\cos \delta = \frac{V - X_q I \sin \phi}{\sqrt{V^2 - 2X_q V I \sin \phi + X_q^2 I^2}} \quad (119)$$

The power equation, (101), of the motor may be written

$$P = VI \cos \phi = \frac{EV}{X_d} \sin \delta + V^2 \frac{X_d - X_q}{X_d X_q} \sin \delta \cos \delta \quad (120)$$

Substituting (118) and (119) in (120), transposing and squaring to eliminate the radical, and simplifying, there results

$$E = \frac{V^2 - (X_d + X_q) VI \sin \phi + X_d X_q I^2}{\sqrt{V^2 - 2X_q V I \sin \phi + X_q^2 I^2}} \quad (121)$$

This is the equation for the compounding curves of the (unsaturated) salient pole motor. The open-circuit voltage *E* may be plotted against the armature current *I*, for any constant pf angle ϕ . If $X_q = X_d$, as in a round-rotor machine, (121) reverts to (116) for no resistance.

The equation for the V -curves is easily found. From (120)

$$VI \sin \phi = \sqrt{V^2 I^2 - I^2 \tilde{I}^2} \cos^2 \phi = \sqrt{V^2 I^2 - P^2} \quad (122)$$

and substituting this in (121) there results

$$E = \frac{V^2 - (X_d + X_q) \sqrt{V^2 I^2 - P^2} - P^2 + X_d X_q I^2}{\sqrt{V^2 - 2X \sqrt{V^2 I^2 - P^2} + X^2 I^2}} \quad (123)$$

This equation permits the open circuit voltage E to be plotted against the armature current I , with the power, P , as parameter. The V -curves of the salient pole machine are of the same general shape as those for the round-rotor motor. If $X_d = X_q$, (122) reverts to (112) for zero resistance.

Problems

1. Carry out in detail the steps leading to (112), (113), (114), and (116) showing exactly how these equations are developed.

2. Show that when armature resistance is neglected that (112) reduces to

$$\sqrt{V^2 - E^2} + 1 = 2\sqrt{E(V - \sqrt{P^2})}$$

and that this is in good agreement with (112) below the stability limit.

3. If armature resistance is neglected, what are the shapes of the boundary curves of the O -curves?

4. A round rotor synchronous motor has a synchronous impedance $Z_s = 0.1 + j1.0$ (per unit) and terminal voltage $V = 1.0$.

(a) Plot its O -curves for $P_n = 0, 0.5, 1.0, 1.5, 2.0, P_{max}$.

(b) Plot the limit of stability curve.

(c) Plot the leading and lagging pf characteristics for $\text{pf} = 1.0, 0.8, 0.6$.

(d) Locate the following points: maximum excitation, maximum armature current, maximum power, armature current at zero excitation.

5. Prove that the theoretical O -curves have a maximum voltage and a maximum current respectively, of

$$E_{max} = \frac{VZ}{R} \quad \text{and} \quad I_{max} = \frac{V}{R}$$

(These are not possible operating points, however, since saturation would vitiate the results.)

6. Using the data given in the example following Sec. 19, plot the V -curves for $P = 0$, and $P = 1.0$ by one of the methods for calculating the excitation. These are true V -curves, as contrasted with the theoretical (no saturation) V -curves described in Sec. 26.

28. Mechanical Oscillations in Synchronous Machines

In the foregoing analysis of synchronous machines the speed, fixed by the frequency, has been assumed to be absolutely constant. There are a number of practical cases, however, for which variations of speed, such as oscillations, are superimposed on the mean synchronous speed of the machine. These variations may be occasioned by sudden changes in the load, or in the output of the prime mover, or they may be inherent in the nature of the load, as in the case of reciprocating compressors whose torque requirements contain decided harmonics. Under certain conditions, the mechanical oscillations of the rotor may cumulatively increase in magnitude and cause the motor to pull out of synchronism and stall. In the case of a generator, a sustained mechanical oscillation may cause perceptible flickering of lights. If the *natural period* of mechanical oscillations of a machine happens to be approximately (say within 20 per cent) equal to that of a pulsating load, there is danger of it pulling out of step. Transient stability studies resolve themselves into the problem of determining whether the sudden removal or application of a load will result in mechanical oscillations of such magnitude as to carry the rotor beyond the point at which the required power can be transferred. It is therefore of great importance to inquire, at least superficially, into the electromechanical transients of synchronous machines. However, a really comprehensive treatment of the subject is outside the scope of this text.

In general, when the torque angle, δ , is changing there are four separate torques acting on the machine rotor:

1. The normal synchronous motor torque
2. The induction motor torque due to the squirrel cage windings in the field poles (the amortisseur winding), as well as the field coils and field collars.
3. The accelerating torque required by the inertia of the rotor
4. The load torque

Each of these torques will be determined, then a general differential equation of motion will be set up, and solutions obtained under certain simplifying assumptions.

The developed power, in watts per phase, of a salient pole synchronous machine, ignoring resistance, is given by (101) as

$$P_m = \frac{EV}{X_d} \sin \delta + V^2 \frac{X_d - X_q}{2X_d X_q} \sin 2\delta$$

where δ is in electrical radians, the corresponding mechanical angle being $\delta_m = 2\delta$ P with $P = \text{No. of poles}$. If n_1 is the synchronous rpm of the machine, the corresponding torque in $lb\text{-ft}$ for an m phase machine is

$$\begin{aligned} T_1 &= \frac{33000}{746} \frac{m}{2\pi n_1} \left[\frac{E V}{X_d} \sin \frac{P\delta_m}{2} + V^2 \frac{X_d - X_q}{2X_d X_q} \sin P\delta_m \right] \\ &= K_0 \sin \frac{P\delta_m}{2} + K_1 \sin P\delta_m \end{aligned} \quad (124)$$

The slope (stability factor) of the torque curve at $\delta_m = \delta_0$ is

$$\left. \frac{dT_1}{d\delta_m} \right|_{\delta_m = \delta_0} = K_0 \frac{P}{2} \cos \frac{P\delta_0}{2} + K_1 P \cos P\delta_0 = K$$

so that for a small oscillation about an angle δ_0

$$T_1(\delta_m) = T_1(\delta_0) + K(\delta_m - \delta_0) \quad (125)$$

Suppose, now, that the revolving field of armature reaction is a maximum at a space angle ωt , reckoned from a stationary reference axis on the armature, Fig. 36. At the same time, suppose the field pole to have an instantaneous speed ω_0 and to lag the armature by the torque angle δ . Then

$$\omega - \omega_0 = \frac{d\delta}{dt},$$

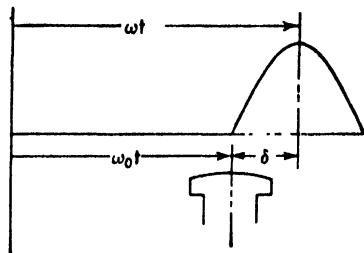


Fig. 36

$$\text{or the slip speed is } s\omega = \omega - \omega_0 = \frac{d\delta}{dt} = \frac{P}{2} \frac{d\delta_m}{dt} \quad (126)$$

For small slips the induction motor torque is proportional to the slip, hence by (Chap. 4, Eq. 38) and (126)

$$T_2 \cong \frac{33000}{746} \frac{mP}{4\pi n_1 R_2' \omega} \frac{d\delta_m}{dt} = H \frac{d\delta_m}{dt} \quad (127)$$

If synchronous and (instantaneous) rotor rpm are n_1 and n_0 respectively, then (126) may be written

$$\frac{\pi P}{60} (n_1 - n_0) = \frac{P}{2} \frac{d\delta_m}{dt} \quad (128)$$

The inertia torque of the rotor (opposing acceleration) then is

$$T_3 = J \frac{d}{dt} \frac{2\pi n_0}{60} = J \frac{d}{dt} \left(\frac{2\pi n_1}{60} - \frac{d\delta_m}{dt} \right) = -J \frac{d^2\delta_m}{dt^2} \quad (129)$$

in which J is the polar moment of inertia of the rotor and that of the connected load (referred to the rotor shaft) in lb-ft². For a ring it is

$$J = \frac{W}{64.4} (r_2^2 + r_1^2)$$

where

r_2 = outer radius (ft)

r_1 = inner radius (ft)

W = weight of ring

Finally, there is the load torque. This may consist of a constant term and a number of harmonics

$$T_1 = T + \sum T'' \sin \lambda t = T_0 + T' + \sum T'' \sin \lambda t \quad (130)$$

where for future convenience the constant term has been expressed as the sum of a term T_0 existing prior to the change in load, and a part T' representing the increment of load placed on the machine by the change.

The condition of torque equilibrium is

$$\left(\begin{array}{c} \text{synchronous} \\ \text{motor} \\ \text{torque} \end{array} \right) + \left(\begin{array}{c} \text{induction} \\ \text{motor} \\ \text{torque} \end{array} \right) = \left(\begin{array}{c} \text{torque to} \\ \text{overcome} \\ \text{inertia} \end{array} \right) + \left(\begin{array}{c} \text{torque} \\ \text{required by} \\ \text{the load} \end{array} \right)$$

that is

$$T_1 + T_2 = T_3 + T_4 \quad (131)$$

Substituting (125), (127), (129), and (130) in (131), and rearranging, yields the differential equation of motion

$$J \frac{d^2 \delta_m}{dt^2} + H \frac{d \delta_m}{dt} + K_0 \sin \frac{P \delta_m}{2} + K_1 \sin P \delta_m = T_0 + T' + \sum T'' \sin \lambda t \quad (132)$$

This equation cannot be solved by analytical methods and recourse must be had to solutions by means of mathematical machines, or involved step-by-step solutions. However, in terms of the approximation of (125) we have

$$J \frac{d^2 \delta_m}{dt^2} + H \frac{d \delta_m}{dt} + K(\delta_m - \delta_0) + T_1(\delta_0) = T_0 + T' + \sum T'' \sin \lambda t \quad (133)$$

This equation is to be solved subject to the initial conditions:

$$\left. \begin{array}{l} \delta_m = \delta_0 \text{ at } t = 0 \\ T' = 0 \text{ at } t = 0- \\ T'' = 0 \text{ at } t = 0- \end{array} \right\} \quad (134)$$

It will be convenient to put

$$\delta_m = \delta_0 + \delta' \quad (135)$$

in which δ_0 is the steady state torque angle just prior to the disturbance. Since under steady state conditions both the inertia torque and the induction motor torque are zero, it follows from (133) and (134) that $T_1(\delta_0) = T_0$. Hence, substituting (135) in (133) reduces the latter to

$$J \frac{d^2\delta'}{dt^2} + H \frac{d\delta'}{dt} + K\delta' = T' + \sum T'' \sin \lambda \quad (136)$$

subject to the initial condition $\delta' = 0$ at $t = 0$.

The solution of an ordinary differential equation with constant coefficients is in two parts: (1) the complementary solution, and (2) the particular integral. The former is the solution of the auxiliary equation

$$J \frac{d^2\delta'}{dt^2} + H \frac{d\delta'}{dt} + K\delta' = 0 \quad (137)$$

Try $Ae^{\gamma t}$ as a solution by substituting it in (137), giving

$$J\gamma^2 Ae^{\gamma t} + H\gamma Ae^{\gamma t} + KAe^{\gamma t} = 0 \quad (138)$$

Cancelling the $Ae^{\gamma t}$, and solving the quadratic for γ , we find the two permissible values to be

$$\gamma_1, \gamma_2 = \frac{-H}{2J} \pm \sqrt{\left(\frac{H}{2J}\right)^2 - \frac{K}{J}} \quad (139)$$

There are three possible cases involved in (139):

Case	Roots γ_1 and γ_2	Type of transient
$\left(\frac{H}{2J}\right)^2 > \frac{K}{J}$	real and distinct	non-oscillatory
$\left(\frac{H}{2J}\right)^2 = \frac{K}{J}$	real and equal	aperiodic
$\left(\frac{H}{2J}\right)^2 < \frac{K}{J}$	complex $(-\alpha \pm j\beta)$	damped oscillatory

If there are no amortisseur windings, $H = 0$, and only an oscillatory solution is possible.

In the damped oscillatory case, the *natural frequency of oscillation* of the rotor is

$$f_0 = \frac{\beta}{2\pi} \quad (140)$$

Since both K and H depend upon the applied voltage, and K also on the excitation, it is evident that β , and therefore f_0 , are not absolutely con-

stant for a given machine. The natural frequency is further affected by the degree of saturation in the machine.

Corresponding to each root of (139) there is an integration constant, and adding the particular integral (see any standard text on *Differential Equations*), the complete solution for the non-oscillatory case is found to be

$$\delta' = A_1 e^{\gamma_1 t} + A_2 e^{\gamma_2 t} + \frac{T'}{K} + \sum \frac{T'' \sin(\lambda t - \theta)}{\sqrt{(K - \lambda^2 J)^2 + \lambda^2 H^2}} \quad (141)$$

$$\text{where} \quad \theta = \tan^{-1} \frac{\lambda H}{K - \lambda^2 J} \quad (142)$$

For the oscillatory case, substitute in (141)

$$\begin{aligned} A_1 e^{\gamma_1 t} + A_2 e^{\gamma_2 t} &= A_1 e^{(-\alpha + j\beta)t} + A_2 e^{(-\alpha - j\beta)t} \\ &= (A_1 + A_2) e^{-\alpha t} \cos \beta t + j(A_1 - A_2) e^{-\alpha t} \sin \beta t \\ &= A e^{-\alpha t} \cos \beta t + B e^{-\alpha t} \sin \beta t \end{aligned} \quad (143)$$

Then for this case

$$\delta' = A e^{-\alpha t} \cos \beta t + B e^{-\alpha t} \sin \beta t + \frac{T'}{K} + \sum \frac{T'' \sin(\lambda t - \theta)}{\sqrt{(K - \lambda^2 J)^2 + \lambda^2 H^2}} \quad (144)$$

It remains to determine the integration constants when the torques T' and T'' are suddenly applied to the machine at $t = 0$. At this instant $\delta' = 0$, and since speed cannot change instantaneously, $d\delta'/dt = 0$. Hence by (144)

$$\delta' \Big|_{t=0} = 0 = A + \frac{T'}{K} + \sum \frac{T'' \lambda H}{(K - \lambda^2 J)^2 + \lambda^2 H^2} \quad (145)$$

$$\frac{d\delta'}{dt} \Big|_{t=0} = 0 = -\alpha A + \beta B + \sum \frac{T'' \lambda (K - \lambda^2 J)}{(K - \lambda^2 J)^2 + \lambda^2 H^2} \quad (146)$$

$$\text{Therefore,} \quad A = -\frac{T'}{K} + \sum \frac{T'' \lambda H}{[(K - \lambda^2 J)^2 + \lambda^2 H^2]} \quad (147)$$

$$B = -\frac{\alpha T'}{\beta K} + \sum \frac{T'' \lambda [\alpha H - (K - \lambda^2 J)]}{\beta [(K - \lambda^2 J)^2 + \lambda^2 H^2]} \quad (148)$$

In the case of a machine without damper windings, $H = 0$, and by (139) it is seen that

$$\alpha = 0 \quad \text{and} \quad \beta = \sqrt{\frac{K}{J}}$$

$$\text{Then by (147)} \quad A = -\frac{T'}{K} \quad (149)$$

$$B = - \sum \frac{T'' \lambda}{\beta(K - \lambda^2 J)} \quad (150)$$

which in (144) gives

$$\delta' = \frac{T''}{K} (1 - \cos \beta t) - \sum \frac{T''}{\beta(\beta^2 - \lambda^2)J} (\lambda \sin \beta t - \beta \sin \lambda t) \quad (151)$$

This equation shows two extremely interesting phenomena. First, due to the sudden application of the constant load increment T'' , there ensues an oscillation at the natural frequency of the machine, causing the torque angle to pulsate by an amount $(2T''/K)$. This in itself may be sufficient to throw the machine out of step. At least for large enough values of T' the oscillation can become critical. Second, if the frequency of the load torque is nearly equal to the natural frequency of the machine, $\lambda = \beta$, mechanical resonance will occur. The last term of (151) is indeterminate for $\lambda = \beta$, since

$$\frac{\lambda \sin \beta t - \beta \sin \lambda t}{\beta^2 - \lambda^2} \Big|_{\lambda = \beta} = \frac{0}{0} \quad (152)$$

But evaluating this indeterminate by differentiating numerator and denominator with respect to β , we have

$$\frac{\lambda \cos \beta t - \sin \lambda t}{2\beta} \Big|_{\lambda = \beta} = \frac{t}{2} \cos \beta t - \frac{1}{2\beta} \sin \lambda t \quad (153)$$

and this is seen to increase without limit as $t \rightarrow \infty$. Even if the ratio λ/β is considerably less than unity, the latter term of (151) may reach high values. It is instructive to plot (152) for a range of values of λ/β between zero and unity. Of course, there is always some damping present, and the exponential decrements of (144) cause the oscillations to die out.

The vector diagram of an oscillating motor is indicated in Fig. 37. Steady state conditions show the excitation voltage E at a torque angle δ_0 and a motor output current I . If, now, the rotor oscillates through an angle $\Delta\delta$ about its mean position, the excitation voltage remaining constant in magnitude, the impedance voltage $(E - V)$ may experience considerable variation, and with it the current

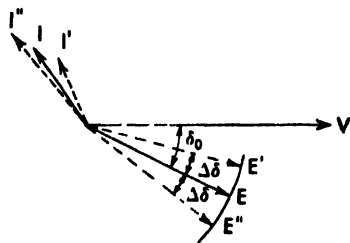


Fig. 37

$$I = \frac{E - V}{jX_s} \quad (154)$$

When $\delta = \delta_0 - \Delta\delta$, the current, I' , is small, and so is the power taken by the motor. The rotor therefore slows down, increasing the angle to $\delta = \delta_0 + \Delta\delta$. At this angle the current, I'' , becomes large, and with it the power, causing the rotor to speed up. The cycle repeats at a natural frequency fixed by the inertia of the rotating parts and by the machine constants, until damped out by the pole face windings, or until the machine falls out of synchronism. This phenomenon is usually called *hunting*. There are three ways in which it can be guarded against: (1) by using a heavy flywheel to reduce the natural frequency to a value safely below the frequency of any incipient harmonic load torques which may be present, (2) by designing the machine with a suitable *stiffness factor*, and (3) by the employment of damper windings of low resistance which will absorb the energy in the oscillation. But the squirrel-cage windings of a synchronous motor are also used for starting, and too low a resistance may militate against desirable starting and pull-in characteristics. Sometimes double squirrel cages are used to gain the advantage of high starting torque and heavy damping effect.

It is not generally feasible to change the stiffness factor of a standard machine materially, owing to the necessity of designing for a specified maximum torque.

Example: A synchronous motor driving a reciprocating compressor has the following data:

200-hp	$W R^2 = 1400 \text{ lb-ft}^2$ (including load)
900-rpm	$R_2' = 0.16$ ohms per phase
60-cycles	$X_d = 0.78$
3 ϕ -Y	$X_q = 0.58$
440-volts (line)	$E = 615$ excitation volts (line)
Eff.-96%	pf = 0.80 lagging

The motor is operating at half load (100-hp) when an additional 100-hp load is suddenly thrown on. This causes the compressor to develop a 50-hp superimposed oscillatory component of torque at a frequency equal to 80 per cent the natural frequency of oscillation of the set. Plot a curve showing the variation with time of the torque angle.

The motor has 8 poles, and therefore the electrical angle is 4 times the mechanical angle. The motor (synchronous) torque is, by (124),

$$T_1 = 7.04 \frac{3}{900} \left[\frac{354 \times 254}{0.78} \sin \delta + 254^2 \frac{0.78 - 0.58}{2 \times 0.78 \times 0.58} \sin 2\delta \right]$$

$$= 2710 \sin \frac{8\delta_m}{2} + 334 \sin 4\delta_m \text{ lb-ft}$$

The torque requirement at half load (100-hp) is

$$T_0 = \frac{33000 \times 100}{2\pi \times 900} = 582 \text{ lb-ft}$$

Equating the synchronous motor torque to the load torque and solving for the initial torque angle, we find $\delta_0 = 2.5$ degrees (mechanical).

The stability factor, (125), is

$$K = 2710 \times \frac{8}{2} \cos \frac{8 \times 2.5}{2} + 334 \times 8 \cos (8 \times 2.5) = 13200$$

The induction motor torque factor, (127), is

$$H = \frac{33000}{746} \frac{3 \times 8}{4\pi \times 900} \frac{254^2}{2\pi \times 60 \times 0.16} = 100$$

The polar moment of inertia of the motor and compressor is

$$J = \frac{W R^2}{g} = \frac{1400}{32.2} = 43.5$$

By (139), the decrement factor and angular velocity are

$$-\alpha + j\beta = \frac{-100}{2 \times 43.5} + j \left[\left(\frac{100}{2 \times 43.5} \right)^2 - \frac{13200}{43.5} \right] = -1.15 + j17.4$$

and by (140) the natural frequency is

$$f_0 = \frac{17.4}{2\pi} = 2.76 \text{ cycles per second}$$

The angular velocity of the compressor pulsation is $\lambda = 0.80 \times 17.4 = 13.9$ radians per second and the torque magnitude of this pulsation is

$$T'' = 0.25 \times 1164 = 291 \text{ lb ft}$$

The constant component of the load increment is

$$T' = 0.50 \times 1164 = 582 \text{ lb ft}$$

The integration constants, by (147) and (148), are

$$A = -\frac{582}{13200} + \frac{291 \times 13.9 \times 100}{[(13200)^2 - 13.9^2 \times 43.5]^2 + 13.9^2 \times 100^2} = -0.028$$

$$\begin{aligned} B &= -\frac{1.15}{17.4} \frac{582}{13200} + \frac{291 \times 13.9 [1.15 \times 100 - (13200 - 13.9^2 \times 43.5)]}{17.4 [(13200)^2 - 13.9^2 \times 43.5]^2 + 13.9^2 \times 100^2} \\ &= -0.047 \end{aligned}$$

Finally, by (144), the angular velocity oscillation is

$$\begin{aligned}\delta' &= -0.028e^{-1.15t} \cos 17.4t - 0.047e^{-1.15t} \sin 17.4t \\ &\quad + \frac{582}{13200} + \frac{291 \sin (13.9t - 16.2^\circ)}{4990} \\ &= 0.054e^{-1.15t} \cos (17.4t - 59.2^\circ) + 0.044 + 0.058 \sin (13.9t - 16.2^\circ)\end{aligned}$$

The torque-angle curve for this motor is shown in Fig. 38. The variation of the angular displacement, δ , (in electrical degrees) is shown in Fig. 39. It is clear that the 25 per cent oscillatory component of the

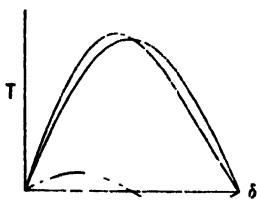


Fig. 38

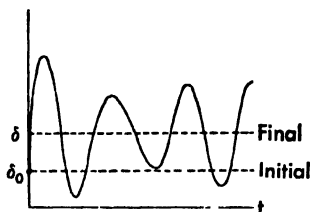


Fig. 39

load torque is responsible for a 65 per cent oscillation in the angle. But the machine stays in step.

Problems

1. In the example of Sec. 28, what value of H would be necessary to prevent oscillations due to a change in load? What effect would this have on the "forced" oscillation due to T'' ? Plot the oscillation.
2. In the example of Sec. 28, suppose $H = 0$. Plot the oscillation.
3. In the example of Sec. 28, suppose T'' to be negative. Determine and plot the oscillation.

20. Starting of Synchronous Motors

Synchronous motor torque, *per se*, is zero at start, and is alternately positive and negative at speeds below synchronous. It is therefore necessary to provide auxiliary means for starting. Early designs actually used separate starting motors, sometimes employing the exciter in this role, or using the d-c generator in the case of motor-generator sets. Very small synchronous motors will start, without load, due to the eddy currents induced in their pole faces, but this torque is inadequate in the larger sizes. Modern synchronous motors are started and brought up to speed as induction motors. For this purpose squirrel-cage windings (also called *amortisseur* or *dumper* windings) are embedded in the pole faces. They perform the dual job of starting the motor and of damping

out transient oscillations in the speed. For the starting function they should have high resistance (in order to provide high starting torque at reasonable starting current), but a high-resistance winding will have a large slip at full load and may prove ineffective in bringing the speed up to a point where the motor will pull into step as a synchronous machine (usually at about 95 per cent speed). Moreover, a high resistance is not suitable for damping out oscillations. Thus the design of the amortisseur winding is a compromise. Double squirrel cage, deep bars, and wound rotor construction have all been employed. In cases where the starting current must be limited, starting compensators, series reactors, or external resistors, may be used, just as in the starting of polyphase induction motors.

The so-called *supersynchronous* motor has been developed for heavy starting duty. Its armature is mounted in cradle bearings and is free to rotate, unless clamped and held stationary by a large brake band. In starting, the brake is released and the armature, revolving backward, is brought up to speed and into step. The brake is then gradually applied, and since the relative speed between rotor and armature remains constant at synchronous speed, the rotor must pick up speed to exactly the same extent that the armature slows down. This is an expensive construction, and used only where necessary.

At standstill, the field winding acts as the secondary of a transformer, of which the armature winding is the primary, and because there are a great number of turns in the field winding, its induced voltage may be dangerous to both life and the insulation. To alleviate this situation, the field winding is sometimes opened at several places during starting, and then automatically reconnected by centrifugal devices as the motor comes up to speed. Or the field may be short circuited through a resistor, but this may result in a torque opposing the acceleration.

A complete analysis of starting phenomena is beyond the scope of this text, since it involves the whole theory of electromechanical transients in synchronous machines. However, if induced field currents and transient reactances be ignored, a crude approximation to the ruling differential equation would be (132) with the $(Hd\delta_m/dt)$ term replaced by the complete expression for induction motor torque. At small values of slip, however, (132) can be taken as it is, and solutions sought for specified initial conditions of δ_m and $d\delta_m/dt$. But a solution in standard form is not known, and therefore dependence must be placed on mathematical machines or step-by-step solutions. In this way criteria have been arrived at as conditions for the pulling-into step of synchronous

motors.* Evidently, the possibility of pull-in depends upon the following factors:

1. Induction motor characteristic of the damper windings
2. Synchronous motor torque
3. Inertia of the rotating parts and the natural period of the motor
4. The torque-speed characteristic of the load
5. The torque angle δ_0 and speed of the motor at the instant the field is energized

A simplified physical idea of pull-in is supplied by Fig. 40. The motor starts as an induction motor, point 1, and has an induction motor

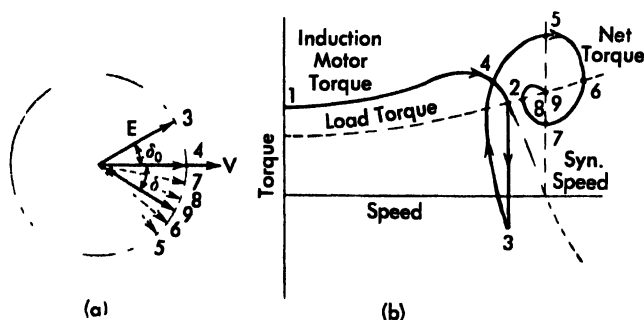


Fig. 40 Oscillations of a synchronous motor pulling into step

torque speed characteristic to point 2 where it intersects the load characteristic, and equilibrium conditions occur at some slip s . Suppose the field is then excited and at this instant the field poles happen to be at an angle δ_0 ahead of the terminal voltage V , Fig. 40a. The machine is then also a synchronous generator having a negative torque, which torque subtracted from the induction motor torque gives a net torque, point 3, considerably less than that required by the load, thus causing the slip to increase. The motor is running at less than synchronous speed, and therefore the torque angle δ is decreasing. There comes an instant, point 4, when δ is passing through zero and the synchronous motor torque is zero, so that the net torque is entirely induction motor torque, and being in excess of the load torque, causes the machine to accelerate. But the angle δ is now negative and continues to decrease because the speed is still below synchronous. This gives synchronous motor (positive) torque, which adds to the induction motor torque to

* Edgerton and Fourmarier "The Pulling into step of a Salient pole Synchronous Motor," *Trans. AIEE*, Vol. 50, p. 769, 1931

yield a net torque which causes the machine to accelerate. When it reaches synchronous speed, point 5, the angle δ is at its greatest negative value. As the speed continues to increase, δ decreases in magnitude, and with it the synchronous torque. Moreover, for speeds in excess of synchronism, the induction motor torque is negative. Thus the net torque rapidly decreases, and at some point 6 is just equal to the load torque. But as δ is continuing to close, the synchronous motor torque decreases still further and the rotor slows down. As the instantaneous speed once more falls below synchronous, δ begins to open up again, the synchronous motor torque increases, and the machine speeds up. Finally, these oscillations die out and the motor settles down to a stable synchronous speed, point 9. The sequence of events may be clarified by the following tabulation, in which the torques are shown as positive, negative, or zero; and a dominating torque by a double sign (+ +).

Point	Angle δ	Syn torque	Induction motor torque	Load torque	Inertia torque	Remarks
1		0	+ +	--		Acceleration
2		0	+		0	Constant speed
3	+	--	+	-	+	Field closed Deceleration
4	0	0	+ +	-	-	Acceleration δ decreasing
5		+ +	0			Synchronous speed
6	-	+ +	-		0	Above syn. speed
7	-	+	0	-	+	Synchronous speed Decelerating
8	-	+	+		0	Below syn. speed
9	-	+	0	-	0	Synchronous speed

Problem: Suppose the angle δ_0 in Fig. 40(a) is *negative* at the instant the field switch is closed. Sketch the torque-speed curve corresponding to Fig. 40(b), and draw up a table of events similar to that shown above.

30. Synchronizing

Before a synchronous machine is connected in parallel with an active bus it should meet three conditions:

1. Equal voltage
2. Same phase sequence, and
3. Identical frequency as on the bus

The procedure for bringing about these equalities, and paralleling the incoming machine at the proper instant, is called *synchronizing*. Equal voltages are indicated by a comparison of the voltmeter readings on the bus and on the incoming machine. Proper phase sequence may be determined once for all when the machine is first installed and is thereafter of no concern. One way in which phase sequence may be determined will be described presently. But to ascertain the exact instant when the frequencies are identical requires special provisions. The frequency of the incoming machine can be held only momentarily at exactly the same frequency as the bus. Suppose the bus frequency is f while that of the incoming machine is $(f + \Delta f)$, and the voltages are of equal magnitude. Then the voltage across the switch is

$$\begin{aligned} e &= V \cos (\omega + \Delta \omega)t - V \cos \omega t \\ &= -2V \sin \frac{\Delta \omega}{2} t \sin \left(\omega + \frac{\Delta \omega}{2} \right) t \end{aligned} \quad (155)$$

The first term of this equation, of frequency $\Delta f/2$, may be regarded as the variable amplitude, or envelope, of the average frequency oscillation represented by the second term. An oscillogram showing the *beat* frequency and the *carrier* frequency is given in Fig. 41. The beat frequency is very low as the machine approaches synchronism.

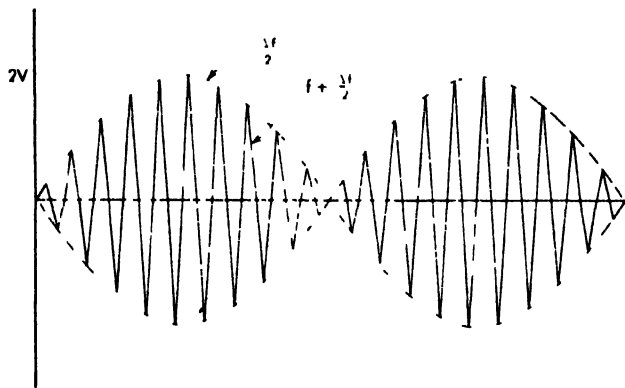


Fig. 41

The simplest method of synchronizing is by means of lamps connected directly, or through transformers, across the open switch terminals. Fig. 42. When the voltage triangles are of the same voltage, phase sequence, and frequency, the switch may be closed. If the voltages are

different, but the other two conditions complied with, all three lamps will glow, the brighter the greater the voltage difference. If the fre-

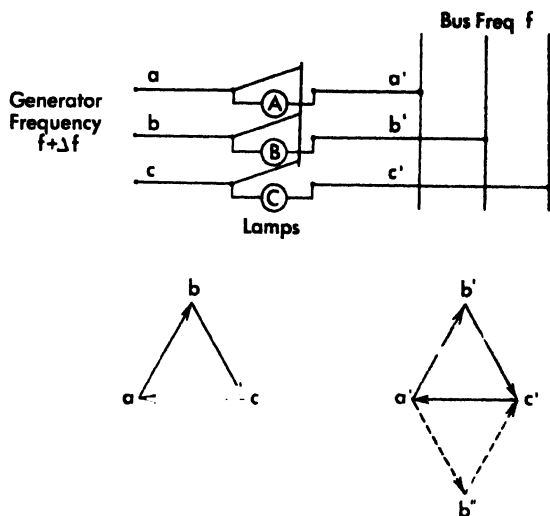


Fig. 42

quencies and voltages are equal, the voltage acting on lamps *A* and *B* will be

$$V_A + V_B = V_{ab} - \begin{cases} V_{a'b'} = 0 & \text{for proper phase sequence } a'b'c' \\ V_{ab} - \sqrt{3}V & \text{for wrong phase sequence } a'b''c' \end{cases} \quad (156)$$

But since the frequencies will differ slightly, the lamps will flicker in unison at beat frequency when the phase sequence is proper. When all lamps are dark the switch should be closed.

Various switchboard instruments, called *synchronoscopes*, have been developed to indicate the proper instant for synchronizing. The Lincoln synchronoscope, Fig. 43, has a field winding excited from the bus, and a split 2-phase armature winding excited by the incoming machine. One of its coils has a resistance and the other a reactance in series. When the bus and machine voltages are in phase, the armature coil having the resistance in series will be centered on the field pole and a vertical pointer will indicate synchronism. If the phase difference is 90 degrees, the other coil will align itself with the field. An intermediate position will be taken up for any other phase difference. If the frequencies differ, the armature will revolve in the clockwise direction if the incoming machine is too fast, and in the opposite direction if the incoming machine is too

slow. Thus the behavior of the instrument pointer indicates whether to speed up or slow down the incoming machine, as well as the most propitious moment for synchronizing.

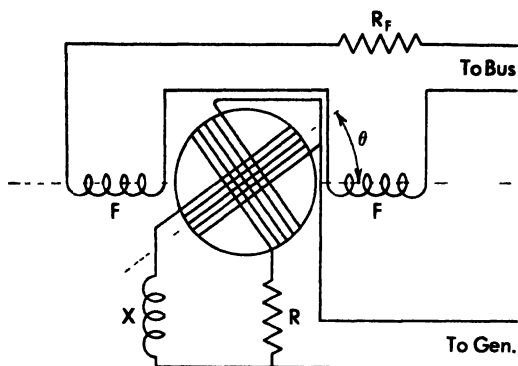


Fig. 43 The synchronoscope.

31. Parallel Operation of Synchronous Machines

When we consider a synchronous machine to be synchronized and connected in parallel with an active bus or another machine, four questions present themselves.

- (1) how does it adjust itself to the bus conditions,
- (2) what happens if its excitation is changed,
- (3) what determines the division of load between it and other machines on the bus, and
- (4) is parallel operation a stable state of affairs?

We shall see that maladjustments are rectified automatically by a circulating current resulting in torques of the proper sign; that changes in excitation have no effect on the flow of power but do change the power factor; that division of load is strictly a matter of the governor settings of the prime movers; and that parallel operation is inherently stable.

Consider two round rotor machines operating in parallel on the same bus, Fig. 44a.* Suppose the bus voltage, V , to be maintained constant by adjustment of the field, E_1 , of machine No. 1. The load current I , and its pf ϕ are given. Suppose the voltage, E_2 , and power, P_2 , of ma

* Single line diagrams, such as in Fig. 44a, are generally used in power work to represent polyphase systems.

chine No. 2 to remain unchanged. The problem is first to determine the initial operating conditions, and then to see how the system will adjust

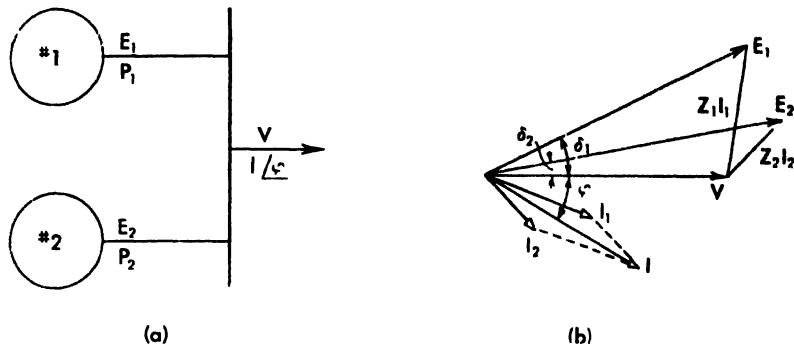


Fig. 44 Parallel operation

itself to various changes. By (68), the power output of No. 2 is

$$P_2 = E_2^2 \frac{R_2}{Z_2^2} - \frac{E_2 V}{Z_2} \cos(\delta_2 + \theta_2) \cong \frac{E_2 V}{Z_2} \sin \delta_2 \quad (157)$$

in which $Z_2 = \sqrt{R_2^2 + X_2^2}$ is the impedance of machine No. 2 and θ_2 is the impedance angle. Since P_2 and E_2 were specified as constant, the angle δ_2 is readily found from (157) as

$$\begin{aligned} \delta_2 &= \cos^{-1} \left(\frac{E_2 R_2}{V Z_2} - \frac{P_2}{E_2 V} Z_2 \right) = \cos^{-1} \left(\frac{R_2}{Z_2} \right) \\ &\cong \cos^{-1} \left(- \frac{P_2 X_2}{E_2 V} \right) = \frac{\pi}{2} \end{aligned} \quad (158)$$

The current supplied by No. machine 2 then is

$$I_2 = \frac{E_2 - V}{Z_2} = \frac{(E_2 \cos \delta_2 - V) + j E_2 \sin \delta_2}{R_2 + j X_2} \quad (159)$$

The current supplied by machine No. 1 then is

$$I_1 = I - I_2 = I \phi - I_2 \quad (160)$$

The excitation voltage of machine No. 1 therefore is

$$E_1 = V + Z_1 I_1 = E_1 \delta_1 \quad (161)$$

The power output of machine No. 1 is

$$P_1 = E_1^2 \frac{R_1}{Z_1^2} - \frac{E_1 V}{Z_1} \cos(\delta_1 + \theta_1) \cong \frac{E_1 V}{Z_1} \sin \delta_1 \quad (162)$$

The conditions given by the above equation are indicated in Fig. 44b.

As a special case, suppose the two machines to be idling on the bus;

that is, the external current to be zero, $I = 0$. Assume further, machine No. 2 to have zero power output and its voltage equal to the bus voltage, $E_2 = V$. Then according to (158), $\delta_2 = 0$, and according to (159) its current is also zero. Hence, $I_1 = 0$ by (160), and $E_1 = V$ by (161). Thus $\delta_1 = 0$ and both machine excitation voltages are in phase with the bus voltage, Fig. 45a.

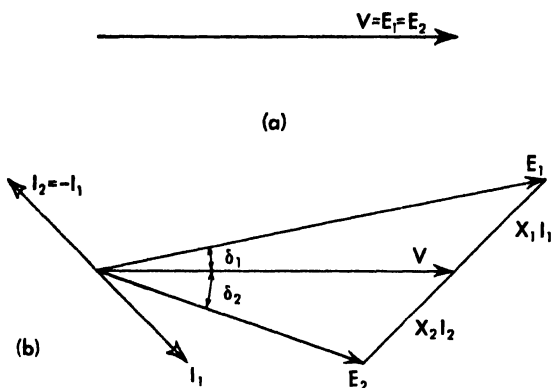


Fig. 45

But suppose $E_2 \neq V$. Then even though $P_2 = 0$, (158) shows a displacement angle δ_2 . Consequently, by (159), a current I_2 flows from machine No. 2, and by (160) an equal and opposite current $I_1 = -I_2$ flows from machine No. 1. In other words, there is now a *circulating current* flowing between the two machines. By (161) this circulating current will cause machine No. 1 to have a displacement angle δ_1 . There is a total angle $(\delta_1 + \delta_2)$ between the machine rotors. The power output, (162), of machine No. 1 is just sufficient to supply the losses, $(R_1 + R_2)I_2^2$. The diagram is shown in Fig. 45b. The circulating current, through armature reaction, decreases the excitation of the generator, No. 1, and increases that of the motor, No. 2.

Returning now to the loaded machines of Fig. 44, suppose the excitation of No. 2 to receive a positive increment ΔE_2 , but that its output, P_2 , remains unchanged. By (158) the angle δ_2 will experience a negative increment $-\Delta\delta_2$, that is, the angle δ_2 will shrink. The current I_2 will also fall back, by (159), and since the load current I remains constant, the current I_1 will be compelled to change its angular position and magnitude. This in turn results in corresponding changes in angle δ_1 and voltage E_1 such that new equilibrium conditions obtain.

Should either machine experience a momentary change of torque

angle, the system will return automatically to its old equilibrium condition. For example, should δ_2 decrease by $\Delta\delta_2$, with E_2 and P_2 unaltered, I_2 will decrease in magnitude, and shift back. This will require I_1 to shift forward and increase in magnitude, which in turn will cause δ_1 to increase by $\Delta\delta_1$. But now No. 1 will have a momentary higher output than is being supplied by its prime mover (assuming that the governor has had no time to act) and will tend to fall back, reducing δ_1 . And No. 2, with a lower power output than being supplied by its prime mover will speed up. Thus both actions tend to reduce the angle between machines and to return them to their equilibrium position. The system is inherently stable if the limits of stability are not exceeded by the momentary change. The change in power output of a machine for a small angular change is approximately

$$\Delta P = \frac{dP}{d\delta} \Delta\delta = \frac{EV}{X} \cos \delta \cdot \Delta\delta \quad (163)$$

This is the power tending to restore the rotor to its previous position.

For the salient pole machine it is

$$\Delta P = \left(\frac{EV}{X_d} \cos \delta + 1^2 \frac{X_d - X_q}{X_d X_q} \cos 2\delta \right) \cdot \Delta\delta \quad (164)$$

The load supplied by a synchronous machine is entirely a matter of the prime mover output, and this in turn depends on the governor setting. Figure 46 illustrates the way in which governor action permits a machine to pick up load. There are shown three *load-speed characteristics* a, b, c . These are approximately straight-line relationships with drooping characteristics, that is, the speed falls with an increase in load. Otherwise the machine would be unstable, for if a slight increase in speed resulted in an increase in output, the speed would continue to increase.

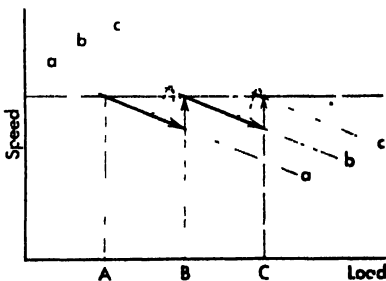


Fig. 46

Now any governor depending on centrifugal force cannot react until it has experienced an actual change in speed. Therefore, if the machine is operating on characteristic a at load A , and the load increases to B , the speed will fall off. When the governor responds to this change in speed, it will shift the prime mover output to characteristic b causing the speed to return to normal. A further increase in load to C will result

in a shift to another characteristic c . Thus the function of the governor is to shift the prime mover characteristic as required to meet the exigencies of the load changes. A very sluggish governor would permit excessive speed changes to accompany changes in load, and might very well allow the machine to fall out of step before the necessary additional prime mover power became available. On the other hand, a very sensitive governor might induce excessive hunting by responding too quickly, thereby causing power pulses. Too sensitive governors attempt to maintain a state of dynamic, rather than static, equilibrium by continually oscillating about the desired mean speed. This tendency is alleviated by dash pots and other mechanical damping devices.

The division of load between machines in parallel is fixed by the governor settings and the load. Referring to Fig. 47, suppose machines

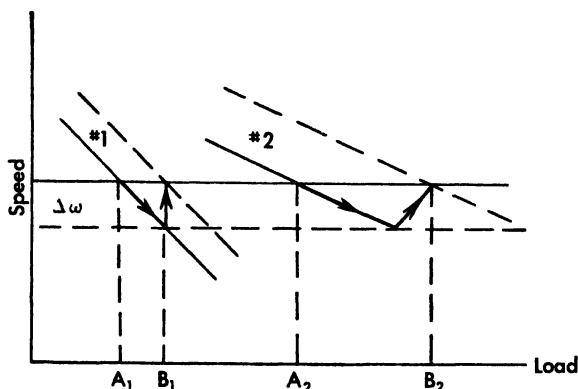


Fig. 47

No. 1 and No. 2 are in parallel operating on the full-line characteristics. If the load increases, resulting in a speed drop, $\Delta\omega$, and the governors do not respond, the new division of load between the two machines will be in different proportions than originally (unless the two characteristics are exactly parallel). But if the governors respond, shifting the machines to the dash line characteristics, the original division of load may be restored. Usually, in large power systems, certain machines operate at a fixed governor setting and constant output, and minor variations in the system load are cared for by one machine which has the responsibility of maintaining constant frequency. If it is desired to change the load on any other machine, its governor setting is changed by a fixed amount. Load division is dictated by considerations of relative efficiencies as well as ratings of the machines.

32. Circle Diagrams of the Synchronous Motor (round rotor)

There are a variety of ways in which circle diagrams may be constructed for the round rotor synchronous motor, of which a few will be discussed in this section. They are all based on the voltage equation

$$V = E + ZI \quad (165)$$

A circle diagram can be developed showing the locus of the armature current, I , as the excitation voltage, E , and its torque angle, δ , are varied. For this purpose select $V = V + j0$ as reference vector, and let $E = E \angle -\delta$ and $Z = Z \angle \beta$. Then (165) may be rewritten

$$I = \frac{V \angle 0}{Z \angle \beta} - \frac{E \angle -\delta}{Z \angle \beta} = \frac{V}{Z} \angle -\beta - \frac{E}{Z} \angle -\delta - \beta \quad (166)$$

or expanded

$$I = \left[\frac{V}{Z} \cos \beta - \frac{E}{Z} \cos (\delta + \beta) \right] + j \left[-\frac{V}{Z} \sin \beta + \frac{E}{Z} \sin (\delta + \beta) \right] \quad (167)$$

Then taking the sum of the squares of the real and imaginary components on both sides of the equation, there results the law of cosines,

$$I^2 = \frac{V^2}{Z^2} + \frac{E^2}{Z^2} - 2 \frac{V E}{Z Z} \cos \delta \quad (168)$$

These equations are interpreted by the vector and circle diagrams of Fig. 48. The voltage vector diagram (V , E , ZI) obviously corresponds to (165). According to (166), the current vector, I , is compounded of the fixed vector $(V/Z) \angle -\beta$ and the vector $(E/Z) \angle -\delta - \beta$ of constant magnitude E/Z and variable angle, δ . As δ varies, this latter vector traces out a circle. That the magnitudes I , V/Z , and E/Z are the three sides of a triangle is further borne out by the law of cosines given in (168).

Now if the excitation voltage, E , is changed in magnitude, the radius, E/Z , of the circle will change, but its center will remain fixed. Thus a series of circles may be drawn representing the loci of the current, I , as function of the torque angle, δ , for different excitation voltages, E . For zero excitation, $E = 0$, the radius of the circle vanishes, and the current has the magnitude and direction $I = (V/Z) \angle -\beta$. If $E > V$, the current is leading for small values of δ , but lagging for larger values of δ . For positive values of δ , the machine becomes a generator. Maximum current occurs when $\delta = \pi$ and the current is then equal to $I_{\max} = (V + E)/Z$. This, however, is far beyond the limits of stability.

A companion circle diagram, Fig. 49, can be developed showing the

locus of I as a function of its power factor angle, ϕ , for different values of power output, P . For this purpose multiply the conjugate of (165) by the current,

$$\hat{V}I = \hat{E}I + \hat{Z}\hat{I}I = \hat{E}I + (R - jX)I^2 \quad (169)$$

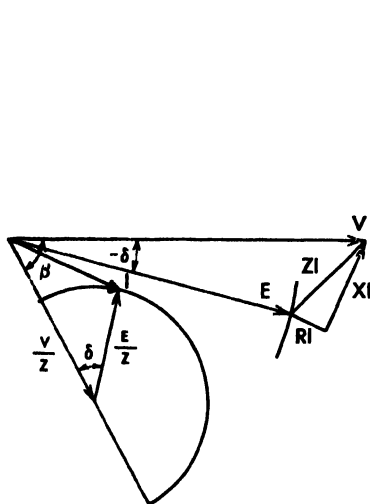


Fig. 48

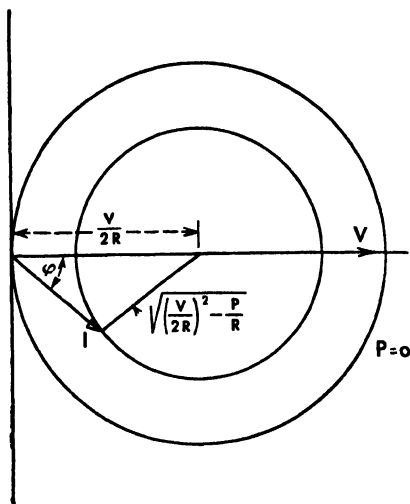


Fig. 49

in which $\hat{E}I = P + jQ$ is the complex power consumed by the counter emf of the motor, while $\hat{V}I = VI(\cos \phi + j \sin \phi)$ is the complex power at the terminals. Therefore,

$$VI \cos \phi + jVI \sin \phi = (P + RI^2) + j(Q - XI^2) \quad (170)$$

The real power then is

$$VI \cos \phi = P + RI^2 = P + RI^2(\cos^2 \phi + \sin^2 \phi) \quad (171)$$

Rearranging and completing the squares, this becomes

$$\left(I \cos \phi - \frac{V}{2R}\right)^2 + (I \sin \phi)^2 = \frac{V^2}{4R^2} - \frac{P}{R} \quad (172)$$

which is the equation of a circle of radius $\sqrt{\frac{V^2}{4R^2} - \frac{P}{R}}$ and with center at $\left(\frac{V}{2R}, 0\right)$. The zero power circle, $P = 0$, has a radius equal to the offset

of its center, and this circle passes through the origin. This is the largest radius that a power circle can have. Maximum power occurs when

by the line OA , on the line of centers OO' , since the excitation circle is tangent to the power circle on this line.

The minimum excitation for any power is given by OB , on the line of centers.

The minimum power factor for any power is given by the point where the current vector is tangent to the power circle.

Maximum power for a fixed excitation occurs at OB , on the line of centers OO' ; for if the torque angle, δ , increases beyond this point, the power decreases as is clear on the diagram.

A different type of circle diagram, in which active and reactive power are the variables, with excitation voltage as parameter, can be derived by taking the excitation voltage E as reference vector and substituting

$$I = \frac{P + jQ}{E} \quad (174)$$

Then (165) may be written

$$V = E + (R + jX) \left(\frac{P + jQ}{E} \right) \\ \frac{1}{E} [E^2 + (RP - XQ) + j(XP + RQ)] \quad (175)$$

Taking the sum of the squares of the real and imaginary components on each side of the equation, and rearranging, there results

$$V^2 E^2 = E^4 + (R^2 + X^2)(P^2 + Q^2) + 2E^2 RP - 2E^2 XQ \quad (176)$$

Dividing through by $R^2 + X^2 = Z^2$ and completing the squares,

$$\left(P + \frac{RE^2}{Z^2} \right)^2 + \left(Q - \frac{XE^2}{Z^2} \right)^2 = \left(\frac{VE}{Z} \right)^2 \quad (177)$$

This is the equation of a circle of radius (VE/Z) and with center at $(-RE^2/Z^2, +XE^2/Z^2)$. This equation is plotted in Fig. 51. The center and radius of the circle are different for each value of excitation voltage, E , but if only the terminal voltage is varied, the center remains fixed and the radius changes. Maximum power for a given excitation occurs where a vertical line is tangent to the circle.

Equation (177) can be modified to give the power and reactive components of current, upon dividing through by E^2 , whereupon it becomes

$$\left(\frac{P}{E} + \frac{RE}{Z^2} \right)^2 + \left(\frac{Q}{E} - \frac{XE}{Z^2} \right)^2 = \left(\frac{V}{Z} \right)^2 \quad (178)$$

Here P/E and Q/E are the current components.

It must be remembered that P and Q , and therefore the current

components, refer to the excitation voltage, E , and not to the terminal voltage, as reference vector.

The terminal watts and vars are

$$P' + jQ' = (P + RI^2) + j(Q - XI^2) \quad (179)$$

A circle diagram for the terminal power and vars can be derived by exactly the same process, but taking V as reference vector. Then

$$I = \frac{P' + jQ'}{V} \quad (180)$$

and (165) becomes

$$E = V - (R + jX) \left(\frac{P' + jQ'}{V} \right) \quad (181)$$

Hence, without difficulty, we find

$$\left(P' - \frac{RI'^2}{Z^2} \right)^2 + \left(Q' + \frac{XI'^2}{Z^2} \right)^2 = \left(\frac{VE}{Z} \right)^2 \quad (182)$$

which is a circle of radius VE/Z and center at $(RI'^2/Z^2, -XI'^2/Z^2)$. As compared with (177), the roles of V and E have been interchanged. The circles of (182) are also shown in Fig. 51. Equation (182) can be

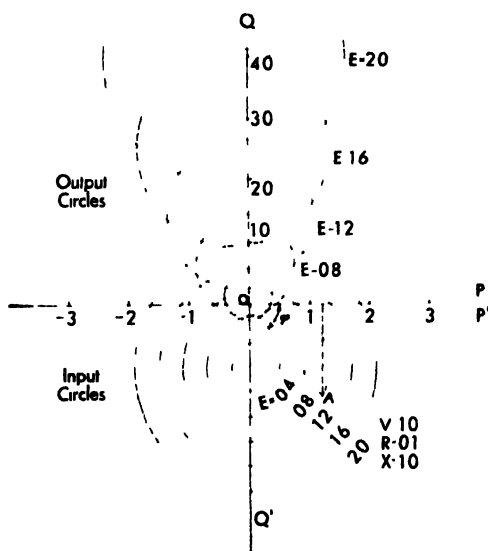


Fig. 51

converted to current scale by dividing through by V^2 , so that

$$\left(\frac{P'}{V} - \frac{RI'^2}{Z^2} \right)^2 + \left(\frac{Q'}{V} + \frac{XI'^2}{Z^2} \right)^2 = \left(\frac{E}{Z} \right)^2 \quad (183)$$

A vertical line on Fig. 51 is a constant power line, and the point A where this line cuts an excitation circle is an operating point. The current is $I = OA/V$, and its power factor angle is ϕ . Hence the data for the construction of V -curves is obtainable from this type of circle diagram. Likewise, curves of power factor as function of excitation, with power as parameter, may be plotted.

Problems

1. The per-unit values of a round rotor synchronous motor are

$$R = 0.10 \qquad X_s = 1.00 \qquad V = 1.0$$

- (a) Construct the composite circle diagram, Fig. 48, for the following excitations:
 $E = 0.2, 0.4, 0.6, 0.8, 1.0, 1.2, 1.4, 1.6, 1.8$, and 2.0 and for the following powers:
 $P = 0.2, 0.4, 0.6, 0.8, 1.0, 1.2, 1.4, 1.8, 2.0$.
 - (b) Using these circle diagrams, construct the O -curves for $P = 0, 0.5, 1.0, 1.5, 2.0$ and P_{\max} .
 - (c) Using the circle diagrams, construct leading and lagging power factor characteristics for $\text{pf} = 1.0, 0.8, 0.6$.
2. (a) For the above machine construct the output and input power circle diagrams, Fig. 49, for the same range of excitations.
 (b) Using the power circles, construct the O -curves and power factor characteristics.
 3. Discuss the relative advantages of the two types of circle diagrams.

33. Losses and Efficiency

The losses which may be chargeable to a synchronous machine are classified in the table on page 321.

Sometimes the increased core loss due to armature current and the skin-effect loss in the conductors are lumped and called *stray loss*. In large central stations some of the losses are reclaimed by using them to heat the intake air for the boilers. The ventilating fan or blower may be necessary only under load, in which case it should be classified as a load-loss.

A complete segregation of the losses requires extensive design data (some empirical), and this is not usually available except to the manufacturer. Nor is it feasible to make a detailed segregation of the losses by test. However, a major separation of the losses is possible through various test expedients and judicial extrapolation of test data.

	No-load Losses	Load Losses
Mechanical	Bearing friction Bearing oil pump Bearing cooling pump Brush friction Windage Ventilating fan	(Ventilating fan)
Excitation	Exciter losses (including losses in its drive) Rheostat losses $R_f I_f^2$ Field loss $R_f I_f^2$ $E_f I_f$	These may change under load because the excitation required depends on the load and its power factor
Iron	Core loss (hysteresis and eddy) Open-circuit field flux (teeth, pole face, core)	Core loss (hysteresis and eddy) Leakage fluxes (teeth, slot wedges, pole face, clamps, spider) Armature reaction (teeth, pole face, wedges, clamps, spider)
Copper	Skin effect due to peripheral variation in the radial component of flux through the conductor	Skin effect caused by slot leakage flux D-c resistance loss in the conductors

To separate the windage and friction from the no load core loss, let the machine be run as an unloaded synchronous motor; and measure the watts input, and current for different values of terminal voltage. Subtract the RI^2 loss of the armature from the input (using a value of resistance about 50 per cent greater than the measured d c resistance at

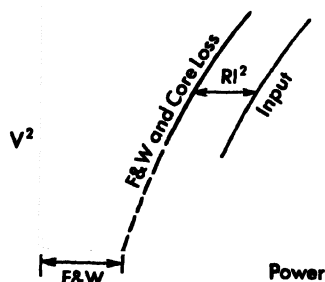


Fig. 52

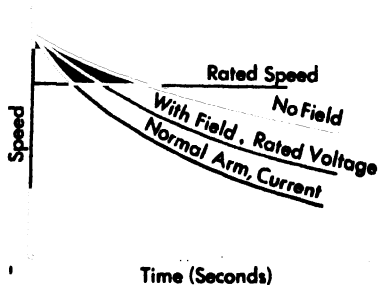


Fig. 53

75 C), and plot the curves of Fig. 52. Evidently the remainder represents friction, windage, and no-load core loss. Assuming the core loss

to vary as the square of the voltage, the lower straight-line portion of the curve may be extrapolated, and where it intercepts the power axis must be the friction and windage, since the core loss would be zero at zero voltage.

If it is possible to drive the generator at synchronous speed by a motor of known efficiency it need be big enough only to supply the losses the losses may be segregated as follows:

- (1) Friction and windage losses are equal to the input to the generator when it is driven at rated speed without excitation.
- (2) The no-load core loss is the additional loss incurred when excitation is applied to the field. Usually a curve is obtained for different values of excitation (field current or open-circuit voltage).
- (3) The armature resistance loss for currents from 25 to 150 per cent rated current are calculated, using measured values of the d-c resistance, corrected for temperature.
- (4) The stray loss (additional iron loss and conductor eddy-current loss due to armature current) is found by short-circuiting the generator terminals, at rated speed, and using just enough excitation to circulate from 25 to 150 per cent rated current, then from the measured loss subtracting the friction and windage, core loss, and resistance loss as found previously.
- (5) The excitation loss is the exciter voltage times the exciter current, or if the field and rheostat resistance are measured, it is $(R_f + R_r)I_f^2$.

In the case of large motors where it is not practicable to determine the losses by the above procedure, the *retardation method* may be used. This method requires the taking of a retardation speed-time curve after the motor is disconnected and allowed to coast to rest. Since the losses must be equal to the rate of change of the kinetic energy,

$$K \dot{\omega} = \frac{1}{737.6} \frac{d}{dt} \left(\frac{J}{2} \omega^2 \right) = \frac{\omega J}{737.6} \frac{d\omega}{dt} = \frac{4.6}{10^7} (W R^2) n \frac{dn}{dt} \quad (184)$$

$K \dot{\omega}$ = kilowatts loss

ω = speed in mechanical radians per second = $\frac{\pi n}{30}$

n = speed in (rpm)

J = polar moment of inertia

$$= \frac{(W R^2)}{32.2} \text{ lb-ft}^2$$

The angular acceleration is measured on the speed-time curve as the slope at rated speed.

By taking a number of curves under different conditions, the losses may be segregated, Fig. 53. First let a retardation curve be taken with no excitation on the machine. The losses are then due to windage and friction. Next let a retardation curve be taken with the armature open-circuited and a field sufficient to give rated terminal voltage at rated speed. The losses are then due to friction, windage and core loss. Finally, let a curve be taken with the armature short circuited and sufficient field to give rated current at rated speed. Under this condition the flux is too small to cause appreciable core loss, and the deceleration is due to friction, windage, copper and stray losses. If the d-c resistance loss is calculated, the stray loss may be isolated.

If the moment of inertia, J , is not known, but the losses are known for some condition, then J may be determined and used thereafter to find the losses for other conditions.

The efficiency of a 3-phase synchronous machine is

$$\text{Eff.} = \frac{\text{output}}{\text{output} + \text{losses}} = \frac{\sqrt{3} VI \cos \phi}{\sqrt{3} VI \cos \phi + 3R_a I^2 + (R_f + R_r) I_f^2 + (W \& F) + \left\{ \frac{P_{\text{core}}}{T_{\text{core}}} \right\} + \left\{ \frac{P_{\text{stray}}}{T_{\text{core}}} \right\}} \quad (185)$$

in which

$3R_a I^2$ = armature copper loss

$R_f I_f^2$ = field loss

$R_r I_f^2$ = field rheostat loss

$W \& F$ = windage and friction

Stray loss = increase in core loss due to load current, and skin effect in conductors (unless the armature resistance R_a includes skin effect)

The copper and stray losses are usually calculated at the standard temperature of 75 C. It should be noted that stray loss is corrected to a standard temperature in an inverse fashion from copper (RI^2) loss, that is

$$\frac{(\text{Copper loss at } T_2)}{(\text{Copper loss at } T_1)} = \frac{(\text{Stray loss at } T_1)}{(\text{Stray loss at } T_2)} = \frac{234 + T_2}{234 + T_1} \quad (186)$$

Problem

A 1000-kva, 3-phase, 60-cycle, 180-rpm, 2300-volt, *Y*-connected alternator has an armature resistance of $R_a = 0.059$ ohms per phase at 25 C. The power output of a d-c driving motor, under several conditions, is:

Alternator	Driving motor
No excitation, open-circuited	6.83 kw.
Rated voltage, open-circuited	19.75 kw.
Rated current, short-circuited	16.52 kw.

The excitation power $[(R_f + R_r)I_f^2 + \text{exciter losses}]$ is 11.41 kw. Determine the (a) windage and friction loss, (b) core loss, (c) armature copper loss, (d) stray loss, (e) and efficiency at 75 C.

8 The Synchronous Converter

1. Introduction

Because of the ease with which voltages can be transformed, and the absence of commutators, alternating current has largely superseded direct current for the generation, transmission, distribution and utilization of electric power. Nevertheless, for certain uses, notably electrolytic processes, railway electrification, elevators, cranes, hoists, steel mill motors, paper mill drives, and similar applications, direct current is either mandatory or highly desirable from the standpoint of close and accurate speed control. In such cases means must be provided for the conversion of an alternating-current supply to direct current. There are a number of ways in which this may be accomplished.

Only the mercury arc rectifier, motor-generator set (synchronous or induction), and synchronous converter are at present of importance in the power field. Many ingenious attempts have been made to produce a satisfactory mechanically driven rectifying commutator, but these have not been an unqualified success. In recent years the mercury arc rectifier has largely displaced the synchronous converter in electrolytic and railway applications; since it has the advantages of better efficiency (particularly in the higher voltage class), can be built for higher voltages, does not require as heavy foundations, has a lower upkeep (there are no rotating parts, or brush and commutator wear), and is competitive in first cost. In certain other applications, such as Ward-Leonard control

systems for steel and paper mill drives, electric shovels, cranes, hoists, etc., motor-generator sets are used. Nevertheless, synchronous converters are installed in numerous plants and constitute a major electrical load in the country. Their theory of operation presents many interesting aspects of circuit and machine theory, some of which are not present in any other electrical machine. For these reasons this chapter is devoted to the consideration of the synchronous converter.

The principal problems presented by the synchronous converter are:

1. Voltage ratio (fixed, in the ordinary converter)
2. Current ratio (fixed, in the ordinary converter)
3. Heating (not the same for all conductors, varies with pf)
4. Losses (much less than in d-c machine of same output)
5. Armature reaction (very small, resulting in a sensitive machine)
6. Power factor (must operate near unity pf to prevent excessive heating)
7. Commutation (commutator subject to flashover)
8. Hunting (poor stability factor as compared with synchronous motor)
9. Parallel operation (additional hazards over d-c and a-c generators)
10. Voltage regulation (inherently good)
11. Voltage control (limited, unless by external or auxiliary means)
12. Starting (d-c side, a-c side, auxiliary motor)

2. Principles of Operation

The synchronous (or rotary) converter is similar structurally to an ordinary d-c generator having an armature tapped at equal intervals

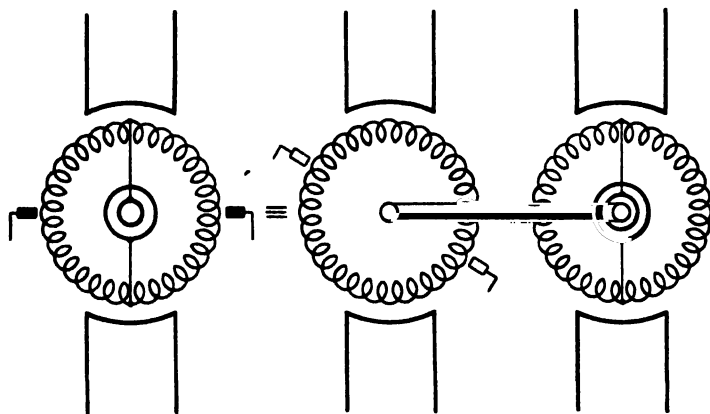


Fig. 1 Evolution of the synchronous converter.

and supplied through slip rings from an a-c source. It may be looked upon as the natural evolution of the synchronous motor generator set, Fig. 1, in which the a-c and d-c armatures have been combined, as well as the two sets of field poles. When the armature rotates at synchronous speed, alternating voltage is induced in the conductors and appears across the slip rings, while direct voltage appears at the brushes due to the rectifying action of the commutator. The alternating current provides the motor action while the armature generates direct current at the commutator brushes. The advantages of such a construction are obvious:

1. One machine has replaced two; with a consequent saving in size, weight, floor-space, and cost.
2. Since motor and generator action occur in the same armature, the shaft need transmit no power, and can be greatly reduced in diameter. Also, it is much shorter, since it supports only one, instead of two armatures.
3. The bearings can be made smaller, and the third bearing and pedestal used with larger size machines is unnecessary.
4. Since motor currents flow in one direction and generator currents in the opposite direction, the two sets of currents tend to cancel, and consequently the output of a given armature is greatly increased over its capacity as an ordinary d c generator.
5. The losses are reduced materially. The armature copper losses are less because the a-c and d c currents tend to cancel. The core, field, and windage losses are less because there is only one machine instead of two.
6. The armature reaction is small, since the a c motor and d c generator currents tend to produce armature reaction in opposite directions, which in a large measure, cancel.

But the disadvantages of the converter as compared to the motor generator set—inflexible voltage ratios, localized heating of armature conductors, tendency of the commutator to flashover, necessity of operating at near unity power factor, hunting and instability under rapid change of load condition, difficulties encountered on sudden reversal of power, etc.—become evident only upon further analysis or operating experience.

The synchronous converter is a very versatile piece of apparatus. In theory, at least:

1. It may be operated as a synchronous motor by supplying a-c to the

slip rings and driving a shaft load. Actually, it has limited capabilities as a motor, because without the d-c in the armature the heating becomes excessive.

2. It may be operated as a synchronous condenser. Here again, it has very limited condenser capacity because of excessive heating.
3. It may be operated as an a-c generator by driving it mechanically and taking power from the slip rings.
4. It may be operated as a d-c motor, but it is limited in this respect by heating.
5. It may be operated as a d-c generator by driving it mechanically and taking power from the commutator. Its capacity is limited by heating.
6. It may be operated as a double current (a-c and d-c) generator by driving it mechanically and taking power from both the commutator and the slip rings. But heating places a severe limit on this possibility
7. It may be operated as an *inverter*, by supplying d-c power to the commutator and taking a-c from the slip rings.
8. It may be operated as a converter, by supplying a-c power to the slip rings and taking d-c from the commutator.
9. It may be operated as combinations of the above.

Actually, however, a machine, designed and adjusted to operate satisfactorily under one set of conditions, will not do so under some other conditions. Heating, commutation, stability, and regulation change radically when the operating conditions are changed.

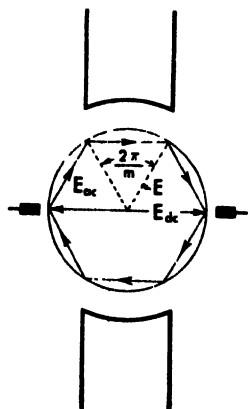


Fig. 2

The *voltage ratio* of a converter may be estimated by assuming the armature conductors to be infinitely distributed, so that the infinitesimal voltage vectors lie on a circle, Fig. 2. The diameter of the circle then represents the direct voltage. If the armature is tapped at m equidistant points per pair of poles, and these points connected to slip rings, the crest values of the alternating voltages between taps are represented by the chords of the circle. From the geometry of Fig. 2 it is clear that

$$\frac{E_{ac(max)}}{E_{dc}} = \frac{E2 \sin \frac{\pi}{m}}{2E} = \sin \frac{\pi}{m}$$

The ratio of the rms alternating voltage to the direct voltage is

$$\frac{E_{ac}}{E_{dc}} = \frac{1}{\sqrt{2}} \sin \frac{\pi}{m} \quad (1)$$

It may be noticed that the ratio of the alternating line-to-neutral voltage, E , to the direct voltage, is simply one-half. Evidently then, the voltage ratio of a converter is a fixed quantity, depending only on the number of phases. Therefore, in order to vary the direct output voltage, the alternating input voltage must be varied by some external or auxiliary means. There are a number of ways in which this can be done. The supply transformer may be provided with taps (perhaps with automatic load ratio control), and the taps changed to meet the load conditions. Or an induction regulator may be inserted in series between the transformer and the converter, and the voltage applied to the slip rings varied by controlling the induction regulator. Or an a-c booster may be connected in series with the converter and its generated voltage added (or subtracted) to the applied voltage. In practice this booster is mounted on the same shaft with the converter armature, and is driven by the converter. Of course, a d-c booster could be used, but it would be far more expensive than the a-c booster. There is still another way—the regulating pole—for changing the voltage ratio, but this will not be considered until later. The fixed voltage ratio compels the use of transformers with the converter.

The *current ratio* of the converter is arrived at from energy considerations. Let

I_{dc} = total direct output current

I_c = a-c coil current (rms value)

η = efficiency

$\cos \theta$ = power factor

P = number of poles

Then by the conservation of energy

$$E_{dc} I_{dc} = \eta m \frac{P}{2} E_{ac} I_c \cos \theta = \eta m \frac{P E_{dc}}{2 \sqrt{2}} \sin \frac{\pi}{m} I_c \cos \theta$$

$$\text{hence} \quad \frac{I_c}{I_{dc}} = \frac{\sqrt{2}}{\eta m P \sin \frac{\pi}{m} \cos \theta} \quad (2)$$

Since the armature is a mesh winding of m phases, the line current is

$$I_{ac} = \frac{P}{2} \left| I_c - I_c \frac{2\pi}{m} \right| = \frac{P}{2} I_c \left| 1 - \cos \frac{2\pi}{m} - j \sin \frac{2\pi}{m} \right|$$

$$= \frac{P}{2} I_c \sqrt{2 \left(1 - \cos \frac{2\pi}{m} \right)} = P I_c \sin \frac{\pi}{m}$$

Hence (2) becomes

$$\frac{I_{a_c}}{I_{d_c}} = \frac{2\sqrt{2}}{\eta m \cos \theta} \quad (3)$$

Thus the current ratio varies inversely with the power factor, but is otherwise a fixed ratio. In applying (2) or (3) to the a-c booster type converter, the factor η must include the energy required to drive the

booster. For example, if the efficiency with the booster unexcited is 0.95, the efficiency at 15 per cent boost would be $\eta = 0.95 - 0.15 = 0.80$. On the other hand, at 15 per cent buck, the "efficiency" factor would be $\eta = 0.95 + 0.15 = 1.10$.

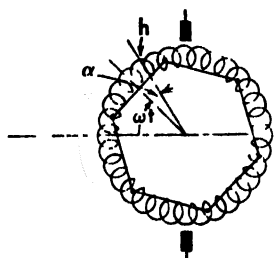


Fig. 3

The *armature heating* of a synchronous converter is a much more

complicated phenomenon than the heating of either a straight a-c or d-c machine. The complication develops because the current flowing in any conductor is the superposition of an alternating sinusoidal current and a reversing direct current. To fix ideas, there is shown in Fig. 3 a

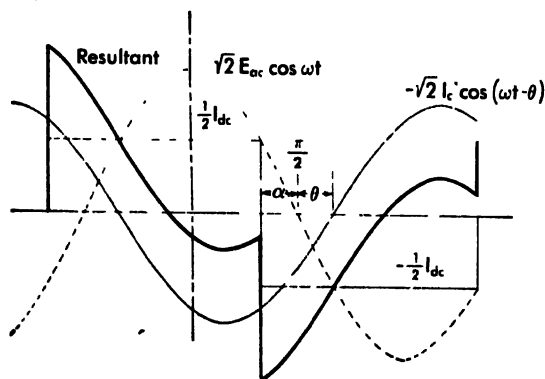


Fig. 4 D-c, a-c, and resultant currents in a conductor.

bipolar Gramme ring armature tapped for six-phase, and with the brushes on neutral. Suppose the center of phase-1 to have moved an angle ωt from the pole axis. Its induced voltage then is $\sqrt{2} E_{a_c} \cos \omega t$ and for a lagging power factor the a-c motor current in each conductor of the phase is

$$- \sqrt{2} I_c \cos (\omega t - \theta)$$

Now consider a particular conductor h of the phase at an angle α from the center of the belt. In addition to its a-c current it will carry a direct current $\frac{1}{2}I_d$ until it passes under a brush and has its current reversed to $-\frac{1}{2}I_d$. This occurs when the center of the phase is at an angle $\omega t = (\pi/2 - \alpha)$. The alternating and direct current relationships for conductor h are then as shown in Fig. 4. The algebraic sum of alternating and direct currents is the resultant current in the conductor. This re-

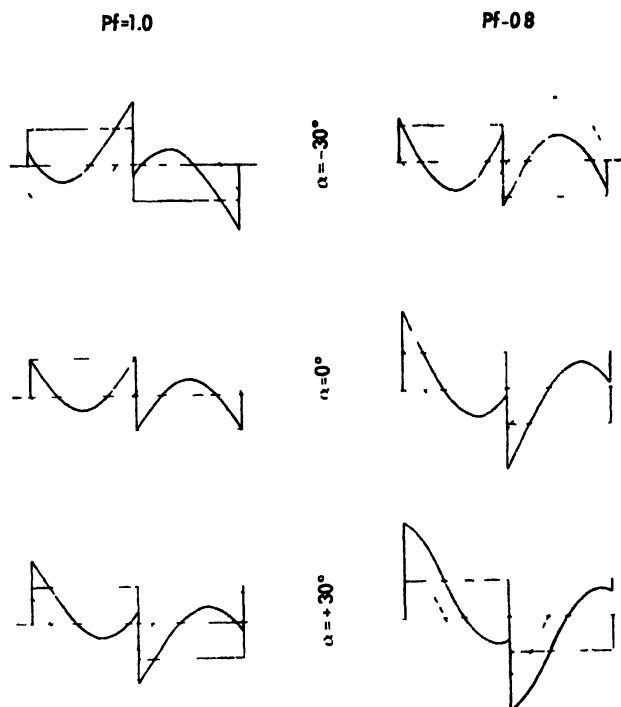


Fig. 5 Effect of power factor and position of conductor on resultant current

sultant is seen to be different for each conductor (that is, angle α) in the phase belt, and to depend also on the power factor angle θ . The lower the power factor, the greater the magnitude of I_d , according to (2), and the more it is displaced with respect to the direct current, according to Fig. 4. The currents in the tap coils, $\alpha = -\pi/6$ and $\alpha = +\pi/6$, and in the mid coil, $\alpha = 0$, are shown in Fig. 5 for power factors of $\cos \theta = 1.0$ and $\cos \theta = 0.80$ respectively.

The coil heating, which is proportional to the square of the currents, is seen to be much greater in the case of the coils near the taps, and to

increase with a departure from unity power factor. Since every coil experiences a different resultant current, the heating of a converter armature is not uniform as in other machines and "hot spots" develop at the tap coils.

The *armature reaction* of the synchronous converter is the resultant of the d-c and a-c armature reactions, and varies from instant to instant. Figure 6 represents a 6-phase converter having full pitch infinitely distributed windings, with the d-c brushes on neutral directly under the interpole.

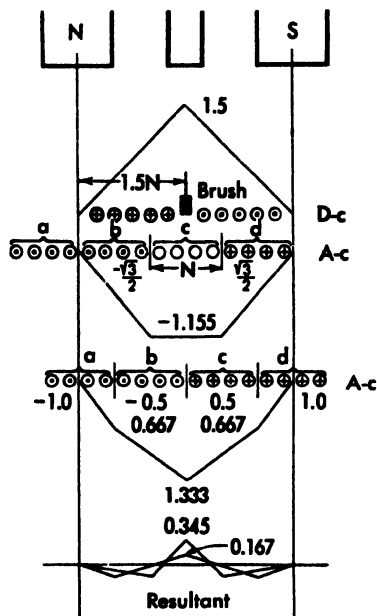


Fig. 6 The d-c, a c, and resultant armature reaction.

The d-c armature obviously is a triangular wave reaching a peak of $1.5NI_d/P$ where $N =$ turns per phase belt. The a-c magnetomotive force per phase belt will then reach a crest value, according to (2), (for $\eta = 1.0$),

$$\begin{aligned}\sqrt{2} I_a N &= -\frac{4}{m \sin \pi/m} \frac{NI_d}{P} \\ &= \frac{4}{6 \sin 30^\circ} \frac{NI_d}{P} = \frac{4}{3} \frac{NI_d}{P}\end{aligned}$$

At $t = 0$, when phase belt c is centered on the interpole, the voltage induced in it is zero, and at unity power factor the current is also zero. The currents in phase belts b and d are $\sqrt{3}/2$ of maximum, and the a c magnetomotive force acting on the interpole is therefore

$$\frac{\sqrt{3}}{2} \frac{4}{3} \frac{NI_d}{P} = 1.155 \frac{NI_d}{P}$$

One sixth of a cycle later the armature has moved 30 degrees and the currents in the phase belts are $i_a = -1.0$, $i_b = -0.5$, $i_c = +0.5$ and $i_d = +1.0$. The a-c magnetomotive force acting on the interpole then is

$$\left(\frac{N}{2} \times 1.0 + N \times 0.5\right) \frac{4}{3} \frac{I_d}{P} = 1.333 \frac{NI_d}{P}$$

The net magnetomotive force under the interpole is then the difference between the d-c and a-c armature reaction and varies between the limits

$$\begin{aligned}& \{1.5 - 1.155 \quad 0.345\} \frac{NI_d}{P} \\ & \{1.5 - 1.333 = 0.167\} \frac{NI_d}{P}\end{aligned}$$

It is evident that the net magnetomotive force pulsates between the above two limits every 30 degrees, or as a 6th harmonic, and thus will cause a "tap frequency pulsation" to appear in the external circuit of the converter when the machine is loaded. These 6th harmonics increase the core loss and the losses in the damper windings.

There is a steady term of armature reaction under the interpole represented by the average of the two extremes, $(0.345 + 0.167) / 2 = 0.256$. This must be compensated by extra turns on the interpole. Its small value, compared to the d-c reaction, is the reason why interpoles were not adopted for converters until after their application to straight d-c machines.

It will also be noticed from Fig. 6 that there is a cross magnetizing magnetomotive force under the main poles. This demands an increased excitation with load (due to saturation), which must be supplied either by increased field excitation, or by reactive alternating current and a change of power factor.

3. Construction

As mentioned in the Introduction, the synchronous converter is structurally similar to a d-c generator with the addition of slip rings tapped at equal intervals to the armature. There must be as many taps per pair of poles as there are phases. Converters have been built with 1, 2, 3, 6, and 12 phases. The more the number of phases, the higher the efficiency, but of course many phases add both electrical and mechanical complications. Thus special multiwinding transformers must be used to provide 6 or 12 phases, and 12 slip rings with their brush rigging results in a long machine with a heavier shaft. For these reasons, most converters on a 3 phase system are *6-phase* machines.

Figure 7 shows a 6-phase *booster type converter*. The a-c booster is an integral part of the machine, but is actually an auxiliary a-c generator having its own armature and field. It acts either as a motor driving the converter, or as a generator driven by the converter, depending on whether it is bucking or boosting the voltage. Now for an ordinary converter, or for a booster converter with zero excitation on the booster, the a-c and d-c armature reactions essentially cancel, and the interpoles need provide only sufficient excitation to effect good commutation. If, however, the converter must also act as a motor or a generator (to the extent that the booster is functioning), the armature reaction is unbalanced and the resultant armature reaction along the d-c brush axes



Fig. 7 A large, modern synchronous converter

a Commutator end

b Slip ring end, showing the booster
(Westinghouse Electric Corporation)

must be neutralized. For this reason, the interpoles of a booster type converter must be provided with *both* series and shunt field windings.

In the ordinary converter, it is usually desirable to use series, as well as shunt windings, on the main poles, so as to obtain some (about 5 per cent) compounding effect. This results not by changing the voltage ratio — which is a fixed quantity — but by causing the converter to draw a leading current when the field excitation is increased, and this leading current drawn through the reactance of the transformers causes a rise in voltage at the slip rings, and of course a proportional rise at the d-c brushes.

A converter is sensitive to hunting, with the possibility of bad commutation, and even flashover of the commutator. For these reasons, all modern converters have heavy *damping windings* in the pole faces. These windings also serve as starting windings if the machine is started from the a-c side.

The tendency for the commutator to flashover on sudden changes of load, or due to disturbances originating on the a-c side, brought about the use of *arcing barriers* between brushes or *arc chutes* around the brushes themselves. These devices do not prevent flashover, but minimize the detrimental effects.

Other unusual construction features of the converter are the provisions for lifting either the a-c or d-c brushes during starting (see Starting).

A word should be said about the transformers which are a necessary part of every converter installation. These are usually 3 phase to 6-phase, the secondaries being connected in star, diametrical, double delta, or double zigzag. On street railway installations and other metropolitan applications, the transformers are usually of the air blast type, in order to avoid the oil fire hazard. In industrial plants, oil filled transformers are generally used. If the alternating supply voltage is more than a few thousand, oil-filled transformers are necessary in any case.

4. The Voltage Ratio

Suppose that the flux density distribution with respect to the quadrature axis of a synchronous converter is given by (Chap. 3, Eq. (2))

$$\beta = \sum \beta_k \sin k \left(\frac{\pi x}{\tau} + \gamma_k \right) \quad (4)$$

and that both the β_k and the γ_k are constant. Then the general equation for the induced voltage [Chap. 3, (18)] reduces to

$$e = - \sum \frac{Nq}{10^8} K_{pk} K_{dk} k \phi_k \frac{\pi}{\tau} \frac{dx_0}{dt} \cos k \left(\frac{\pi x_0}{\tau} + \gamma_k \right) \quad (5)$$

in which x_0 is the position of the center of the coil group.

In an m -phase synchronous converter, let the coil group be taken as one of the phases. Then [Chap. 3, (16)]

$$K_{dk} = \frac{\sin(k\pi q\sigma/2\tau)}{q \sin(k\pi\sigma/2\tau)} = \frac{\sin k\pi' m}{q \sin k\delta} \frac{m}{2} \quad (6)$$

and the rms value of the fundamental ($k = 1$) alternating voltage is, putting $\omega = \frac{\pi}{\tau} \frac{dx_0}{dt}$ for synchronous speed,

$$E_{d1} = - \frac{N\omega}{\sqrt{2} 10^8} K_{p1}\phi_1 \frac{\sin \pi}{\sin \delta} \frac{m}{2} \quad (7)$$

Now consider the belt of conductors between adjacent pairs of brushes as belonging to a "phase belt." For this case $m = 2$. Suppose the brushes to be shifted an angle ξ from the quadrature axis. Then the center of this coil group is located at the brush, that is $\pi x_0/\tau = \xi$. But the velocity of the conductors is $\pi dx_0/\tau dt = \omega$. Hence the voltage between brushes is, by (5),

$$E_{d1} = - \sum \frac{N\omega}{10^8} K_{p1} \frac{\sin k\pi}{\sin k\delta} \frac{2}{2} k\phi_k \cos k(\xi \pm \gamma_1) \quad (8)$$

The ratio of the direct to the alternating voltage then is

$$\begin{aligned} \frac{E_{d1}}{E_{a1}} &= \sqrt{2} \frac{\cos(\xi + \gamma_1)}{\sin \pi/m} + \sqrt{2} \sum \frac{K_{p1}}{K_{p1}} \frac{\sin k\pi}{\sin k\delta} \frac{2 \sin \delta}{2 \sin \pi/m} \frac{2 \phi_1}{\phi_1} k \cos k(\xi + \gamma_1) \\ &= \frac{\sqrt{2} \Delta}{\sin \pi/m} \end{aligned} \quad (9)$$

If the flux distribution is sinusoidal, $k = 1$, and passes through zero at the quadrature axis, $\gamma_1 = 0$, and the brush shift is zero, $\xi = 0$, this expression reduces to the simple relationship given in (1) and usually found in text books. But the development given above shows that the voltage ratio depends on the following factors:

1. The number of phases m in the ratio $\sqrt{2} \sin(\pi/m)$.
2. The brush shift ξ , limited to small values to avoid sparking.
3. The flux shifts γ_1 , which have the same effect as the brush shift, and result in sparking.
4. Harmonics in the flux wave, which do not affect the fundamental of the alternating voltage (7), but may change materially as much as ± 25 per cent the direct voltage (8). This possibility gave rise to the development of the *regulating* (or split) *pole* converter, Fig. 8, in which the main pole is flanked by one or two regulating poles

having separate excitations. By changing the excitation of the auxiliary poles it is possible to change the flux distribution from a flat to a very peaked wave, and thereby change the voltage ratio. However, this type of construction is expensive, and the regulating pole converter is now obsolete

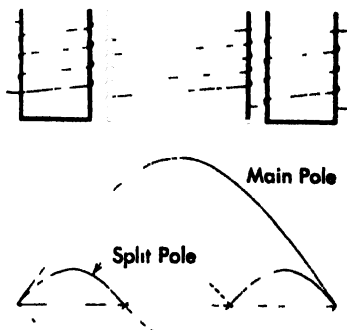


Fig. 8 Regulating pole

5. The Current Ratio

In the case of the a c booster type converter having an auxiliary synchronous generator mounted on the same shaft with the converter and connected in series therewith, let

- E_1 = alternating line voltage at the transformer secondaries
- $+ E_b$ = alternating voltage added by the booster
- E_{ac} = alternating voltage per phase of the converter armature (rms)
- E_d = direct voltage at the brushes
- I_d = total direct current
- I_{ac} = alternating line current (at slip ring) (rms)
- I_c = alternating coil current (in converter winding) (rms)
- P = number of poles
- m = number of phases
- η = efficiency of the machine, booster unexcited
- $\cos \theta$ = power factor

$$\text{Then} \quad I_{ac} = PI \sin \frac{\pi}{m} \quad (10)$$

$$E_1 = E_{ac} + E_b \quad (11)$$

The current ratio of a synchronous converter follows from the law of conservation of energy

$$(\text{d-c output}) = (\text{a-c input})(\text{efficiency}) \quad (12)$$

$$E_d I_d = \frac{P}{2} \eta m E_1 I_c \cos \theta = \eta m \frac{P}{2} (E_{ac} + E_b) I_c \cos \theta \quad (13)$$

Therefore, making use of (9)

$$\frac{I_c}{I_d} = \frac{2E_d}{P\eta m(E_{ac} + E_b) \cos \theta} = \frac{2E_{ac} \sqrt{2} \Delta \sin(\pi' m)}{\eta m P(E_{ac} + E_b) \cos \theta}$$

$$= \frac{2\sqrt{2}\Delta}{\sin \pi/m} \frac{1}{\eta m P (1 + e) \cos \theta} \quad (14)$$

where $e = \frac{E_b}{E_m}$ = per unit boost or buck (15)

In terms of the slip ring currents

$$\frac{I_{ar}}{I_{dr}} = \frac{2\sqrt{2}\Delta}{\eta m (1 + e) \cos \theta} \quad (16)$$

6. Armature Heating

The armature heating in a converter is a more complicated phenomenon than is the armature heating of other machines, because a-c and d-c flow in every conductor. This results in nonuniform heating, the conductors near the taps getting hotter than those near the center of the phase belts. Moreover, the heating is much more sensitive to changes in power factor and to brush shift.

On the assumption of linear commutation with a brush width b , and a brush shift of ξ electrical radians, the direct current in the layer of conductors between adjacent brushes is a trapezoidal wave, as shown in Fig. 9, and may be expressed by the

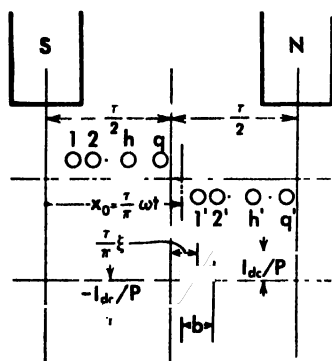


Fig. 9 Distribution of the d-c current

Fourier series (with respect to the direct axis)

$$i_{dr} = \frac{-4}{\pi} \frac{I_{dr}}{P} \sum_{\lambda=1}^{\infty} \frac{\sin (2\lambda - 1)b\pi}{(2\lambda - 1)^2 b\pi} \frac{2\tau}{2\tau} \cos (2\lambda - 1) \left(\frac{\pi x}{\tau} - \xi \right) \quad (17)$$

The alternating (motor) current in a phase coil group is

$$i_{gr} = \sum_n I_n \sin (n\omega t + \theta_n) \quad (18)$$

If the center of the coil group is located at x_0 and the armature is moving at synchronous speed $\omega t = x_0 \pi / \tau$, then the h th coil in the phase belt is located at

$$x_h = x_0 - \frac{q}{2} \sigma - \frac{1}{2} \tau + h\sigma = \frac{\tau}{\pi} \omega t - \frac{q}{2} \sigma - \frac{1}{2} \tau + h\sigma \quad (19)$$

The substitution of (19) in (17) thus specifies the direct current in the h th coil of the phase group at any instant. The resultant current is the sum of the direct and the alternating currents, that is

$$i_h = i_{a_1} + i_{a_2} = \frac{-4}{\pi} \frac{I_d}{P} \sum_1^s \frac{\sin(2s-1)b\pi}{(2s-1)^2 b\pi} \frac{2\tau}{2\tau} \cos(2s-1) \left(\omega t - \xi - \frac{q}{2} + \frac{1}{2} \frac{\sigma}{\tau} \pi - \frac{p\pi}{2} + h \frac{\sigma}{\tau} \pi \right) + \sum_n I_n \sin(n\omega t + \theta_n) \quad (20)$$

The average loss per cycle for this coil is

$$W_l = \frac{1}{\pi} \int_0^\pi R i_h^2 d(\omega t) \quad (21)$$

where R is the resistance of the coil. The substitution of (20) in (21) yields integrals of the following types

$$\left. \begin{aligned} \int_0^\pi \sin^2 ax \, dx &= \pi/2 & \int_0^\pi \sin ax \cdot \cos bx \, dx &= 0 \\ \int_0^\pi \cos^2 ax \, dx &= \pi/2 & \int_0^\pi \sin ax \cdot \sin bx \, dx &= 0 \\ \int_0^\pi \sin ax \cdot \cos ax \, dx &= 0 & \int_0^\pi \cos ax \cdot \cos bx \, dx &= 0 \end{aligned} \right\} \quad (22)$$

$a \neq b$

Hereby (21) becomes

$$W_l = \frac{R}{2} \sum_n I_n^2 + \frac{R}{2} \left(\frac{4}{\pi} \frac{I_d}{P} \right)^2 \sum_1^s \frac{\sin^2(2s-1)b\pi}{(2s-1)^4 b^2 \pi^2} \frac{2\tau}{2\tau} + R \frac{4}{\pi} \frac{I_d}{P} \sum_n I_n \frac{\sin n b \pi}{n^2 b \pi} \frac{2\tau}{2\tau} \sin n \left(h \frac{\sigma}{\tau} \pi - \psi_n \right) \quad (23)$$

in which $\psi_n = \xi + \frac{q}{2} + \frac{1}{2} \frac{\sigma}{\tau} \pi - \frac{p\pi}{2} + \frac{\theta_n}{n}$

Half the first summation is the square of the alternating rms coil current, I^2 .

It may be shown (see Note, end of this Section) that the second summation of (23) is

$$R \frac{I_d^2}{P^2} \left(1 - \frac{2}{3} \frac{b}{\tau} \right) \cong R \frac{I_d^2}{P^2}$$

The last summation cannot, in general, be evaluated. However, since $b/2\tau$ is small and since the higher time harmonics are negligible, no great error is made by taking the *sine* equal to the angle, whereupon the last term becomes

$$R \frac{4}{\pi} \frac{I_d}{P} \sum_n I_n \sin n \left(h \frac{\sigma}{\tau} \pi - \psi_n \right)$$

Hence (23) simplifies to

$$W_l = R I^2 + R \frac{I_d^2}{P^2} + R \frac{4}{\pi} \frac{I_d}{P} \sum_n I_n \sin n \left(h \frac{\sigma}{\tau} \pi - \psi_n \right) \quad (24)$$

The average heating per conductor for the whole armature is

$$W = \frac{1}{q} \sum_1^q W_h = R \left\{ I_a^2 + \frac{I_d^2}{P^2} - \frac{4}{\pi} \frac{I_d}{P} \sum_n \frac{I_n}{n} K_{dn} \sin n \left(\frac{p\pi}{2} + \frac{\theta_n}{n} + \xi \right) \right\} \quad (25)$$

in which $K_{dn} = \frac{\sin(nq\sigma\pi/2\tau)}{q \sin(n\sigma\pi/2\tau)}$ = distribution coefficient

If the a-c harmonics be neglected, ($n = 1$), there is by (14) in (24) and (25)

$$W_h = R \frac{I_d^2}{P^2} \left\{ 1 + \frac{8\Delta^2}{\eta^2 m^2 (1 + e)^2 \cos^2 \theta_1 \sin^2 \frac{\pi}{m}} + \frac{16\Delta \sin(h\sigma\pi\tau - \psi_1)}{\pi\eta m (1 \pm e) \cos \theta_1 \sin \frac{\pi}{m}} \right\} \quad (26)$$

$$W = R \frac{I_a^2}{P^2} \left\{ 1 + \frac{8\Delta^2}{\eta^2 m^2 (1 + e)^2 \cos^2 \theta_1 \sin^2 \frac{\pi}{m}} - \frac{16\Delta K_{d1} \sin(p\pi/2 + \theta_1 + \xi)}{\pi\eta m (1 + e) \cos \theta_1 \sin \frac{\pi}{m}} \right\} \quad (27)$$

The usual text book expressions follow upon substituting:

$\Delta = 1$ (no harmonics in the flux distribution)

$e = 0$ (no booster)

$\xi = 0$ (zero brush shift)

$p = 1$ (full pitch coils)

$K_{d1} = \frac{\sin \frac{\pi}{m}}{\pi m}$ (infinite distribution of conductors)

$\alpha = \left(\frac{q+1}{2} - h \right) \frac{\sigma\pi}{\tau}$

Then (26) and (27) reduce to the approximate relationships

$$W_h \cong R \frac{I_d^2}{P^2} \left\{ 1 + \frac{8}{\eta^2 m^2 \cos^2 \theta_1 \sin^2 \frac{\pi}{m}} - \frac{16 \cos(\alpha + \theta_1)}{\pi\eta m \cos \theta_1 \sin \frac{\pi}{m}} \right\} \quad (28)$$

$$W \cong R \frac{I_a^2}{P^2} \left\{ 1 + \frac{8}{\left(\eta m \cos \theta_1 \sin \frac{\pi}{m} \right)^2} - \frac{16}{\pi^2 \eta} \right\} \quad (29)$$

It is clear from (28) that the heating is a minimum when $(\alpha + \theta_1 = 0)$ and a maximum when $(\alpha + \theta_1 = \pi/2)$. Hence at unity power factor $\theta_1 = 0$, the mid coil ($\alpha = 0$) is cooler than the tap coils ($\alpha = \pi/m$).

Problems

1. Prepare a table showing the *ratio* of the *maximum* to the *minimum* coil heating for $m = 2, 3, 4, 6$, and 12 and the following power factors: $\cos \theta_1 = 1.0, 0.9, 0.8$. Assume an efficiency of $\eta = 0.95$.
2. Prepare a table showing the *ratio* of the *average* converter heating to that which would result from the d-c current alone for $m = 2, 3, 4, 6$, and 12 and $\cos \theta_1 = 1.0, 0.9, 0.8$. Assume $\eta = 0.95$.
3. Prepare a table based on the problem above of *relative ratings* of a given machine used as converter and as a d-c generator.
4. At what power factor will the converter average heating be the same as when operating as a d-c generator?

Note on the summation of a series. The second series in (23) may be summed by three successive integrations of the Fourier series for a rectangular wave, and using the series for a triangular wave to evaluate an intermediate series introduced by the first integration.

The Fourier series for rectangular and triangular waves of unit amplitude are respectively

$$y_1(x) = \frac{4}{\pi} \sum_{n=1}^{\infty} \frac{\sin (2n-1)x}{(2n-1)} \quad (30)$$

$$y_2(x) = \frac{8}{\pi^2} \sum_{n=1}^{\infty} \frac{\sin (2n-1)\pi/2}{(2n-1)^2} \sin (2n-1)x \quad (31)$$

Integrating the rectangular wave (30), there is

$$\begin{aligned} \int_0^x 1 dx &= \int_0^x \frac{4}{\pi} \sum_{n=1}^{\infty} \frac{\sin (2n-1)x}{(2n-1)} dx \\ \therefore x &= \frac{4}{\pi} \sum_{n=1}^{\infty} \left[\frac{\cos (2n-1)x}{(2n-1)} - \frac{1}{(2n-1)} \right] \end{aligned} \quad (32)$$

But by (31) for $x = \pi/2$, where the triangular wave is of unit height,

$$y_2\left(\frac{\pi}{2}\right) = \frac{8}{\pi^2} \sum_{n=1}^{\infty} \frac{1}{(2n-1)^2} = 1 \quad (33)$$

Substituting (33) in (32) and integrating twice

$$\int_0^x \int_0^x \left(\frac{\pi}{2} - x\right) dx = \int_0^x \int_0^x \frac{4}{\pi} \sum_{n=1}^{\infty} \frac{\cos (2n-1)x}{(2n-1)} dx \quad (34)$$

hence

$$\frac{\pi x^2}{4} - \frac{x^3}{6} = \frac{4}{\pi} \sum_{n=1}^{\infty} \frac{1 - \cos (2n-1)x}{(2n-1)^3} = \frac{8}{\pi} \sum_{n=1}^{\infty} \frac{\sin^2 (2n-1)x/2}{(2n-1)^4} \quad (35)$$

and therefore the required series is

$$\sum_{n=1}^{\infty} \frac{\sin^2 (2n-1)x/2}{(2n-1)^4} = \frac{\pi^2 x^2}{32} - \frac{\pi x^3}{48} \quad (36)$$

7. Armature Reaction

The armature reaction of a synchronous converter is made up of a-c and d-c components. The former is of the same nature as that found in a synchronous motor or generator, and the identical equations may be employed to describe it. The d-c armature reaction may be regarded as that due to a 180-degree phase belt excited by a constant current, the center of the coil group being at the brush. Once these two components have been obtained, it is a simple matter to superimpose them.

A-c armature reaction. If the alternating current in a phase group comprises a set of time harmonics, as in (18), that is

$$i_a = \sum_n I_n \sin(n\omega t + \theta_n) \quad (37)$$

in which time is counted from the instant when the coil group is centered on the *S* pole, and θ_n is the internal power factor angle, then the polyphase armature reaction with respect to the stationary axis through the *S* pole is given by L_A , (14) of Appendix II as

$$a_a = 0.4qNm \sum_n \sum_k \frac{K_m}{k} K_{dn} I_n \left\{ \sin \left[(n - k')\omega t + k' \frac{\pi x}{\tau} + \theta_n \right] + \sin \left[(n + k'')\omega t - k'' \frac{\pi x}{\tau} + \theta_n \right] \right\} \quad (38)$$

in which

- q = coils per phase per pair of poles
- N = turns per coil
- m = number of phases per pair of poles
- n = order of the time harmonics
- k = order of the space harmonics
- k' = any value of k for which $(n - k)$ is a multiple of m or zero
- k'' = any value of k for which $(n + k)$ is a multiple of m
- I_n = crest value of the n th time harmonic of current
- τ = pole pitch
- σ = slot pitch
- x = distance measured from the center line through the *S* pole
- $K_m = \sin k p \pi / 2$ = pitch coefficient
- $K_{dn} = \frac{\sin(kq\sigma\pi/2\tau)}{q \sin(k\sigma\pi/2\tau)}$ = distribution coefficient

If only the fundamental time harmonic is present, $n = 1$, and the n -summation in (38) may be dispensed with. The a-c armature reaction under the main pole is found by putting $x = 0$, while that under the interpole

is found by putting $x = \tau/2$. The *average* armature reaction may be found, if desired, by integrating (38) over a pole pitch.

D-c armature reaction. It is convenient to regard the top layer of conductors between adjacent brushes as a 'phase belt,' having its returns in the bottom layer of conductors the pitch angle $p\pi$ ahead. The d-c armature reaction may then be calculated as for two such "phases" displaced by 180 degrees in space from each other, and carrying currents in opposite directions; thus, in a sense, also 180 degrees out of phase in time. Now Eq. (4), Appendix II gives the armature reaction for a coil group carrying a current i . This equation can be applied to determine the d-c armature reaction upon substituting

$$i = -I_a/P \text{ for the first belt}$$

$$i = +I_a/P \text{ for the second belt, 180 degrees ahead of the first}$$

$$x_0 = \frac{\tau}{2} + \frac{\tau\xi}{\pi} = \text{center of the first coil group}$$

$$x_0 = \frac{\tau}{2} + \frac{\tau\xi}{\pi} + \pi = \text{center of the second coil group}$$

$$mq/2 = \text{coils per belt between brushes}$$

$$K'_{ad} = \frac{2 \sin k\pi/2}{nq \sin(k\pi/2r)} \approx \frac{\sin k\pi/2}{k\pi/2} \quad \text{distribution factor}$$

(different from that for the a-c coil group)

Then by (4), Appendix II, for the two coil groups

$$\begin{aligned} a_{ad} = 0.8 \frac{nqN}{2} \frac{I_a}{P} \sum_1 \frac{K'_{ad}K_{ad}}{k} \left[-\cos k \left(\frac{\pi x}{\tau} - \xi - \frac{\pi}{2} \right) \right. \\ \left. + \cos k \left(\frac{\pi x}{\tau} - \xi + \frac{\pi}{2} \right) \right] = -0.8mqN \frac{I_a}{P} \sum_1 \frac{K'_{ad}K_{ad}}{k} \sin \frac{k\pi}{2} \sin k \left(\frac{\pi x}{\tau} - \xi \right) \end{aligned} \quad (39)$$

For unity pitch and infinite distribution, (39) reduces to

$$a_{ad} \cong -\frac{1.6mqN}{\pi P} I_a \sum_1 \frac{1}{k^2} \sin \frac{k\pi}{2} \sin k \left(\frac{\pi x}{\tau} - \xi \right) \quad (40)$$

Since k is always odd, comparison of (40) with (31) shows the d-c armature reaction to be a triangular wave passing through zero at an angle ξ (the brush shift) from the reference axis through the S-pole. The peak value of this triangular wave is $0.2\pi mqNI_a/P$.

Resultant armature reaction. The resultant armature reaction is the sum of the a-c and d-c reactions as given by (38) and (39), and is

$$a = 0.4mqN \sum_1 \frac{K_{pk}}{k} \left[K_{d1} \sum_n I_n \left\{ \sin \left[(n - k')\omega t + k' \frac{\pi x}{\tau} + \theta_1 \right] \right. \right. \\ \left. \left. + \sin \left[(n + k'')\omega t - k'' \frac{\pi x}{\tau} + \theta_1 \right] \right\} \right. \\ \left. - K'_{d1} \frac{2}{p} I_d \sin \frac{k\pi}{2} \sin k \left(\frac{\pi x}{\tau} - \xi \right) \right] \quad (41)$$

For full pitch coils, ($p = 1$), infinite distribution, ($\sigma = 0$), fundamental current only, ($n = 1$), and putting $Z = 2mqN$ as the total number of conductors per pair of poles, (41) becomes

$$a \cong \frac{0.2}{\pi} Z \sum_1 \frac{\sin k\pi}{k'} \frac{2}{m} \left[I_1 m \sin \frac{k\pi}{m} \left\{ \sin \left[(1 - k')\omega t + k' \frac{\pi x}{\tau} + \theta_1 \right] \right. \right. \\ \left. \left. + \sin \left[(1 + k'')\omega t - k'' \frac{\pi x}{\tau} + \theta_1 \right] \right\} \right. \\ \left. - I_d \frac{4}{p} \sin k \left(\frac{\pi x}{\tau} - \xi \right) \right] \quad (42)$$

for odd values of k only. By (14) the alternating current (crest value) is

$$I_1 = \frac{4\Delta}{\sin \pi m} \frac{I_d}{\eta m P (1 + \epsilon) \cos \theta_1} \quad (43)$$

hence (42) becomes

$$a \cong \frac{0.8}{\pi} \frac{Z}{p} I_1 \sum_1 \frac{\sin k\pi}{k'} \frac{2}{m} \left[\frac{\Delta}{\eta (1 + \epsilon) \cos \theta_1} \frac{\sin k\pi}{\sin \pi m} \right. \\ \left. \left\{ \sin \left[(1 - k')\omega t + k' \frac{\pi x}{\tau} + \theta_1 \right] + \sin \left[(1 + k'')\omega t - k'' \frac{\pi x}{\tau} + \theta_1 \right] \right\} \right. \\ \left. - \sin k \left(\frac{\pi x}{\tau} - \xi \right) \right] \quad (44)$$

Since k is always odd, and since $(1 + k)$ is zero or a multiple of m , it follows that

$$\frac{\sin k\pi}{\sin \pi m} = \pm 1$$

the plus sign being associated with k' and the negative sign with k'' . Moreover, the time harmonics $(1 + k)$ are always even (including zero).

Thus the armature reaction of a converter consists of a *triangular* distribution of d.c. reaction, a constant *sinusoidal* distribution of a.c. reaction ($k' = 1$), and a series of *even* time harmonics. The pulsations due to the even time harmonics show up in the oscillograms as the so-called "tap ripple." For unity power factor ($\theta_1 = 0$), no brush shift ($\xi = 0$), neither buck nor boost ($\epsilon = 0$), and a sinusoidal flux distribution

($\Delta = 1$) the steady term of armature reaction under the main pole ($x = 0$) disappears, but the armature reaction under the interpole ($x = \tau/2$) does not vanish under these conditions. For example, in the case of $m = 6$ (44) gives for $x = \tau/2$

$$a_g = \frac{Z}{P} I_d (-0.0595 + 0.0154 \cos 6\omega t - 0.0006 \cos 12\omega t + \dots)$$

Thus a 6th time harmonic pulsation of about one-fourth the magnitude of the steady term exists under the interpole. Due to this pulsation the armature reaction varies from about 10 per cent to 20 per cent of the d.c. armature reaction. The ordinary series winding of the interpole does not neutralize these pulsations of magnetomotive force, but damper windings in the interpole will assist in neutralizing them.

It is interesting to note that under the above ideal case, the space fundamental armature reaction component vanishes entirely. But space harmonics in the flux distribution and in the armature reaction, poor efficiency, buck or boost, departure from unity power factor, and brush shift, all conspire to upset the magnetomotive force balance, and if not properly compensated, will result in poor commutation and possibly flashover.

8. Voltage Control

The foregoing analysis shows that the voltage ratio of a converter is essentially a fixed value, except the harmonic content of the field flux distribution be changed by means of split poles. Since this latter possibility leads to a complicated and expensive construction, it has been found better to control the direct output voltage by varying the alternating input voltage at the slip rings. There are four ways in which this may be accomplished.

A polyphase *induction regulator* may be used in series between the transformer and the converter slip rings. This will give smooth variation of the voltage over any desired range, but necessitates an extra piece of apparatus.

Tap changing transformers offer a simple and inexpensive method of changing the voltage. The tap changing may be arranged for automatic load ratio control. The voltage changes by discrete steps, which may be objectionable, but direct voltages intermediate between those corresponding to the tap steps may be obtained by field adjustments, as described in the next paragraph.

Field excitation changes will cause the converter to draw a leading

current for high and a lagging current for reduced excitation. A leading current drawn through the reactance of the transformer (or a separate series reactor) will result in a rise of alternating voltage at the slip rings. A lagging current will result in a fall of voltage at the slip rings. This method of regulation depends upon a change in power factor in the converter, and as was shown in Section 5, a small departure from unity power factor plays havoc with the armature heating. For this reason voltage control by field excitation is limited to a few per cent, plus or minus. Within these allowable limits the change in excitation may be accomplished by varying the shunt field current, or automatically by means of a series field. In those cases where the voltage range can be satisfied (± 5 per cent), this is the most satisfactory of all the methods of control.

Booster converters have an auxiliary generator whose armature is connected in series with the converter armature, and whose voltage may be added to or subtracted from that of the converter. The booster may be either a d-c or an a-c machine; and it may be either a separate machine or mounted on the shaft as an integral part of the converter. D-c boosters are not used, because the commutators have to be large and expensive to handle the full load currents. A-c, or synchronous, boosters are universally mounted on the main shaft with the revolving armature between the converter armature and the slip rings. A separate field, having the same number of poles as the converter, may be adjusted in either direction so that its voltage is added or subtracted from the slip ring voltage. But when the voltage is additive, the booster is acting as a generator, and must receive its drive from the converter acting as a motor. The converter must, therefore, draw a motor current, above and beyond the current converted to d-c, and this upsets the ampere-turn balance in the armature. The interpoles must therefore be provided with shunt windings to compensate for this unbalance of armature reaction and preserve good commutation.

9. Hunting and Commutation

Hunting in a converter is the same phenomenon as occurs in a synchronous motor; but whereas in the motor the only concern is whether the machine will remain in step or may produce a flicker in the lights, in the converter hunting may be accompanied by violent sparking at the d-c brushes, or even by a flashover of the commutator. The reason for brush sparking is that the magnetomotive force of armature reaction (which is stationary in space under normal conditions) oscillates back and

forth as the armature oscillates about its mean or synchronous speed, and thereby induces voltages in the short-circuited armature coils undergoing commutation. The presence of a commutating pole will accentuate the trouble, because it offers a lower reactance path to the magnetomotive force and permits more flux in the quadrature path. If the voltage induced in the armature coils by the oscillating flux is sufficiently high, the air between commutator segments will breakdown and precipitate a flashover of the commutator.

An abrupt change of load, of a short circuit on the d-c side, may cause a flashover. The d-c armature reaction is instantaneous, but the a-c armature reaction has a time lag due to the inductive circuits, so that there is a momentary unbalance of armature reaction. The rotor torque angle oscillates and sparking or flashover may result. Moreover, if the interpoles have noninductive shunts, the increment of d-c current will flow initially through the shunt, rather than through the high inductance interpole windings, and consequently full compensation is not instantaneously available in the commutating zone.

It is therefore imperative to prevent hunting in a converter. This is done by means of heavy damper windings in the pole faces.

Question: Would increasing the W/R^2 of a converter alleviate sparking due to hunting? Why?

10. Inverters

If the power transmitted through a synchronous converter is reversed, that is, flows from the d-c to the a-c side, the machine becomes an *inverter*. Machines are rarely intended for continual use as inverters, but occasions arise when reverse power must be reckoned with. For example, regenerative braking on electric locomotives fed by synchronous converters may result in temporary reversal of power through the converters.

There is an interesting aspect of inverter action which may result in runaway speeds if the frequency on the a-c side is not fixed. Suppose a converter has a compound field and is operating in parallel with other sources of d-c power, and that its a-c power supply is suddenly cut off, power will reverse and the converter will begin to speed up as a differentially wound d-c motor. If there is an inductive load on the a-c side, the a-c armature reaction will further weaken the field and cause the machine to speed up even more. But the higher the speed the higher the frequency, and the more reactive the load, resulting in still further weakening of the

field. Thus the machine will run away. For this reason, converters should be equipped with speed-limiting devices.

11. Starting

There are three ways of starting a converter.

a. *By an auxiliary motor.* This is an older method in which an induction motor is mounted on an extension of the converter shaft and is used to bring the converter above normal speed. The motor is then switched off and the converter is synchronized at the proper instant as it slows down. This method of starting has been abandoned, because the extra motor and its starting compensator are expensive and the shaft extension to accommodate the auxiliary motor adds to the overall length.

b. *By amortisseur windings.* The damper windings in the pole face are used to start the converter, at reduced voltage, as an induction motor, with the field winding open-circuited; and when synchronous speed is approached the field is excited and the converter pulls into step as a synchronous motor. Certain precautions are usually expedient in starting a converter by this method. The open-circuited shunt field winding should be sectionalized during starting to avoid excessive induced voltages. If the series field has a shunt, this must be opened to prevent heavy circulating currents due to transformer action during starting. The d-c brushes should also be lifted during starting, for otherwise vicious sparking will occur due to the large currents induced in the short-circuited armature coils under the brushes. These currents are accentuated by the presence of interpoles which offer a lower reactance path to the flux caused by the rotating field of armature reaction. (Once synchronism is attained the armature reaction is stationary in space and no longer induces voltages in the field windings or in short-circuited armature coils.) Usually one pair of brushes (narrower than the others) are left in contact with the commutator to provide a source of d-c excitation, and to indicate polarity.

c. *As a d-c motor.* When a d-c source is available, as when machines are operated in parallel, the converter may be started as a d-c motor and synchronized in the usual fashion. The series field winding should be short-circuited or disconnected to obviate the possibility of starting in the wrong direction as a differentially wound compound motor. Also, the a-c side should be disconnected (usually by raising the slip ring brushes) from the transformers, because the frequency is low in the early stages of starting and the transformer impedance correspondingly small, so that heavy alternating currents will flow.

12. Parallel Operation

Dissimilar converters paralleled on the a-c slip rings will not operate properly, because heavy circulating currents will flow between them. But if each converter has its own transformer bank (as is usually the case), no special difficulties are encountered.

In the case of compound-wound machines, equalizer connections must be used as with compound-wound d-c generators.

Load division between converters operated in parallel is effected by changing the direct voltages of the individual machines.

APPENDIX I

The Distribution Summations

This appendix is concerned with finding the sum of certain finite trigonometric series which repeatedly occur in the harmonic analysis of rotating machines. These sums are in fact the pitch and distribution factors. Since

$$\frac{1-z}{1-z} = 1 + z + z^2 + \dots + z^{j-1} = \sum_{r=0}^{j-1} z^r \quad (1)$$

it follows upon replacing z by $e^{-j\alpha}$ that

$$\begin{aligned} \sum_{r=0}^{j-1} \sin(\lambda + r\alpha) &= \sum_{r=0}^{j-1} e^{j(\lambda + r\alpha)} - e^{-j(\lambda + r\alpha)} \\ &= \frac{e^{j\lambda}}{2j} \left(\frac{1 - e^{-j\alpha j}}{1 - e^{-j\alpha}} \right) - \frac{e^{-j\lambda}}{2j} \left(\frac{1 - e^{-j\alpha j}}{1 - e^{-j\alpha}} \right) \\ &= \left[\frac{e^{j\lambda} + e^{-j\lambda}}{2j(1 - e^{-j\alpha})} - \frac{e^{j(\lambda + \alpha)} + e^{-j(\lambda + \alpha)}}{2j(1 - e^{-j\alpha})} \right] \\ &= \frac{\sin \lambda - \sin(\lambda + \alpha)}{2(1 - \cos \alpha)} + \frac{\sin(\lambda + n\alpha - \alpha) - \sin(\lambda + n\alpha)}{2(1 - \cos \alpha)} \\ &= \frac{2 \sin(\alpha/2) \cos[(2\lambda - \alpha)/2] - 2 \sin(\alpha/2) \cos[(2\lambda + 2n\alpha - \alpha)/2]}{4 \sin^2 \alpha/2} \\ &= \frac{\cos[(2\lambda - \alpha)/2] - \cos[(2\lambda - \alpha + 2n\alpha)/2]}{2 \sin(\alpha/2)} \end{aligned}$$

$$= \frac{\sin n\alpha}{\sin \alpha} \frac{2}{2} \sin \left(x + \frac{n-1}{2} \alpha \right) \quad (2)$$

Replacing (α) by $(-\alpha)$

$$\sum_{r=0}^{n-1} \sin (x - r\alpha) = \frac{\sin n\alpha}{\sin \alpha} \frac{2}{2} \sin \left(x - \frac{n-1}{2} \alpha \right) \quad (3)$$

Replacing (x) by $(x + \pi/2)$ in (2) and (3) respectively

$$\sum_{r=0}^{n-1} \cos (x + r\alpha) = \frac{\sin n\alpha}{\sin \alpha} \frac{2}{2} \cos \left(x + \frac{n-1}{2} \alpha \right) \quad (4)$$

$$\sum_{r=0}^{n-1} \cos (x - r\alpha) = \frac{\sin n\alpha}{\sin \alpha} \frac{2}{2} \cos \left(x - \frac{n-1}{2} \alpha \right) \quad (5)$$

If the range of summation is $(1 \leq r \leq n)$, put $r = s + 1$, so that

$$\sum_{r=1}^n \sin (x + r\alpha) = \sum_{s=0}^{n-1} \sin (x + \alpha + s\alpha) = \frac{\sin n\alpha}{\sin \alpha} \frac{2}{2} \sin \left(x + \frac{n+1}{2} \alpha \right) \quad (6)$$

and similarly in the other expressions $(n-1)$ is replaced by $(n+1)$ when the limits of summation are 1 to n rather than 0 to $(n-1)$.

The more general sums, in which the angles do not differ by a regular amount, and in which different amplitudes are involved, are found as follows, using complex numbers:

$$\sum A_r = \sum A_r e^{j\theta_r} = \sum A_r \cos \theta_r + j \sum A_r \sin \theta_r = A_0 e^{j\theta_0} \quad (7)$$

$$\text{where } A_0 = \sqrt{(\sum A_r \cos \theta_r)^2 + (\sum A_r \sin \theta_r)^2} \quad (8)$$

$$\tan \theta_0 = \frac{\sum A_r \sin \theta_r}{\sum A_r \cos \theta_r} \quad (9)$$

Or transforming to trigonometric notation

$$\sum A_r \sin (x + \theta_r) = A_0 \sin (x + \theta_0) \quad (10)$$

$$\sum A_r \cos (x + \theta_r) = A_0 \cos (x + \theta_0) \quad (11)$$

If $A_1 = A_2 = \dots = A_n = A$ and $\theta_r = r\alpha$, then (8) and (9) reduce as follows:

$$\begin{aligned} A_0 &= A \sqrt{\left(\sum_{r=0}^{n-1} \cos r\alpha \right)^2 + \left(\sum_{r=0}^{n-1} \sin r\alpha \right)^2} \\ &= A \frac{\sin n\alpha}{\sin \alpha} \frac{2}{2} \sqrt{\left(\cos \frac{n-1}{2} \alpha \right)^2 + \left(\sin \frac{n-1}{2} \alpha \right)^2} \\ &= A \frac{\sin n\alpha}{\sin \alpha} \frac{2}{2} \end{aligned} \quad (12)$$

$$\theta_0 = \tan^{-1} \left(\tan \frac{n-1}{2} \alpha \right) = \frac{n-1}{2} \alpha \quad (13)$$

APPENDIX II

Armature Reaction*

1. The Magnetomotive Force of a Single Coil

Consider a concentrated coil, Fig. 1, of N -turns, stacking length l , and pitch $p\tau$ whose center is located a distance x_0' from a reference axis. Let

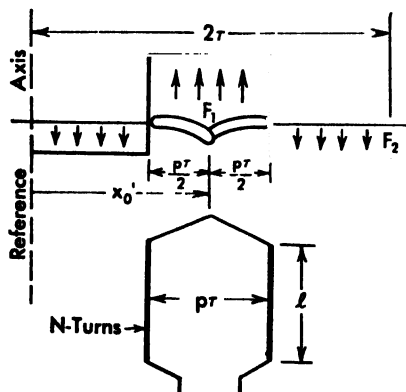


Fig. 1

the pole pitch be τ . The magnetomotive force of the coil is $0.4\pi Ni$. Assuming a uniform air gap of length g , this magnetomotive force will produce a flux which crosses the air gap upward through the coil (of area $p\tau l$) and returns downward through the remaining area $(2 - p)\tau l$. The two paths are therefore in series, and their combined reluctance is

$$\mathcal{R} = \frac{g}{p\tau l} + \frac{g}{(2 - p)\tau l} = \frac{2g}{p(2 - p)\tau l}$$

The flux then is
$$\phi = \frac{mmf}{\mathcal{R}} = \frac{0.2\pi p(2 - p)\tau l Ni}{g}$$

The magnetomotive force drops corresponding to the upward and downward flux paths then are

* Hambleton and Bewley, "The Synchronous Converter," *AIEE Trans*, Vol. 47 (1927)

$$F_1 = \frac{g}{p\tau l} \phi = 0.2\pi(2 - p)Ni$$

$$F_2 = \frac{g}{(2 - p)\tau l} \phi = 0.2\pi pNi$$

Thus it is possible to regard the coil as having its total magnetomotive force distributed in the above proportion, and accordingly represented by an unsymmetrical rectangular wave. This wave, Fig. 1, may be specified piecewise as follows:

$$\left. \begin{aligned} F &= -0.2\pi pNi & \text{for} & \quad 0 < x < \left(x_0' - p\frac{\tau}{2}\right) \\ F &= +0.2\pi(2 - p)Ni & \text{for} & \quad \left(x_0' - \frac{p\tau}{2}\right) < x < \left(x_0' + p\frac{\tau}{2}\right) \\ F &= -0.2\pi pNi & \text{for} & \quad \left(x_0' + \frac{p\tau}{2}\right) < x < 2\tau \end{aligned} \right\}$$

Now over the range ($0 < x < 2\tau$) this distribution may be expressed as a Fourier series

$$F(x) = \sum \left(A_k \sin \frac{k\pi x}{\tau} + B_k \cos \frac{k\pi x}{\tau} \right)$$

The coefficients are evaluated in the usual fashion as

$$\begin{aligned} A_k &= \frac{1}{\tau} \int_0^{2\tau} F(x) \cdot \sin \frac{k\pi x}{\tau} \cdot dx \\ &= \frac{0.2\pi Ni}{\tau} \left[-p \int_0^{x_0' - \frac{p\tau}{2}} \sin \frac{k\pi x}{\tau} dx + (2 - p) \int_{x_0' - \frac{p\tau}{2}}^{x_0' + \frac{p\tau}{2}} \sin \frac{k\pi x}{\tau} dx \right. \\ &\quad \left. - p \int_{x_0' + \frac{p\tau}{2}}^{2\tau} \sin \frac{k\pi x}{\tau} dx \right] \\ &= \frac{0.8Ni}{k} \sin \frac{k p \pi}{2} \sin \frac{k \pi x_0'}{\tau} \end{aligned}$$

$$\begin{aligned} \text{Likewise} \quad B_k &= \frac{1}{\tau} \int_0^{\tau} F(x) \cdot \cos \frac{k\pi x}{\tau} dx \\ &= \frac{0.8Ni}{k} \sin \frac{k p \pi}{2} \cos \frac{k \pi x_0'}{\tau} \end{aligned}$$

Thus the Fourier series for the magnetomotive force is

$$\begin{aligned} F(x) &= 0.8Ni \sum_k \frac{\sin \frac{k p \pi}{2}}{k} \left(\sin \frac{k \pi x_0'}{\tau} \sin \frac{k \pi x}{\tau} + \cos \frac{k \pi x_0'}{\tau} \cos \frac{k \pi x}{\tau} \right) \\ &= 0.8Ni \sum_k \frac{K_{p'}}{k} \cos \frac{k \pi}{\tau} (x - x_0') \end{aligned} \quad (1)$$

in which

$$K_{pk} = \sin \frac{k p \pi}{2} = \text{pitch coefficient of the } k\text{th harmonic.} \quad (2)$$

For a full-pitch coil ($p = 1$) this coefficient is ± 1 . Thus the effect of fractional pitch is to reduce the magnitude of each harmonic of magnetomotive force and possibly reverse its sign. This same coefficient will appear later in an exactly analogous manner in the equations for the induced voltage in a coil in Appendix IV. Curves of the pitch coefficient were given in Fig. 2 of Chapter 3, and accompanied by a discussion of the characteristics and meaning of the coefficient.

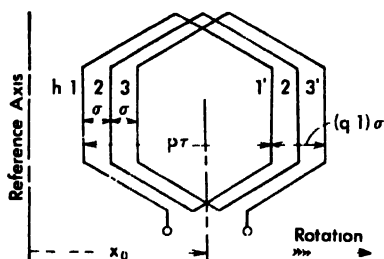


Fig. 2

be at x_0 . Then the center of the h th coil of the group, counting from the trailing coil, is located at

$$x_0' = x_0 - \frac{(q-1)\sigma}{2} + (h-1)\sigma = x_0 - \frac{q-1}{2}\sigma + h\sigma \quad (3)$$

Substitution in (1) then gives the magnetomotive force, or armature reaction, for this h th coil. The magnetomotive force of the entire group of coils therefore is (Appendix I)

$$\begin{aligned} a_g &= 0.8Vi \sum_{k=1}^q \sum_{h=1}^q \frac{K_{pk}}{k} \cos \frac{k\pi}{\tau} \left(x - x_0 + \frac{q-1}{2}\sigma - h\sigma \right) \\ &= 0.8qVi \sum_{k=1}^q \frac{K_{dk}K_{pk}}{k} \cos \frac{k\pi}{\tau} (x - x_0) \end{aligned} \quad (4)$$

in which

$$\begin{aligned} K_{dk} &= \frac{\sin(kq\sigma\pi/2\tau)}{q \cdot \sin(k\sigma\pi/2\tau)} \\ &= \text{distribution coefficient for the } k\text{th space harmonic} \end{aligned} \quad (5)$$

The summation with respect to h in (4) is effected by the general method given in Appendix I, and results in the appearance of the *distribution*

2. The Armature Reaction of a Group of Coils

Several coils belonging to the same phase may be connected in series, Fig. 2, to form a *phase group* or *belt*. Suppose there are q coils of pitch $p\tau$ in the group, with coil sides uniformly separated by the *slot pitch* σ , and let the center of the group

coefficients, (5). These factors also appear in the induced voltage equations, and were discussed in detail in Chapter 3. For the present it is sufficient to observe that K_{at} is a factor generally less than unity whose general effect is to reduce the space harmonics in comparison with the fundamental of armature reaction.

Up to this point nothing has been said about the instantaneous current i . Suppose, now, that the coil group discussed above is assumed to belong to the r th phase of an m -phase winding, and let this phase be supplied with a general (time) harmonic current given by the Fourier series

$$i_r = \sum_n I_n \sin \left[n\omega t + \theta_n - \frac{n2\pi}{m} (r - 1) \right] \quad (6)$$

in which $2\pi/m$ is the time-angle between the fundamental phase currents and θ_n is the phase-angle of the n th time harmonic. The current in the first phase, $r = 1$, is

$$\begin{aligned} i_1 &= \sum I_n \sin (n\omega t + \theta_n) \\ &= \sum (I_n \cos \theta_n \sin n\omega t + I_n \sin \theta_n \cos n\omega t) \\ &= \sum (I_{Qn} \sin n\omega t + I_{Dn} \cos n\omega t) \end{aligned} \quad (7)$$

in which $I_{Qn} = I_n \cos \theta_n$ and $I_{Dn} = I_n \sin \theta_n$ are called the *quadrature* and *direct* components of armature current, and are of significance in synchronous machine theory.

3. The Armature Reaction of a Polyphase Winding

Now if phase 1, Fig. 3, is centered at x_0 , phase r will be centered at $\left(x_0 - 2\tau \frac{r-1}{m}\right)$, and this latter value should be substituted for x_0 in

(4) to give the armature reaction for the r th phase. Then substituting (6) in (4) and summing for all the phases, the resulting armature reaction becomes (putting $K_i = K_{at} K_{pt}$)

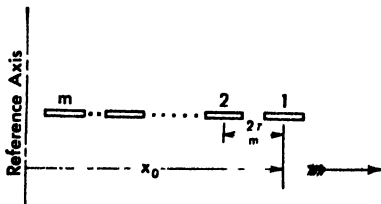


Fig. 3

$$\begin{aligned} a &= 0.8qN \sum \sum \frac{K_i}{k} I_n \sin \left[n\omega t + \theta_n - \frac{n2\pi}{m} (r - 1) \right] \\ &\quad \cos \frac{k\pi}{\tau} \left(x - x_0 + 2\tau \frac{r-1}{m} \right) \end{aligned}$$

$$\begin{aligned}
&= 0.4qN \sum_n \sum_k \sum_1^m \frac{K_k}{k} I_n \left\{ \sin \left[n\omega t + \theta_n + k\pi \frac{x - x_0}{\tau} \right. \right. \\
&\quad \left. \left. - \frac{2\pi}{m} (r-1)(n-k) \right] + \sin \left[n\omega t + \theta_n - k\pi \frac{x - x_0}{\tau} - \frac{2\pi}{m} (r-1)(n+k) \right] \right\} \\
&= 0.4qN \sum_n \sum_k \frac{K_k}{k} I_n \left\{ \sin \left(n\omega t + \theta_n + k\pi \frac{x - x_0}{\tau} \right) \sum_1^m \cos \frac{2\pi(r-1)(n-k)}{m} \right. \\
&\quad \left. - \cos \left(n\omega t + \theta_n + k\pi \frac{x - x_0}{\tau} \right) \sum_1^m \sin \frac{2\pi(r-1)(n-k)}{m} \right. \\
&\quad \left. + \sin \left(n\omega t + \theta_n - k\pi \frac{x - x_0}{\tau} \right) \sum_1^m \cos \frac{2\pi(r-1)(n+k)}{m} \right. \\
&\quad \left. - \cos \left(n\omega t + \theta_n - k\pi \frac{x - x_0}{\tau} \right) \sum_1^m \sin \frac{2\pi(r-1)(n+k)}{m} \right\} \quad (8)
\end{aligned}$$

Now, if α is any integer, then by the methods of Appendix I

$$\sum_1^m \cos \frac{2\pi(r-1)(n+k)}{m} = \begin{cases} 0 & \text{if } (n+k) \neq \alpha m \\ m & \text{if } (n+k) = \alpha m \end{cases} \quad (9)$$

$$\sum_1^m \sin \frac{2\pi(r-1)(n+k)}{m} = 0 \quad (10)$$

Let $k' = \text{any value of } k \text{ for which } (n-k) = \alpha m \text{ or } 0$ (11)
 $k'' = \text{any value of } k \text{ for which } (n+k) = \alpha m$

Then by (9), (10) and (11), equation (8) for the armature reaction referred to the reference axis reduces to

$$a = 0.4qNm \sum_n \sum_k \frac{K_k}{k} I_n \sin \left(n\omega t + \theta_n \pm \begin{cases} k' \\ k'' \end{cases} \pi \frac{x - x_0}{\tau} \right) \quad (12)$$

This is a simple and compact expression for the polyphase armature reaction, with respect to an arbitrary reference axis, of any number of uniformly distributed fractional pitch coils having harmonic excitation. It is understood that the summation \sum_k is to be taken with respect to both k' and k'' . In this form, the magnetomotive force is given as a system of rotating fields (or traveling waves) having velocities with respect to the reference axis of

$$\frac{\pi}{\tau} \frac{d(x - x_0)}{dt} = \begin{cases} -n\omega & k' \\ +n\omega & k'' \end{cases} \quad (13)$$

If the reference axis is on the armature, x_0 is constant and the magnetomotive force for a given harmonic k is seen to sweep around the armature

at a speed inversely proportional to the order k of the space harmonic, and directly proportional to the order n of the time harmonic. The k'' harmonics give rise to *forward* traveling waves, and the k' harmonics to *backward* traveling waves.

Now suppose the armature to revolve at synchronous speed, $x_0\pi/\tau = \omega t$, where time t is counted from the instant when the first phase-group, $r = 1$, is centered on the reference axis, $x_0 = 0$. Then (12) becomes

$$a = 0.4qNm \sum_n \sum_k \frac{K_k}{k} I_n \sin \left[\left(n + \frac{k'}{k''} \right) \omega t + \left\{ \frac{k'}{k''} \right\} \frac{x\pi}{\tau} + \theta_n \right] \quad (14)$$

The constant (non-pulsating) terms of armature reaction are those for which $(n - k') = 0$, and these give, independent of time,

$$a_c = 0.4qNm \sum_n \frac{K_n}{n} I_n \sin \left(\frac{n\pi x}{\tau} + \theta_n \right) \quad (15)$$

This term is sinusoidally distributed and has "direct" (in line with reference axis) and "quadrature" components, in terms of (7), of

$$a_d = 0.4qNm \sum_n \frac{K_n}{n} I_{Dn} \cos \frac{n\pi x}{\tau} \quad (16)$$

$$a_q = 0.4qNm \sum_n \frac{K_n}{n} I_{Qn} \sin \frac{n\pi x}{\tau} \quad (17)$$

It is these terms of armature reaction which, in conjunction with the main field, produce the steady component of flux in the air gap of the machine.

Equation (14) may be resolved into direct and quadrature components in terms of (7),

$$\begin{aligned} a &= 0.4qNm \sum_n \sum_k \frac{K_k}{k} I_n \left\{ \sin \left[\left(n + \frac{k'}{k''} \right) \omega t + \theta_n \right] \cos \frac{k\pi x}{\tau} \right. \\ &\quad \left. + \cos \left[\left(n + \frac{k'}{k''} \right) \omega t + \theta_n \right] \sin \frac{k\pi x}{\tau} \right\} \\ &= 0.4qNm \sum_n \sum_k \frac{K_k}{k} \left\{ \left[I_{Qn} \sin \left(n + \frac{k'}{k''} \right) \omega t \right. \right. \\ &\quad \left. \left. + I_{Dn} \cos \left(n + \frac{k'}{k''} \right) \omega t \right] \cos \frac{k\pi x}{\tau} + \left[I_{Qn} \cos \left(n + \frac{k'}{k''} \right) \omega t \right. \right. \\ &\quad \left. \left. - I_{Dn} \sin \left(n + \frac{k'}{k''} \right) \omega t \right] \sin \frac{k\pi x}{\tau} \right\} \quad (18) \end{aligned}$$

The constant components (16) and (17) follow also from this form, upon segregating the $(n - k') = 0$ terms. In (18) the *direct* components (in

line with the reference axes) are the $\cos k\pi x/\tau$ terms, and the *quadrature* components are the $\sin k\pi x/\tau$ terms, as is evident upon substituting $x = 0$ and $x = \tau/2$ respectively.

In a 3-phase machine wound with 60 degree phase belts (thus in reality a 6-phase machine, $m = 6$) the contributing space harmonics for the fundamental, third, and fifth time harmonics, and the velocities with respect to the armature, are:

k	$n = 1$		$n = 3$		$n = 5$	
	$n - k'$	$n + k''$ vel.	$n - k'$	$n + k''$ vel.	$n - k'$	$n + k''$ vel.
1	0	-1			6	+5
3			0	6 -1		
5	6	+1 5			0	-1
7	-6	-1 7			12	+5 7
9			-6	12 +1 3		
11	12	+1 11			-6	-5 11
13	-12	-1 13			18	+5 13
15			12	18 +1 5		
17	18	+1 17			-12	-5 17
19	-18	-1 19			24	+5 19
21			-18	24 +1 7		

If the armature is moving forward at synchronous speed, $x_0\pi/\tau = \omega t$, then the fundamental space harmonic, which is moving backward at synchronous speed with respect to the armature, is standing still in space. In general, the speed of any space harmonic with respect to a stationary axis is

$$\frac{\pi}{\tau} \frac{dx}{dt} = \omega + \begin{cases} -n\omega & k' \\ +n\omega & k'' \end{cases} = \begin{cases} \omega(n - k') & k' \\ \omega(n + k'') & k'' \end{cases} \quad (19)$$

Negative Sequence Armature Reaction

If the phase sequence of the exciting currents is reversed, so that the phase currents reach their maximum in the order $m - \dots - 2 - 1$ rather than in the order $1 - 2 - \dots - m$, (6) is replaced by

$$i_r^{(-)} = \sum_n I_n^{(-)} \sin \left[n\omega t + \theta_n + n \frac{2\pi}{m} (r - 1) \right] \quad (20)$$

Substituting (20) instead of (6) in (4) their results, corresponding to (12),

$$a^{(-)} = 0.4qNm \sum_n \sum_k \frac{K_A}{k} I_n^{(-)} \sin \left(n\omega t + \theta_n \pm \begin{cases} k'' \\ k' \end{cases} \left\{ \frac{x}{\tau} - \frac{x_0}{\tau} \right\} \pi \right) \quad (21)$$

and corresponding to (14) for a synchronous machine

$$a^{(1)} = 0.4qNm \sum_n \sum_l \frac{K_l}{k} I_{n,l} \sin \left[\left(n + \frac{k''}{k'} \right) \omega t + \left\{ \frac{k''}{k'} \right\} \frac{\pi x}{\tau} + \theta_n \right] \quad (22)$$

Thus the armature reaction equations for negative sequence currents have exactly the same form as those for positive sequence currents, except that k'' and k' have exchanged places, and this entails a reversal in the direction of rotation of the various harmonics.

Zero Sequence Armature Reaction

If all the phases are excited by in phase currents (zero sequence currents), then (6) is replaced by

$$i^{(0)} = \sum_n I_n^{(0)} \sin (n\omega t + \theta_n) \quad (23)$$

Substituting these currents in (4) and summing over all the phases, there results

$$\begin{aligned} a^{(0)} &= 0.8qN \sum_n \sum_l \sum_m \frac{K_l}{k} I_{n,l}^{(0)} \sin (n\omega t + \theta_n) \cos \frac{k\pi}{\tau} \left(1 - x_0 + 2\tau \frac{r}{m} - 1 \right) \\ &= 0.8qN \sum_n \sum_l \frac{K_l}{k} I_{n,l}^{(0)} \frac{\sin k\pi}{\sin k\pi/m} \sin (n\omega t + \theta_n) \cos k\pi \left(\frac{1}{\tau} - \frac{x_0}{\tau} + \frac{m-1}{m} \right) \end{aligned} \quad (24)$$

This expression vanishes unless $k - k'' = \alpha m$ (a multiple of the number of phases), in which case

$$a^{(0)} = 0.8qNm \sum_n \sum_l \frac{K_l'''}{k'''} I_{n,l}^{(0)} \sin (n\omega t + \theta_n) \cos \frac{k'''\pi}{\tau} (1 - x_0) \quad (25)$$

Substituting $x_0 = \omega t$ for a synchronous machine, there results

$$\begin{aligned} a^{(0)} &= 0.8qNm \sum_n \sum_l \frac{K_l'''}{k'''} I_{n,l}^{(0)} \sin (n\omega t + \theta_n) \cos k'''\pi \left(\frac{\pi x}{\tau} - \omega t \right) \\ &= 0.4qNm \sum_n \sum_l \frac{K_l'''}{k'''} I_{n,l}^{(0)} \left\{ \sin \left[(n - k''') \omega t + \frac{k'''\pi x}{\tau} \right] \right. \\ &\quad \left. + \sin \left[(n + k''') \omega t - \frac{k'''\pi x}{\tau} \right] \right\} \quad (26) \end{aligned}$$

For $n = k'''$ there is both a stationary component given by the first part of (26) and a rotating field given by the second part of (26), the latter revolving in the forward direction at *twice* synchronous speed. All other permissible space harmonics give rise to a pair of traveling waves of equal magnitude revolving in opposite directions.

APPENDIX III

Permeances and Flux Density

The air gap of a rotating machine, on which the field and armature magnetomotive forces act to produce flux, may be substantially smooth and uniform as in turbo alternators and induction motors, or quite variable as in salient pole machines. In either case minor irregularities are introduced by the slots and teeth. It is the purpose of this appendix to show how the permeance may be represented by a Fourier series which can be multiplied by the Fourier series of armature reaction to yield an expression for flux density.

1. Uniform Air Gaps

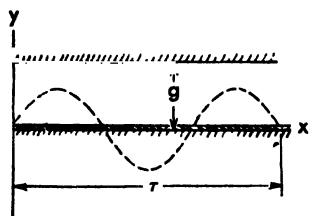


Fig. 1

Figure 1 shows a uniform air gap, g , subjected to a harmonic excitation along the lower boundary. If the excitation is the k th space harmonic, and the pole pitch is τ , it may be shown that the permeance per unit area of the gap is *

$$\phi_{(\mu - a)} = \frac{k\pi g}{\sinh k\pi g} \frac{\tau}{\tau g} \frac{1}{\tau g} \quad (1)$$

As here defined ϕ_g is the factor which multiplied by the magnitude of the armature reaction at any point gives the corresponding flux density

* Bewley, L. V., *Two-Dimensional Fields in Electrical Engineering*, The Macmillan Co., New York, 1948.

on the opposite side of the gap). As thus defined it is a measure of the flux which *crosses* the gap, and not of the flux along the armature surface. The corresponding permeance factor along the armature surface is

$$\phi_{(y=0)} = \frac{k\pi g}{\tanh k\pi g} \tau \frac{1}{g} \quad (2)$$

In either case, (1) or (2), if $k\pi g$ is small compared to the pole pitch, τ , the permeance factor is closely equal to the reciprocal of the air gap, $\phi = 1/g$. Otherwise, these permeance factors for a smooth uniform air gap are constant for a given space harmonic, but differ for each harmonic. When the order of the space harmonic is high the permeance (1) approaches zero (that is, no flux crosses the air gap), while the permeance (2) approaches the value $k\pi \tau$ independent of the gap.

2. Nonuniform Air Gap

In salient pole construction the air gap is not uniform, due to the interpolar space and to the chamfer of the pole faces, Fig. 2. Each space harmonic of excitation will then give rise to a somewhat different flux distribution, and a *sine* wave of magnetomotive force will have a different flux distribution than a *cosine* wave. It is not possible to derive analytical expressions for the permeances of salient pole machines, and in general it is necessary to rely upon free hand field plots.* From such field plots permeance curves, corresponding to particular modes of excitation, Fig. 2, may be drawn and then analyzed into Fourier series. Since the permeance curve for either a harmonic *sine* or a *cosine* distribution of magnetomotive force must be symmetrical about both the pole and interpolar (direct and quadrature axes,) it can contain only *even* harmonics and a constant term. Let

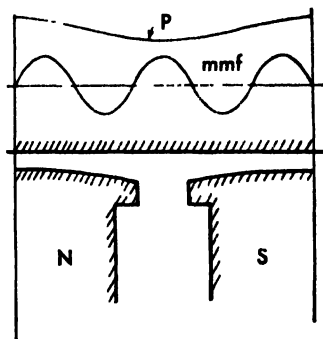


Fig. 2

$\phi = p$ th space harmonic of permeance for the *sine* wave of the k th space harmonic of magnetomotive force.

$\phi = p$ th space harmonic of permeance for the *cosine* wave of the k th space harmonic of magnetomotive force.

* Doherty and Nickle, "Synchronous Machines, I," *IEEE Trans.*, Vol. XLV, p. 912, 1927.

The complete permeances for the k th harmonic of magnetomotive force, expressed as Fourier series, then are

$$\dot{\Phi}_l^s = \sum_p^s \dot{\Phi}_{lp}^s \cos \frac{p\pi x}{\tau} \quad (3)$$

$$\dot{\Phi}_l^e = \sum_p^e \dot{\Phi}_{lp}^e \cos \frac{p\pi x}{\tau} \quad (4)$$

Doherty and Nickle* have shown, from numerous field plots, that these two series are substantially the same. In the majority of cases it is sufficient to take only the constant term and the second harmonic of the series.

3. Flux Density Due to Armature Reaction

Equation (18) of Appendix II gives the armature reaction of a poly-phase winding resolved into its *direct* (in line with the field poles) and *quadrature* (in line with the interpolar axis) components assuming, of course, that the reference axis is taken at the center of a field pole. Multiplying each harmonic by its appropriate permeance series, (3) or (4), there results for the flux density due to armature reaction

$$\begin{aligned} \beta_n = 0.4qNm \sum_p \sum_k \sum_{k'} \frac{K_l}{k} I_n \left\{ \dot{\Phi}_{lp}^s \sin \left[\left(n + \frac{k'}{k''} \right) \omega t + \theta_n \right] \right. \\ \left. \cos \frac{k\pi x}{\tau} + \dot{\Phi}_{lp}^e \cos \left[\left(n + \frac{k'}{k''} \right) \omega t + \theta_n \right] \sin \frac{k\pi x}{\tau} \right\} \cos \frac{p\pi x}{\tau} \quad (5) \end{aligned}$$

This equation gives the flux density with respect to a reference axis through the center of the field pole.

Combining terms, (5) becomes

$$\begin{aligned} \beta_n = 0.2qNm \sum_p \sum_l \sum_{k'} \frac{K_l}{k} I_n \left\{ \dot{\Phi}_{lp}^s \left(\sin [(n - k') \omega t + \theta_n] \right. \right. \\ \left. \left. + \sin [(n + k'') \omega t + \theta_n] \right) \cdot \left[\cos (p + k) \frac{\pi x}{\tau} + \cos (p - k) \frac{\pi x}{\tau} \right] \right. \\ \left. + \dot{\Phi}_{lp}^e \left(\cos [(n - k') \omega t + \theta_n] - \cos [(n + k'') \omega t + \theta_n] \right) \cdot \right. \\ \left. \left[\sin (p + k) \frac{\pi x}{\tau} - \sin (p - k) \frac{\pi x}{\tau} \right] \right\} \quad (6) \end{aligned}$$

This form is the most convenient for synchronous machine theory, and will be made use of in the calculation of synchronous machine armature reaction.

* *Ibid.*

4. Flux Density Due to the Field Poles

The flux density distribution due to the field poles depends on the shape of the pole (chamfer), the pole arc, and the air gap. The distribution is symmetrical about the pole axis, and can accordingly be represented by the Fourier series

$$\beta_f = \sum \beta_{2k-1} \cos (2k-1) \frac{\pi x}{\tau} \quad (7)$$

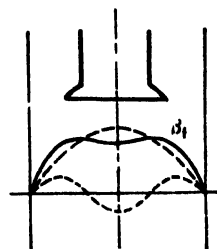


Fig. 3

APPENDIX IV

Induced Voltages

1. Induced Voltage of a Single Coil, *Fig. 1*

Consider a fractional pitch coil with skewed coil sides, the center of which is located at x_0' from an arbitrary reference axis. Then its trailing and leading coil sides are located at

$$x' = \left(x_0' - p \frac{\pi}{2} + y \tan \alpha \right)$$

$$\text{and} \quad x'' = \left(x_0' + p \frac{\pi}{2} + y \tan \alpha \right) \quad (1)$$

in which α is the angle of skew.

Suppose the coil is in a field whose flux density is specified by the representative u th space harmonic

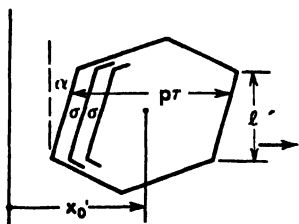


Fig. 1

$$\beta = \beta_u \sin u \left(\frac{\pi x}{\tau} + \gamma_u \right) \quad (2a)$$

$$= \left(\beta_u' \sin \frac{u\pi x}{\tau} + \beta_u'' \cos \frac{u\pi x}{\tau} \right) \quad (2b)$$

In general, this flux density distribution is due to both external causes (i.e., the field poles of an alternator and to the armature reaction of the coils themselves). Moreover, the harmonics of this flux density may be varying in magnitude, $d\beta_u/dt$, and in position, $d\gamma_u/dt$.

The total flux linked with the coil at any particular instant is

$$\phi = \int_{-l/2}^{+l/2} \int_A^{x''} \beta dx dy \quad (3)$$

Substituting (2) for the integrand, and (1) for the limits of (3), and performing the integrations, there results

$$\phi = \frac{2}{\pi} \tau l \frac{\beta_u}{u} K_{su} K_{pu} \sin u \left(\frac{\pi x_0'}{\tau} + \gamma_u \right) \quad (4)$$

in which

$$K_{pu} = \sin \frac{u p \pi}{2} = \text{pitch coefficient of the } u\text{th harmonic} \quad (5)$$

$$\begin{aligned} K_{su} &= \frac{2\tau}{u\pi l \tan \alpha} \sin \frac{u\pi l \tan \alpha}{2\tau} \\ &= \text{skew coefficient of the } u\text{th harmonic} \end{aligned} \quad (6)$$

The pitch coefficient for the flux, and therefore for the induced voltage, is identical with that for the armature reaction, Eq. (2), Appendix III.

Now the flux is a function of x_0' , β_u , and γ_u and in general each of these is a function of time. Then Faraday's law yields for the induced voltage

$$\begin{aligned} e &= \frac{-N}{10^8} \frac{d\phi}{dt} = \frac{-N}{10^8} \left\{ \frac{\partial \phi}{\partial x_0'} \frac{dx_0'}{dt} + \left(\frac{\partial \phi}{\partial \beta_u} \frac{d\beta_u}{dt} + \frac{\partial \phi}{\partial \gamma_u} \frac{d\gamma_u}{dt} \right) \right\} \\ &= -\frac{2\tau l N}{\pi 10^8} K_{su} K_{pu} \left\{ \frac{1}{u} \frac{d\beta_u}{dt} \sin u \left(\frac{\pi x_0'}{\tau} + \gamma_u \right) \right. \\ &\quad \left. + \beta_u \left(\frac{\pi}{\tau} \frac{dx_0'}{dt} + \frac{d\gamma_u}{dt} \right) \cos u \left(\frac{\pi x_0'}{\tau} + \gamma_u \right) \right\} \quad (7) \end{aligned}$$

This equation shows that an induced voltage may result from three different operations:

$$\left. \begin{aligned} d\beta_u/dt, & \text{ pulsation (standing wave) of the flux harmonic} \\ d\gamma_u/dt, & \text{ progression (traveling wave) of the flux harmonic} \\ dx_0'/dt, & \text{ movement of the coil through the flux} \end{aligned} \right\} \quad (8)$$

In a d-c or synchronous generator under balanced steady-state conditions, only the latter term is present. In the rotating field theory of the polyphase induction motor, the penultimate term is the one responsible for the induced voltage. In the transformer only the first term is present. In an a-c commutating motor all three terms may be identified. Moreover, the presence of a term depends upon the selection of the reference axis. For example, if the reference axis in a polyphase induction motor

is taken on the stator, the constant magnitude field is rotating synchronously with respect thereto. But if the reference axis is itself assumed to rotate synchronously, then the field is stationary and constant with respect to such an axis, and the voltage is due to the movement of the conductors through the flux. The different possibilities are discussed in detail in Chapter 3.

It is also clear from (7) that the harmonics of the induced voltage are modified by the skew and pitch coefficients.

An alternative form for the induced voltage results if the flux density substituted in (3) is specified by (2b) instead of (2a). In that case

$$e = -\frac{2\tau l N}{\pi 10^8} K_{su} K_{pu} \left\{ \left(\beta_u' \cos \frac{u\pi x_0'}{\tau} - \beta_u'' \sin \frac{u\pi x_0'}{\tau} \right) \frac{\pi}{\tau} \frac{dx_0'}{dt} + \frac{1}{u} \left(\frac{d\beta_u'}{dt} \sin \frac{u\pi x_0'}{\tau} + \frac{d\beta_u''}{dt} \cos \frac{u\pi x_0'}{\tau} \right) \right\} \quad (9)$$

2. Induced Voltage of a Group of Coils

The total voltage for a phase group of q coils uniformly distributed by the angle σ is found by substituting for the h th coil

$$x_0' = x_0 - \frac{(q-1)\sigma}{2} + (h-1)\sigma = x_0 - \frac{q-1}{2}\sigma + h\sigma \quad (10)$$

where x_0 is the mid-point of the coil group, and then summing (9) over the q coils of the group. Once again making use of Appendix I in effecting this summation, there results

$$e = \sum_{h=1}^q e_h = \frac{-2Nql}{10^8} K_{su} K_{pu} K_{du} \left\{ \left(\beta_u' \cos \frac{u\pi x_0}{\tau} - \beta_u'' \sin \frac{u\pi x_0}{\tau} \right) \frac{dx_0}{dt} + \frac{\tau}{u\pi} \left(\frac{d\beta_u'}{dt} \sin \frac{u\pi x_0}{\tau} + \frac{d\beta_u''}{dt} \cos \frac{u\pi x_0}{\tau} \right) \right\} \quad (11)$$

in which

$$K_{du} = \frac{\sin(uq\sigma\pi/2\tau)}{q \sin(u\sigma\pi/2\tau)}$$

= distribution coefficient of the u th space harmonic (12)

If the armature is revolving with respect to the reference axis (*i.e.* the reference axis taken on the stationary field pole)

$$\frac{\pi x_0}{\tau} = \omega t \quad \text{and} \quad \frac{dx_0}{dt} = \frac{\tau}{\pi} \omega \quad (13)$$

and these values may be substituted in (11) to give the induced voltage in the phase belt of the machine,

$$e = \frac{-2Nql\tau}{\pi 10^8} K_u \left\{ (\beta_u' \cos u\omega t - \beta_u'' \sin u\omega t) \omega + \frac{1}{u} \left(\frac{d\beta_u'}{dt} \sin u\omega t + \frac{d\beta_u''}{dt} \cos u\omega t \right) \right\} \quad (14)$$

in which $K_u = K_{au}K_{pu}K_{du}$ is the overall winding factor for the u th harmonic.

3. Induced Voltage of a Synchronous Machine

Equation (14) gives the induced voltage when the flux density is distributed as a sine and cosine function, according to (2b). In the synchronous machine with stationary reference axis centered on the field pole, the field pole flux density is a cosine function of odd harmonics, Appendix III, Equation (7), and comparing with (2b)

$$\beta_u' = 0 \quad \beta_u'' = \beta_{2l-1} \quad (15)$$

Therefore, the induced voltage due to the field flux is by (14)

$$e_f = \frac{+2Nql\tau\omega}{\pi 10^8} \sum_k K_{2l-1} \beta_{2l-1} \sin (2k-1)\omega t \quad (16)$$

Thus the induced voltage consists of a series of odd harmonics, as reduced by the winding factors K_{2k-1} . At $t = 0$, when the coil is centered on the field pole, the voltage is zero. A quarter cycle later it reaches its positive maximum.

Comparison of (2b) with (6) of Appendix III shows that there are two cosine terms (type β_u'') and two sine terms (type β_u') in the armature reaction flux densities. Substitution of these four terms in the voltage equation (14) yields for the induced voltage due to armature reaction

$$\begin{aligned} e_a = & -\frac{0.4N^2q^2ml\tau\omega}{\pi 10^8} \sum_n \sum_k \sum_p \frac{K_p}{k} I_n \left\{ \right. \\ & \frac{1}{\omega} \left(\cos [(n-k')\omega t + \theta_n] - \cos [(n+k'')\omega t + \theta_n] \right) \cdot \\ & \quad \left[K_{p+1} \cos (p+k)\omega t - K_{p-1} \cos (p-k)\omega t \right] \\ & - \frac{1}{\omega} \left((n-k') \sin [(n-k')\omega t + \theta_n] - (n+k'') \sin [(n+k'')\omega t + \theta_n] \right) \cdot \\ & \quad \left[K_{p+1} \frac{\sin (p+k)\omega t}{(p+k)} - K_{p-1} \frac{\sin (p-k)\omega t}{(p-k)} \right] \\ & - \frac{1}{\omega} \left(\sin [(n-k')\omega t + \theta_n] + \sin [(n+k'')\omega t + \theta_n] \right) \cdot \\ & \quad \left. \left[K_{p+1} \sin (p+k)\omega t + K_{p-1} \sin (p-k)\omega t \right] \right\} \end{aligned}$$

$$+ \frac{c}{k_p} \left((n - k') \cos [(n - k')\omega t + \theta_n] + (n + k'') \cos [(n + k'')\omega t + \theta_n] \right) \\ \left[K_{p+k} \frac{\cos \left(\frac{p+k}{p+k} \omega t \right)}{(p+k)} + K_{p-k} \frac{\cos \left(\frac{p-k}{p-k} \omega t \right)}{(p-k)} \right] \quad (17)$$

This equation is rather formidable, containing as it does the effects of time and space harmonics and permeance harmonics. However, it can be simplified considerably by putting $\frac{c}{k_p} = \frac{c}{k_p} = \frac{c}{k_p}$, since the permeance coefficients for sine and cosine distributions are substantially equal. Doing so, combining terms, and including with (16), there finally results the complete equation for the induced voltage in the winding,

$$e = + \frac{2Nq\tau l \omega}{\pi 10^8} \sum_k K_{2k} \beta_{2k} \sin (2k - 1) \omega t - \frac{0.4N^2 q^2 m l \tau \omega}{\pi 10^8} \sum_n \sum_p \sum_k \frac{K_k}{k} \frac{c}{k_p} \left\{ \right. \\ \left[K_{p+k} \frac{n+p}{p+k'} + K_{p-k} \frac{n+p}{p-k''} \right] I_n \cos [(n+p)\omega t + \theta_n] \\ \left. + \left[K_{p-k} \frac{n-p}{p-k'} + K_{p+k} \frac{n-p}{p+k''} \right] I_n \cos [(n-p)\omega t + \theta_n] \right\} \quad (18)$$

Expanding (18) and substituting I_D and I_Q ,

$$I_n \cos \theta_n \cos (n + p)\omega t - I_n \sin \theta_n \sin (n + p)\omega t = \\ I_{Qn} \cos (n + p)\omega t - I_{Dn} \sin (n + p)\omega t \quad (19)$$

from which it is clear that direct axis components of voltage will be induced only by direct axis components of current, and similarly for quadrature components.

The fundamental voltage in (18) is given by the term $k = 1$ in the field flux, and by the terms $(p = 0, n = 1)$, $(p = 2, n = 1)$, $(n - p = 1)$ in the armature reaction. But the last possibility, $(n - p = 1)$, does not give a time fundamental of voltage associated with a time fundamental current.

The fundamental of voltage induced by the field flux and the fundamental of current is

$$e_1 = + \frac{2Nq\tau l \omega}{\pi 10^8} K_1 \beta_1 \sin \omega t - \frac{0.4N^2 q^2 m l \tau \omega}{\pi 10^8} \sum_k \frac{K_k}{k} \left\{ \right. \\ \omega_{k0} \left[\frac{K_{1'} - K_{1'}}{k'} + \frac{K_{1''} - K_{1''}}{k''} \right] (I_{Q1} \cos \omega t - I_{D1} \sin \omega t) \\ \left. - \omega_{k2} \left[\frac{K_{2'} - K_{2'}}{2 - k'} + \frac{K_{2''} - K_{2''}}{2 + k''} \right] (I_{Q1} \cos \omega t + I_{D1} \sin \omega t) \right\} \quad (20)$$

But $K_{-k} = -K_k$. Therefore,

$$e_1 = + \frac{2Nq\tau l \omega}{\pi 10^8} K_1 \beta_1 \sin \omega t - \frac{0.4N^2 q^2 m l \tau \omega}{\pi 10^8} \sum_k \frac{K_k}{k} \left\{ \begin{aligned} & \left[2 \phi_{k0} \left(\frac{K_k'}{k'} + \frac{K_k''}{k''} \right) - \phi_{k2} \left(\frac{K_{2-k}'}{2-k'} + \frac{K_{2-k}''}{2+k''} \right) \right] I_{Q1} \cos \omega t \\ & - \left[2 \phi_{k0} \left(\frac{K_k'}{k'} + \frac{K_k''}{k''} \right) + \phi_{k2} \left(\frac{K_{2-k}'}{2-k'} + \frac{K_{2-k}''}{2+k''} \right) \right] I_{D1} \sin \omega t \end{aligned} \right\} \quad (21)$$

Equation (21) shows that the fundamental of the voltage in a synchronous machine is the sum of three terms:

- (1) The voltage induced by the field flux
- (2) The armature reaction voltage due to the direct component I_{D1} of the current, which is in phase with the field flux voltage
- (3) The armature reaction voltage due to the quadrature component I_{Q1} of the current, which is lagging the field flux voltage by 90 degrees in time.

As originally defined, θ is the angle by which the current *leads* the voltage, that is

$$\begin{aligned} I_1 \sin(\omega t + \theta_1) &= I_1 \cos \theta_1 \sin \omega t + I_1 \sin \theta_1 \cos \omega t \\ &= I_{Q1} \sin \omega t + I_{D1} \cos \omega t \end{aligned} \quad (22)$$

For this reason, the armature reaction voltage due to I_{D1} in (21) is seen to add to the voltage due to the field flux. For a *lagging* current θ_1 would be negative, I_{D1} would change sign, and its armature reaction would then oppose the field magnetomotive force.

If in (21) the coefficient of $I_{Q1} \cos \omega t$ is called x_Q , and the coefficient of $I_{D1} \sin \omega t$ is called x_D , then that equation takes the form

$$e_1 = E_f \sin \omega t + x_D I_{D1} \sin \omega t - x_Q I_{Q1} \cos \omega t \quad (23)$$

Rewriting (22) and (23) in vector form, with E_f as reference vector, and using rms values for the currents and voltages,

$$I_1 = I_{Q1} \pm j I_{D1} \quad (24)$$

$$E_1 = E_f \pm x_D I_{D1} - j x_Q I_{Q1} \quad (25)$$

The terminal voltage of the machine is the induced voltage, (25), less the armature resistance and reactance drops. The latter comprises the slot leakage reactance and the end-turn reactance. In the present analysis the reactances contributed by the air-gap armature fluxes (sometimes called belt-differential or zigzag reactance, and including also tooth-tip reactances) have already been included with the harmonic

armature reaction terms. The end-turn reactance, being of the same nature as the air-gap reactance, is also best included with the armature reaction terms of (21) by increasing the permeance coefficients somewhat. On this basis there remains only the resistance and slot leakage terms to be added to (25) to give the terminal voltage

$$\begin{aligned}
 V &= E_1 - (r + jx)I_1 \\
 &= E_1 - r(I_{Q1} \pm jI_{D1}) - jxI_{Q1} \pm xI_{D1} \\
 &= E_1 \pm (x_D + x)I_{D1} - j(x_Q + x)I_{Q1} - r(I_{Q1} \pm jI_{D1}) \\
 &= E_1 + X_d I_d - jX_q I_q - rI_1
 \end{aligned} \tag{26}$$

in which $X_d = x_D + x$, $X_q = x_Q + x$ and I_d and I_q have replaced I_{D1} and I_{Q1} respectively.

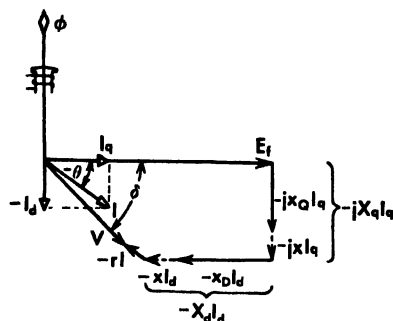


Fig. 2 Salient pole

and X_q . Thus the salient pole machine is characterized by two synchronous reactance components, X_d and X_q .

4. The Round Rotor Machine

For the round rotor machine with uniform air gap the permeance is constant, so that $\phi_{k2} = 0$ and $\phi_{k0} \cong \phi_0$ for all harmonics. Then (21) reduces to

$$\begin{aligned}
 e_1 &= \frac{2Nq\tau l\omega}{\pi 10^8} K_1 \beta_1 \sin \omega t \\
 &\quad - \frac{0.8N^2 q^2 m l \tau \omega \phi_0}{\pi 10^8} \left[\left(\frac{K_1}{k'} \right)^2 + \left(\frac{K_1''}{k''} \right)^2 \right] I_1 \cos (\omega t + \theta_1)
 \end{aligned} \tag{27}$$

Calling x_a the coefficient of I_1 , this equation may be written

$$e_1 = E_f \sin \omega t - x_a I_1 \cos (\omega t + \theta_1) \tag{28}$$

or in vector form, and using rms values,

$$\mathbf{E}_1 = \mathbf{E}_f - jx_a \mathbf{I}_1 \quad (29)$$

The terminal voltage then is

$$\begin{aligned} \mathbf{V} &= \mathbf{E}_1 - (r + jx) \mathbf{I}_1 \\ &= \mathbf{E}_f - r \mathbf{I}_1 - j(x_a + x) \mathbf{I}_1 \\ &= \mathbf{E}_f - (r + jX_s) \mathbf{I}_1 \end{aligned} \quad (30)$$

in which $X_s = x_a + x$ is the synchronous reactance of the round rotor machine. The corresponding vector diagram is shown in Fig. 3.

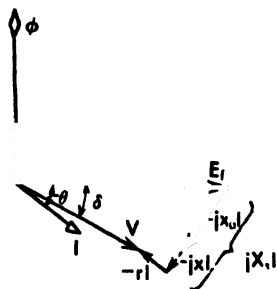


Fig. 3 Round rotor.

5. The Direct and Quadrature Reactances

In accordance with (23) the coefficients of I_{d1} and I_{q1} in (21) have been lumped as reactances x_d and x_q , since they appear in the induced voltage equation in that dimension. These coefficients are called the *direct* and *quadrature* reactance components of armature reaction. They account for all of the flux in the air gap caused by the armature reaction. Using a + and -- sign for the direct and quadrature components respectively

$$\begin{aligned} \begin{cases} x_d \\ x_q \end{cases} &= A \sum \left\{ 2\phi_{k0} \left[\left(\frac{K_k'}{k'} \right)^2 + \left(\frac{K_k''}{k''} \right)^2 \right] \right. \\ &\quad \left. \pm \phi_{k2} \left[\frac{K_k'}{k'} \frac{K_{2-k'}}{2-k'} + \frac{K_k''}{k''} \frac{K_{2-k''}}{2+k''} \right] \right\} \end{aligned}$$

in which $A = 0.4N^2q^2m/\tau\omega \pi 10^8$, and k' is any value of k for which $(k - 1)$ is zero or a multiple of the number of phases; and k'' is any value of k for which $(1 + k)$ is a multiple of the number of phases. Now in a 3-phase machine with 60-degree phase belts, $m = 6$, the permissible values of k' and k'' are

$$\begin{array}{cccccc} k' = & 1 & 7 & 13 & 19 & 25 & 31 \\ k'' = & 5 & 11 & 17 & 23 & 29 \end{array}$$

The harmonic contributions to x_d and x_q may be tabulated as shown on the following page. Considering how rapidly the contributions of the higher harmonics diminish, it is clear that it is sufficient to indicate only the first few harmonics in estimating the armature reaction reactances.

The reactances due to all of the harmonics (except the fundamental) may be segregated and classified as the air gap (belt and zigzag)

k	x_D/A	x_Q/A
1	$2 \Phi_{1,0} K_1^2 + \Phi_{1,2} K_1^2$	$2 \Phi_{1,0} K_1^2 - \Phi_{1,2} K_1^2$
5	$2 \Phi_{5,0} \frac{K_5^2}{25} + \Phi_{5,2} \frac{K_5}{5} \frac{K_7}{7}$	$2 \Phi_{5,0} \frac{K_5^2}{25} - \Phi_{5,2} \frac{K_5}{5} \frac{K_7}{7}$
7	$2 \Phi_{7,0} \frac{K_7^2}{49} + \Phi_{7,2} \frac{K_7}{7} \frac{K_5}{5}$	$2 \Phi_{7,0} \frac{K_7^2}{49} - \Phi_{7,2} \frac{K_7}{7} \frac{K_5}{5}$
11	$2 \Phi_{11,0} \frac{K_{11}^2}{121} + \Phi_{11,2} \frac{K_{11}}{11} \frac{K_{13}}{13}$	$2 \Phi_{11,0} \frac{K_{11}^2}{121} - \Phi_{11,2} \frac{K_{11}}{11} \frac{K_{13}}{13}$
13	$2 \Phi_{13,0} \frac{K_{13}^2}{169} + \Phi_{13,2} \frac{K_{13}}{13} \frac{K_{11}}{11}$	$2 \Phi_{13,0} \frac{K_{13}^2}{169} - \Phi_{13,2} \frac{K_{13}}{13} \frac{K_{11}}{11}$
17	$2 \Phi_{17,0} \frac{K_{17}^2}{289} + \Phi_{17,2} \frac{K_{17}}{17} \frac{K_{19}}{19}$	$2 \Phi_{17,0} \frac{K_{17}^2}{289} - \Phi_{17,2} \frac{K_{17}}{17} \frac{K_{19}}{19}$
19	$2 \Phi_{19,0} \frac{K_{19}^2}{361} + \Phi_{19,2} \frac{K_{19}}{19} \frac{K_{17}}{17}$	$2 \Phi_{19,0} \frac{K_{19}^2}{361} - \Phi_{19,2} \frac{K_{19}}{19} \frac{K_{17}}{17}$

component of the leakage reactance. The fundamental ($k = 1$) reactances are retained as true armature reactions. This classification is of importance when taking saturation into account.

Index

- Ac commutating machines
 - classification 217
 - high resistance leads 223
 - performance characteristics 224
 - principles 216 220
 - repulsion motor 225 229
 - series motor 220 225
- Air gap
 - nonuniform 361
 - uniform 360
- Armature
 - reaction 123 232 233 234 251 254
 - direct 128
 - flux density due to 362
 - group of coils 354
 - negative sequence 358
 - polyphase winding 355
 - quadrature 125 252
 - reactance 129 252
 - single coil 352
 - synchronous converter 332 342 344
 - zero sequence 360
 - windings 104 114
- Autotransformer
 - comparison with transformer 55 56
 - equivalent circuit 54
 - forked 75
 - simple 52 74
 - starting of induction motor 172
- Blocked rotor test
 - polyphase induction motor 155 159
 - single phase induction motor 196
- Capacitor motor 210
- Circle diagram
 - induction motor 160-164
 - synchronous machine 315 320
- Concatenation 182
- Connections
 - delta-delta 80 85 87
 - delta-wye 80 88
 - diagram 64
 - open delta 80 87
 - polyphase 78
 - Scott 80 89
 - single phase 77
 - tee-tie 80 88
 - transformers 80-81
 - wye-delta 80 88
 - wye-wye, 79-85
 - zigzag, 80, 81, 90 92
- Constant current transformer, 60
- Construction
 - induction motor 139 145
 - synchronous converter 333 335
 - synchronous machine 236 249
 - transformer 15 24
- Cross field theory 195 204 208
- Distribution coefficient 117 118 120 122
 - 124 256 336 340 342 343 350 351
 - 366
- Distribution summations 350 351
- Double revolving field theory 195 201 211
 - 213 215
- Double squirrel cage induction motor 179
- Efficient loss
 - in motor 29
 - separation of 30
- Electromagnetic phenomena
 - interrelationship 4 5
- Excitation characteristics 292 296
- Flux
 - density 113
 - induction motor 148
 - rotating machine 114
 - synchronous machine 250 254
- Flaming coefficient 9
- Harmonics
 - induction motor 169 171
- High resistance commutator leads, 275
- Hysteresis
 - effect on wave form 26 27
 - loops 25 26
 - loss 28
 - separation of 30
 - Steinmetz formula 28
- Inductances
 - transformer 38
- Induction generator 190-192
- Induction motor
 - blocked rotor test 156 159
 - circle diagram 160-164
 - constants 155 158
 - construction 139 145
 - core loss 164
 - design constants 164
 - double squirrel cage 179 180
 - equivalent circuits, 150 151, 156
 - flux, 148

- generator, 190-192
- harmonics, 169-171
- magnetizing current, 164
- performance characteristics, 162, 168
- power, 150-154
- principles, 136-139
- reactances, leakage, 165-168
- running light test, 156
- rotating field, 137, 145 148
- rotor, 142-144
- rotor resistance, 153, 155
- slip, 138, 147, 154
- speed control, 181-190
 - changing frequency, 181
 - changing poles, 181
 - concatenation, 182
 - Kramer system, 187-188
 - Leblanc system, 186
 - mechanical, 19
 - rotor rheostat, 182
 - rotor voltage, 186
 - Scherbius system, 189
 - Ward Leonard, 182
- starting, 171 179
 - autotransformer, 172
 - line start, 172
 - wound rotor, 174
 - wye-delta, 174
- stator, 141, 142
- subsynchronous locking, 170
- torque, 154
- vector diagrams, 150
- wound rotor, 174 176
- Instrument transformers, 57-59
- Inverters, 347
- Kramer speed control system, 187
- Leakage
 - flux, transformer, 93
 - reactance, induction motor, 165 168
 - rotating machines, 129-135
 - synchronous generator, 236-237
 - transformer, 94 96
- Leblanc speed control system, 186
- Line start, induction motors, 172
- Machinery, electrical
 - classification of, 1, 2, 3, 4
- Magnetic circuits, 5-9, 25
- Magnetizing
 - characteristics, 8
 - current, induction motor, 164
- Mechanical oscillations, 296-304
- Multiwinding transformers, 65
 - coupling windings, 73
 - independent connections, 70
 - parallel connections, 71
 - regulating transformer, 76
 - series connections, 68
- O-curves, synchronous motor, 292
- Parallel operation
 - synchronous machines, 310-314
 - transformers, 61-63
- Per-unit values, 49-52
- Pitch coefficient, 114, 120 122, 124, 256, 342, 349, 354
- Potier diagram, 268
- Reactance
 - differential, 134-135, 167, 258, 259
 - direct, 236-237, 258, 371-372
 - end turn, 133-134, 166, 259
 - induction motor, 165
 - quadrature, 236-237, 258, 371 372
 - rotating machine, 129-135
 - slot, 130-133, 165, 259
 - synchronous, 236, 258-259, 371
 - transformer, 94-96
 - zigzag, 167
- Reduction factors
 - connection, 119, 120 122
 - distribution, 117, 118, 120 122
 - pitch, 114, 120 122, 124
 - skew, 115, 120 122
- Referred quantities, 49
- Regulation
 - alternator, 265
 - transformer, 44, 46
- Regulating transformer, 76
- Repulsion motor, 225 229
- Resistance
 - windings, 165
- Rotating field
 - armature reaction, 125 128
 - double, 195 201, 211 213, 215
 - induction motor, 137, 145 148
- Rotor
 - definition, 2
 - induction motor, 142-144
 - synchronous generator, 241-242, 248
- Running light test
 - polyphase induction motor, 155
 - single phase induction motor, 199
- Scherbius speed control system, 189
- Scott connection, 80, 89
- Series motor, 220 225
- Shaded-pole motor, 208-210
- Single phase induction motor, 194
 - blocked rotor test, 198
 - calculations, 211
 - capacitor, 210
 - constants, 199
 - cross field theory, 195, 204-208, 213-215
 - double revolving field theory, 195, 211-215
 - equivalent circuits, 198, 200, 207
 - power, 199
 - principles, 194-195
 - shaded-pole, 208

- split-phase, 210
- starting, 208-211
- torque, 199
- transformer and speed voltages, 201-204
- vector diagrams, 205, 206
- Skew coefficient, 115, 120, 365
- Slip, 138, 147, 154
- Speed control
 - induction motor, 181-190
- Split-phase motors, 210
- Starting
 - induction motors, 171-179
 - single phase induction motors, 208-211
 - synchronous converter, 348
 - synchronous motors, 307
- Stator
 - definition, 2
 - induction motor, 141-142
 - synchronous generator, 240, 245-246
- Synchronizing, 307
- Synchronous converter
 - armature reaction, 332, 342, 344
 - construction, 333, 335
 - currents, 331
 - current ratio, 329, 337
 - heating, 330, 338
 - hunting, 346
 - inverter, 349
 - losses, 339, 340
 - principles, 326
 - starting, 348
 - voltage control, 345
 - voltage ratio, 328, 335
- Synchronous generator and motor
 - armature reaction, 232, 233, 234, 251, 254
 - direct, 232, 252, 371
 - quadrature, 232, 252, 371
 - synchronous, 236
 - circle diagrams, 315, 320
 - construction, 238, 249
 - efficiency, 320, 324
 - excitation characteristics, 292
 - flux distribution, armature reaction, 254
 - flux distribution, field pole, 250
 - frequency, 235
 - leakage reactance, 236, 237
 - losses, 320, 324
 - mechanical oscillations, 296-304, 306
 - O-curves, 292
 - parallel operation, 310, 314
 - poles, 249, 250
 - Potier diagram, 268
 - power, 233, 234
 - power transfer, 279, 289
 - equations, 290, 291
 - principles, 231
 - reactances, 258, 259
 - regulation, 266
 - AIEE (old) method, 270
 - ASA method, 272
 - comparison of methods, 275
 - emf method, 269
 - example, 276, 278
 - general method, 273
 - mmf method, 271
 - problems, 278
 - salient pole machine, 274
 - rotor, 241-242, 248
 - salient pole, 235
 - starting, 304
 - stator, 240, 245, 246
 - synchronizing, 307-310
 - torque, 234
 - V-curves, 297
 - vector diagrams, 260, 266
 - voltage, induced, 231, 256, 367
 - windings, 247
- Three winding transformer, 56, 57
- Transformers
 - autotransformer, 52, 56, 74, 75
 - bushings, 23
 - classification, 10, 14, 24
 - coils, 15, 18, 21, 22
 - connections, 63
 - constant current, 60
 - constants, 40, 43
 - construction, 15, 24
 - cores, 15, 16, 17, 18
 - coupling windings, 73
 - delta delta, 80, 87
 - delta wye, 80, 88
 - differential equations, 38
 - efficiency, 45, 46
 - equivalent circuit, 36, 37, 41, 45
 - general equations, 32, 37, 38, 39
 - generalized constants, 47, 49
 - independent connections, 70
 - instrument, 57, 59
 - insulation, 17
 - leakage flux, 93
 - multiwinding circuits, 65
 - open delta, 80, 87
 - parallel operation, 61, 63
 - performance calculations, 44, 46
 - per unit values, 49, 52
 - principles of operation, 12
 - problems, 96, 102
 - ratio, 12
 - reactance, 34, 94, 96
 - referred quantities, 49, 52
 - regulation, 44, 46
 - tee tee, 80, 88
 - tests, 40, 43
 - three winding, 56, 57
 - vector diagram, 36
 - windings in parallel, 71

- windings in series, 69
- wye-delta, 80, 88
- wye-delta-zigzag, 81, 92
- wye-wye, 80, 79-85
- zigzag, 80, 81, 90, 92
- Transformation ratio, 12
- Turbo-generator, 238-243
 - cutaway view, 234
 - rotor, 241-242
 - stator, 240
- V-curves, synchronous motor, 292
- Voltages
 - induced, 34, 111-123, 231, 256, 364-371
 - speed (motional) (cutting), 112
 - transformer action, 111
- Ward-Leonard control, 182
- Wave form
 - effect on of hysteresis, 27, 36
- Windings
 - armature, 104-111
 - coupling, 73
 - diamond, 107
 - direction, 64
 - double-layer, 106
 - fractional slot, 108-111
 - mesh or delta, 105
 - multiple circuit, 106
 - parallel, 71
 - series connection, 68
 - single-layer, 106
 - star or wye, 105
 - wye-wye, 79-85
- Wound rotor induction motor, 174-176, 178
- Wye-delta starting, induction motor, 174
- Y-Y connection, 79-85
- Zigzag
 - autotransformer, 80, 81, 90
 - transformer connection, 80, 81, 92
 - wye-delta, 92

